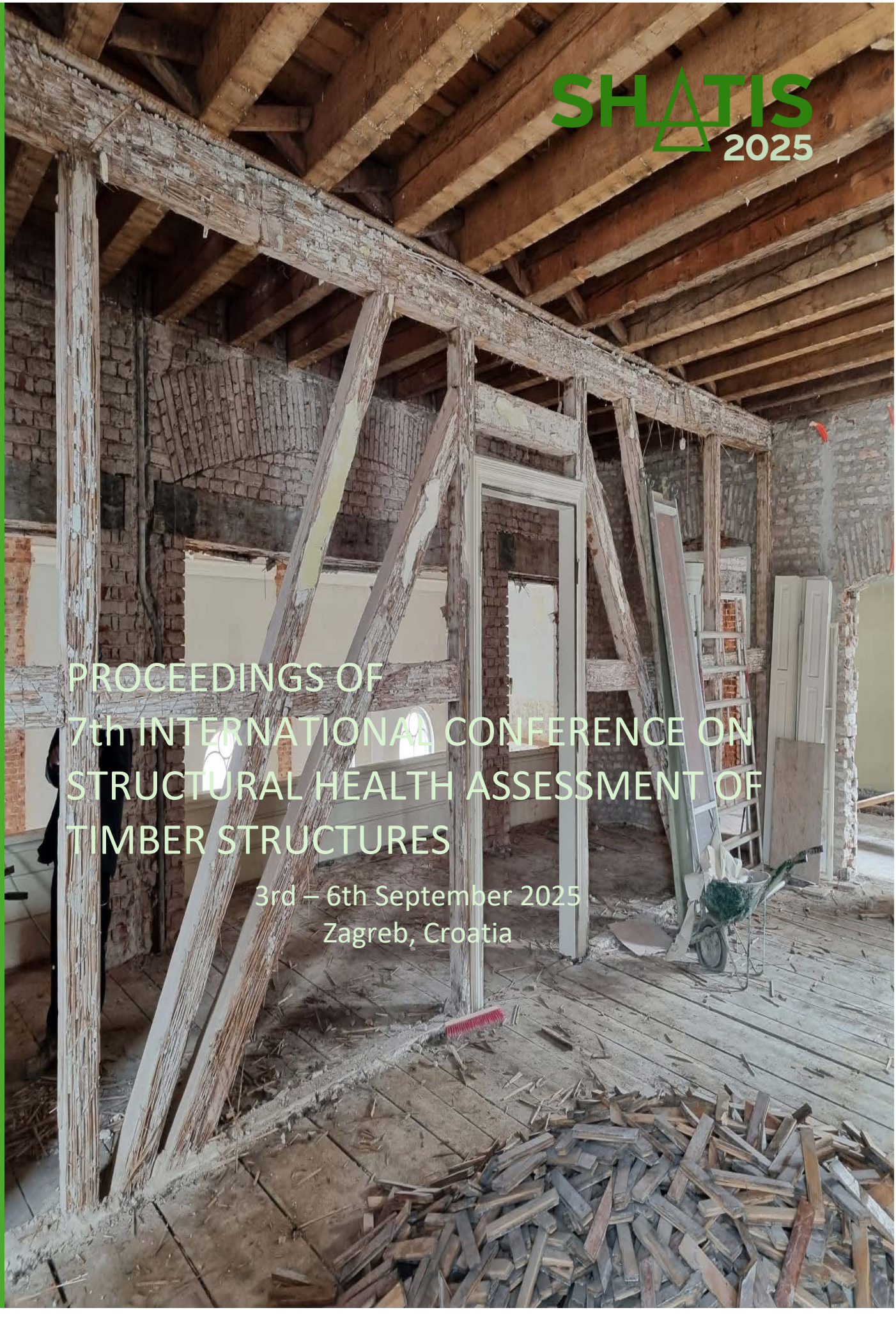

PROCEEDINGS OF 7th INTERNATIONAL CONFERENCE ON STRUCTURAL HEALTH ASSESSMENT OF TIMBER STRUCTURES

3rd – 6th September 2025
Zagreb, Croatia

Proceedings of the SHATIS 2025 – 7th International Conference on Structural Health Assessment of Timber Structures

3rd – 6th September 2025, Zagreb, Croatia

International Conference on Structural Health Assessment of Timber Structures

Editors

prof. Hrvoje Turkulin
University of Zagreb Faculty of Forestry and Wood Technology

prof. Vlatka Rajčić
University of Zagreb Faculty of Civil Engineering

assoc. prof. Tomislav Sedlar
University of Zagreb Faculty of Forestry and Wood Technology

The papers herein are published in the form as submitted by the authors after scientific review. Minor changes have been made to address obvious errors and discrepancies.

Proceedings of SHATIS 2025

Edited by Hrvoje Turkulin, Vlatka Rajčić and Tomislav Sedlar

University of Zagreb

ISBN 978-953-292-091-8 (PDF)

ORGANIZING INSTITUTIONS

University of Zagreb Faculty of Forestry and Wood Technology

University of Zagreb Faculty of Civil Engineering

Studio ARHING d.o.o.

Ministry of Culture and Media of the Republic of Croatia

ICOMOS Croatia

in collaboration/with the support of

Croatian Chamber of Civil Engineers

Croatian Chamber of Forestry and Wood Technology Engineers

Croatian Chamber of Architects

International Scientific Committee on the Analysis and Restoration
of Structures of Architectural Heritage

Croatian center for earthquake engineering

Drvene konstrukcije d.o.o.

SCIENTIFIC COMMITTEE

Maurizio Piazza (University of Trento, Italy)

Ivan Giongo (University of Trento, Italy)

Bohumil Kasal (University of Primorska, Slovenia)

Francisco Arriaga Martitegui (Universidad Politécnica de Madrid, Spain)

Werner Seim (University of Kassel, Germany)

Mariapaola Riggio (Oregon State University, USA)

Gerhard Schickhofer (Institut für Holzbau und Holztechnologie, Austria)

Thomas Tannert (University of Northern British Columbia, Canada)

Philipp Dietsch (Karlsruhe Institute of Technology, Germany)

Beatrice Faggiano (University of Naples "Federico II", Italy)

Maria Rosa Valluzzi (University of Padova, Italy)

Massimo Fragiacomo (Università degli Studi dell'Aquila, Italy)

Guillermo Íñiguez González (Universidad Politécnica de Madrid, Spain)

Maria Adelaide Parisi (Politecnico di Milano, Italy)

Roberto Tomasi (Norwegian University of Life Sciences, Norway)

Alfredo Geraldes Dias (University of Coimbra, Portugal)

José Saporiti Machado (National Laboratory for Civil Engineering, Portugal)

Paulo B. Lourenço (University of Minho, Portugal)

Marius Mosoarca (Politehnica University Timisoara, Romania)

Tomaž Pazlar (Slovenian National Building and Civil Engineering Institute (ZAG), Slovenia)

Robert Jockwer (Chalmers University of Technology, Germany)

Maria Loebjinski (iBHolz Technische Universität Braunschweig, Germany)

Mike Sieder (iBHolz Technische Universität Braunschweig, Germany)

Petr Kuklík (Czech Technical University, Czechia)

Miloš Drdácký (ITAM, Czechia)

Jiři Kunecký (ITAM, Czechia)

Georg Hochreiner (Technische Universität Wien, Austria)

Jerzy Jasieńko (Wroclaw University of Technology, Poland)

Thomas K. Bader (Linnaeus University, Sweden)

Gi Young Jeong (Timber Frame Building Safety Center, Republic of Korea)

Xiaobin Song (Tongji University, China)

Anna Sandak (InnoRenew CoE, Slovenia)

Boštjan Lesar (University of Ljubljana, Slovenia)

Michele Mirra (University of Delft, Netherlands)

Yutaka Goto (Chalmers University of Technology, Sweden)

Kaori Fujita (University of Tokyo, Japan)

Yasemin Didem Aktas (University College London, UK)

Andrii Bidakov (O.M.Beketov National University of Urban Economy in Kharkiv, Ukraine)

MAIN ORGANIZERS

Hrvoje Turkulin (University of Zagreb Faculty of Forestry and Wood Technology, Croatia)

Vlatka Rajčić (University of Zagreb Faculty of Civil Engineering, Croatia)

ORGANIZING COMMITTEE

Mislav Stepinac (University of Zagreb Faculty of Civil Engineering, Croatia)

Vjekoslav Živković (University of Zagreb Faculty of Forestry and Wood Technology, Croatia)

Tomislav Sedlar (University of Zagreb Faculty of Forestry and Wood Technology, Croatia)

Marin Hasan (University of Zagreb Faculty of Forestry and Wood Technology, Croatia)

Andrija Novosel (University of Zagreb Faculty of Forestry and Wood Technology, Croatia)

Jiří Kunecký (ITAM, Czechia)

Jorge M. Branco (University of Minho, Portugal)

Juraj Pojatina (Studio ARHING d.o.o., Croatia)

David Anđić (Studio ARHING d.o.o., Croatia)

Cover photo

Juraj Pojatina (Studio ARHING d.o.o., Croatia)

PREFACE

After the last SHATIS held in Prague, we are pleased to invite all those involved in structural timber engineering who are eager to meet, share experiences, and exchange ideas in Zagreb. The conference is renowned for its passion for timber, shared by an international group of researchers, professional engineers, practitioners, as well as architects, conservators, and restorers. A wide spectrum of themes concerning the assessment, repair, and monitoring of historic and new timber structures provides unique insight into new and modern practices and innovations in the field.

Wood is not only a material or a subject of someone's profession; it truly presents a passion for many professionals who have dedicated their careers, efforts, interests, and knowledge to this fascinating matter. Dealing with historic timber structures in all their complexity inevitably calls for sharing this passion with other colleagues. Old wooden structures, whether they form a part of cultural heritage or present just parts of „common" buildings, call for our endeavours to honour them, to nourish their work with all our care, to pay tribute to generations of builders and carpenters who left us those structures, very often marvels of human achievement. Even the technically uneducated public is fully aware of the beauty, technical advantages, and – in the modern age – environmental benefits of applying wood in building. It is our task to work diligently in order not to disappoint the public and to offer the knowledge by which the wood shall be ever more and ever better used in construction.

However, many of the specifics of historic wood and its structures teach us the almost forgotten aspects of its use, which can be an everlasting inspiration for us and for future generations. Perhaps the time has come for us to make a loop of 100 or more years back, when a carpenter's apprentice needed an hour or two to make a good carpenter's joint. With modern technologies, such joints can be made in minutes. Therefore, we could invest effort in studying how such joints can be made of wood only, which is perfect in an ecological sense, and apply this knowledge to modern and future wood construction.

Following two major earthquakes in Croatia in 2020, a significant number of historic timber structures are now undergoing restoration. As an inseparable part of the conference, site visits will be organised to the most interesting construction and historic timber sites.

The conference could not have been organised without the participation and general support of many institutions and professionals, as well as the assistance of our supporting institutions and the engagement of numerous volunteers who contributed to the meeting's preparation. However, the greatest thanks should go to our authors, reviewers, and numerous experts who are part of our Scientific Committee. The Editors and the Organising Committee warmly express their gratitude. Let us share our passion again in Zagreb and send a motivating message about our conference to future organisers, colleagues, and friends.

Prof. dr. sc. Hrvoje Turkulin

Prof. dr.sc. Vlatka Rajčić

Mr Juraj Pojatina, civ. eng.

TABLE OF CONTENTS

WOOD PROPERTIES, STRENGTH GRADING, ADHESIVE BONDS

TESTING METHODOLOGY - IN SITU AND LABORATORY TESTING

GENERAL ASSESSMENT, DIAGNOSTICS METHODOLOGY

STRENGTHENING, STABILITY AND MODELLING

BIODEGRADATION

STRUCTURAL, REINFORCEMENTS AND RETROFITTING

CROATIAN EXPERIENCES

WOOD PROPERTIES, STRENGTH GRADING, ADHESIVE BONDS

THE EN 17121 IN PRACTICE: REFLECTIONS AND RESULTS AFTER FIVE YEARS OF APPLICATION

Nicola MACCHIONI[1] and Margherita VICARIO[1]

[1] CNR-IBE, Institute of BioEconomy, Sesto Fiorentino (FI), Italy

Invited lecture

ABSTRACT

The EN 17121, which provides guidelines for the on-site assessment of load-bearing timber structures, was published in autumn 2019 after four years of discussions within a committee that brought together specialists from various fields, including civil engineers, architects, and wood technologists. The standard follows a methodology that begins with an archival desk survey and, through a preliminary assessment and report, ultimately leads to the detailed study and diagnostic report.
More than five years after the publication of the standard, this paper reflects on its dissemination, drawing on an analysis of scientific publications on the subject and the practical application of the methodology by CNR-IBE in five significant historical Italian timber structures. In these cases, IBE was tasked with conducting detailed diagnostic surveys, and the resulting diagnostic reports provided valuable insights into the actual application of the standard.

KEYWORDS: EN 17121, on-site assessment, historic timber structures, standard, cultural heritage

INTRODUCTION

Over the centuries, the preservation of large, decorated attics or exposed timber roofs has consistently garnered significant attention, as these elements are regarded as integral to our architectural and artistic heritage. By contrast, the less visible structures, which comprise most of the historical timber heritage, have only recently begun to receive serious consideration for preservation. A significant cultural shift occurred from the 1980s onwards when the first scholars began to recognise ancient roofs and hidden attics as cultural assets. Such structures were increasingly valued as artefacts that offer valuable insights into the evolution of human material culture, through the choice of timber, the design of structural joints, and the organisation of roof frameworks. Timber structures hold, among other things, an essential intrinsic value as a significant carbon sink; for example, the roof timber structure of the Florence Cathedral was built using 360 m^3 of wood, which equates to 270 tons of carbon.
The recognition of historic wooden structures as part of the heritage has had significant consequences. Among these, the need to preserve them where they are and as they are is compatible with structural safety conditions. This has required the development of a comprehensive set of methodologies, protocols, diagnostic tools, principles, and guidelines aimed at providing information on the original nature of the structure and the consequences of its structural history. As the millennium approached, studies carried out from this perspective produced numerous practical examples that became case studies, providing a foundation for discussions aimed at establishing standards documents. The first published standard was the Italian UNI 11119:2004[1]. This was later followed by the European standard EN 17121[2], published in autumn 2019. A document intended for all individuals involved in the conservation of heritage buildings that contain wooden elements, from building owners and responsible authorities to the professionals engaged in such work.

The general aim of the standard is to provide guidelines on the criteria for on-site assessment of load-bearing timber structures in heritage buildings recognised for their cultural and historical significance. The standard is organised into three main sections: a description of the preliminary assessment, a description of the detailed survey, and finally, an informative annexe that lists the current tools for non-destructive testing of timber structures. The standard does not provide guidelines for the design of repairs; nevertheless, it suggests that intervention works should only be undertaken on a heritage structure as a last resort and should have a minimal impact on the building fabric.
This paper aims to analyse practical cases of the standard's application by reviewing available literature and significant Italian historic timber structures surveyed over the last five years by the Institute of BioEconomy of the National Research Council of Italy (CNR-IBE), which is the research institute of the authors. These cases serve as a basis for reflections on the extent of the standard's application and the challenges encountered in its full implementation. This paper will evaluate the entire assessment process described in the standard. Subsequently, five case studies of historic timber structures surveyed by CNR-IBE will be detailed, and the application of the various steps listed in the standard will be examined. The timber structures were examined during a structural diagnosis, following the procedure outlined in the section titled "Detailed survey" in the standard.

AN OVERVIEW OF THE DISSEMINATION OF EN 17121 IN SCIENTIFIC LITERATURE

To analyse the dissemination of the standard in Europe five years after its publication, a review of the available scientific literature was carried out. A potential limitation of this analysis relates to the nature of the standard itself, which is intended as a practical guideline for diagnostic activities. Therefore, the standard may have been used in practice without producing any corresponding publications. This is particularly probable since restoration projects are rarely deemed suitable for publication, and even less often for inclusion in peer-reviewed scientific journals.
The literature review was conducted using Google Scholar, chosen for its broad coverage of scholarly publications, including non-indexed conference proceedings and other grey literature. The search was performed using the term "*EN 17121"*, applied across the full text to retrieve the highest possible number of relevant publications. The review was limited to articles published in English between 2019 and 2025, corresponding to the period following the release of the standard. From the search, 25 journal articles and 14 conference proceedings were selected as relevant to the topic.
Of the 40 selected publications, the distribution by year is shown in the graph in Figure 1. This trend indicates a growing interest in the topic following the introduction of EN 17121 in 2019, with a peak in 2022. Particularly relevant is the contribution of papers presented at the International Conference on Structural Health Assessment of Timber Structures (SHATIS) in its last two editions. All four identified contributions from 2019 came from this conference, three were presented within the session *"From the standards to its practical application: review on standards on structural assessment and examples from practice on the field",* during which the draft standard prEN 17121:2017 was introduced, and one was delivered as part of a keynote lecture. At SHATIS 2022, six papers cited the standard, confirming the increasing dissemination and adoption of EN 17121 within the scientific community.

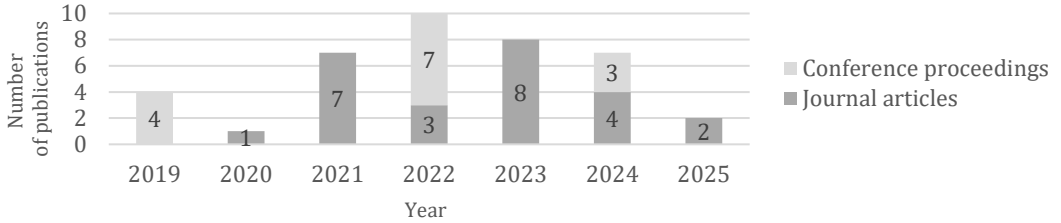

Figure 1. Distribution of papers regarding EN 17121 over the years.

Among the topics addressed in the publications, two main areas of focus can be identified.
One, which is predominant, includes studies dedicated to evaluating and estimating the mechanical performance of timber members in situ. These works refer to the standard as a tool for knowledge, recognising its value in the context of historic timber structures. However, the focus is primarily on the development and application of methodologies and techniques for the mechanical and physical characterisation of the material, using non-destructive (NDT) and semi-destructive tests (SDT) on-site, as well as destructive tests (DT) in the laboratory. The lack of a clear and shared methodology for assigning strength classes for structural calculations remains the most significant issue identified.
The second area of focus concerns the application of the EN 17121:2019. Few papers describe case studies of timber structure diagnosis, following the guidelines of the standard.
Perkovic et al. [3] utilised the paragraph of the standard outlining the comprehensive survey of timber structures, particularly the visual inspection and moisture content measurements. They opted not to employ the visual grading of timber but instead to evaluate the mechanical performance of the timber elements using the dynamic MOE measurement. Arriaga et al. [4] apply the standard to an 18th-century building in Madrid, facing several problems, given by the real accessibility of the timber elements, frequently hidden in the masonry, impeding the visual evaluation of the strength-reducing wood defects. Saarinen et al. [5] applied the entire standard to the timber roof assessment of a Finnish castle, concluding that the standard functions effectively in practice when utilised for complex architectural conservation projects, also including training and students. Lopez et al. [6] reference the standard in the introduction of their paper concerning the assessment of 16th-century timber floors in a Spanish house; however, the authors do not state the application of the standard in their diagnostic activities. Nevertheless, the path followed aligns perfectly with that described in the standard. In the case study presented by Aira-Zunzunegui et al. [7], the preliminary assessment was carried out by a private company. Based on this assessment, the authors subsequently performed a detailed analysis in accordance with EN 17121 and provided recommendations for intervention. MOE, MOR and density were estimated through non-destructive testing (NDT) for the assignment of the strength class. In Turkulin et al. [8], the structural analysis of the roof structure of the Zagreb Cathedral is presented. The detailed survey was conducted following the guidelines of EN 17121, and the strength classes were assigned through a comparative study of various methodologies. These included visual grading and density measurements on drill cores, non-destructive testing (NDT) such as stress-wave, screw withdrawal, and resistance drilling, as well as destructive testing (DT) on medium-sized samples. The study highlights that the assignment of strength classes is the most critical factor for a reliable structural assessment of existing structures. In the work of Henriques et al. [9], it is emphasised that it is necessary to define simplified methodologies and guidelines to enable the effective implementation of the assessment of existing timber structures. For this purpose, a simplified methodology based on EN 17121 is defined and tested on a case study, followed by the structural analysis and the evaluation of potential intervention needs.

APPLYING EN 17121: INSIGHTS FROM ITALIAN CASE STUDIES

Historic timber structures in Italy are mainly flooring or roofing frameworks. The examined timber structures (*Figure 2*) are all roof frameworks of significant historic buildings, mainly in Tuscany (Florence and Prato), with one in Turin. In Florence, these include the roofs of the Cathedral, the San Marco Museum, and the Basilica of Santa Croce. In Prato, the notable structure is the roof of the church of San Francesco. In Turin, the structure under study is the roof of the main hall of Palazzo Madama.
During the detailed survey, the following analyses were carried out: wood identification, measurements of moisture content and moisture gradients, a geometrical survey, evaluation of biotic and abiotic decay, visual structural grading of timber members, and an inspection of structural joints.

Wood identification was initially performed by examining anatomical features visible to the naked eye or with a low magnification lens. If the results appeared unreliable, a small sample was taken for laboratory identification using microscopic examination.
Wood moisture content and moisture gradients were estimated by measuring with electric moisture meters at different points in the structure, specifically as close as possible to the connections to the wall, which are often potential moisture traps.
The geometrical survey focused on measuring the sections of various timber members at different points, at least at the connections to the walls.
The biotic decay was assessed by thoroughly examining the surfaces to determine the existence of insect infestations, thereby estimating the presence of exit holes and potential ongoing attacks. Their depth was gauged using chisel and hammer percussion. Fungal rot attacks, normally not directly visible, were assessed by resistographic inspection through micro-drillings (using an IML Resi PD400), specifically concentrated close to the walls, to inspect the portions of the timber embedded in the walls. The micro-drillings simultaneously allow for the detection of decayed portions and for estimating the section still intact. Abiotic decay consists of mechanical failures that can be observed through careful examination.

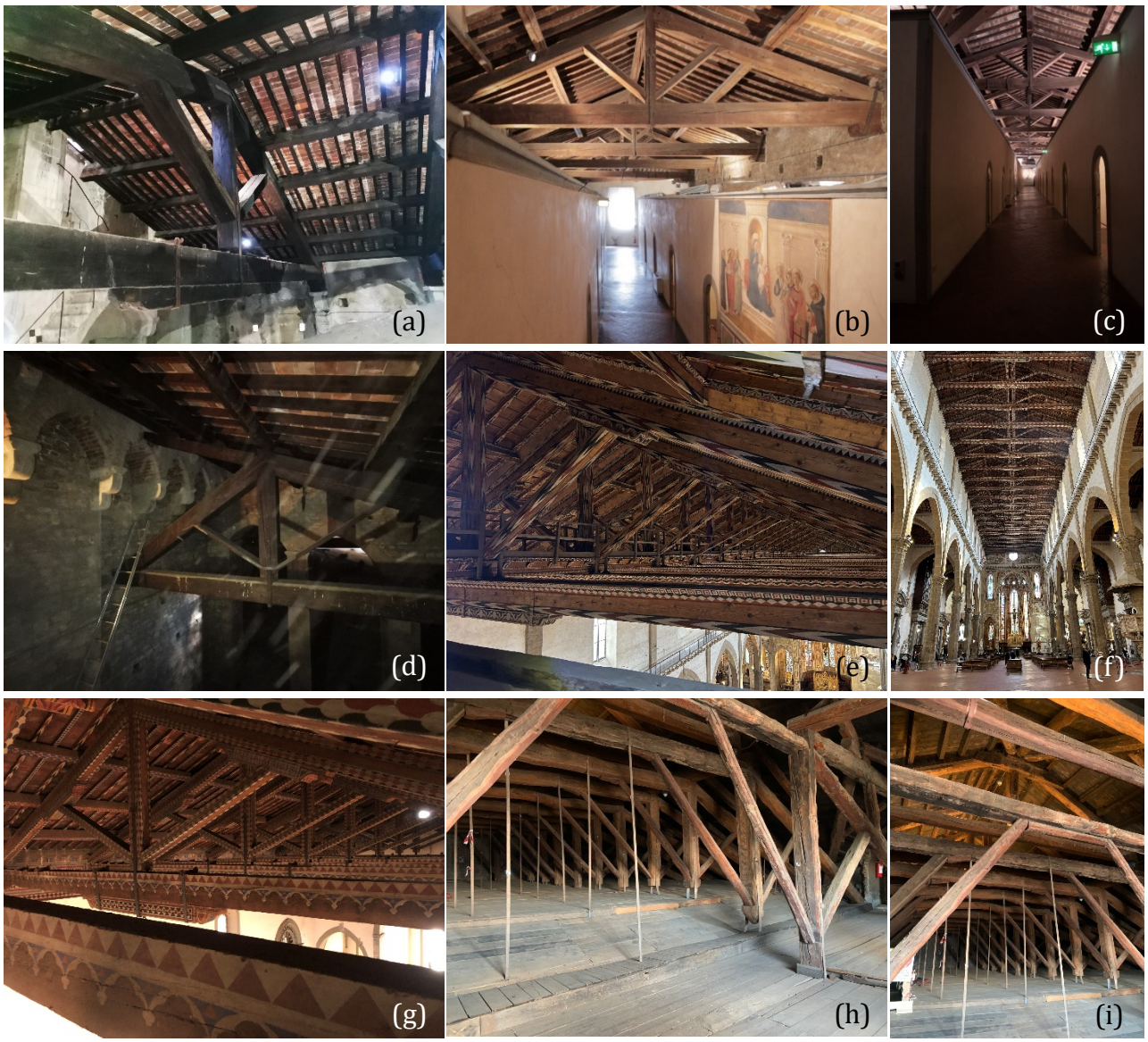

Figure 2. (a) and (d) Truss of central and lateral nave roof at Florence Cathedral; (b) and (c) two aisles of the Museum of San Marco; (e) and (f) Trusses organisation of the central nave roof at Santa Croce Basilica; (g) View of the roof structure of San Francesco in Prato; (h) and (i) Turin, the trusses of the main roof of Palazzo Madama.

Visual grading was performed by closely observing each element's characteristics that reduce mechanical performance and applying these observed features to the grading table published in the Italian standard UNI 11119.
Each mechanical joint in every truss was geometrically measured and analysed. More specifically, the joints that characterise the health of a truss, such as the tie beam-rafter joints, were accurately observed and measured to evaluate their effectiveness.

Florence Cathedral

The analysed timber structures are the roof structures of the central nave and the two lateral naves. The three structures examined are not visible from the church due to the presence of masonry vaults. The roof of the central nave is supported by 19 large Italian trusses, spanning approximately 18 meters (Figure 2a), while the roofs of the two lateral naves are supported by 16 asymmetric trusses, each spanning around 9 meters (Figure 2d). According to the literature, the roof was installed during the last decades of the 15th century, following the completion of the famous dome.
The aim of the work requested by the management of the Cathedral was to acquire a detailed understanding of the timber roof structures for safety reasons. Initially, no restoration work was planned.
About the preliminary assessment, the desk survey was partially conducted during the detailed survey, primarily to explain some peculiarities that arose during the detailed analysis. The preliminary visual survey involved a quick and straightforward observation of the structures to be examined, without indicating specific areas to be highlighted during the detailed analysis. The detailed survey was carried out based solely on a cloud point measured survey of the central nave timber structures. No information was available on the lateral naves timber structures. Since no preliminary information was available, no preliminary structural analysis was conducted.
The detailed survey was quite extensive because it included creating a geometric survey of the side aisles. It should be noted that even when a laser-scanner survey is available, examining the details of the connections between the structural elements is necessary during diagnosis. The survey of the lateral aisles facilitated a thorough study of four almost-ignored horizontal timber structures, most likely designed by Brunelleschi himself to counteract the lateral movements of the walls caused by the dome's load during construction [10].
The data collected from the detailed investigations enabled a comprehensive structural analysis. The management team of the Cathedral of Santa Maria del Fiore now has an essential tool to assist in planning the restoration and maintenance of the church's roofing structures. The first structural restorations are now underway as an initial outcome derived from the data in the diagnostic report.

San Marco Museum in Florence

The San Marco Museum in Florence is located in the monumental part of the homonymous Dominican Convent. The timber structure analysed belongs to the roof covering the former dormitory area of the Dominican friars, situated on the first floor and dating back to the mid-15th century. This area, one of the oldest in the complex, consists of three corridors with 43 cells for friars, arranged along the sides. The entire space is covered by a double-pitched roof supported by 28 traditional Italian trusses, spanning approximately 7 to 9.5 meters in length (Figure 2b). The roof structure, although partially hidden by the cells, remains visible (Figure 2c).
The on-site assessment of the roof structure was carried out as part of the DIA-Smart project, which focuses on innovative approaches to the diagnosis of historic timber structures. The objective was to test new diagnostic methods and to collect data in a structured and queryable format.

As part of the preliminary assessment, some archival information and the results of previous diagnostic investigations on the structure were made available. These provided a general understanding of the structure and helped in planning subsequent activities.
Point cloud surveys, combining laser scanning and photogrammetry, were integrated to obtain a detailed geometric survey. The detailed survey provided an in-depth understanding of the structure, and the collected data were subsequently used both for the development of an HBIM model for information management and for the structural analysis conducted to assess the need for potential interventions.

Palazzo Madama in Turin

Palazzo Madama in Turin has origins dating back to the defensive structure of the east gate of the Roman city of *Augusta Taurinorum* (nowadays Turin). Over the centuries, it was transformed into a typical medieval castle and later into a ducal residence. The analysed structure is the roof system of the central hall, originally a 17th-century ballroom that was then converted into the hall of the first Italian senate. The timber framework is not directly visible due to a false wooden ceiling, which is supported by the upper examined timber trusses (Figure 2h-i).
The diagnostic analysis of the roof structure of the first Senate of the Kingdom of Italy was commissioned from the CNR-IBE to collect the necessary data for designing a new tourist route, including the attic of the Palace and its timber structure. For the management authorities and the designers, it was therefore essential to understand the condition and performance of the entire structure. Regarding the initial stages, the results of a potential desk survey have not been made available, except for some general information on the history of the various elements of the existing structure. The preliminary visual survey involved a specialised inspection of the current timber structure with the designer of the intervention, who explained the project's purpose and the data needed to design a transparent footbridge that would rest on the tie-beams of the wooden trusses. The aims of this brief survey do not entirely align with the objectives of the preliminary survey outlined in the standard.
Conversely, the results of the dimensional survey based on a point cloud generated by a laser scanner were available during the detailed survey, significantly assisting the fieldwork. No preliminary static analysis had been carried out before the detailed diagnostic work.
The most notable results from the diagnostic survey can be summarised as follows. Firstly, a peculiar mixture of wood species, probably linked to different construction phases: spruce (*Picea abies*), larch (*Larix decidua*), and deciduous oak (*Quercus* sp. subgenus *Quercus*). Then, the tie-beams covering a very long span of about 20 meters, made from a single piece without junctions. The tie-beams have an alternating arrangement of different sections: smaller sections (approximately 20 x 30 cm) alternate with larger sections (about 30 x 45 cm), likely due to various construction phases. From a mechanical perspective, two of the smaller section tie-beams were found to be broken due to bending, approximately at mid-span. They are now collaborating only to a limited extent and will need a consolidation before being charged again.

Santa Croce Basilica in Florence

The Basilica of Santa Croce is one of the most important churches in Florence, attracting millions of visitors each year. The timber roof structure of this Franciscan church is visible to visitors and plays a significant role in its architectural decoration, thanks to the painted geometric designs on the timber elements. The central nave's structure consists of 32 trusses that span approximately 18 meters (Figure 2e-f). The side aisles are covered by seven gable roofs, each supported by five decorated beams, covering about 8 meters. According to documents, the roof was installed during the construction of the church between the 13th and 14th centuries, but maintenance work over the centuries has introduced new elements or prostheses.

The management body of the Basilica di Santa Croce had to conduct a detailed survey to evaluate the timber structures supporting the roof. As previously described for the Florence Cathedral, there is no ongoing restoration project for the roof. However, there are two significant differences compared to the Cathedral roof: the Santa Croce timber structure is visible and decorated, making it a prominent decorative element of the church. The second key difference is that, being visible, the timber structure is accessible only via an elevated platform.
A prior archival desk survey has not informed the detailed diagnosis; furthermore, access to the historic information is currently quite complicated. The difficult access to the structures rendered any preliminary survey practically impossible. The measured survey through laser scanning is ongoing, and as a result, the data are not yet available. Without any data, no preliminary structural analysis has been performed.
The detailed survey is ongoing, and currently, more than one-third of the entire church roof has been surveyed. It is evident that over the eight centuries of the building's existence, several structural restorations have occurred. In most cases, the intervention repaired decayed element extremities (both tie-beams and rafters), using connecting prostheses made from the same wood species. Currently, it is not possible to precisely date them (as the archive cannot always provide accurate information) without a detailed dendrochronological analysis. Nevertheless, it is possible to identify the variability and evolution of the metal fasteners used to connect the prostheses. Some of these appear older, made of wrought iron and without screws, while others, more recent, feature screwed fasteners, some with squared nuts and others with hex nuts. Currently, several tie-beams are no longer composed of the original two portions but can consist of three or four with the prostheses. The survey also allowed for describing a peculiar ventilation system, conceived from the beginning to improve the durability of the entire timber structure, which was made with non-durable European fir.

San Francesco Church in Prato

As for Santa Croce, the Franciscan church in Prato, dedicated to San Francesco (St. Francis), is covered by a visible and decorated timber structure. The church is a single nave, covered by sixteen 15-meter-span trusses (Figure 2g). The dendrochronological analysis dated the structure to the second half of the 13th century, followed by a complete roof restoration made at the end of the 19th century. The survey was performed in a double-phase manner. In the preliminary phase, only the connections to the walls were analysed using an elevated platform; later, during the restoration works, all other parts of the trusses were inspected thanks to scaffolding.
Among the selected examples, the activity at the Franciscan church in Prato was the only one suggested by an ongoing restoration project. The restoration of the roof of the Church of San Francesco in Prato was entrusted to an architectural design firm that supervised all the preliminary phases.
Therefore, the detailed diagnostic activity, along with a dendrochronological dating campaign [11], was planned after a thorough analysis of the archives (desk survey) and a visual assessment conducted from an aerial platform, which led to a preliminary structural evaluation.
The initial report highlighted the necessity for a comprehensive diagnosis and set its priorities. During several initial meetings, emphasising the importance of identifying the wood species used, conducting detailed analyses of the truss supports, and accurately recording all structural joints in the wooden components was stressed. Ultimately, recording all defects of each timber member and performing a visual structural grading enabled the creation of a diagnostic report and final structural assessment.
Key issues emerged during the detailed survey, such as some original medieval tie-beams featuring the structural dovetail joint with the original king-posts, crafted from elm wood (*Ulmus* sp.). The sections of the original king-post inserted into the tie-beam remained intact. Based on experience, it was common during the medieval period to construct king-posts from elm wood, particularly in the Florentine region.

A diagnostic result that the authors consider noteworthy pertains to wood species. These results provide essential diagnostic information, as various woods exhibit distinct physical and mechanical properties. Furthermore, they relate to environmental and cultural factors, such as the origin of the raw material, species selection, processing techniques, and transportation. Such issues facilitate a deeper understanding of historical knowledge and practices. In fact, in historic Italian wooden structures, some variability in the woods used is observed, which is connected to the watershed of the rivers flowing through the major cities. Most of the described timber structures are located in the centre of Florence. In Florence, the most widely utilised timber is European fir (*Abies alba*), sourced from the forests near the source of the Arno, the river that crosses Florence [12]. The presence of elm wood (*Ulmus* sp.) is more sporadic, mainly associated with the king-posts in trusses. Sweet chestnut (*Castanea sativa*) wood is also present, but it tends to be found in shorter timber elements. One example of timber structures is found in the city centre of Turin. The rivers reaching the city all originate from the nearby alpine valleys of the western Alps; therefore, it is common to find alpine timbers, such as fir, spruce (*Picea excelsa*), and larch (*Larix decidua*). The presence of oak (*Quercus* sp.) elements from the surrounding plains is not uncommon, especially in monumental buildings [13].

DISCUSSION

The main point from analysing the results is that the preliminary assessment is often overlooked (*Table 1*). This suggests that, in most cases, detailed diagnostic investigations are delegated to specialists without providing any initial results, aside from a survey that may be more or less detailed, covering the organisation of the structure and the sizing of the main elements.

Table 1. In red, the aspects of the preliminary analysis covered during the detailed survey. In black, the same, but done before the detailed survey. In grey, ongoing activities.

Case Study	Desk survey*	Visual survey*	Measured survey*	Preliminary structural analysis*	Preliminary report*	Detailed survey	Diagnostic report
Florence Cathedral	x	x	x			x	x
San Marco Museum	x		x			x	x
Palazzo Madama			x			x	x
Santa Croce Basilica	x		x			x	x
San Francesco Church	x	x	x	x	x	x	x

*** Phases included in the Preliminary Assessment**

The fact that the results of any preliminary operations are not provided could also mean that they have not been performed. Still, it is not considered necessary to make them available to the specialist who will carry out the diagnosis. Our experience, however, indicates that the preliminary analyses required by the standard are not usually performed, except occasionally.

The results show that applying the standard in its entirety, following the described scheme, allows for a more rapid and detailed diagnostic investigation, producing results aligned with the goals of the restoration manager.

Achieving this requires a continuous dialogue based on mutual trust between the designer of the structural restoration and the diagnostic specialist, underscoring the importance of interdisciplinary communication in the restoration of cultural heritage.

What are the reasons why the preliminary investigation phase is generally lacking? The standard is certainly little known to those working in the restoration of ancient buildings, just as the existence of a well-established practice for diagnosing historic timber structures is little known.
Another possible reason is that professionals often have limited familiarity and personal training in wood as a structural material and in wooden structures. Ultimately, there is no practical procedure for applying the standard, and the entire system is perceived as cumbersome and complicated, particularly in light of the potential improvements that could be achieved by following the procedure.
The second major issue stems from both the literature review and the practical diagnostic survey. It concerns what happens after the diagnostic report, specifically its use in generating a reliable structural analysis.
The structural analysis necessitates an accurate assessment of the mechanical performance of each structural member and joint. The standard itself states that it is impossible to obtain a dependable estimate of the mechanical performance of structural joints and therefore recommends verifying whether they remain effective and are geometrically similar to their original shape.
Regarding the mechanical performance of structural members, the standards suggest that each country develop its own visual grading table for the most commonly used structural timbers, in accordance with EN 14081-1:2016, Annex A [14]. Each grade should then have its own mechanical profile.
In Italy, the previously mentioned UNI 11119:2004 standard reports a grading table, and the informative annexe contains a table linking timber species with their respective grades, providing a structural profile based on the allowable tensions. Converting these to characteristic values, as required by EC5, involves applying a safety coefficient that has been empirically established.

CONCLUSIONS

Based on the authors' experience, two main issues require improvement to fully comply with the guidelines of EN 17121.
Although fully following the recommended procedure reduces the time and improves the quality of the detailed diagnostic survey results, the preliminary procedure is very rarely performed, or the results are not made available to the specialised diagnostician.
The on-site visual grading procedures for estimating the mechanical performance of timber members need to be established at the country level for each participating country in the CEN; so far, no country has established these procedures at the national level.

REFERENCES

[1] UNI 11119, Cultural heritage - Wooden artefacts - Load-bearing structures - On site inspections for the diagnosis of timber members, UNI, Milano, Italy, 2004.

[2] EN 17121, Conservation of cultural heritage. Historic timber structures. Guidelines for the on-site assessment of load-bearing timber structures, CEN - European Committee for Standardisation, Brussels, 2019.

[3] N. Perković, M. Stepinac, V. Rajčić, J. Barbalić, Assessment of Timber Roof Structures before and after Earthquakes, Buildings 11 (2021) 528. https://doi.org/10.3390/buildings11110528.

[4] F. Arriaga, C. Osuna-Sequera, M. Esteban, G. Íñiguez-González, I. Bobadilla, In situ assessment of the timber structure of an 18th century building in Madrid, Spain, Construction and Building Materials 304 (2021) 124466. https://doi.org/10.1016/j.conbuildmat.2021.124466.

[5] P. Saarinen, M. Huttunen, L. Laine, P. Savolainen, FOLLOWING THE STANDARDS, FOLLOWING THE STRUCTURES – THE CASE OF LOUHISAARI CASTLE MID 17TH CENTURY ROOF STRUCTURES, in:

Proceedings of the SHATIS 2022 – 6th International Conference on Structural Health Assessment of Timber Structures, 2022.

[6] G. López, P. Vallelado-Cordobés, J.L. Gómez-Royuela, L.-A. Basterra, Diagnosis and assessment of a historic timber structure in La Casa del Corregidor, using non-destructive techniques, Case Studies in Construction Materials 19 (2023) e02311. https://doi.org/10.1016/j.cscm.2023.e02311.

[7] J.R. Aira-Zunzunegui, L. Gonzalo-Calderón, M. González-Sanz, E. Moreno-Fernández, F. González-Yunta, INSPECTION AND DIAGNOSIS OF TIMBER STRUCTURES OF THE BIRTHHOUSE OF JORGE JUAN Y SANTACILIA, in: Proceedings of the SHATIS 2022 – 6th International Conference on Structural Health Assessment of Timber Structures, 2022.

[8] H. Turkulin, T. Sedlar, A. Novosel, J. Pojatina, A. David, Zagreb Cathedral – Structural assessment of timber roof structure, in: Proceedings of the SHATIS 2022 – 6th International Conference on Structural Health Assessment of Timber Structures, 2022.

[9] D.F. Henriques, M.P. Clara, I. Flores-Colen, Inspection and structural assessment of traditional timber floors: a practical systematisation, IJBPA 41 (2023) 675–691. https://doi.org/10.1108/IJBPA-08-2021-0106.

[10] S. Caciagli, M. Degl'Innocenti, N. Macchioni, F. Mannucci, A wooden traction retrofitting system at Florence' Cathedral, conceived by Filippo Brunelleschi, The Construction Historian Issue 8 (2021).

[11] M. Bernabei, F. Marchese, Analysing the medieval roof of the San Francesco's church in Prato (Italy): A dendrochronological interpretation, Journal of Cultural Heritage 54 (2022) 103–107. https://doi.org/10.1016/j.culher.2022.01.014.

[12] N. Macchioni, M. Degl'Innocenti, F. Mannucci, I. Stefani, S. Lazzeri, S. Caciagli, Timber Structures of Florence Cathedral: Wood Species Identification, Technological Implications and Their Forest Origin, Forests 14 (2023) 1733. https://doi.org/10.3390/f14091733.

[13] N. Macchioni, M. Mannucci, The assessment of Italian trusses: survey methodology and typical pathologies, International Journal of Architectural Heritage 12 (2018) 533–544. https://doi.org/10.1080/15583058.2018.1442516.

[14] EN 14081-1, Timber structures. Strength graded structural timber with rectangular cross section. Part 1: General requirements, CEN - European Committee for Standardisation, Brussels, 2016.

STRENGTH GRADING OF TIMBER IN EXISTING STRUCTURES – METHODOLOGY AND CASE STUDY

Gunter LINKE[1/2], Wolfgang RUG[2] and Hartmut PASTERNAK[1]

[1] BTU Brandenburg University of Technology, Faculty of Architecture, Civil Engineering and Urban Planning, Chair of Steel and Timber Structures, Cottbus/Germany

[2] Public expert office W. Rug & VHÖB Laboratory for timber construction and ecological building technology, Eberswalde/Germany

ABSTRACT

The retrofitting and redevelopment of existing structures is of great economic and social importance. A comprehensive assessment of the building's condition is an absolute prerequisite for professional interventions in existing load-bearing structures that do not damage the substance. The assessment of the existing load-bearing capacity is an essential part. The combination of visual and non-/semi-destructive testing methods has proven to be a promising approach. Basic requirements are already included in the drafts of international codes. However, concrete specifications for practical implementation are still missing. This paper presents a method for in situ strength grading. In addition to the basic methodological approach and definite specifications for its implementation, the practical application is presented using the example of tests in the laboratory and in situ.

KEYWORDS: existing timber structures, strength grading, minimum intervention

INTRODUCTION

The rule of minimum interventions in the context of ecological transition nowadays also refers to the material usage during the redevelopment of existing structures. This applies to the replacement of structural components as well as their reinforcement. The knowledge of the constructive conditions – e.g. present damages as well as the material quality – is an unconditional requirement for professional interventions.

In this paper, a new procedure for the assessment of structural timber components as a precondition for their further use is demonstrated. This procedure is designed to meet new contemporary standards, which must be respected on new and existing buildings.

CURRENT STANDARDS FOR THE ASSESSMENT OF EXISTING TIMBER STRUCTURES

The redevelopment, preservation and future use of existing structures is of increasing economic, ecological, and social importance. To ensure professional, substance-careful and economic interventions in existing constructions, a comprehensive assessment of the building condition is required. In the recent past, the latter has increasingly become the focus of research and standardisation. For example, Italy, Switzerland, and Austria published national codes for the assessment of existing structures - especially timber structures - in the period 2004-2013 (see [1]).

In 2015, the Joint Research Centre of the European Union published a first draft of a unified guideline for the assessment of existing structures, which is in line with the regulations of the Eurocodes (see [1, 2]). At the same time, the COST action IE0601 "WoodCultHer" developed a guideline for the assessment

of the structural condition of historic timber structures (see [3]). The basic requirements of both guidelines have since been transferred into European standards (see [4, 5]). The essential procedure includes not only the assessment of the structural geometry, the present loads and influences and any possible damage, but also the determination of the existing material quality. However, the currently available international codes [4, 5] only specify general requirements. The material quality should usually be determined using the strength grading methods developed for new timber.
However, the strict application of these methods is usually not possible *in situ* (see [6]). In practice, therefore, in-situ strength grading is rarely carried out and then only visually and to a limited extent. Usually, the material quality is only estimated and static calculations are carried out assuming an average load-bearing capacity. A reliable assessment of the material quality is thus not possible. Therefore, alternative approaches are necessary. The combination of a visual examination and non-destructive/semi-destructive testing methods is currently the consensus (see [4, 5, 7]). However, concrete specifications for the application of an in-situ strength grading are still not available in the existing regulations.

DEVELOPING A METHOD FOR IN-SITU STRENGTH GRADING

Between 2017 and 2021, a systematic study on the strength grading of timber members in existing structures was carried out at BTU/Cottbus, Germany, in cooperation with HNEE & VHÖB/Eberswalde, Germany (see [8]). The aim was to develop a methodology for in situ strength grading based on the combined use of visual grading and selected ND-/SD-Testing Methods. For this purpose, approximately 900 specimens made from new spruce, pine and oak timber were examined in comparative material tests. These tests included the following test methods.

- visual grading according to DIN 4074-1/-5 [10, 11];
- ultrasonic time-of-flight measurement with the Sylvatest Trio measuring device;
- determination of density on cuboid specimen, core drill samples and with the penetration depth method (test device: “wood pecker wood test hammer”);
- destructive bending tests according to EN 408 [12].

A detailed description of the systematic material tests can be found in [8, 9].
Based on the recorded data sets, two methods for in situ strength grading have been investigated. The first approach was a grading procedure based on the ultrasonic time-of-flight measurement with limiting values for the grading criterion “ultrasonic velocity” (see [8, 9]). The sorting yield showed a significant improvement compared to visual sorting - especially in the strength classes C30/D30 according to EN 338 [13] and higher. However, the correlation between the estimated material quality and the load-bearing capacity determined in destructive tests was still comparatively low. The reason for this is that, on the one hand, there is a relatively low correlation between the ultrasonic velocity and the strength and stiffness properties. On the other hand, the ultrasonic pulse time-of-flight measurement does not include the effects of relevant features that influence the load-bearing capacity - such as knots, slope of grain and cracks. From this, it can be concluded that ultrasonic time-of-flight measurement is suitable in principle for strength grading, but should not be used alone.
As an alternative approach, the applicability of so-called grading parameters was investigated. These grading parameters are already used for the machine grading of new construction timber. However, the applicable European standards currently only consider the natural frequency and the density (see [14]). Furthermore, the investigations by the authors have shown that the direct inclusion of the essential visually measurable growth characteristics is necessary for an accurate estimation of the material quality. Therefore, based on the results of the comparative material tests, grading parameters were derived using a multivariate regression model.

This model enabled the simultaneous evaluation of the measurement results of several non- and semi-destructive test methods. Specifically, the visually measurable growth characteristics like knots (A), slope of grain (FN) and cracks (R), as well as the measurement results of the ultrasonic time-of-flight measurement, the density (ρ) calculated from the penetration depth and determined on drill core samples were included in the analysis. Regarding the ultrasonic time-of-flight measurement, the transmitted electrical voltage (U) as an indicator for the signal attenuation and the dynamic modulus of elasticity (E_{dyn}) were considered in addition to the measured ultrasonic velocity (v). The bending strength (f_m) and the static modulus of elasticity (E_m) served as target values.
To take the particularities of existing structures and the possible implementation of adjusted analysis methods into account, the regression model was set up as a multi-level system (see Figure 1). The extent of the measurements and examinations to be carried out on-site depends on the state of preservation of the components or constructions, their degree of stress and importance for the entire structure, as well as on the conservation value. In general, less extensive investigations are required for subordinate structural components. The main structure and critical components, on the other hand, require a more detailed investigation. This offers the possibility to precisely plan and carry out the necessary investigations in situ. Depending on the extent of the knowledge gained from the strength grading, various adjustments of the verification methods can be made (see [15]).

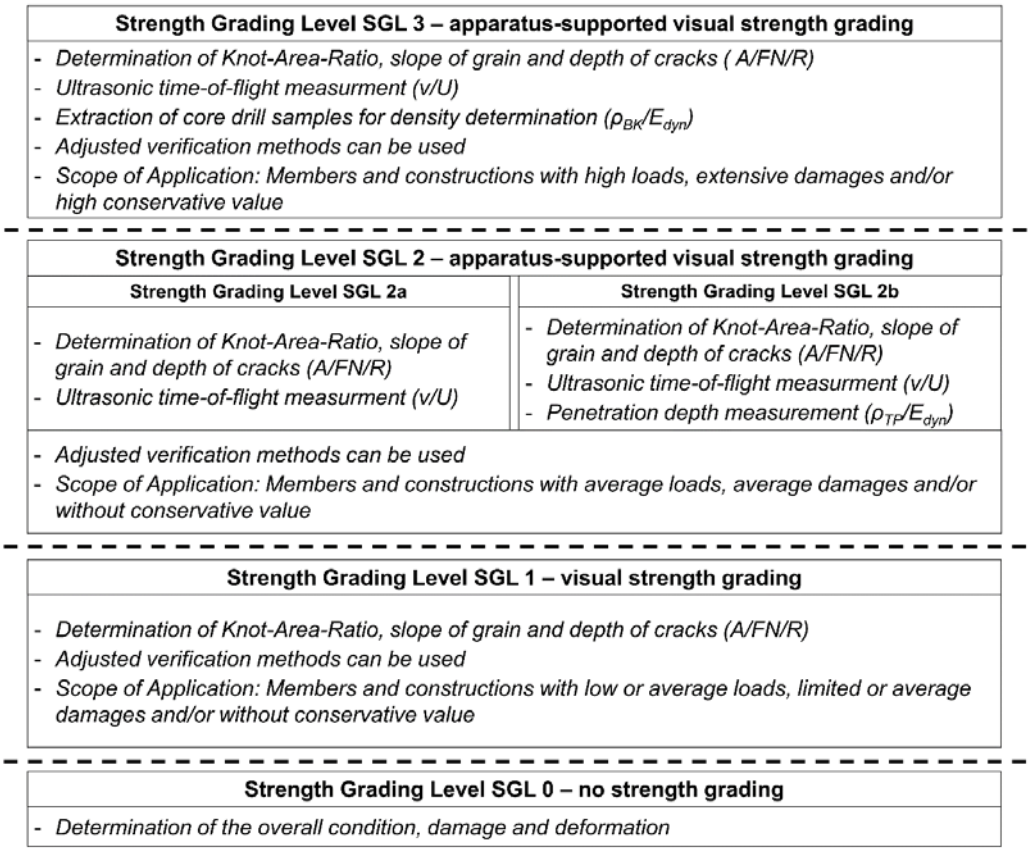

Figure 1. Schematic depiction of the in-situ strength grading method

Several multivariate linear regression equations were set up for the grading levels shown in Figure 1. The above-mentioned characteristics and parameters were put into regression in various combinations with the target values of bending strength and static modulus of elasticity. A total of 87 different combinations were examined for each wood species and target value. Table 1 shows the strongest regressions using the example of the target value static modulus of elasticity. This shows a clear improvement in the correlation through the inclusion of non-destructive and low-impact measurable parameters.

Table 1. Correlation coefficients of the strongest regressions to the target value, static modulus of elasticity (for indirect ultrasonic time-of-flight measurements)

Strength grading level	Grading criteria and corresponding equation	Species Spruce	Pine	Oak
SGL 1	A, FN, R $E_m\,(IP) = a \cdot A + b \cdot FN + c \cdot R + d$	0,294	0,535	0,310
SGL 2a	A, FN, R, v, U $E_m\,(IP) = a \cdot A + b \cdot FN + c \cdot R + d \cdot v + e \cdot U + f$	0,799	0,816	0,878
SGL 2b	A, FN, R, E, ρ $E_m\,(IP) = a \cdot A + b \cdot FN + c \cdot R + d \cdot E + e \cdot \rho + f$	0,834	0,840	0,876
SGL 3	A, FN, R, E, ρ $E_m\,(IP) = a \cdot A + b \cdot FN + c \cdot R + d \cdot E + e \cdot \rho + f$	0,867	0,837	0,887

The equations resulting from the multivariate regression analysis were then used to derive limit values for the grading parameters. For this purpose, an indicating property (IP) for the target value (TP) was calculated for each test specimen using the regression equations mentioned above. These estimated values correspond to the subsequent grading parameters and were placed in a linear regression to the characteristic values of bending strength and static modulus of elasticity determined in the bending test (see Figure 2).

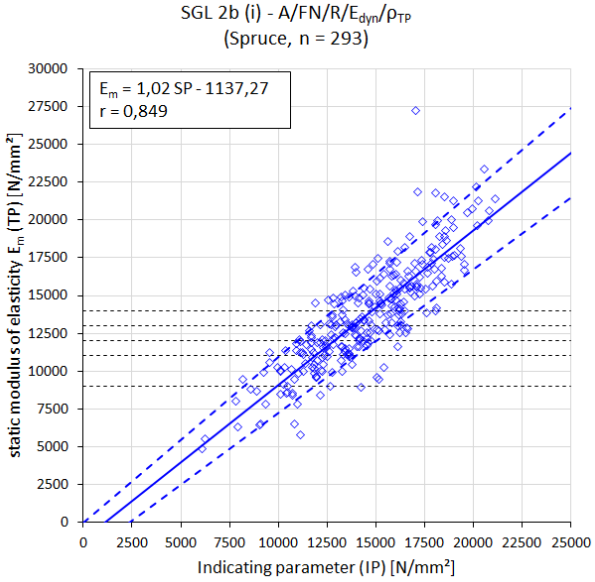

Figure 2. Linear regression between the indicating parameter (IP) and the static modulus of elasticity (TP) – here: Spruce, SGL2b

By converting the established linear regression equations, the limiting values for the grading parameters can then be calculated. For this purpose, the characteristic values of bending strength and static modulus of elasticity specified in EN 338 were used as required target values. The general procedure is shown in the following equations (1)-(3) for the regression shown in Figure 2.

- Regression equation between the indicating parameter (IP) and the static modulus of elasticity (TP):

$$TP(E_m) = 1{,}02 \cdot IP - 1137{,}27 \quad \left[N/mm^2\right] \qquad (1)$$

- Required target property (TP) according to EN 338 for the strength class C24:

$$TP_{Em,req} = 11000\ N/mm^2 \qquad (2)$$

- Limiting Value for the grading parameter for the strength class C24:

$$S_{Em} = \frac{TP_{Em,req} - b_{TP,Em}}{a_{TP,Em}} = \frac{11000\,N/mm^2 + 1137,27}{1,02} \approx 11900\ N/mm^2 \qquad (3)$$

Using the limit values determined in this way, it is then possible to assign individual timber components directly to the strength classes in accordance with EN 338 (see Figure 3). Overall, the application of indirect ultrasonic time-of-flight measurement and the use of the static modulus of elasticity as a target variable proved to be the most suitable.

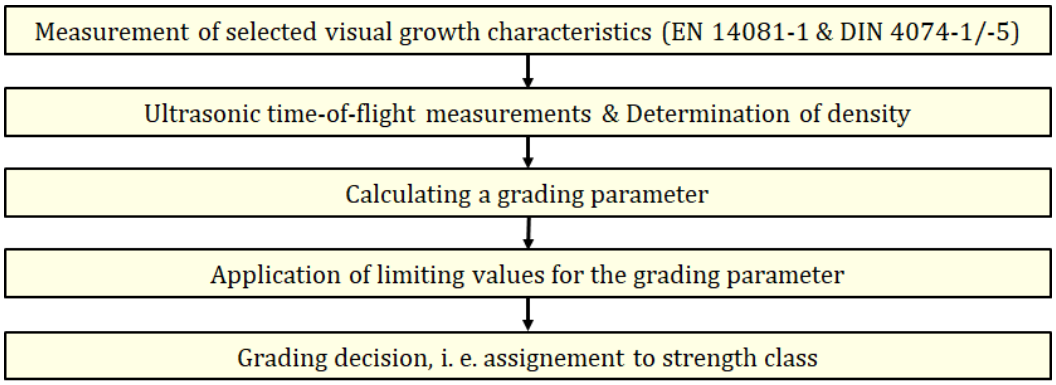

Figure 3. Process of the in-situ strength grading methodology

The application of the in-situ strength grading methodology to the sample material made from new construction timber showed that the material quality can be reliably estimated. The accordance between the assignment to the strength classes according to EN 338 [13], based on the developed grading method, as well as based on the destructive bending tests, was (86 to 96) %.
In addition to the investigations described above, the strength grading methodology was applied in comparative material test on sample material from historical, partially deconstructed timber structures (see [16, 17] and Figures 4 & 5). In the course of this, it was determined that minor adjustments to the methodology are necessary regarding the consideration of the load-bearing capacity-reducing growth and component characteristics.

Figure 4. Fichtenberg High School, Berlin/Germany – left: exterior view; right: interior view of the roof construction

Figure 5. Castel Friedenstein, Gotha/Germany – left: aerial view; right: examined ceiling construction

The additional tests carried out on historic timber components showed that, regardless of the size of the features, their position in the component is also decisive for the load-bearing capacity. Knots, smaller defects, limited organic damage and superficial indentations and notches caused premature failure even if they were relatively small, provided they were in the loaded area. If these circumstances are not considered, the agreement between the estimated and test-determined material quality is only (64 to 79) %. About (10 to 30) % of the components were overestimated.

To eliminate this deficit, the accuracy of the strength grading methodology was adjusted by means of correction factors. The use of a global factor in the range of k_{IP} = (0.80 to 0.95) resulted in a reduction of the overestimation to approx. (0 to 23) %. At the same time, the proportion of underestimated samples increased to approx. (5 to 79) %. This does not represent an improvement in the accuracy and reliability of the results. Using a correction factor k_{vis} = (0.85 to 0.90) related to the individual case resulted in an overestimation of (7 to 10) %. The agreement between the estimated and test-determined material quality was (78 to 85) %. This is acceptable from an engineering point of view.

The application of the factor k_{vis} is recommended for components that have local weak points (i.e. predetermined breaking points) that are not included in the calculation of the grading parameter due to their characteristics or size. This is necessary, for example, in the case of knot accumulations, strong crack formation and unfavourable fibre inclinations in the tensile area - especially in the highly stressed component sections, knots and knot accumulations around load introduction, local cross-section weakening (e.g. cuts/cervical/etc.), and superficial damage to the edge fibres (e.g. axe notches). Its application is shown in the following equation (4):

$$IP_{SGL2b} = k_{vis} \cdot \left(a \cdot A + b \cdot FN + c \cdot R + d \cdot E_{dyn} + e \cdot \rho_{mean} - f\right) \quad (4)$$

with: IP_{SGL2b} ... grading parameter; k_{vis} ... correction factor to consider the prognostic fracture behaviour (recommended: k_{vis} = 0.15); a...f ... coefficients and constants, tabularised in [18] for different wood species; A ... knots [/]; FN ... slope of grain [/]; R ... cracks [/]; v_{mean} ... average ultrasonic velocity [m/s]; U_{mean} ... average transmitted electrical voltage [mV]; E_{dyn} ... dynamic modulus of elasticity [N/mm²]; ρ_{mean} ... average density [kg/m³]

Overall, the application of the proposed grading methodology represents a significant improvement compared to an exclusively visual grading. The examined sample material taken from historic timber structures was underestimated by (61 to 69) % regarding its material quality by an exclusively visual grading. Only (23 to 28) % were assigned to the same strength class based on the destructive bending tests. This can result in considerable load-bearing capacity deficits, which in practice can lead to an unrealistic evaluation of the construction and thus to unprofessional, less substance-careful and uneconomical interventions in the existing constructions. This deficit can be significantly reduced by applying the proposed methodology for in situ strength grading. In the investigated constructions, reserves in the range of (17 to 67) % related to the characteristic bending strength and (7 to 27) % regarding the mean value of the modulus of elasticity were found. The application of the proposed

grading methodology is thus a significant improvement over the current practice in the assessment of present material quality in existing timber structures.

CASE STUDY – THE MARGARETHENHAUS, BERLIN

The practical application of the strength grading methodology was investigated in an additional field survey. This survey was conducted by assessing the material quality of structural timber in several existing structures, such as half-timbered houses, wooden roof constructions, as well as churches and parish houses. One of the investigated structures was the Margarethenhaus of the church community in Berlin-Heinersdorf. The essential results of this field study are presented in the following.
The Margarethenhaus – also known as Margareth-Hall (see Figure 6) – is part of a building ensemble which is listed as built heritage by the Berlin State Monuments Office. The building was erected in the 1920s as a community hall and is currently used by the protestant parish of Berlin-Heinersdorf.

Figure 6. Exterior view of the Margarethenhaus, Berlin, before the extensive redevelopment

The building consists of a two-storey main building with two corner risalits on the western and eastern sides. The second storey of the main building is set back and includes a balcony along the whole length of the building. The roof structure is formed by a pitched roof above the main building and hipped roofs above the risalits. The load-bearing structure of the roof is executed as a purlin roof.
The focus of the field study was on the timber beams of the ceiling above the second storey since extensive redevelopment measurements – including the replacement and reinforcement of individual beams – have been carried out. The roof construction was not considered in this field study since the structure was completely replaced due to extensive biological damage.
The subjects of the investigation were the floor beams in the direct vicinity of the future staircase (see Figure 7). The main floor beams (b/h = 200/260 mm, pine timber) were reinforced with steel profiles (U260) to transfer the additional loads. The present material quality was determined by applying the following non- and semi-destructive test methods:

- visual grading according to DIN 4074-1 [10] with focus on knots, cracks and slope of grain and additional component characteristics, e.g. holes, cross-section reductions;
- indirect ultrasonic time-of-flight measurement with the Sylvatest Trio measuring device;
- determination of density on core drill samples (Ø 15 mm).

The assessed data sets were evaluated according to the strength grading levels SGL 2a and 3, according to Figure 1.

Figure 7. Examined part of the ceiling structure

The assessment of the material quality revealed that significant load-bearing reserves were present. Both strength grading level SGL 2a and SGL 3 resulted in an allocation of the floor beams to the strength class C40 according to EN 338 [13]. The solemn visual grading of the floor beams according to DIN 4074-1 [10] – which is comparable to strength grading level SGL 1 (see Figure 1) – resulted in the allocation to the strength class C24 according to EN 338 [13]. Based on the mechanical properties given in EN 338 [13], the apparatus-supported strength grading revealed load-bearing reserves in the range of 67 % concerning the flexural strength, respectively 27 % concerning the modulus of elasticity. Such reserves can be used to minimise the redevelopment measures, particularly the material usage.

The static calculations for the reinforcement were carried out with the assumption of structural coniferous timber of the strength class C24 according to EN 338 [13]. The utilisation of the load-bearing capacity without consideration of the executed reinforcement is 194 %. Considering the revealed load-bearing reserves, the utilisation decreases to 116 %. Furthermore, the reinforcement measures could be planned more effectively using the in-situ assessed material quality.

To illustrate the benefits of in-situ strength grading for the planning of more substantial, careful and economical redevelopment measures, approximate structural calculations were carried out. These calculations were based on the original redevelopment planning that was carried out, as well as the results of the on-site investigations. The subject of the calculations was the verification of the load-bearing capacity of the floor beams. The results of the in-situ strength grading – i.e. the higher strength class of the timber – were considered.

The results of the approximate calculations have shown that the material usage in reinforcing the floor beams could have been significantly reduced. Instead of reinforcing the beams with steel profiles, U260, much smaller steel profiles would have been sufficient to bear and distribute the assumed loads. According to the approximate calculations, the reinforcement with U120 would have been possible. This reduction of the steel profile cross-section leads to a reduction in material usage of 26 kg/m or 65 %. For the investigated beams, this equals 0,2 t less steel per floor beam. In economic terms, this equals a cost reduction in material usage of around 55 %.

CONCLUSIONS

The study shows that the method for in-situ strength grading derived from tests on new structural timber is suitable for practical application. The laboratory tests on wooden components from historical constructions confirm this conclusion. The existing uncertainties were considerably reduced with the help of additional safety factors, which take the influence of individual growth and structural characteristics on the fracture behaviour into account. The remaining uncertainties are acceptable from an engineering point of view. This is especially the case under consideration of the load-bearing reserves that can be determined and used in the assessment of the structural stability and for the planning of redevelopment measures.

Furthermore, the results of the field study have shown that the application of the in-situ strength grading can be used for the planning of more substantial, careful and economically reasonable redevelopment measures. In the presented case, a significant reduction in material usage would have been possible.

However, the results of the extensive laboratory and field studies also show that the grading process requires expertise not only in the field of visual grading and NDT/SDT measurement but also concerning the load-bearing and fracture behaviour of timber members to evaluate the measurable parameters according to their structural position.

The results of the presented study are currently used to draft the framework for an application guideline. In addition to specifications concerning the practical application as well as the documentation of the results, this will also specify the required personnel qualifications. The implementation of the proposed method into the currently existing standards for the assessment of existing timber structures [4, 5] as part of a detailed on-site survey is possible.

ACKNOWLEDGEMENTS

This research has been funded by private donations and supported by the commitment of engineers of the Laboratory for timber construction and ecological building technology. Furthermore, the authors want to thank the Engineering offices Dr. Krämer (Weimar/Germany), Trabert & Associates (Geisa/Germany) and Seemann (Berlin/Germany), the Thuringian Palaces and Gardens Foundation as well as the Senate Department for Urban Development and Housing of the City of Berlin for their support in the testing and practical application of the investigated methodology.

REFERENCES

[1] M. Loebjinski, G. Linke, W. Rug, H. Pasternak, Evaluation of existing timber structures – Current standards for the assessment and evaluation in Germany and Europe, in: J. M. Branco, H. M. Sousa, E. Poletti (eds.) Proceedings of the 5th International Conference on Structural Health Assessment of Timber Structures SHATIS, Guimaraes, Portugal, 25-27th September (2019) 884-893

[2] S. Dimova, A. Pinto, P. Luechinger, S. Denton (eds.), New European Technical Rules for the Assessment and Retrofitting of Existing Structures – Policy Framework, Existing Regulations and Standards, Prospect for CEN Guidance, Publications Office of the European Union, 2015.

[3] H. Cruz, D. Yeomans, E. Tsakanika, N. Macchioni, A. Jorrissen, M. Touza, M. Mannucci, P. Lorenço, Guidelines for the on-site assessment of historic timber structures, in: International Journal of Architectural Heritage: Conservation, Analysis and Restoration, Volume 9 (2015), Issue 3, 277-289

[4] CEN/TS 17440 (2020), Assessment and retrofitting of existing structures

[5] EN 17121 (2019), Conservation of cultural heritage – Historic timber structures – Guidelines for the on-site assessment of load-bearing timber structures

[6] K. Lißner, W. Rug, Holzbausanierung beim Bauen im Bestand, 2nd ed., VDI Springer, Berlin, 2018

[7] J. Machado, M. Riggio, T. Descamps (eds.), State of the Art Report – Combined use of NDT/SDT methods for the assessment of structural timber members; Université de Mons, 2015

[8] G. Linke, W. Rug, H. Pasternak, Strength grading of structural timber in existing structures with the ultrasonic time-of-flight measurement, in: J. M. Branco, H. M. Sousa, E. Poletti (eds.), Proceedings of the 5th International Conference on Structural Health Assessment of Timber Structures SHATIS, Guimaraes, Portugal, 25-27th September (2019) 589-598

[9] G. Linke, W. Rug, H. Pasternak, Strength grading of structural timber in existing structures – Study on the Apparatus Supported Grading with the ultrasonic time-of-flight measurement, in: I. Vayas, F. M. Mazzolani (eds.), Proceedings of PROHITEC 2021 Protection of Historical Constructions, Athens, Greece, 25-27th October (2021) 3-19

[10] DIN 4074-1 (2012), Strength grading of wood – Part 1: Coniferous sawn timber

[11] DIN 4074-5 (2008), Strength grading of wood – Part 5: Sawn hard wood

[12] EN 408 (2012) – Timber structures – Structural timber and glued laminated timber – Determination of some physical and mechanical properties

[13] EN 338 (2016) – Structural timber – Strength classes

[14] EN 14081-2 (2018) – Timber structures – Strength grading structural timber with rectangular cross section – Part 2: Machine grading; additional requirements for type testing

[15] M. Loebjinski, W. Rug, H. Pasternak, Redevelopment of a wooden roof construction under preservation order, in: J. M. Branco, H. M. Sousa, E. Poletti (eds.), Proceedings of the 5th International Conference on Structural Health Assessment of Timber Structures SHATIS, Guimaraes, Portugal, 25-27th September (2019) 912-921

[16] G. Linke, W. Rug, H. Pasternak, In-situ-Festigkeitssortierung von Holzbauteilen in bestehenden Konstruktionen – eine Fallstudie, in: U. Kuhlmann, et al. (eds.), 9. Doktorandenkolloquium Holzbau Forschung + Praxis, Stuttgart, Germany, 10-11th March (2022) 139-146

[17] N. Luxor, G. Linke, H. Pasternak, New procedure for timber in heritage buildings – the case study of Castle Friedenstein, Gotha (Germany), in: 20th International Forum on World Heritage and Ecological Transition, Naples/Capri, Italy, 8-10th September (2022)

[18] G. Linke, Festigkeitssortierung von Holzbauteilen beim Bauen im Bestand – Ein Beitrag zur substanzschonenden Erhaltung historischer Gebäude (Dissertation); Brandenburgische Technische Universität Cottbus-Senftenberg, Fakultät für Architektur, Bauingenieurwesen und Stadtplanung, 2024

EXPERIMENTAL STUDY ON TORQUE EVOLUTION IN NORWAY SPRUCE LOGS DURING DRYING

Jiři KUNECKÝ[1] and Michal KLOIBER[1]

[1] Institute of Theoretical and Applied Mechanics of the Czech Academy of Sciences, Prosecká 809/76, 190 00 Praha 9, Czech Republic, email: {kunecky,kloiber}@itam.cas.cz.

ABSTRACT

This study investigates the development of torque in Norway spruce logs during drying, with a particular focus on the influence of spiral grain. Two full-scale logs, sawn from green timber and equipped with a custom restraint setup, were subjected to controlled drying from the fibre saturation point down to 12% moisture content. One end of each log was fully fixed to eliminate all degrees of freedom, while the opposite end was restrained using a system of eight steel wires arranged to permit indirect measurement of induced torsional loads. Monitoring included optical displacement tracking and vibrational analysis of the steel wires, with Fast Fourier Transform (FFT) employed to extract eigenfrequencies and estimate internal forces. Preliminary results revealed significant torque generation, reaching approximately 40 Nm per beam during the one-month drying period. These findings highlight the structural relevance of drying-induced stresses in green timber with spiral grain and underline the need for careful consideration in engineering applications. A more detailed evaluation of the results will be presented at the conference.

KEYWORDS: spiral grain, torque, green wood, drying.

INTRODUCTION

Spiral grain is defined as a helical orientation of wood fibres around the longitudinal axis of a tree stem. According to EN 844-8, it is a qualitative feature where fibres deviate spirally around the pith of the wood, either left- or right-handed, or alternating along the stem [1]. This grain deviation is a natural growth characteristic influenced by species, environment, and possibly genetic factors, and has significant implications for the mechanical behaviour of wood. Measurement of spiral grain is standardised by EN 1310 and EN 48 0204, which define procedures for evaluating the grain angle on 1-meter sections of logs, based either on visible fibre orientation (on debarked logs) or bark grooves (on barked logs). The deviation is expressed in centimetres per meter or as a percentage of deviation from the longitudinal axis [2]. Many aspects regarding spiral grain as a phenomenon have been described by Harris et al. [3], and practical measurement and implications are discussed thoroughly in [4].

The motivation was practical: to assess the forces within a structure if a beam with pronounced spiral grain is installed in the green state and subsequently dries. What is the magnitude of the resulting torque, and what internal forces might be induced within the construction? For this reason, we conducted a laboratory experiment using two logs made of green timber, allowing them to dry while measuring the forces generated during the process.

METHODOLOGY

Two logs were prepared from Norway spruce with nominal cross-sectional dimensions of 12 × 14 cm and a length of 400 cm. Each log was installed in a test rig with one end rigidly fixed, effectively eliminating all degrees of freedom to prevent any movement or rotation. The opposite end was secured using eight galvanised steel wires, each with a diameter of 2 mm, arranged in a pre-defined configuration as shown in Figure 1. This setup enabled the transfer of any torsional or longitudinal forces generated during drying into measurable tension in the wires, facilitating quantification of the internal loads induced by shrinkage and spiral grain effects. The logs were monitored throughout the drying process, beginning from the fibre saturation point (green wood condition) down to a target moisture content (MC) of 12%. The experiment was conducted in a controlled indoor testing hall, where the average temperature was maintained at approximately 23 °C, and the relative humidity remained stable at around 50%. These environmental conditions were chosen to simulate standard indoor drying scenarios and ensure consistent moisture loss across the duration of the test.

Monitoring of the displacements was carried out using optical measurement techniques [6], as well as through the analysis of vibrations in the steel wires. The recorded signals were processed using Fast Fourier Transform (FFT) to determine the eigenfrequencies, enabling indirect estimation of the forces generated during the drying process. The implementation was done using NumPy/ScipPy libraries [5].

Figure 1. Beams in the testing hall equipped with ArUco markers [6] for precise displacement monitoring.

RESULTS

The results are not presented here in full detail; a more comprehensive analysis will be provided during the conference. However, preliminary findings for the first two specimens are summarised in Table 1. The values have been computed using a string formula and will be calibrated using a universal testing machine.

Table 1: Sum of forces over time

Days	Beam 1 [N]	Beam 2 [N]
0	893.3	901.8
7	954.8	608.2
12	931.4	1135.1
19	1208.0	2052.6
26	1788.8	2799.7
33	2552.7	3175.0
40	3003.3	3470.5

CONCLUSION

The experimental results demonstrate that the drying process in timber—particularly in logs exhibiting pronounced spiral grain—can generate substantial torsional loads, with torque values reaching approximately 40 Nm for the studied beams in one month of monitoring. This highlights the importance of considering drying-induced internal forces when designing or evaluating timber structures, especially when green wood is used. These preliminary findings provide a basis for understanding the mechanical behaviour of drying logs under restrained conditions. A more detailed analysis, including additional data and implications for structural applications, will be presented in the upcoming conference presentation.

ACKNOWLEDGEMENT

The research was supported by the project "Wooden structures prevention and maintenance for heritage conservation purposes" NAKI III, reg. No. DH23P03OVV005, provided by the Ministry of Culture of the Czech Republic.

REFERENCES

[1] EN 844-8 – European Standard. *Round and sawn timber – Terminology – Part 8: Features of round and sawn timber – Spiral grain.*

[2] EN 1310 & EN 48 0204 – European Standards. *Round and sawn timber – Method of measurement of features – Includes measurement of spiral grain in cm/m or as a percentage.*

[3] Harris, J. M. (1989). *Spiral grain and wave phenomena in wood formation*. Springer-Verlag.

[4] Kloiber, M., Kunecký, J., & Kotmel, M. (2023). *Prediction of timber twisting based on measured spiral grain of spruce logs*. In Proceedings of the World Conference on Timber Engineering (WCTE 2023), Oslo.

[5] Virtanen, P., Gommers, R., Oliphant, T. E., Haberland, M., Reddy, T., Cournapeau, D., ... & van der Walt, S. J. (2020). *SciPy 1.0: Fundamental algorithms for scientific computing in Python.* Nature Methods, 17(3), 261–272. https://doi.org/10.1038/s41592-019-0686-2.

[6] Bontemps, A., Godi, G., Fournely, E. et al. (2024) *Implementation of an Optical Measurement Method for Monitoring Mechanical Behaviour.* Exp Tech 48, 115–128. https://doi.org/10.1007/s40799-023-00636-2

CHALLENGES AND DEVELOPMENTS IN STANDARDIZING STRUCTURAL RECLAIMED TIMBER IN EUROPE

Musaab Ahmed MAHJOUB[1] and Dario PARIGI[1]

[1] Department of the Built Environment, Aalborg University, Denmark

ABSTRACT

The reuse of structural timber from demolition is increasingly seen as a key strategy for sustainable construction and the circular economy. Technical standardisation for reclaimed structural timber in Europe is lagging. In this contribution, we review the current challenges, limitations, and recent advances in testing and grading reclaimed timber. The lack of harmonised standards is a main issue, as existing European norms for strength grading (e.g. EN 14081) were designed for new timber and explicitly restrict regrading of previously used members. High variability in species, condition, and mechanical properties of salvaged wood leads to uncertainty in structural performance. Visual grading tends to over-reject reclaimed timber, while machine grading calibrations for new wood may not directly apply. Non-destructive testing (NDT) techniques are emerging as promising tools to bridge these gaps. NDT methods can non-invasively assess properties like stiffness and detect defects, and have shown success in predicting strength. The findings indicate that while significant challenges remain in harmonising standards for reclaimed timber, recent research and standardisation proposals are laying the groundwork for reliable grading and re-certification procedures. This will ultimately facilitate safer and wider reuse of structural timber in Europe.

KEYWORDS: reclaimed timber, non-destructive testing, circular economy, standardisation

INTRODUCTION

Reclaimed timber offers substantial sustainability advantages by extending wood's service life and preserving embodied carbon [1]. In Europe, interest in reusing structural wood is supported by circular economy policies and the push for low-carbon construction [2]. Structural reclaimed timber – such as beams, columns, and joists salvaged from old structures – could substitute for new lumber if reliable methods exist to assess and certify its structural properties. However, the practice today is hampered by the lack of clear technical standards and guidelines [3]. Unlike newly milled timber, which is governed by well-established European norms, reclaimed wood does not yet benefit from a harmonised standard for testing, grading, or documentation of its properties. This gap raises safety and liability concerns, as engineers must ensure that reused elements meet structural requirements despite unknown history and inherent variability [1]. A major challenge is that current grading standards were written for virgin timber and are often inapplicable to reclaimed materials. The primary European standard for strength grading, EN 14081, explicitly states that timber members which have already been graded and used structurally should not be regraded to assign a new class [4]. Furthermore, EN 14081 and related standards assume certain conditions (such as known species, source, and regular section sizes) that reclaimed timbers may not satisfy [5]. Reclaimed beams frequently come in assorted dimensions and species mixes, sometimes with surface damage, holes or checks from prior use. These factors complicate direct application of standardised visual grading (which relies on visible knot size,

slope of grain, etc.) or machine grading (which relies on mechanical measurements like dynamic modulus of elasticity) that were calibrated on new, defect-free lumber populations [1]. As a result, there is currently no unified European procedure to certify the load-bearing capacity of reclaimed timber, and practices vary by country or project.

This paper provides an overview of the key technical issues hindering the standardisation of structural reclaimed timber in Europe and examines recent developments aimed at overcoming these issues. The focus is on (1) the current limitations of grading and testing standards for reclaimed timber and the consequences of these gaps, (2) the variability and mechanical characterization of reclaimed wood material, (3) advances in non-destructive evaluation techniques to improve assessment, and (4) new proposals that are paving the way toward harmonized European guidelines for reclaimed structural timber.

METHODOLOGY

This study was conducted as a comprehensive literature review and synthesis of recent findings on the assessment and standardisation of reclaimed structural timber. The methodology involved surveying peer-reviewed journals, conference proceedings, technical standards, and project reports. Key search terms included *reclaimed timber*, *reused structural wood*, *strength grading*, *non-destructive testing (NDT)*, and *standardisation*. By synthesising insights from these diverse sources, we outline the current limitations in technical guidelines and highlight innovative methods (including NDT techniques) that have been proposed to evaluate reclaimed timber.

RESULTS

To better illustrate the literature survey results, we can summarise key aspects in Table 1.

Table 1. Insights found from the literature survey.

Aspect	**Findings from the literature**
Grading & testing standards	- Visual grading rejects most reclaimed elements [6]. - Visual grading underestimated the true bending strength on average by 50-54% [7]. - Standards assume undamaged, uniform wood and do not account for defects (nails, splits, large knots, wane), hence are inadequate for reclaimed timber [1][2]. - Visually graded old wood has higher true safety margins if it passes the current conservative visual grading standards [7].
Material variability	- Reclaimed wood comes from diverse sources (various species, sizes, past loads, treatments) [1], [2]. - It is difficult to obtain a representative sample of reclaimed timber for testing [8].
NDT techniques	- Techniques applied for new timber, like ultrasound and longitudinal vibration, can be applied for reclaimed timber [6], [9], [10]. - NDT techniques like visual imaging can identify defects that could govern strength [9].
Harmonization proposals	- No completed EU standard yet, but draft guidelines are emerging [11]. - Norway's SIRKTRE project has a draft NS 3691 (parts 1-3) for reused wood grading [11], [12], [13], [14].

When free of decay or excessive damage, old timber can retain mechanical properties comparable to new wood. A comprehensive review by Cavalli et al. [15] noted that changes in bending modulus of elasticity (MOE) for aged wood ranged from slight decreases to slight increases, depending on species and history. Similar findings can be found in [16], where no significant differences in the static modulus of elasticity were found between cross-laminated timber panels manufactured from recovered and new timber. These findings are good news for reuse, indicating that age alone does not necessarily degrade wood. However, it can be noticed that current visual grading methods tend to be conservative for old wood. In [6], two standards (French NF B52001-1 and German DIN 4074-1) applied to reclaimed Norway spruce resulted in a high rejection rate (95%). In [7], 56 reclaimed spruce beams were evaluated with two visual standards, namely the draft Norwegian rule (prNS 35691-3) and the Nordic INSTA 142 (for new timber). It was found that these standards significantly underestimated the true bending strength on average by 50-54%. This conservatism means visually graded old wood, if it passes, generally has a higher true safety margin. However, it also implies that a lot of sound wood could be rejected, unless supplemental testing is used to justify its capacity. In [10], visual grading according to the Italian rule for new wood (UNI 11035) and (UNI 11119) for old wood was applied. It was concluded that both rules need to be modified before using them for reclaimed wood.

Reclaimed structural timber is inherently more variable than new timber [2], and this variability poses challenges for assessment and standardisation. Sources of variability include differences in original species and grade, varying age and growth characteristics, and diverse service histories (loading, environmental exposure, alterations such as holes or notches [1]). The resource is far less homogeneous than the graded lumber produced in modern sawmills. In [8], it is emphasised that a major difficulty in this field is obtaining representative samples of reclaimed wood for testing, given that each batch can differ markedly. Many research studies to date have necessarily worked with small samples, often sourcing timber from a single structure or a limited set of demolitions, e.g.[6], [10], [9], [17]. This makes it difficult to generalise results and calibrate broadly applicable grading rules.

Given the impracticality of destructive testing on every reclaimed beam (since the goal is to reuse them, not break them), non-destructive testing has become a cornerstone of reclaimed timber assessment [1]. NDT methods enable evaluators to estimate mechanical properties and detect internal defects without damaging the piece [18]. The literature review shows a range of NDT techniques being adapted and combined for this purpose. The most applied techniques are those also used in grading new timber: longitudinal vibration (dynamic MOE measurement by tapping or resonance) and ultrasonic wave transmission [6], [9], [17]. In [6], NDT methods, particularly vibration and ultrasound, showed promising potential with moderate to strong correlations (R^2 between 0.60 and 0.77) for estimating the modulus of elasticity and bending strength. However, caution should be considered as the sample size was only 19 Norway spruce (*Picea abies* (L.) Karst.) beams. In [9], 40 reclaimed timber beams from two different sites were tested. It was found that ultrasound velocities measured at the mid span of the beams were most predictive, with correlation coefficients of 0.56 for modulus of elasticity (MOE) and 0.73 for modulus of rupture (MOR). In [17], 81 salvaged beams from a historical building site were considered. Vibration and acoustic techniques, in combination with visual strength grading and wane extension, were used to predict MOE and MOR. The research achieved comparable results to new timber for MOE/MOR prediction by combining longitudinal vibration tests and wane extension (R^2 = 0.71 for MOE, R^2 = 0.43 for MOR).

Density measurement is another important parameter; techniques like drilling resistance (resistograph) or X-ray scanning can estimate density and detect internal voids or decay [19]. Beyond stiffness and density, NDT is also used to identify defects that could govern strength. Visual imaging (enhanced by high-resolution photography or 3D scanning) can document the size and location of knots,

cracks, nail holes, or biological damage [20]. X-ray or CT (computed tomography) scanning can reveal internal features like hidden nails, cracks, or insect galleries that are not visible on the surface [1].

Despite the current gaps in formal standards, the landscape is rapidly evolving through various proposals aimed at establishing quality control for reclaimed timber. At the national level, a landmark development is Norway's NS 3691 draft series. It provides a comprehensive framework for evaluating reclaimed timber to ensure its quality, safety, and suitability for reuse in construction and wood-based products. NS 3691-1 [12] lays the groundwork by defining key terms and establishing general rules for evaluating reclaimed timber. It specifies that reclaimed timber includes wood from deconstructed constructions, packaging, or offcuts, but excludes byproducts from sawmills or forestry. NS 3691-2 [13] outlines procedures for evaluating the presence of damage and impurities, including embedded metal elements and localised decay, with guidelines for removal or downgrading based on severity. It recommends non-destructive techniques, such as metal detection, to aid in internal quality assessment without damaging the timber. NS 3691-3 [14] is focused on visual strength grading, essential for determining if reclaimed timber can be used in load-bearing structures or as elements in engineered wood products like glued laminated timber or cross-laminated timber. The standard adopts a pragmatic principle: reclaimed elements can retain their original strength class if no critical defects are observed; otherwise, a downgrade (e.g., by one class) is recommended. This conservative, safety-focused philosophy recognises that visual grading tends to underestimate strength, thus offering an implicit margin of safety.

CONCLUSION

The reuse of reclaimed structural timber offers significant sustainability benefits but is hindered by the lack of harmonised European standards. Current norms, such as EN 14081, do not effectively accommodate reclaimed materials due to their inherent variability and complex assessment requirements. Non-destructive testing techniques (vibration, ultrasound, CT scanning) provide promising solutions for reliable evaluation without damaging the timber. Initiatives like Norway's NS 3691 standard demonstrate viable pathways towards dedicated guidelines for reclaimed timber grading. Continued collaboration among research, industry, and standardisation bodies is essential to establish robust and scalable certification procedures, promoting wider and safer reuse of structural timber in construction.

REFERENCES

[1] M. Tamke, T. Svilans, J. A. J. Huber, W. Wuyts, and M. R. Thomsen, "Non-Destructive Assessment of Reclaimed Timber Elements Using CT Scanning: Methods and Computational Modelling Framework," in *The 1st International Conference on Net-Zero Built Environment*, M. Kioumarsi and B. Shafei, Eds., Cham: Springer Nature Switzerland, 2025, pp. 1275–1288. doi: 10.1007/978-3-031-69626-8_107.

[2] M. Smith, "Use of Recycled and Reclaimed Timbers," in *Reuse of Materials and Byproducts in Construction*, A. Richardson, Ed., in Green Energy and Technology. , London: Springer London, 2013, pp. 111–149. doi: 10.1007/978-1-4471-5376-4_5.

[3] D. P. Pasca, A. Aloisio, Y. De Santis, H. Burkart, and A. Øvrum, "Visual-based classification models for grading reclaimed structural timber for reuse: A theoretical, numerical and experimental investigation," *Engineering Structures*, vol. 322, p. 119218, Jan. 2025, doi: 10.1016/j.engstruct.2024.119218.

[4] *Timber structures – Strength graded structural timber with rectangular cross section – Part 1: General requirements*, Report or Standard, Brussels., 2019.

[5] D. F. Llana, G. Turk, C. Osuna-Sequera, and G. Iñiguez-González, "RECOVERED TIMBER GRADING SYSTEM," in *World Conference on Timber Engineering 2025*, Brisbane, Australia: World Conference on Timber Engineering 2025, 2025, pp. 3460–3465. doi: 10.52202/080513-0424.

[6] D. F. Llana, G. Íñiguez-González, M. Plos, and G. Turk, "Grading of recovered Norway spruce (Picea abies) timber for structural purposes," *Construction and Building Materials*, vol. 398, p. 132440, Sept. 2023, doi: 10.1016/j.conbuildmat.2023.132440.

[7] M. Kauniste, A. Just, E. Tuhkanen, and T. Kalamees, "Assessment on Strength and Stiffness Properties of Aged Structural Timber," *sace*, vol. 34, no. 1, pp. 62–74, Feb. 2024, doi: 10.5755/j01.sace.34.1.35534.

[8] G. Iñiguez-González, D. F. Llana, D. Ridley-Ellis, V. Torres, and F. Arriaga, "REUSE OF WOOD IN STRUCTURAL PRODUCTS – A GAIN?," in *World Conference on Timber Engineering 2025*, Brisbane, Australia: World Conference on Timber Engineering 2025, 2025, pp. 3452–3459. doi: 10.52202/080513-0423.

[9] I. Viken and K. Sejersted, "Reclassification of Historical Timber with Non-Destructive Testing and Machine Learning".

[10] M. Nocetti, G. Aminti, M. Vicario, and M. Brunetti, "Mechanical properties of ancient wood structural elements assessed by visual and machine strength grading," *Construction and Building Materials*, vol. 411, p. 134418, Jan. 2024, doi: 10.1016/j.conbuildmat.2023.134418.

[11] "Framework for Quality Documentation for Reusing Structural Timber Components," in *Lecture Notes in Civil Engineering*, Cham: Springer Nature Switzerland, 2025, pp. 1301–1312. doi: 10.1007/978-3-031-69626-8_109.

[12] *NS 3691-1:2025 Evaluering av returtre - Del 1: Terminologi og generelle regler*, 2025.

[13] *NS 3691-2:2025 Evaluering av returtre - Del 2: Urenheter*, 2025.

[14] *NS 3691-3:2025 Evaluering av returtre - Del 3: Visuell styrkesortering*, 2025.

[15] A. Cavalli, D. Cibecchini, M. Togni, and H. S. Sousa, "A review on the mechanical properties of aged wood and salvaged timber," *Construction and Building Materials*, vol. 114, pp. 681–687, July 2016, doi: 10.1016/j.conbuildmat.2016.04.001.

[16] D. F. Llana, V. González-Alegre, M. Portela, and G. Íñiguez-González, "Cross Laminated Timber (CLT) manufactured with European oak recovered from demolition: Structural properties and non-destructive evaluation," *Construction and Building Materials*, vol. 339, p. 127635, July 2022, doi: 10.1016/j.conbuildmat.2022.127635.

[17] A. Cavalli *et al.*, "MOE and MOR assessment of in service and dismantled old structural timber," *Engineering Structures*, vol. 125, pp. 294–299, Oct. 2016, doi: 10.1016/j.engstruct.2016.06.054.

[18] Z. Azzi, H. Al Sayegh, O. Metwally, and M. Eissa, "Review of Nondestructive Testing (NDT) Techniques for Timber Structures," *Infrastructures*, vol. 10, no. 2, p. 28, Jan. 2025, doi: 10.3390/infrastructures10020028.

[19] D. F. Llana, G. Íñiguez-González, M. Plos, and G. Turk, "Grading of recovered Norway spruce (Picea abies) timber for structural purposes," *Construction and Building Materials*, vol. 398, p. 132440, Sept. 2023, doi: 10.1016/j.conbuildmat.2023.132440.

[20] M. Lukovic *et al.*, "Probing the complexity of wood with computer vision: from pixels to properties," *J. R. Soc. Interface.*, vol. 21, no. 213, p. 20230492, Apr. 2024, doi: 10.1098/rsif.2023.0492.

APPLICATION OF A STOCHASTIC MODEL FOR PREDICTING THE BENDING STRENGTH OF GLUED LAMINATED TIMBER BEAMS MADE FROM EUROPEAN HORNBEAM

Jelena LOVRIĆ VRANKOVIĆ[1], Ivana UZELAC GLAVINIĆ[1], Ivica BOKO[1] and Neno TORIĆ[1]

[1] University of Split, Faculty of Civil Engineering, Architecture and Geodesy

ABSTRACT

This study presents a stochastic model for predicting the bending strength of glued laminated timber beams made from European hornbeam (*Carpinus betulus L.*) harvested in Croatian forests. The model is based on a two-dimensional numerical simulation that integrates ANSYS and MATLAB software tools, aiming to generate variable mechanical properties both along individual laminations and across the entire glued laminated timber beam. Global mechanical properties were derived from tensile tests conducted on the laminations. To simulate local variability along each lamination, a first-order autoregressive model was used, incorporating the cross-correlation between the modulus of elasticity and tensile strength parallel to the grain. The proposed model replicates the bending test procedure following the EN 408 standard and enables the determination of the 5th percentile of bending strength, which represents the characteristic value used in structural design.

KEYWORDS: stochastic approach, European hornbeam, glued laminated timber, finite element method, bending strength

INTRODUCTION

Wood is an anisotropic material due to its natural growth and structural irregularities such as knots, grain deviations, redheart, etc. Those defects result in significant variability in stiffness and strength within the element. Glued laminated timber (GLT), as an engineered wood product, offers greater potential in terms of strength and stiffness compared to solid timber elements. One of the key properties is the *laminating effect*, which refers to the smaller values of the coefficient of variation (COV) for GLT compared to the COV of the individual laminations. The *size effect* explains the reduction in bending strength in larger beams due to a higher probability of defects caused by natural growth, which can be described by Weibull's weakest link theory. Numerous studies have investigated the tensile strength of laminations and finger joints in relation to the mechanical potential of GLT. Part of that research focused on experimental testing of laminations and GLT beams, while another part included numerical modelling using stochastic approaches to establish a connection between the 5th percentile of lamination tensile strength and the 5th percentile of GLT bending strength.

The use of stochastic methods within the finite element method (FEM) dates back to the 1980s, when the relationship between GLT bending strength and mechanical properties of laminations and finger joints was established [1]. Each lamination was divided into segments and assigned a modulus of elasticity (MOE) and tensile strength based on the density and knot size. Knot spatial distribution and finger joints were not included due to limited experimental data. Failure criteria were based on Weibull's weakest link theory, where failure occurs when the first element breaks. Distribution functions for stiffness and strength were obtained using Monte Carlo simulations.

The Karlsruhe Calculation Model was developed in 1985 based on extensive research into the variability of spruce laminations (*Picea abies* L.) and finger joints [2]. This research determined correlations between strength, MOE, density, and knots, enabling better simulation of mechanical properties using regression models. Compression-zone laminations were modelled as plastic materials, and the failure criterion allowed for force redistribution and localised failure before global fracture. The spacing between finger joints was generated randomly based on a statistical distribution [3]. The updated failure criterion allowed failures at the knot and finger joint positions in the tension zone with redistribution of internal forces. Several years later, additional bending tests of GLT beams of varying heights were conducted, leading to new correlation equations between mechanical properties [4], along with improvements in knot distribution and location. Following a comprehensive calibration phase, equations (1) and (2) were formulated to relate GLT bending strength to the strength of the finger joints and laminations, and these were later incorporated into the European standard EN 14080 [5]:

$$f_{m,g,k} = -2.2 + 2.5 f_{t,0,k}^{0.75} + 1.5 \cdot \left(\frac{f_{m,j,k}}{1.4} - f_{t,0,k} + 6 \right)^{0.65} \quad (1)$$

where $f_{m,g,k}$ presents the characteristic bending strength of GLT, $f_{t,0,k}$ is the characteristic tensile strength parallel to the grain, and $f_{m,j,k}$ presents the characteristic bending strength of the finger joint, with the condition:

$$1.4 \cdot f_{t,o,k} \leq f_{m,j,k} \leq 1.4 \cdot f_{t,o,k} + 12 \quad (2)$$

In 1989, Govindarajoo [6] implemented an effective cross-sectional method for calculating load-bearing capacity, yielding results similar to the FEM. In 1992, Hernandez et al. developed [7] the PROLAM model, which was based on effective stiffness. The modelling process included generating lamination lengths, MOE, and tensile strength for 61 cm lamination segments, as well as for finger joints. Finger joint positions were determined by random generation of lamination lengths, and their properties were defined using regression equations. Spatial and cross-correlation of mechanical properties were considered. This approach was more efficient than FEM but lacked segment-to-segment interaction, leading to underestimation of bending strength (~5%) and overestimation of MOE (~14.5%).

Recently, global warming and climate change have led to the expansion of deciduous forests (oak, beech, hornbeam), which exhibit better mechanical properties than conifers. As a result, over the past 20 years, extensive research has been conducted on hardwood-based structural products. The EU's wood-based industries have recognised their potential and are increasingly incorporating them into regulations. In this context, the "European Hardwoods for the Building Sector" (EU Hardwoods) project was launched in 2017 by Holzforschung Austria, University of Ljubljana, MPA Stuttgart, and FCBA Simonin Sas to evaluate the suitability of hardwood species (beech, oak, chestnut, ash) for structural applications [8].

In response to the changing climate and afforestation policies leading to increased hardwood shares in European forests, Blass et al. [9], [10] developed the first version of the Karlsruhe Calculation Model applicable to beech and mixed glulam composed of softwood and hardwood. A comprehensive experimental study on approximately 2000 beech laminations was conducted to establish distributions and correlations between lamination and finger joint mechanical properties. New regression equations were introduced compared to previous models. This version was implemented in Abaqus and applied a more conservative failure criterion, i.e. beam failure occurred if any bottom lamination segment failed, disallowing redistribution of internal forces.

In 2014, Fink developed a probabilistic model using MATLAB software [11]. Variability along the beam was due to knots, with the remaining "clear wood" treated as homogeneous. Finger joints were modelled as segments with knot-like reductions (20–30%). The material was isotropic, and ductility in the compression zone was not considered. The failure criterion allowed multiple element failures before

total fracture, triggered at 1% stiffness loss. The model showed a strong correlation with experiments where knot positions, strength of finger joints, and dynamic MOE were known. It was later extended [12] using fracture mechanics, incorporating fracture energy and smeared crack theory.
In 2017, Kandler and Fussl [13] presented a model using the Karhunen-Loève theorem for generating MOE, with laser scanning to define fibre orientation. Finger joints were not considered in this model. Tapia developed the Stuttgart Stochastic Strength Glulam Model for predicting bending strength and applied the XFEM method to simulate the initiation and propagation of a discrete crack in each segment of the beam [14]. Vida et al. [15] studied beams of various classes and sizes using effective stiffness. For the first time, a 3D model included two types of discrete cracks via cohesive surfaces: vertical cracks within laminations and horizontal cracks between laminations (traction-separation law), enabling continuous crack formation. The model was validated through experimental testing of beams with known lamination morphology and knot cluster positions, modelled with reduced stiffness and strength. This automatically included the laminating and size effects.
In 2018, the European Organisation for Technical Assessment published European Assessment Document EAD 130320-00-0304 ″Glued laminated timber made of solid hardwood″, which covers glued laminated timber made of several hardwood species [16]. To avoid a great testing effort, the characteristic value of the flatwise bending strength of the GLT, $f_{m,g,\mathrm{flat},k}$, shall be determined from the strength and stiffness properties of the laminations using formulae:

$$f_{m,g,k} = a_1 + a_2 f_{t,0,\mathrm{l},k}^{e_1} + a_3 \cdot \left(f_{t,0,\mathrm{j},k} - f_{t,0,\mathrm{l},k} + a_4\right)^{e_2} \quad (3)$$

where $f_{t,0,\mathrm{l},k}$ is the characteristic tensile strength of laminations, $f_{t,0,\mathrm{j},k}$ presents the characteristic tensile strength of finger-jointed laminations, and a_1, a_2, a_3, a_4, e_1 and e_2 are the model parameters determined by means of a material model based on Finite-Element calculations and Monte-Carlo simulations of the stochastic lamination properties. Annex C [16] gives basic principles of the strength model for GLT made from hardwoods.
In the last few years, local hardwood from Croatia has been investigated for the production of the GLT [17]–[19]. Since experiments assume considerable financial costs, a numerical model should be applied. The following sections provide the steps in modelling glued laminated timber beams in bending using a stochastic approach within a finite element model. Also, a specific dataset of European hornbeam harvested from Croatian forests is used.

METHODOLOGY

Firstly, the generation of global material properties is implemented, including the modulus of elasticity $E_{t,0}$, tensile strength parallel to the grain $f_{t,0}$, compression strength parallel to the grain $f_{c,0}$ and the length of each board. The distributions for tensile strength and MOE parallel to the grain were derived from tensile tests conducted on laminations from European hornbeam (*Carpinus betulus L.*) [20], while the data for compressive strength parallel to the grain were taken from the literature [21] and defined by the following expression:

$$f_{c,0,k} = 11{,}54 + 4{,}41 f_{t,0,k}^{0,5} \quad (4)$$

Lamination lengths were generated using a lognormal distribution. This procedure includes generating samples from a standard normal distribution, applying Cholesky decomposition to obtain correlated variables, and finally transforming each variable to the actual lognormal distribution.
After the generation of global material properties, the local characteristics for each lamination were defined. The laminations were divided into segments 100 mm in length. The stiffness of the segments within each lamination was generated using an autoregressive model. The resulting values were then

corrected to align the local segment stiffness with the global stiffness of each lamination, following the approach in [22]. To generate strength values along the laminations, a vector autoregressive model with cross-correlation was applied.
The model was implemented in ANSYS 2021 R2 [23]. The simply supported GLT beam, with dimensions 80x160x3000mm, is composed of 6 laminations without finger joints. Two-dimensional elements (PLANE183) were used. To derive the cumulative distribution function, two distinct configurations of laminations through the height of the GLT beam were used. The results of the tensile tests on the laminations include the classification into four tensile strength classes [20]:

1) $f_{t,0,k} \geq 51MPa$
2) $40MPa \leq f_{t,0,k} < 51MPa$
3) $32MPa \leq f_{t,0,k} < 40MPa$
4) $28MPa \leq f_{t,0,k} < 32MPa$.

In the first configuration, the outer zones (25% of the beam height) consisted of laminations from the highest strength classes, while the inner laminations were of the third strength class. In the second configuration, the outer zones were composed of laminations from the second strength class, whereas the inner zone contained laminations from the fourth strength class. Boundary conditions were defined according to the EN 408 standard [24] for four-point bending tests, and the loading was applied through displacement control. The stochastic distribution of mechanical properties caused an imbalance in load transfer between the two loading points, which was mitigated by introducing a reference control point and imposing linked displacements between nodes, following the method in [22]. The computation is conducted iteratively, increasing displacement in each step, and terminating the analysis once the maximum force drops by more than 2%.

RESULTS

A stochastic approach has been applied for modelling two configurations of inhomogeneous GLT beams in four-point bending. The total force applied to the beam is used to calculate the bending strength of the GLT beam. Table 1 gives the main statistics for the bending strength of the first and second configurations, including minimum and maximum values for bending strength and characteristic bending strength.

Table 1. Main statistics of the bending strength for the first and second configurations.

Configuration	**Min – max bending strength (MPa)**	**Characteristic bending strength (MPa)**
First configuration	72,1 – 102,5	69,7
Second configuration	60,4 – 90,8	58,2

Figure 1 shows the stress profiles through the selected GLT beam under four-point bending. Monte Carlo simulations are performed by calculating the bending strength for each set of randomly assigned parameters. Repeating this process with varying parameter values yields the bending strength distribution of the GLT beam. Once all simulations are completed, the cumulative distribution function (Figure 2) is derived, from which the 5th percentile bending strength is determined.

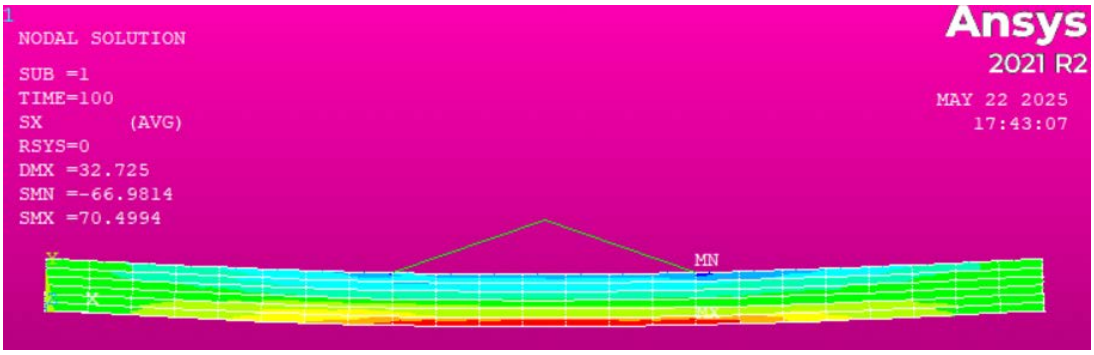

Figure 1. Stresses for the selected GLT beam under the four-point bending test

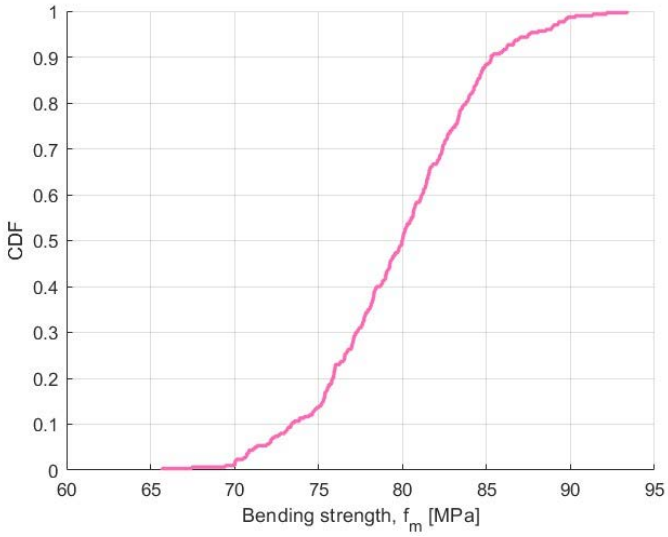

Figure 2. Cumulative distribution function (CDF) of bending strength for the second configuration

DISCUSSION

The simulated results were compared with findings from the literature [22] on GLT made from beech. The characteristic bending strengths obtained for the first and second configurations showed slightly better performance than in the referenced study, where the characteristic bending strength was 58.8 MPa for beech GLT with a beam height of 200 mm, using T42 and T22 grade laminations. It should be noted that the simulated GLT beam has a lower height compared to the beam in the reference study, which emphasises the significance of the size effect. Following Eurocode 5 [25] and the EAD [16], an adjustment to the bending strength is required for GLT beams with heights below 600 mm, reflecting the influence of the size effect on structural performance.

CONCLUSION

Due to the high financial demands of experimental testing, recent studies emphasise the potential of computational models for estimating the mechanical properties of GLT. Over the past few decades, various probabilistic finite element models have been developed and refined to incorporate structural irregularities, allowing more accurate predictions of bending strength. Numerous experimental studies have been statistically analysed to establish relationships between the mechanical property distributions of individual laminations and those of the wood-based structural products. The 2D numerical model presented in this study combines ANSYS and MATLAB software to generate global and

local variable mechanical properties along the beam's geometry. This model numerically simulates the four-point bending test of glued laminated timber beams following the EN 408 standard and determines the 5th percentile of bending strength, which represents the characteristic value. Experimental validation is required to confirm the reliability of the numerical results. Furthermore, additional experimental investigations are necessary, particularly those including the quantification of structural defects such as grain deviation, in order to incorporate these parameters into the numerical model and enhance the accuracy of characteristic bending strength predictions.

ACKNOWLEDGEMENTS

This work was supported through the following projects: IRI-2 KK.01.2.1.02. 0330 "Increasing the development of new products in the timber industry used in civil engineering"; KK.01.1.1.02.0027, a project co-financed by the Croatian Government and the European Union through the European Regional Development Fund—the Competitiveness and Cohesion Operational Programme. The authors gratefully acknowledge Graz University of Technology for their valuable support and guidance throughout the experimental testing of laminations made from European hornbeam.

REFERENCES

[1] R. O. Foschi and B. J. D., "Glued-laminated beam strength: A model," *ASCE J. Struct. Div.*, pp. 1735–1754, 1980, [Online]. Available: https://doi.org/10.1061/JSDEAG.00054

[2] J. Ehlbeck, F. Colling, and R. Gorlacher, "Einfluß keilgezinkter Lamellen auf die Biegefestigkeit von Brettschichtholzträgern," *Holz als Roh- und Werkst.*, vol. 43, pp. 333–337, 1985, doi: 10.1007/%2202607817.

[3] H. J. Larsen, "Strength of glued laminated beams, Part 5. Report No. 8004," 1980.

[4] J. Ehlbeck and F. Colling, "Biegefestigkeit von Brettschichtholz in Abhängigkeit von Rohdichte, Elsatizitätsmodul, Ästigkeit und Keilzinkung der Lamellen, der Lage der Keilzinkung sowie von der Trägerhöhe. Tech. Rep.," 1987.

[5] E. commitee for Standardization, "EN 14080; Timber Structures—Glued Laminated Timber and Glued Solid Timber—Requirements.," 2013

[6] R. Govindarajoo, "Simulation modeling and analyses of straight horizontally laminated glulam timber beams," Civil Engineering Dept., Purdue University, West Lafayette, 1989.

[7] R. Hernandez, D. A. Bender, B. A. Richburg, and K. S. Kline, "Probabilistic Modeling of Glued-Laminated Timber Beams," *Wood Fiber Sci.*, vol. 24 (3), pp. 294–306, 1992.

[8] P. Linsenmann, "European Hardwoods for the Building Sector Reality of today - possibilities for tomorrow," 2016.

[9] H. J. Blaß, M. Frese, P. Glos, P. Linsenmann, and J. Denzler, "Biegefestigkeit von Brettschichtholz aus Buche, German. Tech. rep. Karlsruher Institut für Technologie (KIT)," 2005. doi: 10.5445/8ZS/1000001371.

[10] H. J. Blaß and M. Frese, "Biegefestigkeit von Brettschichtholz-Hybridträgern mit Randlamellen aus Buchenholz und Kernlamellen aus Nadelholz. German. Tech. rep. Karlsruher Institut für Technologie (KIT), 55," 2006. doi: 10.5445/ 8ZS/1000005148.

[11] G. Fink, "Influence of varying material properties on the load-bearing capacity of glued laminated timber," 2014. [Online]. Available: https://doi.org/10.3929/ethz-a-010025751

[12] L. Blank, G. Fink, R. Jockwer, and A. Frangi, “Quasi-brittle fracture and size effect of glued laminated timber beams,” *Eur. J. Wood Wood Prod.*, pp. 667–681, 2017, doi: 10.1007/s00107- 017-1156-0.

[13] G. Kandler and J. Fussl, “A probabilistic approach for the linear behaviour of glued laminated timber,” *Eng. Struct.*, vol. 148, pp. 673–685, 2017, doi: 10.1016/j.engstruct.2017.07.017.

[14] C. Tapia Camú, *Variation of mechanical properties in oak boards and its effect on glued laminated timber: application to a stochastic finite element glulam strength model*. 2022. [Online]. Available: http://nbn-resolving.de/urn:nbn:de:bsz:93-opus-ds-121287%0Ahttp://elib.uni-stuttgart.de/handle/11682/12128

[15] C. Vida, M. Lukacevic, J. Eberhardsteiner, and J. Fussl, “Modelling approach to estimate the bending strength and failure mechanisms of glued laminated timber beams,” *Eng. Struct.*, vol. 255, 2022.

[16] EOTA, “EAD 130320-00-0304 Glued Laminated Timber Made of Solid Hardwood,” p. 30, [Online]. Available: www.eota.eu

[17] I. Uzelac Glavinić, I. Boko, J. Lovrić Vranković, N. Torić, and M. Abramović, “An Experimental Investigation of Hardwoods Harvested in Croatian Forests for the Production of Glued Laminated Timber,” *Materials (Basel).*, vol. 16, no. 5, 2023, doi: 10.3390/ma16051843.

[18] J. Lovrić, I. Boko, I. U. Glavinić, N. Torić, and M. Abramović, “The Time-Dependent Behavior of Glulam Beams from European Hornbeam,” *Buildings*, vol. 13, 1864, 2023.

[19] I. Boko, I. U. Glavinić, N. Torić, T. Hržić, J. L. Vranković, and M. Abramović, “Potential of Hardwoods Harvested in Croatian Forests for the Production of Glued Laminated Timber,” *Int. J. Struct. Civ. Eng. Res.*, vol. 12, no. 4, pp. 131–134, 2023, doi: 10.18178/ijscer.12.4.131-134.

[20] J. Lovrić Vranković, I. Uzelac Glavinić, I. Boko, and N. Torić, “An experimental investigation on the tensile properties parallel to the grain of European hornbeam (Carpinus betulus L.) boards [Manuscript submitted for publication],” 2025.

[21] A. Kovryga, P. Stapel, and J. W. G. van de Kuilen, “Mechanical properties and their interrelationships for medium-density European hardwoods, focusing on ash and beech,” *Wood Mater. Sci. Eng.*, vol. 15, no. 5, pp. 289–302, Sep. 2020, doi: 10.1080/17480272.2019.1596158.

[22] C. Tapia Camu and S. Aicher, “A Stochastic Finite Element Model for Glulam Beams of Hardwoods A STOCHASTIC FINITE ELEMENT MODEL FOR GLULAM BEAMS OF HARDWOODS,” in *In WCTE 2018 - World Conference on Timber Engineering. World Conference on Timber Engineering (WCTE)*, 2018, p. 9.

[23] “ANSYS, Inc., Release 2021 R2, Canonsburg, PA, USA, 2021.”

[24] E. commitee for Standardization, “EN 408:2010+A1:2012 Timber structures - Structural timber and glued laminated timber - Determination of some physical and mechanical properties,” 2012.

[25] E. commitee for Standardization, “Eurocode 5: Design of timber structures -- Part 1-1: General -- Common rules and rules for buildings (EN 1995-1-1:2004/A2:2014).” 2014.

TESTING METHODOLOGY - IN SITU AND LABORATORY TESTING

STRUCTURAL HEALTH ASSESSMENT OF AMSTERDAM TIMBER PILE FOUNDATIONS – FROM BACTERIAL DECAY TO RESIDUAL SERVICE LIFE ESTIMATION

Jan-Willem G. VAN DE KUILEN[1], Wolfgang F. GARD[2], Geert J. P. RAVENSHORST[2], Michele MIRRA[2], Giorgio PAGELLA[2] and Maria FELICITÀ[3]

[1]Technical University of Munich / Delft University of Technology
[2]Delft University of Technology, NL
[3]previous: Delft University of Technology, NL, current: ETH Zürich, CH

Invited lecture

ABSTRACT

Wooden pile foundations are present in many historic towns in Europe and beyond. The technology for making such foundations was developed primarily in southern Europe but spread rapidly to other locations, with ever-better-performing technologies for creating them. In the area of Venice, Italy, the piles are relatively short, whereas in many cities around the Netherlands, the wooden piles can be up to around 15m. Oftentimes, horizontal wood members are placed on top of the piles, acting as the structural interface between the upper structure and the piles. Many of the current foundations in Amsterdam and other medieval cities in the Netherlands were built from 1600 onwards. As there are indications that their end-of-service life is nearing, assessing the state of the wood, its mechanical properties, and the remaining load-carrying capacity is fundamental, as the economic consequences of failure of foundations below bridges, quay walls, and buildings can be colossal. Consequently, a fundamental analysis is required, addressing the type and extent of mechanical degradation resulting from long-term loading (duration of load effect), in combination with an assessment of the size and severity of biological or physical decay. The combined effect is responsible for the remaining load-carrying capacity and, consequently, for the remaining service life or for the assessment of possible reuse of the foundation. The assessment of this remaining load-carrying capacity is performed using an integral damage accumulation model, which takes into account the severity of time-dependent biological degradation and the wood quality, as measured by underwater microdrilling, combined with the mechanical load components (dead load, traffic loads), and the duration of the load effect. As such, the structural analysis approach differs from current design standards for new timber structures and aligns with the principles outlined in ISO Standard 13822 for the assessment of existing structures.

KEYWORDS: timber pile foundations, bacterial decay, wood assessment, residual service life estimation

INTRODUCTION

Timber as a structural material may be found in many buildings and structures around Europe, with a current age of sometimes more than 500 years. Already in the Roman era, foundations were made with timber, both by means of horizontal beams under brick walls and vertical piles for deeper foundations. Timber can be found in the foundations of famous heritage buildings, such as the Royal Palace in Amsterdam, the Netherlands, and bridges (Fig. 1). In these cases, timber foundations are the true foundations of cultural heritage, and therefore, their economic and technical importance is significant. A complication in the assessment is that pile foundations are difficult to inspect and maintain, and yet

many thousands of buildings, bridges and quay walls depend on them. Assessing such structures for their safety and serviceability requires, first of all, a method that addresses the 'state of the material' with a sufficiently high accuracy. Advanced calculation models can only be helpful if they consider the history of the structure, the quality and strength of the wood, but also the loads on the structure over

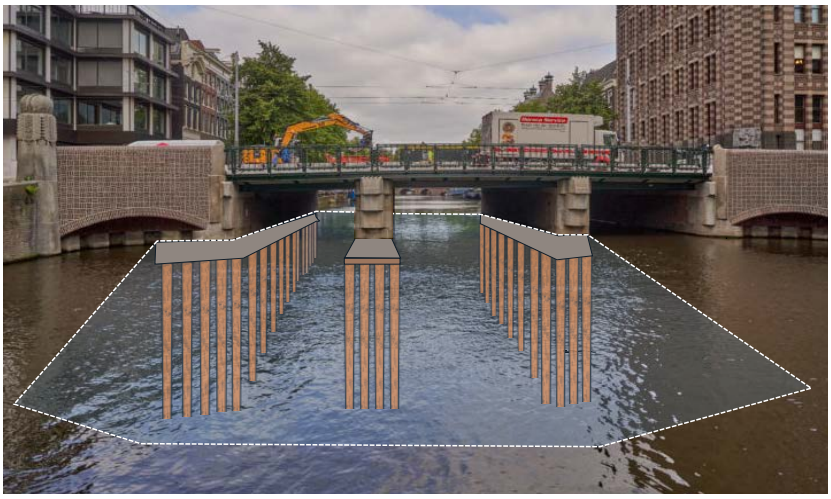

Figure 1. Artist impression of a timber pile foundation under a bridge in Amsterdam, NL

history, and expected future loads are important in the assessment procedure. Although most of the timber foundations known worldwide are in very good condition, assessments of their quality and load-carrying capacity are often necessary. Various design and maintenance aspects must be considered to assess the quality of the foundation, as bridges often feature multiple designs under a single bridge, having been widened over time to accommodate increasing traffic. In order to deal with all these aspects related to the state of this infrastructure from both a mechanical and a durability point of view, a comprehensive research program has been set up with the final goal to develop an integral method that includes all steps necessary to reliably assess a foundation and predict residual service under specified loading conditions. It includes methods for assessing the state of foundations based on reliable measurement and assessment methods, among which is the development of underwater microdrilling equipment, allowing for an indication of wood quality to be obtained in situ by a trained diver without the need to bring samples to a laboratory. To determine the current capacity in compression and the stiffness of the piles, recovered piles were analysed using microscopy, FTIR, CT scanning, and longitudinal vibration before full-scale mechanical testing was carried out. These methods are not discussed further in this paper. Data obtained from these tests have been paired with micro-drilling readings to estimate the cross-sectional material strength properties of a partially degraded pile, as well as the remaining load-carrying capacity of the entire pile. A non-linear damage approach for estimating the remaining structural capacity and service life has been developed, integrating biological degradation processes and time-variant loading.

METHODOLOGY

The analysis of the residual load-carrying capacity of timber piles in foundations requires a complete integral analysis regarding both wood and soil and their interaction. The principal mechanical system is shown in Figure 2 [1].

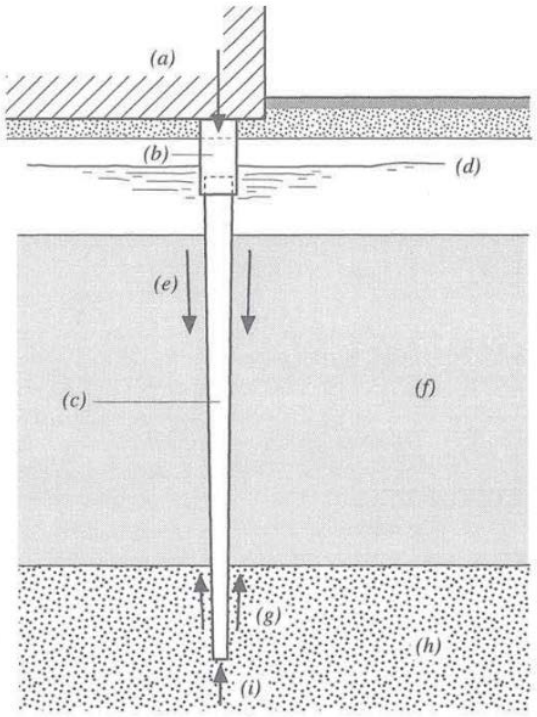

(a) Load
(b) Concrete extension pile (not present in older foundations)
(c) Timber pile (Species, Length, Taper, ...)
(d) Water table
(e) Negative skin friction
(f) Soil type (incl. time dependent behaviour, negative skin friction…)
(g) Positive skin friction
(h) Soil type (incl. time dependent behaviour, skin friction…)
(i) Pile tip

Figure 2. Scheme for a tapered timber pile structural analysis [1]

In order to determine the residual load-carrying capacity and remaining service life, the following parameters require a thorough analysis, always in light of the scope of structural reliability:

- Understanding timber pile strength and quantification of effects of biological degradation in completely submerged piles;
- In-situ measurement of piles using an appropriate and reliable method at reasonable costs;
- Interpretation and extrapolation of results for an entire pile and/or groups of piles;
- Load history in relation to the current state of the foundation;
- Development of a method to predict the load carrying capacity 'as is' and its possible future service life and use.

TIMBER PILES

The quality of timber piles in the Netherlands is regulated in a special standard, the Dutch NEN 5491:1983 "Quality requirements for timber piles" [2]. This standard regulates that only spruce, larch, and Douglas Fir species are allowed, where a batch of 'spruce' may contain both Spruce (Picea abies) and Fir (Abies alba). Pine piles have been forbidden for use in new foundations, but are still present in existing foundations. Piles are primarily loaded in compression, and the relationship between growth characteristics, such as knottiness and growth ring width, as practical measures for the compression strength, is not very pronounced. Consequently, the quality requirements in the standard are not very strict where these growth characteristics are concerned. The major restriction on knots is that the knot area, measured as the sum of knot diameters divided by the circumference, must be smaller than 0.5 and that the maximum permitted diameter of a single knot is 1/12 of the circumference or 50 mm. Other restrictions relate to fissures and the straightness of the pile, with a maximum deviation in the middle of the pile of half the middle diameter, as this is relevant for both installation and possible pile buckling in weak soil layers when the pile is installed. Additionally, permissible deviations in size are specified for both the circumference and length of the piles. The content of the timber piles standard has been

primarily based on practical applications and experiences. However, the situation with degrading piles in Amsterdam has called for a more profound analysis of the compression strength. For use as a timber pile, it is essential to understand that a timber pile is essentially an upside-down tree. This means that a longitudinal variation in compression strength will be evident along the length of the pile, just as it is along the length of the tree. In the upper parts of the tree, the proportion of juvenile wood in the cross section is higher than in the lower part of the tree, where the tree has formed more mature wood in the cross section, as well as thinner growth rings in the sapwood, leading to higher density as well. Consequently, there is a difference in compression strength between the head and the tip of the pile, which is about 2.5 MPa, with spruce showing a difference of about 1.4 MPa and pine of 4.2 MPa [3,4]. The location of the various wood tissues inside a tree over the cross-section when used as a pile is shown in Figure 3.

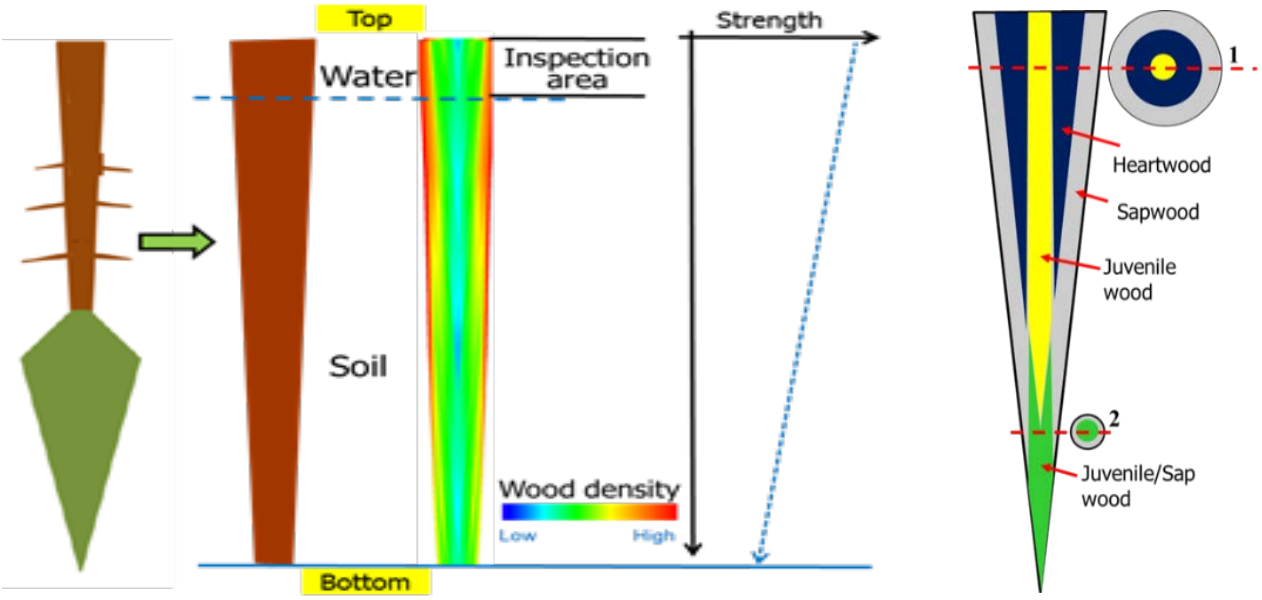

Figure 3. Sketch of a sound tree stem as foundation pile upside down; possible density development along the length of the pile, possible strength development along the length with accessible inspection zone at the top of the piles, On the right: wood tissue distribution in a pile.

Bacterial degradation in timber piles: Core-drilling versus Microdrilling

The scope of bacterial degradation research was related to the development of an in-situ measurement protocol based on underwater microdrilling, rather than traditional core-drilling, with the provision that microdrilling measurements would be and should be favourable compared to core-drilling. In accordance with Dutch practical guidelines for the assessment of existing pile foundations [6-9], in-situ

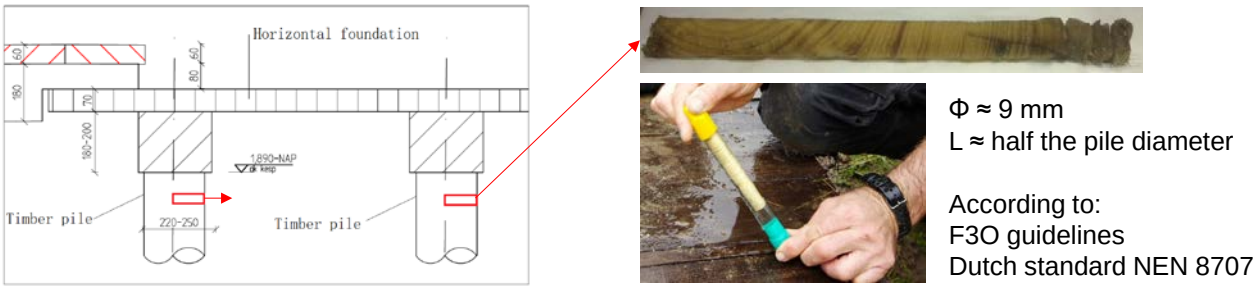

Figure 4. Location and example of a core drilling sample taken by a diver from the head of the pile.

measurements to determine the state of piles were done by core-drilling, just below the head of the pile, see Figure 4.

Based on the drilled core, an estimate of the depth and severity of deterioration was made. In a second step, the remaining 'healthy' cross-section was consequently used for the verification of the load-carrying capacity based on the characteristic strength of timber piles with modified safety factors. In this procedure, a number of uncertainties were present, among others:

- The method was based on a relationship between water content and the strength of pine sapwood. In contrast, the majority of piles present are spruce, which is less vulnerable to bacterial decay than pine due to its relatively open structure.
- The method of core-drilling is labour-intensive and expensive, as a diver needs time and energy to take the sample, while working under the waterline and taking two cores per pile at two different heights.
- The drill core results represent only a single location within an entire pile, measured from the outside to the pith.
- The drill core needs to be visually assessed by experienced personnel using a microscope, possibly leading to subjective classification of the level of decay, depending on the laboratory performing the work, as well as on the storage time that may influence the water content of the core.
- Using a microdrill allows for a better assessment of a pile cross-section, as four quadrants can be measured in the same time frame as a single drill core can be taken.

As a result of this procedure, large numbers of bridge and quay wall foundations had to be classified as 'unsafe', which was not consistent with practical experiences within the city boundaries under the control of the engineering offices of the Municipality of Amsterdam. Consequently, a new measurement method was required, and the method chosen was underwater microdrilling.

A fundamental study on bacterial decay was performed by Varossieau in 1949 [5] from the Centre of Materials Research in the Netherlands, which later became part of TNO, the Netherlands Organization of Applied Scientific Research. Various stages of bacterial decay were identified in old wood that had been in service in soil while below the groundwater table. One of the conclusions of this work was that bacterial decay starts relatively quickly and within the first couple of years after being installed in the soil. The bacterial decay can be identified from the black areas in Figure 5, where the cell wall is degrading.

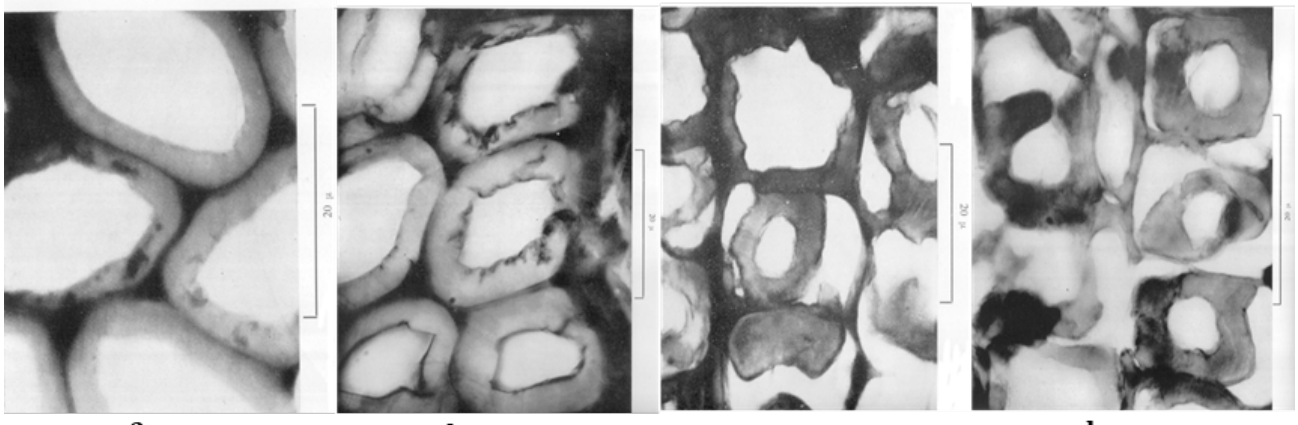

Figure 5 ***a.*** *Onset of bacterial decay in the cell wall,* ***b.*** *S3 layer decayed and S2 layer affected,* ***c.*** *Cell wall collapse visible,* ***d.*** *Cells completely decayed and collapsed [3].*

More recent images have been obtained directly from retrieved piles from Amsterdam foundations, where light microscopy was used to observe birefringence as an indication of decay (see Figure 6), and density measurement using CT-Scanning (see Figure 7).

Figure 6. Left: Representative example of a slice with no decay based on the adopted classification. Smooth cell walls are present (1), showing bright colours because of intensive birefringence; erosion channels are absent and smooth walls are also observable within the cell lumen (2).

Right: Representative example of a slice with severe decay based on the adopted classification. Isolated sound cells (1) still showing birefringence and brighter colour are present, within a matrix of degraded cells (2), showing no birefringence. Presence of V-shaped notches in the few remaining partly sound cell walls can also be observed.

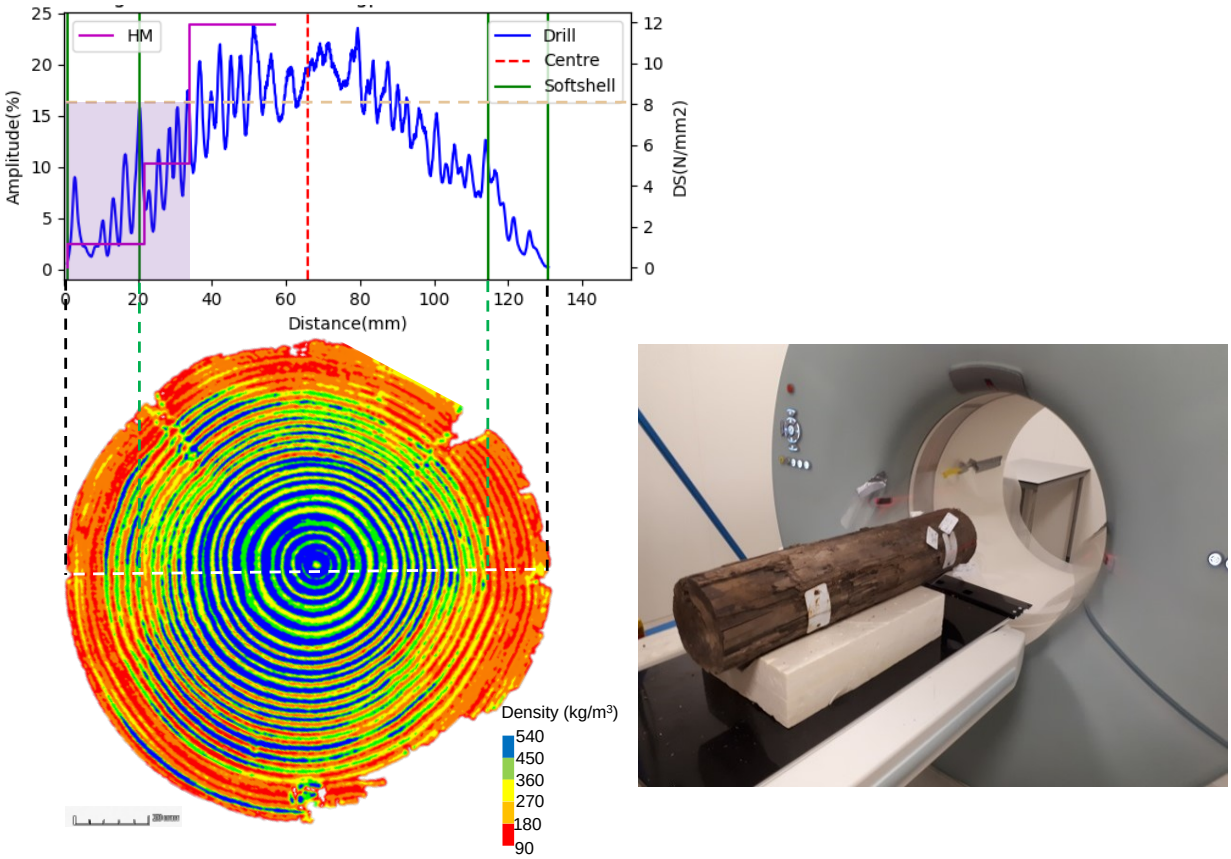

Figure 7. Comparison between the RPD signal, the core drill profile, and a CT scan on the same cross section for the tip of a pile of Bridge 30 in Amsterdam. Both RPD and HM (Core drill) soft shells are highlighted in the graph above. Dotted line white: RPD measurement along the cross section.

After analysing a number of piles, it was decided to break down the microdrilling signals into five levels, each representing 20% of the sound wood density, and to determine the softshell thickness as governed by the lowest two classes. This approach was chosen to align with the Municipality of Amsterdam's current practice and to make historical core drill data accessible for future analysis. An important finding relates to the fact that no bacterial degradation was found in the heartwood portions of the extracted piles. This means that the rate of degradation (or penetration) of the decay front has either stopped or is severely reduced after reaching the sapwood-heartwood transition. However, at the pile tip, the cross-section is primarily sapwood. Whether there is a correlation between biological decay at the pile head and pile tip is still a matter of study. Further analysis of the remaining healthy cross-section gave the following relationship between the short-term strength of wet timber piles and the remaining cross-section [13]:

$$f_{c,0,d,wet} = 14.74e^{0.0182(A_{sound}-100)} \quad (1)$$

Load and stress predictions inside the pile and at the tip

One of the more challenging questions relates to the prediction of the load-carrying capacity at the pile tip, which is generally the design governing section of a pile. As timber piles are tapered, the cross-sectional stress will increase over depth, depending on the soil conditions related to the skin friction. In order to see the load and stress distribution along the length of timber piles, a separate in-situ test series was performed with new wood piles, equipped with distributed fibre optic sensors (DFOS). These allow strain measurements when the pile is loaded, allowing for an accurate estimate of the actual stress distribution.

Three spruce and three pine foundation piles instrumented with DFOS were driven into the soil in a testing field in Amsterdam and axially loaded in compression. Since DFOS provides strain information, calculating the stress distribution in the piles requires knowledge of their stiffness properties, which inherently vary from the head to the tip. Consequently, the piles were extracted, and their overall wet dynamic elastic modulus ($E_{c,0,dyn,wet}$) was determined through frequency response measurements. Subsequently, the piles were segmented, and for each segment, the mechanical properties were determined, and their variability along the pile was studied, in particular for the static modulus of elasticity ($E_{c,0,stat,wet}$). This enabled a comprehensive assessment of the actual in-situ stress distribution

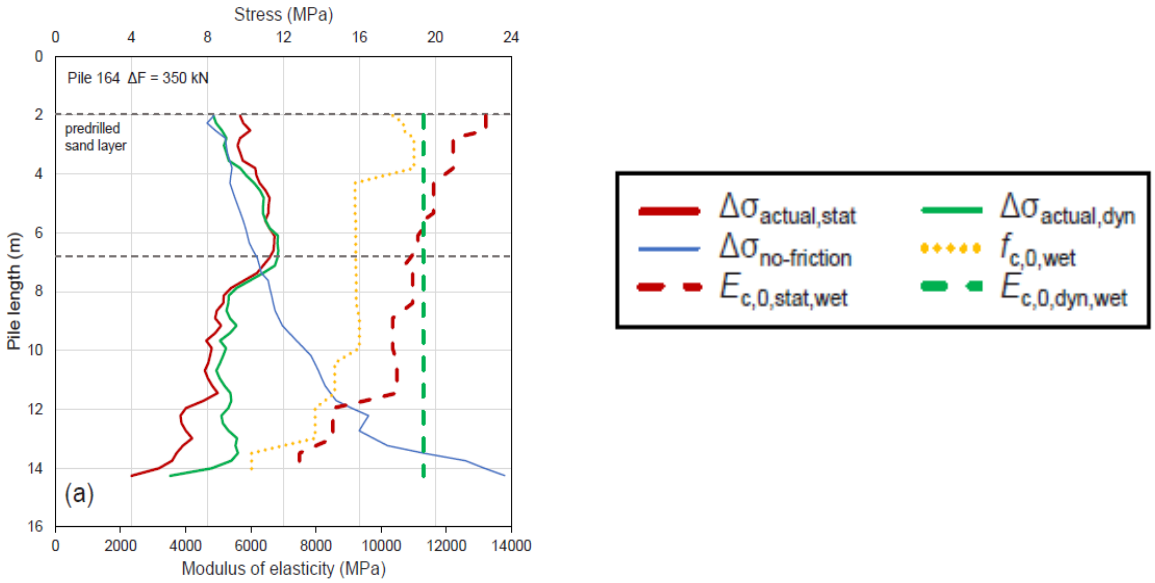

Figure 8. Stress development in a pile taking into account the MoE over the length

along the length of the piles, calculated with DFOS strains and the pile stiffness values. An example of the stress development along the pile axis is shown in Figure 8, showing a decrease in stress closer to the pile tip, highlighting the influence of skin friction and the variation in modulus of elasticity over the pile length. This is an important finding, as the pile tip has lower strength, so the ratio of stress over strength is counterbalanced by a reduced stress level at this point inside the pile [14].

A second issue relates to the stress distribution inside the pile. Due to the degradation of the outer side of the pile (the soft shell), the stress distribution in the cross-section will be altered, and more stress will be taken up in the centre part of the pile. This is a time-dependent process that is visualised in Figure 9. It means that the stress ratio in the remaining sound part will increase over time, which will increase the accumulation of damage over time as the stress ratio over strength increases.

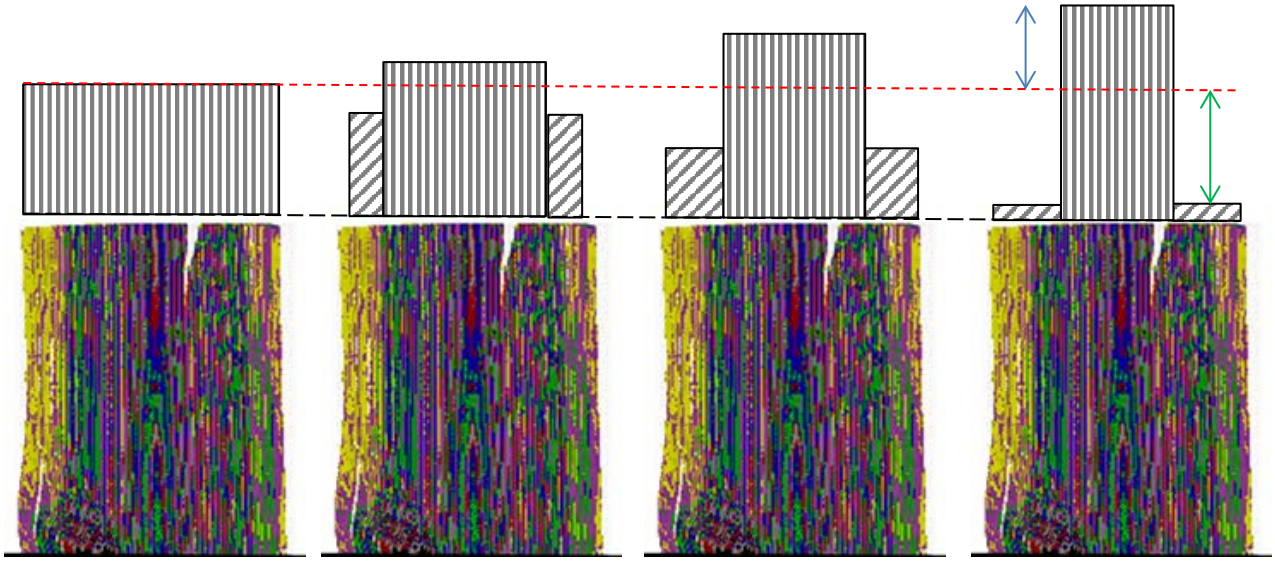

Figure 9. Time related redistribution of stresses in a pile cross section caused by increasing softshell thickness

RELATION TO EURCODE 5 AND DAMAGE ACCUMULATION MODELLING

Background of Eurocode 5: Duration of load classes

The long-term strength may reach a state where the creep rate starts to increase, leading to structural failure. The time span from the beginning of loading until the failure is called the 'time to failure' (T_f). This time to failure is related to the load level, where the load level is generally defined as the ratio between the applied stress and the timber strength, whereas this strength value is generally taken as the mean short-term strength. The latter is the strength as found in standardised tests for the determination of wood properties. The standardised tests, used for the assignment of wood into strength classes such as C18 or C24 (NEN-EN 338 Structural Timber - Strength classes), are based on bending tests (determination of bending strength and modulus of elasticity), or alternatively on tensile tests (determination of tensile strength and modulus of elasticity, as well as the wood density. The assignment to strength classes is based on tested sawn wood, not roundwood. Other properties than the tested ones, such as compression strength, shear strength, etc., are based on established relationships between the various properties (EN 384).

In the case of timber piles, the characteristic value of the short-term compression strength has been derived on the basis of a limited set of data on new saturated piles. The assumed characteristic strength values for spruce piles were practically based on a single subsample only [10, 11] with a mean tip

diameter of around 140 mm. For reasons of consistency of use in structural design codes, the result for the compression strength of piles had been modified and published as a 'dry' characteristic compression strength value, which is then converted by the structural engineer using the ratio for dry-wet strength as specified in Eurocode 5. However, this wet-dry characteristic strength value conversion is primarily based on bending strength ratios for dry vs. wet strength (Service Class 1/2 vs. 3), whereas for compression strength, the ratio between dry and wet strength is probably higher and is expected to be in the order of 30-35% [15]. Furthermore, several assumptions in the assessment procedure were based on the design procedures for new timber structures as specified in Eurocode 5 [12], not taking into account the effects of how 'damage' actually accumulates in wood under long-term loading.

Equations relating the load level to the time to failure are generally straight lines on a logarithmic time scale:

$$\frac{\sigma(t)}{f_s} = C_1 - C_2 log T_f \qquad (2)$$

in which:
$\sigma(t)$ = the stress in time, generally taken as constant in a time to failure test
f_s= the short-term strength of the material from standardised tests
T_f = the time to failure
C_1, C_2 = constants obtained from a regression analysis of test data on time to failure

Values for C_1, C_2 can be found in literature. With respect to time to failure, sometimes reference is made to what is called the 'Madison equation', reading:

$$\frac{\sigma(t)}{f_s} = 0.7416 T_f^{-0.4635} + 0.183 \qquad (3)$$

This is a hyperbolic curve, but it leads to a comparable result with respect to the time of failure in relation to the applied load level. A major difference is that this equation predicts that a stress level below 0.183 will lead to an infinite time to failure, but this is far beyond the life of normal timber structures. It can be seen as a base stress level below which no damage accumulation occurs. These two equations, together with the k_{mod} values as given in EN 1995, are graphically shown in Figure 10.

From the graph, it can be observed that the long-term strength values (kmod) as given in EC5, coincide well with the derived time to failure lines by P.E. Wood [17, 18]. However, the reference period is restricted to 50 years (permanent loading), whereas foundation piles in Amsterdam have been in service for up to around 400 years. Due to the logarithmic nature of the time to failure process, the relative load level is quite sensitive for a given period of service life. As an example, for wet conditions and a reference period of 50 years, EN 1995 specifies a value of 0.5. At this 0.5 level, however, the theoretical prediction of the mean time to failure based on the regression equation of wood [17] gives an equivalent estimated mean time to failure (service life) of about 300 years.
For pile foundations, and in general for existing timber structures that need to be assessed, it is crucial to have a good estimate of the ratio (also known as the 'load level') between the actual permanent load and material strength. As can be seen from Figure 10, if the load level is around 0.5 (or 50%), the expected failure time is around 50 years, but if the load level is about 0.4 (40%), the expected failure time is more than 1100 years. Consequently, for historical pile foundations, a good and accurate estimate of the load level and its history is essential. If the determined stress level is overestimated, the allowed service life is too short and high investment costs for service life extension are incurred.

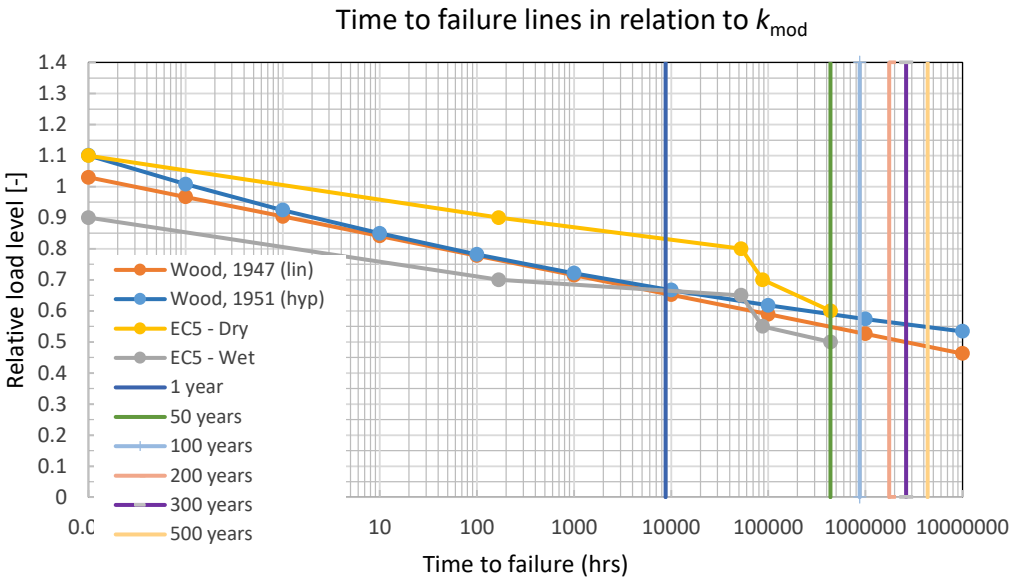

Figure 10. Time to Failure lines of wood in hours, with Eurocode 5 load duration classes. The green vertical line indicates 50 years duration of dead load. The purple vertical line indicates 300 years of age, which is comparable to the (current) oldest bridge foundations.

The use of this long-term strength phenomenon in the verification of the strength of timber is regulated in design standards such as NEN-EN 1995 - Eurocode 5 Timber structures, through the factor k_{mod}, relating the characteristic strength to the design strength:

$$\sigma_{c,0,d} \leq k_{mod} \frac{f_{c,0,k}}{\gamma_M} \tag{4}$$

This equation can be used when structures are designed with new wood. It can be rewritten as:

$$\gamma_M \frac{\sigma_{c,0,d}}{f_{c,0,k}} \leq k_{mod} \tag{5}$$

This equation is equal to equation 2, and consequently, k_{mod} in Eq. 5 can be seen as a representative value for the time to failure equation, apart from any safety factors. For applications such as timber piles that are in the saturated state, the k_{mod} value relates to Service Class 3 in Eurocode 5 (wet conditions).

In EN 1995, Table 1 is given specifying values for k_{mod} as a function of the load duration and the service class. Each load acting on a structure has to be assigned to a 'load duration class'. Foundations are generally considered to be loaded by permanent loads, for which EC5 specifies load duration class permanent (self-weight), when the accumulated duration of the characteristic load exceeds 10 years.

Table 1. Load-duration classes and loading examples in Eurocode 5.

Load-duration class	Order of accumulated duration of characteristic load	Examples of loading
Permanent	more than 10 years	self-weight
Long-term	6 months – 10 years	Storage
Medium-term	1 week – 6 months	imposed floor load, snow
Short-term	less than one week	snow, wind
Instantaneous		wind, accidental load

As the reference period for structural safety levels is generally taken as 50 years, pile foundations aged 100 or more years clearly fall outside of this generally accepted time range. This means that for existing structures, when analysed for structural safety and remaining service life, the standard approaches as given in design codes have to be handled with care and are sometimes not even applicable.

Modelling of the residual service life and load carrying capacity using a damage accumulation approach

In the case of pile foundations primarily loaded in compression, a different approach should be taken as the load case is specific, and the timeframe extends far beyond the 50-year reference period as assumed in Eurocode. A complicating factor is the change in stress and mechanical properties and/or geometry over time due to biological degradation, as indicated in Figure 9. A safe approximation is always that biologically degraded material has zero strength and stiffness, even though this could be used when more data on the strength of degraded wood and its mechanical behaviour becomes available [24, 28]. The physical background explanation of equation 2 can be found in many papers related to damage accumulation modelling [18-23], with an extension to the influence of degradation in [24-26]. The basis of damage accumulation modelling is found in the assumption that each load acting over a certain time period will lead to a certain 'damage' inside the material. Equation 2 is the solution of a linear damage accumulation model that can be used as a basis for more elaborate damage accumulation modelling and long-term strength analysis [18-24]. Equation 2 is the solution on which Eurocode 5 is based as a time to failure equation of the following exponential damage accumulation equation. When integrated for α starting at 0 (zero damage) and going to 1 (failure) while time t reaches T_f:

$$\frac{d\alpha}{dt} = \exp\left(-a + b\frac{\sigma(t)}{f(t)}\right) \tag{7}$$

in which $\sigma(t)$ is the stress over time and $f(t)$ the strength. Integrating for constant loading ($\sigma(t) = c$, dead load and $f(t)$ = the short term strength = f_s) gives:

$$\int_0^\alpha d\alpha = \int_0^t exp\left(-a + b\frac{\sigma}{f_s}\right) dt \Rightarrow \alpha = t \cdot exp\left(-a + b\frac{\sigma}{f_s}\right) \tag{8}$$

With $\alpha = 1$ (failure) and $t = T_f$, this results in:

$$T_f = exp\left(-a + b\frac{\sigma}{f_s}\right) \tag{9}$$

or, written as a traditional 'time to failure' line, similar to equation (2):

$$\frac{\sigma}{f_s} = \frac{a}{b} - \frac{1}{b} ln\, T_f. \tag{10}$$

This equation is valid for a determinate value of the strength and a constant load during a period Δt. Equation 10 means that the coefficients in the traditional straight time to failure lines for new sound wood:

$$\frac{\sigma}{f_s} = \frac{a}{b} - \frac{1}{b} ln\, T_f = C_1 - C_2\, ln\, T_f \text{ and thus } C_1 = \frac{a}{b} \text{ and } C_2 = \frac{1}{b} \tag{11}$$

The important item in the traditional damage accumulation models is the ratio between applied load and short-term strength. The latter is relatively easy to estimate, and in practice, a fixed value for the short-term strength f_s may be assumed, even though there will be a natural scatter in material properties. For existing structures, a priori information is generally available, which can be used in the

analysis [27]. Oftentimes, the wood species and quality can be determined or estimated from in-situ analysis, even though beams sometimes cannot be accessed from all sides and assumptions may have to be made. However, for many species, the relationship between quality, grade, and strength is known, and strength values can be estimated more accurately from in-situ analysis than just taking the strength class or the minimum grade value. Within the framework of assessing pile foundations, estimates of the wood quality and strength are now based on the interpretation of microdrilling results as measured on the pile head, even though the verification of the load-carrying capacity has to be done along the complete pile. This means that for the expected governing cross-section at the pile tip, uncertainties will remain.

In addition to the mechanical load, the time-dependent degradation caused by bacterial decay can now be integrated into the damage accumulation equation. Integration of equation 7 then has to be done in multiple time steps covering the history of the foundation, both from a solicitation as well as from a resistance point of view. Additional assumptions may account for the expected delay time for degradation. It is yet to be determined whether bacterial decay starts directly after pile installation, or if there is a delay time, which may be different for sap- and heartwood [24]. Also, rates of sapwood decay are assumed to be higher for pine than for spruce, due to the more open structure of pine.

Similarly challenging is the load history. Estimates can be made based on the historic use of the structure. Whereas self-weight can be estimated quite accurately, live loads over time are more complex to address. For the loads, a number of approaches are available, see for instance the JCSS Model Code [29], Eurocode 1 [30] and ISO 2394 [31] that give guidance. For the problem under study here, long-term loading and time to failure, a Ferry-Borges-Castagneta (FBC) model [29] is more than sufficient. A fully random load system requires time-consuming integration and is not necessary for the majority of cases, certainly not for the bridges in Amsterdam, where the main load component is dead load. However, over the period of up to 300 years, bridges have certainly seen an increase in loads over time, especially related to traffic loads by trams and other heavy vehicles. Also, bridges were regularly widened when traffic increased, so a single foundation may consist of various configurations. In Figure 11, two out of eight examples of cross sections of bridge foundations are shown covering the time span to be analysed. The original one from 1727, and the current one, where the bridge widening works from 1886 to 1922 are added, and the original 1727 bridge is incorporated. The current period covers the load levels for the timespan 2020 – 2120, so it covers the coming 100 years with respect to the expected loads.

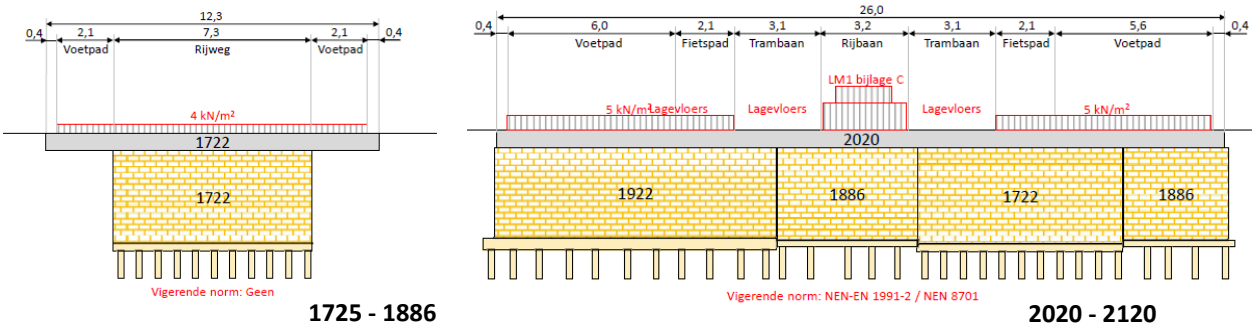

Figure 11. Bridge 30, Left: cross section and max. load from 1727 to 1886. Right: cross section, including additions and modifications from 1886 and 1922, incl. max. loads from 2020 to 2120.

The damage accumulation equation 7 is primarily intended for mean strength and constant load values, whereas in real-life structures, such conditions are not typically encountered. However, it allows modelling of the time variant loading on an actual structure as a time sequence of constant loads with varying amplitude, for instance, in accordance with the FBC-Load model approach. A fixed value for the

short-term strength f_s or the value from equation 1 may be used. Alternatively, a random value out of the known statistical distribution of pile strengths can be generated. Consequently, the important item in the traditional damage accumulation model, being the ratio between applied load and short-term strength, can be generated, and its contribution to the accumulation of damage can be accounted for, allowing also for sensitivity and failure studies. The algorithm with which the damage accumulation per time step can be calculated is given in [24, 25] for piles that are degrading and in [26] for cracked timber beams.

CONCLUSIONS AND OUTLOOK

The Municipality of Amsterdam is confronted with a portfolio of bridges with timber pile foundations that need to be assessed for both structural safety and serviceability. As the current assessment method proved not sufficiently accurate and reliable, a large research program has been initiated to improve the timber pile assessment methods as well as the structural calculation methods.

Regarding timber piles, the method of underwater microdrilling has been developed and introduced in the daily operations. It replaces the method using drill cores, which are labour-intensive for divers and require microscopy and water content determination in a laboratory environment, in order to estimate the state of deterioration based on experiences with the species pine. The newly developed method using microdrilling allows for a more accurate and comprehensive assessment of the 'softshell' independent of the wood species. This method is not only faster and easier to perform by divers, but it also directly covers four quadrants of the cross-section instead of 1, and is more economical as post-sampling laboratory work is no longer required. In addition, as the measurements are being monitored in real-time, possible errors can be directly observed by the technicians, who can then instruct the divers to take action.

One of the prime challenges is understanding both the complexity of the timber piles themselves, as well as the variability in biological (bacterial) degradation. From the cross-section of a pile, different tissue areas can be distinguished using a microdrill. After extensive testing, the microdrill profile as measured could be directly used to estimate a reliable strength profile over the pile cross-section as well as the pile's wet material strength. This value can be directly used to estimate the current state of the foundation, as the measured profile serves as a direct input parameter in the calculation model. This model determines the load-carrying capacity and the remaining service life under the given load conditions, which include both dead and live (traffic) loads.

The measured profiles provide comprehensive output on decayed wood caused by microorganisms, sapwood, heartwood, juvenile wood, compression/reaction wood, as well as the early- and latewood within a growth ring. Furthermore, the position of the pith and the number of annual rings can be determined, allowing for an estimate of the sapwood portion, which in turn is related to the time of development of the softshell. The parameters have been investigated and correlated with the stiffness and load-carrying capacity in compression along the entire pile.

In addition to the introduction of this in-situ measurement method, a new method for calculating the mechanical state of the timber piles has been introduced, allowing for a more accurate estimate of the wood material strength over the length of the pile and around the pile tip in particular. A considerable number of tests on both retrieved and new piles have been performed, providing a scientific basis for the new approach and offering valuable insights into material stresses along the pile shaft. For the verification of the load carrying capacity, both 'as is' and its future development, the transition is underway to implement the concept of damage accumulation modelling. The current calculation method, as given in Eurocode 5, does not apply to structures that have been preloaded for such a long time. This requires the implementation of the new algorithms.

The analysis of the current state and remaining service life of Amsterdam pile foundations is extremely complicated, as it depends on a great number of influencing factors. The method for calculating the state of the foundation and its remaining service life under various load and structural safety scenarios is being developed in a step-by-step manner and is still ongoing.

As it is a time-dependent issue, the estimation of the (remaining) service life involves the assessment of the behaviour of wood under a mixture of loadings, which can be of mechanical, physical, biological and/or chemical in nature. The service life of structures can be determined using several approaches that have been classified by the Joint Committee on Structural Safety (JCSS). The most complicated approaches comprise so-called level III calculations, where for each variable of the structure (e.g., strength, stiffness, durability, and loads), the actual or an estimated statistical distribution of the parameter is used. For wood, such distributions are often unknown or have a high uncertainty level due to the large natural scatter. The consequences of these uncertainties are that extremely high safety levels are aimed for, which often are not supported by practical evidence from existing structures. The parameters that can be used in the model can be updated as soon as new knowledge becomes available, for instance, in relation to pile strength and stiffness distributions, as well as within pile variation along the pile axis.

For foundations, the main load component is dead load, where variable loads from traffic are also present, but over the history of 100-300 years, they seem to be less relevant at first glance. However, traffic loads have been increasing, especially over the last 150 years, so this may become more important, especially regarding the older foundations. Equally important is to get an accurate estimate of the constant dead load over the pile's history and the point in the pile where the highest stress level occurs. In that case, the damage equation is more straightforward to solve. The failure process is then governed for long-term static loading, without having the complexities of random variable loading.

The assessment of parameters affecting the load-bearing capacity remains, however, complex. Measurable assessment parameters are limited, since only a very small 'window' of approx. 10% of the entire pile at the top is available for assessment, from which an estimate for the entire pile must be made. The complete cycle of analysis is shown in Figure 12.

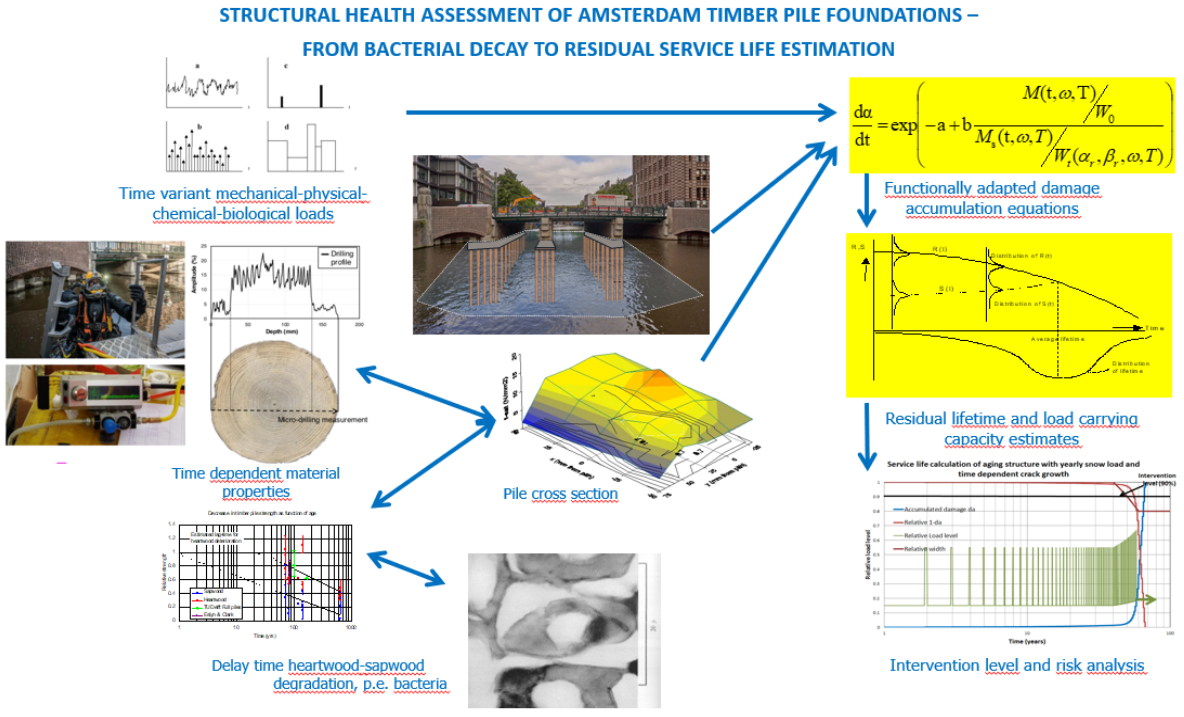

Figure 12. Overview of the project from the bacterial decay level to the complete

Future work may consider a more profound analysis of the interaction of wood and soil at the pile tip, the correlation between decay at the pile head and the pile tip, as well as the behaviour of piles with a soft shell under quay walls loaded in compression and bending.

ACKNOWLEDGEMENTS

The Municipality of Amsterdam is gratefully acknowledged for their year-long support in making this project possible.

REFERENCES

[1] Timber Piles, J.W.G. van de Kuilen, Lecture E18, Timber Engineering STEP 2, Eds. Blass et al. 1995.

[2] NEN 5491:1991 Quality Requirements for Timber - Timber Piles

[3] Influence of initial plant density on sawn timber properties for Douglas-fir (Pseudotsuga menziesii (Mirb.) Franco), Andreas Rais, Werner Poschenrieder, Hans Pretzsch, Jan-Willem G. van de Kuilen, Annals of Forest Science (2014) 71:617–626 DOI 10.1007/s13595-014-0362-8

[4] Strength grading of saturated softwood foundation piles, Pagella,P., Ravenshorst, G.J.P., Mirra, M., Van de Kuilen, J.W.G., , INTER Paper 57-6-1, Padova, Italy, 2025

[5] Opgegraven en aangetast hout vanuit biologisch oogpunt bezien, Varossieau, W.W., CIMO Delft, 1949 (in Dutch).

[6] F3O (2011) F3O Richtlijn: Onderzoek en beoordeling van houten paalfunderingen onder gebouwen. Rap-portnummer: 978-90-816732-1-1 (in Dutch).

[7] NEN 8707 (2018) Assessment of the structural safety of an existing structure during renovation and rejection - Geotechnical constructions, Nederlands Normalisatie-instituut (NEN).

[8] Klaassen R.K.W.M. (2008) Bacterial decay in wooden foundation piles – Patterns and causes: A study of historical pile foundations in the Netherlands. International Biodeterioration & Biodegradation.

[9] Van de Kuilen J.W.G. (1994) Bepaling van de karakteristieke druksterkte van houten heipalen. Rapportnum-mer 94-con-RO271. Delft: Toegepast-Natuurwetenschappelijk Onderzoek (in Dutch).

[10] EN 384:2016 Structural timber - Determination of characteristic values of mechanical properties and density

[11] Stapel,P., Van de Kuilen, J.W.G., Ravenshorst,G.J.P., Influence of sample size on assigned characteristic strength values. 2011, CIB W18, proceedings paper 44-17-1,2011, Alghero, Italy.

[12] EN 1995 – Eurocode 5 – Design of timber structures

[13] Innovative application of micro-drilling for the assessment of decay and remaining mechanical properties of historic wooden foundation piles in Amsterdam, G. Pagella, G.J.P. Ravenshorst, M. Mirra, W.F. Gard, J.W.G. van de Kuilen, Developments in the Built Environment 19 (2024) 100514

[14] Assessment of in-situ stress distribution and mechanical properties of wooden foundation piles instrumented with distributed fiber optic sensors (DFOS), M. Felicita, G. Pagella, G.J.P. Ravenshorst, M. Mirra, J.W.G. van de Kuilen, Case Studies in Construction Materials 20 (2024) e03139

[15] Wood Handbook . FPL–GTR–190, Forest Products Laboratory, USDA.

[16] Wood, L.W., 1947. Behavior of wood under continued loading. Eng. News-Rec. 139, 108–111.

[17] Wood, L.W., 1951. Relation of Strength of Wood to Duration of Load; Report No. 1916. Forest Products Laboratory: Madison, WI, USA.

[18] Gerhards, C.C., 1979. Time-related effects on wood strength: A linear cumulative damage theory. Wood Sci. 11, 139–144.

[19] Caulfield, D.F., 1985 A chemical kinetics approach to the duration-of-load problem in wood. Wood and fibre science, Vol. 17. No. 4, pp. 504-521

[20] Kuipers, J., 1986. Effect of age and/or load on timber strength. CIB-W18 Timber Structures, paper 19-6-1, Florence, Italy

[21] Foschi RO, Yao R.C., 1986. Another look at three duration of load models. CIB/W18, Paper 19-9-1, Florence, Italy.

[22] Van der Put, TACM., 1986. A model of deformation and damage processes based on the reaction kinetics of bond exchange. CIB-W18, Paper 19-9-3, Florence, Italy.

[23] Van der Put, TACM, 1989, Deformation and damage processes in wood, PhD Thesis TU Delft, 1989

[24] Van de Kuilen J.W.G., 2007. Service life modelling of timber structures. Mat. & Struct. DOI 10.1617/s11527-006-9158-0

[25] Van de Kuilen, J.W.G. Beketova-Hummel, O. Pagella, G. Ravenshorst, G.J.P. Gard, W.F., 2021. An integral approach for the assessment of timber pile foundations, WCTE 2021, Santiago de Chile, Chile.

[26] Van de Kuilen, J.W.G., Gard, W.F, 2013, Damage assessment and residual service life estimation of cracked timber beams, Advanced Materials Research Vol. 778, pp. 402-409

[27] ISO 13822:2010 Bases for design of structures — Assessment of existing structures

[28] M. Lee, Cross-sectional analysis of the mechanical and physical properties of spruce foundation piles, MSc thesis TU Delft.

[29] JCSS Probabilistic Model Code, ISBN 978-3-909386-79-6.

[30] EN 1990 - Eurocode: Basis of Structural Design.

[31] ISO 2394 - General principles on reliability for structures.

ASSESSMENT OF HISTORICAL TIMBER TRUSSES USING NON-DESTRUCTIVE TESTING (NDT) PENETRATION METHODS

Yilién CABRERA MARTÍN[1], Vittoria BORGHESE [2], Claudio SEBASTIANI[1], Carlo BAGGIO[1] and Silvia SANTINI[1]

[1] Department of Architecture, Roma Tre University, Rome, Italy
[2] Department Building Materials and Structures, Netherlands Organisation for Applied Scientific Research, Delft, Netherlands

ABSTRACT

The correct diagnosis of timber structures of buildings in the urban historical centres contributes to heritage conservation. This research evaluated the importance of accurate wood species identification as the starting point of the visual inspection and assessed the effectiveness of combining non-destructive penetration tests to estimate wood density. The results demonstrated that incorrect species identification compromises the accuracy of density estimates obtained with instruments and of the maximum stress of the on-site classification via visual inspection, leading to incorrect material characterisation. Statistical analysis of combined Woodpecker and Resistograph results indicated that using a nonlinear correlation would improve the coefficient of determination, which should be demonstrated with a larger sample.

KEYWORDS: Non-Destructive Testing (NDT), historical solid timber structure, assessment.

INTRODUCTION

Many inherited buildings in historical city centres have solid timber roofs and floor structures, either entirely or partially, emphasising the importance of a reliable diagnosis in heritage conservation. Precisely evaluating the structural condition without compromising the aesthetic integrity of the elements, considering that wood is an organic, heterogeneous, hygroscopic, anisotropic, and porous material, poses a challenge for specialists in the field [1] [2] [3].

Technical standards related to the diagnosis of historic timber structures are based on visual inspection [5] [6]. The established procedure begins with species identification and culminates in classification according to evaluated strength based on detected defects and the identified species type [6] [7]. Errors in this first step would compromise the structure's assessment even when visual inspection is supplemented with non-destructive tests (NDT); verifying this is one of the objectives of the present research.

NDT are recognised by technical standards [5] [6] as a supplement to visual inspection for determining physical and/or mechanical parameters that allow estimation of the strength of ancient timber structures. [6] [7] Combining tests is advisable to leverage each method's advantages, as they behave differently depending on fibre orientation and material properties [2] [3] [8].

Density is a physical property that can be used as an indicator of timber's mechanical properties [9], [10], [11]; its relationship with them is strong and varies according to the loading direction relative to the fibre, the type of stress, and moisture content [12] [13]. This is validated by studies highlighting its importance in classifying wood by mechanical strength [5] [6] [14] [15] [16]. With the density estimates

obtained through NDT, it is possible to estimate the modulus of elasticity (MoE) and compare it to the value derived from the in-situ classification according to normative standards based on visual inspection, thereby establishing an estimation range for structural assessment.
Several NDT exist to determine in-situ timber density [8] [17] [2] with Drill Resistance and Pin Pushing methods concurrent in several studies [7] [18] [19] [20]. Their advantages include ease of operation, instantaneous results, and minimal invasiveness. Both methods are penetration-based, making them candidates for correlation to achieve better density estimates, the second research objective. The former yields a complete reading across the element's cross-section with reasonable to low correlation to density, while the latter is superficial with reasonable to good density correlation, especially in compression perpendicular to the grain [12].
If a strong correlation is established between Drill Resistance and Pin Pushing, supported by statistical methods due to variability in solid wood characteristics and combining two different techniques [7] [21] [22] [23] [24], one could achieve a better density estimate for the element by averaging sectional measurements.

METHODOLOGY

The object of study was taken as the component elements of three of the eleven trusses that form the roof structure, and six purlins, in a historic building located in Rome, built at the end of the nineteenth century (Figure 1).

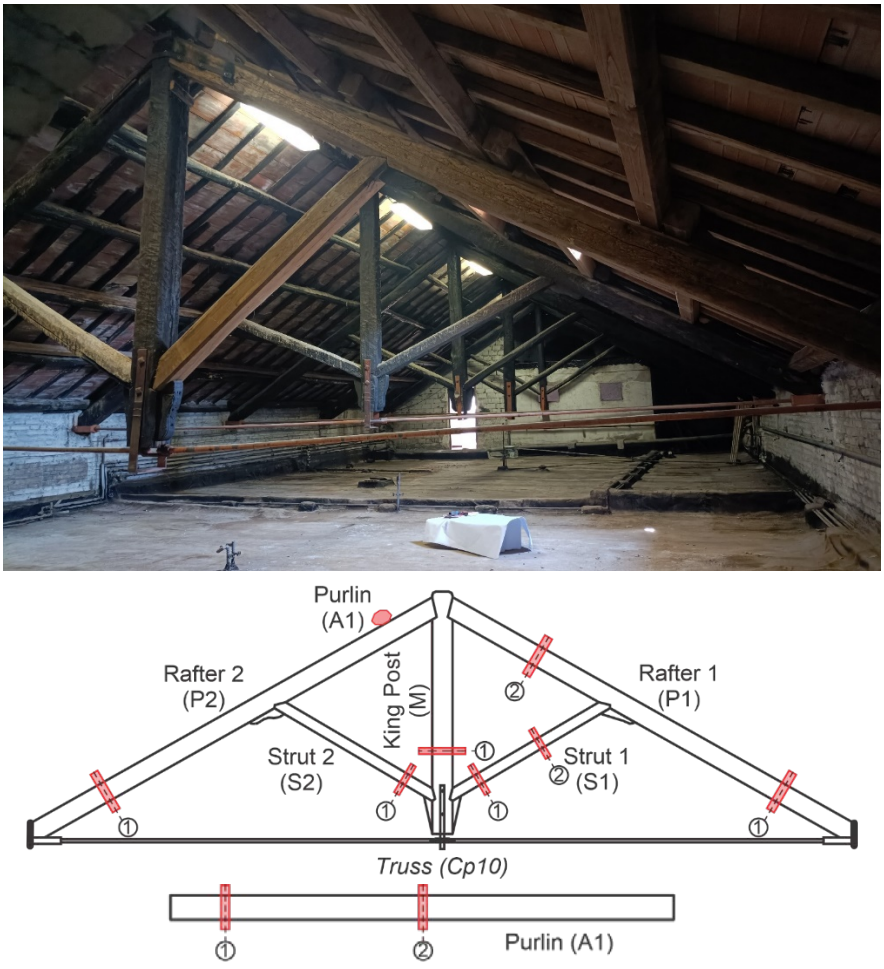

Figure 1. Truss selected for the study with marked test sections.

Visual inspection was accompanied by instrumental tests: hygrometry (Huepar M01 Moisture Meter (Leiwotec), equipped with probes for surface moisture readings suitable for wood), thermography (HIKMICRO G40 Handheld Thermography), and penetration tests using the Resistograph (IML-RESI PD400-Series) and the Woodpecker (Woodpecker 1.0 DRC S.r.l.). This article focuses in detail only on the latter two instruments, as they relate directly to the stated objectives.
The starting point was an architectural survey accompanied by visual inspection without laboratory species identification tests. Once it was verified with the moisture meter that the wood averaged 11.30% moisture content across all element faces, close to the 12% stipulated by standards [25], penetration tests were carried out.
Tests were conducted in seven cross-sections distributed across all truss members: three on the strut, one on the king post, and three on the rafter; and two sections on the purlin (Figure 1). Section selection points were based on surface conditions: absence of knots, nails, or other surface elements, minimal or no biological degradation, and conditions feasible for instrument operation.
For each section, tests were performed with the Resistograph and then the Woodpecker, ensuring they covered the same surface area for comparative analysis and to meet one of the research objectives. This was not possible on the king post due to surface conditions (Figure 2).

Figure 2. Woodpecker and Resistograph tests on the same cross-section.

The Resistograph is equipped with a 3 mm flat steel needle that drills through the entire cross-section. Drilling speed and rotation vary according to wood hardness; in this case, a rotation speed of 3000 rpm and a feed rate of 1000 mm/min were used, assuming a hardwood.
During drilling, the tool measures material resistance at every 0.1 mm, and data are stored by the instrument's control unit. These measurements are presented as a graph with depth (P) on the x-axis and resistance (R), expressed as a percentage, on the y-axis.
For each section, according to its particularities, two to three perforations were made transversely: two perpendicular and one diagonally (Figure 3). The resulting profiles were obtained through the processing of the data, extracted from the instrument with the PD-Tools PRO software, and with Microsoft Office Excel. The graphs were obtained that showed the behaviour of the amplitude of the drilling resistance (R, expressed in %).
The friction coefficient was not applied to instrument results since the wood moisture content was below 12%. Results were cleaned only at the graph's end, where R values approached zero, indicating exit from the section. No such trend was observed at the start of the graph; thus, all results were considered as they corresponded to sections overlapping with Woodpecker tests.
Accurate species identification was verified via average cleaned drill resistance values (R_{mDEP}) for each section. These values were used in density estimation correlations for different species to compare results. The correlations used for White Oak and Poplar are from Brunetti, Aminti, Vicario, and Nocetti [26], whereas for Chestnut, they are from Borghese, Santini, and Sguerri [20], as these references were performed with more samples than the first. (Table 1)

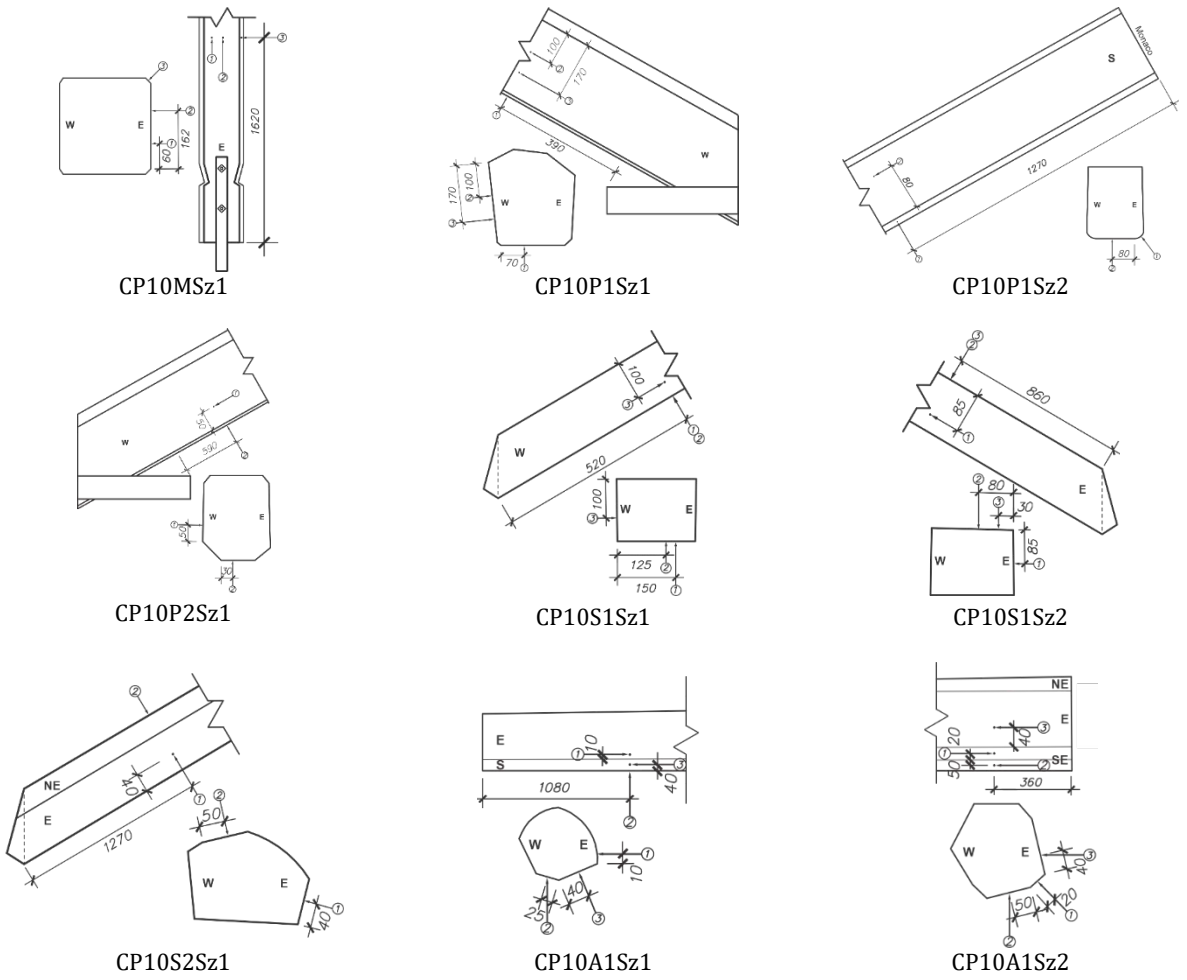

Figure 3. Truss member sections of CP10, indicating test positions and quantities with Resistograph.

Table 1. Correlations used for density estimation with Resistograph IML-RESI PD400-Series

Correlation for White Oak [26]	Correlation for Poplar [26]	Correlation for Chestnut [20]
D (Kg/m^3) =0,12Rm+233 (1)	D (Kg/m^3) =0,23Rm+76 (2)	D (Kg/m^3) =14,71Rm+295,15 (3)
R^2=0.76	R^2=0.94	R^2 =0.82

The Woodpecker is a timber penetrometer with a percussion rod housing a 50 mm long, 2.5 mm diameter hardened steel nail (60 Rockwell), with a 35° conical tip. This study used the manufacturer's correlation to determine Chestnut density based on nail penetration.

Tests were performed according to the manufacturer's instructions. On each section's surface, a 3×3 grid of nine points spaced 3 cm apart was drawn (Figure 4). Five hammer blows were applied at each point to drive the nail. Once all nine nails were inserted, the remaining nail length was measured to determine penetration, and manufacturer correlation was used to estimate surface density for each section, processed in Excel.

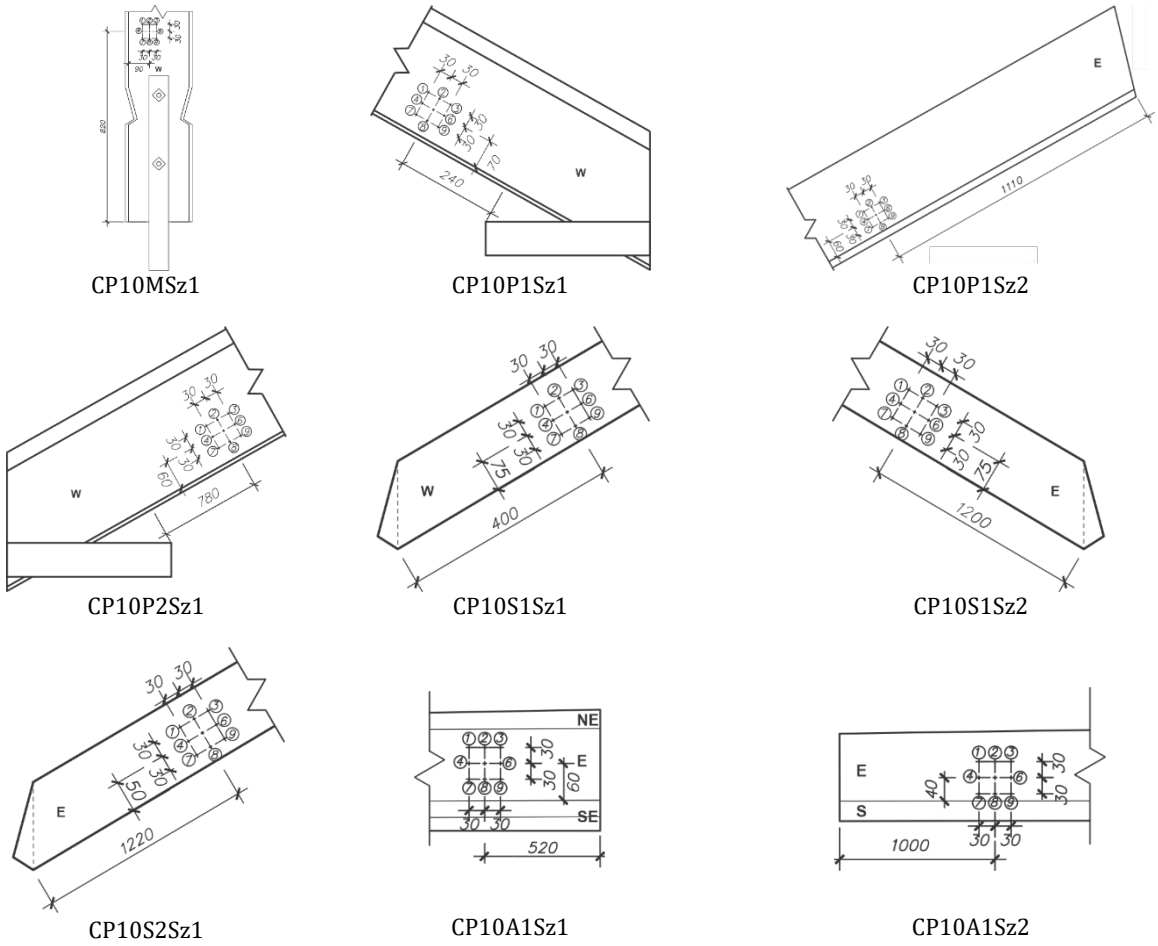

Figure 4. Truss member sections of CP10, indicating test positions and quantities with Woodpecker.

The results of both instruments, for the chestnut species, were organised in a table, in Excel, distributed horizontally for each section and vertically every 0.1mm of penetration into the wood. In this way, the mean for each instrument in the same penetration length was obtained, whose minimum value, among all the sections, was taken as a limit parameter for the analysis of the variables perforation resistance (R), density obtained by the Woodpecker (D_{Wp}) and penetration depth (P).
The behaviour of the variables was analysed based on the means obtained. Linear regression was used as a statistical method, with Excel, which was illustrated with scatter plots, which allowed observing the resulting trends, equations and correlations. With the same tool, a regression data analysis was carried out to adjust the model and verify the results obtained.

RESULTS

Applying different correlation laws to Resistograph results yielded varying densities for the same section (Table 2). Results differed by a factor of two between White Oak and Poplar, and Chestnut showed the same factor relative to White Oak (Figure 5).

Table 2. Resistograph results by section for each element and density calculation using three correlation laws: white oak, poplar, and chestnut

Element	Section	Test	R_m (%)	$R_{m,DEP}$ (%)	$R_{mSection}$ (%)	$R_{mDEPSection}$ (%)	$\rho_{Section}$ White Oak (Kg/m3)	$\rho_{Section}$ Poplar (Kg/m3)	$\rho_{Section}$ Chestnut (Kg/m3)
CP10	M Sz2	R1	17,09	17,63	17,39	17,66	235,12	80,06	554,94
		R2	18,07	18,07					
		R3	17,00	17,28					
	P1 Sz1	R1	14,74	15,20	16,27	16,84	235,02	79,87	542,89
		R2	16,36	17,25					
		R3	17,70	18,08					
	P1 Sz2	R1	18,03	18,58	17,66	18,08	235,17	80,16	561,16
		R2	17,29	17,58					
	P2 Sz1	R1	17,41	18,91	17,63	18,70	235,24	80,30	570,29
		R2	17,85	18,50					
	S1 Sz1	R1	18,30	18,42	18,37	19,51	235,34	80,49	582,09
		R2	18,61	20,90					
		R3	18,19	19,20					
	S1 Sz2	R1	20,26	21,00	19,40	20,43	235,45	80,70	595,73
		R2	16,83	17,42					
		R3	21,10	22,88					
	S2 Sz2	R1	16,60	17,11	15,82	16,67	235,00	79,83	540,31
		R2	15,05	16,22					
	A1 Sz1	R1	23,85	26,06	25,43	26,73	236,21	82,15	688,32
		R2	27,29	27,55					
		R3	25,16	26,57					
	A1 Sz2	R1	31,65	33,88	26,97	28,73	236,45	82,61	717,80
		R2	25,48	26,19					
		R3	23,79	26,13					
CP16	M Sz1	R1	20,96	21,61	23,17	23,98	235,88	81,52	647,88
		R2	25,37	26,35					
	P1 Sz1	R1	21,40	22,21	22,37	23,01	235,76	81,29	633,68
		R2	23,75	24,37					
		R3	21,96	22,47					
	P1 Sz2	R1	19,82	20,53	19,77	20,63	235,48	80,74	598,61
		R2	19,71	20,73					
	P2 Sz1	R1	18,40	19,16	19,19	19,73	235,37	80,54	585,43
		R2	20,00	20,48					
		R3	19,16	19,56					
	S1 Sz1	R1	16,42	17,48	15,61	16,95	235,03	79,90	544,54
		R2	15,20	16,92					
		R3	15,21	16,46					
	S1 Sz2	R1	17,35	18,64	17,62	18,74	235,25	80,31	570,86
		R2	18,67	19,67					
		R3	16,85	17,92					
	S2 Sz2	R1	18,48	19,27	16,84	18,27	235,19	80,20	563,95
		R2	15,21	17,27					
	A1 Sz1	R1	11,49	12,49	12,01	13,03	234,56	79,00	486,84
		R2	13,19	14,32					
		R3	11,35	12,28					
	A1 Sz2	R1	13,84	14,91	14,58	15,38	234,85	79,54	521,35
		R2	14,40	15,19					
		R3	15,50	16,03					
	A2 Sz1	R1	20,56	21,67	18,33	19,65	235,36	80,52	584,24
		R2	17,96	19,02					
		R3	16,46	18,27					
	A2 Sz2	R1	20,56	21,02	19,57	20,28	235,43	80,66	593,43
		R2	18,57	19,53					
		R3	20,38	21,48					
CP21	M Sz1	R1	22,67	23,03	22,13	22,50	235,70	81,18	626,18
		R2	22,04	22,38					
		R3	21,67	22,09					
	P1 Sz1	R1	18,63	19,24	17,68	18,34	235,20	80,22	564,97
		R2	16,78	17,32					
		R3	17,62	18,47					
	P1 Sz2	R1	20,77	21,79	18,63	19,45	235,33	80,47	581,22
		R2	19,11	19,71					
		R3	16,00	16,84					
	P2 Sz1	R1	19,97	20,47	19,39	20,25	235,43	80,66	592,97
		R2	19,69	21,69					
		R3	20,49	20,84					
		R4	17,43	17,98					
	S1 Sz1	R1	19,85	21,65	19,93	21,47	235,58	80,94	610,90
		R2	19,02	20,44					
		R3	20,93	22,30					
	S1 Sz2	R1	21,05	22,18	18,12	19,12	235,29	80,40	576,46
		R2	15,34	16,43					
		R3	17,97	18,76					
	S2 Sz1	R1	14,02	14,96	14,15	15,06	234,81	79,46	516,62
		R2	14,02	14,67					
		R3	14,40	15,54					
	A1 Sz1	R1	18,96	20,02	18,82	19,62	235,35	80,51	583,76
		R2	18,69	19,22					
	A1 Sz2	R1	19,72	20,97	19,84	21,23	235,55	80,88	607,39
		R2	20,66	21,90					
		R3	19,15	20,81					
	A2 Sz1	R1	19,64	20,41	20,22	21,20	235,54	80,88	607,01
		R2	20,79	21,99					
	A2 Sz2	R1	17,94	18,78	19,81	20,94	235,51	80,82	603,22
		R2	20,28	21,84					
		R3	21,22	22,20					

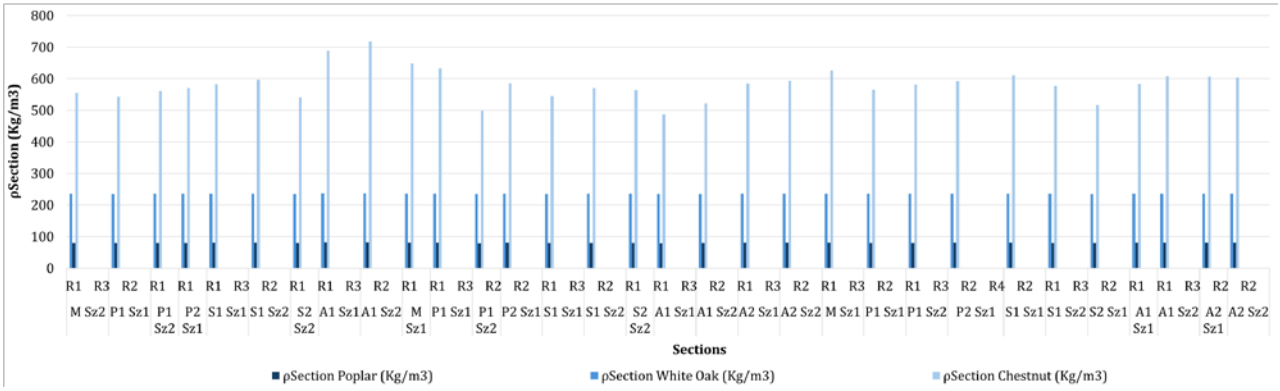

Figure 5. Density behaviour using Resistograph correlation laws for different species

Linear regression between Woodpecker density and Resistograph drill resistance at drilling depths from 0 to 15.30 mm yielded an R^2 of 0.77. (Figure 6a) Their behaviours relative to penetration were R^2 = 0.48 and R^2 = 0.71, respectively. (Figure 6b)

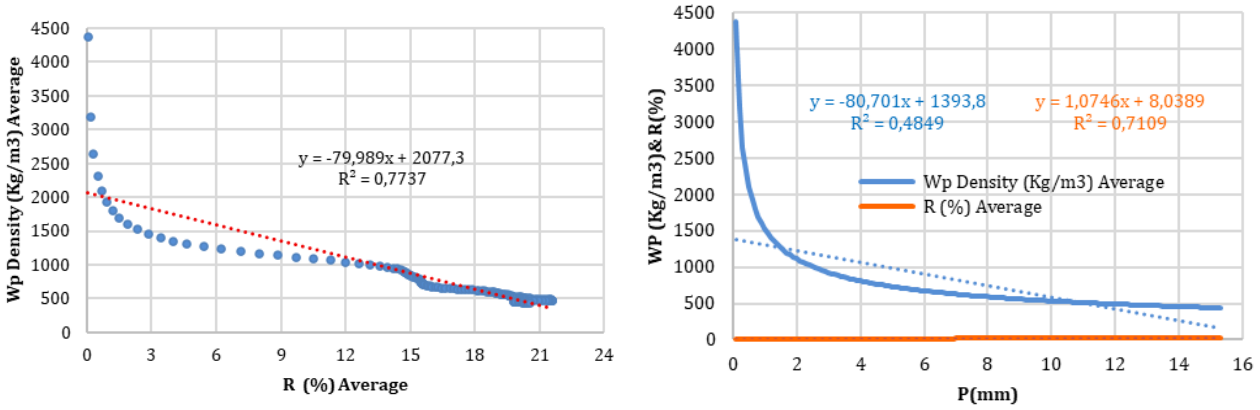

(a) *(b)*

Figure 6. Regression curve between Woodpecker density and Resistograph drill resistance (a). Regression curve of Woodpecker density and Resistograph drill resistance relative to penetration depth (b)

Adjusted regression analysis between Woodpecker density and Resistograph drill resistance showed an adjusted R^2 of 0.77, 0.0015 lower than R^2, with a standard error of approximately 245 kg/m^3 (Figure 7a). Woodpecker density versus penetration yielded an adjusted R^2 of 0.48, 0.0034 lower than R^2, with a standard error of approximately 369 kg/m^3 (Figure 7b). Resistograph drill resistance versus penetration depth had an adjusted R^2 of 0.71, 0.0019 lower than R^2, with a standard error of approximately 3.05 %. (Figure 7c) Data dispersion around the trend line was nonlinear, especially for penetration depth versus Resistograph drill resistance.

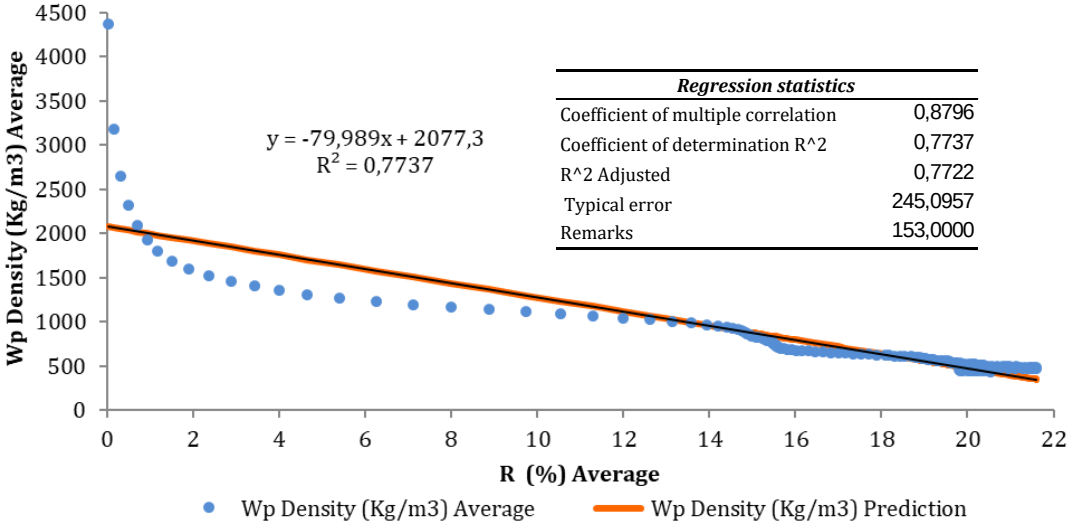

(a)

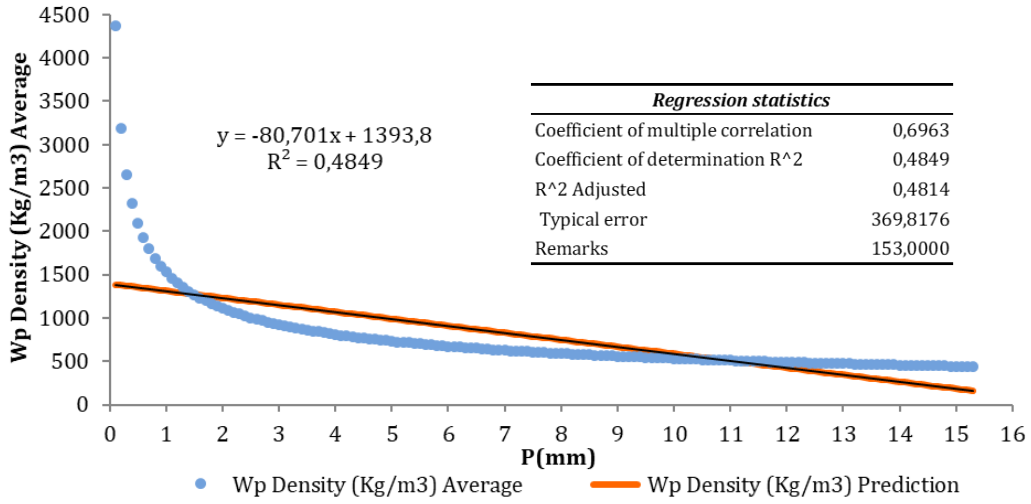

(b)

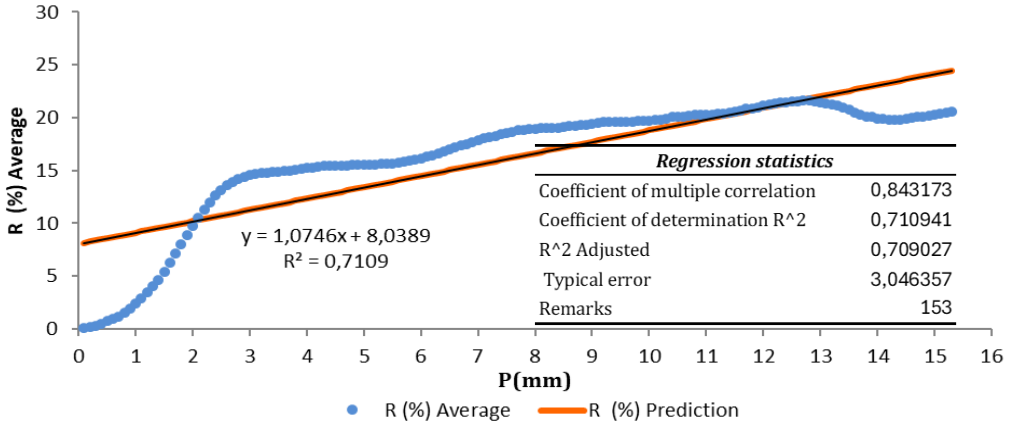

(c)

Figure 7. Adjusted regression curve between Woodpecker density and Resistograph drill resistance (a). Adjusted regression curve between Penetration depth and Woodpecker density (b). Adjusted regression curve between Penetration depth and Resistograph drill resistance (c)

DISCUSSION

The variability of estimated densities for the same section of the element, when applying correlation laws made for different species of wood, demonstrates the importance of a correct identification of the type during the first stage of diagnosis. Conducting a technical assessment on an old timber structure based on properties associated with a different species of wood than the actual one can lead to overestimating or underestimating its bearing capacity, resulting in erroneous construction actions that neglect the principle of heritage conservation.

The debugging of the data obtained from the Resistograph, when these tend to zero, varies the results, although not substantially. This procedure allows the elimination of the readings made by the equipment outside the cross-section, allowing the real values of the section to be obtained.

The calculated correlation between the density of the Woodpecker and the drilling resistance of the Resistograph is not reliable, for the size of the sample studied, despite having a linear equation with an R^2 above 0.75 due to the value of the typical error yielded by the analysis of regression data. The results obtained, however, do not deny the existence of a correlation between the parameters of both instruments.

The behaviour of Woodpecker density and Resistograph drill resistance with respect to penetration depth is different, and both have an R^2 under 0.75. The graphs in Figures 6b and 7b show that the density of the Woodpecker with respect to the depth of penetration is almost linear and with little dispersion, which suggests the need for a few adjustments in the correlation of estimation of the Woodpecker density and/or an increase in the sample size to prove this. The behaviour of the resistance to the Resistograph drilling, as shown in Figures 6b and 7c, differs, exhibiting an undefined and sinuous pattern that suggests a nonlinear correlation might better describe the results.

CONCLUSION

The study focused on the component elements of three of the eleven trusses and purlins, forming the roof structure of a historical building in Rome. Following an initial visual inspection, instrumental tests were carried out to further assess the condition of the timber elements, with particular attention given to Woodpecker and the Resistograph.

It is important to have a visual inspection in the assessment of old timber structures, with a correct identification of the species. This depends entirely on the experience of the specialist, his skills and the conditions of the site. Taking into account the complexity of the matter, the years required to train this specialist, and the few that exist capable of making an identification of the species in situ, the use of laboratory tests that confirm the species is recommended since they are not very invasive and ensure an accurate result, despite implying an increase in the budget of the technical assessment.

The Woodpecker and the Resistograph are instruments whose parameters are variously associated with the penetration length of the cross-section of the elements. The behaviour of the dispersion of the results with respect to the linear correlation suggests the use of another type of function whose curve better describes its trace, especially for the Resistograph, always accompanied by a data analysis that verifies the behaviour of the forecasts.

It is prudent to corroborate the analysis made on a larger sample and demonstrate the exact relationship between the density of the Woodpecker and the drilling resistance of the Resistograph to know the effectiveness of the combination of both tools in the estimation of the density of structural elements in wood. The debugging of the results of the Resistograph in the length of the cross-section, if it is carried out, must be done with caution, and its result should not be used as the only value for obtaining mechanical parameters through correlations.

REFERENCES

[1] Suirezs TM, Berger G. *Descripciones de las propiedades físicas y mecánicas de la madera*. Misiones: Universidad Nacional de Misiones; 2009. [Online]. Available from: https://editorial.unam.edu.ar/images/documentos*digitales/f5*978-950-579-154-5.pdf (Accessed Nov 28, 2024).

[2] Osuna-Sequera C, Llana DF, Esteban M, Arriaga F. Improving density estimation in large cross-section timber from existing structures optimizing the number of non-destructive measurements. *Constr Build Mater.* 2019 Jun;211:199–206. https://doi.org/10.1016/j.conbuildmat.2019.03.144

[3] Hasníková H, Kuklík P. Various non-destructive methods for investigation of timber members from a historical structure. *Wood Res.* 2014;59(3):411–20. [Online]. Available from: https://www.woodresearch.sk/wr/201403/04.pdf (Accessed May 23, 2025).

[4] UNI 11119:2004. *Beni culturali – Manufatti lignei – Strutture portanti degli edifici – Ispezione in situ per la diagnosi degli elementi in opera*. July 2004.

[5] UNE-EN 17121:2020. *Conservación del patrimonio cultural. Estructuras históricas de madera. Directrices para la evaluación in situ de estructuras portantes de madera*. March 2020. [Online]. Available from: https://tienda.aenor.com/norma-une-en-17121-2020-n0063444 (Accessed May 27, 2025).

[6] Riggio M, Forestieri A, Di Renzo F, et al. In situ assessment of structural timber using non-destructive techniques. *Mater Struct.* 2014 May;47(5):749–66. https://doi.org/10.1617/s11527-013-0093-6

[7] Faggiano B, Marzo A. A method for the determination of the timber density through the statistical assessment of ND transverse measurements aimed at in situ mechanical identification of existing timber structures. *Constr Build Mater.* 2015 Dec;101:1235–40. https://doi.org/10.1016/j.conbuildmat.2015.08.088

[8] Azzi Z, Al Sayegh H, Metwally O, Eissa M. Review of Nondestructive Testing (NDT) Techniques for Timber Structures. *Infrastructures.* 2025 Feb;10(2):28. https://doi.org/10.3390/infrastructures10020028.

[9] Arriaga F, Wang X, Íñiguez-González G, Llana DF, Esteban M, Niemz P. Mechanical Properties of Wood: A Review. *Forests.* 2023 Jun;14(6):1202. https://doi.org/10.3390/f14061202

[10] Ross RJ, Forest Products Laboratory. *Wood handbook: wood as an engineering material*. Madison (WI): U.S. Department of Agriculture, Forest Service, Forest Products Laboratory; 2010. https://doi.org/10.2737/fpl-gtr-190

[11] Bartolucci B, De Rosa A, Bertolin C, Berto F, Penta F, Siani AM. Mechanical properties of the most common European woods: A literature review. *IGF-ESIS.* 2020;54:18. https://doi.org/10.3221/IGF-ESIS.54.18.

[12] de Oliveira Feio AJ. *Inspection and Diagnosis of Historical Timber Structures: NDT Correlations and Structural Behaviour* [PhD thesis]. Braga: Universidade do Minho; 2005. [Online]. Available from: https://repositorium.sdum.uminho.pt/bitstream/1822/14697/1/2006*PhD*ArturFeio.pdf (Accessed Jan 10, 2025).

[13] Giordano G, Ceccotti A, Uzielli L. *Tecnica delle costruzioni in legno: caratteristiche, qualificazione e normazione dei legnami da costruzione, progettazione e controllo delle strutture lignee tradizionali, applicazione dei moderni metodi di calcolo alle nuove tipologie costruttive*. 4th ed. Milano: Hoepli; 1993.

[14] Togni M. *Elasticidad y resistencia de vigas de madera antiguas de gran sección: estimación con metodologías no destructivas aplicables in situ*. 1995..

[15] Seco JIF-G, Díez R, Hermoso E, López CB, Casas JM. Caracterización de la madera de E. globulus para uso estructural. *Bol Inf CIDEU.* 2007;(4):91–100. [Online]. Available from: https://dialnet.unirioja.es/descarga/articulo/2723431.pdf (Accessed May 28, 2025).

[16] Ramón G, Basterra A, Casado M, Acuña L. Análisis de las técnicas de diagnóstico de madera estructural en edificios existentes y propuesta de integración orientada al proyecto. *Jorn Investig Constr.* [Online]. Available from: https://maderas.uva.es/files/2019/03/2005-Ram%C3%B3n-et-al-An%C3%A1lisis-de-TecDiag-orientada-al-proyecto-1-Torroja.pdf (Accessed May 28, 2025).

[17] Schimleck L, Evans R, Hector G, et al. Non-Destructive Evaluation Techniques and What They Tell Us about Wood Property Variation. *Forests.* 2019 Sep;10(9):728. https://doi.org/10.3390/f10090728.

[18] Cavalli A, Togni M. Monitoring of historical timber structures: state of the art and prospective. *J Civ Struct Health Monit.* 2015 Apr;5(2):107–13. https://doi.org/10.1007/s13349-014-0081-8.

[19] Feio AO, Machado JS, Lourenço PB. Compressive behavior and NDT correlations for chestnut wood (Castanea sativa Mill.). In: *Proceedings of the 4th International Seminar on Structural Analysis of Historical Constructions*; 2005. p. 369–75. [Online]. Available from: https://books.google.com/books?hl=it&lr=&id=FWC1DwAAQBAJ&oi=fnd&pg=PA369 (Accessed May 17, 2025).

[20] Borghese V, Santini S, Sguerri L. Sustainable assessment: a contribution to improve the reliability of NDT on old chestnut purlins. In: *World Conference on Timber Engineering (WCTE 2023)*; Oslo, Norway; 2023. p. 957–66. https://doi.org/10.52202/069179-0131.

[21] Vega A, Dieste A, Guaita M, Majada J, Baño V. Modelling of the mechanical properties of Castanea sativa Mill. structural timber by a combination of non-destructive variables and visual grading parameters. *Eur J Wood Wood Prod.* 2012 Nov;70(6):839–44. https://doi.org/10.1007/s00107-012-0626-7

[22] Maulud D, Abdulazeez AM. A review on linear regression comprehensive in machine learning. *J Appl Sci Technol Trends.* 2020 Dec;1(2):2. https://doi.org/10.38094/jastt1457.

[23] Braun MT, Oswald FL. Exploratory regression analysis: a tool for selecting models and determining predictor importance. *Behav Res Methods.* 2011 Jun;43(2):331–39. https://doi.org/10.3758/s13428-010-0046-8.

[24] Santini S, Baggio C, Sguerri L. Sustainable interventions: conservation of old timber roof of Michelangelo's Cloister in Diocletian's Baths. *Int J Archit Herit.* 2023;17(3):500–17. https://doi.org/10.1080/15583058.2021.1938747.

[25] UNI 11204:2007. *Beni culturali – Manufatti lignei – Determinación de la humedad*. 2007. [Online]. Available from: https://store.uni.com/uni-11204-2007 (Accessed May 22, 2025).

[26] Brunetti M, Aminti G, Vicario M, Nocetti M. Density estimation by drilling resistance technique to determine the dynamic modulus of elasticity of wooden members in historic structures. *Forests.* 2023 Jun;14(6):1107. [Online]. Available from: https://www.mdpi.com/1999-4907/14/6/1107 (Accessed Apr 28, 2025).

INVESTIGATION OF ADHESIVE BONDLINE HEALTH IN CLT PANEL USING NDT AND SDT TECHNIQUE

Václav SEBERA[1], Luděk PRAUS[1], Jan ZLÁMAL[1], Patrik NOP[1] and Mojtaba V. HASSAN[1]

[1] Department of Wood Science and Technology, Faculty of Forestry and Wood Technology, Mendel University in Brno, Zemědělská 3, 613 00, Brno, Czech Republic

ABSTRACT

Timber structures made of cross-laminated timber (CLT) have become more frequent in Europe over the last 30 years. The CLT panel is held together by an adhesive bond that may be impaired by production or degraded by mechanical, environmental and biotic factors that intensify their effects in time. Therefore, it is necessary to know whether a debonded adhesive bondline occurs in the construction. The paper aims at defectoscopic analysis of CLT panels of spruce and beech with designed imperfections in adhesive bonding with the help of non-destructive and semi-destructive techniques (NDT and SDT). The panels were examined using acoustic wave propagation across the panel using both standard point-to-point and tomographic approaches, and using resistance microdrilling. The results show that an impaired bondline can be easily detected using ultrasound techniques such as time of flight or modified acoustic tomography. However, resisting microdrilling did not prove to be an appropriate tool to locate the impaired bondline.

KEYWORDS: cross-laminated timber, acoustic wave, speed of sound, resistance microdrilling, adhesive bondline, imperfection

INTRODUCTION

The damage to the bondline between layers in CLT creates a cavity in its mass, preventing the ultrasound wave from propagating through it in its ideal path. The use of a dry two-probe instrument to detect cavities in timber has been proven effective for a long time [1]. Shortly after, this technique was applied to the detection of defects in bondlines of GLT beams [2]. The authors successfully detected impaired thick glue lines (1.5 mm), but for thin ones (~0.1 mm), they found that ToF significantly increased, even despite so-called kissing bonds that may occur even without adhesive. Using a two-probe system and analysis of the ultrasound signal going through a historically glued timber beam was demonstrated too [3]. The authors found that the contact system can capture and roughly locate the delamination. The application of the ultrasonic technique in an investigation of impaired glue lines in CLT was given in [4]. The authors found that a drop in sound velocity due to imperfection is greater than the one caused by knots and resin pockets, and that imperfection may be located with high accuracy. The usage of ultrasonic testing to assess the stiffness of CLT panels made of wood at various ages and conditions was shown recently [5]. Their work showed that when wood of lower quality is present in a CLT panel, the ultrasonic technique may reveal it well, even though it overestimates the values compared to those obtained by other vibrational techniques, such as frequency-resonance.

METHODOLOGY

Tested specimens consisted of 10 cross-laminated timber (CLT) panels, 5 of which were made of Norway spruce (*Picea abies*) and five were made of European beech (*Fagus sylvatica*), all with about 10% of moisture content. All CLT panels had three layers of the same thickness (~ 27 mm), so the total size was 800 x 800 x 82 mm^3. Within both groups of CLT panels, each panel was different in terms of its gluing, following gluing scenarios were produced: A1 - CLT panel was fully glued, i.e. side- and edgewise; A2 - CLT panel was glued only between layers (boards main sides), but edges were not glued; B - CLT panel was glued only between layers and, at the same time, an imperfection of 10% of total panel area was introduced in the center of the panel between top and middle layer; C - CLT panel was glued only between layers and, at the same time, an imperfection of 40% of total panel area was introduced in the center of the panel between top and middle layer; D - CLT panel was glued only between layers and, at the same time, an imperfection of 40% of total panel area was introduced at the side of the panel between top and middle layer (see Figure 1left). The polyurethane (PUR) glue was used for all CLT panels; the manufacturing pressure was 0.8 MPa.

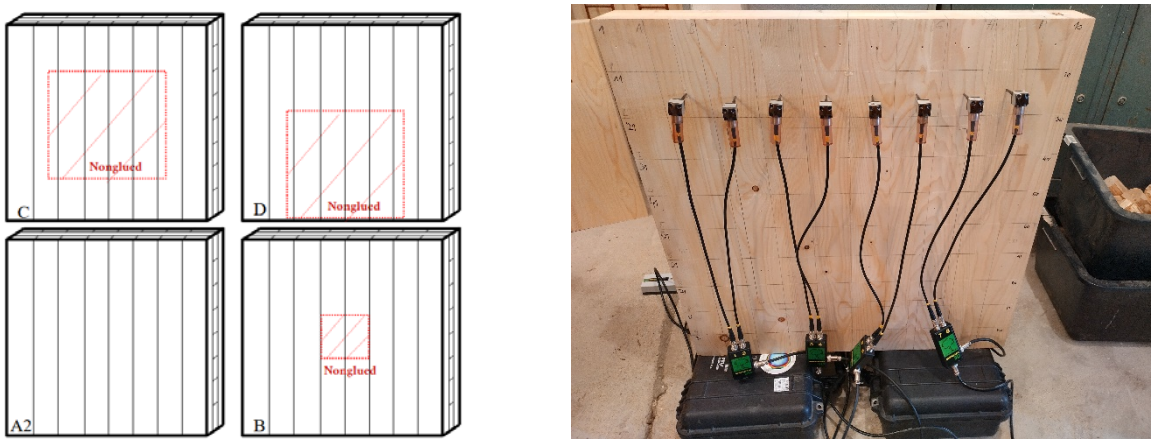

Figure 1. Manufactured scenarios of CLT panels (left), measurement of CLT panel using acoustic tomography

The panels were divided into 100 squares (10x10), and each square was examined using a time-of-flight device (Fakopp Enterprise, Hungary) and an acoustic tomograph (ArborSonic 3D Acoustic Tomograph, Hungary) having 16 probes. Each measured square was measured 5 times using both devices, so the mean value of the travel time of the ultrasound signal could be obtained. The mean values were then processed into heatmaps and evaluated by ANOVA.

RESULTS

Results obtained using the Fakopp ToF technique are displayed in Figure 2 as a heatmap for both spruce and beech CLT panels. It can be seen that the designed imperfection in bonding is visible as yellow spots within the panel structure. The imperfection of 10% in the panel centre is difficult to distinguish, but for imperfections of 40% panel size, it is quite easy. There are also spots showing higher ToF due to the higher quality of wood (stripes in spruce CLT panel with 10% imperfection in the centre). The statistical analysis confirmed that the ToFs between locations of glued and impaired bondlines differ at a level of significance of 0.05. The microdrilling technique proved not to be an appropriate tool for detecting delamination in the CLT panel's lamellae, as it was unable to determine the drop in microdrilling due to the presence of a cavity. The microdrilling data of the designed cavities were obscured by the variability of data provided by the material (tree rings, etc.).

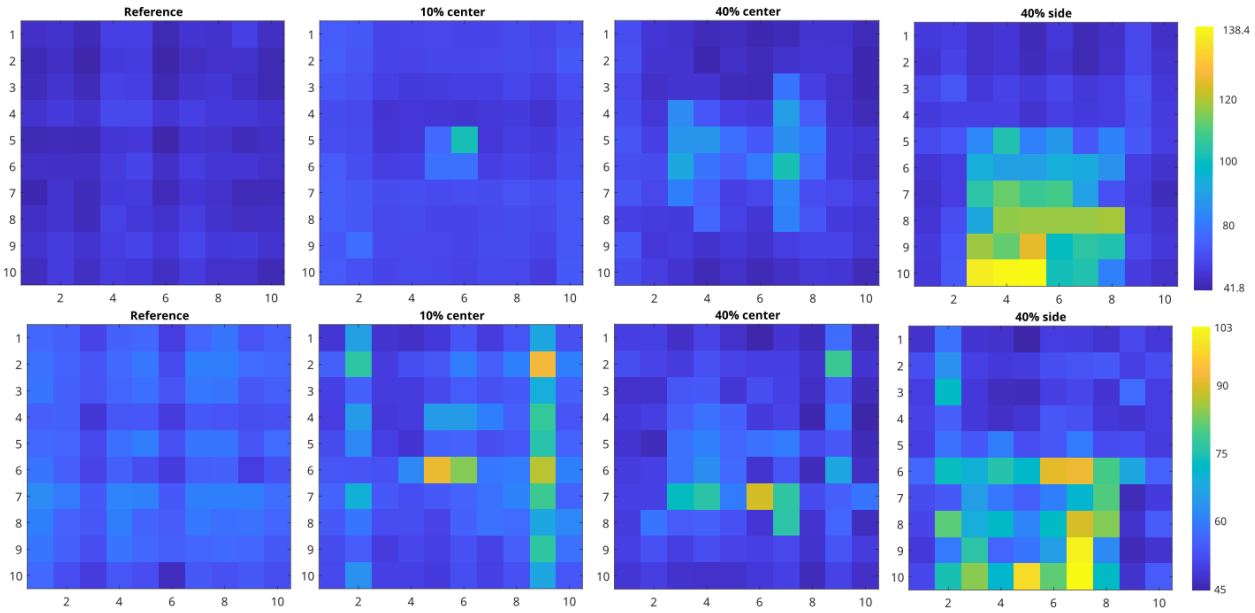

Figure 2. Time of flight (μs) of ultrasound signal in spruce CLT (bottom) row and beech CLT panels (top row). The yellow colour denotes a longer time of ultrasound flight - it matches the developed imperfections.

CONCLUSION

The work brings the following conclusions: a) acoustic techniques utilising ToF of ultrasound can be used to detect impaired adhesive bondlines in CLT with statistical relevance; b) resistance microdrilling has limited capacity in the detection of impaired adhesive bondlines.

ACKNOWLEDGEMENT

The work was supported by the project "Improvement and diagnostics of adhesive bondline used in multi-story timber buildings" (LUC23065) funded by the Ministry of Education, Youth and Sports of the Czech Republic.

REFERENCES

[1] Hasenstab, A., M. Krause, B. Hillemeier, and C. Rieck. 2006. "Ultraschallecho-Messungen an Holz." Holz als Roh- und Werkstoff 64 (6): 475–81. https://doi.org/10.1007/s00107-006-0124-x.

[2] Aicher, Simon, and Gerhard Dill-Langer. n.d. "Non-Destructive Detection of Glue Line Defects in Glued Laminated Timber."

[3] Neuenschwander, Jürg, Sergio J. Sanabria, Philipp Schuetz, Robert Widmann, and Mareike Vogel. 2013. "Delamination Detection in a 90-Year-Old Glulam Block with Scanning Dry Point-Contact Ultrasound." Hfsg 67 (8): 949–57. https://doi.org/10.1515/hf-2012-0202.

[4] Concu, Giovanna, Massimo Fragiacomo, Nicoletta Trulli, and Monica Valdès. 2017. "NON-DESTRUCTIVE ASSESSMENT OF GLUING IN CROSS-LAMINATED TIMBER PANELS." In , 559–69. Bristol, UK. https://doi.org/10.2495/SDP170491.

[5] Zhang, Lu, Alan Tiemann, Tonghao Zhang, Tom Gauthier, Kevin Hsu, Mustafa Mahamid, P. K. Moniruzzaman, and Didem Ozevin. 2021. "Nondestructive Assessment of Cross-Laminated Timber Using Non-Contact Transverse Vibration and Ultrasonic Testing." European Journal of Wood and Wood Products 79 (2): 335–47. https://doi.org/10.1007/s00107-020-01644-4.

MULTISENSOR SHM OF A WOODEN CANOPY WITH MECHANICALLY CROSS-LAMINATED ROOF STRUCTURE

Sadra SHAHSAVAR[1], Ine KNOOPS[1], Jose Gouveia HENRIQUES[1], Bram VANDOREN[1] and Eline VEREECKEN[1]

[1]UHasselt, Construction Engineering Research Group, Agoralaan, 3590 Diepenbeek, Belgium

ABSTRACT

With the rising interest in circularity, there is an increased focus on the life-cycle assessment of structures. The monitoring of structures makes an important contribution herein because it enables early damage detection. To gain insight into the information that can be retrieved from continuous monitoring of a timber structure, at the ACB^2 lab of Hasselt University, a wooden canopy has been equipped with different types of sensors, providing continuous monitoring information. This paper will discuss the sensor readings and information that can be extracted from these readings, such as relationships between sensor data and sensor locations.

KEYWORDS: Structural Health Monitoring, Statistical Data Analysis, Wooden Canopy

INTRODUCTION

Structural Health Monitoring (SHM) is gaining increasing interest, also for timber structures [1], [2], [3]. Data obtained from SHM systems can help in improving the understanding of the structural behaviour of the monitored structure, and can be used to detect defects or possible damage. Measurements often applied to timber structures are those tracking the moisture content of the wood, since moisture has an important influence on fungal decay and hence on the service life of these structures [4].
To investigate the benefits of SHM applied to timber structures and the knowledge that can be gained from the obtained data, a wooden canopy outside the ACB^2 laboratory of the Construction Engineering Research Group of Hasselt University has been equipped with different sensors to monitor its behaviour over time. The (preliminary) results of this monitoring campaign will be discussed in this paper.

INVESTIGATED STRUCTURE AND SHM SYSTEM

In this research, an outdoor wooden canopy structure is investigated (Figure 1 (a)). This canopy structure is a prototype for a much larger structure to be built as a covering for bus stops along the new public transport line connecting the city centres of Hasselt and Maasmechelen (Belgium). The composite roof of this structure is made of four layers of timber beams (3.8 cm in height), arranged in a waffle-like structure, with the beams mechanically connected to each other at each crossing. A cross-section of the roof structure is visualised in Figure 1 (b). The roof is covered with a ply sheathing layer and a bitumen finishing layer, and supported by four timber columns, connected to the roof by a ball joint.

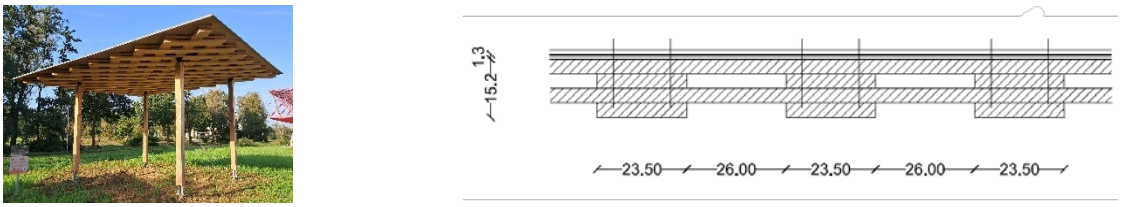

a) Global view *b) Cross-section of the roof (dimensions in cm)*

Figure 1. The investigated wooden canopy structure

The canopy is equipped with different sensors, according to the layout visualised in 2 and 3. Here, the sensors indicated with "T" are Dwyer RHP sensors, which measure the temperature and relative humidity of the air. T1 is located on top of the roof structure, and T2 is located under the roof. The sensors listed with "H" are Evikon E2353 sensors and measure the moisture content of the wood based on conductivity measurements with screw electrodes with pins of 15 mm length for the roof and 25 mm length for the columns. The measurement range is from 7 to 20% with a resolution of 0.01% and an accuracy of +-1%. For the roof, the sensors are located in the lowest layer of the roof structure. Only H2 has been positioned in another layer, i.e. the lower side of the ply sheathing. This additional sensor has been placed in a location that has a priori been identified to be contaminated with mould (see Figure 4). Due to inappropriate detailing or execution, at this point in the structure, there is local saturation with water, resulting in visible fungal decay. Furthermore, the dominant side for driving rain is south-west, meaning column C2 is most exposed to this driving rain and a priori column C3 is assumed to be less exposed. Hence, it is chosen to equip these two columns with humidity sensors.

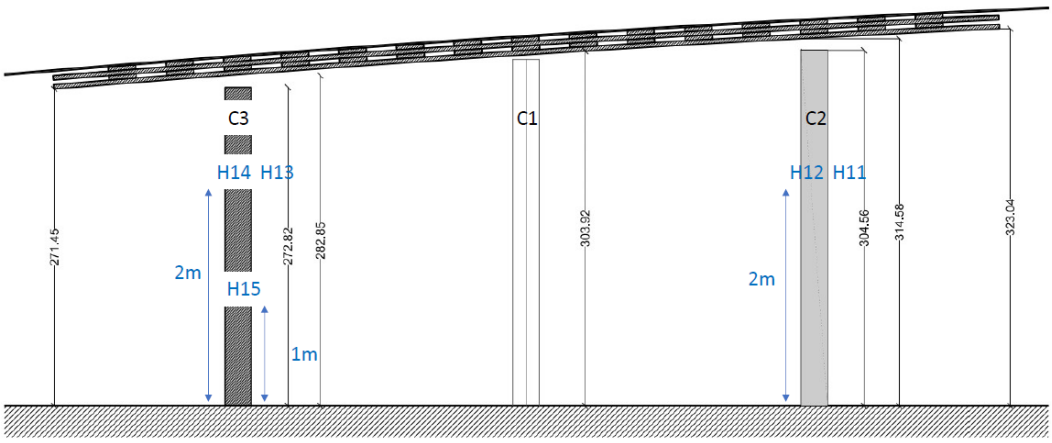

Figure 2. Sensor layout of the canopy: sensor locations on the columns

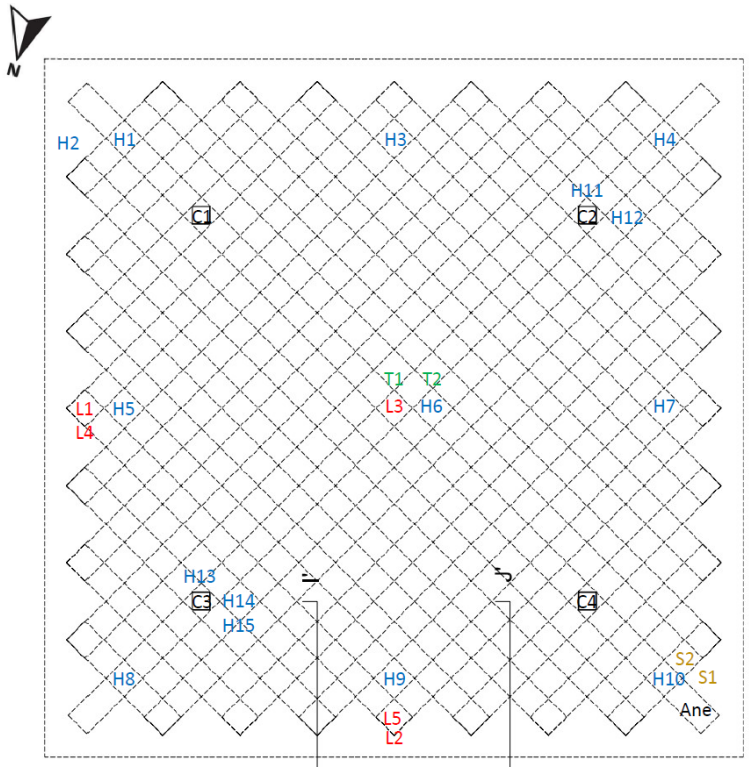

Figure 3. Sensor layout of the canopy: sensor locations on the roof

Sensors indicated with an "L" are lasers of the type Baumer OM30-P0550.HV.AUN, measuring the deformations. They have a measuring range of 500 mm and a linearity error of +-1.25 mm. These sensors measure the deformations at the lowest layer of the roof structure. L4 and L5 measure horizontal deformations, whereas L1 to L3 measure vertical deformations. Sensors indicated with an "S" are VELEK OFTF-NITK sensors and measure the surface temperature of the structure (one above and one below the roof). "Ane" indicates an anemometer (Reichelt Windgeber PCE-WS V), measuring the wind speed (on top of the roof). The latter anemometer and surface temperature sensors were installed more recently than the others. At the moment of writing this paper (March 2025), the data from the anemometer is not available yet. The data from the surface temperature sensors are still rather limited in time and will be included in future analysis.

Figure 4. Sensors H1 (in the lower timber beam) and H2 (in the ply sheathing), with H2 located in visible mould

SHM RESULTS

As indicated in Figure 3, the vertical deformations are measured along three points in the structure. These deformations are visualised in Figure 5. Here, it can be seen that the overall change in deformation in the middle of the roof (L3) is generally higher than at the sides of the roof (L1 and L2). The deformations of L1 are also closely aligned with those of L2. In all deformation measurements, clear fluctuations in the deformations are also visible, following daily temperature/humidity cycles.

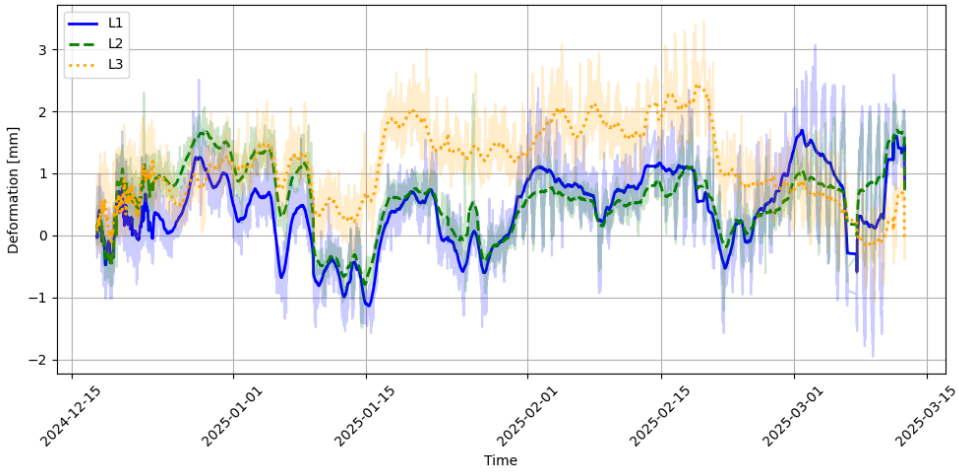

Figure 5. Measured vertical deformations of the roof. The dark lines represent the 1-day moving average.

The measured horizontal deformations are visualised in Figure 6. Again, daily fluctuations and seasonal trends can be observed in these data. In general, both sensors show the same trend, but in opposite directions. Nevertheless, the small-scale fluctuations are more minor for L5 than for L4, indicating that L4 might be more susceptible to changes in temperature or relative humidity of the environment.

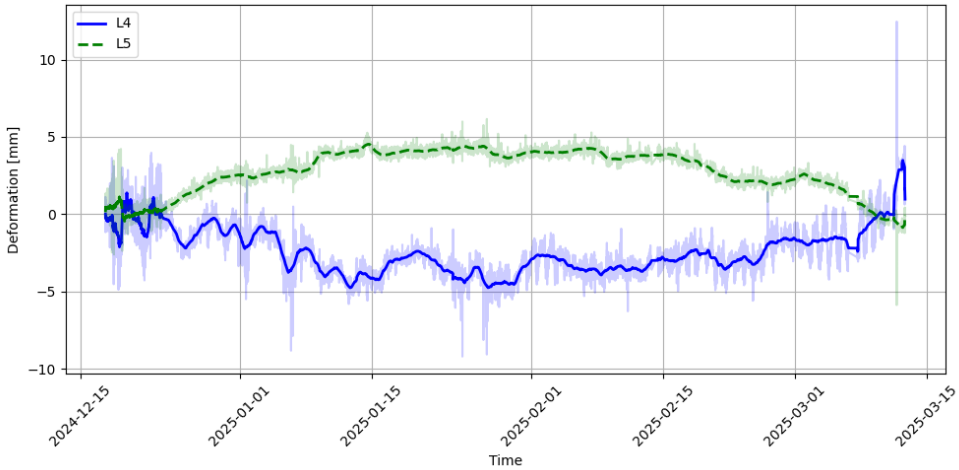

Figure 6. Measured horizontal deformations. The dark lines represent the 1-day moving average.

The moisture content on the roof has been measured at 10 locations. These results are visualised in Figure 7. Here, it can be seen that for H2, which has been placed in the mould, the moisture content remains constant around 20% (the upper limit of the sensor). For the other humidity sensors, it can be seen that these sometimes also reach the 20% limit, linked to very wet outdoor conditions (snow/rain). In general, with spring approaching at the time of analysing these data (March 2025), the sensors also indicate the drying of the structure, with local fluctuations related to daily temperature changes. The relationship between the outdoor environment and the moisture content of the timber is also visualised

in Figure 8 for sensor H6. Here it can be seen that, indeed, lower relative humidity (RH) results in lower moisture contents in the timber, whereas higher RH, together with lower temperatures, results in higher moisture content in the timber. Furthermore, it could be observed that the moisture content of 20% is only reached for temperatures between -3 and +12°C. This observation could be beneficial, since according to [4], favourable conditions for fungal development are temperatures between 25 and 32°C and moisture contents of 20% and higher. Nevertheless, it should be noted that these observations are based solely on measurements taken in winter and the early spring. Hence, the very high temperatures of 25°C and higher have not been reached yet.

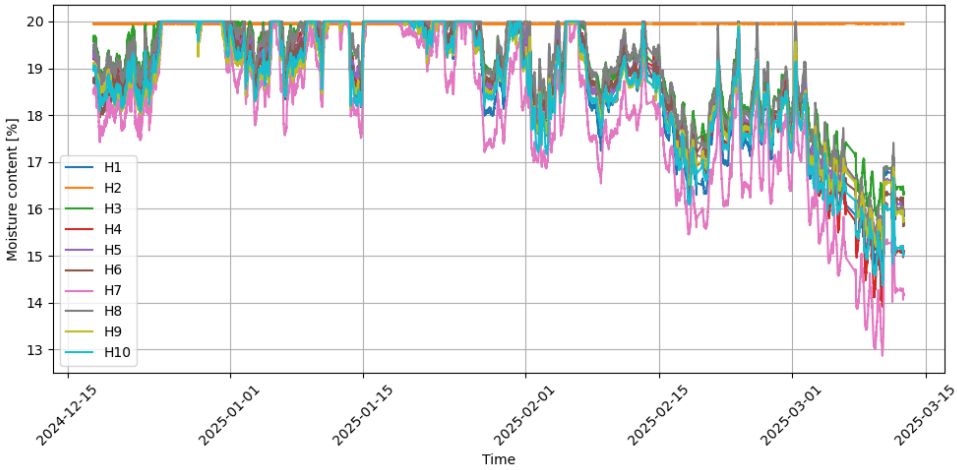

Figure 7. Moisture content at the roof

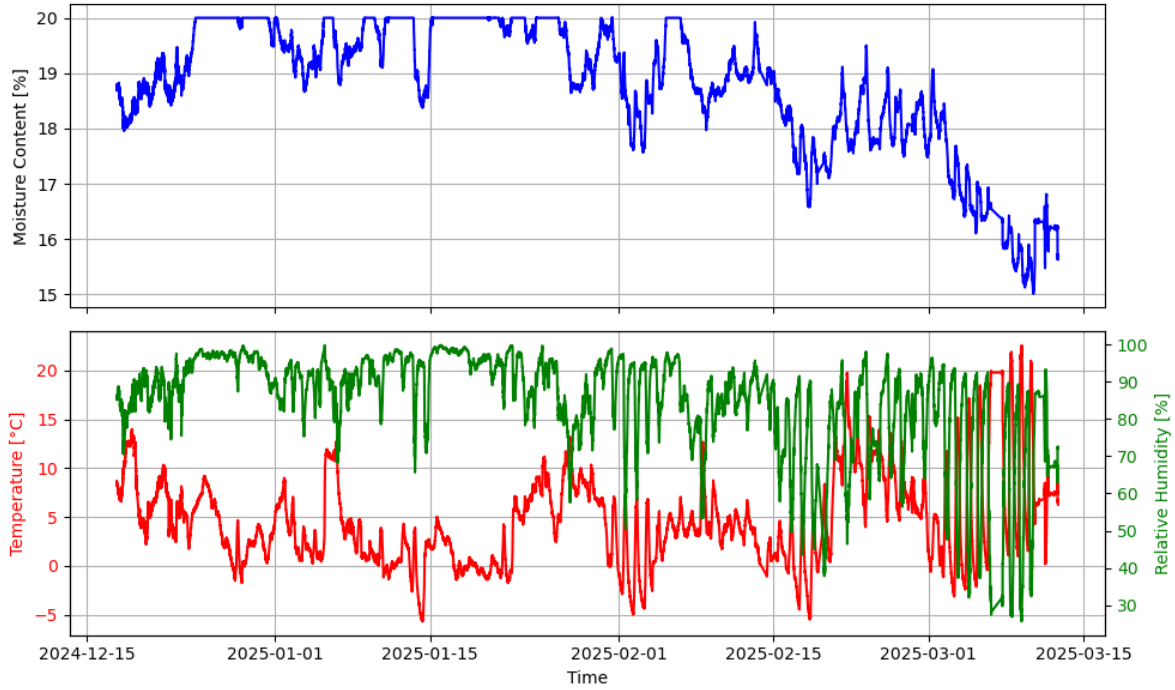

Figure 8. Moisture content at the roof for sensor H6, together with outdoor temperature and relative humidity measured with sensor T2

In Figure 9, the moisture content (MC) measurements of the columns are also provided. Here, it is evident that column C2, being most exposed to wind and direct rain, dries significantly more than column C3, which is better protected against environmental influences. In column C3, the upper sensors indicated moisture contents of 20% and only started drying very recently, whereas sensor H15, i.e. the lowest sensor, has been indicating drying and hence lower MC a few weeks earlier. These unexpected

high MCs, especially compared to column C2, indicated that there would be local leakages in the roof close to this column. These were not visible at the moment of sensor installation, but could be observed at later stages, after looking for signs of leakage, since the SHM results indicated these high MCs. Hence, the SHM system on this canopy, serving as a prototype for a much larger structure, points out critical points in the design, such as the roof/column connection being prone to leakage.

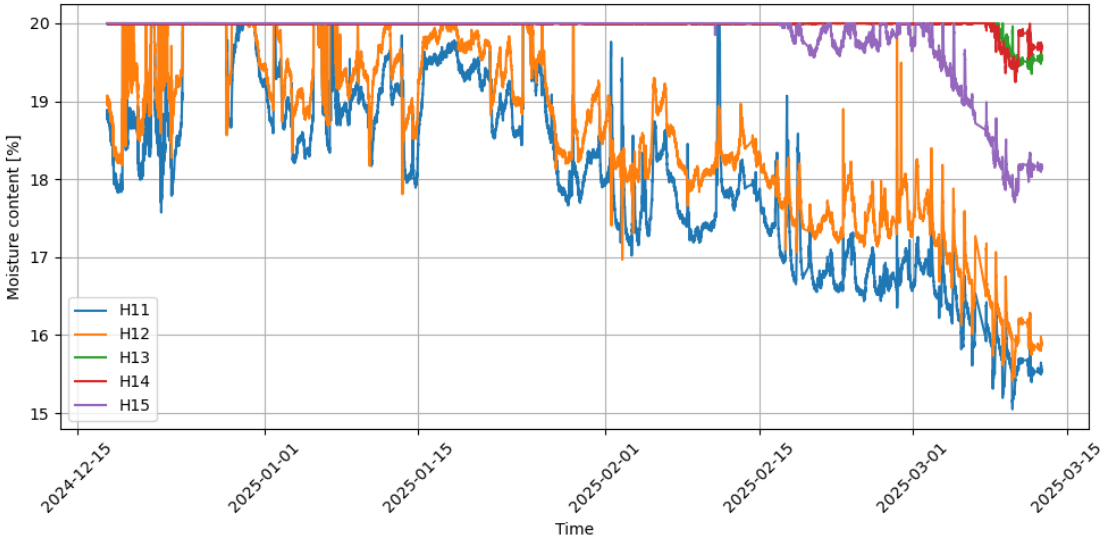

Figure 9. Moisture content in the columns

DISCUSSION OF THE RESULTS

An investigation is conducted to determine the extent to which a relationship exists between the moisture content and deformation measurements of the canopy and environmental conditions, such as temperature and relative humidity. In Figure 10 (a), the vertical deformations of the roof are visualised as a function of the timber moisture content, measured at the exact location. Based on this data, no global trend can be observed. The R^2 values for a linear relationship between both variables range from 0.06 (for L2) to 0.11 (for L3). The relationship between deformations and relative humidity of the environment is given in Figure 10 (b). Here, it can be observed that a higher relative humidity of the environment generally leads to a higher deformation. Nevertheless, very low R^2 values for a linear relationship are also found, ranging from 0 (for L3) to 0.08 (for L2).

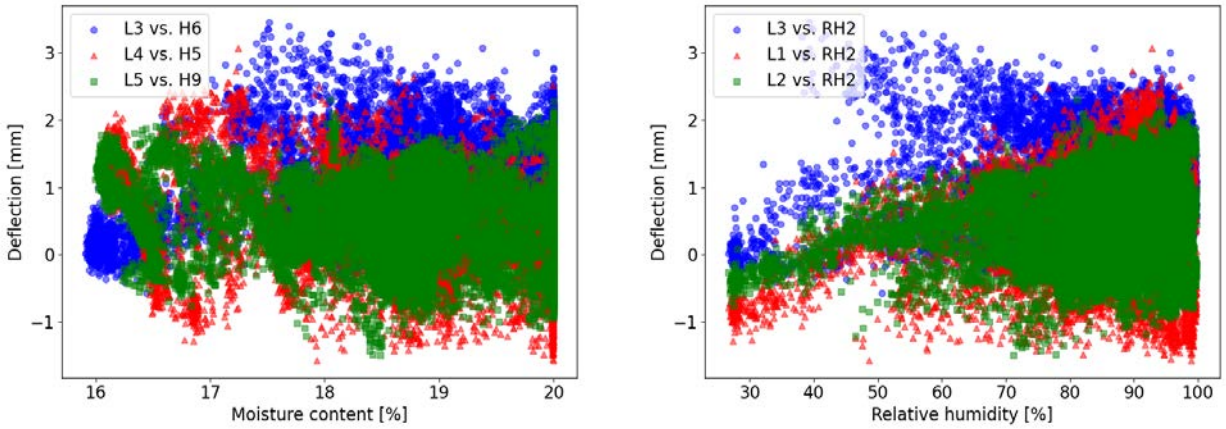

a) Roof deflection as a function of timber moisture content

b) Roof deflection as a function of relative humidity of the environment

Figure 10. Roof deflection as a function of (a) timber moisture content and (b) relative humidity of the environment

In Figure 11, the moisture content of the roof is provided as a function of the relative humidity of the environment. Here, it can be seen that there is indeed an increase in moisture content with an increase in humidity, but there is a lot of scatter in the results. The scatter could possibly be ascribed to temperature effects (see also Figure 8).

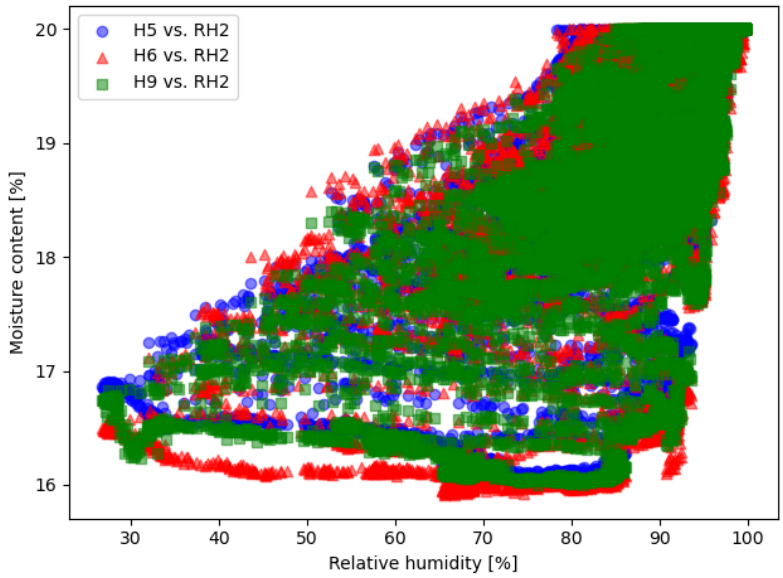

Figure 11. Moisture content of the roof as a function of the relative humidity of the environment

In Figure 12 (a), the moisture content of the timber is plotted as a function of the relative humidity and temperature of the environment. In Figure 12 (b), the same plot is visualised for the deformation of the roof as a function of the relative humidity and temperature of the environment. Even though trends can be observed in these 3D plots, no proper (simple) relationship can be fit to these curves. When applying polynomial (2nd degree), exponential, power-law or sigmoidal models, each provides an insufficient fit (with R^2 values up to 0.3 for the deformations and 0.5 for the moisture content).

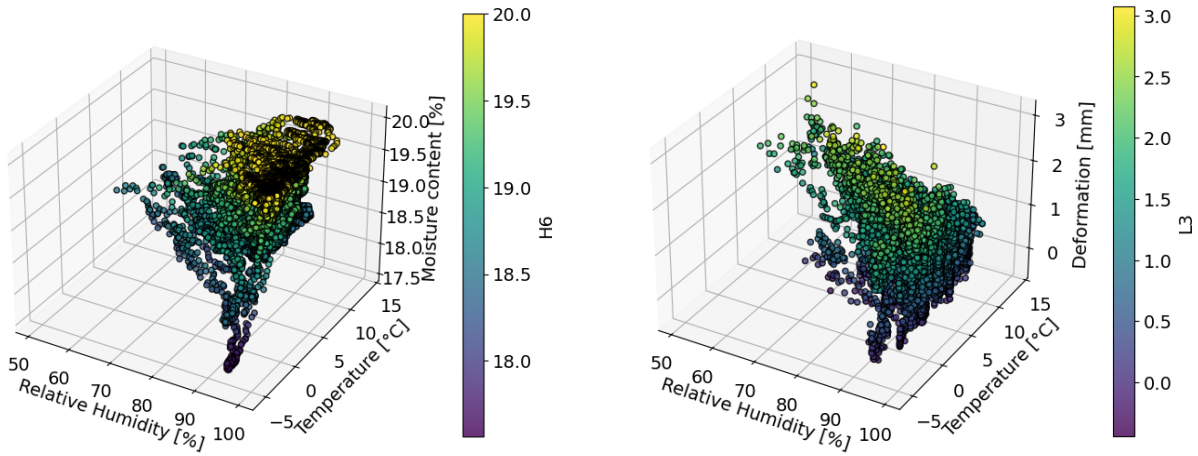

a) Moisture content as a function of RH and T

b) Vertical deflection as a function of RH and T

Figure 12. Influence of the relative humidity and temperature of the environment on (a) moisture and (b) vertical deflection of the roof

SPATIAL CORRELATION BETWEEN MEASUREMENTS

At the roof of the canopy, nine humidity sensors are placed (i.e. sensors H1 and H3 to H10, H2 is located in the ply sheathing), with approximately equal spacing in both directions. From these humidity measurements, for each point in time, the semivariogram (γ) of the results is evaluated, representing the spatial autocorrelation between the datapoints as a function of the lag τ, i.e. the spatial distance between datapoints. From all these experimental semivariograms, the mean experimental semivariogram and median experimental semivariogram are evaluated. To these semivariograms, a theoretical correlation model is fitted, for which the correlation length ρ_l and standard deviation σ are determined. Different fitting procedures are applied (curvefitting and maximum likelihood procedures, both with and without accounting for correlation [5]). In general, the curve-fitting procedures resulted in theoretical semivariograms that provided the closest fit with the (mean or median) experimental semivariogram. This fit is evaluated based on the least-squares differences between the experimental and theoretical semivariogram. Within this curve-fitting method, also different correlation models are accounted for, i.e. an exponential correlation model, a Gaussian correlation model and a linear correlation model [5]. Based on the evaluation of the least-square differences, the Gaussian model according to equation (1) provided the best fit.

$$\gamma(\tau) = \sigma^2 \left(1 - \exp\left(-\frac{|\tau|^2}{\rho_l^2}\right)\right) \tag{1}$$

The results were slightly different for a fit to the median semivariogram compared to a fit to the mean semivariogram. The standard deviation σ was about the same (0.37 vs. 0.39). The correlation length ρ_l ranges from 3.3 m (fit to the median) to 2.9 m (fit to the mean). The resulting plots are also provided in Figure 13 (a). It should be pointed out that the derived correlation lengths indicate that spatially, the different measurement points are not closely related to each other, since their spacing is larger than the correlation length. This is in contrast to the high correlation found between the different sensors when evaluating the correlation matrix of the whole dataset (see Figure 13 (b)). Nevertheless, this correlation matrix also contains the time-dependent correlation, which will be very high for all these sensors, due to the equal exposure conditions. It should also be noted that this evaluation of the correlation length is based on limited spatial data points (three in each orthogonal direction) and may only be valid for this specific structural configuration.

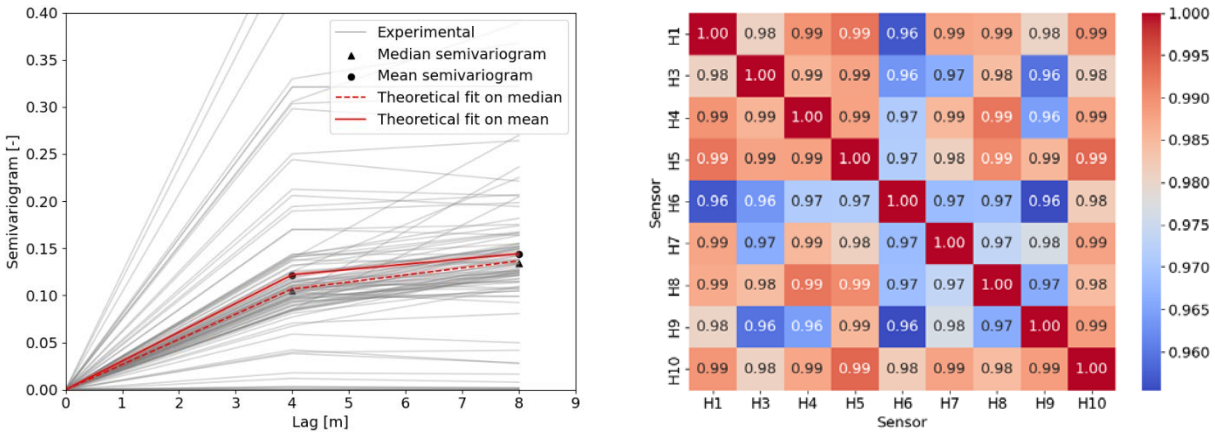

a) Experimental and fitted theoretical semivariograms *b) Correlation matrix for humidity sensors on the roof*

Figure 13. a) Experimental and fitted theoretical semivariograms (with the lag, the horizontal distance between data points); and (b) correlation matrix for humidity sensors on the roof

DAMAGE DETECTION

For detecting damage, the focus could be on two points, i.e. the risk of fungal decay by measuring both the moisture content of the timber and the temperature, and detecting exceptional deformations. In this section, the focus will be on the latter. Detecting excessive deformations based on the monitoring data can be a challenge, due to the fluctuations in the measurements following daily temperature and/or humidity cycles. Nevertheless, it has been indicated in the previous sections that no clear relationship between the environmental parameters and the humidity could be derived. Hence, in this section, the method based on robust principal component analysis (PCA) as described in [6] is applied. In this method, a PCA model describes the variation in data in terms of its so-called principal components, without requiring knowledge of the inputs that drive this variation. This method enables the evaluation of a time-dependent error term *e* that accounts for the misfit between model predictions and observed behaviour of the structure. Under the assumption of a sufficient amount of training data, a PCA model with multiple components will be more effective in modelling the natural variation in the input data compared to other methods, such as correction for environmental effects by linear regression, as such enabling more accurate damage detection [6].

In the graphs provided below, the misfit is provided for the measured deformations of the wooden canopy together with the [-3σ, +3σ] intervals, with σ the standard deviation of the misfit errors. In Figure 14, the results are provided accounting for all five deformation measurements (L1 to L5). Datapoints are alternately added to the training set and validation set (i.e. data points 1, 3, 5, 7... are training data and 2, 4, 6, 8... are validation data). As such, a broader range of environmental conditions is covered in the training data. In Figure 15, the distinction is made between the horizontal and vertical deformation measurements.

To visually detect outliers from graphs like those in Figures 5 and 6, thresholds are necessary to determine which deformations are too large to be considered unusual and trigger an automated warning based on the data. Nevertheless, defining these thresholds is not always that straightforward. The advantage of the methods described in this section is that they could trigger such automated warning events by detecting deformations outside the [-3σ, +3σ] intervals. For these intervals to be appropriate, it would be suggested to extend the training data to at least cover a whole year and hence all seasons. Based on the described analysis, for the horizontal deformations, clear peaks exceeding the [-3σ, +3σ] intervals could be observed. These resulted from placing a ladder against the canopy to place additional sensors.

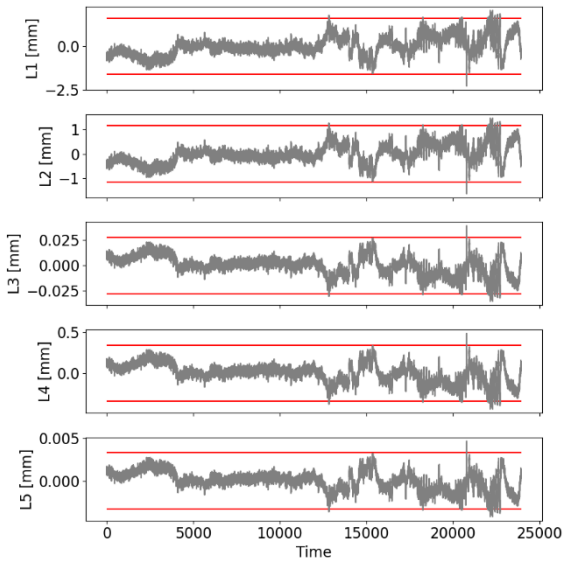

Figure 14. Evolution of the robust PC model misfit as a function of time for all deformation measurements.

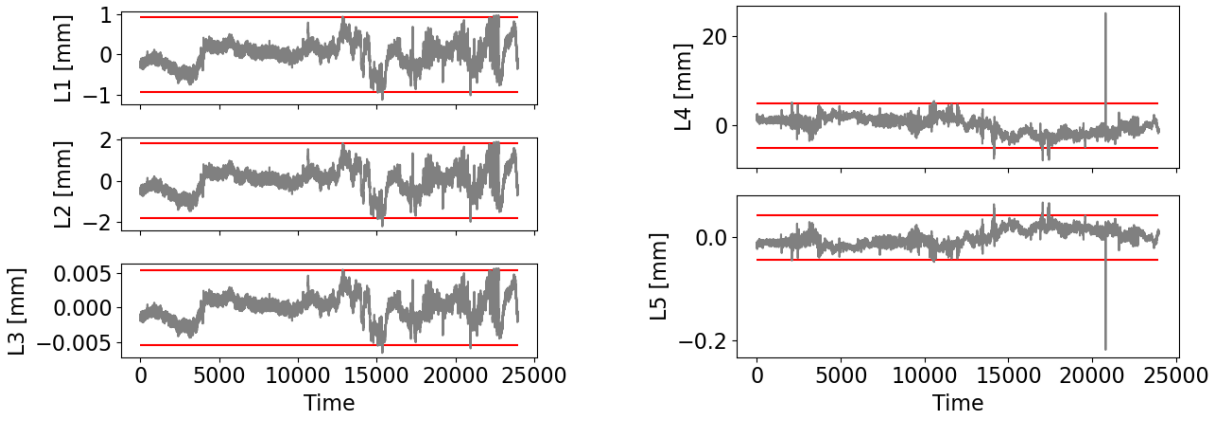

a) Vertical deformation measurements *b) Horizontal deformation measurements*

Figure 15. Evolution of the robust PC model misfit as a function of time for (a) vertical deformation measurements and (b) horizontal deformation measurements

CONCLUSIONS AND FURTHER RESEARCH

This paper describes the preliminary results of a monitoring campaign applied to an outdoor timber canopy. Moisture content and deformation of the structure were recorded, together with environmental parameters such as relative humidity and air temperature. The sensor readings could indicate when severe moisture conditions (20%) were reached. Local leakage in the structure could be detected by measuring unexpectedly high moisture contents at one of the columns of the structure.

When considering the moisture content of the roof, highly correlated data were generally obtained. Nevertheless, this high correlation was mostly ascribed to the same environmental exposure, as it was derived that the spatial correlation between the different sensors is rather low. Hence, for this specific structure, it could be concluded that sensor locations should be mostly decided on based on structural changes (i.e. locations prone to leakage) and environmental exposure. Locations with similar structural detailing and the same environmental exposure, i.e. the sensors in the roof, showed very similar moisture contents. Nevertheless, for the columns, being located under critical connection points prone to leakage, much larger deviations in moisture contents were found. Here, also variation over the height was observed, as the lower sides of the columns started drying earlier than the higher sides (closer to the leak).

Once sufficient additional sensor data is acquired, i.e. wind speed measurements and surface temperature measurements of the canopy structure, more relationships could be derived. For example, relations between horizontal deformations and wind speed (due to the torsional instability of the structure) could be derived. Furthermore, the relationships in this work could be refined further, replacing the temperature of the environment with the surface temperature. Also, when data will be available over a longer time span (one to multiple years), seasonal variations could be investigated, possibly enabling future predictions of the deformation behaviour, as for example done in [7].

In future research, a 3D model of the structure will be generated with FEM software. This model could then be used to simulate the deformations, while investigating the influence of the local (nominal) E-modulus of the wood and the joint stiffness, taking into account spatial variation of the moisture content and hence of the stiffness properties. Results from such a model could then be compared with the measurement results.

REFERENCES

[1] B. Franke, S. Franke, and A. Müller, "Case studies: long-term monitoring of timber bridges," *J Civ Struct Health Monit*, vol. 5, no. 2, pp. 195–202, Apr. 2015, doi: 10.1007/s13349-014-0093-4.

[2] C. Larsson, O. Abdeljaber, Å. Bolmsvik, and M. Dorn, "Long-term analysis of the environmental effects on the global dynamic properties of a hybrid timber-concrete building," *Eng Struct*, vol. 268, Oct. 2022, doi: 10.1016/j.engstruct.2022.114726.

[3] C. Brischke, A. O. Rapp, R. Bayerbach, N. Morsing, P. Fynholm, and C. R. Welzbacher, "Monitoring the 'material climate' of wood to predict the potential for decay: Results from in situ measurements on buildings," *Build Environ*, vol. 43, no. 10, pp. 1575–1582, Oct. 2008, doi: 10.1016/j.buildenv.2007.10.001.

[4] M. Verbist, L. Nunes, D. Jones, and J. M. Branco, "Service life design of timber structures," in *Long-term Performance and Durability of Masonry Structures: Degradation Mechanisms, Health Monitoring and Service Life Design*, Elsevier, 2018, pp. 311–336. doi: 10.1016/B978-0-08-102110-1.00011-X.

[5] W. Botte, E. Vereecken, and R. Caspeele, "Numerical and Experimental Investigation of a Correlation Model to Describe Spatial Variability of Concrete Properties," *ASCE ASME J Risk Uncertain Eng Syst A Civ Eng*, vol. 9, no. 4, Dec. 2023, doi: 10.1061/ajrua6.rueng-1100.

[6] K. Maes, L. Van Meerbeeck, E. P. B. Reynders, and G. Lombaert, "Validation of vibration-based structural health monitoring on retrofitted railway bridge KW51," *Mech Syst Signal Process*, vol. 165, Feb. 2022, doi: 10.1016/j.ymssp.2021.108380.

[7] C. Larsson, O. Abdeljaber, Å. Bolmsvik, and M. Dorn, "Long-term analysis of the environmental effects on the global dynamic properties of a hybrid timber-concrete building," *Eng Struct*, vol. 268, Oct. 2022, doi: 10.1016/j.engstruct.2022.114726.

EXPERIMENTAL ASSESSMENT OF DAMAGE IN TIMBER ELEMENTS USING A MODAL TESTING HAMMER

Sergio J. YANEZ[1], Elson HERMOSILLA[1], Roberto ESCOBAR[1] and Erick SAAVEDRA-FLORES[1]

[1] University of Santiago of Chile (USACH), Faculty of Engineering, Civil Engineering Department, Chile

ABSTRACT

The reliable assessment of structural integrity in timber members is crucial to ensure safety and extend service life. This work evaluates the sensitivity of Experimental Modal Analysis (EMA) to chemical damage in radiata pine beams subjected to controlled immersion in hydrogen peroxide (H_2O_2). The methodology employs free–free boundary conditions and impact hammer excitation with triaxial accelerometers to extract modal parameters. Intact and damaged states are compared through natural frequencies, mode shapes, and modal damping ratios, with frequency response functions processed in Dewesoft®. Reference values for density and static modules of elasticity are obtained via an E-Grader device, enabling direct comparison between dynamic and quasi-static stiffness estimations. The global severity of damage is quantified through a stiffness reduction factor κ, derived from the ratio of pre- and post-damage modal frequencies across the first six flexural modes. Results indicate a progressive reduction of natural frequencies (≈3–6% after 24 h, 6–10% after 48 h, and 10–15% after 72 h), corresponding to global stiffness losses between 5% and 28%. These findings confirm that frequency-based modal indicators provide robust and reproducible measures of stiffness degradation, even under chemically induced deterioration. The proposed procedure establishes a traceable, non-destructive framework for structural health monitoring of timber components, with potential applications in maintenance planning and performance-based design.

KEYWORDS: damage detection, timber elements, modal analysis, modal hammer.

INTRODUCTION

Timber is increasingly employed in civil engineering owing to its favourable strength-to-weight ratio, renewable origin, and low embodied carbon footprint [1,2]. However, its structural performance depends strongly on the integrity of the lignocellulosic microstructure and its sensitivity to environmental or chemical agents [3]. Degradation processes, whether due to moisture variation, biological attack, or chemical exposure, often manifest as reductions in stiffness, which compromise load-carrying capacity and alter dynamic response characteristics [4]. Vibration-based methods, widely applied to concrete and steel structures [5,6], have recently been adapted to timber, offering non-destructive evaluation (NDE) of stiffness loss and damage severity.

This study investigates the potential of modal testing with an impact hammer to quantify global stiffness degradation in timber beams subjected to chemical deterioration. Controlled immersion in 30% hydrogen peroxide was used to induce measurable stiffness loss, while pre- and post-exposure comparisons provided robust intra-sample controls. The analysis focuses on the correlation between static modules of elasticity and dynamic modal parameters.

METHODOLOGY

Twenty radiata pine beams (≈2 m length, rectangular cross-section) were immersed in 30% H_2O_2 solutions for 24 h, 48 h, and 72 h, corresponding to increasing damage levels. For each specimen, the static modulus of elasticity was determined via three-point bending using an E-Grader device. Modal testing was performed under free–free conditions using a suspended experimental setup, excitation with an instrumented modal hammer, and response measurement via a triaxial accelerometer. Five excitation points (0L, 0.25L, 0.50L, 0.75L, 1.00L) were selected to excite the first six flexural modes. Three valid impacts are performed at each point, and the results are averaged to increase coherence and improve the signal–to–noise ratio (SNR).

Frequency response functions (FRFs) were acquired and processed in a Dewesoft® data acquisition system, applying quality criteria such as coherence ($\gamma^2 \geq 0.90$) and modal stability analysis. Multi-degree-of-freedom identification was performed using the Least Squares Complex Frequency (LSCF) method, with AutoMAC and synthesis error employed for validation [5,7]. For each beam, natural frequencies from intact and damaged states were compared. A stiffness reduction factor κ was computed as:

$$\kappa_n = (f_n, post / f_n, pre)^2 \quad (1)$$

Where f_n, pre and $f_n, post$ are the nth natural frequencies before and after treatment. Global stiffness severity was then defined as $1 - \kappa$, averaged across validated modes. Group-level differences were assessed via analysis of variance, complemented by bootstrap confidence intervals.

RESULTS AND DISCUSSION

Initially, the modal testing hammer was calibrated by comparing the theoretical expressions for natural frequency with experimental results in intact timber samples. Table 1 shows the natural frequencies obtained from the first six modes of vibration. The theoretical expressions are based on the well-known Euler-Bernoulli theory for a beam. After the modal hammer is calibrated, chemical damage is induced. Experimental results showed systematic reductions in modal frequencies with increasing immersion time. After 24 h, frequency decreases ranged from 3–6%; after 48 h, 6–10%; and after 72 h, 10–15% or higher. These reductions corresponded to global stiffness losses of 5–10%, 10–18%, and 18–28%, respectively. Variations were mode-dependent, with higher-order flexural modes showing greater sensitivity to stiffness deterioration.

Table 1. Theoretical and experimental frequencies for intact timber samples.

Mode	Theoretical frequency (Hz)	Experimental frequency (Hz)	Error (%)
1	40.28	42.10	-4.5%
2	111.02	105.00	5.4%
3	217.67	210.40	3.3%
4	359.79	353.70	1.7%
5	537.49	529.70	1.4%
6	750.66	712.70	5.1%

Typical modal parameter extraction using a stabilisation diagram is shown in Figure 1. The algorithm identified six structural modes with their corresponding frequencies, damping ratios, and confidence levels. The stabilisation diagram (left) validates them, while the 3D indicator plot (right) highlights the

resonance peaks. The first mode occurs around 49 Hz, and higher modes appear roughly every 100–200 Hz. The damping ratios range from 0.3 to 0.8, which are relatively high, suggesting material damping or instrumental noise. Finally, the stabilisation diagram confirms that the selected frequencies are consistent.

The consistency between static modulus reductions and frequency-based stiffness factors validated the approach, although systematic differences were observed, likely due to rate-dependent effects and damping contributions. Importantly, the intra-sample design minimised the influence of timber heterogeneity, ensuring that changes could be attributed primarily to chemical degradation.

The proposed methodology offers several operational advantages: (i) non-destructive assessment under free–free conditions, reducing boundary-condition uncertainties, (ii) robust modal validation through coherence and AutoMAC, and (iii) integration of static and dynamic measures, enhancing traceability. Nonetheless, limitations include the global (non-localised) nature of stiffness estimation and the need for calibration when extrapolating to in-situ timber elements with different support conditions.

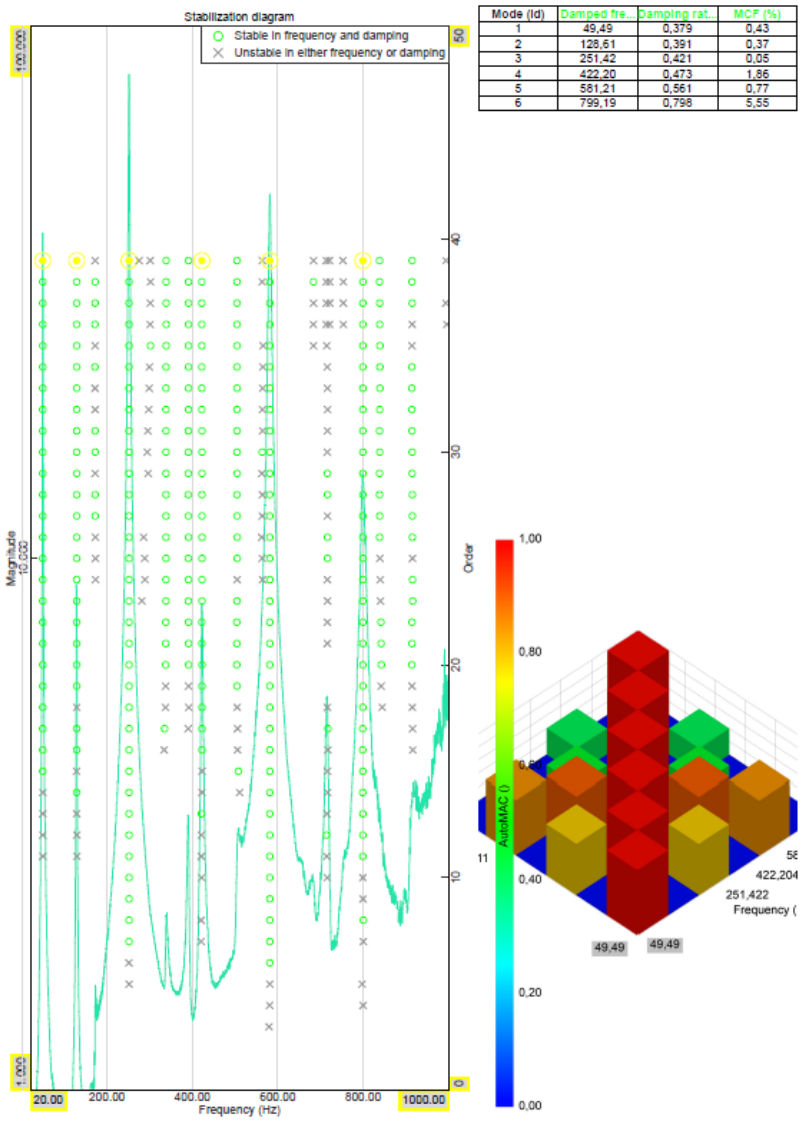

Figure 1. Typical modal parameter extraction using a stabilisation diagram

CONCLUSIONS

This study demonstrates that impact-hammer modal testing provides a reliable and sensitive means to quantify chemically induced stiffness degradation in timber beams. The stiffness reduction factor $1-\kappa$ emerges as a robust global indicator of structural integrity, consistent with static modulus estimations. By integrating non-destructive modal testing with reference quasi-static parameters, the approach establishes a reproducible framework for structural health monitoring of timber components. These results support the wider adoption of vibration-based methods for performance-based assessment, maintenance planning, and durability studies in timber engineering.

REFERENCES

[1] Liu, R., Yao, L., Gong, Y., & Wang, Z. (2025). Life Cycle Assessment with Carbon Footprint Analysis in Glulam Buildings: A Review. Buildings, 15(12), 2127.

[2] Tupenaite, L., Kanapeckiene, L., Naimaviciene, J., Kaklauskas, A., & Gecys, T. (2023). Timber construction as a solution to climate change: A systematic literature review. Buildings, 13(4), 976.

[3] Kumar, A., Jyske, T., & Petrič, M. (2021). Delignified wood from understanding the hierarchically aligned cellulosic structures to creating novel functional materials: a review. Advanced Sustainable Systems, 5(5), 2000251.

[4] Lanata, F. (2015). Monitoring the long-term behaviour of timber structures. Journal of Civil Structural Health Monitoring, 5(2), 167-182.

[5] Meruane, V., Yanez, S. J., Quinteros, L., & Saavedra Flores, E. I. (2022). Damage detection in steel–concrete composite structures by impact hammer modal testing and experimental validation. Sensors, 22(10), 3874.

[6] Cedeño-Rodríguez, M. D., Yanez, S. J., Saavedra-Flores, E. I., Guzmán, C. F., & Pina, J. C. (2025). Vibration-Based Damage Prediction in Composite Concrete–Steel Structures Using Finite Elements. Buildings, 15(2), 200.

[7] Kouroussis, G., Fekih, L. B., & Descamps, T. (2017). Assessment of timber element mechanical properties using experimental modal analysis. Construction and Building Materials, 134, 254-261.

CASE STUDIES - ASSESSMENT, STRENGTHENING, RECONSTRUCTION

THE USE OF TIMBER AS REINFORCEMENT OF MASONRY BUILDINGS AGAINST EARTHQUAKE - TRADITIONAL AND MODERN METHODS - CASE STUDIES FROM GREECE

Elefteria TSAKANIKA[1]

[1] National Technical University of Athens, School of Architecture, Greece

Invited lecture

ABSTRACT

This paper reviews the typology and structural role of historic horizontal timber reinforcement systems in masonry walls (tie beams, lacings, and ring beams). Case studies from Greece are presented, focusing on restoration methods in historic buildings, where timber is used to enhance the diaphragmatic action of roofs and floors. Techniques for connecting these diaphragms to the original timber tie-beam systems, and for anchoring tie beams to masonry walls and non-load-bearing timber elements (e.g., window frames and decorative features), are also discussed. These interventions, which utilise, preserve, and reinforce the original timber elements of both historic and contemporary masonry buildings, can enhance their seismic performance while providing reversible, lightweight, and cost-effective solutions. Moreover, these solutions can be effectively applied in the construction of new masonry structures.

KEYWORDS: horizontal timber reinforcements of masonry, timber lacings/tie-beams/ring-beams, timber diaphragms, timber earthquake-resistant reinforcements

INTRODUCTION

In many countries worldwide, the load-bearing systems of heritage buildings are predominantly composed of unreinforced masonry, combined with timber roofs and floors. Post-earthquake studies of masonry structures have demonstrated that these buildings are highly vulnerable (Figure 1), with the timber roof and floor systems playing a decisive role in their seismic response [1, 2]. In Greece, and across regions extending eastward as far as India, a continuous horizontal system of timber ties or lacings —a horizontal grid of longitudinal and transversal timbers embedded within the masonry —was historically employed to reinforce stone or adobe walls [1,3]. This system, acting as a structural "*belt*" at various heights (Figure 2), is regarded as the earliest timber-based seismic reinforcement technique for masonry buildings, with evidence of its continuous use from prehistoric times through the 20th century [3,4]. The floors and roofs were nailed onto these timber ties, enhancing the connection and cooperation between walls (*box-like behaviour*), reducing out-of-plane displacements, and in many cases preventing partial or total collapse [1,5,6].

During recent decades, however, the timber elements of historic structures in Greece—roofs, floors, timber-framed walls, and horizontal lacings—were often inadequately studied and, in many restoration projects, were removed and replaced with reinforced concrete slabs. Post-earthquake field surveys and documentation conducted over the last decades have confirmed significant structural failures in several of these interventions (e.g., hammering effects). Significant problems have also been observed where timber roofs and floors were connected to masonry walls using poorly constructed concrete ring beams

(oversized sections, insufficient anchorage to the masonry), as well as in cases where masonry walls were not reinforced with timber ties [6] (Figure 2).

Figure 1: Vrisa village in Mytilini, Greece. 2017 earthquake. Severe damage and partial collapses were observed in masonry buildings reinforced with concrete slabs and concrete tie-beams at roof level, and in masonry buildings without timber lacing [6].

In this paper, the historical horizontal timber reinforcing system of masonry walls is briefly discussed, with examples from Greece presented, focusing on restoration projects of historic buildings where timber is used to enhance the diaphragmatic action of timber roofs and floors (Figure 3). The original timber tie beam system (lacings, or ring beams) is reused to connect these diaphragms to the walls (Figures 4, 5, 6) or to timber non-load-bearing elements (e.g., window frames and decorative features) (Figure 7), in order to increase the earthquake resistance of masonry structures.

TIMBER TIE BEAMS (LACINGS / RING BEAMS) IN MASONRY

The timber ties, ring beams, or lacings—terms used in English to describe the horizontal timber reinforcement system of masonry—are referred to in modern Greek as *xylodesia*, meaning the tying of the building with wood. The timber ties, ring beams, or lacings—terms used in English to describe the horizontal timber reinforcement of masonry—are referred to in modern Greek as *xylodesia*, meaning the tying of the building with wood. Even during the ancient and Byzantine periods, this reinforcing system was known as *ιμάντωσις*, derived from the verb *ιμαίνω*, meaning "to tie" [3, 4, 6]. Since antiquity, this term has accurately described its primary structural function: connecting the walls at multiple levels like a continuous "*belt*," [1] which prevents the outward collapse of the walls and the subsequent failure of the roof and floors inside the building, one of the most common and hazardous failure modes of masonry buildings under seismic loading.

Figure 2: a) The typical horizontal timber reinforcement system of masonry [8]. The timber lacings are used at least at the level of the floor and the roof. They are also placed at the level of the lintel, the sill, and the middle height of the masonry piers between the openings. b), c), d), e) Masonry buildings in Greece (stone and adobe) reinforced with timber lacings. Special attention is given to tying the corners of the buildings, as well as the roof and floor structures, to the timber lacings. [4,5].

In addition to its primary structural function, the horizontal timber reinforcement embedded in masonry enhances both the seismic and overall performance of masonry buildings through several mechanisms: it increases the ductility as well as the shear and flexural capacity of the inherently brittle masonry, delays the initiation and propagation of cracks, and connects the outer and inner leaves of the masonry through the cross elements [4,5]. Furthermore, timber lacings that are well connected with the timber frames of openings (windows and doors) can significantly reinforce the masonry surrounding these vulnerable areas against seismic forces [7, 8, 12].

TIMBER AS EARTHQUAKE REINFORCEMENT OF MASONRY BUILDINGS - TRADITIONAL AND MODERN METHODS. CASE STUDIES FROM GREECE

The structural performance of a masonry building under lateral loads (earthquakes, ground movements etc.) is strongly influenced by the in-plane stiffness of the floors and roofs. Their seismic response can be significantly enhanced by improving their diaphragmatic action, particularly by establishing an effective connection between these diaphragms and the masonry walls.

This paper presents examples from Greece, concerning restoration projects of historic buildings reinforced against earthquake, using:

- Timber applied through various methods (planks and plywood), to improve the diaphragmatic action of existing or new timber roofs and floors (Figure 3) [8,9,10,11].

Figure 3: a) Benizelos mansion in Athens. Application of 20mm plywood over the ceiling, with both layers screwed onto the ceiling beams of the roof (horizontal plane) [8]. b) Kaloutsiani Mosque in Ioannina. Application of plywood over the interior visible timber planks. The inclined timber diaphragm, anchored to the masonry walls through timber-tie beams (red circles), was used to enhance the seismic resistance of the angular porch, especially against out-of-plane forces [9].

- Different techniques are used to connect the horizontal beams of the diaphragmatic timber roofs and floors to embedded masonry timber ties, utilising screws, steel plates, straps, etc. (Figure 4c) [8,9,11,12].
- Various methods to connect the timber ties to the masonry beneath, either more expensive (e.g., use of stainless steel or timber dowels) (Fig. 4c, 4d, 5a), or easy to apply (e.g., use of transversal timber elements embedded in the walls under the longitudinal ones, at floor and roof levels (Figure 5b) [8,9,11,12]. This anchorage method provides a low-cost alternative in situations where metal rods are unavailable. The use of cross timbers improves the connection between the two faces of three-leaf masonry and enhances the collaboration and cohesion of the timber grid with the surrounding masonry, functioning as a type of mechanical anchorage within the wall. Special care must be taken to establish the connection of these timber diaphragms with the walls that are parallel to the floor beams or with the gable walls of a two-pitched roof (Figure 6) [8,12].

- Different techniques are used to connect the timber tie-beams along the height of the masonry (Figure 4a) to the load-bearing timber-framed walls of the buildings, establishing their collaboration and ensuring a "*box behaviour*" of the building during seismic actions. (Figure 7) [8].
- Different techniques for connecting the timber lacings along the height of the masonry, to non-load-bearing timber elements of the building (window, door frames, decorative elements, non-load-bearing timber-framed walls, etc.). Their contribution to the overall behaviour of the building may be important in the event of a strong seismic event, serving as a second line of defence, which is not usually included in calculations (Figure 8) [7,12].

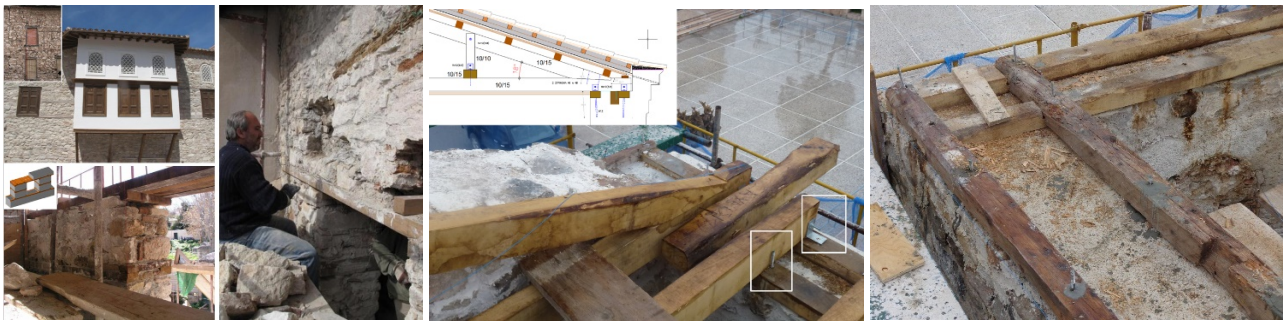

Figure 4: a), b) Benizelos mansion in Athens. Reconstruction of the timber lacing system along the height of the walls in areas that had been destroyed due to later interventions [8]. Bailos House, in Chalkis. c) The ceiling beams of the roof were connected to the timber lacings at the top of the walls, using steel angles or screws [11]. c), d) connection of the timber tie beams at the top of the masonry walls, accomplished using stainless steel rods of 12mm diameter every 80-100cm, fixed slightly inclined in the masonry with non-shrinkage mortar [11].

Figure 5: Hagi Mehmet Aga Mosque in Rhodes. a) Timber dowels (d=14mm) were used instead of steel dowels to connect the timber lacings to the masonry beneath, since steel dowels had often caused significant damage to the porous stones of Rhodes. Benizelos Mansion in Athens and the Turkish mansion in Rhodes [11]. b) In these cases, the usual cross timbers of the lacing system—normally placed above the longitudinal elements— were instead embedded within the masonry beneath the longitudinal timbers and connected to each other with screws (d = 8 mm) [8,12]. c) Timber floor beams screwed onto timber lacings anchored into masonry with stainless rods [11].

Figure 6: a) Kefallonia (2014), b) Mytilini (2017). Typical gable collapses caused by earthquakes. Bailos House in Chalkis. c), d) Timber lacings anchored with steel rods to the masonry are used to connect the gable to the roof inclined diaphragm, through the purlins that are screwed onto the timber tie beams [11].

The presented interventions and strengthening solutions were selected by the study groups [8,9,10,11,12] on a case-by-case basis, aiming for compatibility with the original structural system, minimum interventions, while reinforcing the buildings against earthquake through the use of lightweight, reversible, and low-cost timber diaphragms at the floor and roof levels. This strategy also involved utilising, restoring, or reconstructing the existing traditional timber lacing system. The same principles can also be applied in modern masonry construction practice.

Figure 7: Benizelos Mansion in Athens. Connection with screws of the last post of the load bearing timber-framed walls of the building to the tie beams along the height of the masonry walls, using carbon steel screws (system WT) [8].

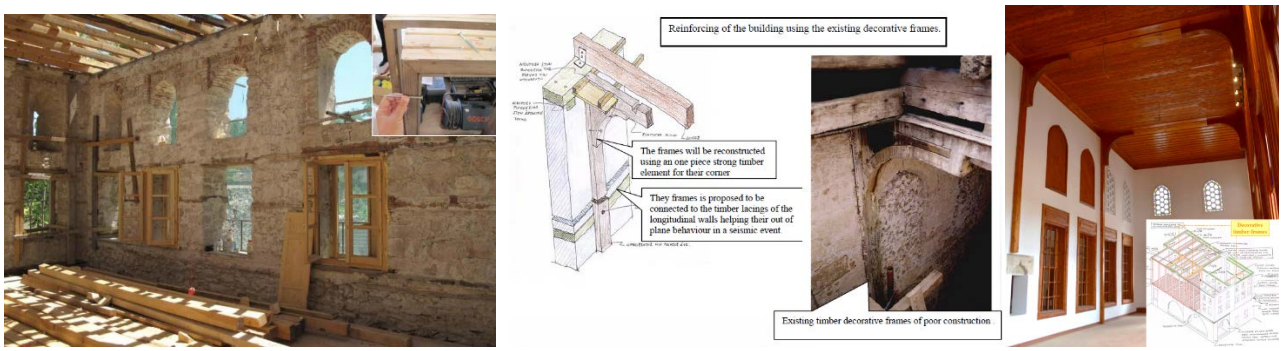

Figure 8: Benizelos Mansion in Athens. a) The connection of the window timber frames (their "sewing"), with several screws to the timber reinforcing system of the wall at the level of the lintel, the sill and at the middle height of the piers, provides additional confinement to the surrounding stone piers and consequently, increases the strength of the surrounding masonry wall [8]. Turkish Mansion in Rhodes. b), c), d) The decorative non-load bearing timber frames, through proper design and reinforcement, were used as additional strengthening systems of the masonry walls (out-of-plane action), for the seismic improvement of the building [12].

CONCLUSION

For heritage buildings, repair and/or reinforcement is preferred over total structural replacement with new elements of concrete, steel, or even timber. Each restoration solution has advantages and disadvantages in terms of conservation philosophy, architectural and aesthetic considerations, structural performance, safety, and technological or constructional quality. Economic factors, such as intervention cost and the availability of specialised personnel, can also influence the selection of the final method. The interventions and reinforcements presented in this paper offer reversible, lightweight, and cost-effective solutions for the structural and non-structural timber elements of masonry buildings, preserving and reinforcing the original structural system of existing masonry buildings, whether heritage or not. These solutions can also be effectively applied in the construction of new masonry buildings. Additional research is necessary to provide solid evidence for the inclusion of

both existing and new timber and masonry structures in building standards, focusing on the use of light timber diaphragms and the broader application of timber as a multifunctional reinforcement material.

REFERENCES

[1] Touliatos, P., 2005. The box framed entity and function of the structures. The importance of wood's role. In: Tampone, G. (Ed.), *Proceedings of the International Conference: Conservation of Historic Wooden Structures*, Florence, Italy, vol. 1, pp. 52–64.

[2] Keller, A., Parisi, M.A., Tsakanika, E., Mosoarca, M., 2020. Influence of historic roof structures on the seismic behavior of masonry structures. *Proceedings of the Institution of Civil Engineers – Structures and Buildings*, Themed Issue: Role of structural timber in the earthquake protection of masonry buildings.

[3] Tsakanika-Theohari, E., 2006. Ο δομικός ρόλος του ξύλου στην τοιχοποιία των ανακτορικού τύπου κτηρίων της Μινωικής Κρήτης [The structural role of wood in masonry of the palatial architecture of Minoan Crete]. PhD Dissertation, National Technical University of Athens, Greece.

[4] Tsakanika, E., 2017. Minoan structural systems. Anti-seismic characteristics. The role of timber. In: *Out of Rubble: Interdisciplinary Perspectives on Minoan Earthquakes*, AegIS-UCL-INCAL-CEMA, KU Leuven, Belgium, pp. 267–304.

[5] Touliatos, P., Vintzileou, E., Tsakanika, E., et al., 2005. Investigation of timber reinforced masonry. Research Program - National Technical University of Athens (NTUA)/Earthquake Protection and Planning Organization (EPPO), Athens (in Greek).

[6] Tsakanika, E., 2018. Timber-framed structures in Greece and their earthquake response. Timber frames reinforced by masonry or timber reinforcements of masonry? In: *Proceedings of International Conference: Anti-seismic Vernacular Heritage of Anatolia and Beyond*, ICOMOS Turkey, ICOMOS ISCARSAH Committees, 18–20 July 2018, Kastamonu, Turkey.

[7] Tsakanika, E., 2019. Load and non-load bearing timber-framed structures in Greece. Their aseismic role. In: *Proceedings of SHATIS 2019 - 5th International Conference on Structural Health Assessment of Timber Structures*, 25–27 September 2019, Guimarães, Portugal.

[8] Tsakanika-Theohari, E., Mouzakis, H., 2010. A post-Byzantine mansion in Athens. The restoration project of the timber structural elements. In: *Proceedings of the 11th World Conference on Timber Engineering (WCTE 2010)*, Trento, Italy.

[9] Psylla, N., Tsakanika, E., Mouzakis, H., Kouimtzioglou, T., 2020. Το Τζαμί της Καλούτσιανης στα Ιωάννινα. Δομική τεκμηρίωση και στατική μελέτη αποκατάστασης [The Kaloutsiani Mosque in Ioannina. Structural documentation and restoration design]. *Hellenic Society for Research and Promotion of Scientific Restoration of Monuments (ETEPAM).* (2022). *6th National Conference on Restoration, dedicated to the memory of Kalliopi Theocharidou, 13–16 October 2022,* Thessaloniki, Greece.

[10] Touliatos, P., Tsakanika, E., Tsouras, V., 2010. Μελέτη και κατασκευή νέας στέγης στο Τέμενος Γαζή Χασάν Πασά στην Κω [Design and construction of a new roof at the Gazi Hasan Pasha Mosque in Kos]. In: Stefanidou, A. (Ed.), *Αποκατάσταση των οθωμανικών μνημείων στην Ελλάδα [Restoration of Ottoman Monuments in Greece],* University Studio Press, Thessaloniki, pp. 251–266.

[11] Kourmadas Y., Tsakanika E., 2020. The Use of Timber in the Construction of the Bailo House. Themed Issue 'Venetian and Ottoman Heritage in the Aegean: The Bailo House in Chalcis, Greece'. N. D. Kontogiannis, S. S. Skartsis (eds.). «*Architectural Crosroads Studies in the History» Vol.8, Brepols Publishers n.v. Turnhout,* Belgium, 2020, pp. 157-167.
http://www.brepols.net/Pages/ShowProduct.aspx?prod_id=IS-9782503584096-1

[12] Tsakanika, E., 2005. Methodology concerning the restoration of historical buildings. Case studies: The Turkish Mansion and the Hagi Mehmet Aga Mosque in Rhodes. In: Tampone, G. (Ed.), *Proceedings of the International Conference: Conservation of Historic Wooden Structures*, Florence, Italy, vol. 2, pp. 194–203.

STRUCTURAL STRENGTHENING OF THE TIMBER ROOFS OF THE NATIONAL PALACE OF SINTRA, PORTUGAL

Tiago ILHARCO[1], Bruno QUELHAS[1], Alexandre COSTA[1], João CORTÊS[2] Jorge SOARES[1] and João DOUTEL[1]

[1]NCREP, Consultoria em Reabilitação do Edificado e Património, Porto, Portugal
[2]Parques de Sintra - Monte da Lua, S.A.

ABSTRACT

Right at the heart of the town's historical centre, the National Palace of Sintra stands as the only medieval royal palace left in Portugal, integrating a set of buildings of various architectural styles. The place is located in a rocky acropolis at the foot of Sintra's mountain range, within the Cultural Landscape of Sintra, classified as a World Heritage Site by UNESCO in 1995. The ensemble of volumes of its present configuration, whose origins date back to the early 13th century, is the result of successive building campaigns and modifications that were executed over the years.

Since 2012, the palace has been managed by Parques de Sintra – Monte da Lua, S.A. (PSML), a publicly funded company, responsible for managing the most important cultural values located within the Cultural Landscape of Sintra. Among those values in the National Palace of Sintra, together with the Park and National Palace of Pena, the National Palace of Queluz, and the Moorish Castle. The management of these cultural values, heterogeneous in their nature, represents a tremendous challenge. This responsibility requires a constant setting of priorities and a careful allocation of the available technical and financial resources. Thus, it is imperative to optimise planning and management tools, which are crucial for establishing long-term perspectives to guide the company's operations. To achieve that, PSML developed and implemented Management Plans for Built Heritage, a strategic tool focused on the monitoring, conservation and rehabilitation of built heritage. Within the assets under the care of PSML, the National Palace of Sintra was linked with significant intervention needs, essentially due to the poor state of conservation of the roofs, a segment which is considered of utmost priority in order to prevent heritage loss.

This paper describes the process adopted to define the structural intervention of the different timber roofs that compose the palace. The intervention had as its main objective the preservation of the existing structural elements through the implementation of strengthening and/or replacement measures. This process included the structural characterisation, the identification of existing structural damages and the structural analysis of each of the roofs.

The structural strengthening project, whenever possible, resorted to traditional materials and techniques in order to guarantee the preservation of the building's identity and, at the same time, the respect for the principles of reversibility, compatibility and reduced intrusiveness of the interventions. Following this logic, a series of actions common to all the structures and specific strengthening or replacement measures for each of the roofs were proposed. Whenever it was necessary to build a new structure, this was considered to be self-supporting and installed parallel to or above the existing structure.

KEYWORDS: assessment, timber, roof, strengthening, heritage

INTRODUCTION

This paper describes the process which was carried out to analyse and develop the structural intervention on the timber roofs of the National Palace of Sintra, located within the Cultural Landscape of Sintra, classified as a World Heritage Site by UNESCO since 1995.
Since 2012, the palace has been managed by Parques de Sintra – Monte da Lua, S.A. (PSML), a publicly funded company, responsible for managing the most important cultural values located within the Cultural Landscape of Sintra. Among those values in the National Palace of Sintra, together with the Park and National Palace of Pena, the National Palace of Queluz, and the Moorish Castle. The management of these cultural values, heterogeneous in their nature, represents a tremendous challenge. This responsibility requires a constant setting of priorities and a careful allocation of the available technical and financial resources. Thus, it is imperative to optimise planning and management tools, which are crucial for establishing long-term perspectives to guide the company's operations.

To achieve that, PSML developed and implemented Management Plans for Built Heritage, a strategic tool focused on the monitoring, conservation and rehabilitation of built heritage. This plan, being focused on the building as an asset, encompasses not only the entire civil infrastructure — structure, roofs, windows, doors, electrical installation, piping, and all its components — but also the specific equipment installed within it — HVAC, kitchen and hotel equipment, among others.

No building can be exempt from measures to limit its deterioration. Exposure to atmospheric agents and usage conditions causes all construction materials and technical installations to degrade. Only through the implementation of periodic structural assessment and monitoring of the conservation state, together with regular maintenance, is it possible to prolong the life and integrity of buildings. Indeed, the implementation of these procedures is fundamental, given that the early detection and resolution of anomalies prevents the need for more costly and intrusive interventions, which would have a greater impact on the heritage value of the building. Therefore, the Management Plan for Built Heritage aims to function as a strategic, operational, and updatable tool, which identifies the conservation and maintenance goals for the built heritage and the actions needed to achieve them. The plan is developed according to the following objectives:

- Implementation of methodologies that reduce future interventions and anticipate possible heritage losses;
- Coordination of preventive and corrective actions;
- Compliance with the legal safety requirements of the different pieces of equipment;
- Prioritisation of corrective actions according to the risk of heritage loss.

Within the assets under the care of PSML, the National Palace of Sintra was linked with significant intervention needs, essentially due to the poor state of conservation of the roofs, a segment which is considered of utmost priority in order to prevent heritage loss.

The main objective of the project was the conservation of the different structures that constitute the palace's roofs, fully preserving, whenever possible, the existing structural elements.
The proposed intervention was based on a geometric survey, structural characterisation and identification of the existing structural damages through the structural assessment work performed. After analysing the state of conservation and the structural behaviour of each roof, the necessary strengthening or replacement measures were defined, in order to cause the least possible impact on the existing structure, ensuring compliance with the project and the principles dictated by the International Charters and Recommendations (ICOMOS, 2004).

GENERAL DESCRIPTION OF THE BUILDING

The National Palace of Sintra, dating from the early 13th century, is located on a rocky acropolis, at the foot of Sintra's Mountains, which was transformed over time into a series of platforms at different heights upon which the various volumes that make up the palace complex were built. These volumes, of different shapes and sizes, currently form an organic complex interconnected with numerous gardens and interior courtyards, which stand as a unique example of medieval architecture, being the only example of a Portuguese palace from the Middle Ages to survive with its architectural form almost intact (Fig. 1a).

According to some historians, the National Palace of Sintra, whose origins date back to the Arab dominion of Sintra, is thought to be one of the two fortresses that the Arabs built in this town, as referred to by the Arab geographer Al-Bakri: "Sintra has two castles of extreme solidity". What can be seen today is the result of successive building campaigns promoted by the monarchs who inhabited the palace over eight centuries. The different construction periods make one of the palace's characteristics its architectural diversity, with Gothic, Mudéjar and Manueline styles predominating.

a)

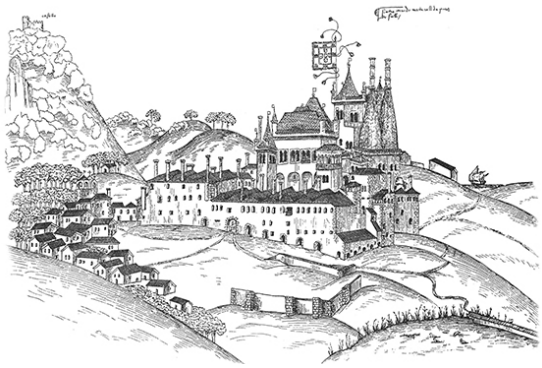

b)

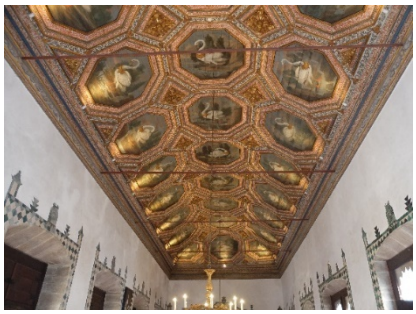

c)

d)

e)

f)

g)

h)

Figure 1. Photos of the palace and some of the most characteristic elements and divisions of the complex

Throughout its history, there were three major periods of occupation of the palace, corresponding to the reign of D. Dinis (14th century), D. João I (15th century), and D. Manuel I (between the 15th and 16th centuries) (Fig. 1b). In each period, the monarch's intervention comprised the adaptation of the existing buildings and the construction of new, connected to the existing ones. There is historical evidence that some of the buildings did not resist the heavy earthquake of 1755, that caused great structural damage to the palace, especially to the tallest structures, which led to the loss of the great tower that had stood above the Sala dos Árabes (Arab Room) (Fig. 1b). Nonetheless, a great restoration campaign was set in place, with particular concern to respect the original plan of the building, and most of the structures were subsequently restored and rebuilt, although some underwent modifications with respect to their original configuration (the great tower was never rebuilt).

The interior of the palace has spaces of great heritage value, such as the Sala dos Cisnes (Swan Room) (Fig. 1c), the Sala das Pegas (Welsh Room) (Fig. 1d), the Sala dos Brasões (Coat-of-Arms Room) (Fig. 1e), and the Quarto D. Afonso VI (King Afonso VI's Room) (Fig. 1f).

Regarding the exterior, the imposing 33-meter-high conical chimneys located in the northeastern area of the complex stand out above the main structure of the palace (Fig. 1h) and serve as a distinctive trademark of the building.

STRUCTURAL ASSESSMENT

Due to the magnitude of the project, the structural assessment work on the several roofs of the National Palace of Sintra was divided into three phases (Fig. 2a), and its main objective was to geometrically characterise the existing structural elements and obtain information on their state of conservation. One of the main obstacles to executing these works was the limited access to the roofs, conditioned by the preservation of existing valuable constructive elements and the need to avoid interfering with the palace's activities, namely, tourist visits. For this reason, the access to the roofs was primarily done from the exterior, through the execution of survey windows in the roof (Fig. 2b), which were accessed via auxiliary vertical elements, namely scaffoldings (Fig. 2c). The location of these survey windows was defined specifically for each roof based on the identified critical areas and to cover the largest possible area and the greatest diversity of structural elements. On some roofs, it was possible to access the interior and conduct a complete survey of the structure (Fig. 2d).

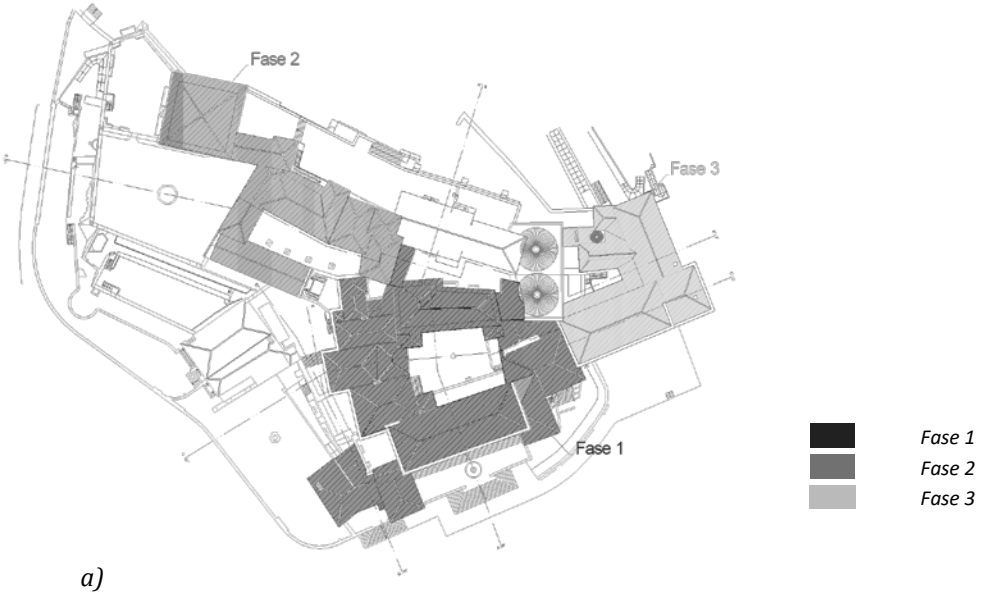

a)

b) c) d)

Figure 2. General plan of the palace with the location of the different survey phases and general photos of the access routes

GEOMETRIC SURVEY AND STRUCTURAL CHARACTERISATION

The vertical supporting structure of the buildings consists of load-bearing walls of ordinary, irregular stone masonry. The stone elements are generally of limestone origin, although there are indications that granite from the excavations executed to create the different platforms may have been used (Sousa, 2013).

Regarding the timber roofs, these are made up of solid pine, chestnut, and, occasionally, oak timber structures. During the structural assessment, it was observed that the structures follow a logical pattern and can be divided into three groups.

The first group corresponds to roofs formed by a single, generally older, structure that supports the exterior cladding and the ceiling. Although there are exceptions, these structures generally consist of simple trusses composed of two chords and one or more struts and ties (Fig. 3a). More recent elements were also observed on these roofs, introduced as strengthening or replacement measures.

The second group includes roofs consisting of two structures, usually independent: an older lower structure that supports the ceiling and a more recent structure that supports the exterior cladding (Fig. 3b). In general, like those corresponding to the first group, both structures consist of simple trusses composed of two rafters, struts and ties.

The third and last group corresponds to roofs that were replaced and are currently composed of a single or double more recent independent structures (Fig. 3c). Some of them are reconstructions of the older structures, while others have a structural configuration similar to the one used in current buildings.

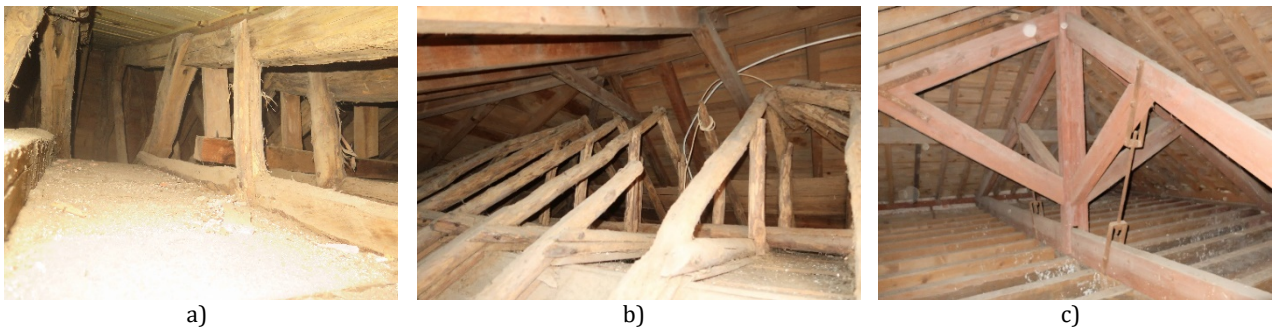

a) b) c)

Figure 3. Examples of the geometry of the existing structures that make up the roofs of the palace

NON-DESTRUCTIVE IN-SITU TESTING

The visual survey was complemented by in-situ non-destructive testing, which provided information on the state of conservation of the structural elements and information on the different wood species.
The internal and superficial preservation of the timber structural elements was verified through resistance drilling machine tests (Fig. 4a), which also allowed the extent of biotic attacks to be assessed. These tests were evenly distributed among the different structures, with some differences depending on the accessibility to the structure.

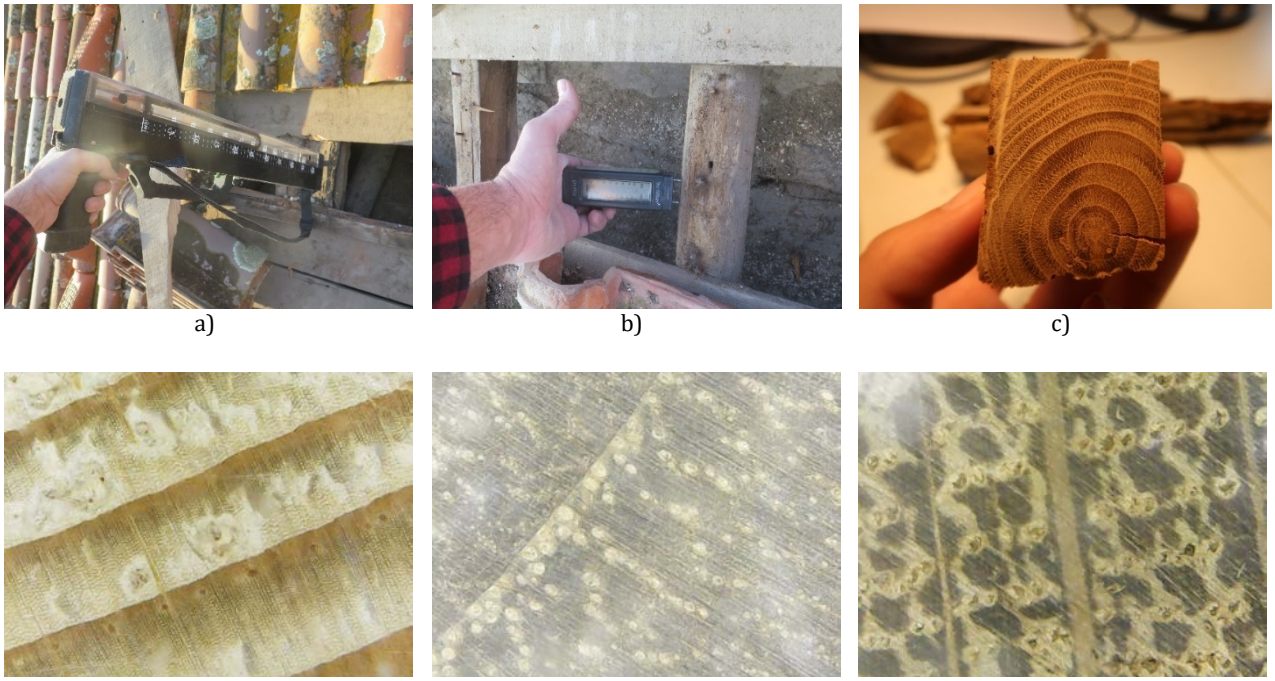

a) b) c)

d)

Pine, Pinus pinaster or Pinus sylvestris *Chestnut, Castanea Sativa mil* *Oak, Quercus robur*

Fig. 4 – Non-destructive in-situ tests carried out during assessment work

The resistance drilling machine tests were complemented with tests using the hygrometer (Fig. 4b), which allowed determining the existing water moisture content of the wood, giving indications of possible water ingress into the interior and the consequent potential to cause damage of biotic origin.
Regarding the identification of the wood species, this was carried out by extracting samples from the specific existing structural elements (Fig. 4c), where the removal of part of the section would not cause or aggravate structural problems. The configuration of the roof structure, combined with the poor state of conservation of some elements, significantly conditioned this process, preventing the possibility of carrying out a more exhaustive identification. Subsequently, the microstructure of the wood samples was analysed following the methodology developed by Cantinieaux (Cantinieaux, 2019), Fig. 4d).
The samples extracted were identified as softwood (pine, *Pinus pinaster* or *Pinus sylvestris*) or hardwood (chestnut, *Castanea sativa* Mill, and occasionally oak, *Quercus robur*).

STATE OF CONSERVATION: MAIN PATHOLOGIES AND STRUCTURAL DAMAGE

Part of the visual survey process involved identifying structural damage and determining its intensity and extent. This work revealed that the structures exhibit varying states of conservation, determined by their structural configuration, exposure to atmospheric agents and construction date.
The main damages observed are related to the attack of biotic agents, especially fungi (Fig. 5a), woodworms (anobiids) (Fig. 5b), and social insects (termites) (Fig. 5c). As a consequence of this attack,

material degradation of the structural elements is visible, which is significant in areas of high-water moisture content and in the oldest structural elements, which have been exposed for a long time to the attack of these agents. The intense material degradation caused, in some cases, deformation and even rupture of the structural elements (Fig. 5d, 5e and 5f).

a) b) c)

d) e) f)

DANOS ESTRUTURAIS	
ELEMENTOS DE MADEIRA	
Degradação por ataques de termitas	M1
Degradação por ataque de fungos xilógafos	M2
Degradação por ataque de caruncho	M3
Deformação	M4
Degradação da estrutura de suporte de tecto	M5
Rotura apoio	M6
Fendas de secagem significativas	M7
Entrada de água	M8
ELEMENTOS METÁLICOS	
Corrosão das chapas metálicas e dos pregos	D1

g)

Figure 5. Example of the main damages identified during the structural assessment (a, b, c, d, e and f) and the mapping of damages carried out on the structural plan of each of the roofs (g)

During the structural assessment other damages were also observed, with minor relevance, such as (i) the presence of drying cracks and knots; (ii) general degradation of the metallic connecting elements due to corrosion; (iii) the existence of inadequate strengthening systems implemented after the construction, that do not materialize an improvement in the structural performance; (iv) the existence of an inadequate structural configuration with main elements supported by secondary structures, as well as structures that transmit high horizontal forces to the load-bearing stone masonry walls, potentially compromising their stability.

The structural configuration of the roofs led, in some cases, to the appearance of cracks in the vertical, load-bearing stone masonry walls. These cracks are a consequence of the transmission of horizontal loads that cause out-of-plane deformation of the walls. Water infiltration from the roof structure was also observed, especially in exposed areas or where water accumulation occurs due to the roof's configuration, coupled with the lack of an adequate drainage system. All observed damages were located and identified on the structural plan of each of the roofs (Fig. 4g), in order to provide a comprehensive overview of the most affected areas of the palace complex and to help understand their possible causes.

STRUCTURAL INTERVENTION: MAIN ACTIONS

An ancient building of high heritage value, such as the National Palace of Sintra, requires careful intervention compatible with existing materials and construction systems. Therefore, the proposed intervention involved, whenever possible, the use of traditional materials and techniques, ensuring the preservation of the building's identity and respect for the principles dictated by the International Charters and Recommendations, by promoting solutions that are generally reversible, compatible, and minimally intrusive. In particular, all elements to be introduced, especially new structures or materials, will be carefully evaluated to ensure they do not damage or alter the functioning or physical and chemical stability of the existing construction elements.

The main proposed actions arise from the results of the structural assessment, as well as the structural requirements identified in the structural analysis to meet current regulatory requirements. The main objective of these actions is to preserve the existing structures and extend their useful life.

As with the structural characterisation, the intervention measures can be divided according to each of the identified roof groups. However, a series of comprehensive actions was proposed for the structures of the entire complex.

Regarding the roofs consisting of a single structure (the first group), the intervention will have the primary objective of preserving the entire structure, with strengthening measures or replacement of elements showing advanced deterioration or with identified structural needs.

For roofs composed of two independent structures (the second group), the intervention is primarily based on the conservation of both structures and the strengthening of the lower structure by suspending it from the newer upper structure (Fig. 6). The upper structure will be subject to specific strengthening or replacement measures, avoiding its complete replacement.

Finally, for roofs that were recently built and are in a good state of conservation (the third group), only the measures common to all roofs will be implemented.

The intervention measures proposed within the project and common to all roofs are (i) treatment against biotic attack and fire of all existing elements to be conserved; (ii) improvement of the joints between existing timber elements; (iii) verification of the need for strengthening or replacement identified in the project, once the structures are exposed and all elements have been cleaned; (iv) replacement of existing elements when strictly necessary in order not to compromise the stability of the remaining elements, always resorting first to new elements parallel to the existing ones or grafts; (v) installation of vapor-permeable and waterproof fabric on the entire roof; (vi) installation, or repositioning where existing, of ceramic tiles, supports and wooden cladding.

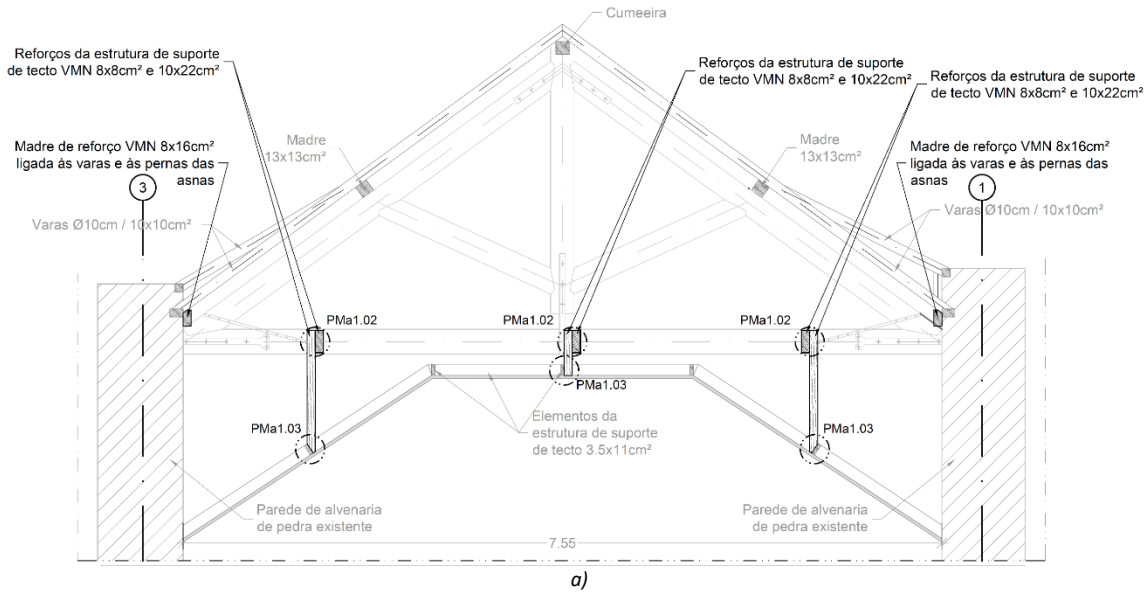

a)

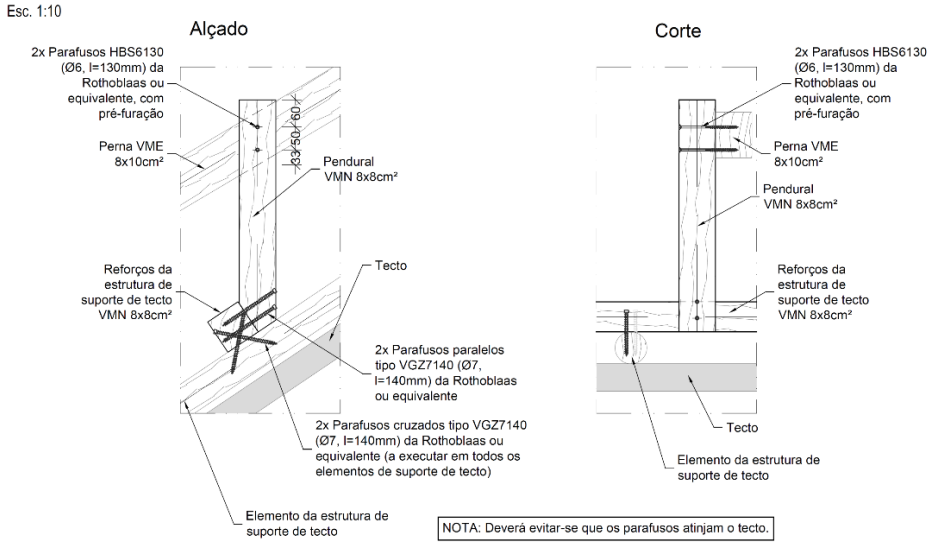

b)

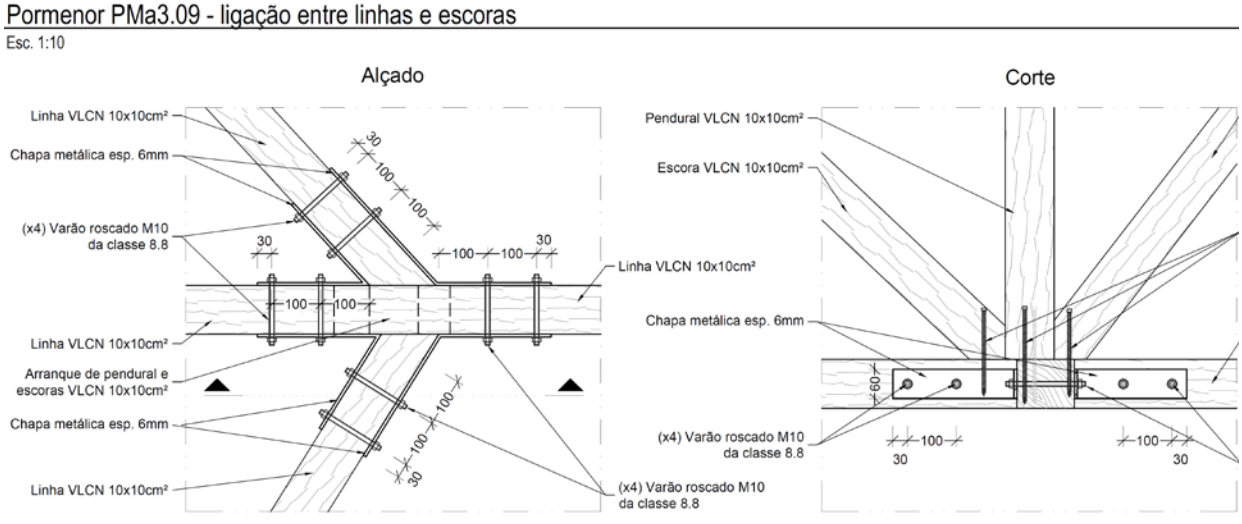

c)

Figure 6. Example of an intervention proposal developed for the palace´s roofs.

a) b)

Figure 7. An example of the intervention executed in one of the timber roofs of the palace.

FINAL CONSIDERATIONS

This paper presents an example of an intervention in the National Palace of Sintra, a building of high heritage value, focusing specifically on the timber roof structures. Structural assessment is presented as the central element for the development of this type of project, based on an initial bibliographic search and a subsequent visual survey, complemented by sampling and non-destructive *in situ* testing. This work allowed the characterisation of the existing structure, the identification of the structural damages and their structural analysis.

To address these damages, a set of structural interventions was proposed in the strengthening project. In these interventions, whenever possible, traditional materials and techniques were used, ensuring the preservation of the building's identity while simultaneously respecting the principles of reversibility, compatibility and low intrusiveness. In this sense, the interventions in the structural strengthening project are based on the conservation of the existing structures with appropriate treatment and the implementation of the necessary strengthening or localised replacement measures. In cases where the existing structure shows advanced deterioration, a new self-supporting structure will be built parallel to or at a higher level than the existing one, which will also serve as a strengthening and suspension structure for the existing elements to be preserved.

REFERENCES

[1] Cantinieaux, C. (2019). Wood species identification guide – technical report, NCREP. Porto, Portugal.

[2] ICOMOS (2004). Recommendations for the Analysis, Conservation and Structural Restoration of the Architectural Heritage of ICOMOS, Portugal.

[3]NCREP (2020). Structural Assessment – phase 1. Porto, Portugal.

[4] NCREP (2020). Structural Strengthening Project – phase 1. Porto, Portugal.

[5] NCREP (2020). Structural Assessment – phase 3. Porto, Portugal.

[6] NCREP (2020). Structural Strengthening Project – phase 3. Porto, Portugal.

[7] NCREP (2021). Structural Assessment – phase 2. Porto, Portugal.

[8] NCREP (2021). Structural Strengthening Project – phase 2. Porto, Portugal.

[9] Sousa, A., y Do Carmo, M. (2013). História da Construção – Arquitectura e Técnicas Construtivas. CITCEM y LAMOP. Braga, Portugal.

REASSESSMENT OF THE ARCHITECTURAL ALTERATIONS OF THE WOODEN CHURCH IN BĂTEȘTI: A STUDY BASED ON FIELD SURVEY AND TRACES ANALYSIS

Yudai YAZAWA[1] and Shinichi HAMADA[1]

[1] Nagoya Institute of Technology, Faculty of Architecture

ABSTRACT

The wooden church in Bătești, located in Timiș County, Romania, is an architecturally and historically significant structure whose construction history remains insufficiently documented. Although historical records mention an expansion of the pronaos by approximately 3 meters in 1858, no detailed architectural survey had been conducted until now. This study presents the findings of a field survey involving precise measurements and documentation of construction traces at the site. The investigation revealed wall elements and door structures likely added during later phases of expansion, suggesting a more complex development process than previously assumed. However, certain physical evidence does not fully correspond with oral historical records, indicating the requirement for further clarification. Future research should aim to reconcile these discrepancies by identifying original materials through dendrochronological analysis and by carefully examining the roof truss traces to ensure historical consistency.

KEYWORDS: wooden church, measurement survey, trace survey, expansion, field survey

INTRODUCTION

While Europe has traditionally been characterised by stone and brick architecture, wooden buildings have been present since ancient times, particularly in regions surrounding the Carpathian Mountains. In Romania, a significant number of wooden structures have survived, among which the wooden churches of the Maramureș and Moldavia regions have been inscribed on the UNESCO World Heritage List for their exceptional cultural value.[1][2] Dr. Alexandru Baboș's research on the wooden churches of Maramureș is particularly notable, offering a comprehensive study of the wooden church building tradition in the region from the 17th to the early 18th century.[3] Although many other wooden churches exist throughout Romania beyond these well-known areas, research has largely focused on regional characteristics or artistic aspects.[4] Studies specifically addressing construction methods, later renovations, and the architectural technologies and values embodied in these buildings remain limited. In the Banat region, Dr. Nicolae Săcară has conducted a survey of wooden churches, but his work provides only an initial overview.[5] In contrast, more detailed research into the architectural planning and development processes of wooden churches has been carried out in the Crivina de sus area by Dr. Vladimir Obradovici.[6] In this context, the wooden church in Bătești, located in Timiș County, represents a valuable yet understudied example of wooden ecclesiastical architecture in western Romania.

Bătești is a village which is a part of the town of Făget and is situated in the historical region of Banat, an area known for its diverse cultural heritage and architectural traditions. Within this village stands

the wooden church known as Biserica de lemn “Cuvioasa Paraschiva” [7], a structure believed to have been relocated in the mid-18th century from the now-extinct village of Veţa, which once existed in the surrounding region. Archival records indicate that the church underwent structural changes following its relocation, with a significant expansion of the pronaos by about three meters in 1858.[8][9] While there are scattered descriptions of the Bătești like this, little is known about its origins, the precise date of its construction in Veţa, or the timing of interventions such as re-roofing, timber replacement, or structural alterations. The absence of detailed architectural documentation has further contributed to the lack of clarity regarding the church's cultural and heritage significance. The church has not attracted scholarly attention, although its age and distinctive features, and no comprehensive studies have been conducted to examine its construction methods and techniques. This paper aims to fill that gap by re-examining the historical and architectural significance of the Bătești through a combination of on-site measurements and trace investigations. The study focuses in particular on the possibility of physical planar modifications to the structure over time.

METHODOLOGY

This study focuses on the changes to the floor plan of the wooden church in Bătești. It has been suggested that the original proportions were disrupted by the extension of the pronaos by three meters in 1858. To investigate this possibility, particular attention was directed toward changes in the church's plan over time. Fieldwork was conducted through direct measurement using a measuring tape, with a focus on obtaining accurate dimensions of planar elements. Special attention was paid to the location of the partition between the naos and pronaos, the position of the iconostasis, and the joining methods, dimensions, and arrangement of the wall components. The study also includes a trace investigation focusing on beam marks preserved in the upper sections of the walls. These traces are interpreted as physical evidence of earlier structural configurations, possibly indicating the original placement of the iconostasis or internal partitions.

Figure 1. The picture of field measurement activities

RESULTS

At the wooden church in Bătești, detailed field measurements and trace investigations were conducted. The architectural survey, carried out using direct measurements and 3D scanning [10], resulted in the production of precise architectural drawings, including floor plans, cross-sections, and elevations. These documents enabled an accurate representation of the current spatial organisation and structural elements of the church. In parallel, the trace investigation identified and classified various construction

traces. These included beam notches, column mortises, marks on the interior wall surfaces, and indications of weathering, all of which were carefully recorded in situ and mapped onto the architectural drawings. The survey confirmed the positions of key structural components, such as columns, girders, and beams, and provided evidence of modifications, including alterations to the entrance area and the door. This combined investigation clarified the construction techniques used in the original phase of the building, as well as subsequent interventions. The data collected serves as a foundation for further analysis of the church's construction history and typological classification within the broader context of wooden churches in the Banat region. Detailed results are presented below.

Measurements

All four sides were measured, and the dimensions were directly annotated onto the photographs. Drawings reflecting distortions were created from the 3D model, while details such as member positions and joints were recorded onto the drawings based on the field measurements.

Figure 2. The pictures, when measured

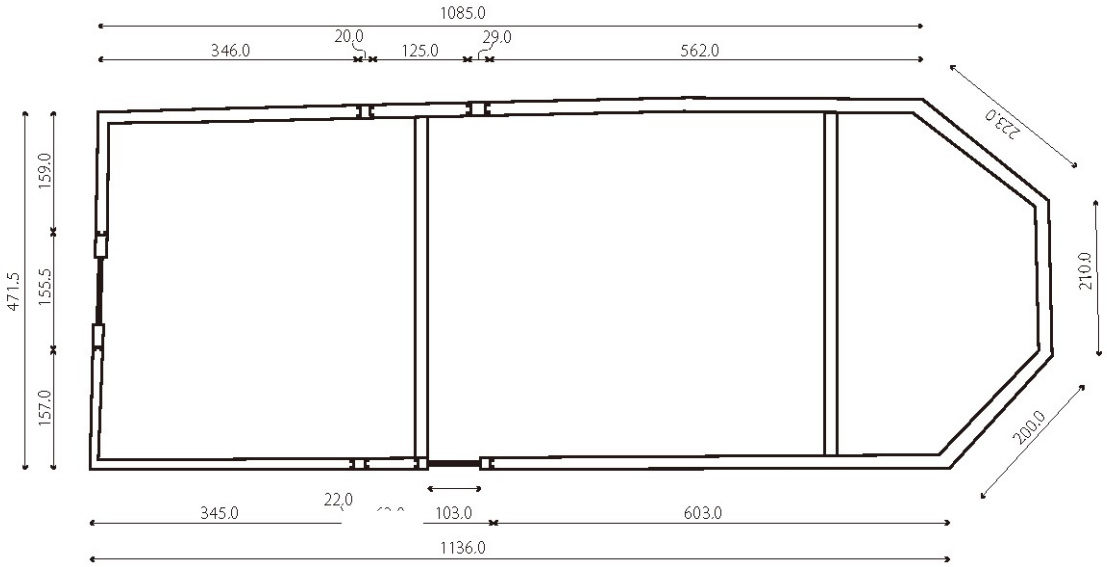

Figure 3. The floor plan of the Bătești Scale 1:100

Traces

Some traces remain on the upper planks where the beams of the partition between the naos and the pronaos were located. The following figure presents these traces plotted on the floor plan. And each material is named according to its directions, parts name, or numbers. For example, the column placed on the northern side is described as Nc1 or Nc2.

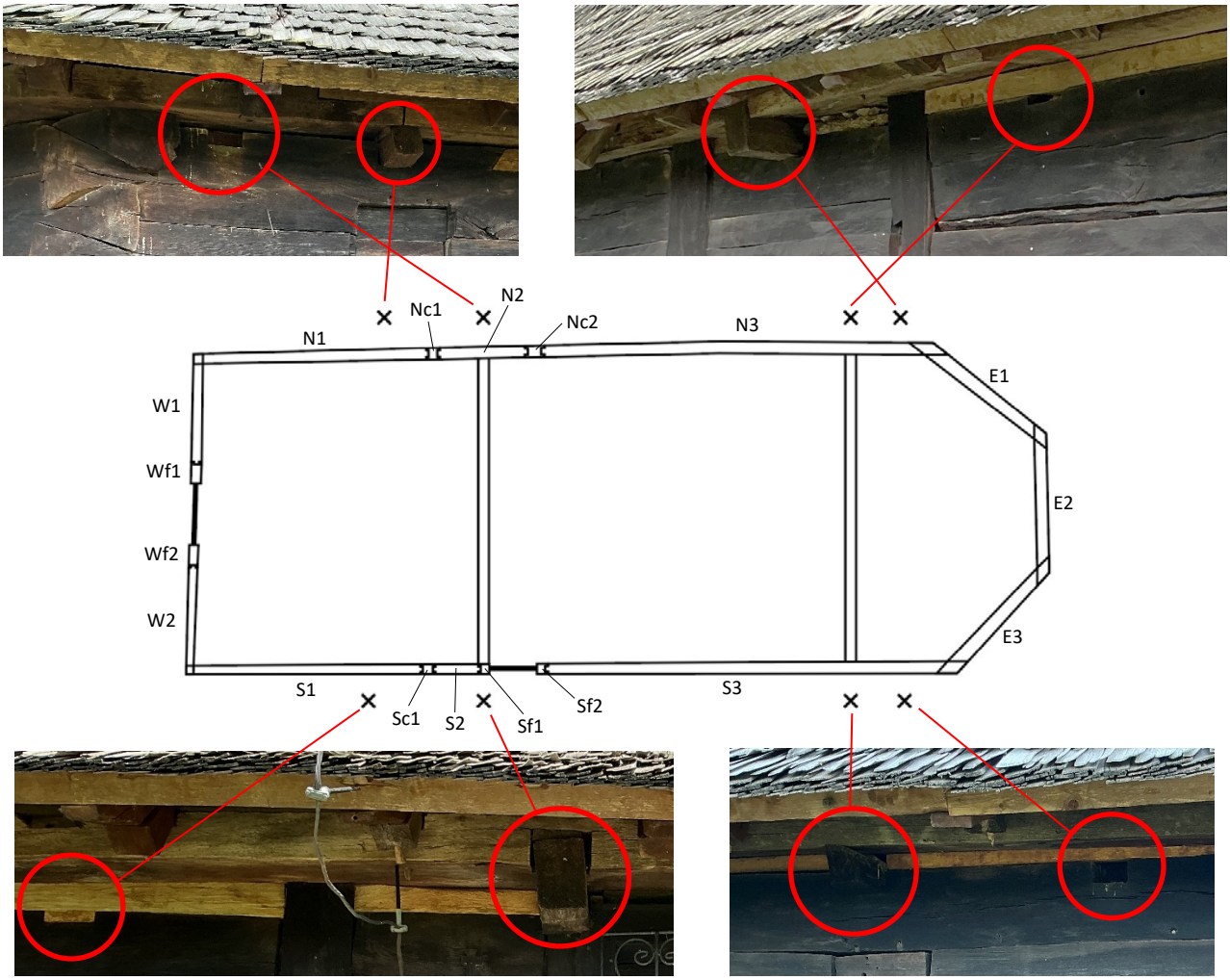

Figure 4. The traces plotted on the floor plan

The following figure illustrates the structure and material continuity of the girders and beams on the timber planks. Similarly, each material is identified by its colour and direction, or by its part name, such as Blue north, Red beam, etc.

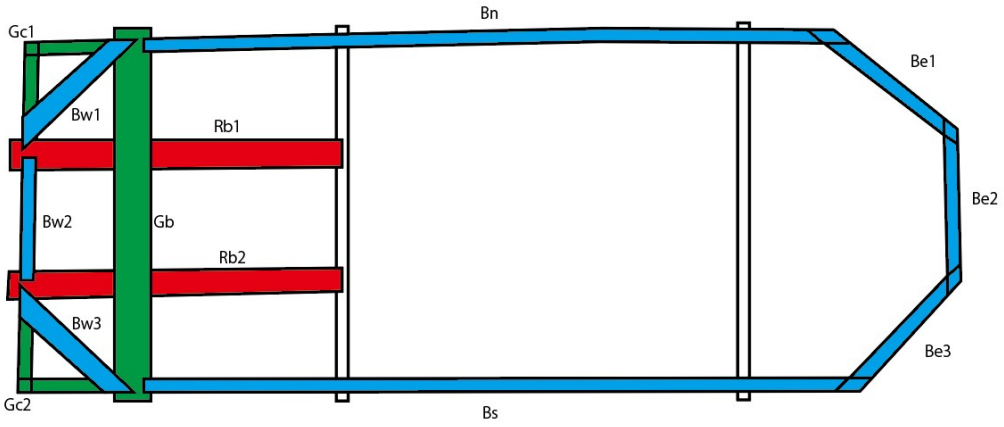

Figure 5. Structure of the beams and girds placed on the upper planks

DISCUSSION

Through on-site investigations, data such as plan drawings, structural diagrams of beams and girders, and trace mappings were collected. This chapter examines the historical significance of the wooden church in Bătești based on this information.

One of the most distinctive features of the church is the framing of the girders and beams in the pronaos. Generally, when the front of the church is configured as a rectangle, diagonal members are not included, and members such as Bn and Bs extend directly to the front wall. However, in the wooden church in Bătești, Bn and Bs are each constructed from a single piece of timber, which terminates at the position of Gb and then connects to Bw1, Bw2, and Bw3.

Typically, Gb functions as the base of the bell tower, but in this case, the bell tower is positioned further east, above Rb1 and Rb2. Gb is located at 132 to 183 cm from the front wall, with centre measurements indicating 150.5 cm. Why was this unusual configuration adopted? Clues to this question can be found by examining the traces of beams for the partition between the naos and pronaos, particularly those remaining on N1 and S1. The current partition is put over N2 to Sf1, located 53 cm and 69 cm from Nc2, respectively, on the northern side. In contrast, the beam traces on N1, S1 are located 54 cm and 70 cm from Nc1, Sc1, respectively—measurements that closely match those of the current partition. Moreover, the width of Nc1 and N2 is about 145 cm, which corresponds closely to the position of Gb from the front wall.

Figure 6. The pictures of the location of Gb and the beams for the partition

These observations indicate that Nc1 and N2 may have been added later. If this hypothesis holds, N1 would have originally connected directly to Nc2, implying that the front was set back by approximately 145 cm, aligning with the current position of Gb. In this arrangement, Bn and Bs, which are single timbers, terminate at the front.

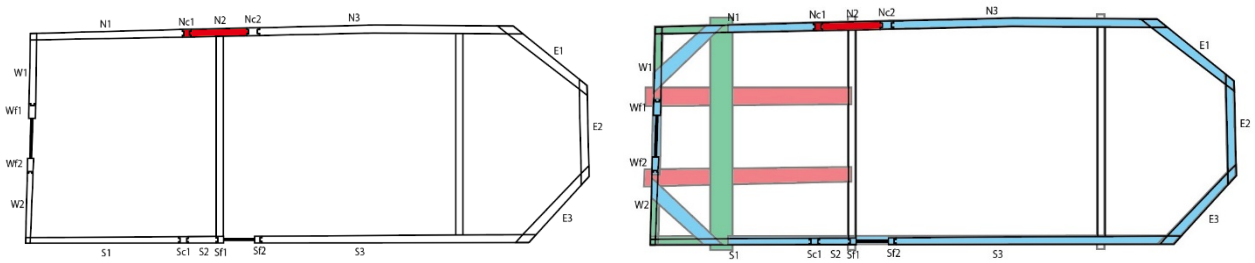

Figure 7. Structure of the beams and girds placed on the upper planks

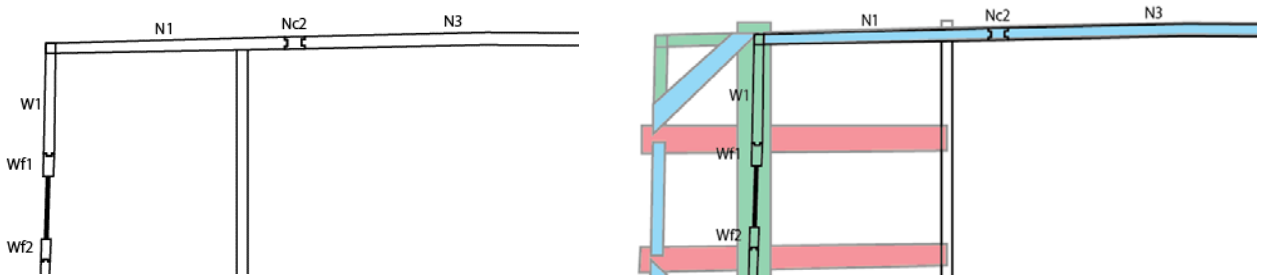

Figure 8. Structure of the beams and girders placed on the upper planks

Considering symmetry, there should be corresponding post-construction elements on the southern side as well. Indeed, the members corresponding to Nc1 on the southern side are Sc1, while the location equivalent to N2 and Nc2 aligns with the midpoint of the southern door for women. At present, however, no member corresponds directly to N2. Nevertheless, on the outer frame of the southern door, Sf2, there is a trace suggesting that material was cut away to fit the door, with the remaining width of the member being 29 cm—matching exactly with Nc2. This implies that Sf2 was originally positioned similarly to Nc2.

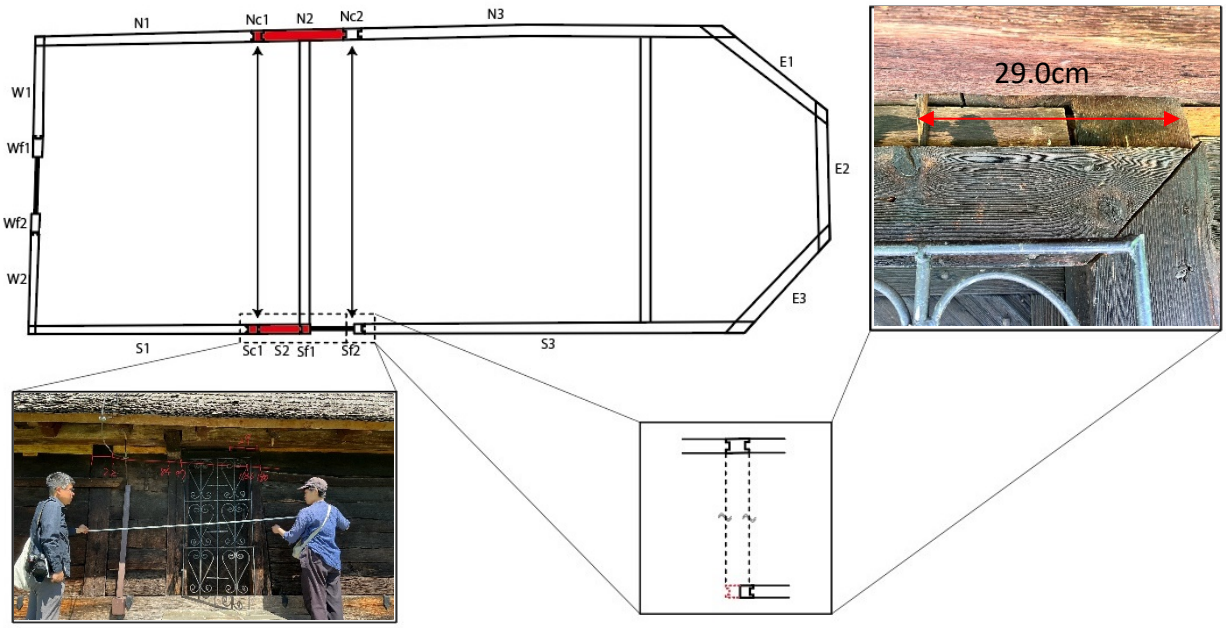

Figure 9. Structure of the beams and girds placed on the upper planks

In summary, the elements on the north side (Nc1, N2), and their counterparts on the south side (Sc1, S2, Sf1, and the door) are considered later additions, suggesting they were part of an expansion phase. Thus, it is necessary to consider what the former floor plan of the wooden church looked like before this expansion. If it is assumed that Nc1 and N2 on the north side, and Sc1, S2, Sf1, and the southern door on the south side are later additions, then N1 and S1 would have connected directly to Nc2 and Sf2, respectively. In this scenario, the position of the partition beams would have remained unchanged, and only the pronaos would have been reduced in size. Additionally, regarding the framing of the girders and beams, the front was set back to the position of Gb and Rb1, Rb2, Gb, and Bw1, Bw2, Bw3, which are currently within the interior, would have originally protruded outdoors. This hypothesis is also supported by the fact that these members exhibit significantly more weathering than other interior elements.

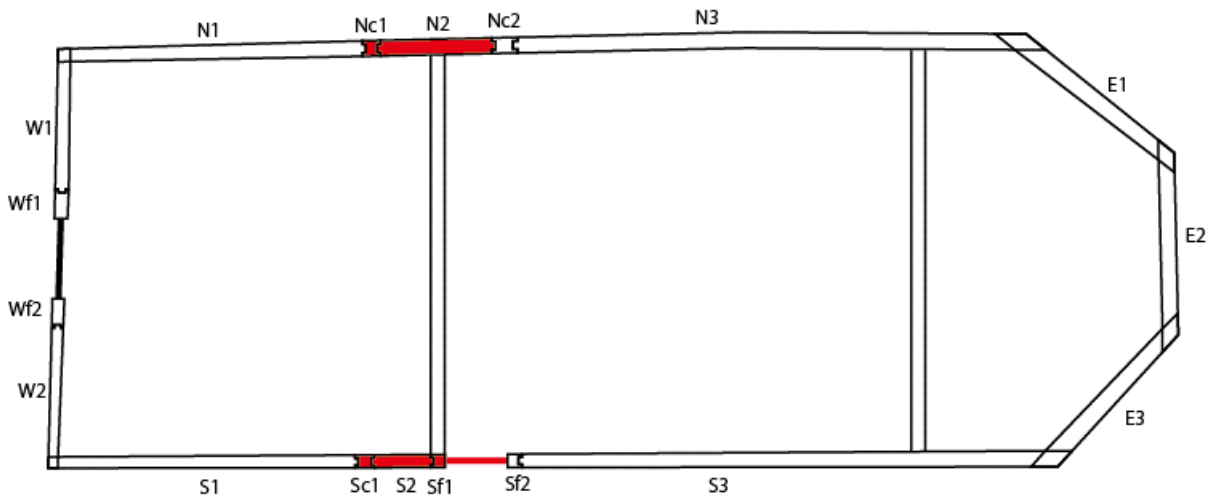

Figure 10. The parts added later

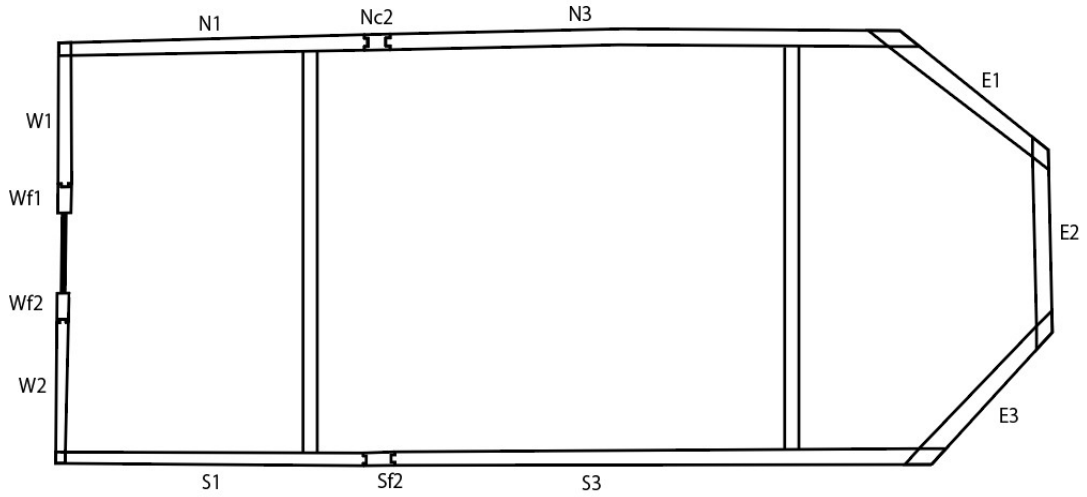

Figure 11. The restoration plan

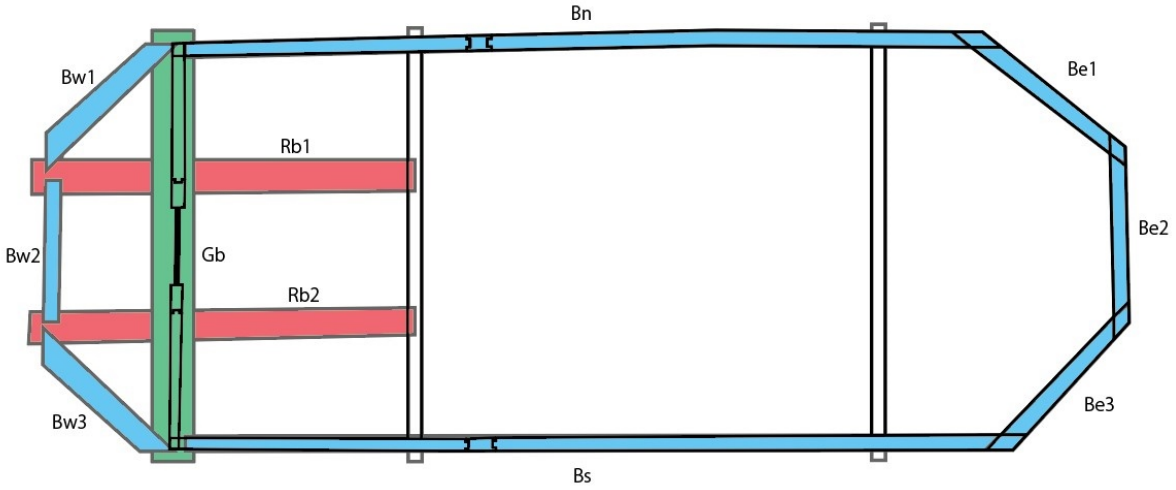

Figure 12. The fitting of the floor plan and beam frame in the restoration plan

Furthermore, this configuration is consistent with other wooden churches in the Bătești area, such as those in Povergina and Margina, which feature deep overhanging eaves at the front. Although the precise

date of this transformation is unclear, it can be reasonably inferred that at some point, the church was approximately 1.5 meters shorter in length compared to its current state.

Figure 13. The wooden church in Margina (left) and Povergina (right)

CONCLUSION

Despite the recognised historical significance of the wooden church in Bătești, detailed aspects of its architectural evolution have mainly remained unclear. Through the present on-site investigation, including detailed measurement surveys and trace analyses, evidence has been uncovered indicating that the floor plan was extended by about 1.5 meters from its earlier configuration.

Historically, it has been recorded that the pronaos of the Bătești wooden church was expanded by about 3 meters in 1858. Although the size of this recorded extension differs from the about 1.5-meter expansion revealed by the current survey, it remains undetermined whether this discrepancy is due to an error in the historical record or if the expansion process occurred in a few distinct phases. Nevertheless, the existence of an earlier floor plan, about 1.5 meters shorter than the current state, has been substantiated through the present study.

As for future research, key issues include examining the restoration proposal, including the cross-section and elevation, the identification of the original construction materials through dendrochronological analysis, further investigation of traces related to the roof truss system and other structural elements, and comparative studies with other wooden churches in the surrounding regions.

REFERENCES

[1] UNESCO World Heritage Convention, Wooden Churches of Maramureş, https://whc.unesco.org/uploads/nominations/904.pdf, accessed 14.5.2025.

[2] UNESCO World Heritage Convention, Churches of Moldavia, https://whc.unesco.org/uploads/nominations/598bis.pdf, accessed 14.5.2025.

[3] Alexandru. B, (2004), Tracing a Sacred Building Tradition, Wooden Churches, Carpenters and Founders in Maramureş until the Turn of the 18th Century, Doctoral Thesis (monograph), Department of Architecture and Built Environment, History of Architecture, Lund University.

[4] Coriolan. P, Bisericile de lemn din judeţul Arad, Tipografia şi Institutul de arte grafice Ios. Drotleff, 1927.

[5] Nicolae Săcară, BISERICILE DE LEMN ALE BANATULUI, Timişoara: Excelsior, 2001.

[6] Vladimir. O, (2020), SALVGARDAREA BISERICII MONUMENT DE LEMN DIN CRIVINA DE

SUS. ROLUL ARHITECTULUI ÎNTR-UN PROCES MULTIDISCIPLINAR, Doctoral Thesis, faculty of architecture, Universitatea Politehnica Timişoara.

[7] Ministerul Culturii, Lista monumentelor istorice din România, https://www.cultura.ro/lista-monumentelor-istorice

[8] Nicolae Săcară, BISERICILE DE LEMN ALE BANATULUI, Timişoara: Excelsior, 2001, pp.25-30.

[9] DIRECŢIA PENTRU CULTURĂ, Cărările credintei-Biserici de lemn monument-istoric din judeţul Timiş, https://biblioteca-digitala.ro, pp.31-33

[10] Biserica de lemn „Cuvioasa Paraschiva" din Bătești (TM-II-m-A-06179), autor arh. Cosmin Bloju, scanare finanțată de Consiliul Județean Timiș pentru Arhiepiscopia Timișoarei.

FIELD AND LABORATORY TESTING OF 170-YEAR-OLD TIMBER SPECIMENS: CASE STUDY OF A WHARF IN TRONDHEIM, NORWAY

Katarzyna OSTAPSKA[1], Guillermo ÍÑIGUEZ-GONZÁLEZ[2], Daniel F. LLANA[2], Kacper WASILEWSKI[3], Dag DENSTAD[5], Kamil ZALEGOWSKI[3], Jan PELCZYNSKI[3], Tomaž PAZLAR[4], Andrea LUCHERINI[4]

[1] Sintef Community, Trondheim, Norway, katarzyna.ostapska@sintef.no
[2] Timber Construction Research Group, Universidad Politécnica de Madrid (UPM), Spain
[3] Warsaw University of Technology, Faculty of Civil Engineering, Warsaw, Poland
[4] Slovenian National Building and Civil Engineering Institute (ZAG), Ljubljana, Slovenia
[5] Rambøll, Trondheim Norway,

ABSTRACT

Non-destructive and destructive laboratory tests are compared with non-destructive field measurements of timber elements in a building case study of the adaptive reuse of a 170-year-old timber wharf building from Norway Spruce located in Trondheim, Norway. Several testing and imaging techniques are used: ultrasound and stress wave Time-of-Flight, resistance to drill, moisture content, LIDAR scanning, acoustic resonance, four-point bending, and shear destructive tests. Estimated material properties are utilised in numerical models for system strength prediction: a roof portal frame. The combination of non-destructive testing techniques is assessed in terms of prediction value based on destructive testing verification. The equivalent strength class or strength profile of the original timber elements within the historical building from ca. 1857 in downtown Trondheim is estimated for future adaptive reuse projects of similar buildings in the row alongside the Nidelva river.

KEYWORDS: historic timber, existing structures, Norway spruce, non-destructive testing, LIDAR scanning for wood

INTRODUCTION

Trondheim is a coastal city in Norway, which has had a strong merchant tradition since the 17th century. Then, the row of merchant buildings along the river Nidelva was built as part of the oldest timber district, Bakklandet. Many old wharf buildings in Trondheim were out of use but are currently a focus of combined efforts of public and private actors for renovation and adaptive reuse of the district with respect for its heritage value [1].

Figure 1. Façade (left), and roof structure before and after renovation for adaptive reuse, Brygge 15, Trondheim

One of the buildings recently adapted for reuse, Brygga 15, shown in Figure 1, is from 1857 but has undergone renovation in the 1980s, Figure 2, when the inner timber structure on four stories was replaced with concrete, causing the timber flanks on all sides to deviate from horizontal position over time [1]. Thus, in the current adaptation, reinforcement of the roof structure was introduced. Brygge 15 is depicted from the riverfront in Figure 1 (left), and the top floor with roof frames before and after the adaptation is shown (centre and right). As many similar existing timber buildings will require renovation and adaptation, and their historical character and value are of importance, the assessment of the mechanical properties of the original timber is necessary. Some of the timber specimens can be acquired for testing, but the logistical, labour and laboratory costs are high. Thus, a campaign of different non-destructive and destructive tests was performed on the timber acquired from one wharf. A visual strength grading standard [1] has been recently released in Norway to support the effort toward timber upcycling and resource conservation. Among other proposals for grading [2]. Nevertheless, the current standardisation framework does not facilitate the reuse of recovered wood [3], even though its technical feasibility is being confirmed by ongoing research [4].

Figure 2. Brygge 15 during adaptation: replacement of rotten timber (left), concrete structure from the 1980s.

METHODOLOGY

Timber pieces of Norway spruce (*Picea abies* (L.) Karst.) were salvaged from the wharf and transported to the laboratory for a non-destructive testing (NDT) campaign followed by a destructive four-point bending test according to the European standard EN408 [5]. In total, four laboratory-tested roof specimens, see Figure 3, and three field-tested roof specimens, see Figure 4, were analysed in this work.

Timber beams were scanned with LIDAR to store geometry data and visual characteristics for further analysis and to assess cross-sectional dimensions more accurately for stiffness and strength estimation. See examples of scans in Figure 3. NDT included: ultrasound pulse velocity (UPV) (Pundit Lab 200, Proceq), acoustic stress wave time (Microsecond Timer - MST, Fakopp, Bt), local density (Resistograph, Rinntech), moisture content (Lignometer, Lignomat), and acoustic stress wave resonance (Resonance Lumber Grader, Fakopp Bt.).

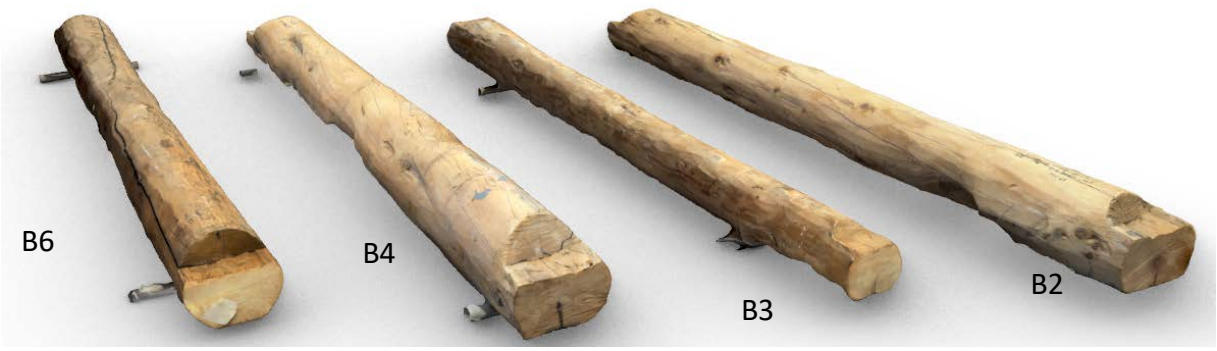

Figure 3. LIDAR scans of specimens B2, B3, B4, and B6 tested in the laboratory and recovered from Brygge 15, Trondheim

Figure 4. Specimens S1, S2, S3 measured in situ after adaptation (renovation), Brygge 15, Trondheim

Time-of-Flight $\boldsymbol{t_f}$ measured both with UPV and MST is used to obtain the ultrasound wave speed $\boldsymbol{v}$ at the measured distance L, and together with density ρ, the dynamic modulus of elasticity *MOE_dyn* is calculated according to equation (1).

$$v = \frac{L}{t_f} \rightarrow MOE\_dyn = \rho \cdot v^2 \qquad (1)$$

Eigenfrequency f found in longitudinal acoustic resonance of a specimen of length L, is used to obtain MOE_dyn according to equation (2):

$$v = \frac{2fL}{n} \rightarrow MOE\_dyn = \rho \cdot v^2 \qquad (2)$$

Imaging was done with an in-built iPhone LIDAR based on direct time-of-flight measurement of reflected light. Scan processing was performed in Rhinoceros3D CAD software on imported mesh models.

Figure 5. Set-up for destructive four-point bending test with typical failure in bending: fibre splitting.

Destructive testing was carried out following EN408 [5] with a four-point under static load conditions, see Figure 5. Force-displacement curves were obtained with displacement at the load cell position. The formula for the modulus of elasticity was modified to account for that using the following equation (3):

$$y_a = \frac{Pl^3}{6EI} \cdot \frac{bx_a}{l^2} \cdot \left[1 - \left(\frac{b}{l}\right)^2 - \left(\frac{x_a}{l}\right)^2\right], \qquad y_b = \frac{Pl^3}{6EI} \cdot \frac{bx_b}{l^2} \cdot \left[1 - \left(\frac{a}{l}\right)^2 - \left(\frac{x_b}{l}\right)^2\right] \tag{3}$$

The symbols and distances used in Equation 3 are depicted in Figure 6.

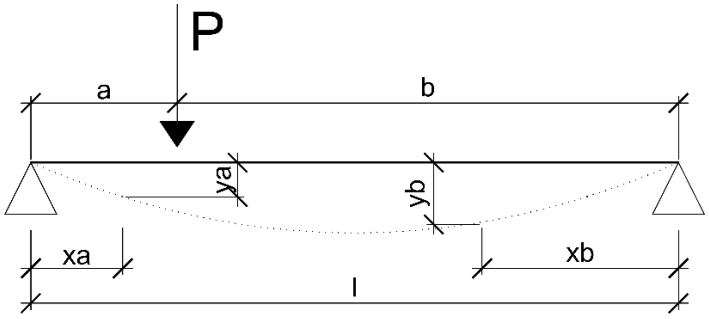

Figure 6. Euler-Bernoulli beam deflection model, see equation (1).

LIDAR scans of the laboratory specimens were analysed in CAD software (Rhinoceros3D) to extract information about the cross-sectional properties, i.e. height, section modulus and centroid, following the methodology described in [6]. The data were subsequently used within the same software to perform Finite Element Analysis (FEA) using beam elements. The FEA models of the four selected beams (B2, B3, B4, B6) were built and loaded with the respective peak forces obtained in the destructive 4-point bending test. Based on the calculated bending moments and geometrical properties, the maximum tensile stresses were estimated along the fibre direction at the peak load just before failure. The scan geometry and the resulting FEA model with a series of extracted cross-sections are shown in Figure 7.

Based on the results of the non-destructive and destructive testing, and data post-processing, the material properties of static Modulus of Elasticity (MOE_st) and bending strength (Modulus of Rupture, MOR) were applied to the material model in the numerical analysis of the building roof frame using finite elements in commercial software Abaqus [7]. The numerical model was based on 3D geometry, and solid continuum elements were used. One portal frame, after adaptation, see Figure 8, was modelled in variants with and without steel reinforcement.

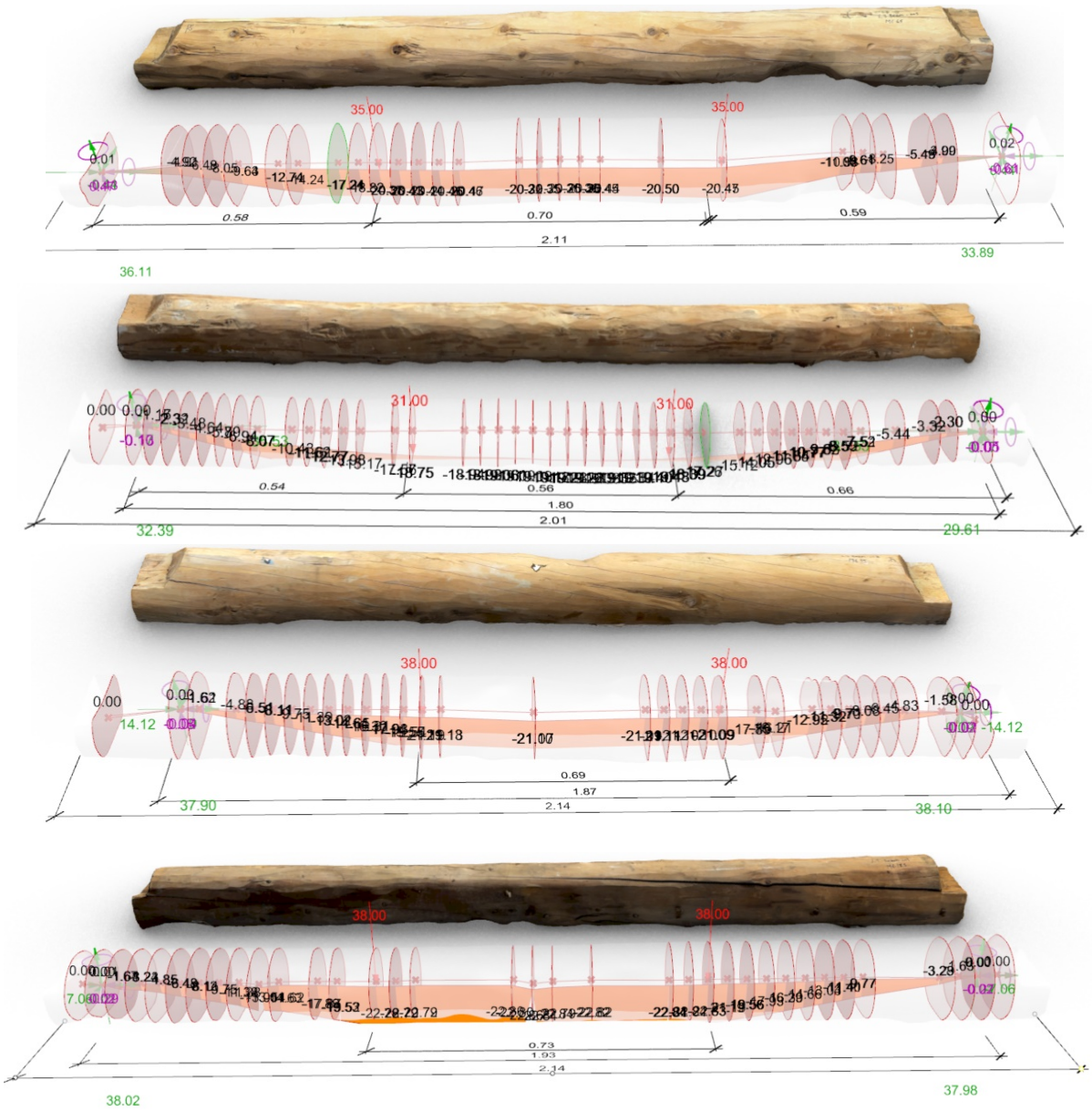

Figure 7. Bending moments and deflection in FEA based on scanned geometry of specimens from top: B2, B3, B4, B6. Green numbers represent reaction forces [kN], red numbers applied load [kN], and maximum moments at failure of each specimen from top to bottom are 20.5kN, 18.8kN, 21kN, and 22.8kN.

Steel connectors were modelled with a linear isotropic elastic material model and Young's modulus of E=210 GPa, and Poisson ratio of ν=0.3. Wood material was modelled as pseudo-orthotropic with nine material parameters. The design load value for the combination of snow load and self-weight of the roof layers is assumed to be 4 kN/m^2. Model geometry and discretisation, i.e. mesh, are depicted in Figure 9. A global mesh size of 20 mm was used.

Static analysis with non-linear geometry was performed, and load was applied uniformly as traction over the surface of the top common rafter for the snow and load case, respectively. Boundary conditions were applied at the middle cut as symmetry and at the base of all columns by blocking displacements, see Fig. 8.

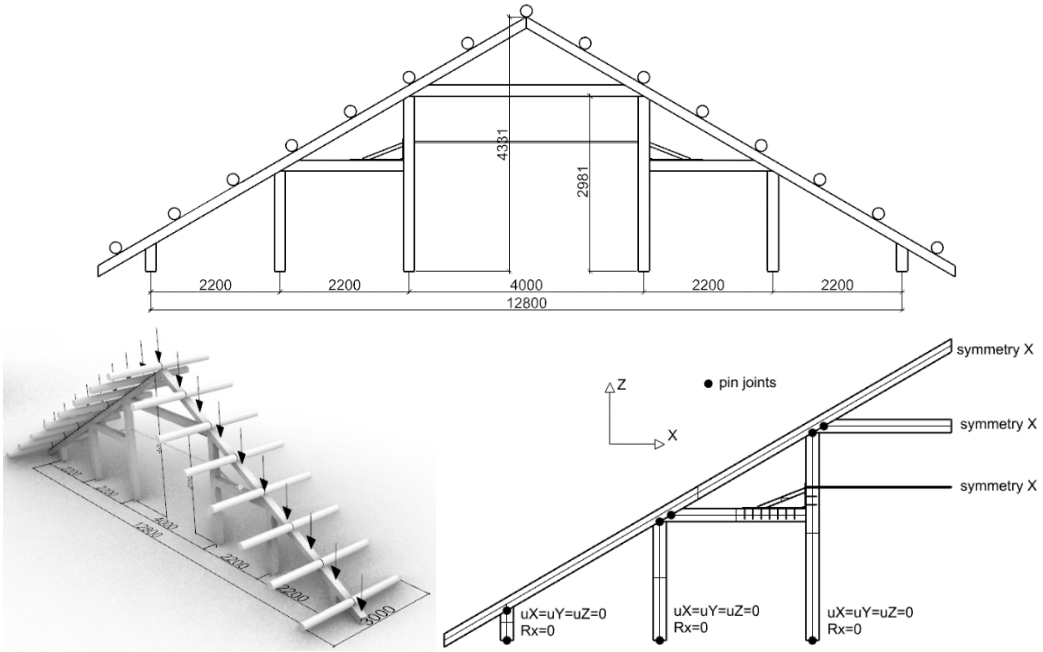

Figure 8. Roof portal frame geometry after adaptation (top) and assumed load transfer via roof beams to rafter for snow and self-weight (bottom left) and boundary conditions assumed in the numerical model (bottom right)

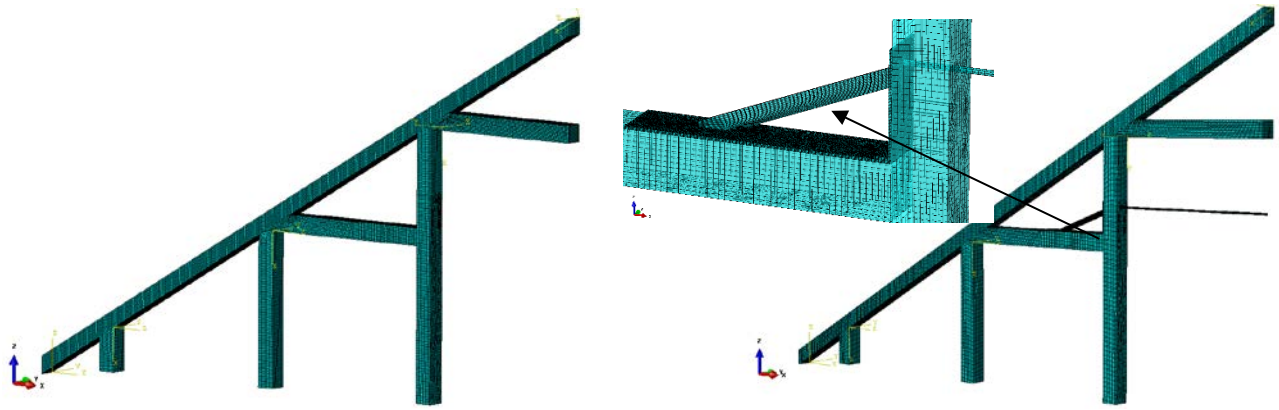

Figure 9. FE Model and discretisation of half of the frame with steel reinforcement (right) and without (left).

RESULTS

Density profiles obtained by Resistograph for three cross-sections in each laboratory specimen are recorded, and some are shown in Figure 10. Sudden drops in profiles indicate cracks, while peaks indicate knots. Density is visibly higher at the outer growth rings.

The variation in density within profiles is higher than the variation between mean density profiles for all specimens, as shown in Table 1. This is reflected in the growth ring pattern, as can be observed in Figure 11.

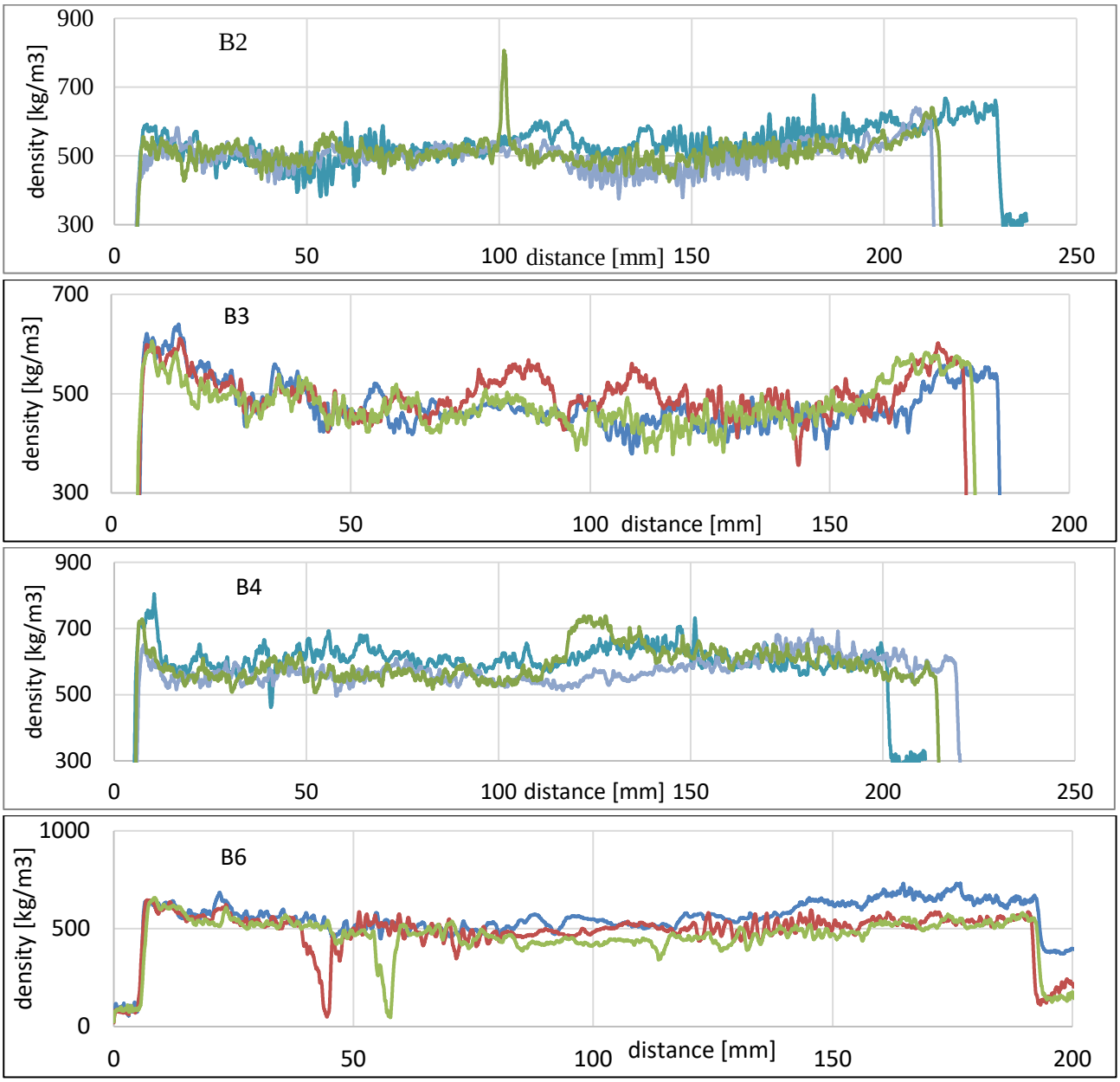

Figure 10. Examples of density profiles of specimens B2, B3, B4, and B6.

Table 1. Density statistics: coefficient of variation (COV) for each profile and between mean profiles for each beam.

ID	profile	1	2	3	mean	COV
B2	ρ_{avg} [kg/m^3]	539	511	502	**517**	3.7%
	COV	8.0%	6.6%	6.6%	7.1%	
B3	ρ_{avg} [kg/m^3]	480	500	481	**487**	2.3%
	COV	9.1%	7.7%	8.6%	8.5%	
B4	ρ_{avg} [kg/m^3]	593	612	574	**593**	3.1%
	COV	8.2%	6.6%	6.2%	7.0%	
B6	ρ_{avg} [kg/m^3]	563	513	488	**521**	7.4%
	COV	12.7%	9.1%	10.7%	10.8%	

Figure 11. Specimen ends images from LIDAR scan.

Force-displacement curves from four-point bending tests for four selected beams are shown in Fig. 12.

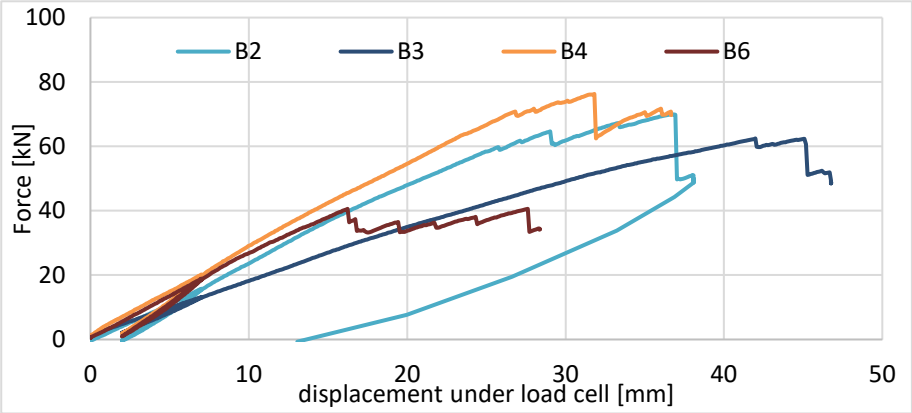

Figure 12. Force-displacement (load cell) curves for specimens B2, B3, B4, and B6.

Table 2. Peak force and load cell extension for selected specimens under the 4-point bending test EN 408.

ID	Fmax [kN]	U [mm]
B2	69.9	36.7
B3	62.4	42.0
B4	76.2	31.8
B6	40.6	16.2

Span between supports for all beams was 1,900 mm, and point load distances were 730-750 mm. A considerably lower peak force was recorded for specimen B6. A summary of the results for laboratory testing of recovered specimens from the wharf building is presented in Table 3. Averaged density from three Resistograph drill curves (Table 1) is also shown, MOE_st and MOR are calculated following the EN408 [5], and Moisture Content (MC) is measured simultaneously with measuring the Time-of-Flight of the ultrasound wave.

Table 3. Results of non-destructive and destructive tests of specimens from Brygge 15.

ID	L x b x h [mm]	MC [%]	Density [kg/m^3]	MOE_dyn UPV [MPa]	MOE_st [MPa]	MOR [MPa]	MOR_FEA [MPa]	MOR/ MOR_FEA
B2	2,075x188x155	17	514	13,831	9,513	34	41.3	1.21
B3	2,200x180x148	7	489	10,914	7,519	55	59.8	1.09
B4	2,155x175x200	10	593	12,668	7,734	30	30.5	1.02
B6	2,100x183x183	17	509	11,387	3,384	22	25.3	1.15
	Mean	13	526	12,200	6,468	35	39.2	1,12
	Std. dev.	±4.4	±40	±1140	±1922	±12	±13	±0.07

Dynamic Modulus of Elasticity (MOE_dyn) is obtained indirectly from ultrasound pulse velocity and density. Modulus of Rapture based on scan geometry and finite element analysis (MOR_FEA) is between 2-21 % higher than MOR obtained based on nominal geometry and analytical beam model. Static modulus of elasticity is 33% lower than the dynamic one based on pulse velocity measured with Pundit

Lab 200. Results of non-destructive measurements performed in the field on three beams in the roof structure: S1, S2 and S3, are summarised in Table 4. Mean dynamic modulus of elasticity obtained from UPV, MST and resonance is calculated.

Table 4. Results of non-destructive and destructive tests of selected beams from Brygge 15.

ID	L x b x h [mm]	MC [%]	MOE_dyn (UPV) [MPa]	MOE_dyn (MST) [MPa]	Max diameter knot [mm]	MOE_dyn (resonance) [MPa]	MOE_dyn mean [MPA]
S1	2,115 x 215 x 180	15	13,292	12,083	50	11,022	12,132
S2	4,160 x 170 x 170	13	12,869	13,797	20	13,820	13,495
S3	2,130 x145 x 180	14	13,292	12,207	30	11,487	13,329
	Mean	14	13,151	12,696	33	12,110	12,958
	Std. dev.	±0.8	±199	±780	±12	±1224	±607

Based on the laboratory testing of the four specimens from the building with non-destructive and destructive methods, the estimation of the MOE_st and MOR of the specimens in the field was made. Considering the low number of tested samples, the rough estimation of the MOE_st of the specimens in the field is made based on the mean dynamic MOE by reducing it by 47 % and equals around 6,880 MPa. A value of 7 GPa was used in numerical analysis as longitudinal Young's modulus E_L, with radial and tangential moduli E_R, E_T, shear moduli G and Poisson's ratios ν listed in Table 5.

Table 5. Engineering constants for the orthotropic material model of wood.

E_L	E_R	E_T	G_{LR}	G_{LT}	G_{RT}	ν_{LR}	ν_{LT}	ν_{RT}
7,000	200	200	450	450	30	0.5	0.8	0.8

Following the property values of Strength Classes defined in EN338 [8] and visual grading stated in [1] for softwood, the timber would be assigned to C22 or higher, considering the mean value of strength and C14, considering the mean value of stiffness. MOE_{dyn} was obtained from NDT lab tests (Table 1), and NDT in-situ tests (Table 2) were consistent.

Results of the numerical analysis of the portal frame with and without steel reinforcement under snow load and self-weight show the stabilising effect of the steel bracket and rod, compare deformations in Figure 13 and longitudinal and shear stresses in the rafter in Figures 14 and 15. Longitudinal stresses are reduced by 26% in the reinforced frame, and shear stresses are reduced by 8%. The effect in timber-timber connections was modelled as pinned, with rotations in the frame plane allowed between timber elements and bending moment transfer was neglected. Displacements in the steel rod are 1.6 mm, and maximum Mises stresses in the steel bracket are 270 MPa, as shown in Figure 16.

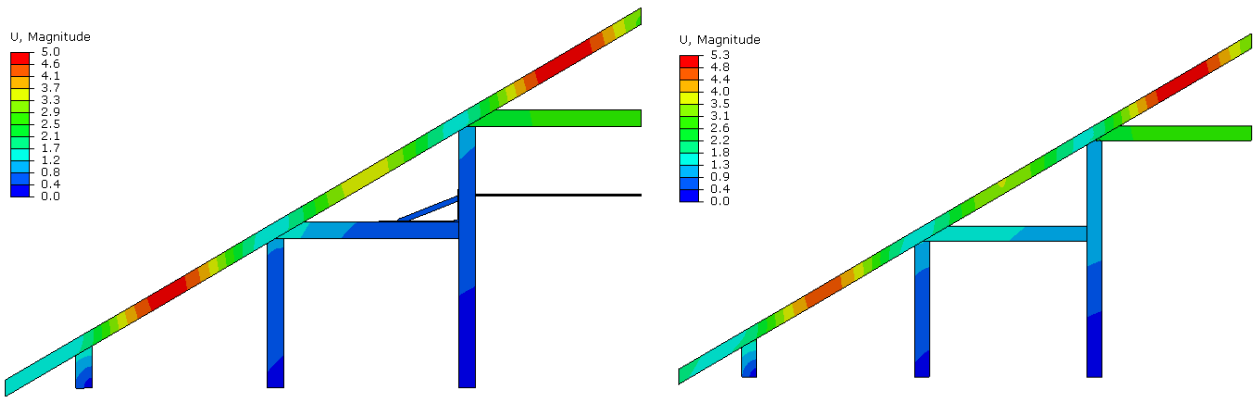

Figure 13. Deformation in timber under snow load in reinforced (left) and unreinforced (right) portal frame.

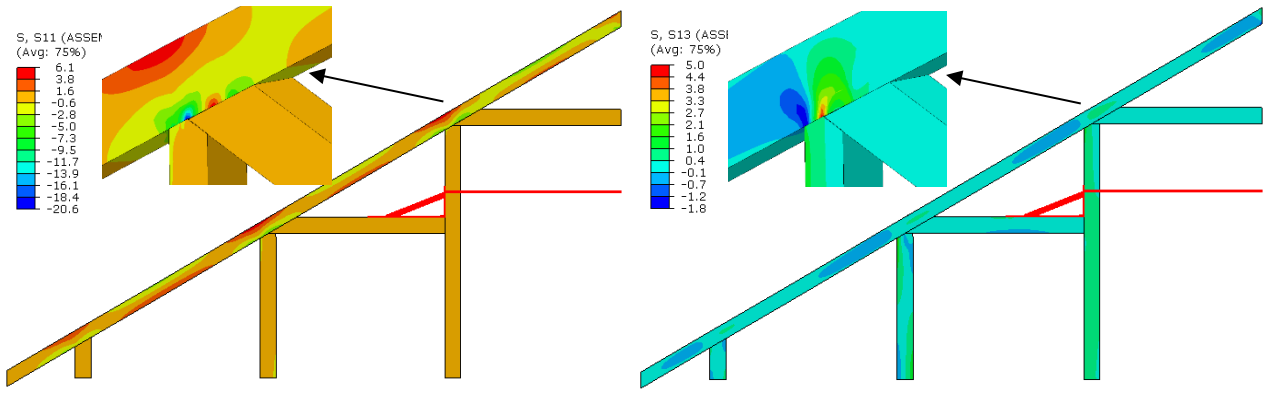

Figure 14. Longitudinal and shear stresses in timber under snow load in a reinforced portal frame.

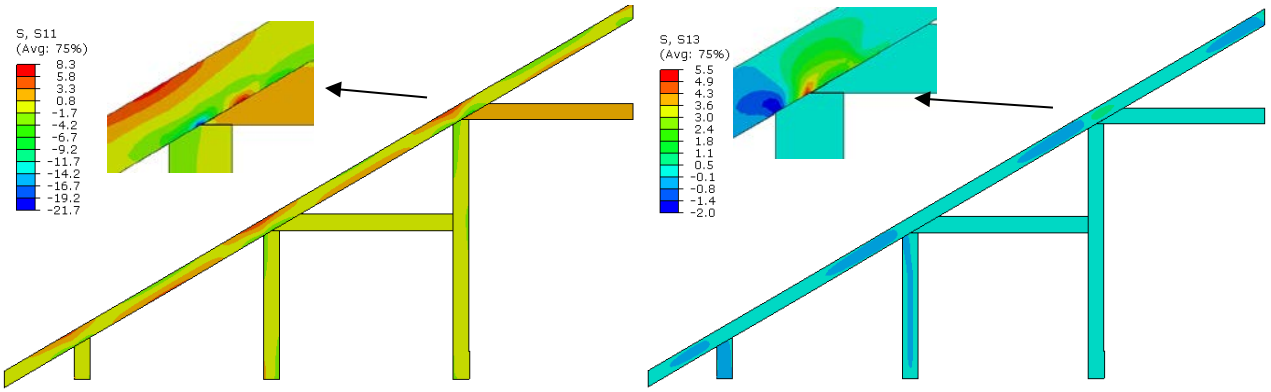

Figure 15. Longitudinal and shear stresses in timber under snow load in an unreinforced portal frame.

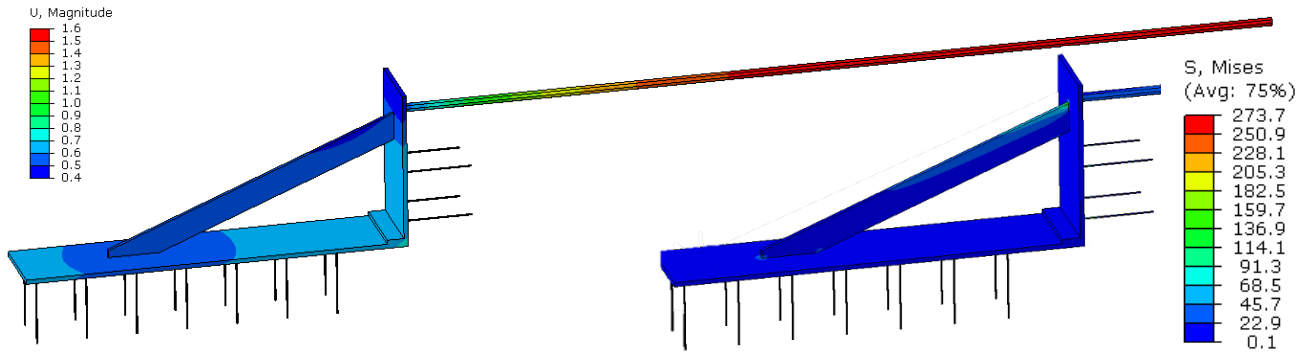

Figure 16. Displacement (left) and Mises stresses in steel elements (right).

CONCLUSION

Old timber pieces from a 170-year-old wharf building located at the riverfront in Trondheim were found to have enough strength for adaptive reuse under local environmental loads, equivalent to a new timber strength class of C22. Stiffness was decreased, mostly by the presence of cracks and knots, to an equivalent new timber strength class of C14, while density was on average 526 kg/m^3, equivalent to the maximum new timber strength class of C50. A mean static longitudinal Young's modulus of 7 GPa was used in the numerical analysis of the building timber frame based on the comparison between laboratory and field non-destructive tests. Introduction of reinforcing steel brackets and tendons was found to lower longitudinal stresses in timber by 26% and shear stresses by 8%. Geometrical defects and cracks require special care, and scanning with LIDAR has been found to be a promising method for

supporting stiffness estimation with more accurate geometry. NDTs such as density profiles and ultrasound speed estimation alone are not a sufficient indicator of global stiffness. Further work is needed on the automated incorporation of crack and knot information to provide reliable stiffness and strength estimation methods without requiring excessive and costly destructive testing campaigns in the laboratory.

ACKNOWLEDGEMENT

The work is part of the TiReX project (ForestValue2 Joint Call 2023) and it has received funding from the European Union's Horizon Europe under grant agreement No. 101094340, a joint call with financing from NFR (Norway), NCN (Poland, grant no. 2023/05/Y/ST8/00176), MICIU (Spain, PCI2024-153432), Ministry of Higher Education, Science and Innovation (MVZI) of the Republic of Slovenia (Slovenia, C3360-24-45201). We would like to acknowledge the cooperation of the building owner and investor, Olav Thon Gruppen, and the general contractor, Consto Trøndelag AS.

REFERENCES

[1] Evaluation of reclaimed timber, Part 3: Visual strength grading, NS 3691-3:2025, Norsk (bokmål)

[2] Recovered timber grading system, Llana, D.F.; Turk, G.; Osuna-Sequera, C.; Íñiguez-González, G., WCTE2025. June 22-26. Brisbane, Australia. https://doi.org/10.52202/080513-0424

[3] Reuse of wood in structural products – a gain?, Íñiguez-González, G.; Llana, D.F.; Torres, V.; Arriaga, F, WCTE2025. June 22-26. Brisbane, Australia. https://doi.org/10.52202/080513-0423

[4] TiReX project`s blog: www.tirex.info

[5] EN 408:2010+A1:2012, Timber structures - Structural timber and glued laminated timber - Determination of some physical and mechanical properties, CEN.

[6] Reclaimed timber assessment supported by LIDAR scanning, Pelczynski J., Ostapska K., Arendt P., proceedings of 14th WCTE 2025, Brisbane, https://doi.org/10.52202/080513-0148

[7] Smith, Michael. ABAQUS/Standard User's Manual, Version 6.9. Providence, RI: Dassault Systèmes Simulia Corp, 2009

[8] EN 338:2016, Structural timber – Strength classes, CEN

HYBRID STRUCTURAL REPAIR AND CAPACITY CHANGES TO A HISTORIC SCIENTIFIC ERA TIMBER FRAME

Rick K. COLLINS[1], Nicole M. COLLINS[1] and Michael PRAST[2]

[1] Firmitas

[2] Fire Tower Engineered Timber

ABSTRACT

Adapting large historic timber-framed structures for new purposes presents numerous considerations and challenges. The shift from one use to another (i.e., private agricultural to event centre/museum with public access) is more involved than specifying repairs. It necessitates detailed planning and the collaboration of many specialised building professionals. This is a case study detailing a process we have successfully replicated for many buildings in the Midwest region of the United States. It outlines the work from initial feasibility investigations and early assessments through to project planning stages and completion. The 1898 Manhattan Round Barn is a 20-sided, 30.48m (100') diameter cattle barn that is currently undergoing a complete structural reconstruction. It will become an events centre with full public access.

KEYWORDS: Heavy timber, repair technique, historic, adaptation, re-use, transitional framing, plank-on-plank

INTRODUCTION

Context and History: The 1898 Manhattan Round Barn, an architectural gem, was constructed using reclaimed materials sourced from the 1893 Chicago World's Fair. This unique 20-sided timber building is a testament to the ingenuity that arose from the social and economic transitions of the time. In the latter half of the 19th century, a significant surge occurred in the construction of round and polygonal barns and similar "scientific" structures across the United States. This phenomenon was primarily centred in the Midwest, particularly in states such as Illinois, Iowa, Indiana, Wisconsin, Michigan, and Minnesota. The trend persisted robustly for about 25 years, reflecting a shift in agricultural practices, industrialisation, and architectural design.

While these structures were marketed as relatively affordable and quick to construct, the reality was quite different. The construction of round barns, including the Manhattan Round Barn, proved to be labour-intensive. They required considerably more staging and scaffolding than traditional rectangular barns in the region. These structures often involved intricate designs and new techniques, which, while innovative, presented significant challenges to builders, working without precedent to follow.

This barn is situated at the top of a floodplain, resting on the remnants of an ancient glacial lake. The original foundation consisted of solid, hard local limestone; however, the building was set at grade, resulting in significant damage to the wood materials in the lower sections. Due to the type of plank-on-plank construction for the lower walls, they acted like sponges, absorbing water. This eventually led to

the slow destabilisation of the outer perimeter of the building as it settled into the earth. By 2008, the situation had grown increasingly critical. The current owner, a municipal parks department (the Manhattan Park District), recognised the urgent need for action to preserve this historical structure.

Figure 1. The 30.48m (100ft) diameter Manhattan Round Barn [photo C. Bill Thorpe, 2024].
The construction of these barn structures symbolises the advances of the Industrial Revolution, serving as a bridge between mid-19th-century and mid-20th-century construction methods in North America.

METHODOLOGY

Our methodology can be divided into four distinct but interrelated phases.

1. Documentation and Discovery: In 2008, we were engaged to assess the structure and report on its construction and condition. We continued a low-tech, low-cost approach to ongoing consulting and advisement, periodically over the course of the next fifteen years, assisting the client as they planned use and phased the project, and worked with the community to secure financing and support for the project. Our periodic visits and assistance enabled light, affordable, yet ongoing documentation and analysis of the building's deterioration and changes in condition. These touch-points also supported the owner in budgeting, shaping community perception, building communication, and fundraising.

The Manhattan Round Barn, with its impressive 30.48m (100ft) diameter and 20-sided design, was built in a late 19th-century style typical in the Chicago area, known locally as “plank-on-plank” construction. This technique involved laying flat nominal lumber—ranging from 2x4s to 2x10s—and stacking and nailing these together to form walls. This method not only reflects the construction practices of the time but also illustrates the state of the economy, cultural interests, and timber industries in North America. It embodies the positive and negative impacts of the industrial scientific age in the American Midwest.

The latter is evident in the hybridisation of methods: many of these buildings incorporated both plank-on-plank construction and traditional timber frame construction, utilising precisely cut mortise and tenon joinery pinned with wood pegs. The architectural sophistication of these barns often included truss designs and other components that were characteristic of the late 19th-century industrial age. Such features often included hardware such as bolts, washers, nuts, metal strapping, and tension rods. The Manhattan Round Barn exemplifies this blend of traditional craftsmanship and innovative building techniques, marking it as a significant artefact of its era and justifying its potential designation as a National Landmark.

2. Development, Scope of Work: In 2020, our firm was selected to carry out a more comprehensive, in-depth structural assessment, including a more detailed, updated feasibility report for restoration. Our analysis utilised 3D scanning, density drilling, soil testing and a general value engineering review. The focus of this study was to ensure that the building could meet current code requirements for public use within the specified external parameters and the available budget. When buildings transition from agricultural to commercial use, it is essential to reevaluate their floor systems, walls, and roofs to account for the increased floor, wind, and snow loading requirements associated with their new designation. This was the case for the Manhattan round barn.

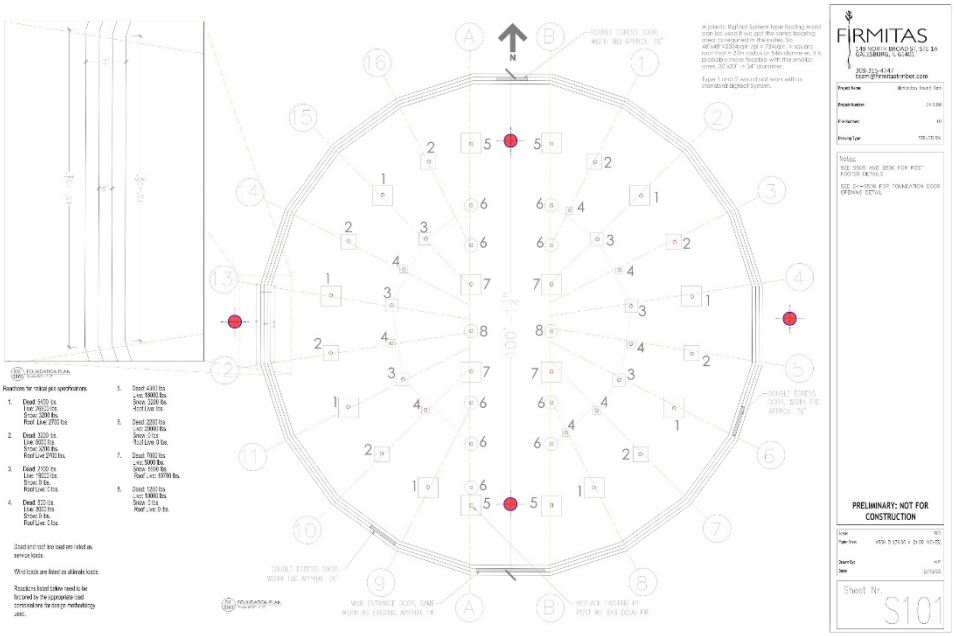

Figure 2. Foundation Plan Overview – Transitional elements are evident in the Manhattan Round Barn, which not only features timber frame joinery and mechanical fasteners from the industrial age but also employs plank-on-plank and platform-style construction. What we witness with these structures is the emergence of a new era in agricultural farm buildings.

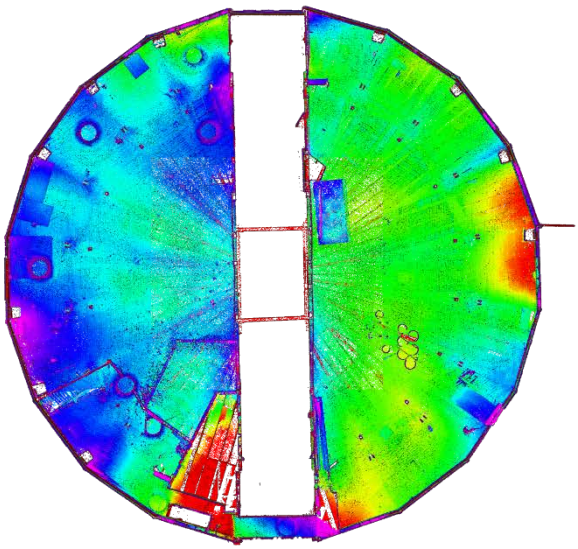

Figure 3. Scanned floor plan, level 1 – used to illustrate "as is" conditions and a baseline to communicate about the work and the structure with the client and others on the building team.

As is typical of the buildings we work on, there was a need to reinforce the roof system to accommodate the requirements for increased snow and wind loads. Additionally, we needed to increase foundation and floor capacities. For the Manhattan Round Barn, the only viable solution to comply with current local building codes while maintaining the budget was to remove the entire existing limestone foundation and install a poured concrete foundation. This new foundation consists of a continuous 4-foot-deep wall, elevating the building by a minimum of one foot above grade. The previous building had been set at grade, which directly contributed to its deterioration and structural issues.

Initial engineering assessments indicated the need to reinforce the roof system with additional timbers. We devised a cost-effective set of repair parameters that included constructing a new truss system of heavy timber along each diagonal, radiating outward from the centre of the barn. This approach not only ensures structural integrity but also maintains the aesthetic qualities of the original design. Furthermore, we determined to increase the floor capacity to 100 pounds per square foot by adding an extra joist in each bay, spaced at a minimum of 12 inches on centre. This adjustment is crucial in accommodating the new loading requirements associated with public use.

3. Defining Methodology: Our creative approach to the methodology of this particular restoration process was driven by the need to achieve the desired high-quality outcome as economically as possible. This involved dividing the building in half and innovating. Following the compass points, the long aisleway runs north-south, allowing for a straightforward division into east and west halves. The overall construction process entails lifting the building by as much as 11 inches in some places to achieve a level floor. This challenging task is accomplished using 20,000-pound hydraulic shoring columns, which facilitate the hydraulic lifting at predetermined points. Once one side of the building is elevated, the limestone foundation is removed and salvaged for potential future use. Excavation for new footings is conducted, followed by the framing of the new exterior wall.

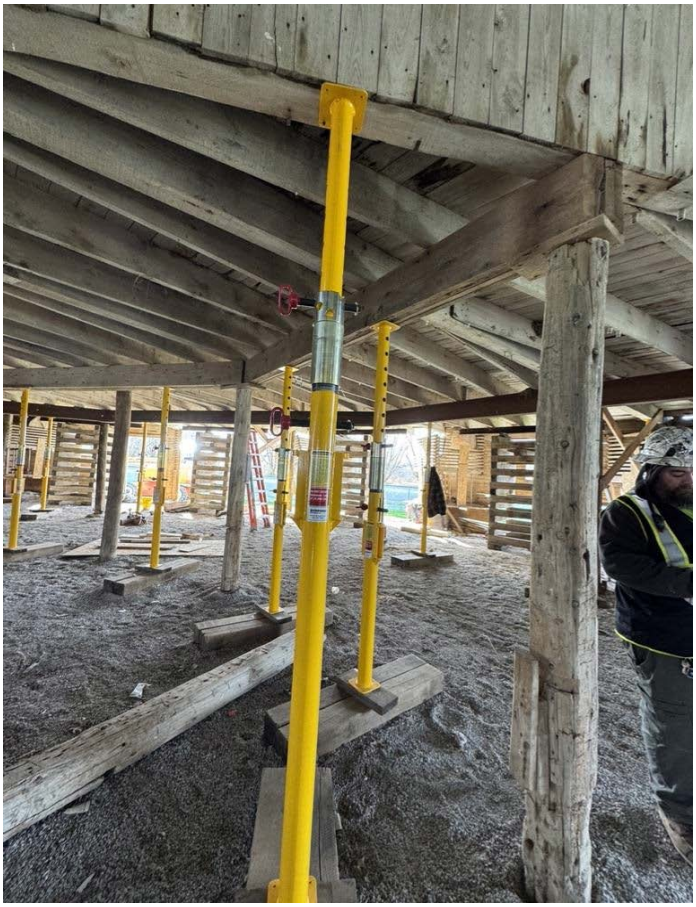

Figure 4. Hydraulic shoring in the foreground with wood cribbing towers visible in the background.

Due to future needs, code requirements, and budget, the original lower wall, which was nail-laminated plank-on-plank, was not rebuilt. A new stud-style 2” x 6” platform wall is being constructed to replace the plank-on-plank wall. This new wall will be reinforced with plywood to increase its shear strength and will be anchored securely to the existing foundation with embedded anchors. The previous structure lacked any hold-downs for wind; the region is prone to high winds and tornadoes.

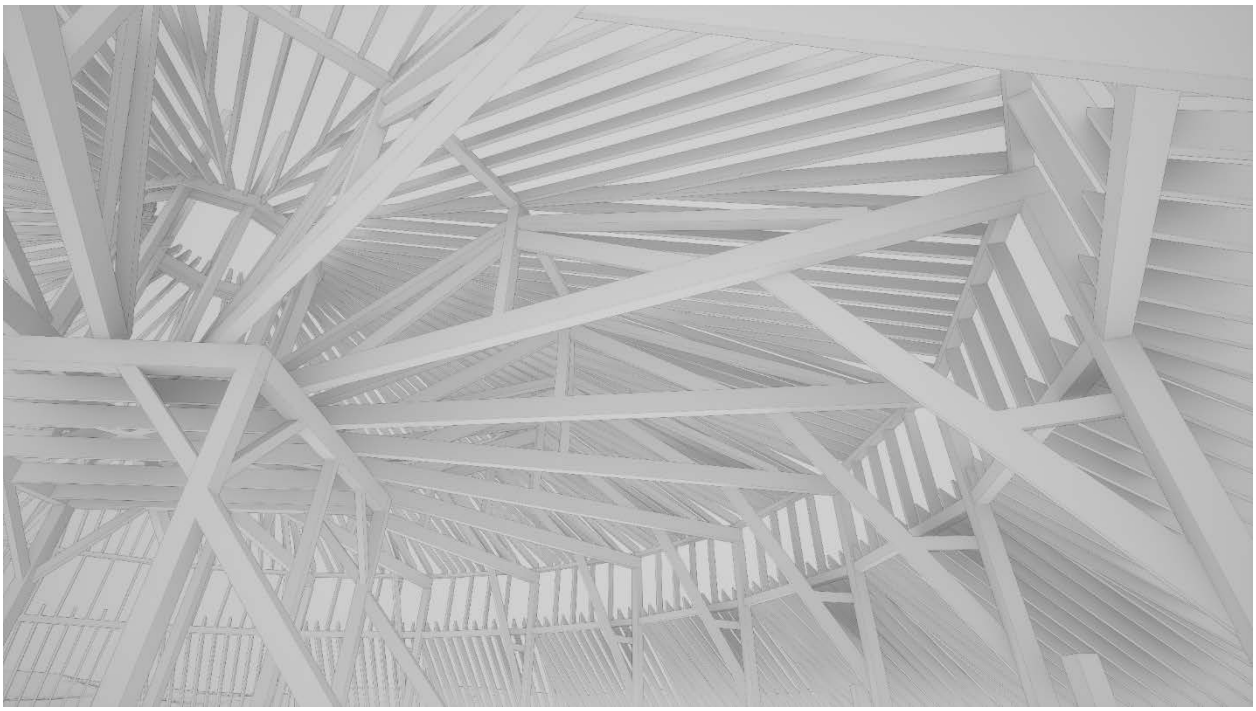

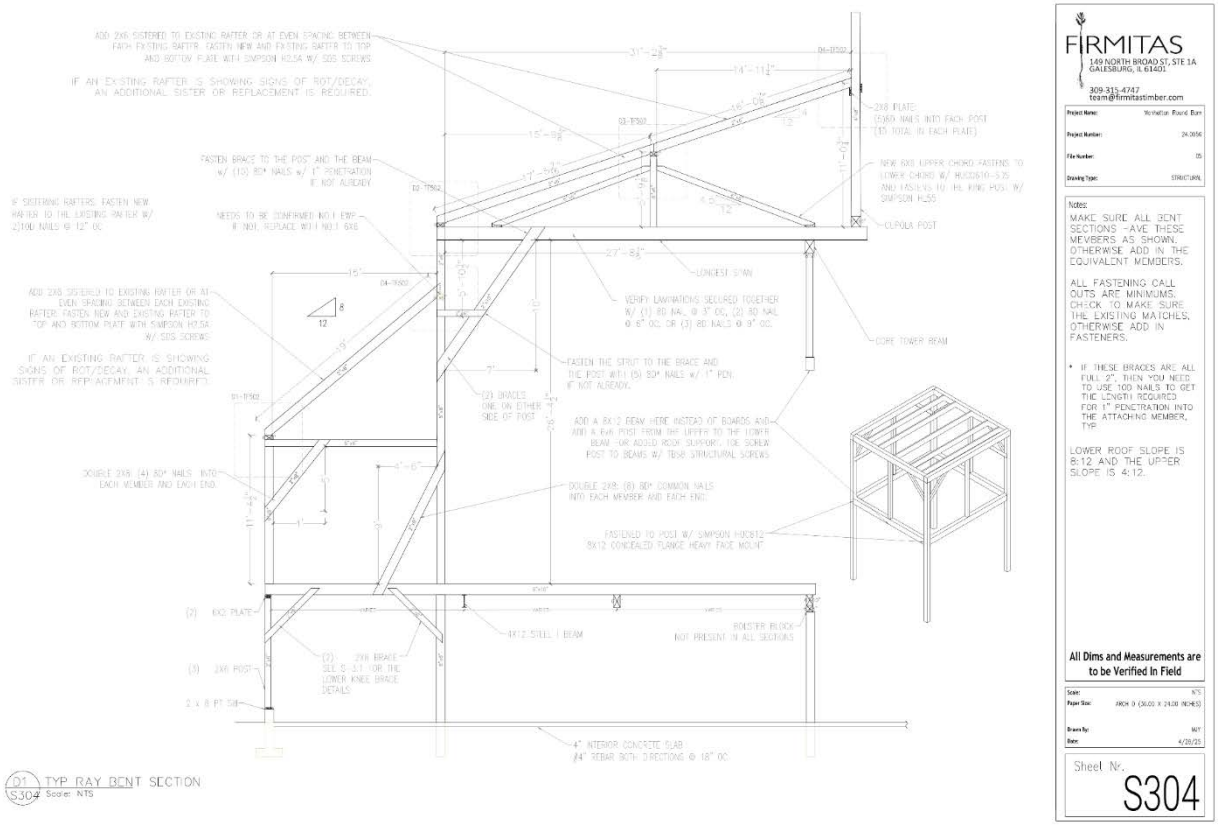

Figures 4 and 5. A rendering at the top, and a typical bent section.

The new plywood layer will also serve to connect the first and second floors, allowing for the reinstallation of new white pine shiplap siding, which will match the original historic aesthetic of the barn. Internally, all original posts will be removed and reinstalled on new footings. The second-floor deck will be reinforced with an additional joist to meet the increased load requirement of 100 pounds per square foot (4788 pascals). Additionally, truss work will be implemented at the third level to further increase the building's capacity to handle snow and wind loads.

4. Implementation: We commenced work on this important project several months ago, and the restoration is well underway. As we progress, our goal remains to honour the historic significance of the Manhattan Round Barn while ensuring its structural integrity and continued functionality for future generations. We assure quality in the work in two ways. The first is by integrating input and knowledge from all trades and building professionals involved in the planned methodology. There is a clear path for those completing the work to follow, grounded in the collective experience of the group. The second is by choosing partners that share our (and our client's) values and interests as much as possible. The restoration of this barn is not just about preserving a building; it is about preserving a piece of history that reflects the agricultural practices and architectural innovations of its time. Through this project, we all contribute to the ongoing narrative of rural architecture and the enduring legacy of the agricultural community in the Midwest.

Figure 6. The restoration of the Manhattan Round Barn

CONCLUSION

In most of our projects, technological tools play a crucial role in the documentation and planning stages of restoring historical structures. We have found that their thoughtful integration enhances our precision and efficiency, and ultimately lowers the cost of this work. We have also found that if our team is not mindful and able to blend simple (traditional techniques) with these relatively new capabilities, the baseline costs to clients can rise to an unattainable level for many. The same pattern occurs as we design and specify repairs and methodologies for completing the work itself. A practical knowledge of traditional low-tech technologies, as well as modern materials, hardware, and techniques, enables a team to create thoughtful, targeted plans that are efficient, achievable, and contextually relevant.

REFERENCES

[1] https://edition.pagesuite.com/tribune/article_popover.aspx?guid=5430a26b-2c1d-4353-a590-f051721e4778

[2] https://www.manhattanparks.org/parks-and-facilities/round-barn-far

ANALYSIS OF CHANGES IN STRENGTH AND DAMAGE TO THE LAMINATED WOOD STRUCTURE OF A LARGE ELECTRICAL COMPLEX OPERATING IN THE OPEN AIR

Andrii BIDAKOV[1],Dmitrii KOCHKAREV[2] and Oksana PUSTOVOITOVA[1]

[1] O.M.Beketov National University of Urban Economy in Kharkiv, Ukraine;
[2] National University of Water Environment Engineering

ABSTRACT

The condition of timber structures during long-term operation and methods for assessing the influence of various factors on their strength and rigidity are extremely important, especially for special-purpose structures. The developed domestic approaches to the study and analysis of old timber are based on the works of Prof. Vadim Fursov and his PhD students within the framework of the electrophysical complex project implemented in the Kharkiv region in 1985 and actively monitored until 2017. The accumulated data are of particular interest, as the timber structures of the complex objects had different design schemes and were exposed not only to climatic loads but also to the action of an electric field from high-frequency currents. The electrophysical complex, or high-voltage test facility GINT-12-30, was awarded the status of National Heritage of Ukraine in 2001 [2].

KEYWORDS: old timber, strength parameters, electrophysical complex, gluelam, operating coefficients

INTRODUCTION

Timber structures in Eastern European practice in different periods had different degrees of popularity and, accordingly, attention to their research. As a rule, such research and development was associated with the number of state programmes in this area. During the 1960s, timber structures were even undesirable in mass construction, and active development was observed in reinforced concrete structures intended for use in the residential and industrial sectors. Timber structures were only used when their use was optimal, like in the chemical industry and agriculture, for storing mineral fertilisers. A non-standard rational solution was to use the timber structures in the electrophysical complexes exposed to the atmospheric moisture, ultraviolet radiation, and high-frequency currents.

In domestic practice, the experience of observing timber structures in old buildings was limited due to military actions, fires, and the fight against the church, which destroyed many old temple buildings. The reliability of data on the nature and intensity of the impacts to which timber structures were subjected during the service life of surviving buildings was unknown, which complicated the establishment of objective factors influencing damage to wood and structural units.

The development of the GINT-12-30 electrophysical installation, namely the structures made of glued laminated timber (GLT) of six towers with dimensions of 6*6 m in plan and heights of 27, 33 and 36 m, as well as the terminal device (ОУ) in the form of a wall 30 m high, 6 m thick and 50 m wide (see Fig. 1), set the task of operating the structures for at least 15 years. The structures of the complex were made of GLT with a maximum cross-section of 300-500 mm at the Krasny Oktyabr plant in Arkhangelsk (Russia) in 1984-1985 and assembled in the Kharkiv region in 1987.

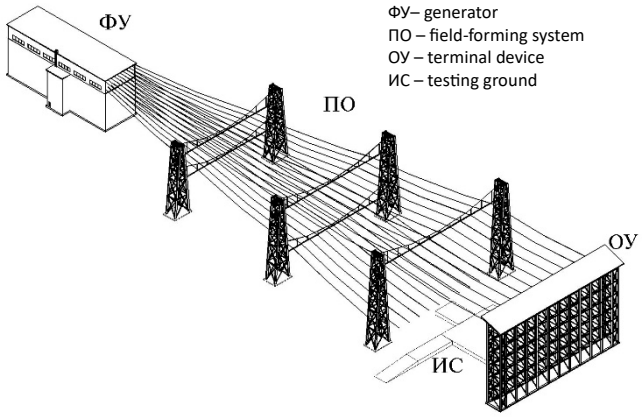

Figure 1. General diagram of the GINT-12-30 electrical complex

Active work during the development of the complex structures and their subsequent examinations under the supervision of Prof. V.V. Fursov, conducted for over 30 years, allowed the collection important data on the intensity of damage accumulation and the nature of its distribution along the framework of objects of the structural tower-shaped systems and the spatial structure of the wall or the terminal device (ОУ). The generator (ФУ) is a two-story building, isolated from atmospheric influences, featuring an electric-gas chamber that creates a powerful electric shock (~10,000 A and a voltage of ~5 MV). Metal and reinforced concrete structures were unacceptable due to the requirement for dielectricity, radio transparency and magnetic permeability, and the percentage of fastening metal according to the technical specifications had to be below5–7% of the weight of the material used. Therefore, for the first time in domestic practice, fibreglass rods were used in connections as dowels, and glued-in steel rods were used in open-air conditions for fastening tower branches to the foundation (Fig. 2-c), a project carried out with the direct participation of Prof. S.B. Turkosovsky.

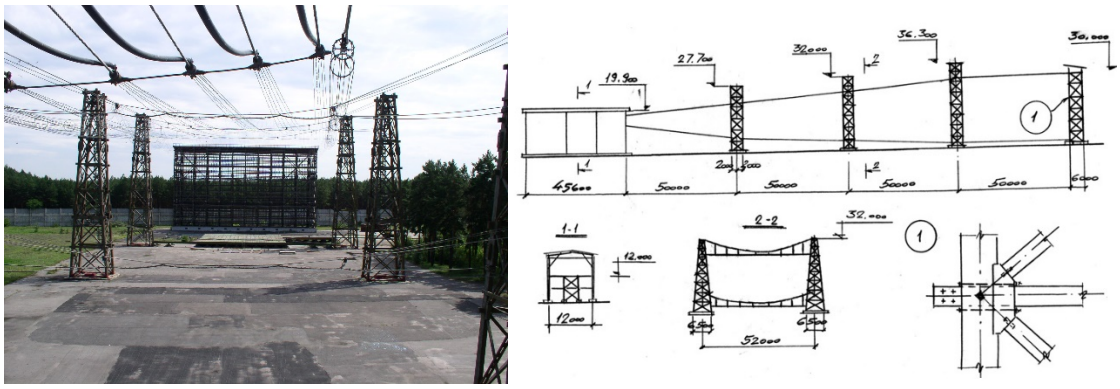

a) terminal device and towers b) general scheme of the complex

c) support fastening on inclined glued-in rods) examination 2011 (Prof. Fursov and PhD-student Bidakov)

Figure 2. Layout of the electrophysical complex towers and the terminal device

The solution of the connections and their development was largely associated with the choice of calculation schemes and installation methods. The tower lattice was designed so that the main direction's diagonals absorbed horizontal loads, including thrust from technological impacts and wind, while the secondary direction's diagonals were exposed only to wind loads. The diagonals were connected to the tower posts by resting on glued intermediate elements, or cushions, in which the boards were placed vertically. The posts of the lattice of the main direction were solved in the form of glued beams passing through special windows arranged in the cushions and the main tower posts.
The main criterion in choosing the solutions for the connections was the ease of assembly, the possibility of evacuating atmospheric moisture, and natural ventilation. Also provided were options for strengthening the nodes and frame elements by installing glued rods, limiting the development of defects and splitting when a discharge flows through. Particular attention was paid to the formed cracks, since they accumulated moisture and changed the electrophysical characteristics of the installation. For this purpose, it was envisioned to fill the cracks and crevices with polymer concrete in the form of epoxy putty (epoxy resin, 20%; hardener, 5%; cement, 27%; dry sand, 48%). Subsequent surveys conducted between 1990 and 2014 confirmed the effectiveness of the measures taken.

METHODOLOGY

The developed design of timber structures for open-air operation envisaged inspection of load-bearing structures by technical personnel responsible for operation at least once a year (in spring). Unscheduled inspections were typically performed in cases where, during the regular inspection, either individual defects in elements or units were detected or significant deformations were noted. Geodetic control of the overall geometry of structures and physical visual inspection of units, including measurements of cracks and local warping, were accepted as primary and mandatory. The assessment of the technical condition of the structure, based on the relative deflections of its elements within a specified range of values, is presented in Table 1, which was developed as the basis for systematic inspections.

Table 1. Technical condition of structures in dependence on the magnitude of deflections of elements

Type of constructive elements	Relative deflections of elements			
	SNiP [1]	Current repairs	Major repairs	Emergency condition
Floorings, sheathings	1/150	1/150….1/100	1/100….1/75	1/50
Rafter legs	1/200	1/200….1/150	1/150….1/100	1/60
Roof purlins	1/200	1/200….1/150	1/150….1/100	1/75
Floor beams	1/250	1/250….1/150	1/150….1/100	1/100
Roof beams	1/200	1/200….1/150	1/150….1/100	1/100
Composite arches on flexible ties (in quarters of the span)	1/250	1/250….1/200	1/200….1/100	1/150
Truss	1/300	1/300….1/200	1/200….1/150	1/175
GLT beams	1/300	1/300….1/250	1/250….1/200	1/175
Thin-walled shell vaults (in quarters of the span)	1/200	1/200….1/150	1/150….1/100	1/100
Deformation in connections, mm	Up to 1	1,5	2-3	3-4

Inspections of the GINT-12-30 electrophysical complex were conducted intermittently at the personal initiative of Prof. V. V. Fursov (in 1993, 1994, 1996, 1999, 2002, 2005, 2011, and 2014), who led inspections with various groups of PhD students. GOST 27751-80 (Art. SEV384-97) "Reliability of Building Structures and Foundations" formulates this point of the state of building structures as follows: "... when, in order to ensure normal functioning for the main purpose, it is necessary to use restrictions and special control over the state of structures, ...". Normal functioning of the complex is the presence of

an electric shock. The elements with cracks remain the most vulnerable in terms of the electrical strength of the insulating structures, as shown in Fig. 3.

Figure 3. Cracks in structural elements and nodes during inspection in 2011

The depth of wood damage by rot was determined by inserting a sharp metal rod and recording the percentage of its destruction. To determine the change in wood strength over time, compression and bending tests were performed on samples at various angles. All the selected samples had no damage from rot but did have cracks.

RESULTS

One of the important results, taking into account the specifics of the GLT structureoperation, was the establishment of the dependence of the wood's electrical strength on humidity (Fig. 4). When exposed to a full pulse wave, the average discharge voltage of dry wood with a sample length of 2–3 m is about 600 kV/m, and wet – 300 kV/m. For dry wood samples 10–12 m long, the average discharge voltage decreases to 180 kV/m, and in the rain, to 150 kV/m. In calculations, the pulse strength of wood supports is taken to be equal to 100 kV/m along the discharge path through the wood.

The conducted studies of standard samples of "old" timber showed that the strength characteristics corresponding to viscous destruction (compression along and perpendicular to the grain) do not differ significantly from the results obtained during testing of new timber. However, under conditions of brittle destruction (tension, bending, and shear), the strength indicators sharply decrease their values. The discrepancies in individual cases range from 16% to 22%.

Statistical processing of tests conducted in different years (see a dissertation by N. Kovlev) showed that the coefficient of variation for viscous destruction (compression and, especially, compression perp) is

characterised by a smaller scatter and ranges from 6.5% to 9.5%, with only slightly higher values in some cases. In studies on chipping, the variation V coefficient increases sharply, which is apparently explained by an increase in the number of internal microcracks that occur in wood due to cyclic atmospheric effects (swelling, shrinkage). This effect is especially characteristic of very dry wood (W = 5% 8%), when the scatter of strength indicators is especially large. When moistening the samples to the saturation point of the fibres, V decreases proportionally to the moisture content due to the phenomenon known as "plasticization" with water.

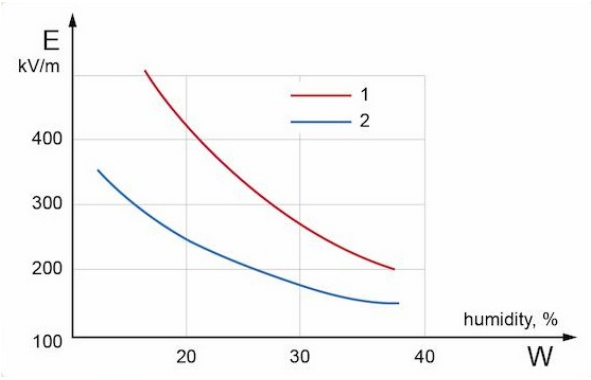

Figure 4. Dependence of the wood's electrical strength on humidity (*wave 1/40 kV/m*).

Compression tests of specimens with different grain orientation relative to the direction of the acting force with the 15˚step in angle change were carried out on specimens of different cross-sections: standard (2x2x3 cm), increased (2x2x6 cm) and large (9x9 cm and 12x12 cm); in the latter not the entire set of angles was considered, but only 0°, 45° and 90°. Fig. 5 shows graphs of changes in the wood strength under compression, tension and bending at different angles for new and old wood. Curve "1" was obtained according to SNiP [1], and curve "2" according to the tensorial equation (1). All series of tests were carried out using specimens cut from new or old wood that was undamaged by rot, allowing for a more reasoned comparison of the strength characteristics of the series tested in different years.

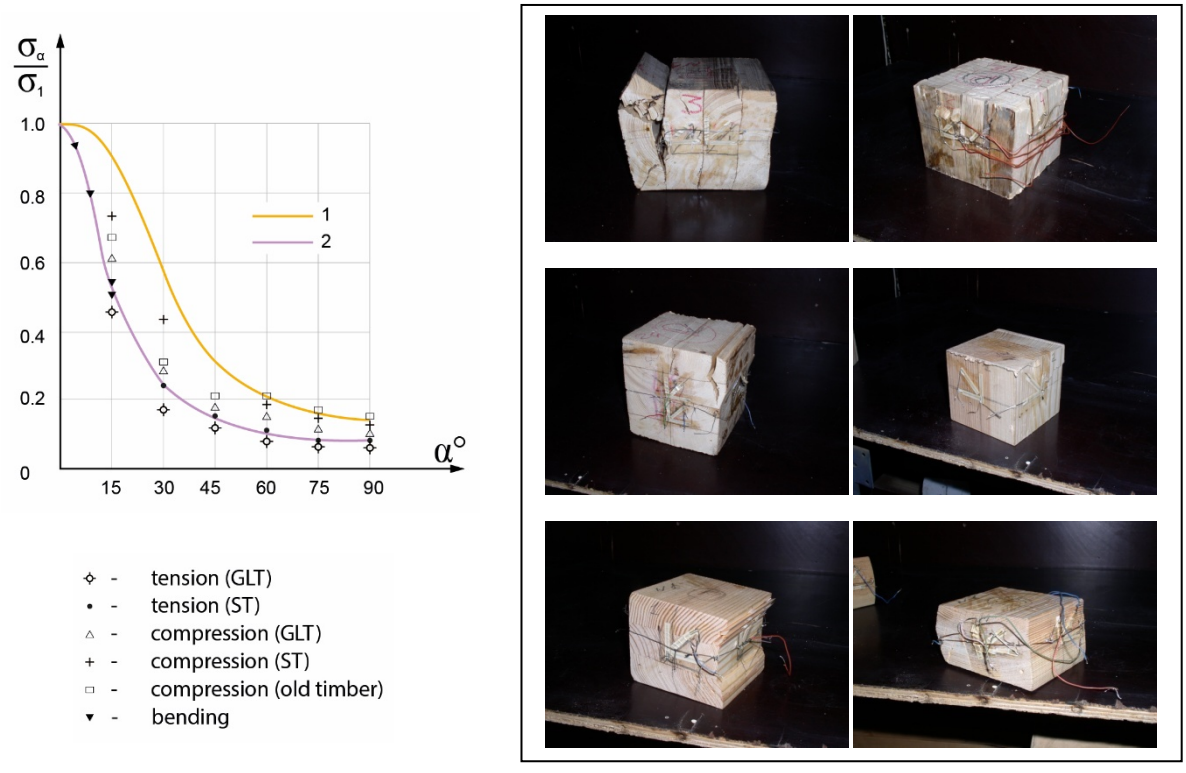

Figure 5. Combined diagram of elastic anisotropy of wood (*a*) *and the nature of sample destruction* (*b*)

Large samples exhibited longitudinal cracks with varying opening sizes ranging from 2 to 3.5 mm, with a penetration depth into the section of up to 43 mm. When making samples, the outer zones of the original beam were discarded, so the core zones fell into the section.

For samples of old wood, a sharper decrease in strength was noted at angles from 15° to 30°, after which a kind of alignment of all curves occurred. In this case, the modulus of elasticity E of "old" wood for angles corresponding to the natural oblique grain (~6º) decreases in strength characteristics more sharply than in new wood. The nature of destruction in all large samples, without exception, was the same: delamination of the cross-section began in the direction of the crack, after which the destruction of a smaller part of the divided volume occurred. The split passed through the core. It does not seem correct to judge the influence of the scale factor on the strength characteristics of "old" wood, although this issue was extremely interesting to many researchers between 1960 and 1985. During that period, the works of B. Madsen [14] and Prof. Yu. M. Ivanov [15, 16] became known, as well as the correspondence between the two scientists, which included discussions on approaches to accounting for the scale factor. The tests conducted on old wood show a sharp drop in the strength limits for samples with a cross-section of 60x60 mm, although its further decrease for samples of 90x90 mm was smooth.

In parallel with the assessment of the strength of "old" wood, a study of its deformation properties was conducted. Analysis of the strain gaging results showed that the modulus of elasticity of "old" wood increases somewhat during operation, which is especially evident when compared with the same indicators of new wood. However, as the cross-section of the samples increases, the value of E decreases. This fact was first noted by N.L. Leontiev [12, 13], who studied the behaviour of wood over time. Poisson's ratios generally retain their values and are within the confidence intervals, but have a certain tendency to decrease. In this regard, the ratio of the modulus of elasticity to the Poisson's ratio of "old" wood increases, which indicates a certain change in the deformation properties. However, one should not forget about the greater heterogeneity of "old" wood, caused by the appearance and accumulation of microstructural damage and microcracks due to shrinkage during operation.

During the reconstruction of the GINT-12-30 electrophysical complex, samples 1,200 to 1,400 mm long were cut out from real dismantled glued-to-laminated beams with a cross-section of 140x600 mm and a length of 4,700 mm, consisting of three and four boards with a cross-section width of 55–56 mm and a height of 90, 60 and 127 mm. The elastic deformation was approximately 0.5 of the destructive load. The nature of the destruction of the experimental beams and the arrangement of the strain gauges are shown in Fig. 6.

a) beams under load and at the moment of destruction

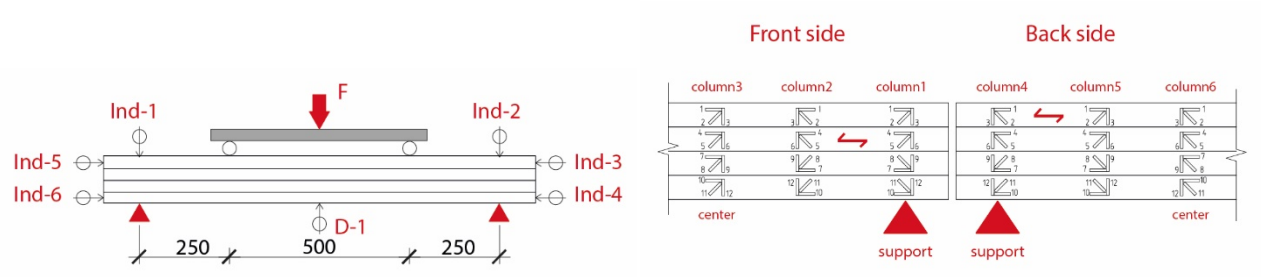

b) scheme of beams tests by bending *c) scheme of strain gauges on the beams*

Figure 6. Destruction of experimental beams (*a*) *and arrangement of strain gauges*(*b*).

The processing of strain gauge readings was carried out according to the recommendations of Prof. E.K. Ashkenazi[3].

$$\sigma_x = \frac{E_x(\varepsilon_x + \mu_{yx}\varepsilon_y)}{1-\mu_{xy}\mu_{yx}} \quad (1)$$

$$\sigma_y = \frac{E_y(\varepsilon_y + \mu_{xy}\varepsilon_x)}{1-\mu_{xy}\mu_{yx}} \quad (2)$$

$$\tau_{xy} = G_{xy}\gamma_{xy} \quad (3)$$

$$\gamma_{xy} = 2\varepsilon_{45} - \varepsilon_x - \varepsilon_y \quad (4)$$

$\varepsilon_x, \varepsilon_y, \varepsilon_{45}$, respectively, the readings of the group of strain gauges in the grain direction are x, perpendicular to the grain direction – y, 45 – the readings of the diagonal strain gauges.

Fig. 7 shows the stress-deflection graphs obtained from the readings of deflection meters and indicators. Within the elastic work limits of glued beams, the discrepancies in deflections between the experimental and calculated deflections at the first stages of loading were 12–14%. As the stress approached the proportionality limit, this discrepancy decreased to 4–5%.

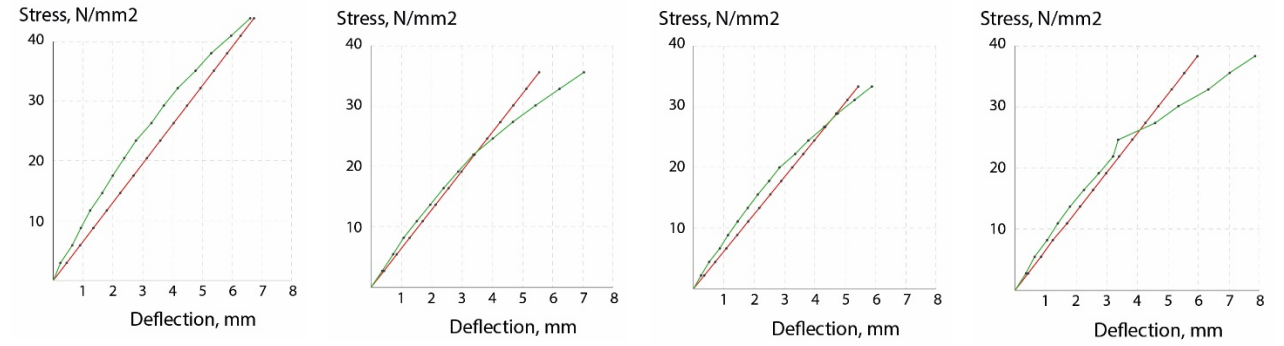

a) b) c) d)

Figure 7. Stress-deflection graphs of experimental beams

The diagrams were obtained from the strain gauges, σ_x corresponds to traditional data with a shift of the neutral axis to the tension zone, then the transverse stresses σ_y, representing values close to a rectangle, at higher stress levels are characterised by a curvilinear dependence with the appearance of two-digit curvilinear diagrams, see Fig. 8.

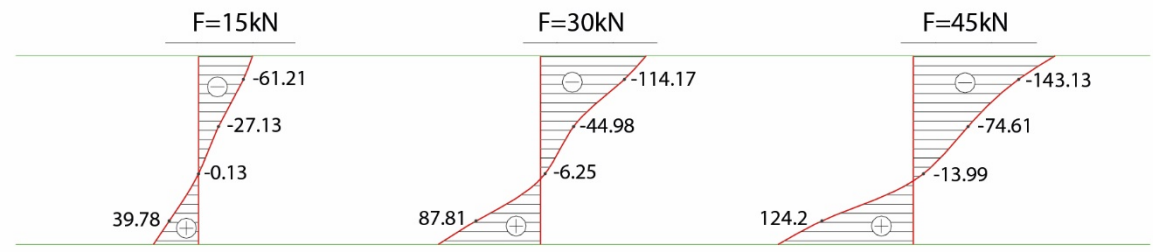

a) diagrams σ_x

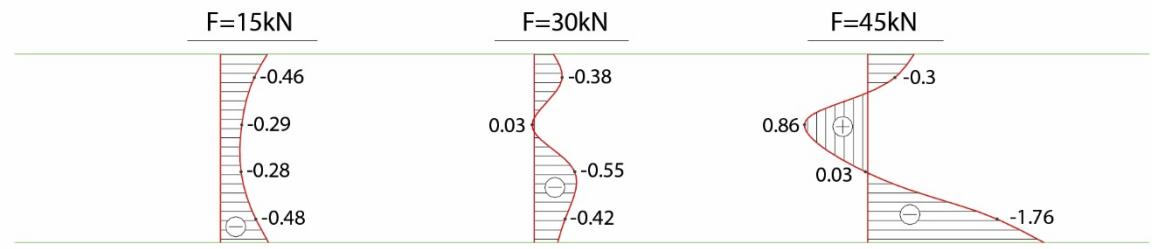

b) diagramsσ_y

Figure 8. Diagrams of normal stresses at different loading levels

According to V. M. Kochenov [17], the highest shear stresses in longitudinal sections of bending elements weakened by cracks can decrease by up to 20% depending on the total crack depth and the type of load. These data were confirmed for elements with a section height of 1/20 and a total crack depth of 1/3–1/2 of the section width. With an increase in the section height of elements to 1/10, the stress reduction reaches 30%.

Cracks in parts of timber structures that operate through shearing (for example, in a notch) can significantly reduce the bearing capacity of the connection due to a decrease in the working shearing planes. In this case, the effect of cracks can be mitigated by reducing the size of the shearing area. The number of such cracks in connections should be limited.

The strength characteristics of wood over-moistened with water are reduced even at a humidity exceeding the saturation point of the fibres. However, in this case, the relationship between humidity and strength is nearly linear. At a humidity lower than the saturation point of the fibers, this relationship is exponential (Fig. 9). Also, the conducted studies of samples of old wood for compression showed an increase in strength with a decrease in temperature, see the graph in Fig. 9-b), where curve "3" comes fromN.L. Leontyev [12] and curve "4" – from Prof. Fursov V.V.

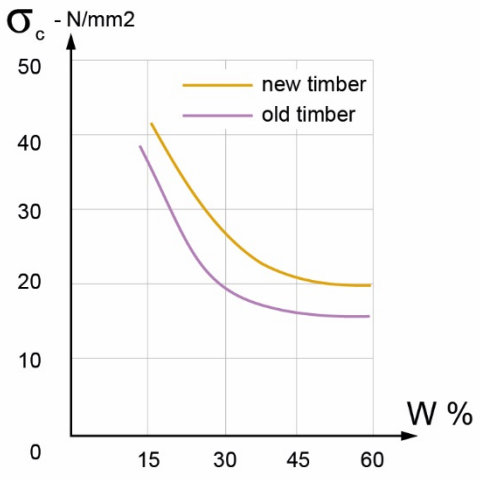

a)

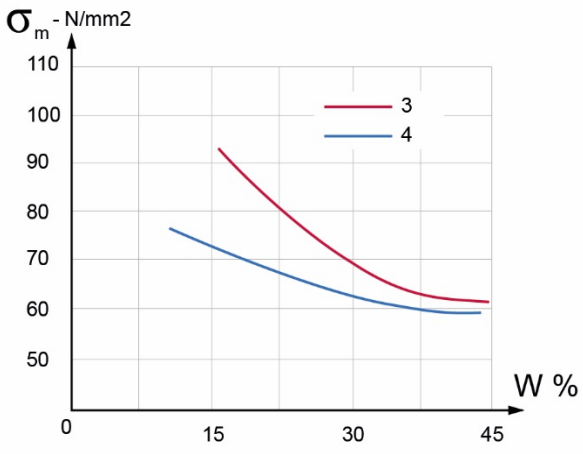

b)

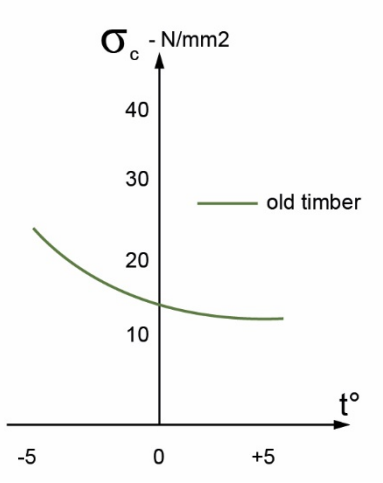

c)

Figure 9. The influence of temperature and humidity conditions on the strength properties of "new and old" wood: a) compression, b) bending under different humidity conditions, c) compression at different temperatures.

Based on the tests conducted and the obtained characteristics of short-term and long-term strength, it is possible to determine the design resistance for wood after its long-term use: Re, for various types of stress-strain state. Taking into account the values of design resistances or strength of wood existing in the standards in force at that time [1], it is easy to determine the operational coefficient Ke = R^e/R, the values of which are given in Table 2.

Table 2. Operational coefficients for "old" wood

№	Type of stress state	K_e	K_e[1]	Notes
1	Bending	0,80	0,75	
2	Tension	0,55*	0,60	In public and civil
3	Compression	0,90	0,90	buildings
4	Compression perp.	0,90	0,95	
5	Shear	0,75	0,70	
6	Module of elasticity	0,90	0,75	

Note: in point 2 (column 3*), data from only one control series were processed.

For the first time in the electrophysical complex, the latest high-strength material of that period, such as wood plastic with a high content of binding glue and very thin layers of veneer, was used. Also, during the development of the GINT-12-30 complex, calculation approaches were developed using volumetric deformation modules necessary to take into account the complex stress state arising both in the elements of the structure and in the nodal connections.

CONCLUSION

The conducted studies on wood samples at different stages of operation, along with 40-year observations of the GLT structure under the supervision of Prof. Fursov, revealed the nature of the change in strength under various stress states. It is possible that the values of reduced strength of old or long-term operating wood somewhat increase due to the operation of the structure under conditions of electromagnetic pulse and high-frequency current, which, during the operation of the complex, heat the wood due to passing currents. As a consequence, crack formation was possibly more intense and, as

a result, wood strength was lower than it would be in the case of a bridge structure operation. The conducted tests of the beams showed that, within the limits of elastic work, the discrepancies in deflections between experimental and calculated deflections at the first stages of loading were 12–14%. As the stress approached the limit of proportionality, this discrepancy decreased and made up 4–5%. The diagrams were obtained from the readings of the transverse stress sensors σy, which are close to a rectangle, but at higher stress levels are characterised by a curvilinear dependence with the appearance of two-digit curvilinear diagrams.

Tests of samples for compression with temperature changes showed that the compressive strength of wood increases significantly for frozen samples and depends to a greater extent on the moisture content of the wood. The operating factors obtained for old wood under various types of stress states reflect the values of strength reduction (Table 2), but without gradation depending on the duration of operation.

REFERENCES

[1]SNiP II 25-80. 1980. Timber Structures, State Committee of the USSR for Construction Affairs.

[2]https://web.kpi.kharkov.ua/molnia/ru/sklad-instituta/eksperimentalnaya-baza-2/

[3] Ашкенази Е.К. Анизотропия древесины и древесных материалов. М.- Лесная промышленность.- 1978.- 221с. (Ashkenazi E.K. Anisotropy of wood and wood materials. M. - Forest industry. - 1978. - 221 p.)

[4] Фурсов В.В., Ковлев Н.Н. Безметальные изоляционные конструкции электро-физических установок// VII Украинская научно-технич. конференция: «Металлические конструкции»: «Взгляд в прошлое и будущее» К. 2004, т.2. Стр. 167-173. (Fursov V.V., Kovlev N.N. Metal-free insulating structures of electro-physical installations// VII Ukrainian scientific and technical. conference: "Metal structures": "A look into the past and the future" K. 2004, v.2. Pp. 167-173.)

[5] Фурсов В.В., Кошмай Н.Д., Ковлев Н.Н. Влияние влажности на прочностные и упругие характеристики древесины. //Сб. научных трудов ОГАСА «Современные строительные конструкции из металла и древесины». Одесса., 2006 г., с. 246-251. (Fursov V.V., Koshmay N.D., Kovlev N.N. Effect of humidity on strength and elastic characteristics of wood. // Collection of scientific papers of OGASU "Modern building structures made of metal and wood". Odessa., 2006, pp. 246-251.)

[6]Фурсов В.В., Абдурахимов Р.Ф. Исследование безметальных нагельных соединений растянутых элементов башен объектов электротехнического назначения. //В сб. “Применение пластмасс в строительстве и городском хозяйстве” IV Украинской науч.-техн. конф. Харьков. ХГАГХ.-1996.-с.56-58 (Fursov V.V., Abdurakhimov R.F. Research of metal-free dowel connections of tension elements of towers of electrical engineering facilities. // In the collection “Application of plastics in construction and municipal services” of the IV Ukrainian scientific-technical conf. Kharkov. KhGAGH.-1996.-pp.56-58)

[7]Фурсов В.В., Ковлев Н.Н., Стародубов С.Н. Испытания клееных балок электрофизических установок. // Сб. Научных трудов Международного симпозиума «Современные металлические и деревянные конструкции(нормирование, проектирование и строительство). Брест, 2009г. с. 336-341. (Fursov V.V., Kovlev N.N., Starodubov S.N. Testing of glued beams of electrophysical installations. // Collection of scientific works of the International Symposium "Modern metal and wooden structures (standardization, design and construction). Brest, 2009. pp. 336-341.)

[8] Фурсов В.В., Ковлев Н.Н., Кошмай Н.Д.,Стародубов С.Н. Исследование клееной древесины на сжатие после длительной ее эксплуатации. //Сб. научных трудов ОГАСА «Современные строительные конструкции из металла и древесины». Одесса., 2005 г.т.1, с. 247-252. (Fursov V.V.,

Kovlev N.N., Koshmay N.D., Starodubov S.N. Study of glued timber compression after its long-term operation. // Collection of scientific works of OGASU "Modern building structures made of metal and wood". Odessa., 2005, v.1, pp. 247-252.)

[9] Фурсов В.В., Кошмай Н.Д., Ковлев Н.Н. Исследование модуля объемной деформации клееной древесины. //Сб. научных трудов ОГАСА «Современные строительные конструкции из металла и древесины». Одесса., 2006 г., с. 240-246. (Fursov V.V., Koshmay N.D., Kovlev N.N. Study of the modulus of volumetric deformation of glued timber. // Collection of scientific works of the OGASU "Modern building structures made of metal and wood". Odessa., 2006, pp. 240-246.)

[10]Фурсов В.В., Ковлев Н.Н. Учет сложного напряженного состояния клеенных деревянных конструкций.// VKONFERENCJANAUKOWA. DREWNOIMATERIAŁY DREWNO POCHODNEW KONSTRUKCJA CHBUDOWLANYCH, Szczecin 17-18 maja 2002r, c.25-30

[11]Фурсов В.В. Работоспособность деревянных конструкций при различных загружениях и эксплуатационных воздействиях. // Докторская диссертация. Полтава-1996.-441с. (Fursov V.V. Performance of wooden structures under various loads and operational impacts. // Habilitation Doctoral dissertation. Poltava-1996.-441s.)

[12] Леонтьев Н.Л. Длительное сопротивление древесины. - М.- 1957.- 132с. (Leontiev N.L. Long-term resistance of wood. - M. - 1957. - 132 p.)

[13] Леонтьев Н.Л. Упругие деформации древесины. - М.- Л.-1952.- 117с. (Leontiev N.L. Elastic deformations of wood. - M.- L.-1952.- 117s.)

[14]B. Madsen, A. H. Buchanan. Size effects in timber explained by a modified weakest link theory. Canadian Journal of Civil Engineering, April 1986. https://doi.org/10.1139/l86-030

[15] Иванов Ю.М. Предел пластического течения древесины. // -М.- Стройиздат.- 1948.-с.6-27. (Ivanov Yu.M. Limit of plastic flow of wood. // -M.- Stroyizdat.- 1948.-p.6-27.)

[16]Иванов Ю.М. О длительной прочности древесины по результатам испытанияобразцов крупного размера. // Известия вузов. “Лесной журнал”.- 1978.- т1. (Ivanov Yu.M. On the long-term strength of wood based on the results of testing large-sized samples. // News of universities. “Forestry magazine”. - 1978. - v1.)

[17] Коченов В.М. Несущая способность элементов и соединений деревянных конструкций. - М.- 1953.- 320с. (Kochenov V.M. Bearing capacity of elements and connections of wooden structures. - M. - 1953. - 320 p.)

GENERAL ASSESSMENT, DIAGNOSTICS METHODOLOGY

THE EARTHQUAKE-RESISTANT WOODEN BUILDING CULTURE IN ANATOLIA – AN EVALUATION OF THE FORMATION CONDITIONS

Hülya DIŞKAYA

Mimar Sinan Fine Arts University

Invited lecture

ABSTRACT

The Anatolian peninsula has been confronted with numerous severe and destructive earthquakes for centuries due to its location on the Mediterranean Seismic Belt. Wood, an easily accessible building material, has gained importance over time for its lightness, flexibility and tensile strength. In this study, the formation conditions of the traditional earthquake-resistant wooden structures of the Anatolian Peninsula, which has been one of the most important centres of attraction throughout history for different cultures, were examined. It can be said that the structural formation of the settlement, which dates back about 13.000 years, matured through a process of trial and error through interaction with different elements. In this context, it can be concluded that the conditions shaping the formation of multi-layered living spaces on these lands are geographical structure, natural disasters, building materials, modes of production, economy and beliefs, as well as migrations, wars and invasions experienced in the historical process. This study focuses on syntheses based on historical and archaeological readings regarding the effects of these determinant elements on structural and architectural development.

KEYWORDS: Earthquake-resistant, wooden building culture, formation conditions, Anatolia

INTRODUCTION

Türkiye is a settlement surrounded on three sides by the sea, formed by the union of the Thracian and Anatolian peninsulas, which were once the sea Tethys itself [1]. Because of its location on the Mediterranean Earthquake Zone, the region has experienced numerous powerful and destructive earthquakes over the centuries [2]. Wood, an easily accessible building material, has become increasingly important due to its lightness, flexibility, and tensile strength. The use of wood, either alone or in combination with natural building materials such as stone, brick, and adobe, has not only produced earthquake-resistant structures but also created an architecture that respects human life and is in harmony with nature in terms of spatial aspects. Despite its seismic nature, the region's favourable climate, abundant water and natural resources have made it a suitable settlement for many cultures. Consequently, it has a multi-layered structure in terms of history, geography, and beliefs.

The Anatolian Peninsula, including Thrace, comprises seven climatic zones, each with its own unique geographical characteristics. These regions exhibit unique settlement patterns due to their topographic and climatic differences and the natural disasters they encounter. Within each region, these differences, with their positive and negative aspects, balance each other while shaping the socio-economic structure [3]. Archaeological excavations are increasingly providing clear information about the cultures that lived, settled, and intermingled with each other in this region [4]. However, when examining the surviving building stock across all climatic zones of Thrace and Anatolia, it becomes clear that, despite the diversity of cultures that have settled in these lands throughout history, a unique structural and

architectural language has emerged over the course of time. Multi-layered archaeological and structural studies reveal that the later settlers in the region formed a synthetic language based on their interactions with indigenous cultures [5]. It is observed that the factors guiding the formation of the structural systems and architecture of the buildings that have survived to this day, creating a composite environment by connecting them, are also reflective of a life in harmony and respect for nature [6].
The aim of this study is to understand the conditions that shaped the structural and architectural systems of the wooden or wood composite structures in Anatolia. Multi-layered analysis and archaeological research demonstrate that physical and human geographies were decisive factors in the formation of the settlements. By understanding the elements that create a multi-input environment, it will be possible to design new earthquake-resistant living spaces for future generations that are respectful of the past and in harmony with nature.

METHODOLOGY

The traditional Anatolian house is a confluence of many elements during a rather long historical process; these can be listed as: physical geography and topography, seismic structure, climate, material abundance and types, load bearing systems, architectural plan types, human geography, historical geography and layers, production methods, and living space design determined by beliefs. This study selected a few of the most significant elements and adopted them as the structural and architectural foundation. Maps have also gained importance as indicators through which the interactions of these elements can be monitored.

Physical geography and seismic structure of Anatolia

Surrounded on three sides by the Black, Aegean and Mediterranean seas, the Anatolian Peninsula generally has the characteristics of a plateau and is located between the 36th and 42nd meridians north and the 26th and 45th parallels east [7]. The North Anatolian Mountains border it to the north and the Taurus Mountains to the south (Figure 1) [8]. The continuous movement of the Arabian Plate in the northeast is blocked by the countermovement of the Eurasian Plate from the north, and this has led to the formation of the North Anatolian and East Anatolian fault lines, Figure 2 [9].

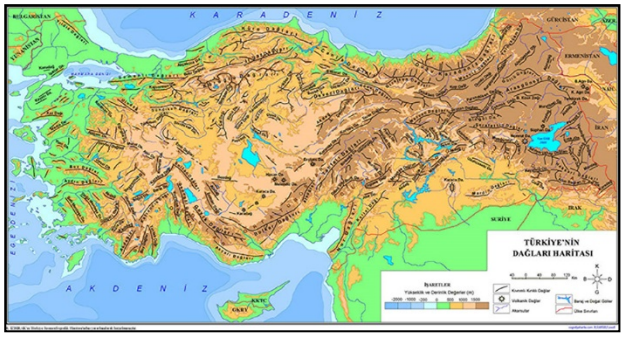

Figure 3. Landforms of Türkiye. (http://cografyaharita.com)

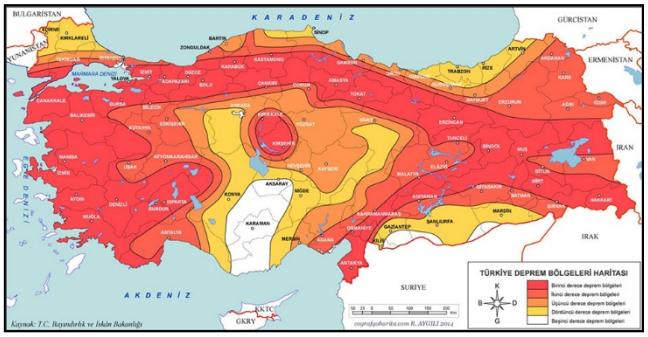

Figure 4. Earthquake Zones of Türkiye, (http://cografyaharita.com)

Relationship between forests and wooden structure settlements

The abundance of easily accessible material was one of the most effective factors in determining both the traditional structure type and fault lines. When the map showing earthquake zones in Figure 2 [9], forest assets in Figure 3 [10] and the distribution of traditional wooden or wood composite buildings in Figure 4 [11] are examined, the relationship between these three concepts could explain why 75% of traditional buildings in Türkiye are timber and 25% are masonry [6].

Figure 5. Distribution of forest assets in Türkiye (T.R. Ministry of Environment and Forestry)

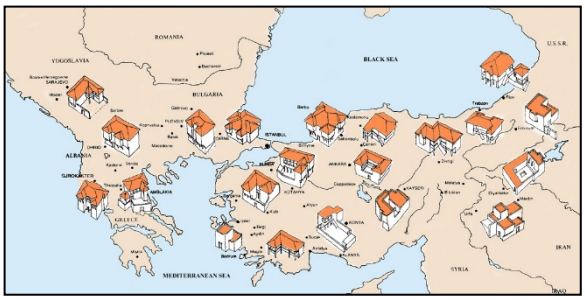

Figure 6. Traditional house distribution in Türkiye (Eruzun, C., Interpretation: Dışkaya, H.)

It is determined that timber material, including decorative parts is used in 90% of traditional structures in Türkiye, and it has been observed that from the coasts up to an altitude of 1.000 meters, deciduous trees, and up to an altitude of 2.000 meters, coniferous trees, have been used for timber constructions in the Black Sea, Marmara, Aegean and Mediterranean regions and northern parts of Inner Anatolia & Eastern Anatolia [11]. The masonry structures were built in the southeast, eastern and some eastern settlements of Central Anatolia; the mud brick structures were built in the central and western parts of Eastern Anatolia [3].

Historical geography

It can be understood that the aspects of historical geography that concern humans are directly related to the settlement processes and the formation of layers. According to the archaeological excavations, it is seen that movements resulting from tribal migrations, wars, and invasions acted as a catalyst for cultural interactions [12]. The map showing the settlements of Anatolia during the Hittite Empire period can help us understand the existence of various cultures in these lands (Figure 5) [13].

Figure 7. Hittite time map of Anatolia (https://www.wikiwand.com/tr/articles/Arzava)

RESULTS

According to archaeological and geographical investigations, the traditional Anatolian house is a product of a continuum in a rather long historical process, with the integration and cultural interaction of the indigenous population with later settlers who immigrated to these fertile lands over time. Thus, the conditions that constitute the traditional building, in terms of their relations with each other, can be listed as: topography and settlement, architectural plan type correlation with predecessors, the effect of living spaces of immigrants, and load-bearing system design with the effect of constructional materials.

Topography and settlement correlation

It appears that the structures were topographically located at the foothills of mountains and hills in traditional Turkish settlements. The purpose of this layout appears to ensure resistance against earthquakes and floods by being on solid ground, while ensuring equitable access to oxygen, light, and view through tiered settlement. This situation should have provided the opportunity to detect external threats and the ability to monitor planting and production areas. Examples of stepped settlements can be seen in Figure 6 for Safranbolu in the northern Anatolia region and Figure 7 for Birgi cities in the western Anatolia region.

Figure 8. Topographic settlement of the houses in Safranbolu (Foto: Dışkaya, H.)

Figure 9. Topographic settlement of the houses in Birgi (Foto: Dışkaya, H.)

Relationship between archaeological findings and architectural definitions

The descriptions of archaeological finds have been an important factor in the reflection and dissemination of the historical chronology of past lifestyles and structural forms. This could cover a wide area, including the depiction of weapons in hunting rituals, musical instruments in religious or social rituals, such as wedding ceremonies, and structural definitions. The resources that provide the link between archaeological finds and architecture can be ordered as follows [14], [15], [16]: archaeological finds of structural foundations, gaps in the horizontal or vertical missing wooden load-bearing elements in the walls, post-fire remains and traces of building materials, hieroglyphic and cuneiform texts from earlier periods, usually written on clay or, very rarely, bronze tablets, architectural depictions on various vessels, structural models made of clay material and reliefs made on stone [17].

Development of architectural plan types

It can be said that the two main elements that shape the Turkish house are the room arrangement and the sofa layout. The room was the central hub where main activities, such as eating, sleeping, and bathing, took place. Meanwhile, the sofa served as the manufacturing area of the house, where all household production occurred, and the rooms opened onto it.

Data obtained from archaeological excavations can provide important information about the evolution of rooms and the sofa during the development of Turkish house plan types, even if the time difference is quite large. Comparing the plan of the Bronze Age residence in Beycesultan, dating back to 5000 BC, in Figure 8 [14], with the plans of the Halil Ağa Mansion in Bursa, dating back to the early 17th century, in Figure 9, can provide an idea of the planimetric influence and development of architecture in Anatolian lands.

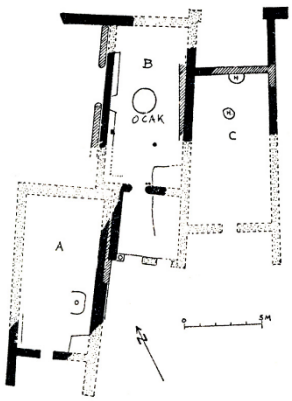

Figure 10. Plan of the Bronze Age House, Beycesultan (Naumann, R.)

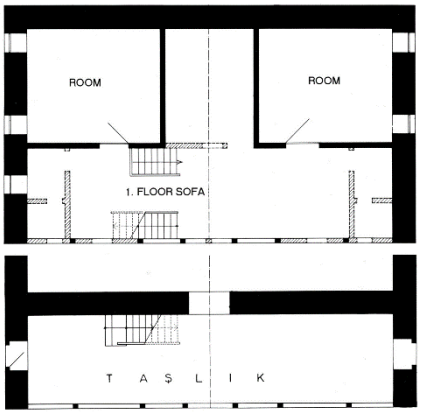

Figure 11. Halil Ağa House, Bursa (Eldem, S. H. E., Interpretation: Dışkaya, H.)

Furthermore, when the spatial configurations of tents belonging to nomadic communities in Anatolia and Thrace are compared with the room layouts of traditional houses, it is seen that shared spatial meanings and harmony are very similar (Figure 10) [14].

In addition, when the interior design of the tents of nomadic tribes and traditional houses in Anatolia and Thrace is compared, shared spatial meanings and alignment also play an important role in the room layout Figure 10 [18].

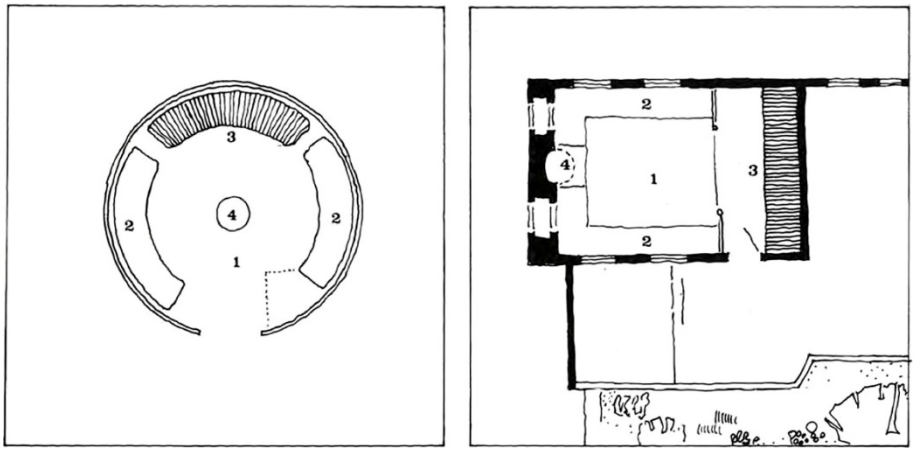

Figure 12. Spatial use of a nomadic tent and a room of a traditional Turkish house (Küçükerman, Ö.)

The Anatolian house, which features a room, common area, courtyard, and sofa setup, expands modularly as the number of family members increases. In this relationship, architectural plan types are classified according to the sofa layout as: without a sofa, with an outer sofa, with an inner sofa, and with a central sofa (Table 1) [3].

Table 2. Planimetric evolution of Turkish House, (Eldem, S. H., Interpretation: Dışkaya, H.)

Relationship between archaeological findings and architectural definitions

While finding concrete traces of wood in archaeological sites is difficult due to its perishable nature, voids and holes in foundations and walls, and traces of burnt wood found in excavations provide significant evidence of its use.
Archaeological data and examination of the surviving traditional building stock reveal three types of structural uses of wood in Anatolia: structures constructed entirely of solid wood with logs and block timber; timber framed structures with no infill or infilled with stone, brick, and adobe; and in the composite structures, the wooden beams were used as stabilisers and binders in foundations and masonry.

Construction with solid wood

This technique, commonly employed in the Black Sea and Mediterranean mountainous regions, utilises two types of wood based on the processing method. In the first one, the trunks were used in their natural condition or peeled (Figure 11). In the second type, the trunks were cut into a rectangular shape (Figure 12). However, in both cases, the wood was connected using an interlocking technique with wooden nails.

Figure 13. A log building from Günpınar village (Photo: Küçükbaş, A.)

Figure 14. A block building from Rize (Photo: Dışkaya, N.)

Timber-framed structures

Timber-framed buildings are the most developed structures in earthquake zones, distinguished by their lightweight and ductile structure. They are found in the Black Sea, Marmara, Aegean, Mediterranean, Central, Eastern, and Southeastern Anatolia regions of Türkiye. The lightest structures were constructed in the Marmara region. These structures were built in two ways, depending on the climatic conditions: stone, brick or adobe infilled (hımış) and unfilled (wood cladding or lath and plaster) systems, generally consisting of 2 or 3 storeys with a timber frame structure sitting on a semi-masonry basement and foundation. The main structure of framed structures consists of three main load-bearing elements: horizontal, vertical and diagonals.

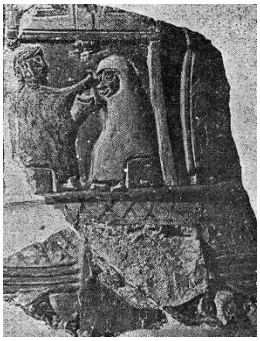

Figure 15. Sacred wedding depiction on Bitik Vase 16th-17th century BC (Darga, M.)

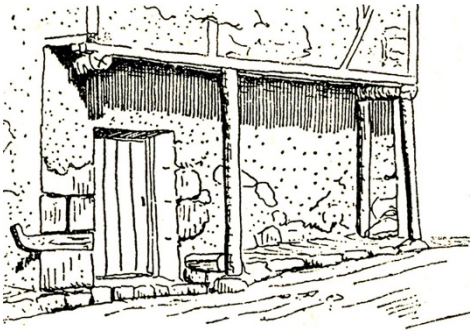

Figure 16. A house illustration from Boğazköy/Çorum (Nauman, R.)

When archaeological data and living examples are examined comparatively, it is seen that the building depictions on ceramic vessels continued until the mid-20th century. Figure 13 [5] shows an example of an infilled framed structure with an external sofa depicting a sacred wedding ceremony on a vase from Bitik Höyük, 16th-17th century BC. The illustration in Figure 14 [14] shows a similar structure that can be found throughout Anatolia.

Accordingly, the 18th-century BC bath pot found at Acem Höyük, shown in Figure 15 [5], is an informative and unique illustration of an earthquake-resistant wooden load-bearing system consisting of wooden joists on headers, placed on wooden posts, and parapets made of diagonal timbers that carried a mudbrick infilled wall [5]. The measured drawing of a Turkish mansion in Figure 16 [3] shows the continuity of tradition despite the time difference of about three thousand five hundred years.

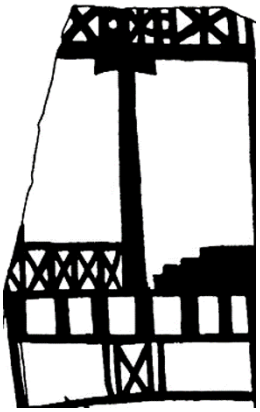

Figure 17. Skeletal system depiction from a Hittite Bath pot 18th century BC, (Darga, M.)

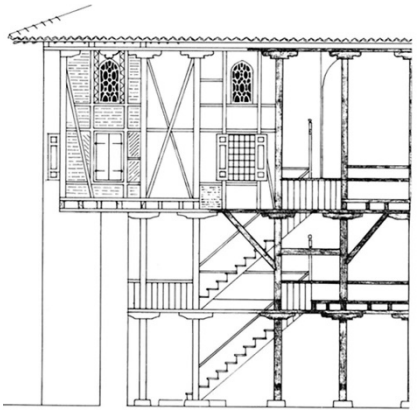

Figure 18. Murad House from the 17th century, Bursa, (Eldem, S. H.)

Composite structures with wooden beams

Wood was an important lacing element in masonry structures, stabilising the walls while bearing vertical loads and maintaining interconnection between structural materials. An example of the timber usage in masonry walls was obtained from the excavations in Zincirli Hilani Tower, 10th century BC, shown in Figure 17 [14]. The traditional continuity in using this structure can be seen in the 19th-century still-standing wall detail from a house in Birgi (Figure 18), from inner western Anatolia, and a house in Erzurum from eastern Anatolia (Figure 19).

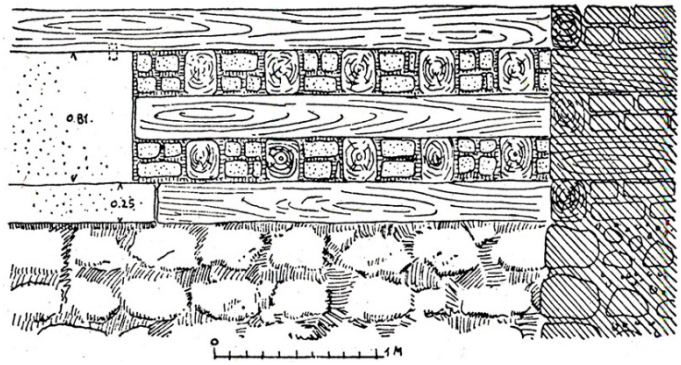

Figure 19. Zincirli, Hilani III, Tower wall from 10th century BC (Nauman, R.)

Figure 20. A house in Birgi, (Foto: Dışkaya, H.)

Figure 21. A house in Erzurum, (Foto: Dışkaya, H.)

DISCUSSION

The study reveals that earthquake-resistant housing production in Anatolia has developed within a multi-component historical process. Regardless of how abundant the data are, it is clear that collective memory serves a specific purpose and function for the benefit of humanity. This situation demonstrates the necessity of looking at the history of cultural production on a global scale from a multifaceted perspective.

CONCLUSION

Traditional houses reflect the spaces where people settled down, carried out their production economy, and continued their social and cultural lives, providing the opportunity to access both tangible and intangible information about past periods. Anatolian settlements, with a history of 13.000 years, have been fertile lands that have witnessed and hosted the transition and rooting of different cultures. It is observed that the culture of shelter and life that emerged here has continued throughout history by enriching and developing its own language. Although their numbers are gradually decreasing, these structures continue to exist today, not only physically but also spiritually, reflecting the past and shedding light on the future.

While earthquakes are inevitable in these lands, Anatolian wooden buildings, with their earthquake-resistant structural systems that respect nature and humanity, deserve to be preserved and serve as inspiration for the future due to their unique architectural and structural features and the values they embody.

REFERENCES

[1] Türkiye fiziki coğrafyası. Türkiye'nin jeolojik özellikleri. [course notes online] [cited 2025 May 10]; 6: [38 screens] Available from: URL https://acikders.ankara.edu.tr/pluginfile.php/85522.

[2] Celep, Z. and N. Kumbasar, Introduction to Earthquake Engineering. Beta Publishing, Istanbul, 2004, p. 22,23,24,25,26.

[3] Eldem, S. H. Turkish House Ottoman Empire Period. TAÇ Foundation, Istanbul. 1984, p. 95, 100.

[4] Yakar, J. Anadolu'nun Etnoarkeolojisi Tunç ve Demir Çağlarında Kırsal Kesimin Sosyo Ekonomik Yapısı, Homer Kitabevi, Istanbul. 2007, p. 15, 33-83.

[5] Darga, A. M. Hitit Mimarisi/1, Yapı Sanatı, Arkeolojik ve Filolojik Data, 1985, p. 60.

[6] Dışkaya, H. The Evolution of Earthquake-Resistant Timber Constructions in Anatolia Based on Archaeological Data, Annals of Geophysics, 62, 3, SE336, 2019; doi: 10.4401/ag-7996, p. 3-6.

[7] The geographical coordinates of Türkiye. [cited 2025 June 02]; Available from: URL https://www.gysakademi.com/pdfler/ders/turkiye_cografyasi.pdf.

[8] Landforms of Türkiye. [cited 2025 May 02]; Available from: URL http://cografyaharita.com/haritalarim/2a-turkiye-fiziki-haritasi.jpg

[9] Earthquake Zones of Türkiye. Figure 2 Available from: URL http://cografyaharita.com/haritalarim/4iturkiye-deprem-bolgeleri-haritasi.png.

[10] Forest distribution of Türkiye. [cited 2025 June 12] Available from: URL http://www.ogm.gov.tr.

[11] Eruzun, C. Turkey: Pilgrimage to cities, In: Process Architecture. Tokyo, 1990, p. 59.

[12] Gümüşçü, O. Tarihi Coğrafya, Kavramlar-Tarihçe-Kaynaklar-Mekan-Metod, Yeditepe. Istanbul, 2014, p. 163-165.

[13] The map of Anatolia in the Hittite Empire period BC 2000 [cited 2025 May 12]; Available from: URL www.wikivand.com.

[14] Naumann, R. Eski Anadolu Mimarlığı, Türk Tarih Kurumu, Ankara, 1985, 197, 106, 359.

[15] Yakar, J., Garzon, J.L. The Survival of Ancient Traditions in the Popular Architecture of North-Central Turkey, Expedition Magazine. 18(2), 1976.

[16] Seeher, J. Hattuša Mudbrick City Wall: A Reconstruction Work. Ege Publication, Istanbul, 2007, p. 17, 20, 21.

[17] Dışkaya, H. The evaluation of earthquake-resistant timber-framed buildings in Turkey according to the regional distribution. Proceedings of the 2nd International Conference on Protection of Historical Constructions PROHITECH'14. Mazzolani, F. M., Altay, G. (Ed.). Boğaziçi University Publishing, Istanbul. 2014, p. 676.

[18] Küçükerman, Ö. Kendi Mekanının Arayışı İçinde Türk Evi, Turkish House in Search of Spatial Identity, Apa Ofset Basımevi ve Sanayi Ticaret A.Ş. Istanbul. 1985, p. 62.

ROOF STRUCTURE OF THE BELL TOWER OF ST. MICHAEL'S CHURCH IN VIENNA - EXPERIENCES WITH OBVIOUS NEED FOR REINFORCEMENTS

Georg HOCHREINER

TU Wien, Institute of Mechanics of Materials and Structures

ABSTRACT

In 2022, the rectory of the parish of St. Michael's Church in Vienna was faced with a report on the overall health, as well as plan documents containing reinforcements of the historic timber structures as part of the bell tower. The report, signed by an engineering office following an on-site inspection by a carpenter, included a proposal for reinforcements. This measure is expected to prevent structural failure due to wind actions, such as rocking. Notably, the historic structure, built in 1596, has remained intact and without significant issues until the present day. Against the background of missing sound facts for decision-making, an agreement with all stakeholders on a more professional procedure for fact-finding was reached. A more comprehensive inspection on site and subsequent structural assessment revealed, that the timber structure was rather prone to slide than to rock and structural integrity could be proved by more accurate structural modelling and realistic loading scenarios according to the provisions of EN 1990 [2] and EN 1991-1-4 [3] Therefore, the characteristic of this monument could be preserved without further changes respective amendments.

KEYWORDS: Historic timber structures, structural modelling, reinforcements

INTRODUCTION

In 2022, the rectory of the parish of St. Michael in Vienna [1] was faced with a report on the health as well as the need for reinforcements of the historic timber structures being part of the bell tower. The report was generated by a carpenter as a member of an engineering office after a brief inspection on site, signalling quite good health of the historic timber structure. However, it was completed by a proposal for reinforcements with heavy steel elements and numerous modern fasteners, which should prevent rocking and therefore failure of the structure due to wind actions. Although no immediate need for repair was stated in this report, the institutions were stressed by the fact that the procurement should be provided within two weeks. The approval was already given by the superior building department of the diocese, but not from the National Heritage Agency (Bundesdenkmalamt, BDA) due to still missing argumentation on the real need and effectiveness of the provisions and the fact that the historic structure has been installed in 1596 and has been maintained without significant changes and problems until today. Furthermore, the characteristics and appearance of the monument might suffer from the implementation of modern structural elements.

Given the background of missing sound facts for decision making and the danger of corrupting an important historical monument, the track of repair based only on personal feeling was stopped, and an agreement on a more professional procedure was found with the BDA. A comprehensive structural assessment, now based on the results of a profound documentation of the structure by both laser-scan and supplementary hand measurements, should reveal if repair or respective strengthening of the

existing structure would be necessary at all. This pilot project should serve as a template for future projects.

BUILDING HISTORY

The existence of the tower was documented first in 1400. In 1525, a big fire in the city of Vienna also partially damaged the roof structure. Finally, an earthquake in 1590 destroyed the upper part of the tower. The reconstruction was finished in 1598. In 1626, a rack for bells was installed. During the siege of Vienna by the French army in 1809, the roof structures were damaged several times by bullets and had to be repaired. In 1825, the roof structure had to withstand a heavy storm event. As a consequence, it has been strengthened by additional wooden structural elements in the lower part and the roof covering was renewed. This procedure was repeated in 2000 due to the same reason. Although the roof covering has been replaced and the structure below has been accessible from both inside and outside, the load-carrying structure of the tower has not been documented so far.
Concluding, the roof structure, installed more than 400 years ago, has successfully withstood extreme weather without causing global dislocation or damage to the surrounding buildings.

TYPOLOGY OF THE STRUCTURAL SYSTEM

The typology of the wooden structure is in line with those commonly used in the context of rectangular ground plans. Following the drawings in Fig. 1 and Fig. 2, the wooden structure of the tower may be segmented into an upper and a lower part.

Upper part of the timber structure

The upper part represents the actual roof structure with a height of about 26m and a diameter of about 6 m at the basement at level-4 on top of a masonry wall made of limestone.

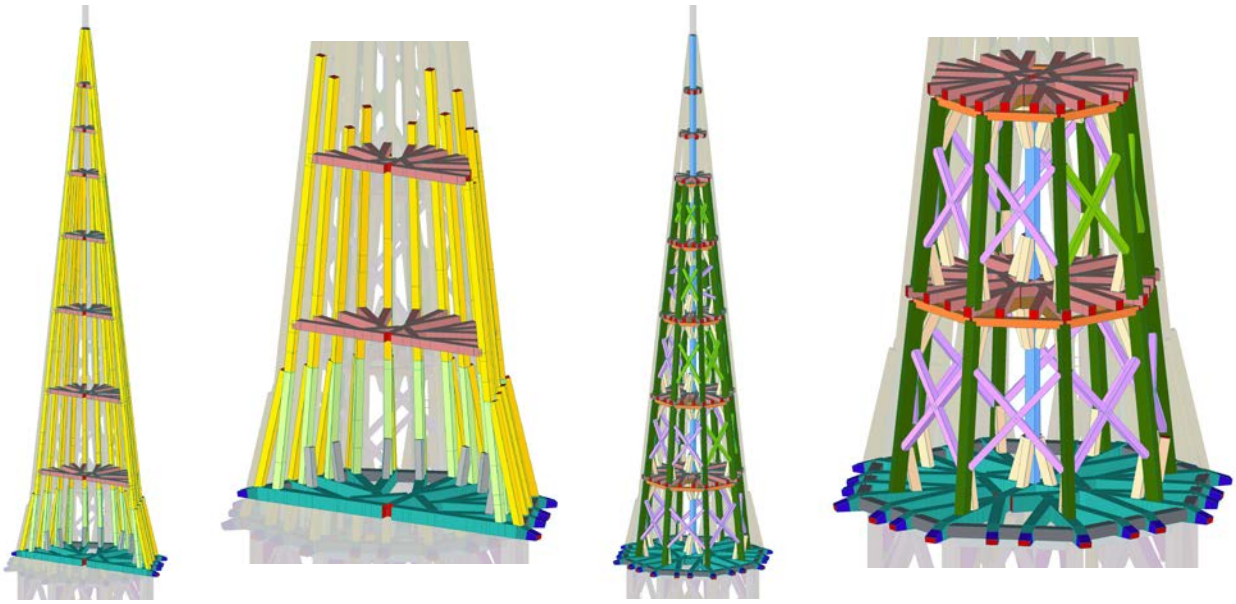

a) Main roof structure *b) Subsidiary structure for installing and bracing*

Figure 1. Typology of the upper structural system

According to Fig. 1a, the structural concept matches a roof consisting of rafters and several levels of collar beams. In its original stage, all angle rafters had a length of more than 22m. In general, such structures have little stiffness against horizontal loads. Therefore, the functionality of bracing had to be added in the context of an additional, frame-like substructure, according to Fig. 1b, in the German

language called "*Liegender Stuhl*". This substructure has also been necessary for the period of installation on-site. Each platform consists of radially allocated elements in the context of the underlying framework and could be used by carpenters during the installation of the long rafters. Bracing elements in terms of St. Andrew's crosses have been installed in every storey between each slightly inclined column of the subsidiary frame structure. Due to the installation of several radial beams in one plane, only two orthogonally crossing beams could be continuous with overlapping at the crossing point. The bending stiffness of this beam grid in the vertical direction and the vertical column at the centre of rotation had to be limited to the height of one storey. Continuity of this column is only possible, respectively necessary for the last three storeys, to work as a cantilever and take the cross on top of the tower.

Upper part of the timber structure

The lower part of the wooden structure, with a height of 17.5 m and a diameter of 5.5 m, is inside the masonry walls and therefore protected against wind load. Surprisingly, this part of the original structure has primarily been strengthened by further elements after the storm in 1825. It is obvious that the amendments from that intervention could also be removed without consequence for the overall stability.

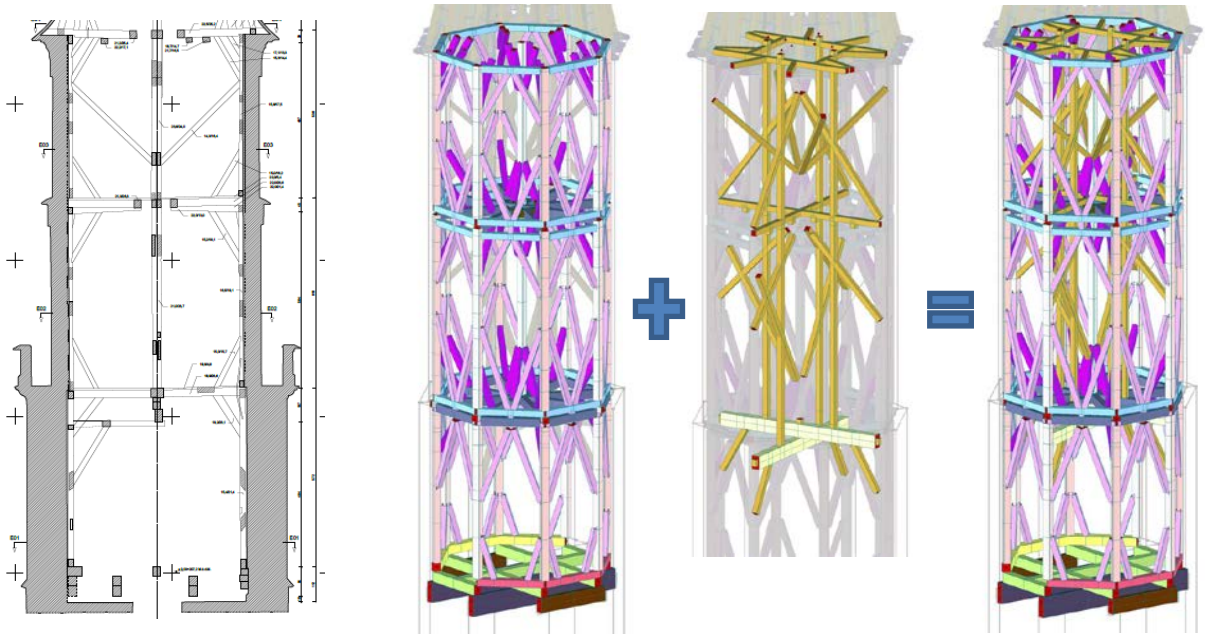

a) Stone wall structure *b) Timber structure inside: Initial system + add-ons*

Figure 2. Typology of the lower structural system

The only job of this part of the wooden structure, according to Fig. 2b, is to host the rack for the bells at the bottom end and to take the vertical load of the column at the centre of rotation at its top end at level-4. Although each vertical column is directly placed below an angle rafter, the direct transfer of compressive vertical loads from the upper part to the lower part is excluded due to a gap of about 2cm between the top end of the columns and the radially allocated elements as a basement for the rafters above. It seems that only knee bracings are intended to additionally support the transfer of vertical loads from rafters above.

Typology of connectors

The typology of the connections is adapted to the needs of the structural elements: *Dovetail connectors* have been used for the bracing elements in terms of diagonal crosses and the connections between collar beams and rafters. *Scarf joints* have been used for the elongation of beams. Shear forces are usually

transferred by *mortise and tendon* joints, which are typically secured in place with *wooden pegs*. Knee braces at the bottom and top end of the slightly inclined columns and rafters at the bottom end at level-4 are only linked by step joints with additional stabilisation by forged nails. Sometimes, the angle rafters are linked to the inclined columns by bolts.

METHODOLOGY OF FACT-FINDING

Before starting the whole process of building documentation, a checklist with content has been formulated to ensure complete information for the stage of structural analysis, and the final decision-making about the need and typology of strengthening:

- All structural elements should be documented, including material specifications such as species, dimensions of the cross-sections, and spatial orientation of the beam axis.
- The typology of connections should be documented either in terms of additional drawings or catalogues with references to the global documentation.
- The documentation should also include notes on local damage and degradation of structural elements and connections resulting from moisture impact or war-related events.
- Just for completeness, carpenter marks that are only relevant during the manufacturing and assembly process should also be documented.

Laser scanning and transfer to a geometrical model

The assessment of geometrical data has been realised by terrestrial 3D laser scans from both inside the structure and outside via drones. During the hearing with potential contractors concerning building documentation, options for adequate and efficient documentation were discussed:

- The generation of a 3D-geometric model based on the point cloud was estimated to be too cumbersome with respect to the 3D-representation of local connections and, therefore, too expensive.
- Following, it was agreed to document the spatial structure in terms of numerous 2D drawings according to Fig. 3. As a consequence, the composition of a 3D structure has been forwarded to the stage of structural modelling.
- The only spatial aspect in the 2D drawing, according to Fig. 3, was the enrichment by layers, to organise and simplify the visualisation of overlapping elements on demand.

Unfortunately, the software packages for an automated conversion of a 3D-point cloud to a structural model without personal contributions or respective mistakes, according to the work of Taskin [4], were not available at that time. For this special project, the time consumption of seven months due to the manual conversion process would have been reduced to a maximum of one week. The special software, according to the work of Taskin, supports the automated generation of datasets representing the structural system in terms of dimensions and beam axis with only rigid links between neighbouring beam elements. This dataset can immediately be exported to a commercial engineering software for subsequent postprocessing, such as hinge specification, application of external loading scenarios, or completion of supporting devices.

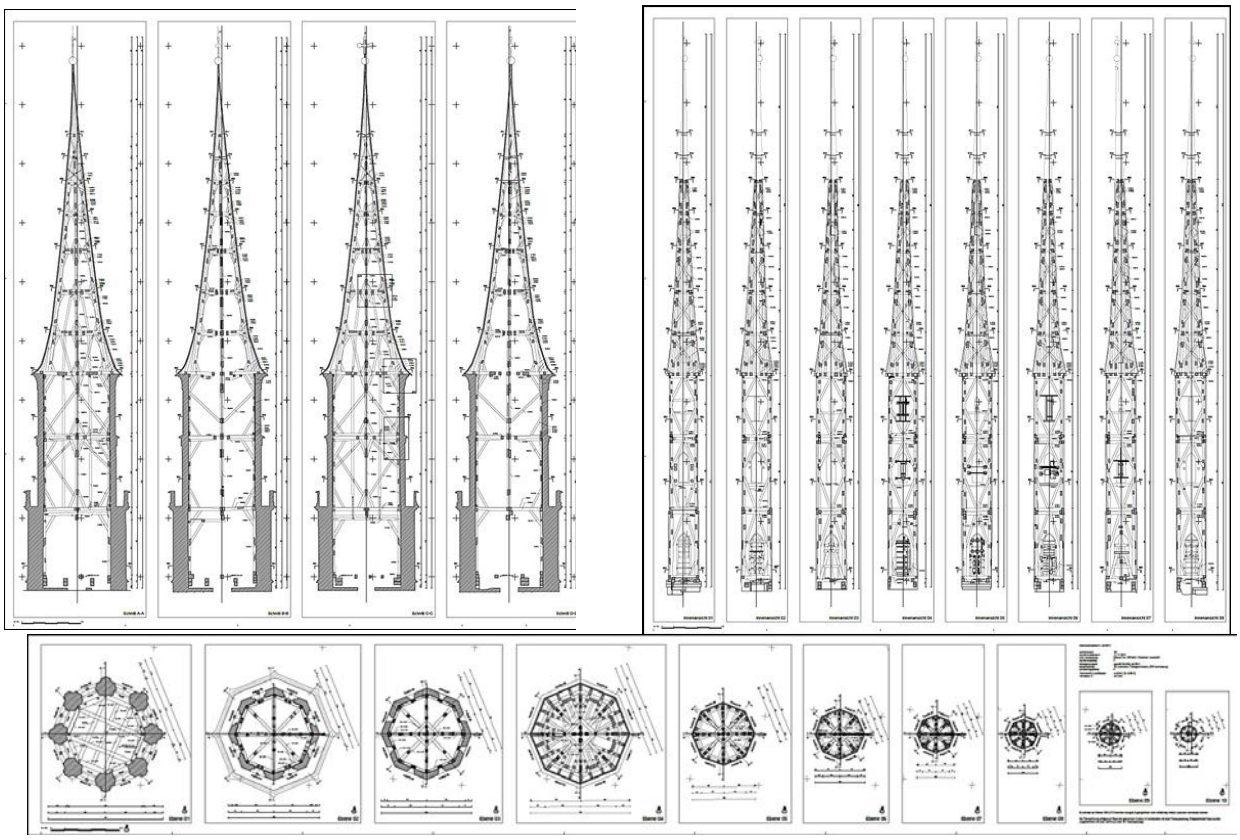

Figure 3. Geometrical database for structural modelling (Plan documents from EKG Baukultur)

Further investigations concerning the typology of connections

3D laser scanning is perfect for the identification of structural elements with the orientation of the beam axis in space and dimensions. Nevertheless, it is nearly impossible to identify the final length of the structural element and the typology of the intersection. In many cases, these critical domains cannot be seen from all sides, and the interior may only be estimated. Therefore, each connection must be re-investigated on site, and the typology and respective special dimensions of the sub-cross-section must be documented in either catalogues, references, or additional special drawings. This stage is cumbersome and cannot be replaced by the application of special software packages. The result in terms of add-ons in 2D plans can be seen in Fig. 4a.

This fact-finding should not only contain the regular connections, but also those from later repair or exchange of damaged structural elements. Sometimes, essential connections are missing or have not been repaired. In this case, an alternative transfer of forces has to be identified. Supplementing photos according to Fig. 4b-g is helpful at the stage of classification of the structural performance, when back in the office.

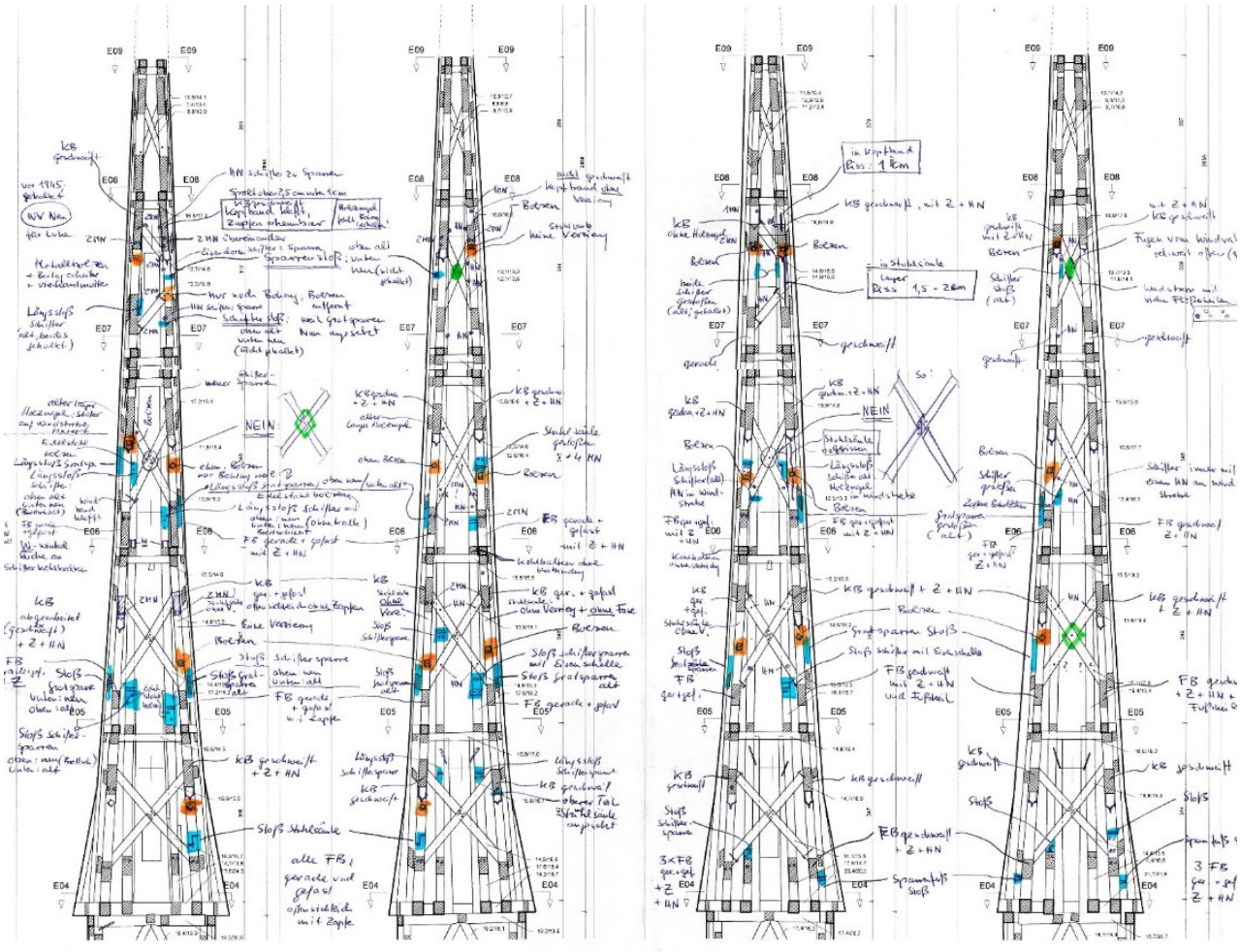

a) Second stage of manual documentation on site

b) Bolts

c) Nails

d) Tie-elements

e) New materials

f) Degradation

g) Mistakes

Figure 4. Subsequent investigation on the local performance of connections for final structural modelling

Adequate structural modelling

Structural modelling has to be organised as follows:

- In general, each structural model should *start with the initial geometry* following the master plans and symmetry of the structure. Therefore, the data from the laser scan, which still represents the already deformed geometry, must be adjusted by engineering judgement in line with the designer's intention. It can be assumed that substructures have been realised in a perfect way with stressless beams and straight beam axes allocated along absolutely allocated vertical or horizontal planes.
- The categorisation of individual material profiles helps to directly separate original from added structural elements. Usually, different material models have to be defined for 1D- and 2D-elements.
- The typology of the historic connections implies the *use of rigid connecting elements* for both realistic modelling of structural elements, as they are built, and the correct transfer of internal forces. Hinges have to be formulated at the location of load transfer.

a) Repair in 1825 and 2000 *b) Repair of rafters (l), radial beams (m) and diagonals (r)*

Figure 5. Numerous repairs over centuries

- The categorisation of special settings for hinges is highly recommended. Even if settings are identical, the implementation of several categories supports visual checks of input data for groups of similar structural elements. According to Fig. 5b, it is also helpful to get a survey on the irregular distribution of further connections induced by repair.
- The structural model must also incorporate 2D elements, such as wooden cladding or masonry walls, to be applicable in the context of CFD. Otherwise, the wind might pass through the single structural elements, resulting in much lower wind load for the whole structural system.

The most important benefit of a detailed structural model is its transparency regarding the flow of forces and the availability of all results for the verification stage, eliminating the need for hand-calculation of intermediate results.

Adequate modelling of load scenarios

The specification of wind loads according to EN 1991-1-4 [3] is restricted and does not meet the requirements of the characteristic of pyramidal bell towers:

- According to Table 7.1.1 in EN 1991-1-4, the specification of wind loads for non-circular cross sections in dependency of the flow parameter according to Reynolds is only possible in terms of resulting forces. Nevertheless, the distribution of compressive and tensile forces along the perimeter is necessary for the identification of a realistic load distribution among the affected structural elements.
- The slenderness of the structure must be considered in relation to its impact on the typology of either a dominating laminar or turbulent wind flow characteristic.

- The reaction forces have been derived from tests in wind channels on samples with constant dimensions along and wind flow only perpendicular to the beam axis, but no wind flow around the ends. At least, the upper roof structure represents the typology of a test configuration with wind flow also around its end. The effect is roughly communicated by reduction factors again for samples with constant dimensions.
- For urban areas, the reference height above ground may be set to the average level of the surrounding buildings.

Since the detailed distribution of wind loads acting on a polygonal spire is not included in EN 1991-1-4, realistic wind loads had to be derived from software, which should be based on CFD [5]. The wind profile was taken from the national appendix to EN 1991-1-4. The setting for RWIND-2 in RFEM can be taken from Fig. 6.

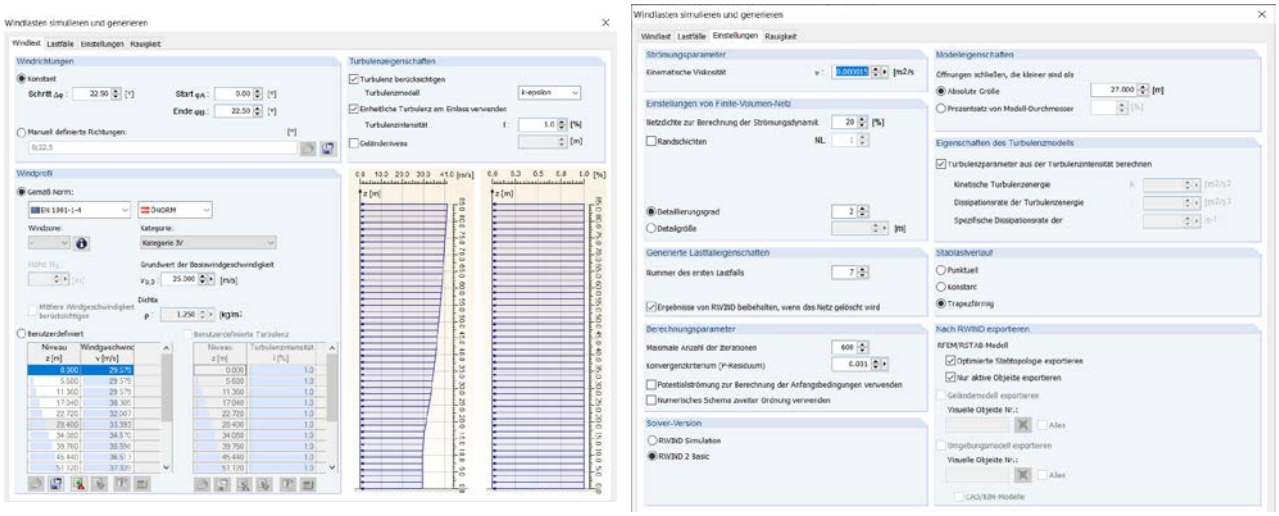

a) Vertical wind profile *b) Further settings for RWIND-2*

Figure 6. Setting for RWIND in RFEM

For an assessment by CFD, the structural model has to be extended by another type of finite element mesh to handle the aspects of fluid dynamics. Structures consisting of single-beam elements have to be covered by a skin to close openings. Otherwise, the wind might go through the structure with numerous openings and end up with much too small wind forces. Depending on the version of the structural engineering software RFEM, the surfaces may be either planes suitable only for load introduction without any structural performance or 2D-elements, such as those used for wooden cladding, which serve as both an element for load introduction and a component in the context of structural load transfer.

As a proof of concept, the results from CFD calculations by RWIND-2 [5] have been compared to the provisions of EC1-1-4 [3].

The distribution of tensile and compressive forces directly exported from RWIND-2 to RFEM is demonstrated in Fig. 7b for two different wind directions at three different levels according to Fig. 7a. Both the intensity and sign of load are qualitatively comparable to the results for a perfect circular cross section as demonstrated in Table 7.27 of EN 1991-1-4 according to Fig. 7c.

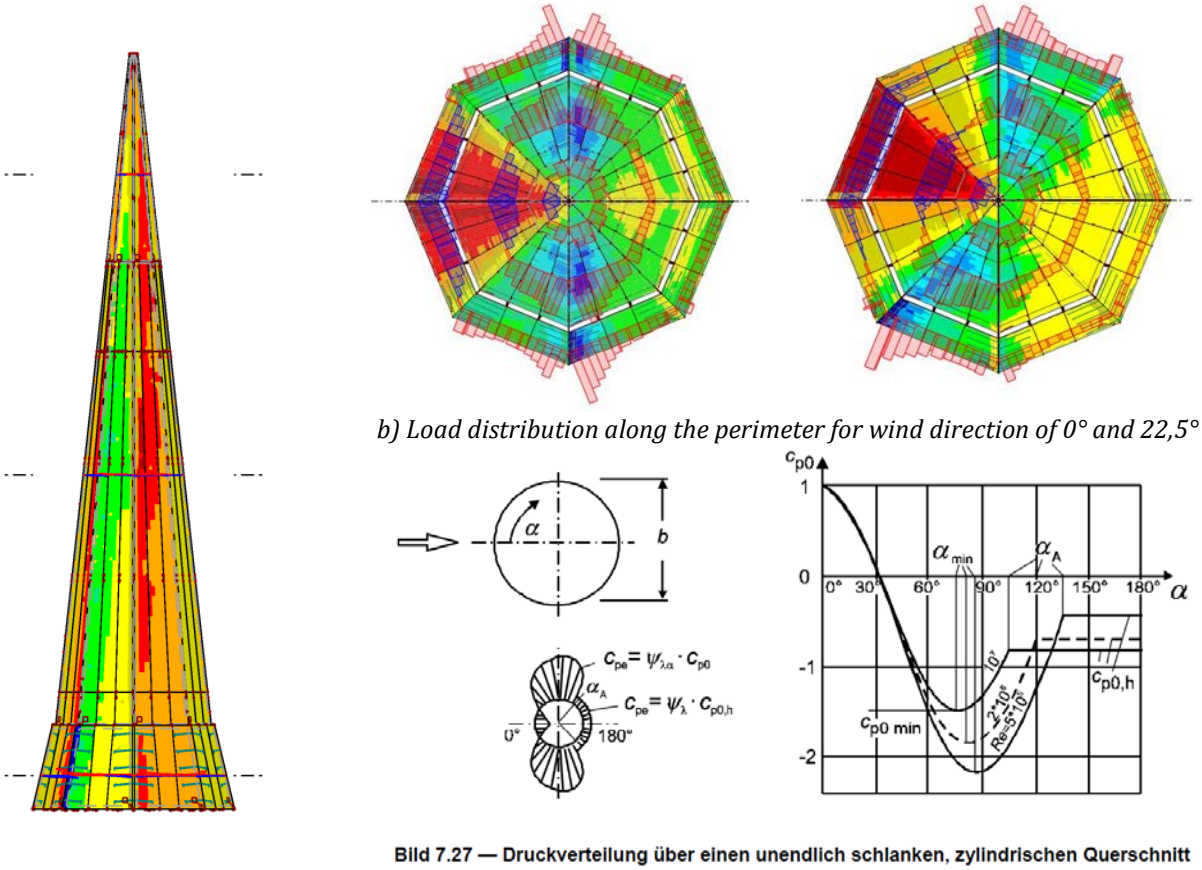

b) Load distribution along the perimeter for wind direction of 0° and 22,5°

Bild 7.27 — Druckverteilung über einen unendlich schlanken, zylindrischen Querschnitt

a) Wind profiles at three levels *c) Comparative load distribution for circular cross sections*

Figure 7. Wind load at the surface of the roofing structure

Structural analysis

Given the background of numerous nonlinearities like contact, friction, asymmetric slip curves and optional ductile behaviour of connections, superposition of single load cases is excluded, and the assessment must be based on load combinations in line with the requirements for second or third order analysis. In any case, the local and global aspects of instability have to be checked.
Incremental load application is highly recommended for the case of nonlinearities as well. Possibly, several types of solvers have to be evaluated to end up with reliable results and acceptable computational costs.

RESULTS AND DISCUSSION

The repair procedure is unknown, but it can be estimated that damaged structural elements have been removed. The surrounding structure then redistributes internal loads according to the newly generated situation. Additionally, gaps and voids have been closed by an adjusted new member that perfectly fits the new volume. As a consequence, stress in new members will only be induced by subsequent external loads, but not by loads applied earlier. This fact also seems to be the reason why the peak of the tower is out of the centre of rotation and inclined to that side of the structure, which exhibits the most locations with repair.

Internal forces had to be calculated for each wind direction due to the asymmetry of the structure induced by nearly randomly distributed connections in the context of repair. This fact can easily be demonstrated in terms of reaction forces of the upper timber structure at level-4 for the load

combination of only dead-load according to Fig. 8a and several other wind directions according to Fig. 8b respective Fig. 8c.

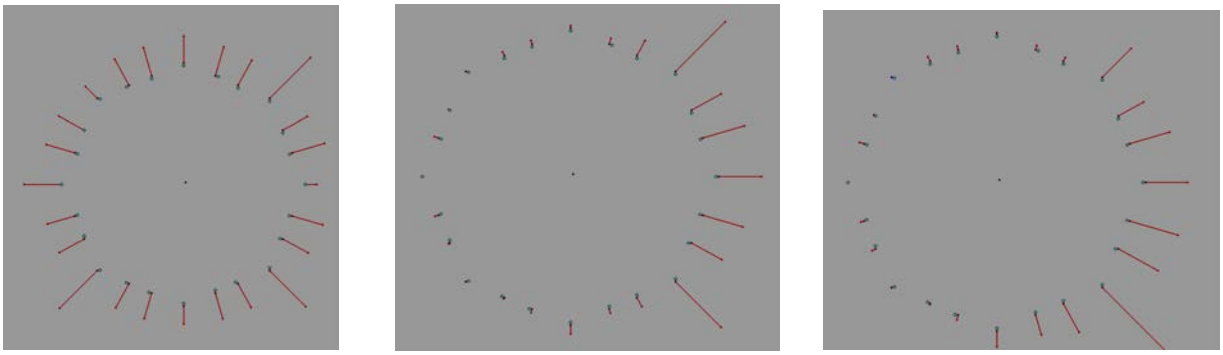

a) Only dead load *b) Dead load and wind from 0°* *c) Dead load and wind from 22,5°*

Figure 8. Vertical reaction forces of the upper roofing structure at level-4

It should be mentioned that according to EN 1990, the reaction forces for all wind directions have been calculated with partial safety factors of 1,0 for dead-load and 1,5 for wind-load. Even these significantly elevated wind loads only induce quite moderate tensile forces in some tie-elements.

The essential result of the structural assessment reveals that the timber structure was rather prone to sliding than to rocking, and structural integrity can be proved by more accurate structural modelling and realistic loading scenarios in line with the provisions of EN 1991-1-4. However, if the historic tie-elements made of forged iron bars according to Fig. 9 might have been inspected as well, the finding of no rocking during the time slot of 400 years could have been proved even without structural assessment.

a) Allocation of tie-elements within the structure *b) Details from the tie connectors with dowel-type end specification*

Figure 9. Initial concept of a tie-connection to prevent rocking

As a matter of prevention, each continuous angle rafter has been connected to the vertical column below according to Fig. 9a. The dowel-type ends of such tie-elements, according to Fig. 9b, are slightly inclined to induce the effect of pretension while being pushed into the timber matrix. Barbs should ensure stable fixation. The absence of embedment deformations indicates that this anchorage system has never been activated, even during heavy storm events.

It should be noted that the tie-elements at level-4 could not have been installed later due to insufficient workspace. Furthermore, it should be noted that, for the same reason, installing the proposed new concept of reinforcing elements would have been impossible.

CONCLUSION

The case study of St. Michael's Church demonstrates that authorities for monument conservation should also incorporate the discipline of structural engineering, rather than relying solely on the proclaimed experience of carpenters based on past realisations. Carpenters are experts in realisation but not in fact-finding in the context of assessment by structural modelling in order to identify the need or type of appropriate reinforcements for historic timber structures. In any case, the effectiveness of reinforcements must be guaranteed, with a minimum number of interventions, thereby saving costs for monument conservation.

Even a comprehensive documentation and qualitative assessment of this historic timber structure would have revealed that in order to prevent global rocking of the upper part, a well-designed subsystem of tie-elements had already been implemented in 1589, but it has never been activated within the timeframe of about 400 years. In conclusion, the characteristics of this monument could be preserved without further changes or amendments.

REFERENCES

[1] Website of St. Michael's Church in Vienna, https://www.michaelerkirche.at, accessed 13.04.2025.

[2] EN 1990: Eurocode 0 - Basis of structural and geotechnical design.

[3] EN 1991-1-4: Eurocode 1 - Actions on structures - Part 1-4: General actions - Wind actions

[4] Taşkın Özkan, 3D Modelling of Historic Timber Structures from TLS, PhD thesis 2025

[5] RWIND-2: Program for the generation of wind loads based on CFD; www.dlubal.com

DENSIFICATION OF WILHELMINIAN BUILDINGS: STRUCTURAL BOUNDARY CONDITIONS AND SCHEME FOR EVALUATING THE LOAD-BEARING CAPACITY OF EXISTING BUILDINGS

Dominik MATZLER[(1) (*)], Gerhard SCHICKHOFER[2] and Andreas RINGHOFER[1, 2]

[1]holz.bau forschungs gmbh, Graz, Austria

[2]Institute of Timber Engineering and Wood Technology, Graz University of Technology, Austria

* corresponding author; dominik.matzler@holzbauforschung.at

ABSTRACT

The increasing demand for densification in inner cities (here: Wilhelminian-era buildings) requires well-founded, resource-efficient structural design solutions. This paper examines the key structural conditions and proposes a framework for assessing the load-bearing capacity of such buildings in the context of densification. The focus lies on foundations, masonry, and historic ceiling constructions.
Based on the FFG research project "Holz-On-Top", a two-stage evaluation scheme is introduced: *"Case A: Preservation of the existing roof structure*" and *"Case B: Dismantling and densification using modular timber constructions"*. For this purpose, a systematic decision-making model is presented that considers structural, legal and heritage preservation regulations. This article provides planners with a structured basis for assessing the structural capacity of Buildings from the Wilhelminian era in the context of vertical extensions, supporting decisions regarding the preservation or ordination of existing buildings in inner-city areas.

KEYWORDS: Buildings from the Wilhelminian era, urban densification, building within existing structures, structural capacity assessment

INTRODUCTION

With the ongoing trend of urbanisation, the demand for housing is steadily increasing in many cities, including in Austria. Cities such as Vienna and Graz have been experiencing continuous population growth. As of the beginning of 2025, the population reached approximately 9.2 million, representing a 0.4% increase compared to the previous year [1]. The degree of urbanisation also rose by 2.2% over the same period [2].
Given the limited availability of land and ecological challenges such as increasing soil sealing in suburban areas, vertical extension and urban densification of well-connected inner-city areas (e.g. so-called “Wilhelminian blocks”) [3] are becoming increasingly important.
The aim of the research project *“Holz-On-Top – Urban Densification with Modular Timber Constructions”* was to demonstrate the suitability and performance of timber as a building material for vertical extensions or roof space densification. To this end, the structural characteristics of typical Buildings from the Wilhelminian era were systematically analysed [4], and a practice-oriented evaluation scheme [5] was developed to assess the structural capacity and suitability of existing buildings for densification measures, which are presented in the following sections.

CONSTRUCTIVE CHARACTERISTICS OF BUILDINGS FROM THE WILHELMINIAN ERA AS A BASIS FOR URBAN DENSIFICATION

When planning a vertical extension or densification of an attic storey, it is essential to examine the existing building's structural features. This is necessary to develop appropriate strategies for assessing and verifying the building's load-bearing capacity and structural stability, and to prevent irreversible damage to the existing structure.

Typical structural elements of Buildings from the Wilhelminian era that are particularly relevant for densification include:

- Foundations
- Walls/Masonry (including façade elements such as cornices, and chimneys)
- Ceilings (type, support conditions, and anchorage)

Further characteristics not listed here can be found in [4].

Foundation

During the construction of Buildings from the Wilhelminian era in the 19th century, the choice of foundation type was primarily determined by the soil type, rather than the soil strength. For sites with "good" soil conditions, shallow foundations (typically strip footings) were generally sufficient for residential buildings. In contrast, for "poor" soil conditions, deep foundations such as pile foundations or caisson wells were used (see Figure 1). The selection of the foundation type typically followed a decision matrix, as illustrated in Figure 2.

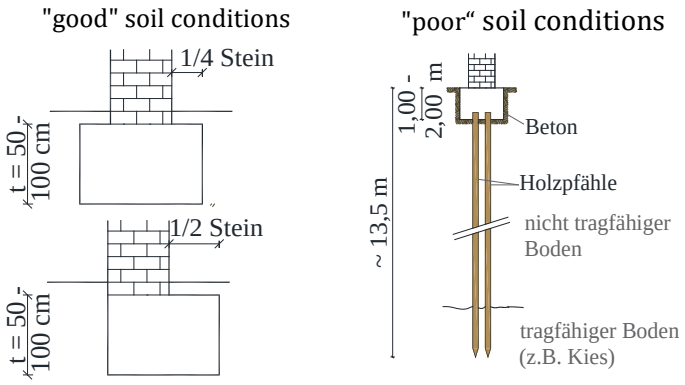

Figure 1. Typical foundation types for Wilhelminian-style buildings: strip foundation and pile foundation [1] [2]

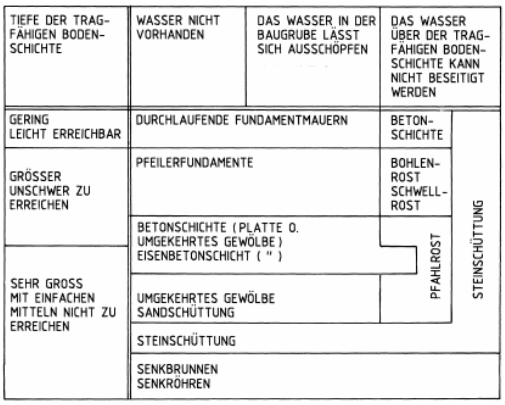

Figure 2. "Selection matrix for determining the most suitable type of foundation" around 1900 [6]

For strip footings, the foundation width a [8] was calculated in such a way that, even under eccentric loading, the foundation remained fully in compression, i.e. the acting normal force N remained within the core zone, satisfying $e \leq a/6$

$$\sigma = \frac{N}{a} \cdot \left(1 \pm \frac{6 \cdot e}{a}\right) = \frac{N}{a} \cdot \left(1 \pm \frac{6 \cdot \frac{a}{6}}{a}\right) < k \qquad (1)$$

$$\rightarrow a > \frac{2N}{k} \qquad (2)$$

Table 1. Design bearing stress limits k for strip footings [7][9]

historical soil classification	design bearing stress limits k [MN/m²]
"good"	0,25 - 0,50
"less good"	0,15 - 0,25
"bad"	0,00 - 0,15

Walls

In Buildings from the Wilhelminian era, the exterior walls, the central wall, and the staircase walls are typically load-bearing. The gable walls, which connect the exterior walls, serve a separating and fire-protective function. The central wall is of particular structural significance in the context of vertical extensions, as it plays a crucial role in transferring vertical loads, although it is often interrupted by chimneys and wall openings in the floor plan [3].

The walls of these buildings were predominantly constructed using single-leaf, unreinforced masonry, typically made from standard-format bricks, either industrially or manually produced, bonded with lime mortar containing locally sourced aggregates [11].

Regarding wall thicknesses, construction tables from around 1900 [12] and the Viennese Building Code of 1890 (see [6], [4]) specify typical wall dimensions, depending on the tract depth (threshold: 6.5 m) and the respective ceiling type.

For ceiling spans under 6.5 m, construction in the attic storey (knee wall area) typically began with a wall thickness equivalent to one brick length (29 cm), based on the Austrian standard brick format as defined in the 1883 Viennese Building Code [4].

Thereafter, the masonry was widened by half a brick length every two storeys (see Figure 3). For spans exceeding 6.5 m, the wall thickness was increased by an additional half brick length. This approach resulted in outer basement walls reaching thicknesses of up to one metre, starting from the attic storey downward.

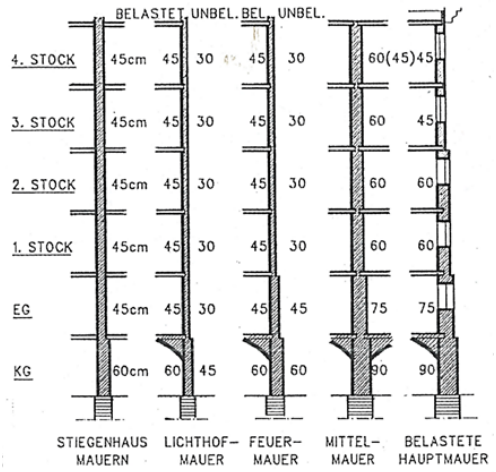

Figure 3. Illustration of the masonry thicknesses by wall type [5]

The thickness of the gable walls was typically 45 or 60 cm in the basement, 45 cm in the uppermost full storey, and 30 cm in the attic. Gable walls were not increased in thickness from storey to storey, as they generally did not serve a load-bearing function [10].

Preliminary Estimation of the Vertical Load-Bearing Capacity of Masonry

In practical applications, reference values for masonry compressive strength can be useful for the preliminary estimation of vertical load-bearing capacity. For this reason, in [4], compressive strength values based on the "σ-permissible" (deterministic) safety concept were compared with those derived from the current semi-probabilistic safety concept and a conversion factor was established.

The component compressive strengths were obtained from sources [6], [10], [5] and [7], and conservative estimates were made using a mean brick compressive strength of $\sigma_{Z,mean}$= 10.0 N/mm² and a mean mortar compressive strength of $\sigma_{M,mean}$= 1.00 N/mm².

The procedures of ÖNORM B 3351:1983 [8] and [16] were applied to convert the values from a purely deterministic safety concept to a semi-probabilistic safety concept, ensuring comparability. The results are presented in Table 2.

Table 2. Comparison of masonry compressive strengths from [4]

	$\sigma_{permissible}$	$\sigma_{\mu.05}$	f_k	f_k	f_k
Determination according to	ÖNORM B 3351:1983 [17]	-	ÖNORM B 3350:1994[17] Eq. (4)	ÖNORM B 3350:1994[17] Eq. (7)	ÖNORM B 4008-1:2018 [18]
Masonry compressive strength [N/mm2]	0,80	2,41	2,67	2,68	2,14

The calculated deterministic value of σ_{zul}= 0.80 N/mm^2 lies within the range of typical permissible compressive stresses for masonry made of artificial stone units (approximately 0.70–1.40 N/mm^2), as stated in [7]. The comparison yields a conversion factor of approximately 3.0 between the old (deterministic) and the current safety concepts.
For a preliminary estimation of the vertical load-bearing capacity, the characteristic compressive strength of masonry constructed as bonded solid brickwork with normal mortar can be estimated using ÖNORM B 4008-1:2018 [18], Equation (C.4), as follows:

$$f_k = 0.80 \cdot 0.60 \cdot {f_b}^{0,65} \cdot {f_m}^{0,25} = 0.80 \cdot 0.60 \cdot 10.0^{0.65} \cdot 1.00^{0.25} \approx 2.00 \text{ N/mm}^2 \quad (3)$$

However, it should be noted that this value serves only as a preliminary structural estimate and does not replace a qualified masonry assessment.

Ceiling constructions

In 19th-century residential buildings, ceilings can be categorized into solid (masonry) and timber constructions. The former were typically implemented as barrel vaults (Tonnengewölben) or Prussian caps (Preußischen Kappen) above basement levels, primarily to improve airtightness and moisture resistance. The vault thickness d was determined based on empirical values, examples of which are provided in Table 3.

Table 3. "Experience values for masonry vaults for normal loads (e.g. living spaces)" [12]

Span s (m)	Arch thickness d (dimension in stone lengths)		Reinforcing belts
	f =s/2	f< s/2	
up to 4	1/2	1/2	without
4-6,30			1/1
over 6.30	1	1 1/2	1 to 2

In the intermediate storeys, so-called Tramdecken (beam-and-fill ceilings) were commonly used, which can be classified into various types: standard beam ceiling (gewöhnliche Tramdecke), false beam ceiling (Fehltramdecke), transverse beam ceiling (Tramtraversendecke), and beam ceiling with infill elements such as cross battens or reed mats (Tramdecke mit Einschub / Kreuzstaken / Windelboden).
This ceiling type consists of hewn beams (or Träme) spaced at regular intervals, typically clad with boarding on both the top and bottom sides, with the cavities filled with loose infill material.
The floor structure was constructed as follows: above the beams, a formwork was installed, onto which approximately 8 cm of infill material was applied. On top of this, leveling battens were often added, followed by the installation of the subfloor (Blindboden) [9]. Typical dimensions of these ceilings are summarised inTable4 .

Table 4. Cross-sectional dimensions of beams for residential beam ceilings (Tramdecken) (with 10 cm infill height, live load 250 kg/m^2), depending on beam spacing and tract depth [12] [12]

Tram distance	Tram thickness [cm]	16/18	16/21	16/24	18/24	18/26	21/26	18/29	21/29	24/29	24/32
e = 80 cm	Tract depth [m]	3,45	4,05	4,60	4,90	5,30	5,70	5,90	6,40	6,85	7,55
e = 90 cm		3,25	3,80	4,35	4,60	5,00	5,40	5,60	6,05	6,45	7,14

In Austrian attic storeys, the predominant ceiling type is the *Dippelbaumdecke* (Dippelbaum ceiling). It consists of fir or spruce beams, sawn or hewn on three sides, and laid edge to edge (*Mann an Mann*). In some historical building codes, the Dippelbaum ceiling was prescribed as the uppermost storey ceiling [20], as it offered superior load-bearing capacity compared to other ceiling types and was better able to support debris loads from the roof structure in the event of a fire. The fire resistance of the ceiling was further improved by adding an 8 cm thick layer of clay or a traditional attic floor topping (*Dachbodenpflaster*). Typical structural heights of Dippelbaum ceilings are illustrated in Figure 4.

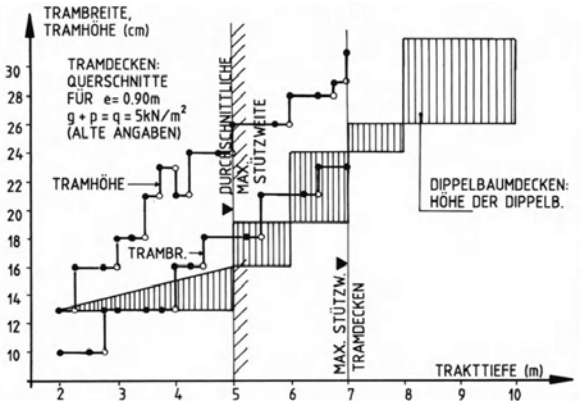

Figure 4. Cross-sectional dimensions of Dippelbaum and beam-and-fill ceilings [6]

SCHEME FOR EVALUATING THE LOAD-BEARING CAPACITY OF BUILDINGS FROM THE WILHELMINIAN ERA FOR URBAN DENSIFICATION

As part of the FFG research project *"Holz-On-Top"*, an assessment scheme was developed in the form of a flowchart to evaluate the structural capacity of Buildings from the Wilhelminian era for vertical extensions and densification. Since densification involving one- or two-storey additions typically requires the removal of the existing roof structure, the scheme is divided into two parts with the following aims:

- Case A: Preservation of the existing roof structure
- Case B: Dismantling of the existing roof structure

An overview of the scheme is shown in Figure5, with the full version presented in Figure 7.

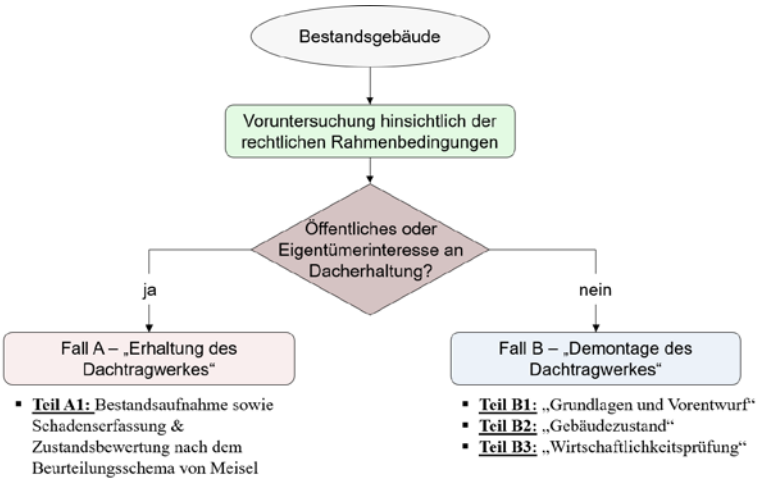

Figure 5. Overview of the evaluation scheme for assessing the structural capacity of Buildings from the Wilhelminian era for urban densification

Case A applies to roof structures considered worthy of preservation due to their historical, structural, or artisanal value. If there is no public or professionally justified interest in preservation, Case B calls for the dismantling of the existing roof structure to allow densification using modular timber construction.

BRIEF DESCRIPTION OF THE FLOWCHART

Both branches of the flowchart (Case A and Case B) are preceded by a preliminary assessment of the applicable legal framework, including heritage protection laws, building regulations, and relevant guidelines. This initial assessment also determines whether there is an interest, either from the public or the building owner, in preserving the roof structure, or whether dismantling of the existing roof structure is permissible.

Case A: Preservation of the Existing Roof Structure

If there is public interest in preserving the roof structure, or if applicable regulations prohibit its removal (due to technical or cultural-historical significance) a condition survey and damage assessment must be carried out in accordance with the flowchart (Case A).

This is followed by a structural condition evaluation of the roof framework, using the assessment method developed by A. Meisel [21], which is based on a school-grade-style rating system (1 = very good condition to 5 = imminent hazard). The evaluation identifies the need for repair or intervention. Based on the findings, appropriate restoration or reinforcement measures can then be implemented.

Condition Assessment of the Roof Structure According to Meisel [15]

The assessment method developed by Meisel (see [21], p. 45ff) for historic timber roof structures in Graz is based on a clearly structured grading system, as illustrated in Figure 6.

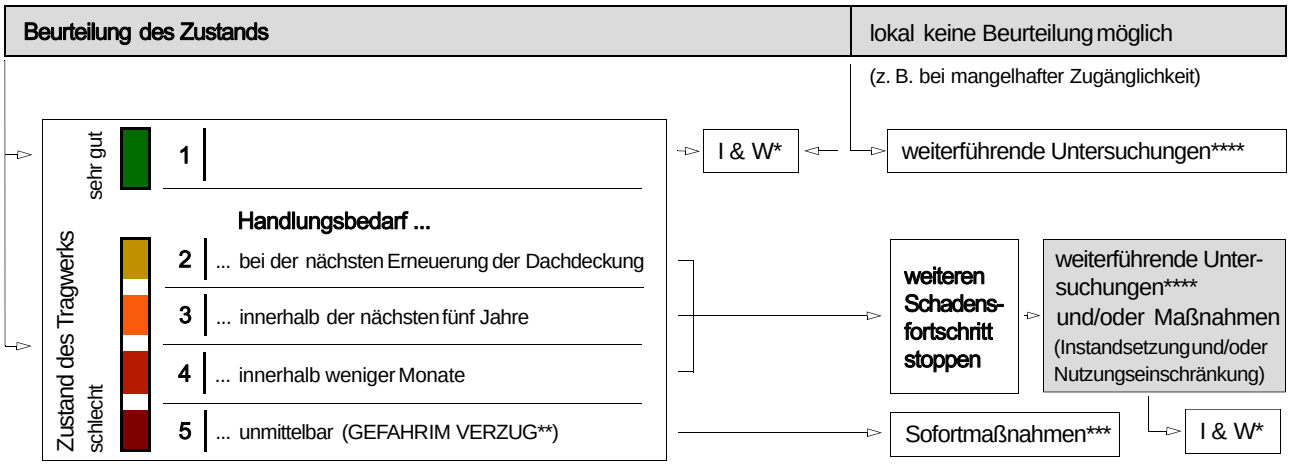

* ... I & W: regelmäßige Inspektion und Wartung
** ... Definition: *Von einer baulichen Anlage ist mit hinreichender Wahrscheinlichkeit eine Gefährdung von Menschen in absehbarer Zeit zu erwarten.*
*** ... z. B. Evakuierung
**** ...Unter „weiterführende Untersuchungen" werden hier insbesondere baustatische Analysen verstanden.

Figure 6. Illustration of the grading system for evaluating historic roof structures by Meisel [21]

The assessment method developed by Meisel [21] is divided into three categories, with a maximum total score of 5 points:

- Damage consequence class: This category considers the structural significance of the roof or its components in the context of potential failure scenarios, as defined in ÖNORM EN 1990:2013 [22]. A maximum of 1 point can be awarded.
- Structural safety: This category evaluates factors such as the load-bearing system and its condition, visible damage and defects, structural indeterminacy, alterations and previous repairs, biological deterioration of timber (e.g. fungal or insect attack), failure of joints or

members, design deficiencies, excessive deformations or cracks, and any signs of progressive deterioration. A detailed explanation of the assessment criteria is provided in Section 3.4.4 of [21]. A maximum of 4 points can be awarded.

- Test loads: This category accounts for exceptionally high loads or targeted load testing, under which no structural damage has occurred so far. In this case, 1 point may be deducted from the total score.

Based on the total score, conclusions can be drawn about the condition of the roof structure and the corresponding need for intervention. The score levels have the following meanings [21]:

1 … Very good condition, no action required
2 … Action recommended during the next scheduled roof renovation
3 … Action required within the next five years
4 … Action required within a few months
5 … Immediate action required ("imminent hazard")

According to Meisel [21], regular inspection and maintenance are necessary even for roof structures in very good condition (score 1). For structures scoring between 2 and 4 points, further deterioration should be prevented through targeted investigations—such as structural analyses—and appropriate repair or reinforcement measures. Structures in very poor condition (score 5), where an "imminent hazard" is present, require immediate emergency measures. These may include, for example, evacuation. "Imminent hazard" is defined as the condition of a structural system in which there is a reasonable likelihood that people will be endangered in the foreseeable future [21].

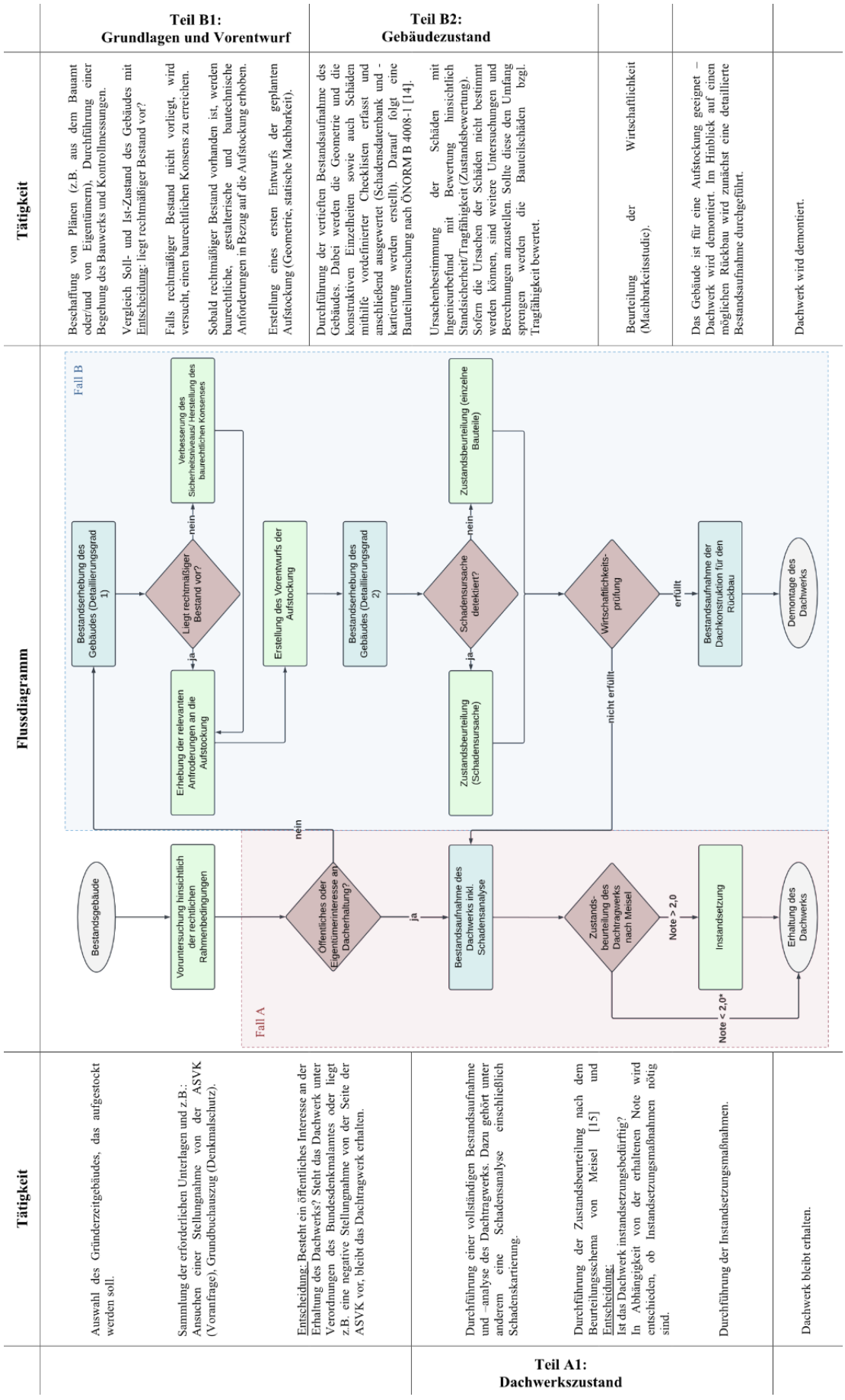

Figure 7. Flowchart of the evaluation scheme for assessing the structural capacity of Buildings from the Wilhelminian era for urban densification

Case B: "Dismantling of the Roof Structure"

If it is determined that there is no public or other interest in preserving the roof or roof structure, "Case B" of the flowchart must be applied. "Case B" consists of three sub-sections: *Part B1* ("Fundamentals and Preliminary Design"), *Part B2* ("Building Condition") and *Part B3* ("Economic Viability Assessment").

As part of *Part B1 "Fundamentals and Preliminary Design",* a building survey is carried out with a low level of detail. In addition to collecting building documentation (archives or building authorities), an initial inspection of the building including control measurements is conducted. The aim is to verify the actual and target condition (keyword: legal conformity (rechtmäßiger Bestand)). Furthermore, the relevant design, building code, and structural requirements for the extension are recorded. Based on the collected information, a preliminary design for the vertical extension can be developed.

As part of *Part B2 "Building Condition"*, the building survey is carried out with a comprehensive level of detail. This includes the following steps:

- Comprehensive survey of the building (level of detail 2)
- Creation of damage mapping and database
- Component investigation in accordance with ÖNORM B 4008-1 [10]
- Determination of the cause of damage
- Condition assessment of the building with regard to structural safety
    - Case a) Assessment of damage causes
    - Case b) Assessment of component damage

The aim of Part B2 is a comprehensive inventory of the building (recording all dimensions and construction details for the structural verifications), whereby the damage to the components is also relevant. For this purpose, dedicated checklists [23] were developed as an aid, summarising the typical construction elements of the 19th century from historical building tables [4], [8], [12] and[24] for each storey or room.

Once the recorded damage has been mapped and compiled in a database, the component inspection in accordance with ÖNORM B 4008-1:2018 [10] can be carried out, based on the collected data and the preliminary structural design. Based on the inspection levels (KL 1: limited knowledge level [20% of KL3], KL 2: normal knowledge level [50% of KL3], KL 3: full knowledge level), ÖNORM B 4008-1 B.5.3.2 [10] defines the scope of on-site and component-specific investigations.

The aim is to document the dimensions of the load-bearing structure, the materials used and their properties, as well as all defects and damage at the time of inspection, in order to determine the causes of damage to the building.

For this purpose, assessment schemes [25], [26], [27], [28], [29], [30] and[31] were compiled from the literature, from which evaluation categories were derived (extent of damage, impact on structural stability, need to restrict use, need for action). These categories are used to classify the causes of damage or component damage according to a grading scale from 1 to 5 (1 = very good condition, to 5 = imminent hazard). In both cases, whether evaluating the causes of damage or the damage to individual components, the overall score corresponds to the highest individual rating. A detailed explanation of the grades and their meanings within the evaluation categories can be found in Table 5.

For completeness, the evaluation scheme was supplemented with *Part B3: "Economic Viability Assessment"*, which is also a key factor in deciding whether densification of the existing structure is feasible, or whether the additional applied loads would require reinforcement measures that are too costly, in which case densification would be inadvisable. However, this aspect was not covered within the scope of the research project.

Table 5. Assessment grades for the condition of the building or its components, with explanations

Grade	Description	Extent of Damage	Impact on Structural Safety	Usability Restriction	Need for Action
1	Very good condition	No or very minor damage. Cosmetic flaws	aesthetic imperfections.	The defect/damage has no impact on the structural safety of the component or structure. The structural safety is ensured.	No restrictions on use required.
2	Good condition	Minor damage or defects on one or more components	with no signs of deterioration.	The defect/damage affects the structural safety of the component	but not the overall structure. Structural safety is ensured.
3	Moderate condition	Moderate damage to components	or several minor damages showing deterioration.	The defect/damage affects the structural safety of the component	with only minor effect on the overall structure.
4	Poor condition	Severe damage to components.	The defect/damage affects the structural safety of both the component and the structure. Further damage may soon endanger safety.	Restrictions on use may soon be necessary.	Repair work should begin as soon as possible.
5	Imminent hazard	Very severe damage/immediate failure of components or the entire structure. Missing load-bearing elements.	Structural safety of both the component and the building is no longer ensured.	Immediate restrictions on use or complete closure until repair work is completed.	Immediate initiation of repair or installation of fall protection required. Emergency measures during inspection

SUMMARY AND CONCLUSION

Densifying Buildings from the Wilhelminian era is a forward-looking strategy for reducing soil sealing in the urban periphery. The results of the Holz-On-Top research project has shown that focusing more deeply on building within existing structures will be essential in the future.

This article first focuses on the structural characteristics of Wilhelminian buildings that are particularly relevant for densification. Building on this foundation, a practice-oriented evaluation framework has been developed to enable the systematic assessment of existing structures' load-bearing capacity. This framework is intended to support planners and professionals in reliably and methodically assessing the structural suitability of Wilhelminian buildings for vertical extensions.

ACKNOWLEDGEMENTS

This project is funded by the Austrian Forest Fund, an initiative of the Federal Ministry of Agriculture and Forestry, Climate and Environmental Protection, Regions and Water Management, and carried out as part of the THINK.WOOD program of the Austrian Wood Initiative.

REFERENCES

[1] A. Kolbitsch, Altbaukonstruktionen, Wien: Springer-Verlag, 1989.

[2] R. Ahnert, K. H. Krause, Typische Baukonstruktionen von 1860 bis 1960, Band 1, Beuth-Verlag, 2009.

[3] K. Hollinsky, LV Bautechnische Analysen und Statik historischer Baukonstruktionen, Technische Universität Wien : Institut für Kunstgeschichte, Bauforschung und Denkmalpflege, 2019.

[4] Bauordnung für die k.k. Reichshaupt- und Residenzstadt Wien, Landesgesetz- und Verordnungsblatt für das Erzherzogthum, Wien, 17.01.1883.

[5] W. Kirchmayer, R. Popp, A. Kolbitsch, Dachgeschoßausbau in Wien, Wien: Verlag Österreich, 2011.

[6] H. Bargmann, Historische Bautabellen: Normen und Konstruktionshinweise 1870 bis 1960, Hamburg: Werner Verlag, 2001.

[7] G. Achs, et. al., Erdbeben im Wiener Becken Beurteilung Gefährdung Standortrisiko, Wien: VCE Holding GmbH, 2011.

[8] ÖNORM B 3351:1983, Wände, aus Ziegeln oder Betonsteinen gemauert, Wien: Austrian Standards International, 1983.

[9] C. Riccabona, Baukonstruktionslehre 1, Wien: Manz Verlags- und Universitätsbuchhandlung, 1992.

[10] ÖNORM B 4008-1: 2018, Bewertung der Tragfähigkeit bestehender Tragwerke, Teil 1:Hochbau, Wien: Austrian Standards International, 2018.

[11] P. Horst, Festigkeitsanalyse ausgewählter Schwerpunkte von historischem Mauerwerk, Diplomarbeit, Staatliche Studienakademie Glauchau, 2013.

[12] A. Pech, A. Kolbitsch, F. Zach, Baukonstruktionen: Decken, Band 5, Wien: Springer-Verlag, 2020.

[13] A. Meisel, Historische Dachwerke – Beurteilung, realitätsnahe statische Analyse und Instandsetzung. Dissertation, Technische Universität Graz, 2015.

[14] holz.bau forschungs gmbh, „Holz-On-Top“ - Checklisten zur Zustandsbewertung von Gründerzeitgebäuden, Graz, 2024.

[15] R. Ruhrberg, Schäden an Brücken und anderen Ingenieurbauwerken Ursachen und Erkenntnisse, Dortmund: Verkehrsbl.-Verl, 1994.

[16] Bundesministerium für Verkehr und digitale Infrastruktur, Richtlinie zur einheitlichen Erfassung, Bewertung, Aufzeichnung und Auswertung von Ergebnissen der Bauwerksprüfungen nach DIN 1076, 2017.

[17] Schweizerischer Verband der Strassen- und Verkehrsfachleute (VSS), Gesamtbewertung von Kunstbauten, Bundesamt für Strassen, 2014.

[18] RVS 13.03.11 - Qualitätssicherung bauliche Erhaltung, Überwachung, Kontrolle und Prüfung von Kunstbauten - Straßenbrücken, 2011.

[19] Bevölkerung von Österreich von 2015 bis 2025 (in Millionen Einwohner) [Graph], Statistik Austria, 11. Februar, 2025. [Online]. Verfügbar: https://de.statista.com/statistik/daten/studie/19292/umfrage/gesamtbevoelkerung-in-oesterreich/.

[20] Urbanisierungsgrad in Österreich von 2013 bis 2023 (Anteil der Stadtbewohner an der Gesamtbevölkerung) [Graph], World Bank, 28. Juni, 2024. [Online]. Verfügbar: https://de.statista.com/statistik/daten/studie/217716/umfrage/urbanisierung-in-oesterreich/.

[21] J. Janković, Erhebung der konstruktiven Randbedingungen von Gründerzeitgebäuden als Grundlage für die Nachverdichtung von Dachräumen in modularer Holzbauweise, Masterarbeit, Technische Universität Graz, 2023.

[22] G. Flatscher, M. Augustin und W. Luggin, Holzbau_Kompakt - Leitfaden zur Wartung und Instandhaltung von Hallen- und Dachtragwerken aus Holz, Wien, Österreichischer Ingenieurholzbauverband (IHBV), 2018.

[23] I. Pirstinger, Gründerzeitstadt 2.1. Die Nachverdichtung von Gründerzeitquartieren - Ein Modell, Dissertation, Technische Universität Graz, 2013.

[24] holz.bau forschungs gmbh, "Holz-On-Top" - Leitfaden & Bewertungsschema zur Beurteilung der Tragfähigkeit von Gründerzeitgebäuden für eine Nachverdichtung, Graz, 2024.

[25] ÖNORM B 3350:1994, Tragende Wände - Berechnung, Bemessung und Ausführung, Wien: Austrian Standards International, 1994.

[26] ÖNORN EN 1990:2013 - Eurocode: Grundlagen der Tragwerksplanung, Wien: Austrian Standards International, 2013.

[27] RVS 13.71. Überwachung, Kontrolle und Prüfung von Kunstbauten - Straßenbrücken, Österreichische Forschungsgemeinschaft Straße und Verkehr (FSV), 1995.

[28] „RI-ERH-ING - Richtlinien für die Erhaltung von Ingenieurbauten - Richtlinie zur einheitlichen Erfassung, Bewertung, Aufzeichnung und Auswertung von Ergebnissen der Bauwerksprüfungen nach DIN 1076," 22 02 2017. [Online]. Available: https://www.bast.de/DE/Publikationen/Regelwerke/Ingenieurbau/Erhaltung/RI-EBW-PRUEF-Erhaltung.pdf?__blob=publicationFile&v=4. [Zugriff am 14 06 2023].

[29] „H. Daub, Hochbaukunde. Teil 3: Stiegen, Türen, Fenster, Abfuhr der Abfallstoffe, Vorbauten, Heizung, Lüftung, Fundamente, Holzbau, Eiserner Fachwerksbau, Leipzig und Wien: Franz Deuticke, 1905".

[30] „H. Daub, Hochbaukunde. Teil 2: Träger, Stützen, Mauern, Decken, Leipzig und Wien: Franz Deuticke, 1909".

[31] „H. Daub, Hochbaukunde. Teil 1: Baustoffe, Leipzig und Wien: Franz Deuticke, 1910".

REDISCOVERING TRADITIONAL CONSTRUCTION STRATEGIES FOR THE SUSTAINABLE CONSERVATION OF HISTORIC TIMBER STRUCTURES

Margherita VICARIO[1], Sara MARRANI[2] and Nicola MACCHIONI[1]

[1] CNR-IBE, Institute of BioEconomy, Sesto Fiorentino (FI), Italy

[2] Opera di Santa Croce, Architectural Heritage Protection Department, Florence, Italy

ABSTRACT

Due to its natural properties and versatility, wood has been one of the earliest materials used in construction. However, as an organic material, it is highly vulnerable to biological degradation, especially when exposed to water leakage and high humidity. Ancient builders and carpenters were aware of these challenges and developed solutions to prolong the lifespan of timber structures. They employed strategies that we would now define as sustainable, such as the careful selection of wood species and the design of construction details that integrated passive design principles and risk-reduction strategies. Over time, much of this practical knowledge has been lost. To ensure the sustainable conservation of timber structures, it is crucial to rediscover and critically reinterpret these traditional building strategies.

The timber roof structure of the Basilica di Santa Croce in Florence provides a notable example of such knowledge, as the builders designed a specific natural ventilation system to prevent the accumulation of water and moisture, protecting the wooden elements from decay. Through this and other examples, the study aims to highlight the importance of rediscovering historical building practices in contemporary conservation, advocating for the integration of traditional and sustainable methods in the restoration of heritage buildings.

KEYWORDS: historic timber structures, cultural heritage, sustainable conservation, natural ventilation, biotic decay

INTRODUCTION

Wood has historically been one of the most widely used construction materials, valued for its mechanical performance, ease of processing, and broad availability across different regions [1]. In historical architecture, its use was widespread for structural elements such as roofs and floors, where timber frameworks often represent well-developed structural solutions that reflect both refined craftsmanship and an empirical understanding of material behaviour. However, as an organic material, wood is inherently susceptible to biological degradation, particularly when exposed to moisture, water infiltration, and extreme environmental conditions. These factors can lead to fungal growth and insect attack, both of which contribute to biotic decay and may compromise the structural integrity and long-term durability of wooden components. Despite this, numerous timber structures have survived the centuries, remaining efficient up to our times.

Understanding the nature of degradations, the conditions under which they occur, and the traditional methods developed to mitigate them is essential for the conservation of historic timber structures [2–

4]. At the same time, this knowledge can also offer valuable insights for the design of more durable and resilient contemporary timber architecture.

BIOTIC DECAY AND COMMON VULNERABILITIES OF HISTORICAL TIMBER STRUCTURES

Biotic degradation in timber structures is caused by biological agents such as insects and fungi [5]. Among the most common wood-boring insects affecting historic architectural elements are Anobiidae, Cerambycidae, and termites. In the case of anobids and cerambycids, their presence is often revealed by small exit holes and fine frass deposits. Insect attack is often perceived as the main threat to timber structures, but its structural impact is frequently overestimated [6], especially when the infestation is superficial (Figure 1a). In many cases, deterioration progresses slowly and may remain inactive for extended periods unless environmental conditions favour insect development. More concerning is termite infestation, whose destructive capacity can indeed be severe. Unlike other wood-boring insects, termites can cause extensive internal damage while leaving few visible signs on the surface, making early detection challenging (Figure 1b). Their colonies can remain active for years, progressively compromising the structural integrity of timber elements, especially in warm and humid climates. In most cases, fungi are the principal agents of wood deterioration [7]. Wood-decay fungi, including brown rot, white rot, and soft rot species, require high wood moisture content to grow and are generally more widespread and structurally damaging than insect infestations, though they are often less apparent in their early stages (Figure 1c). Poor ventilation, high relative humidity, and prolonged moisture exposure create ideal conditions for fungal attack, making this form of biotic degradation particularly insidious in historic timber structures. Fungal attack typically occurs in areas where moisture accumulates, particularly at interfaces between timber and other materials or in poorly ventilated zones where water tends to become trapped. The hygroscopic nature of wood, which allows it to absorb and release moisture from the surrounding environment, makes it vulnerable in such conditions, especially when exposed to condensation, infiltration, or capillary rise.

a b c

Figure 22. Different types of biotic decay in wooden beams (a) galleries and exit holes of anobiid and cerambycid beetles in the outer part, corresponding to the sapwood; (b) termite damage affecting almost the entire cross-section, except for the outer layer, the knots, and the pith; (c) fungal decay affecting the inner part.

In many historic structures, signs of decay often appear in predictable areas, such as beam ends embedded in masonry or contact with other materials, overlapping wooden elements, zones that are poorly ventilated or impermeable, where condensation may form and moisture cannot evaporate. Some

timber assemblies, initially poorly designed, exacerbate these vulnerabilities. Moreover, modern interventions, such as the application of impermeable coatings, the sealing of ventilation paths, or the replacement of traditional breathable materials, have often worsened the issue by compromising the effectiveness of historic passive systems.

TRADITIONAL PASSIVE DESIGN PRINCIPLES AND RISK REDUCTION STRATEGIES

Historical builders were well aware of the risks associated with timber degradation. Their approach was shaped by practical knowledge of material performance and by a resource-conscious mindset, where maximising durability was a necessity due to the high value of raw materials and the labour required for construction [3,8].

Written evidence of this knowledge also appears in historical treatises, where authors from various periods show a deep understanding of timber use in architecture. The first is Vitruvius, who in the 1st century BCE, outlines essential insights into the use of this material in his *De Architectura*. In his Books, Vitruvius emphasises the importance of selecting appropriate materials, properly seasoning timber, and protecting structures from moisture as fundamental strategies for long-lasting construction [9]. His remarks on the vulnerability of certain wood species to humidity and the importance of thoughtful planning reveal a remarkably advanced sensitivity to material behaviour. Although he does not explicitly address biological decay, his focus on keeping structures dry and designing components that are replaceable and maintainable aligns closely with contemporary concepts of passive risk mitigation. Many later authors revisited his writings, adopting some of his recommendations and updating them with the knowledge of their times. In the mid-15th century, in his treatise *De Re Aedificatoria*, Leon Battista Alberti provides specific instructions on how to reduce the risk of deterioration in beam ends, which he identifies as the most vulnerable part of the structure [10]. He recommends that beams rest on perfectly horizontal and solid surfaces, that direct contact between the wood and lime be avoided, and that small openings be left to avoid timber decay caused by exposure to a poorly ventilated environment. He also suggests placing well-dried brushwood, charcoal, or a mixture of olive press residue and olive pits. Other authors instead suggest burning the ends that will be embedded in the masonry, coating them with pitch, or covering them with very thin sheets of lead [11,12].

Following the advances of structural mechanics in the 18th century, practical knowledge based on empirical understanding was gradually replaced by more rigorous mathematical approaches, grounded in a deeper understanding of material behaviour and structural forces.

The gradual loss of empirical knowledge related to traditional construction techniques, combined with the use of new materials often incompatible with historic structures, has led in several cases to interventions that have compromised the original effectiveness of the solutions developed by ancient builders. Today, the growing focus on sustainability and energy-efficient building practices has led to a renewed interest in the field of resource-conscious approaches and traditional strategies developed by ancient builders [13,14]. While several studies have investigated the early forms of passive environmental control aimed at human comfort and the effect on indoor microclimate of historic buildings [15], less attention has been given to the systematic study of strategies specifically designed to preserve materials and mitigate the risks of degradation.

In the context of historic timber structures, several traditional construction details emerge as key strategies for mitigating degradation risks, particularly those aimed at controlling moisture accumulation around wooden elements. Among the simplest and most common solutions were ventilated masonry pocket details, which allowed air circulation around structural elements, helping to keep moisture levels below the threshold for fungal growth. As shown in Figure 2, especially when the structure is not exposed, the pocket where the truss rests within the wall is enlarged to minimise the contact surfaces between the timber and the masonry. This configuration helps prevent moisture

accumulation and promotes air circulation around the embedded timber element. This simple strategy not only contributes to risk mitigation but also facilitates inspection of the structural area most vulnerable to deterioration.

Figure 23. Examples of enlarged masonry pockets at the truss ends

When the roof structure is exposed, for aesthetic reasons, the masonry pocket where the truss rests is often in direct contact with the timber elements. In some cases, to mitigate the risk, the adopted solution was to create a ventilated cavity within the masonry, in contact with the outside through small ventilation holes (Figure 3a). Otherwise, the portion of timber in contact with the masonry is susceptible to deterioration phenomena, such as those visible in Figure 3b. In this example, water infiltration through the roof covering created the conditions for fungal attack. When the masonry surrounding the end of the truss was opened for a detailed inspection, an area with visible fungal decay on the tie beam end was found, along with a particular inverted C-shaped stone element positioned above the rafter to prevent direct contact with the masonry.

a b

Figure 24. (a) Ventilated cavity in the masonry; (b) Inverted C-shaped stone above the rafter and the fungal decay on the tie beam end

Another widespread strategy was the use of sacrificial elements, such as sleepers or thin wooden boards, designed to absorb damage in place of more critical structural components. As shown in Figure 4a, a sleeper positioned below the corbel serves both to distribute structural loads and to reduce the contact surface between the timber and the masonry, thereby limiting potential deterioration mechanisms. Similarly, in Figure 4b, the elements are positioned vertically on either side of the truss members to isolate the timber components from the adjacent masonry. These additional elements were usually made from more durable wood species, which, although less suitable in terms of size and availability for the main structural components of the trusses, were chosen precisely for their resistance and protective function.

a b

Figure 25. (a) Wood sleeper below the corbel; (b) Vertical wood boards on either side of the truss members

THE TIMBER ROOF STRUCTURE AND PASSIVE VENTILATION SYSTEM OF THE BASILICA OF SANTA CROCE IN FLORENCE

More advanced approaches included the integration of natural ventilation systems within the roof structure. These systems were designed to promote continuous airflow, thereby reducing the risk of condensation and helping to maintain dry conditions. A notable example is the complex ventilation system identified in the timber roof of the Basilica of Santa Croce in Florence, which reflects a remarkably sophisticated understanding of building physics, long before such principles were formally codified in modern science.

The Basilica of Santa Croce in Florence is one of the largest Franciscan churches in the world. Already in the first half of the 13th century, the first Franciscans settled in Florence, choosing a marshy area north of the Arno River. With the progressive increase in the number of faithful, the church was rebuilt several times until construction of the current building began in 1294, based on a design by the architect Arnolfo di Cambio. The construction lasted for about a century, and the church was finally consecrated in 1443 [16,17]. The building features a Latin cross plan: the transept, on which the main chapel is set, flanked by five chapels on each side, intersects with the three naves. The central nave is separated from the side aisles by octagonal pillars and pointed arches (Figure 5a).

The roof structure, as in several ancient Franciscan churches, consists of exposed timber framing, with the exception of the chapels in the transept, which are vaulted. The central nave has a double-pitched roof, supported by a primary framework of 31 trusses that carry the secondary framework composed of purlins, three for each slope and two at the ridge (Figure 5b). The purlins in turn support joists

arranged parallel to the slope direction, on which the wooden boarding rests, completed by battens positioned where the boards meet side by side. Resting on the truss tie beams, centrally positioned, is a walkway that runs along the entire length of the basilica. Decorative geometric motifs in white, black, and red adorn the entire wooden roof structure and the walkway. Additional wooden elements, such as closure boards, frames, and cover battens, complete the structure, serving both functional and decorative purposes (Figure 6b).

a b

Figure 26. Basilica di Santa Croce (a) the central nave; (b) detail of the timber structure of the central nave

The trusses follow the traditional Italian typology, consisting of a tie beam, rafters, king post, and struts. They rest on wooden corbels, which are themselves supported by stone corbels (Figure 6a). Set at a height of over 35 meters, the trusses span approximately 22 meters, forming a monumental, imposing, and richly decorated structure that reflects exceptional craftsmanship and knowledge of the material used. All structural elements, except for the corbels, are made of silver fir (*Abies alba*), the most commonly used species in historic structures in the Florence area due to its local availability. Although it has good mechanical properties, it exhibits relatively low natural durability.

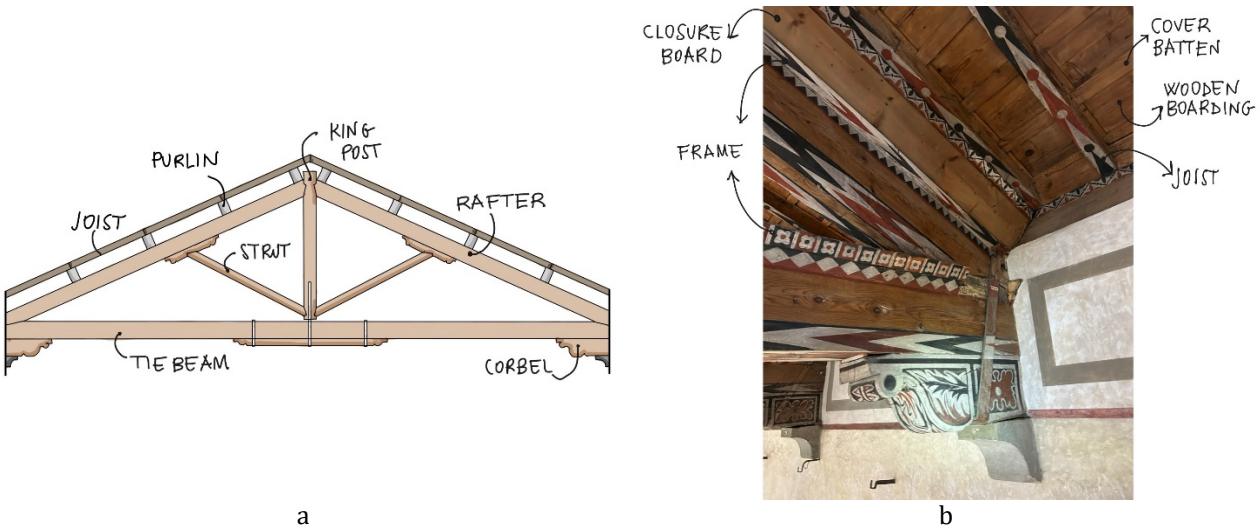

a b

Figure 27. (a) Diagram of the timber structure of the central nave; (b) additional wooden elements

As previously highlighted, the ancient builders were well aware of the main risks associated with the conservation of timber structures. Given the considerable scale of the structure, the challenges

associated with accessing such heights, and the significant costs involved in interventions, both in workforce and materials, specific measures were adopted to prevent deterioration processes that could compromise the structural integrity of the entire roof system.
Particularly noteworthy is the construction detail concerning the area where the trusses rest within the masonry, as well as the configuration of the rafters and ridge beams, which together constitute an effective natural ventilation system. At the level where the trusses rest on the perimeter walls of the Basilica, there is a corridor whose floor serves as the bearing surface for the wooden corbels and trusses. This space is enclosed by two walls, one facing the church interior and the other facing outward, forming a continuous cavity that runs the full length of the central nave (Figure 7). The cavity, accessible through a door located at the intersection between the transept and the central nave, allowed for direct inspection of the truss ends and their ventilation.

a b c

Figure 28. (a) Diagram of the natural ventilation system at the end of the truss; (b) the cavity along the nave; (c) the cavity with ventilation openings on the exterior masonry

The extrados of the rafter, the closure boards, the joists, and the wooden boarding together form a continuous channel that extends up to the two ridge beams located on the sides of the king post head.

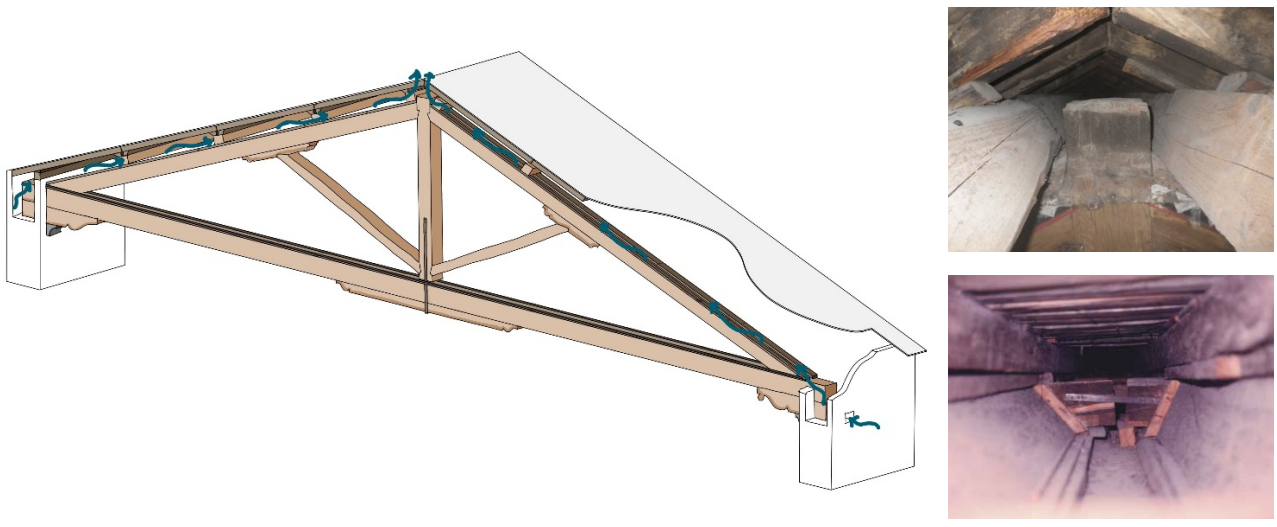

a b

Figure 29. (a) Diagram of the ventilation system; (b) channels above the head of the king posts and the rafters

The space created above the heads of the king posts, enclosed by the closure boards and the wooden roof boarding, forms a second longitudinal channel that runs along the entire length of the central nave, with openings located at the ridge (Figure 8b). These three channels, together with the ventilation openings located on the exterior masonry at the level of the truss ends and the openings at the ridge, created a ventilation system that drives air upward through the chimney effect (Figure 8a).
Furthermore, the strategies implemented in the construction of the roof structure reduce contact points between wooden elements and other materials, thereby minimising the risk of moisture traps. Thanks to this system, the ends of the truss resting within the masonry do not come into direct contact with other materials and benefit from natural ventilation. Additionally, the rafters are not in direct contact with the roof covering but are overlain by a ventilated channel.
The ongoing on-site assessment of the timber structure has shown that the ventilation system has allowed some original elements to be preserved to this day. At the same time, the presence of numerous prostheses and replacement interventions demonstrates how a lack of maintenance compromises the effectiveness of the system. In cases of infiltration through the roof covering, the ventilation system can mitigate the effects but cannot completely prevent them.
To date, 21 of the 31 trusses forming the roof structure of the central nave have been inspected. As shown in Table 1, moisture content (MC) values recorded at the ends of corbels, tie beams, and rafters remain well within safe limits, significantly below the critical threshold of 18% associated with fungal risk. A slight increase of 0.5% is observed at the north-facing supports compared to those on the south side. It is worth noting that the measurements were conducted between November and January, a period typically associated with the highest risk of moisture accumulation. The MC values reflect a generally stable moisture condition across the inspected components and indicate the effectiveness of the system.

Table 3. Moisture content values

Period of inspection	Number of elements inspected	Mean MC (%)	Max MC (%)	Min MC (%)	Mean MC (north) (%)	Mean MC (south) (%)
Nov - Jan	107	12.0	14.0	10.6	12.3	11.7

The analysis of the roof of the Basilica of Santa Croce highlights an advanced design approach for its time, based on a deep understanding of materials and their long-term behaviour. The integration of a natural ventilation system, conceived to promote drying and aeration of the timber elements, evidences a technical awareness aimed at preventing deterioration. This system, together with construction details aimed at minimising vulnerable zones, represents a significant example of sustainable design where functional, technical, and aesthetic aspects are carefully balanced.

CONCLUSION

The assessment of historic timber structures and the evaluation of biotic degradation reveal not only the vulnerabilities of the wood structure, but also the ingenuity of traditional builders in mitigating those risks. These passive solutions, based on empirical knowledge and conscious use of resources, are of considerable relevance today, particularly in the context of heritage conservation and sustainable building practices.
The example of the Basilica of Santa Croce is particularly significant, as it illustrates how advanced design strategies, such as natural ventilation systems and reduced contact between timber and masonry, were employed to prevent moisture accumulation and delay degradation. These measures also demonstrate a deep understanding of building materials and reflect an intentional response to the

intrinsic vulnerability of the available material. Builders were well aware that silver fir, despite its favourable structural properties and broad availability, has low natural durability and is highly susceptible to fungal attack in humid environments.
This case study illustrates how ancient builders were not merely replicating inherited forms, but instead adapting solutions with intent and precision, based on both the performance of local materials and the challenges posed by long-term maintenance. Rediscovering and reinterpreting these traditional practices allows for more informed and respectful interventions. The longevity of historic timber structures relies not only on the initial quality of materials and craftsmanship but also on continuous maintenance, diagnostic assessment, and an appreciation for the historical logic that shaped these systems.

ACKNOWLEDGEMENT

The Basilica di Santa Croce in Florence is owned by the Fondo Edifici di Culto, which is managed by the Direzione Centrale degli affari dei culti e per l'amministrazione del Fondo Edifici di Culto del Ministero dell'Interno.

REFERENCES

[1] R. Ennos, The Age of Wood: Our Most Useful Material and the Construction of Civilization, Simon and Schuster, 2020.

[2] K.E. Larsen, N. Marstein, Conservation of historic timber structures: an ecological approach, Riksantikvaren, Oslo, 2016.

[3] G. Tampone, Il restauro delle strutture di legno: il legname da costruzione, le strutture lignee e il loro studio, restauro, tecniche di esecuzione del restauro, HOEPLI EDITORE, 1996.

[4] J.C.F. de Melo Júnior, M. Vicario, N. Macchioni, Global Trends in Wood Heritage Research: A Bibliometric and Scientometric Analysis, Forests 16 (2025) 326. https://doi.org/10.3390/f16020326.

[5] J.A. Martín, R. López, Biological Deterioration and Natural Durability of Wood in Europe, Forests 14 (2023) 283. https://doi.org/10.3390/f14020283.

[6] M. Brunetti, G. Aminti, B. Pizzo, M. Vicario, M. Nocetti, Evaluation of Timber Degradation Caused by Insects to Quantify the Mechanical Strength of Load-Bearing Elements, International Journal of Architectural Heritage 19 (2025) 633–643. https://doi.org/10.1080/15583058.2024.2362727.

[7] N. Macchioni, M. Mannucci, The assessment of Italian trusses: survey methodology and typical pathologies, International Journal of Architectural Heritage 12 (2018) 533–544. https://doi.org/10.1080/15583058.2018.1442516.

[8] C. Bertolini Cestari, T. Marzi, Conservation of historic timber roof structures of Italian architectural heritage: diagnosis, assessment, and intervention, International Journal of Architectural Heritage 12 (2018) 632–665. https://doi.org/10.1080/15583058.2018.1442523.

[9] Vitruvio, I dieci libri dell'architettura tradotti e commentati da Daniele Barbaro (1567), Il Polifilo, Milano, 1987.

[10] L.B. Alberti, L'architettura, De re aedificatoria (1485), Il Polifilo, Milano, 1966.

[11] S. Serlio, I sette libri dell'architettura (1584), A. Forni, 1978.

[12] V. Scamozzi, L'Idea dell'Architettura universale (1615), tip. Borroni e Scotti, 1838.

[13] S. Lidelöw, T. Örn, A. Luciani, A. Rizzo, Energy-efficiency measures for heritage buildings: A literature review, Sustainable Cities and Society 45 (2019) 231–242. https://doi.org/10.1016/j.scs.2018.09.029.

[14] M. Correia, L. Dipasquale, S. Mecca, eds., VERSUS: Heritage for Tomorrow: Vernacular Knowledge for Sustainable Architecture, Firenze University Press, 2014. https://doi.org/10.36253/978-88-6655-742-5.

[15] M. Pretelli, K. Fabbri, eds., Historic Indoor Microclimate of the Heritage Buildings, Springer International Publishing, Cham, 2018. https://doi.org/10.1007/978-3-319-60343-8.

[16] F. Moisé, Santa Croce di Firenze. Illustrazione storico-artistica, Tipografia Galileiana, 1845.

[17] U. Baldini, B. Nardini, Il complesso monumentale di Santa Croce: la basilica, le cappelle, i chiostri, il museo, Nardini Editore, Firenze, 1983.

COMPARATIVE STUDIES ON GLUED LAMINATED TIMBER WITH NON-SYNTHETIC ADHESIVES UNDER CONSIDERATION OF USAGE-RELATED EFFECTS ON THE LOAD-BEARING CAPACITY

Tommy BÖRNER[1], Gunter LINKE [2], Jörg RÖDER[1] and Wolfgang RUG[2]

[1] FHP University of Applied Sciences Potsdam/Germany

[2] Expert office Prof. Dr.-Ing. W. Rug, Eberswalde/Germany

ABSTRACT

With the application for patent DRP No. 197773 in 1906, the Grand Ducal master carpenter Otto Hetzer (1849-1911) laid the foundation for the development of glulam as it is known today. Its innovative construction method not only led to a significant reduction of material usage in timber constructions, but also to a development without which today's timber engineering would not be so efficient and competitive. A lack of knowledge about historical glulam constructions repeatedly leads to the demolition of these important buildings and testimonies to engineering creativity. This article serves to expand the state of knowledge about historical glulam and nature-based adhesives. The question of how historical glulam constructions can be preserved in the context of current standardisation and which special features must be taken into account in the course of this will also be examined.

KEYWORDS: historic glued laminated timber, load-bearing capacity, non-synthetic adhesives

INTRODUCTION

Changes in the construction industry must also accompany the energy transition and the declared goal of climate neutrality. The focus is on the use of resource-saving building materials and construction methods. Timber, as a renewable raw material, offers a variety of possible uses. In view of the ever-increasing demand for natural materials, board stacking elements, for example, can already contribute to the production of low-emission constructions. Natural adhesives such as casein glue were also used at the beginning of glulam production. In order to test their possible uses in today's constructions, glulam beams manufactured at the beginning of the 20th century were examined for their load-bearing behaviour. The preservation of historic roof structures is not only important from a monument preservation and economic point of view, but they are also still very efficient structures compared to today's timber engineering. As explained below, the increasing age of a timber structure in engineering construction makes it more difficult to prove its stability. The first timber construction standard in Germany was introduced in 1919 as DIN 104 "Wooden beams for small houses". Due to the mandatory compliance with the standard regulations valid at the time of construction, in conjunction with the year of manufacture of the structure, it is possible to understand the applied static design rules and to evaluate them from today's perspective. For engineering structures from the time before the introduction of binding standards, the consideration is difficult from a static point of view. Even before the standardisation in the construction industry, regional building regulations were in force, which required experimental proof of load-bearing behaviour even for new construction methods. Finding these documents and assigning them to the construction to be evaluated is only possible in very rare cases. In order to be able to make well-founded statements about the load-bearing behaviour of

historical glulam beams, central purlins in glulam construction taken from a roof truss built at the beginning of the 20th century were examined.[1]

PREVIOUS STUDIES ON HISTORIC GLUED LAMINATED TIMBER

At the beginning of the 20th century, the woodworking trade was in a time of upheaval, with the traditional carpentry trade developing into timber engineering through innovative inventions. Structural findings from other construction methods (supporting structures made of iron/steel and reinforced concrete) and the transition from carpenter's timber joints to fasteners such as ring dowels, rod dowels or bulldog toothed plates now enable carpenters and engineers to produce wood-saving and high-performance supporting structures. In 1906, the year of the patent application for the first glued wooden components intended for series production by the Grand Ducal Court Carpenter Otto Hetzer, there was still no uniform standardisation in Germany. The building police regulated specifications for the type and execution of a building. At that time, new construction methods with dowelled or glued wood were tested for their suitability by materials testing institutes or the Royal Materials Testing Office. Through the granting of licenses in Germany and Europe, the trials on Hetzer trusses also expanded. As early as 1908, the engineering company Terner & Chopard from Zurich received its licence to manufacture supporting structures using the Hetzer construction method. One of the clients for structures in Hetzer construction was the Swiss Federal Railways (SBB), which financed a test on two trusses on a scale of 1:3 to prove the load-bearing capacity. This shape of the trusses was then to be used for the new locomotive depot of the S.B.B. in the Aebimatt in Bern. Further experiments followed in 1919/1920 at the Swiss Federal Laboratories for Materials Science and Technology in Zurich. The results of these test series in Germany and Switzerland are available in publications in the Central Gazette of the Building Administration and the Swiss Construction Newspaper, which are still available today. [2] [3] In addition to tests, the Hetzer trusses were also statically verified, taking into account dead loads, snow loads and wind loads. However, the assumptions made were not always completely correct, as the example of the riding hall in St. Moritz shows. There, the four main trusses, which were designed as three-hinged arches, had to be reinforced using subsequently installed tension straps, as the first deformations were already showing. [4]

In the field of glueing technology, the first steps towards the production of synthetic adhesives were already taken at the beginning of the 20th century, but casein or glutin glue were usually used. These glues, which dissolved in water, were already used in ancient Egypt and antiquity to glue wood and other materials. For industrial processing, casein glue is preferable to glutin glue, as casein glue can be processed without prior heating of the glue and the wooden lamellae to be joined. Likewise, casein glue is more water-resistant than glutin glue. At the beginning of the 20th century, there were many different approaches to developing a waterproof glue. Without a more detailed description of the composition of the glue, Hetzer uses a "binding agent that is not soluble in moisture" developed by him to produce his binders. This is basically casein-based. In the course of the further development of synthetic resin adhesives in the thirties and forties, nature-based glulam glued laminated timber was increasingly displaced. With the introduction of DIN 1052:1969-10, DIN 68141:1969-10 [5] [2] [6] [7]"Timber joints; Testing of glues and glue joints for load-bearing timber components, quality conditions" was published. During this period, casein glue also found its last explicit mention in standardisation. [1]

The current findings in the handling of historical glulam are based on a few studies on Hetzer binders. In 2011/2012, for example, tests were carried out at the University for Sustainable Development in Eberswalde on the strength of the adhesive joints on Hetzer trusses. 258 glue joints were used for evaluation. [8]. The tests were carried out based on the standard in force at the time DIN EN 392:1996 (today DIN EN 14080:2013-09 [9] [10]). The evaluation showed that the average shear strength of the adhesive joints was 4.3 N/mm^2 and 4.9 N/mm^2 (depending on the component under consideration) and would therefore not meet today's requirements. Also at the University for Sustainable Development in

Eberswalde, comparative studies were carried out on glulam glueing with natural and synthetic resin glues in 1999 as part of a sub-project of the research project "Comparative considerations of European building product standards with national conditions". Here, tensile and compression shear samples, as well as delamination blocks and boards made of spruce and pine wood, were tested using various adhesives. These include modified casein glue (addition of 3% emulsifiable MDI) with and without the addition of preservatives. The results show that casein glue has comparable strengths to synthetic resin bonding when dry. However, the casein glue compounds quickly lose strength after exposure to moisture and heat (various test methods). The determined tensile shear strengths (dry state) were between 4.3 and 6.3 N/mm^2.

A very interesting and important case study in this context is the Aebimatt locomotive depot in Bern. Even before their construction, tests were carried out on the load-bearing capacity of the trusses (see above). In 2007, an expert report recommended the replacement of all trusses, and the construction was temporarily secured using tree trunks. [11]. At the same time, the Swiss Federal Laboratories for Materials Science and Technology (EMPA) tested the shear strength of the existing adhesive joints and possible crack repair with a 2-component PUR system. [12] The strength of the apparently still intact adhesive joints was determined on twelve drill cores, yielding values of 8.9 N/mm^2 and 9.3 N/mm^2 (with the drill cores divided into inner and outer samples). Laboratory tests on crack repair on a removed beam section showed that in old delamination joints, the impurities that are difficult to remove lead to lower adhesive joint strengths than would be the case with crack repair on new glued laminated timber. The reinforcement of the girders with fully threaded screws and glued-in GSA anchors led to an increase in the existing shear strength; nevertheless, the normatively prescribed minimum values were not reached. A second appraisal from the company Indermüle Bauingenieure showed that the stability can be restored by installing tension straps and individual crack repairs. For this purpose, the planned concept was implemented on one of the 50 trusses and a load test was carried out. [11] [12] The renovation was completed in the summer of 2022, showing that even Hetzer constructions that are over 100 years old can be upgraded to today's requirements with little (cost) effort. After reviewing the image material on the website of the company involved, SSA Architected AG BSA SIA from Basel, the renovation primarily involved installing steel tension bands to absorb the horizontal forces in the transom area resulting from the arch's shape.

Insufficient knowledge about the load-bearing behaviour of historical glulam constructions, combined with the increased requirements imposed by applicable standards, repeatedly leads to their demolition. The current standard for glulam and beam laminated timber is DIN EN 14080:2013-09 [9] in conjunction with the normative references listed therein.

THE KAISERIN AUGUSTE VIKTORIA LYZEUM, BERLIN

Hetzer constructions usually consist of two opposing glulam trusses, which together form a main load-bearing structure. By stringing together several containers at a distance of several metres (depending on the available purlin cross-sections), the supporting structure for the actual roof structure, consisting of purlins and rafters, is created. The test specimens examined formed the central purlins of a multi-standing roof truss. The roof truss construction spanned the auditorium of the Kaiserin Auguste Viktoria-Lyzeum (today Fichtenberg-Oberschule) in the Berlin district of Steglitz-Zehlendorf, which was completed in 1912. In a further series of tests, the arch girders of the assembly hall ceiling construction were also examined more closely. In the present example, the five main trusses have a centre distance of up to 7m. Typical of this construction method is that the trusses, which were set up in pairs, were designed as three-hinged frames or arches, depending on the shape of the trusses. In the case of hall structures, the containers are often designed in such a way that they are supported directly on the foundations. The auditorium of the Fichtenberg High School is located on the second floor, so that the five main trusses were supported on the outer walls, made of brick masonry. In the narrower sense, the

execution described above only applies to the fifth main trusses above the stage of the auditorium; the other four containers form a suspended truss construction, with the individual laminated beams acting as struts [see Figure 1]. Over the length of the main trusses, three further purlin strands were arranged between the foot and ridge purlin. Each purlin strand consists of four individual glulam beams with a support width of around 6.3 m between the first and second main containers and around 7.0 m between the remaining containers. The central purlins are designed as headband supports, reducing their span for mathematical verification of the distance between the headbands of a purlin. The glulam purlins have a variable cross-section, the height of which increases towards the middle of the beam and consequently takes on the shape of a fish-belly beam in the middle area. The purlins are not supported directly on the main trusses, but on squared timbers attached to the sides of the trusses, which have a cross-section of 8/16 cm. Due to the vaulted ceiling construction of the auditorium, the head bands of the first middle purlin layer are less widely flared than those of the second and third middle purlin layers. Some of these purlins were secured before disposal during the dismantling of the roof structure, so that the load-bearing capacity of these Hetzer trusses could be determined experimentally. For the bending tests to be carried out, the test specimens are to be supported in the middle of the existing tenon hole in order to obtain the installation-related support width in the tests. This results in 2 test specimen series. Series 1 (6 test specimens) comprises the first central purlin layer with a support span of approx. 4.59 m and Series 2 (7 test specimens) that of the second/third central purlin layer with a support span of approx. 4.02 m [see Figure 2]. [13]

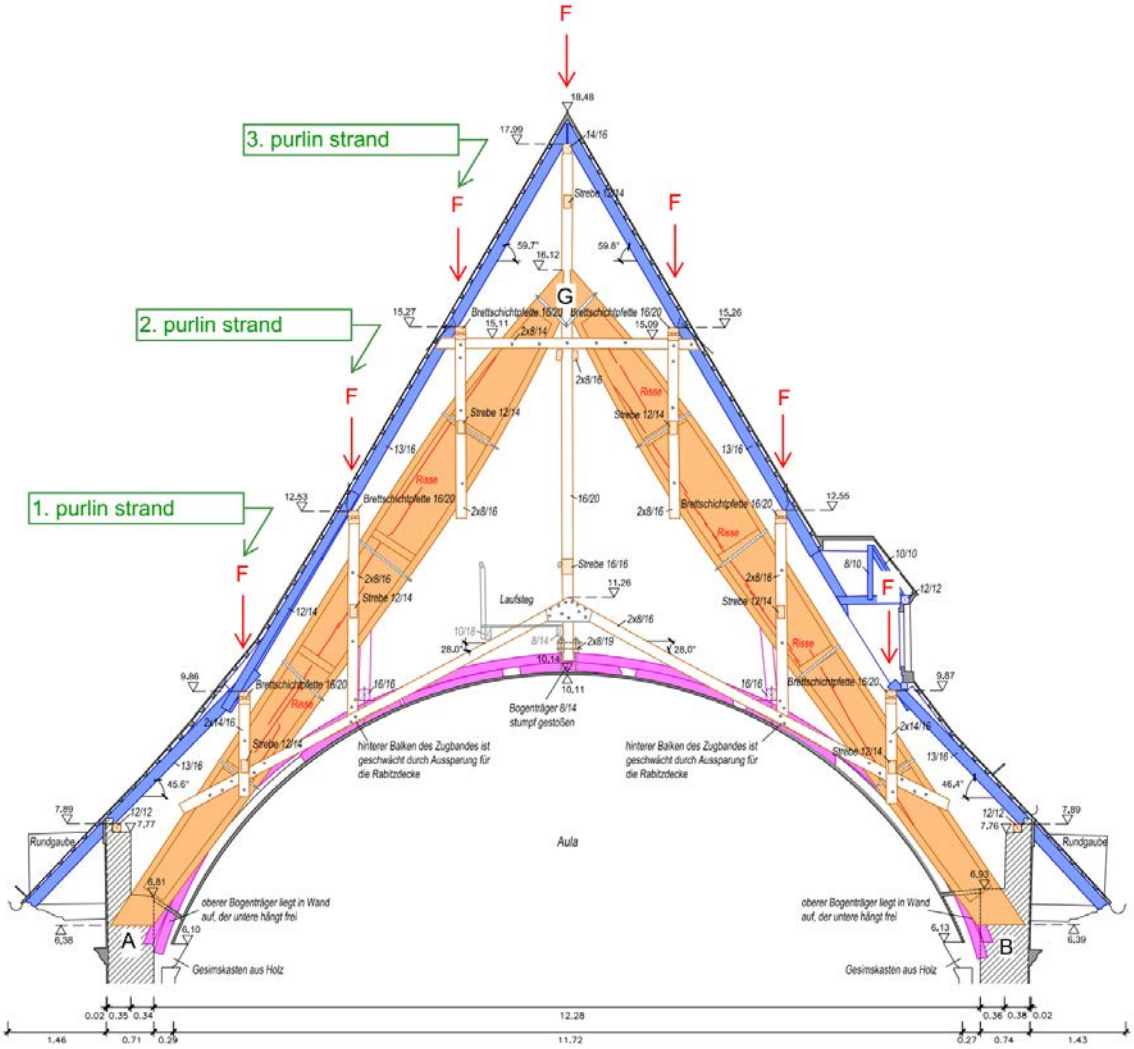

Figure 1. Sectional view of the 4th main truss

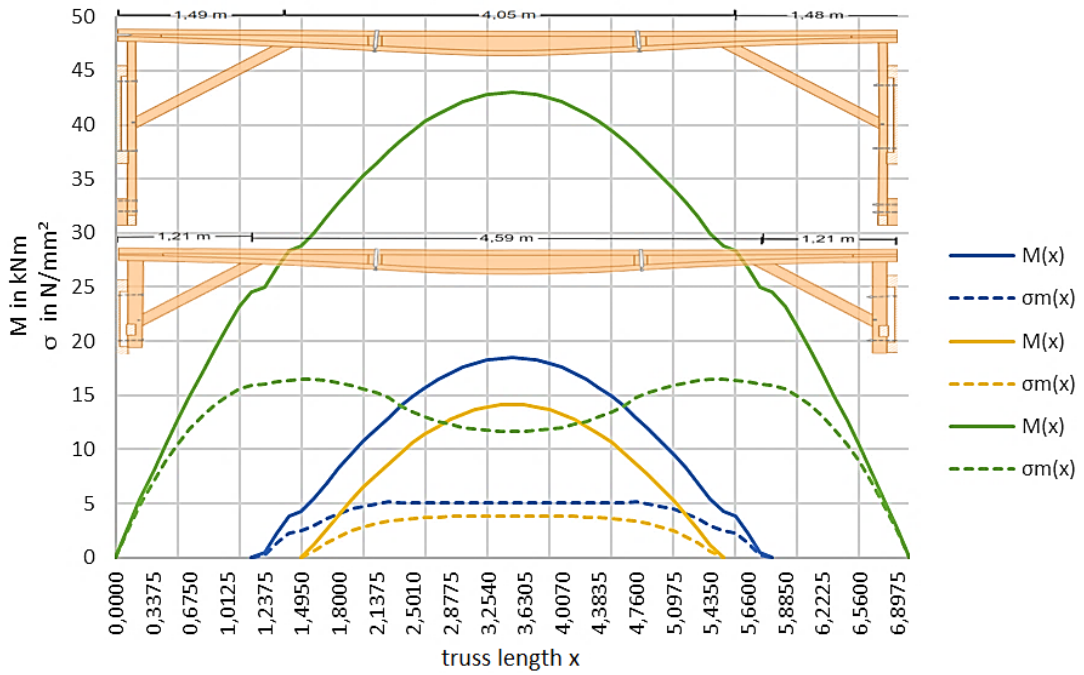

Figure 2. Bending moment and stress along the truss length (blue ... 1st purlin strand; yellow ... 2nd purlin strand; green ... 3rd purlin strand)

In the area of the trusses, the purlins have a cross-sectional height of 20 cm, which increases to 40 cm towards the middle. The cross-section itself has the shape of a double T-beam with upper and lower chords about 16 cm wide and a bar about 6 cm wide. The curved lower chord consists of three individual 2.7 cm thick board slats glued together. The bar and upper chord are made of solid wood and connected to each other and to the lower chord by glue. During the condition assessment, individual nails were also found as a connection between the support components. However, due to the small number and size, it can be assumed that these were more likely to be used for temporary fixation of the individual layers before clamping them in the glueing presses. In addition, the presence of 2 different, opposite radii of curvature on the lower chord can be determined. At the turning points of the radii, the girders are reinforced by timber and steel clasps inserted and glued between the upper and lower chords. From the inventory by the FPK engineering company [14], it can be seen that cross-section reinforcements were also present in the area of the supports. Due to the improper removal of the purlins, the carrier ends were already separated during reception. Under certain conditions, headband straps can be regarded as hinged supports on two supports, whereby the distance between the centres of the headband connections is used as the support width. The centre purlins are stressed by the constant loads from the roof covering (battens and roof tiles) and the rafters, as well as by their own weight. In addition, there are variable loads of the effects of snow and wind. The loads from roof covering, rafters, snow and wind are distributed as a constant line load over the girder length. The dead weight is reflected as a parabolic load with a maximum in the middle of the beam due to the beam geometry. The design is currently carried out in accordance with the specifications of the DIN EN 1995-1-1 [15] and DIN EN 1995-1-1/NA [16]. Along with the changed cross-sectional area, the resistance moment to bending W also changes(X) from the support to the centre of the beam. In the middle of the girder, it has its maximum with the largest cross-sectional area. The shape of the centre purlins thus also corresponds to the course of the bending moment M(X), which is also largest in the middle of the beam. In order to simulate the behaviour of the beam under the installation conditions, the bending moment and the resulting bending stress σm(x) are calculated at regular intervals over the length of the carrier. It was found that the greatest bending stresses do not occur in the middle of the field, but already before (beams without head straps). Towards the middle, the bending stress then decreases again. According

to this procedure, the entire carrier without headbands was considered on the one hand and the area between the headbands on the other. In the simulation for the first central purlin layer, the greatest bending stresses occur precisely in the area that wooden inserts and steel clasps have reinforced. The reinforcement measures were not included in the calculation of the bending stress. The voltage peaks when viewed without headbands are exactly in the range of the headband connections. The girders of the second middle purlin position, on the other hand, have the maximum directly in the middle of the field. This shows that the wood-saving adaptation of the beam shape to the bending moment curve leads to stress peaks outside the centre of the beam, but can be compensated for by the use of headbands. The resulting changes in the maxima in the bending stress were then taken into account by strengthening the beam cross-section in the affected areas.

PRELIMINARY TESTS AND ADHESIVE JOINT STRENGTH

For the mathematical verification of the center purlins, the distance between the head straps is used as the span, whereby the support points for the four-point bending test to be carried out are also defined. The beams were shortened to an appropriate size, and the sections were provided with the beam number, as well as the note "li" for the left section and "re" for the right section. These remaining lengths were thus available for the planned preliminary tests. The individual lengths varied from over one metre to approx. 20 cm, which in view of the sometimes considerable previous damage, did not allow the removal of suitable sample material in some cases. 390 samples could be used to test the compressive strength in the direction of the grain, bulk density and wood moisture content. To determine the shear strength of the adhesive joints based on DIN EN 14080/ Pendant D [9] 95, test specimens could be fed into the experiment. For the microscopic determination of the wood species used, thin sections were obtained with the help of a microtome in order to produce the microscopic preparations. For this purpose, individual pieces of wood were cooked for several hours in advance. Based on the macroscopic and microscopic characteristics, the wood species spruce used was determined. With an average wood moisture value of $\omega m.0 = 9.52\%$, the mean value of the bulk density is rm, $9.52 = 0.414$ g/cm^3 and the compressive strength in the direction of the grain fc,m, $9{,}52 = 48.48$ N/mm^2. At the beginning of the 20th century, protein-based glues were mainly used in the woodworking industry. These include glutin glue (based on collagen from animal by-products) and casein glue (based on caseins from milk). In the production of glutin glue from animal bones, the calcium phosphate contained in it is dissolved depending on the process, so that the subsequent glue contains little or no phosphorus. The caseins all contain phosphorus, which is not split off during the production process of the glue. In the first step, microchemical protein detection can rule out the use of artificial adhesives. In the second step, phosphate detection can be used to distinguish between glutin and casein glue. However, this detection is highly error-prone, as impurities and/or admixtures (e.g. phosphate-containing flame retardants) can lead to positive phosphate detection even in glutin glues, especially in the case of very old adhesive compounds. In order to be able to further differentiate between glutin and casein glue, microscopic examinations, infrared spectroscopy and extensive chemical analyses are necessary. The final laboratory report [17] on determining the type of glue used in the substrate to be tested is important for distinguishing between glutine and casein glue, but it did not produce a clear result. What is certain is that the glue used was produced on a protein basis and contains phosphate. The positive phosphate detection, as well as the higher agreement with the casein reference spectrum, indicate the use of a casein-containing glue, as well as the preservation of the adhesive joint after several hours of cooking for the preparation of thin-section preparations.

To investigate the adhesive joint strength, test specimens with an edge length of ≈ 50 mm were cut. Due to the previous damage to the beam ends, it was not possible to subject all adhesive joints from each section to the tests. The mean shear strength of all specimens was fv,m,ges = 7.52 N/mm^2, with a dispersion of 1.74 N/mm^2 to 12.90 N/mm^2—a standard deviation of 2.87 results in a coefficient of

variation of 38.19%. Under Section 5.5.5.2.3 "Shear strength of adhesive joints" of the DIN EN 14080, a minimum shear strength of 6 N/mm² with at least 74% fibre breakage is required for individual values. A total of 62 specimens fulfil the minimum value of the standard of 6 N/mm² with an average value of 9.31 N/mm², without further consideration of the fibre breakage percentage. According to Section D.7 of Annex D, the test report does not have to provide any information on the proportion of fibre breakage. For results of 4 to 6 N/mm², the fibre fracture percentage must be 100% (see Table 10 in [9]). Pure fibre breakage (100%) describes the failure of the binding forces (cohesive forces) of neighbouring wood cells, so it only occurs outside the adhesive joint and the subsequent boundary areas [see Figure 3]. [9]

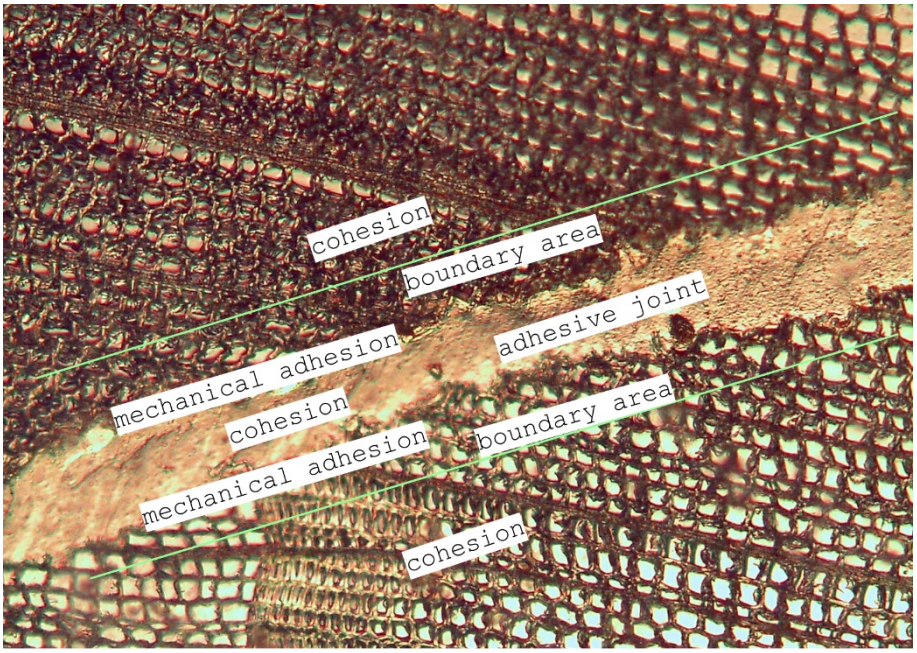

Figure 3. Microscopic cross-section of a glue joint

The binding forces between molecules, both within the wood and within the adhesive, are called cohesion. The form-fitting connection of glue with the adjacent wood cells is called mechanical adhesion. If the fracture takes place exclusively in the adhesive joint (0% fibre breakage), the cohesive forces in the glue have failed. There is a boundary area between the adhesive joint and the wooden surfaces to be joined, in which, in the event of failure, it must be defined whether it is a failure of the adhesive joint or the wood cells. In the most common cases of failure of the fracture surfaces examined here, the fracture meandered between the adhesive joint and the boundary areas. When viewed with UV light, this leads to a map-like distribution of glue and wood surfaces. Even just one row of wood cells would thus be assigned to the fibre fracture percentage, but this would actually mean a failure of the mechanical adhesion forces and would have to be assigned to the failure of the adhesive joint. [18]

DETERMINATION OF THE LOAD-BEARING CAPACITY BY 4-POINT BENDING TESTS

A total of 13 beams were available to determine the bending strength and the flexural elastic modulus. As already described, the different arrangement of the headbands in the first and second/third central purlin position results in two different support widths for the S 1 and S 2 series. The tests were carried out in accordance with DIN EN 408. [19] To measure the deflection of the beam during the test, displacement transducers were attached to the lower chord in the area of the supports, load application points and in the middle of the beam. In order to determine the global flexural modulus of elasticity according to DIN EN 408, the curve portion of the force-displacement diagram in the range between 0.1* Fmax,est and 0.4Fmax,est must be subjected to a regression analysis, whereby the correlation coefficient must be greater than 0.99. This condition was met in all bending tests carried out. Thus, the modulus of elasticity for all beams was determined between an applied load of F ≈ 7.8 kN to F ≈ 18.2 kN,

which at an assumed maximum load of FEst = 52.00 kN corresponds to a factor of 0.15* Fmax,est and 0.35* Fmax,est . The assumed maximum load fixed was calculated beforehand and adjusted based on preliminary tests. According to DIN EN 384, there is a modulus of elasticity of E[20]m,0,mean = 6,201.97 N/mm^2 and a 5% quantile of Em,0,k = 4,155.31 N/mm^2. The flexural strength was determined based on Section 19 of DIN EN 408 [19]. The bending strength to be calculated corresponds to the maximum bending stress in the beam at the time of failure. Due to the existing beam geometry and load situation in the 4-point bending test, the maximum bending stress does not occur in the middle of the beam, but in the area of the load application points. Here, the bending moment reaches its maximum value, whereas the resistance moment to bending is lower than in the middle of the beam. The characteristic value of the bending strength according to DIN EN 14358 f is[21]m,k = 3.96 N/mm^2. The determined bending strengths are to be regarded as lower than the actual bending strengths of the beams, since all of them failed in the 4-point bending test due to a failure due to shear in the area of the supports and not due to a bending fracture. This means that at the time of failure, it was not the bending strength of the beams that was exceeded, but the shear strength of the timbers used or that of the glue joints.

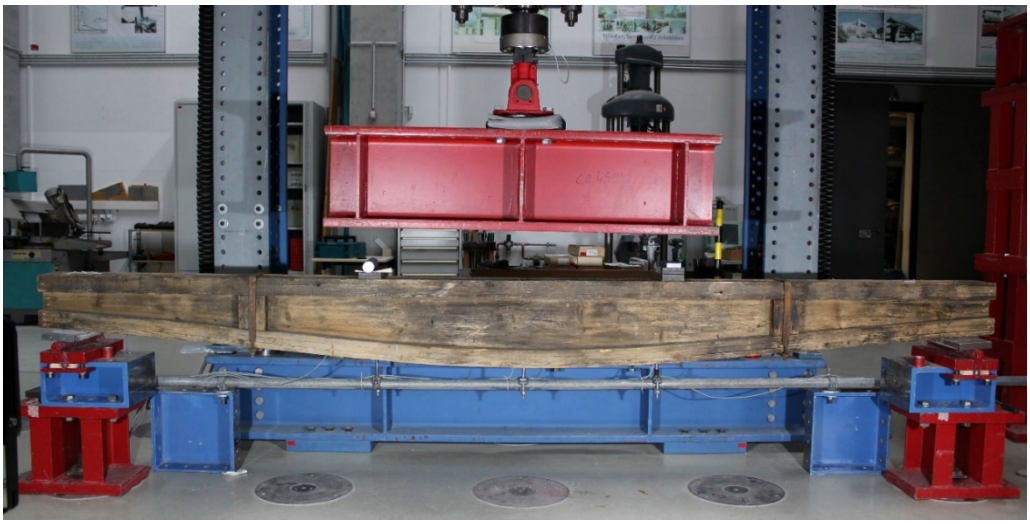

Figure 4. Bending tests

The support points chosen were the tie-in points of the head straps at that time, where no cross-sectional reinforcements were attached at the time of construction. The evaluation of the bending tests has also shown that the I-shaped cross-section with decreasing web height and large cross-sections of upper and lower chords leads to an atypical shear stress distribution [see Figure 5].

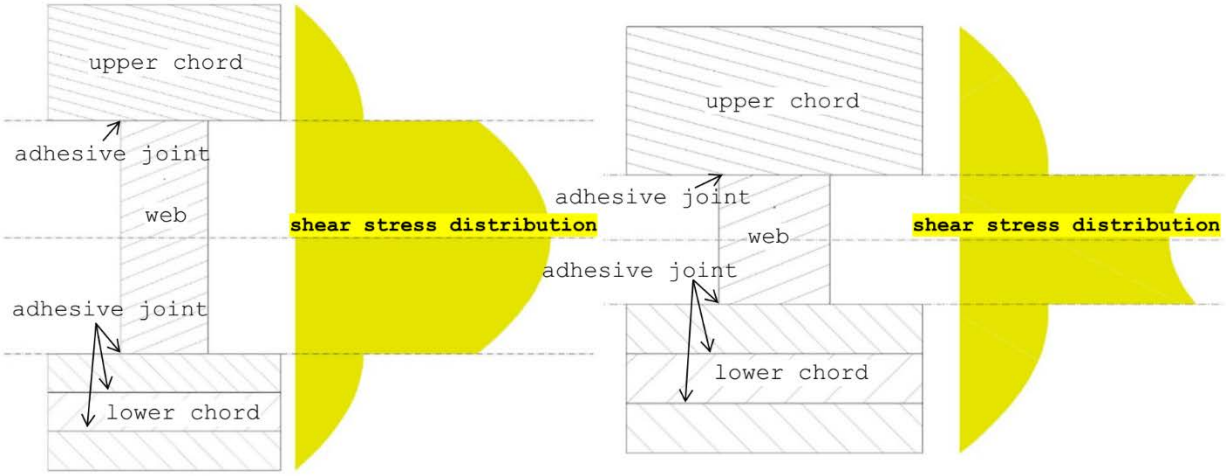

Figure 5. Typical shear stress

SUMMARY AND CONCLUSION

The example of the Aebimatt locomotive depot for a still existing Hetzer structure considered at the beginning shows that even after more than 100 years of service, it is possible to upgrade and maintain these constructions according to today's standards. Demolition, often carried out due to a lack of resilient strength values compared to historical glued laminated timber, should not be endorsed from an economic and ecological perspective. Instead, the number of experimental investigations on historical glulam must be increased in order to be able to assess the load-bearing capacity in a well-founded manner and thus avoid dismantling in the future. The results of the presented study contribute to this requirement. In the 4-point bending test, the beams failed early on thrust in the area of the supports. For further bending tests on Hetzer beams, the cross-sections in the support area were to be reinforced in order to determine the real bending strengths. In the original installation situation, wooden inserts were glued to the bar at the end of the beam above the support between the upper and lower chords. The evaluation of the bending tests has also shown that atypical shear stress distributions occur in the I-shaped cross-section with decreasing web height, and large cross-sections of upper and lower chords in contrast. The maximum stresses do not occur in the middle of the bar as usual, but in the adhesive joints between the bar and the lower or upper chord. In further tests, possibilities for increasing shear in areas at risk of shear should therefore be investigated, e.g. by using fully threaded screws. It is also recommended to carry out a chemical analysis of the near-surface layers of wood in order to be able to draw conclusions about the use of wood and flame retardants, which could possibly have an influence on the adhesive joint strength. In addition, the shear surfaces of the adhesive joint test should be examined for inactive bonding even before the test. For example, it is possible to adjust the shear strength based on the remaining area (e.g. for results of $f_v < 6$ N/mm^2). With the help of UV light, the inactive adhesions can be identified as darkly discoloured areas. The microscopic and macroscopic analyses have mainly shown the use of spruce wood for the production of beams, although the use of fir wood could not be ruled out. This corresponds to today's normative requirement that glulam must be made from one type of wood. Here, fir and spruce are considered together as one type of wood. The failure to provide proof of the load-bearing capacity is not due to an inadequate original design of the beams and insufficient strength of the nature-based glue, but rather to the previous damage affecting the load-bearing capacity during the inappropriate dismantling and the unfavourable interim storage. The Hetzer construction method is a groundbreaking invention today, as it was in the past. The material-saving cross-sections, which are tailored to the intended use, can still make a contribution to resource-saving construction today, if necessary, also with artificial adhesives. In addition, the use of protein-based glues, especially from plant-based raw materials, cannot be ruled out in predefined environmental conditions and should be further investigated.
Through intensive research and cooperation with the monument protection authorities, it should be possible in the future to prevent the further demolition of historic glulam constructions.

REFERENCES

[1] Rug, W., *Ausgewählte historische Bemessungs- und Konstruktionsnormen von 1917 bis 2007..* [Ed.] DIN Deutsches Institut für Normung e.V. Berlin : Beuth Verlag GmbH Berlin Wien Zürich, 2016. Bd. Holzbau im Bestand.

[2] Rug, W., 100 Jahre Hetzer-Patent. *Construction Technology 83.* 2006, Issue 8, pp. 533-540.

[3] Chopard, C., Bruchversuche mit Hetzerbindern. Schweizeriche Bauzeitung. 1913, vol. 61/62, issue 22, pp. 291-295.

[4] Maissen, M., Gramegna, F.and Holzer, S. M. , Pioniergeist und Optimismus - Die Hetzer-Dachkonstruktion der Reithalle von St. Moritz. Bündner Monatsblatt. 4 2019, pp. 355-375.

[5] Sutermeister, E., Das Kasein - Chemie und technische Verwertung. Berlin : Springer Verlag Berlin Heidelberg GmbH, 1932.

[6] Gesteschi, Th., Handbibliothek für Bauingenieure Der Holzbau. [Ed.] R. Otzen. Berlin : Springer-Verlag Berlin Heidelberg GmgH, 1926.

[7] Kühne, H., 70 Jahre geleimte Holz-Tragwerke in der Schweiz. Swiss engineer and architect. 1979, vol. 97, 32-33.

[8] Rug, W., Linke, G. and Winter, L., Untersuchungen zur Festigkeit der Klebefugen von historischem Brettschichtholz. Bautechnik 90. 2013, Heft 10, S. 651-659.

[9] EN 14080 (2013) - Timber structures - Glued laminated timber and glued solid timber - Requirements; German version

[10] Deppe, H.-J., Vergleichende Untersuchungen an Brettschichtholz(BSH)-Verleimungen mit Natur- und Kunstharzen im Kurzzeitversuch nach internationalen Standards ... und Ermittlung der Langzeitbestädigkeit. Fachhochschule Eberswalde. Stuttgart : Fraunhofer IRB Verlag, 2000.

[11] Indermüle Bauingenieure. www.i-b.ch. https://www.i-b.ch/referenzen/sanierungen/depot-aebimatt-bern., accessed 11.06.2022.

[12] Richter, K., Risi, W. and Gehri, E., WHFF Projekt Nr. 2007.05 Klebestofftechnische Sanierung von Brettschichtholz: Ergänzende Untersuchungen zur Ermittlung der statischen Wirksamkeit von Klebestoffsanierungen, Abteilung Holz. Dübendorf : EMPA, 2011.

[13] Linke, G., et al. Bestand statt Austausch - Untersuchungen zum Trag- und Verformungsverhalten von historischen Brettschichtholzbauteilen. Bauingenieur. 2022, Bd. 97, 9.

[14] FPK-Ingenieurgesellschaft mbH. Fichtenberg Oberschule, Berlin Steglitz - Bestandsaufnahme Dachstuhl. [Planzeichnung M 1:50]. 2016.

[15] EN 1995-1-1 (2010) - Eurocode 5: Design of timber structures - Part 1-1: General - Common rules and rules for buildings; German version

[16] EN 1995-1-1/NA (2013) - National Annex - Nationally determined parameters - Eurocode 5: Design of timber structures - Part 1-1: General - Common rules and rules for buildings

[17] Fuchs, Chr., Identifizierung eines Klebstoffs. Stadt/Bau/Kultur, Fachhochschule Potsdam. Potsdam : s.n., 2022. Untersuchungsbericht.

[18] Habenicht, G., Kleben - Grundlagen, Technologien, Anwendungen. 5. Auflage. Wörthsee/Steinebach : Springer Berlin Heidelberg New York, 2006.

[19] EN 408 (2012) – Timber structures – Structural timber and glued laminated timber – Determination of some physical and mechanical properties

[20] EN 384 (2022) – Structural timber - Determination of characteristic values of mechanical properties and density; German version

[21] EN 14358 (2016) – Timber structures - Calculation and verification of characteristic values; German version

JOINT ANALYSIS, EVALUATION AND REMEDIAL ACTIONS IN HISTORIC TIMBER STRUCTURES – THE EXPERT'S ROLE ON SITE

Hrvoje TURKULIN[1], Juraj POJATINA[2], Tomislav SEDLAR[1] and Andrija NOVOSEL[1],

[1] University of Zagreb, Faculty of Forestry and Wood Technology

[2] Studio ARHING d.o.o., Zagreb

ABSTRACT

Evaluation and analysis of joints in situ are critical in assessing the condition of a historic timber structure. Such assessments enable a holistic evaluation of the system's structural integrity and identify essential methods for necessary repairs or upgrades, thereby supporting effective maintenance throughout the building's lifespan. Standard EN 17121 (2019) highlights key considerations for determining the role of each joint, evaluating its fitness, and identifying indicators of potential deficiencies. However, the standard does not provide explicit steps for joint assessment—such as detailed measurements, tolerances, or precise definitions of joint failure causes—nor does it offer guidance for repairs or reinforcement. Consequently, the in-situ judgment of experienced professionals (typically both wood technologists and structural engineers) is vital for reliable joint evaluation and effective remedial action. This paper analyses different traditional joint types and shares insights from remedial work undertaken on Croatian heritage buildings following the 2020 earthquakes.

KEYWORDS: traditional carpentry joints, joint failures, joint repairs, strengthening, replacements

INTRODUCTION

The condition of the joints is vital for the stability of the structure; they transfer loads between structural components and directly support the overall integrity of the structure. There is extensive literature on traditional carpentry wood joints; general references (e.g. [1], [2], [3]) provide comprehensive lists which cannot be detailed here. Valuable insights can also be found in historical texts (e.g. [4]). Traditional carpentry joints are often considered rigid elements in structural assemblies, but the viscoelastic properties of wood make the joints somewhat ductile ([1], [5]). Carpentry joints thus contribute fundamentally to the stability and longevity of historic structures, allowing them to dissipate peak stresses by their geometry (load transfer) and by wood deformation within proportional limits. Traditional joints, refined over centuries of carpentry practice, were tailored for specific requirements in binding structural elements.

When analysing traditional wood joints, it is not only important to understand the various forces acting on the joint, but also the different properties of wood in its natural anatomical composition. Different planes in a wood structure (radial, tangential to the rings, and longitudinal - along the fibres) have radically different mechanical properties, which should be taken into account when analysing joint geometry and attempts to avoid joint failures due to weaknesses in wood's natural structure. A wood technologist and experienced carpenter will also know the difference between various wood tissues (e.g., sapwood presenting the biological hazard, juvenile and reaction wood having some poorer mechanical properties than mature heartwood, latewood proportion affecting shrinkage, but also the mechanical properties). Therefore, the choice of the type and construction of the joint for a particular

purpose is an essential virtue for the skilled carpenter. However, the craftsmanship additionally enhances the role of the carpenter's skills in making the joint. Correctly chosen and composed, but poorly executed joints may show deficiencies over the lifespan of the structure solely due to the errors in making the joint (leaving the gaps, loosening of the joint due to shrinkage of wet-installed wood, lack of adequate friction within joint planes due to poorly executed geometry of the joint, etc.).

Standard EN 17121 (2019) Conservation of cultural heritage – Historic timber structures – Guidelines for the on-site assessment of load-bearing structures [5], in chapter 5.8 (Detailed survey of timber joints), clearly states that "existing joints in historic structures may be considered adequate for the loads they carry and will not require detailed assessment ... except when they show clear deficiencies or damage." However, this standard also identifies aspects of joint quality for evaluation, including wood damage caused by loads in the least resistant anatomical directions, depending on the load and fibre orientation (compression across or at an angle to the grain, shear along the grain, and tension across the grain). The standard further emphasises the importance of workmanship, including the selection of appropriate joints, sound original design, precise timber fitting, and adequate fastener spacing and positioning (avoiding fasteners too close to the end or edge). It also highlights the presence and location of fasteners, adequate beam bearing, and load alignment. Finally, it stresses attention to changes in joints over time (corrosion of metals, timber shrinkage, creep, biological degradation, crushing, movement, and deformation from overloading) or due to human modification. Notably, chapter 5.8 gives little consideration to the effects of moisture, which negatively affects wood's mechanical performance, whether by moisture fluctuations impacting anatomical planes in the joint, or by shrinkage from drying of wet-installed wood in original joints or repairs (such as prostheses).

In addition to visual examination and test drilling, structural soundness analysis is essential for joint assessment. This determines whether a joint is suitable and capable of transferring system loads. Each joint is part of a structural system: from continuous or straightforward beams to various 2D or 3D truss arrangements. In traditional carpentry, joints are far more complex to analyse than in other timber or construction materials. Developed over extensive periods of human and technical progress, traditional timber joints integrate material properties, durability needs, and strength criteria, and they have survived the test of time. Their complex geometry is also challenging to calculate or to model numerically. Expertise is therefore vital in assessing the structural function of traditional timber joints.

Joint evaluation and the identification of deficiencies do not end with documentation; experts in wood technology and civil engineering, working in conjunction with conservators, apply their extensive knowledge of repair and improvement methods. There is considerable literature on modelling and testing the mechanical properties of traditional joints (e.g. [1], [7], [8]), though most experiments use new wood. Aged wood differs, having experienced creep, cracking, and moisture fluctuations; it has not been kiln-sterilised, and its strength diminishes with time (e.g., reduced modulus of elasticity). Significant literature also addresses repair and reinforcement (general references in English include [2], [8]; in Italian, [9]; and in German, [10]). The choice of remedial action depends on timing, restoration objectives, and carpenter availability. Proposals for repair methods depend on practical considerations, such as whether roofing can be removed or if work must be done from inside only; accordingly, available techniques must be selected. This paper presents our experience with joint repairs in historic Croatian buildings after the 2020 earthquakes. In most cases, we recommended traditional techniques appropriate to the structure's era to preserve its character and appearance. We also preferred joints used elsewhere in the structure and used the same wood species and texture when possible, although time constraints and a scarcity of carpenters sometimes required using sawn rather than hewn prostheses.

METHODOLOGY

The joints were inspected by visually observing the exterior and measuring the gaps using callipers (a tool for measuring the distance between two opposite sides of an object), feeler gauges (thin, precise measuring strips), and measurement lenses (magnifying lenses for small distances). The internal structure of the joint was analysed using resistance drilling (where a small drill measures the resistance of wood to assess internal conditions) in multiple directions, allowing identification of joint type, dimensions of individual segments, joined surfaces, and tolerances between them. Biological damage was assessed by visual inspection, microscopic examination of sanded and polished samples extracted with core drills (cylindrical drill bits for removing a sample), and cultivation tests (laboratory growth tests to detect the presence of fungi or bacteria).

RESULTS

Inadequately chosen joints

Figure 1 a)-c). Upper Town High School (origin of the Zagreb University, 1695). The sequence of failures begins with inadequately chosen joints: the strut is too shallowly lapped on the post without a dowel, there is a too-small dovetail lap with the collar, and the collar does not adequately "catch" the purlin on top of the post. These lead first to shear failures at the upper left dovetail lap joint, followed by rotation of the post due to shear failure in the collar. As the collar tie fails, a crack forms in the post, and the post inclines outward (upper left). The lower sketch shows the incorrect layout of the rafter on the collar, which subsequently fails in shear. The right sketch presents a better solution for queen-post structures. Red lines indicate possible remedial measures. Iron clamps are not sufficiently strong and secure for binding the elements, particularly not in softwoods.

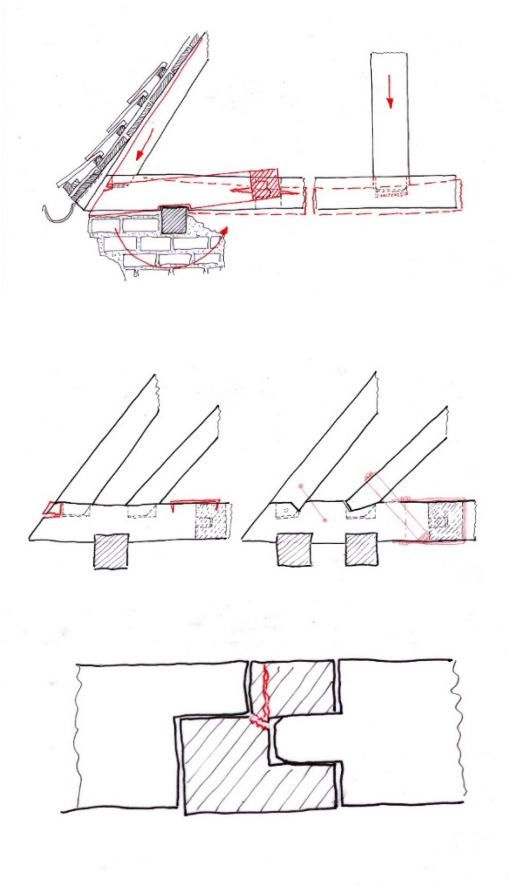

Figure 2 a)-c). The brittle bending failure of the grid beam is attributed to the inadequate positioning of the rafter at the end of the tie beam, resulting in eccentricity that causes upward spur rotation. The tie beam further bends due to insufficient support beneath the queen post (upper right). Right: the current configuration with a single wall plate (left), and the proposed configuration with two wall plates and iron braces (right).

Figure 3 a) and b). The joints in the perimeter grid are positioned inadequately. Failure results when the lap joint and tenon coincide in plane, causing wood to fail in shear and tension perpendicular to fibres.

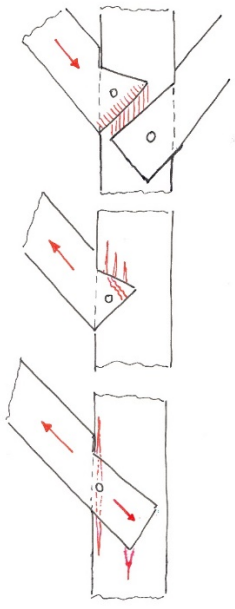

Figure 4 a)-c). Church of St. Michael Archangel, Preloščica, 1832. Shown here are examples of curiously misshapen blind dovetail laps of knee brackets. The structural problems are as follows: depending on the load, the wood fails in compression perpendicular to fibres (compression) or splits in shear or tension perpendicular to fibres (tension). Additionally, positioning wooden pegs too close to the edge of the post can cause the post to split along its grain. These issues suggest that the church was presumably built by local carpenters with limited experience in carpentry.

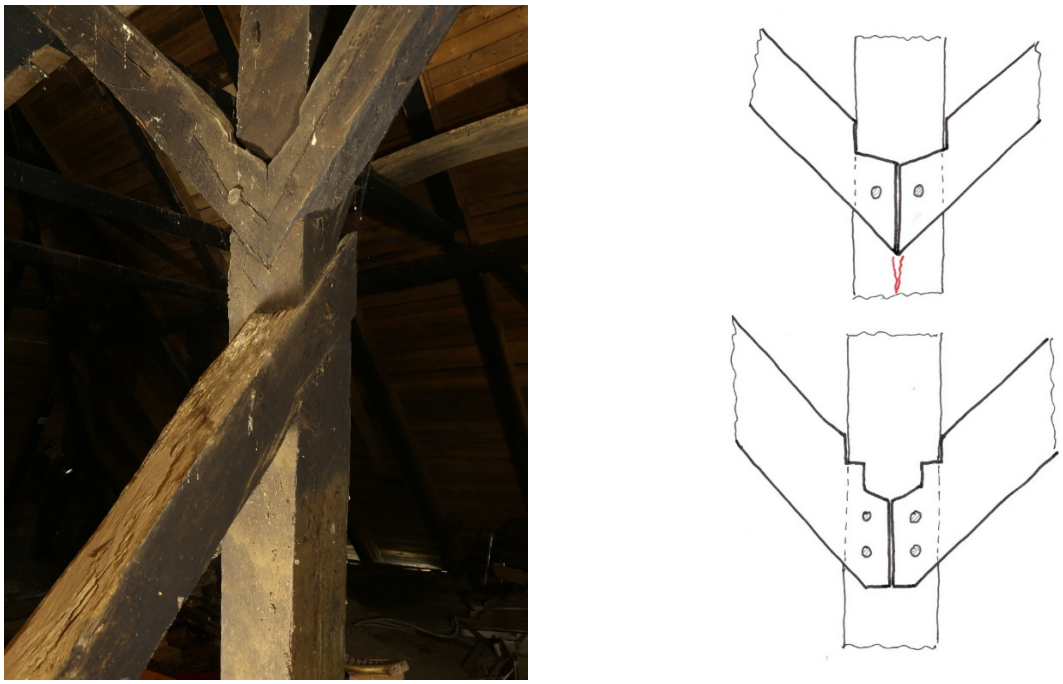

Figure 5 a) and b). Dovetail lap joints have too small an angle (<10°). When positioning two adjoining dovetail laps, poor alignment can cause wedge-like action, resulting in splitting of the post. To address this issue, refer to the suggested joint for this purpose located at the lower right.

Well-chosen joints, inadequate craftsmanship

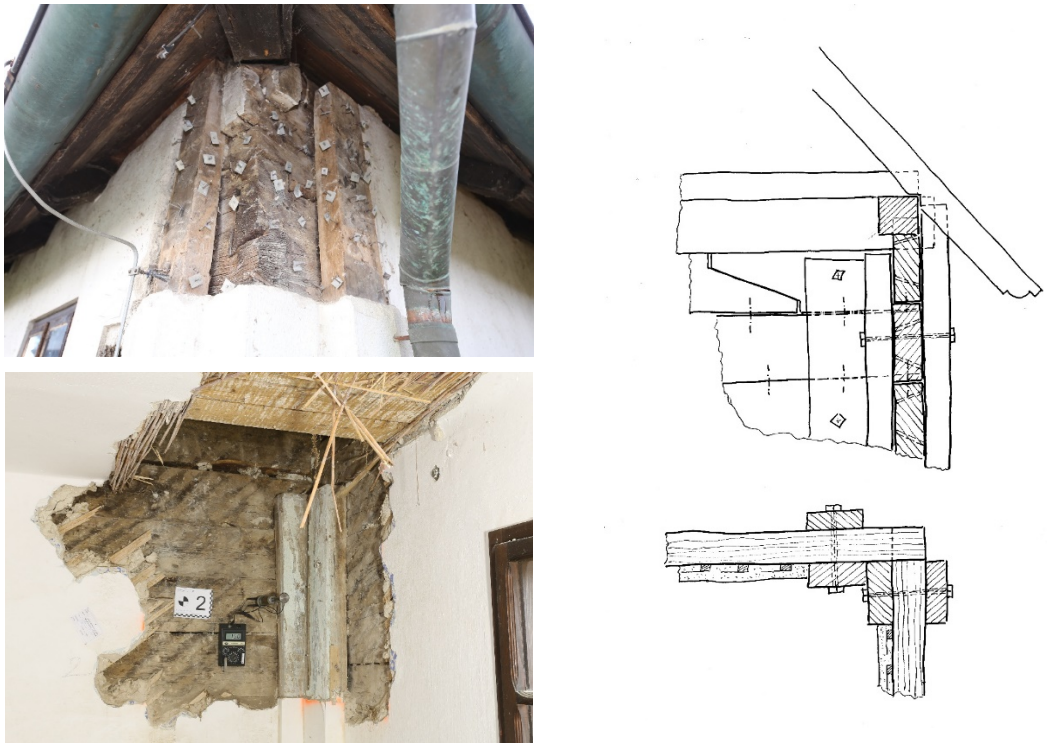

Figure 6 a)-c). Corner of the parish house in Mala Gorca (around 1830s). Initially, poor craftsmanship of the corners (dovetail notched joints) rendered the walls unstable. To address this, the walls were adequately, though not stylishly, improved by binding them with vertical planks and through the use of threaded bolts. Later, in the late 19th century, they were reinforced and plastered on both sides.

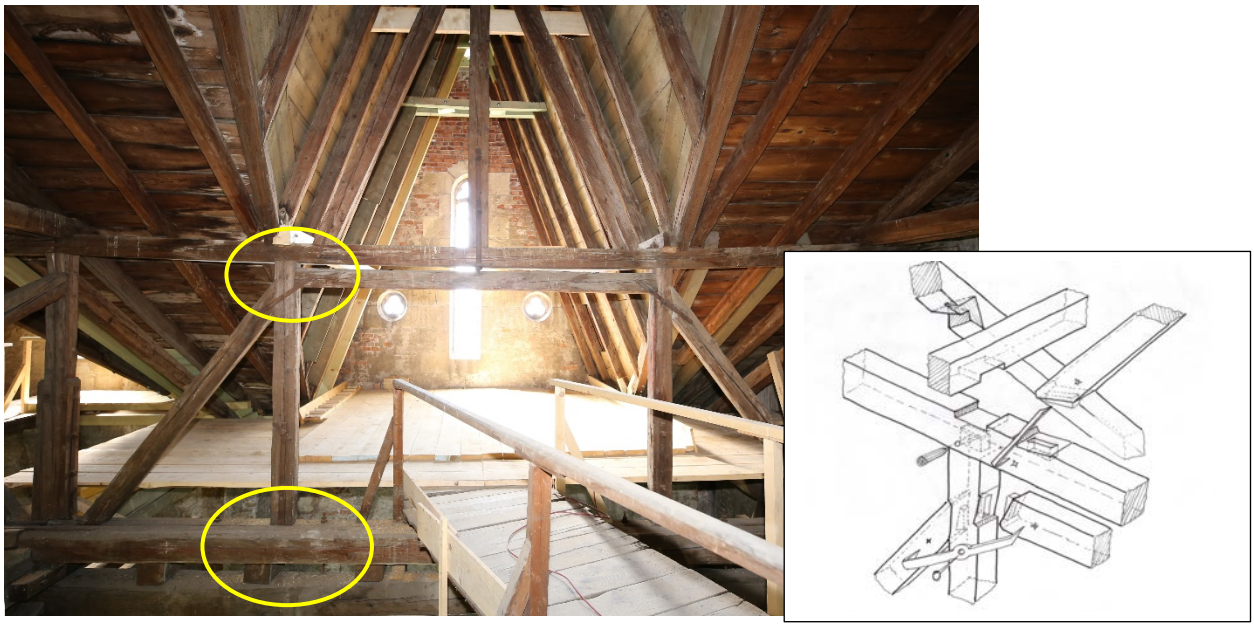

Figure 7 a)-c). Structure above the side aisle of the Zagreb Cathedral (1898). Each of the four segments of the roof with side gable walls spans approximately 6 m. To address this span, the solution involved constructing a beam-like structure, featuring wooden beams as flanges and wooden blocks with through bolts as a web (see lower detail). However, the structure deflected, partly due to the drying of the wood and the pressing of bolt washers into soft firwood, and partly due to the eccentricity of the loading. Additionally, the minimal end-grain surfaces of the queen posts caused compression crushing perpendicular to the fibres of the collar beam (left).

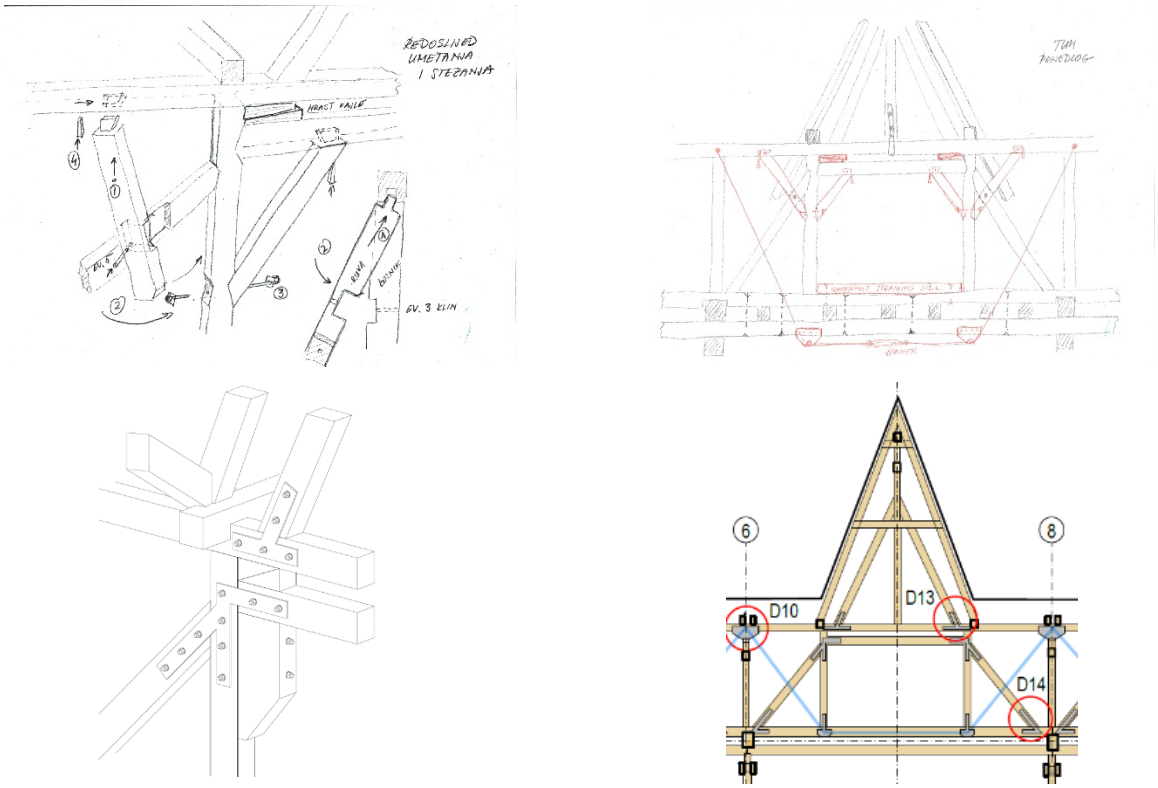

Figure 7 a) – d). Upper: Sketches from the initial "brainstorming" process, which explored solutions such as carpentry reinforcements (left) and the use of steel cables to uplift the entire structure. Lower: Following these explorations, details of the executed joints and final stabilisation methods of the structure are shown.

Biological damage to supports

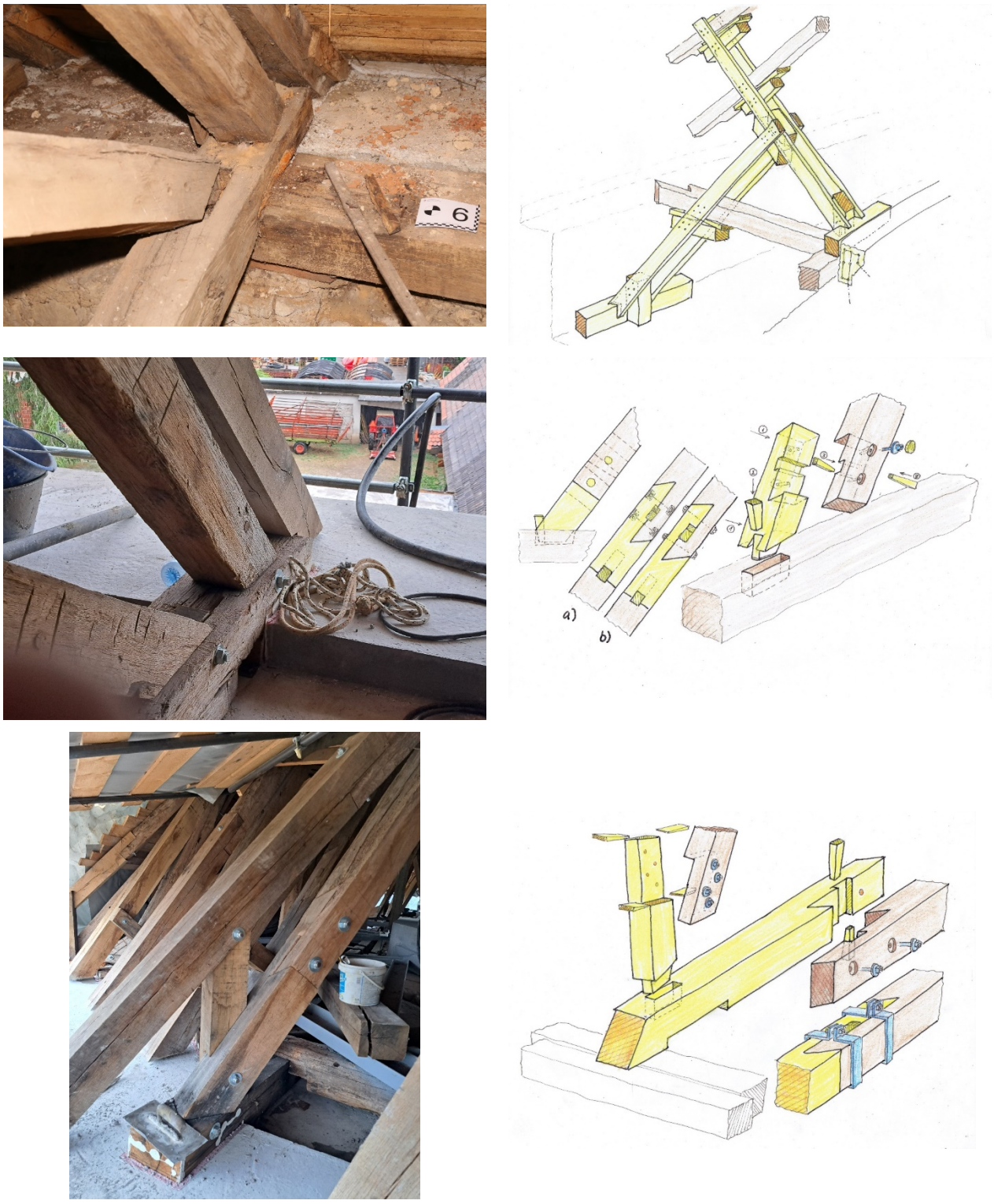

Figure 8 a) – f). Church of the Ascension of the Blessed Virgin Mary in Pokupsko (late 1700s). The Oakwood structure was damaged by distortion and opening of the joints and by biological damage (upper left). A reinforced concrete ring girder replaced wall plates, and rotten elements were partly replaced with prostheses. Tie beams and struts are now insulated in the concrete; the sprockets with birdmouth joint sit on the end of the beams (end grain opened for drying). Tenons and stop-splayed scarf joints with keys or wedges were used in reconstruction. These joints are fixed with threaded rods instead of the original wood pegs for reasons of better tightening and strength. Right column: Experts' sketches for the execution of joints and discussions with carpenters.

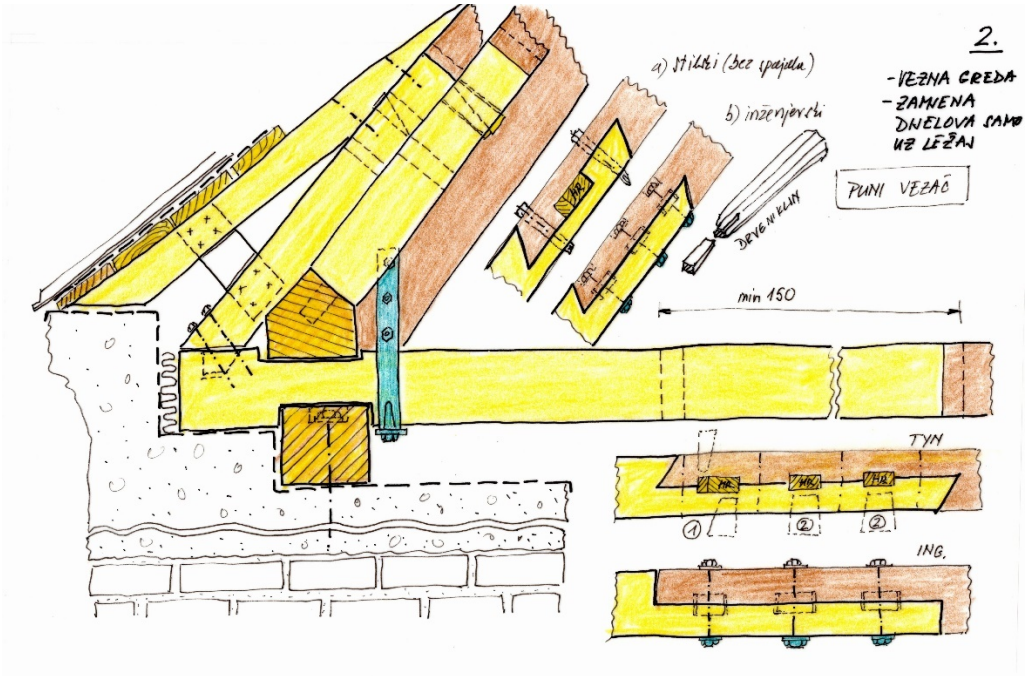

Figure 9 a) and b). Požega, Cathedral of St. Teresa of Ávila (1752). Due to the position of the dome, the roof was built as a reclining truss (in German "liegender Stuhl "). This popular structure relies heavily on load transfer to the wall supports, with tie beams installed only at the roof ends. Initially, the wall plate was laid in the brickwork; however, in later restorations, plaster or concrete was also used. This sequence exposed the wood at the supports to deleterious moisture risks and subsequent biological degradation. Once damage occurred, sketches of suggested replacements—including the installation of a concrete ring girder, a new ventilated and insulated wall plate, and prostheses for principal rafters and reclining struts—guided the engineer and carpenters in designing the final reconstruction.

Well-chosen joints, perfect craftsmanship

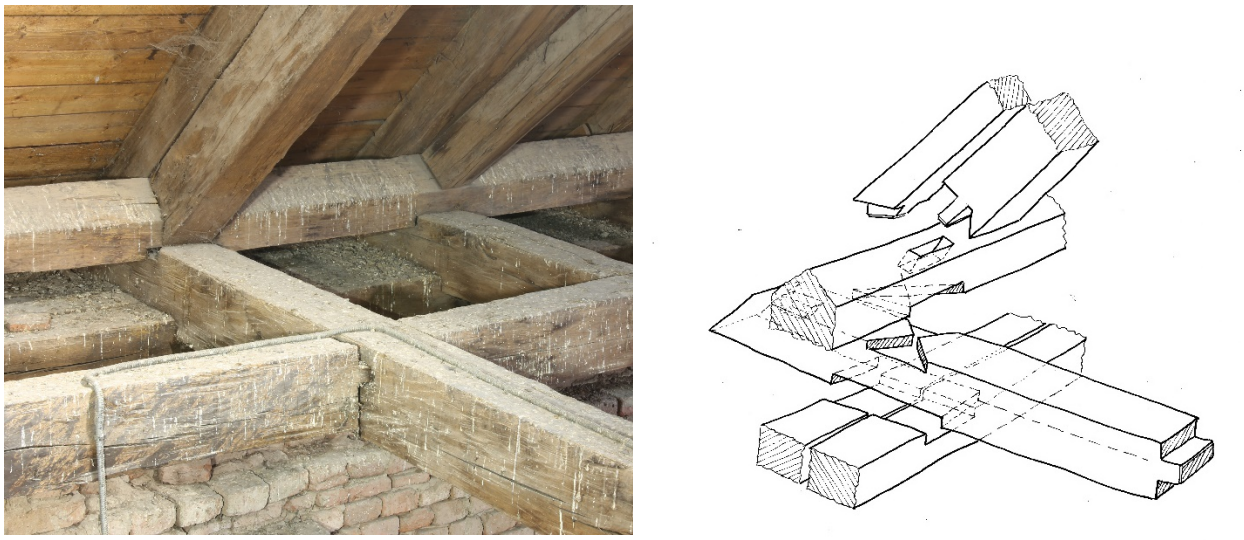

Figure 10 a) and b). Ivanić Grad, St. Peter the Apostle (1831). This is another example of a reclining truss. Initially, the double-wall plates exhibit biological damage, while the joints remain generally intact. The sketch on the right side shows a well-constructed assembly, with good execution of joints. The tie beams are correctly half-lap notched to wall plates, and the main beam is efficiently lapped with a crossed-tenon lap joint. As a result, even when wall plates are damaged, the joints and the rest of the structure remain stable. Such an assembly in oak wood, well-executed, presents a complex of very good stability in all directions; good craftsmanship ensures that there is no splitting or shear in the wood.

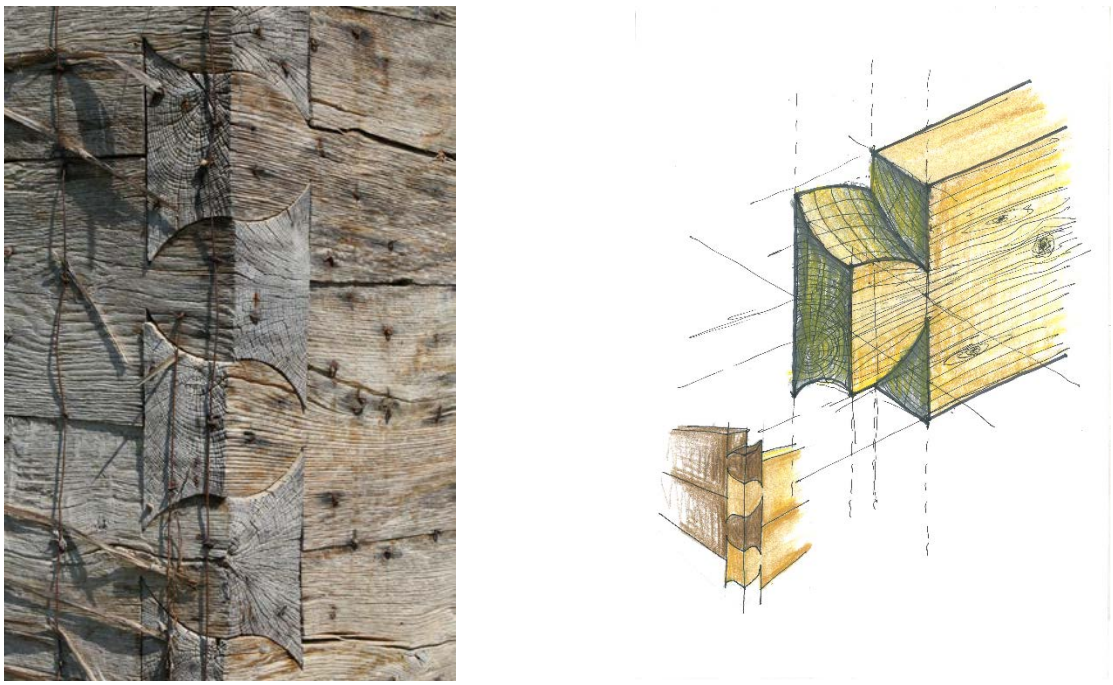

Figure 11 a) and b). Special type of dovetail corner joint (in German "Klingschrott") of a wooden Chapel of St. Mary (Brkiševina, central Croatia, early 1800s).

Figure 11 presents a rare dovetail corner joint with curviplanar cheeks of the tenons. The joint is very rarely found in literature; it was also rarely used, mainly in the alpine region (Bavaria, Austria, Switzerland [14]) and eastern European countries to build representative houses or churches. The photograph demonstrates excellent craftsmanship in the hand-making of these delicate joints. However, the joint possesses significant advantages over standard dovetailed corner joints:

· The joint has larger contact surfaces between the cheeks of the dovetail, which contribute to the strength and tightness.

· The curviplanar cheeks distribute the load in a spatial, not a linear, form. As a result, the stresses along the fibres do not occur in a single anatomical plane of wood, and the risk of shear is significantly reduced.

· The shoulders are as wide and the cheeks as long as straight dovetail tenons, but the connection between elements is longer.

The joint exhibits a notable self-tightening property: as the wood dries, the joint does not open but instead tightens toward the inner corner. In case of cracks or attempted failure, the shape of the joint blocks the propagation of cracks, preventing them from spreading through the connection. This sequence of self-tightening and crack blocking contributes to the joint's durability.

The engineer noted the strongly jointed walls in the small chapel. To preserve them, he decided to lift and relocate the structure during work on the foundations and new concrete slab. After repairing the foundations, the chapel can be lifted back into place.

The Zagreb Cathedral

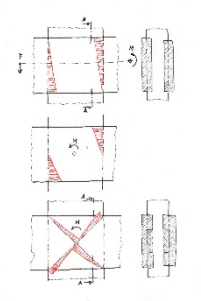

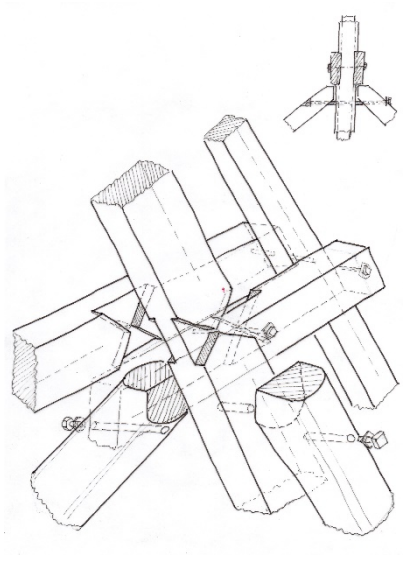

Figure 12 a) – c). The Zagreb Cathedral of Assumption of Blessed Virgin Mary (last reconstruction 1898). Joint of the principal rafter with double collar and wind-braces. A simple half-lap joint is prone to compression crushing when a moment is acting on the joint. When secured with bolts, the joint has smaller areas of compression perpendicular to the fibres, but the forces can be greater, although the bolts also provide the desirable friction. A cross-tenon lap joint, applied here, has 34% greater contact surfaces. Additionally, the compression in the shoulders is at 45°, which renders the compression strength (Hankinson's formula) approximately 26% greater than compression perpendicular to the fibres. In theory, a cross-tenon lap joint can withstand approximately 1.8 times greater stresses than a simple half-lap joint.

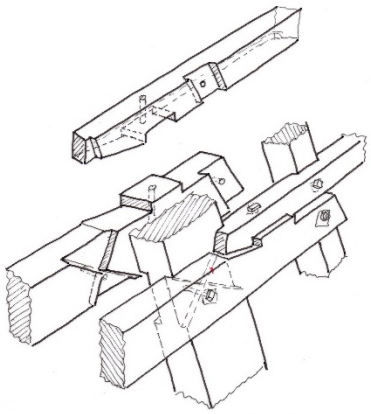

Figure 13 a) and b). Analysis of the joint between the principal rafter, double collars, and purlin to the side aisle. The crossed tenon lap joint between collars and rafter is very stable, with multiple half-lap joints secured by iron bolts. Interlocking in all three directions was assessed first. Subsequently, no wood failure—either in shear or in tension perpendicular to the grain—was recorded at any stage.

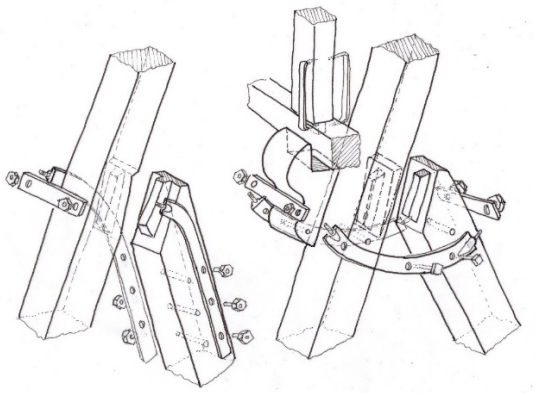

Figure 14 a) and b). Connection detail at the intersection of the principal rafter, main strut, and purlins. The main strut is tenoned approximately 2 cm into the principal rafter and further reinforced by a notched mortise-and-tenon joint to prevent lateral displacement. In the event of structural failure, loosening of the mortise-and-tenon joint would likely precede subsequent displacement, which would be restricted by the cleat and iron stirrup. The cleat and main strut are secured by a robust iron stirrup at the points of compound and I-beam purlin interface. These meticulously executed joints exhibit tight tolerances, high functionality, and exemplary craftsmanship, resulting in reliable structural stability.

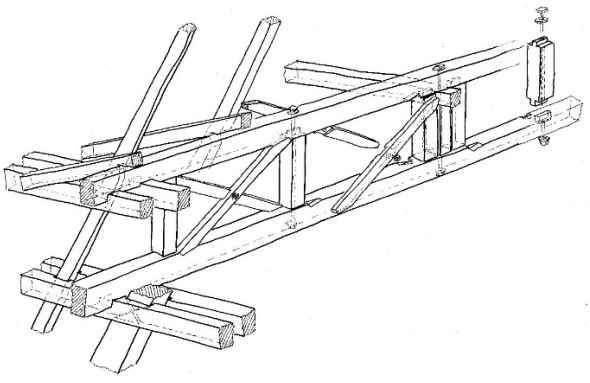

Figure 15 a) and b). At a span of 6.5 meters between the trusses, only a truss configuration is structurally feasible for the purlin. Minimal deflection is observed, while the roofing plane remains properly aligned. The precise assembly sequence of the complex joint is reflected in the firm and tight joints, demonstrating superior workmanship.

Figure 16 a)–c). Notable deviation from conventional engineering practice. The tie beams exhibit inverse deflection (left). Rather than maintaining a gap between the king post and tie beams, the beams are fitted with stirrups that induce upward tension toward the post (middle). Consequently, the entire truss assembly is tensioned, initiating at the tie beams and subsequently tightening each truss joint in progression.

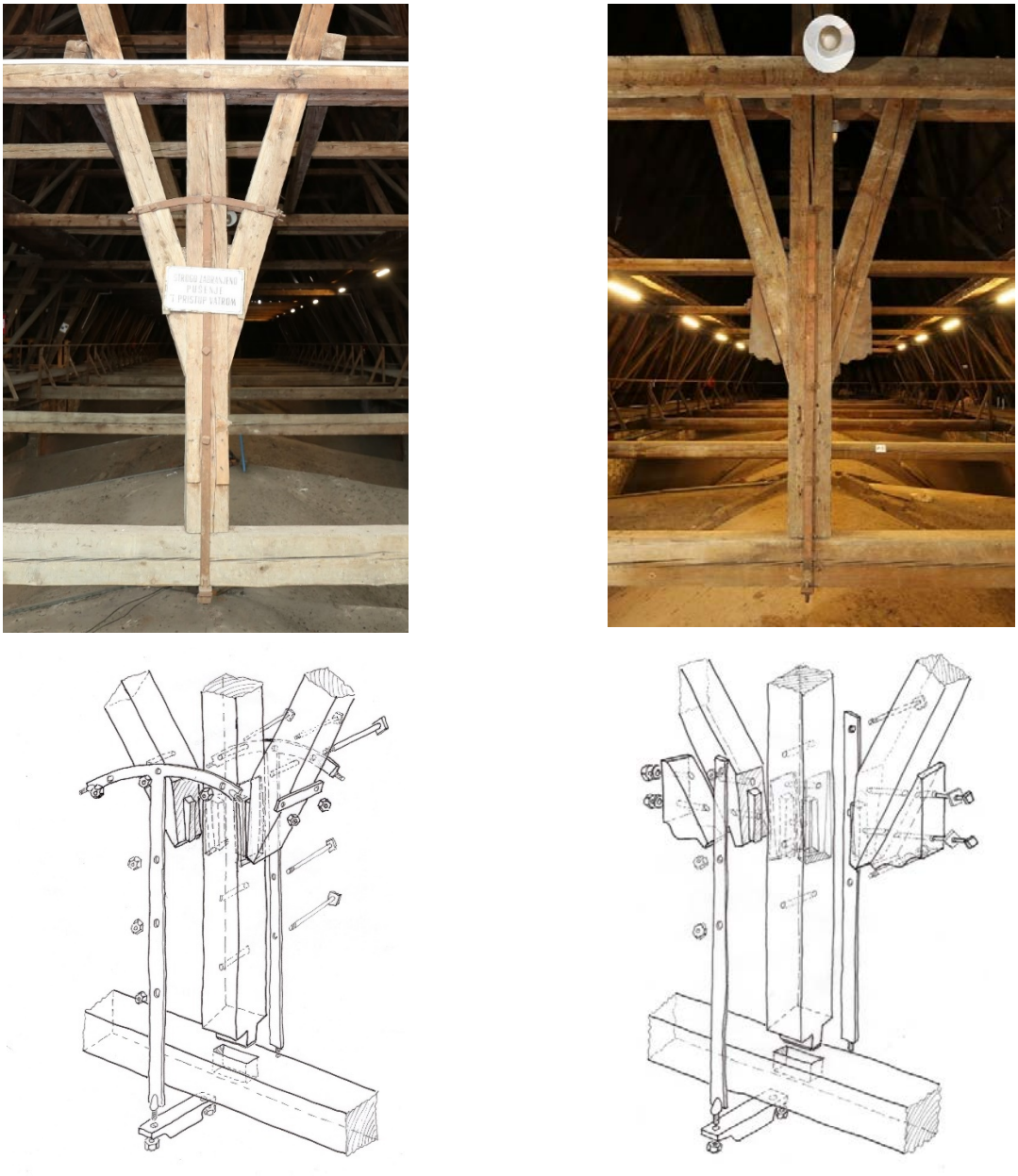

Figure 17 a) – d). This analysis shows the jointing sequence between the king post, tie beam, and supporting struts of the main aisle (two variants). The connections begin with housing and notched mortise and tenon joints, followed by the fitting of heavy ironmongery to secure tightness in all joints. Perfect craftsmanship and joint condition are observed.

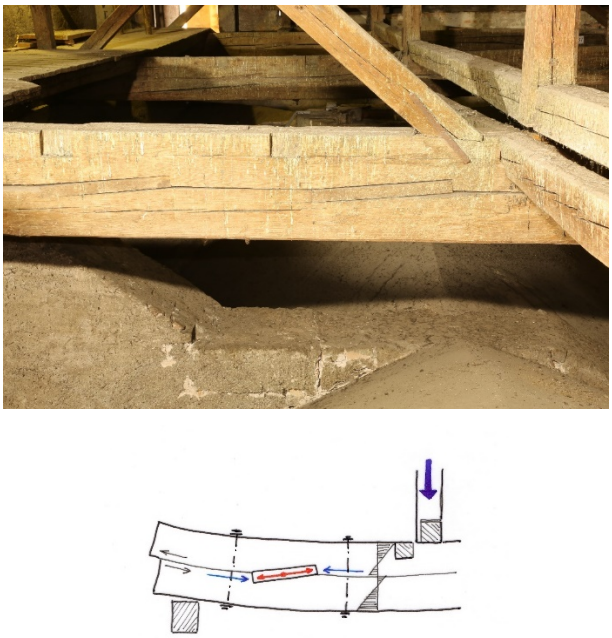

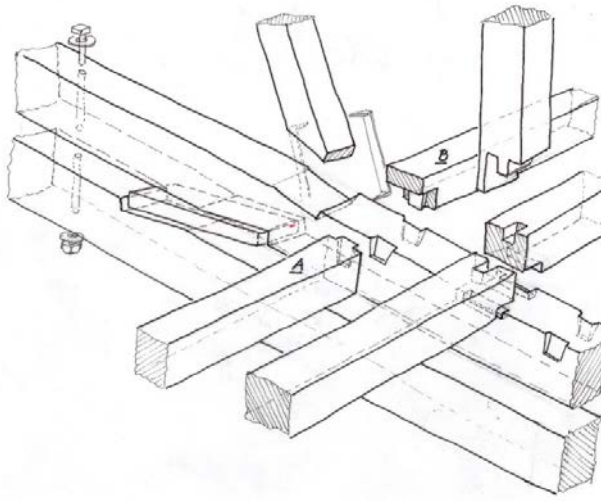

Figure 18 a) – c). An interesting complex is found in the roof of the side aisle of the Cathedral. The king post rests on a double beam with longitudinal stabilisers. Notice the insertion of skew blocks. They transfer the tension stresses of the upper beam to the compression side of the lower beam and vice versa [11]. This makes the double beam a true composite member. The stiffness and perfectly tight joints were affected only after the double beam sank into the wall insert due to extensive rot.

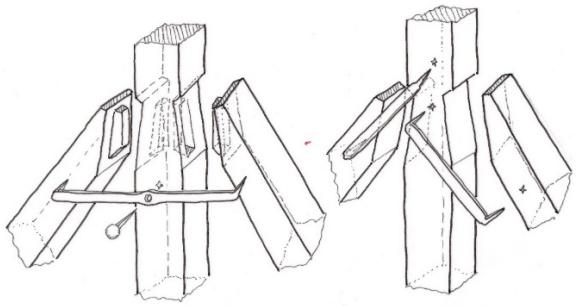

Figure 19 a) and b). Connections of the principal rafters to the king post at the ridge. Various solutions were found. The option seen in the photograph and the left sketch used housed notched joints with mortise and tenon. These were secured either by stirrups or by clamps with a central bolt. The solution on the right, a simple notched joint with clamps, was not firm enough and opened over time.

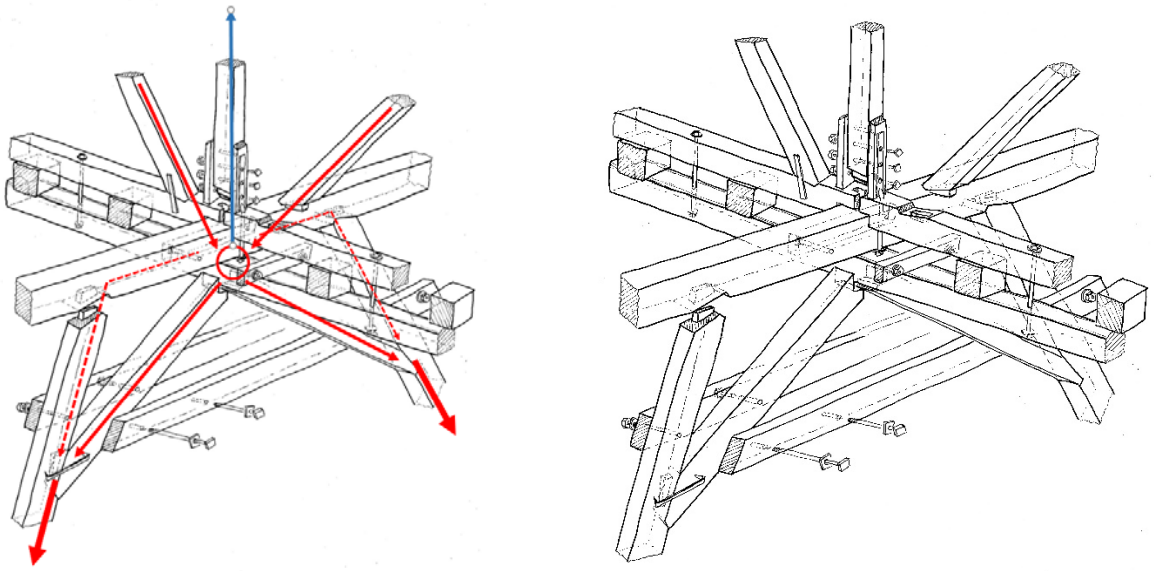

Figure 20 a) – c). Side aisle of the Cathedral. This is an example of a carpenter's ingenuity in complex spatial jointing. It features a composed I-beam, a queen post above, and a reclining truss underneath the joint. The forces are distributed evenly and transferred to the foundation (left sketch). The composed beam has lost some integrity due to the shrinkage and sinking of nut washers in the softwood, but it remains functional. Other joints, secured by iron connectors, still perform perfectly.

Figure 21. The work of an expert on-site consists of careful observations, crawling on the floor, and hanging from the trusses (the structural framework that supports the roof). The expert approaches the object with a camera and light, as well as measurement tools and scientific instruments used to assess its structural integrity. The process concludes with a discussion among all the involved parties, including carpenters, to achieve a satisfactory outcome for all. Photo by J. Pojatina.

DISCUSSION

In twenty-odd buildings that we evaluated over the last four years, the condition of joints (the connections between wooden structural elements) was carefully inspected, and in cases of poor connections, remedial measures were considered and proposed. By far the greatest volume of damage was found on the wall supports due to biological damage (such as condensation, roof leaking, and lack of ventilation). Particularly, the wall plates (horizontal wooden members built into brickwork or plaster to support roof timbers) and the non-ventilated ends of tie-beams (horizontal beams preventing the roof from spreading) were affected to the extent that the overall structural integrity was jeopardised. Some joints were well chosen for the purpose, but are now loosened or broken due to the inadequate design of the whole structure. Most often, the reason for this can be found in too-thin members (e.g.,

collars, spurs, or purlins, which are horizontal or diagonal wooden roof elements) that underwent deformations due to prolonged loads and creep (slow deformation under constant stress). Such altered geometry also affected the joints, whether well-chosen and made or not.

Building on these observations, only a small number of wrongly chosen joints were found, which indicates that, in most roof structures, carpenters from central Europe, or Croatian craftsmen trained in the central-European tradition, were engaged in the works. On the other hand, roofs can be found that are still in very good condition after centuries of use; their joints are tight and fit for the purpose. There are also examples of exceptional joints and exquisite craftsmanship evident in many cases (as in [12] and [13]), which represent a good guideline for evaluating other churches or monumental buildings from former periods in Croatia.

Whenever a poor or biodegraded joint complex (a group of interrelated joints) was identified, the joint analysis was presented to the engineer designing the remedial measures. In most cases, the solutions followed the recommendations from the restaurators' field (specialists in restoration and conservation) to install the prostheses (structural replacements) or reinforcements in accordance with the period of built. If possible, the members (individual wooden elements) and their joints were used for repair that can be found elsewhere on the structure, or in structures from the same period.

Craftsmanship significantly impacts the quality of joints; presented are examples of good joints (effective types of connections) that were poorly executed. The tolerances (gaps allowed in the fits between parts) enabled the movements within the joined surfaces and damage (loosening and falling out of wood pegs, shear failures, or compression perpendicular to fibres, which is crushing of wood against its grain).

Finally, in an attempt to further underline the fil rouge of this paper, it is important to interpret the title expert as a concept, not a specific person. It is obvious that an expert presents several different individuals with their respective fields of competence, each possessing the necessary expertise. Traditional carpentry joints, with all their complexity, require a versatile experience for a high-level assessment and a significant amount of in situ work by various professionals. Therefore, it is most important to create a collaborative environment for every heritage project.
We hope that our analytical work on the joints may serve as an indication for future restoration works.

CONCLUSION

Despite the good outlines for joint analysis and evaluation provided in the standard EN 17121, the role and experience of the expert with versatile knowledge (wood technologist, structural engineer, conservationist, and even carpenters) on site remain crucial for the proper assessment of the joints. Careful analysis of the selection of the type of joint for each function and quality of construction, taking into account the load distribution and anatomical directions of wood, moisture effects, and craftsmanship, as well as the condition of building ironmongery, should all be taken into consideration. The result should also anticipate the possible methods of restructuring and repair, taking into account the carpenter's skills and the practicality of their work in a restricted space. When dealing with historic buildings, the remedial aspects should preferably follow the demands for authenticity; therefore, the choice of wood species for prostheses and joint repairs should, as much as possible, follow the status of the original building period. Exceptions, however, must sometimes be taken as a sound compromise (e.g., steel reinforcing elements) when the long-lasting stability and functionality of the structure might be endangered, particularly in regions of high seismic risk.

REFERENCES

[1] Branco, J.; Descamps, T. (2015): Analysis and strengthening of carpentry joints. Construction and Building materials, 97: 34-47.

[2] Branco, J.; Dietsch, Ph.; Tannert, T. (2021): Reinforcement of Timber Elements in Existing Structures. State-of-the-Art Report of the RILEM TC 245-RTE. Cham: Springer Nature Switzerland AG. https://doi.org/10.1007/978-3-030-67794-7

[3] Müller, A.; Vogel, M.; Lang, S.; Sauser, F. (2016): Historische Holzverbindungen (in German). Bericht 74FE-F.006967-FB-01 A. Bern: Berner Fachhochschule, Institut für Holzbau, Tragwerke und Architektur. P. 1-68.

[4] Warth, O. (1900): Konstruktionen in Holz. Leipzig: J.M. Gebhard's Verlag. Reprint in Edition "Libri rari" by Verlag Th. Schäfer, Hannover, 1982.

[5] EN 17121 (2019): Conservataion of cultural heritage – Historic timber structures – Guidelines for the on-line assessment of load-bearing structures. CEN, 28 pp.

[6] Ceraldi, C.; D'Ambra, C.; Lippiello, M.; Sandoli, A.; Prota, A. (2021): Reinforcing stop-splayed scarf joints with timber pegs: Role of slenderness. In: Proceedings of the 8th ECCOMAS Thematic Conference on Computatioinal Methods in Structural Dynamics and Earthquake Engineering (Papadrakakis, M.; Fragiadakis, M. Eds). Athens, Greece 27 – 30 June 2021. Pp 15.

[7] Karolak, A.; Jasieńko, J.; Raszczuk, K. (2020): Historical scarf and splice carpentry joints: state of the art. Heritage Science 8: 2-19. https://doi.org/10.1186/s40494-020-00448-2.

[8] Branco, J.; Verbist, M.; Tsakanika, E. (2021): Reinforcement of traditional carpentry joints. In: J.Branco, Dietsch, P.; Tannert, T. (eds.): Reinforcement of Timber Elements in Existing Structures, RILEM State-of-the-Art eports 33, 247-271

[9] Tampone, G. (1996): Il restauro delle strutture di legno. Milano: Ulrico Hoepli Editore S.p.A.

[10] Mönck, W.; Erler, K. (2004): Schäden an Holzkonstruktionen. Analyse und Behebung (4. Auflage). Berlin: Huss-Medien GmbH

[11] Rug, W.; Thoms, F.; Grimim, U.; Eichbaum, G.; Abel, S. (2012): Untersuchungen zur Biegetragfähigkeit von verzahnten Balken. Bautechnik 89 (1): 26-36.

[12] Kunecky, Hasniková, H.; Kloiber, M.; Fajman, P.; Kuklík, P.; Sebera, V.; Tippner, J. (2015): Lapped scarf Joints for Repairs of Historical Structures. Result of applied research – design method. Prague: Ministry of Culture of the Czech Republic, pp. 72. DOI: 10.21495/73-4

[13] Weiss, W. (2019): Fachwerk – Bautraditionen in Mitteleuropa. Stuttgart: Fraunhofer IRB Verlag

[14] ××× (2015): Altes Holz – neu gedacht. Zuschnitt 57. Wien: proHolz Austria

STRUCTURAL HEALTH ASSESSMENT OF TIMBER STRUCTURES: A GRADUATE LEARNING EXPERIENCE

Mariapaola RIGGIO[1], Autumn BATTISTI[2], Opeyemi Elisabeth ODULE[2], Shane JOHNSON[2] and Anthony NEWTON[2]

[1] Associate Professor, Wood Science and Engineering, Oregon State University, Corvallis, OR, USA

[2] MS student, Wood Science and Engineering, Oregon State University, Corvallis, OR, USA

ABSTRACT

This paper presents an educational experience within the Wood Science and Engineering graduate program at Oregon State University. The Structural Health Assessment and Monitoring of Timber Structures is a course that introduces interdisciplinary topics, including structural evaluation and non-destructive testing. A key component is a hands-on project where students assess an existing timber building, working with real client requests to develop a tailored assessment plan. The course is based on a structured, multi-stage assessment procedure that includes desk surveys, visual inspection, material characterisation, and evaluation of damage and decay. Students apply a variety of non-destructive and semi-destructive techniques during their field study. In a recent case study of historical glulam portal frames, students identified the timber species as Douglas Fir and the adhesive as likely phenol-resorcinol. The assessment revealed issues such as delamination and localised brown rot, one instance of which had compromised the load-bearing capacity of a structural element. The findings provided the building owner with actionable insights, highlighting areas needing immediate intervention and others warranting ongoing monitoring. This practical experience allows students to apply theoretical knowledge to real-world challenges. Emphasising critical thinking and decision making, the course prepares students with the practical skills essential for application in engineering and other related fields.

KEYWORDS: structural health assessment, historical glulam, graduate curriculum

INTRODUCTION

Timber structures, both historic and contemporary, play a central role in the built environment, reflecting a broad spectrum of architectural, material, and cultural values. As the use of engineered wood systems in modern construction continues to expand, so too does the demand for specialised knowledge in evaluating and maintaining timber structures throughout their service life. At the same time, the conservation of architectural timber heritage and the growing interest in the reuse of reclaimed wood elements have amplified the need for reliable, technically sound approaches to structural health assessment. In these contexts, ranging from large-span glulam systems to centuries-old roof trusses, practitioners are increasingly called upon to assess the performance, safety, and durability of timber elements under uncertain or evolving conditions.

Recognising these challenges, the Wood Science and Engineering graduate program at Oregon State University (OSU) has developed an advanced course titled Structural Health Assessment and Monitoring of Timber Structures. The course introduces students to interdisciplinary concepts and tools for in situ

evaluation of timber systems, emphasising a holistic, multi-level approach to diagnosing the physical and mechanical condition of structural elements. Through a combination of lectures, field exercises, and hands-on work with a real client and case study building, students gain direct experience with the methods and decision-making processes required to conduct meaningful structural assessments.

This paper presents the structure, content, and pedagogical rationale of the course, highlighting its integration of visual inspection strategies and non-destructive and semi-destructive testing techniques. The course project is also presented as a concrete example of student tasks and learning outcomes, illustrating how experiential learning fosters technical competence and critical thinking in structural health assessment. By documenting this educational experience, we aim to contribute to the broader discourse on graduate-level curricula that bridge material science, conservation practice, and engineering.

CONTENT OF THE COURSE

The course Structural Health Assessment and Monitoring of Timber Structures is structured to provide graduate students with a comprehensive and applied understanding of how to evaluate the condition and performance of timber systems in service. Delivered through a combination of student-led lectures, group assignments, and a real-world case study, the course introduces students to a multi-scale, multi-method approach to structural assessment, emphasising the integration of diverse diagnostic tools and interpretive strategies.

The course begins with an introduction to the scope and procedures of in-situ assessment, focusing on the importance of visual inspection as a first-level tool for identifying potential issues and informing subsequent investigative stages. Students are introduced to the challenges of working with timber structures, particularly those with limited documentation or uncertain service histories, and begin developing inspection strategies based on document review and site observations [1], [2], [3]. In the second week, students conduct a guided on-site visual inspection of a selected case study building. Working as a team, they assess areas of visible damage or deterioration and propose targeted sampling plans for wood species identification and moisture content evaluation. This first-hand experience reinforces the need for systematic observation and critical thinking in navigating incomplete or ambiguous field conditions. Subsequent weeks expand the technical repertoire of the students through focused study of both semi-destructive and non-destructive testing techniques. Students analyse various semi-destructive testing (SDT) methods from the literature [4], [5] and select the most appropriate approach to estimate the mechanical properties of the timber elements in their assigned case study, subsequently developing a tailored testing plan specific to their project. In the following weeks, students are introduced to non-destructive testing (NDT) techniques based on electromagnetic [6] and mechanical wave propagation [7], [8]. They then select appropriate methods and utilise available tools, such as infrared thermal imaging and ultrasound devices, to extract relevant information from their case study. In the final technical module, students focus on applying localised semi-destructive testing methods for characterising decay and damage, using techniques such as resistance drilling [9], [10].

After acquiring theoretical knowledge of the different techniques and designing a detailed plan for each assessment stage, students return to the site to implement their testing strategies in practice. Following a series of site visits for data collection, students prepare both a formal presentation and a comprehensive final report documenting their structural health assessment study.

CASE STUDY: CONDITION AND PERFORMANCE EVALUATION OF HISTORIC GLULAM PORTALS FOR CIRCULAR ECONOMY APPLICATIONS

Figure 30. The Oak Creek Building

The case study presented in this paper focuses on the structural health assessment of glued laminated timber (glulam) portals within the Oak Creek Building (OCD) on Oregon State University's (OSU's) Corvallis campus (Figure 1), a facility currently housing office spaces, laboratories, and wood shops serving multiple departments and colleges. Constructed in the early 1950s, this building incorporated glulam technology, a then-emerging structural solution in the United States. Over time, natural ageing and environmental exposure have taken a toll on the structure, with visible signs of decay and several previously repaired elements, making a thorough condition assessment both necessary and timely. The evaluation focuses on the glulam portals along the east and west wings of the OCB, 18 in the east wing and 13 in the west. Each portal features 13.7-meter-long double-pitched cambered beams and two 4.4-meter-tall, tapered columns, with the columns exposed on the building's exterior.

By systematically evaluating these critical load-bearing elements, this assessment aims to inform facility administrators on maintenance and intervention priorities, enabling safer operation and more efficient planning for the building's future. Furthermore, the evaluation of the glulam elements' suitability for reuse supports a data-driven cost-benefit analysis, offering insights into potential circular economy applications.

Beyond this specific case, glulam represents relatively young structural technology within the broader timber industry, with many early installations now approaching the end of their service lives.

METHODOLOGY

During the desk survey phase, students reviewed the building's original blueprints, historical records, and technical documents relevant to glulam, including manufacturing standards from the era of the building's construction. This investigation helped identify the likely manufacturer and key material characteristics of the glulam portals under study.

During the visual inspection, students examined the spatial layout, material characteristics, construction details, and environmental exposure of the portals. Additionally, the inspection focused on identifying visible signs of deterioration that could affect the structural integrity or longevity of the timber elements, including surface damage, delamination, moisture staining, and other indicators of potential distress. Repairs and modifications to the inspected beams and columns were also documented. The presence, type, and distribution of degradation and damage in the inspected elements were documented using thematic maps.

The wood species was identified based on anatomical analysis of a wood sample. Local moisture content was measured on accessible columns using a resistance moisture meter with insulated probes, calibrated for Douglas-fir based on surface temperatures recorded by a thermal camera.

To establish a baseline for each accessible column, stress-wave time-of-flight measurements perpendicular to the grain were taken. This method provides an approximate indication of the wood's mechanical properties and helps screen for decay or damage by analysing stress-wave velocity. The tests were conducted using Proceq's Pundit 200 ultrasonic pulse velocity system with 54 kHz transducers, with measurements taken at five points along the height of each column, parallel to the laminations. Stress-wave velocity readings were compared across all columns and against published industry benchmarks [11], [12], [13] to assess the condition of the glulam's wood.

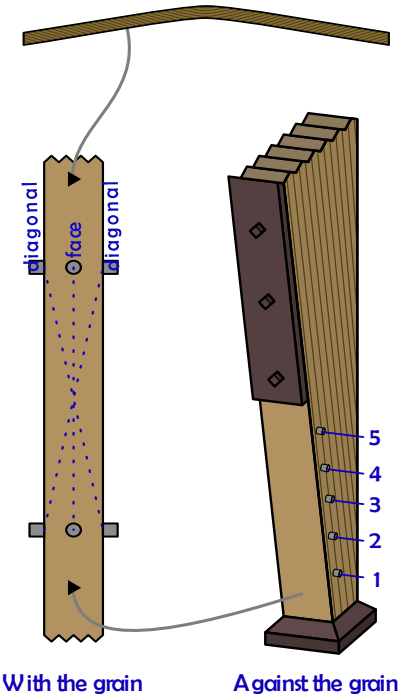

Figure 31. A diagram illustrating where stress wave velocity is measured. The left illustrates the outer face of a column or the lower face of a beam for along the grain assessment, while the right illustrates the setup for against the grain variability testing.

Moisture content readings were also factored in, as higher moisture typically increases mass and density without boosting stiffness, which can lower velocity. The impact of moisture content on velocity across the grain was mitigated using a second-degree polynomial approximation as detailed in [14], shown in Equation 1 and Equation 2 where a, b, and c are constants from the polynomial fit from [14], MC is the moisture content which you are estimating the velocity for(12% was used in this paper), $v_L(MC)$ represents the fitted velocity along the grain as a function of moisture content, v_m is the measured velocity across the grain, MC_m is the measured moisture content, and $v_T(MC)$ represents approximated velocity across the grain as a function of moisture content.

Equation 2: $$v_L(MC) = a + b \times MC + c \times MC^2$$

Equation 3: $$v_T(MC) = v_m \frac{v_L(MC)}{v_L(MC_m)}$$

To estimate the mechanical properties of the glulam members, stress-wave velocity was measured along the grain of the sampled beams or columns to determine their dynamic modulus of elasticity. Measurements were taken on the same face of the glulam (external lamination) as well as diagonally across the two opposite faces of the member (Figure 2).

Equation 3 provides an approximate conversion between velocity across the grain ($\boldsymbol{v_T}$) and velocity along the grain ($\boldsymbol{v_L}$), based on the assumption—supported by Dackermann et al. [7]—that velocity across the grain is typically between one fifth and one third of the velocity along the grain. Building on this, Equation 4 introduces a correction factor for diagonal measurements, where the measured diagonal velocity ($\boldsymbol{v_d}$) is adjusted to estimate its equivalent velocity along the grain ($\boldsymbol{v_L}$), assuming the effect on velocity is proportional to travel along each axis.

Equation 5 is then used to approximate a dynamic modulus of elasticity, assuming a density ($\boldsymbol{\rho}$) of 479 kg/m^3 approximated from the Wood Handbook [15].

Equation 4: $$v_T \approx \frac{4}{15} v_L$$

Equation 5: $v_L \approx \sqrt{((\frac{15}{4} \times \frac{0.172\text{m}}{1.014\text{m}})v_d)^2 + (\frac{1\text{m}}{1.014\text{m}}v_d)^2} = 1.174v_d$

Equation 6: $E_{\text{dyn}} = \rho v^2$

All stress-wave velocity measurements are taken within-lamella, and so should not be significantly affected by, or be an indicator of, the health of the glue line boundaries.

Samples were also taken to assess glue line quality and perform tensile Young's modulus tests on meso-specimens. Glue line quality can be evaluated using block shear tests as described in [16], while tensile tests help correlate the sample tensile strength of extracted clear wood samples with the bending strength of the timber components [4]. Although the samples were extracted from the elements, the tests were not performed; therefore, results from these tests are not included in the following section.

RESULTS

Figure 32. The Oregon Forest Research Laboratory (later renamed the Oak Creek Building), captured soon after completion in 1956 [17], showing a sunshade circumnavigating the perimeter of the building.

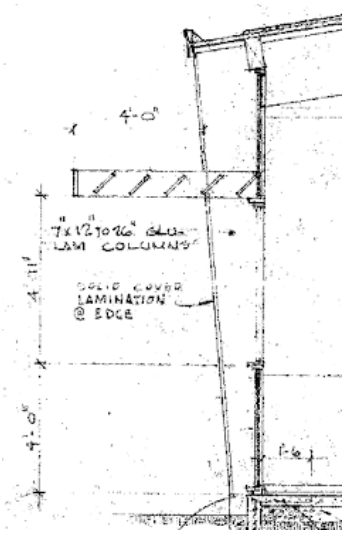

Figure 33. James L. Payne's 1956 blueprint, including the sunshade [18].

The building's construction likely adhered to the 1954 Timber Construction Standards by the American Institute of Timber Construction, which included glulam products [19]. The first glulam-specific manufacturing standard was Commercial Standards CS 253-63 [20]. Since then, standards have evolved significantly in terms of requirements for lumber grading, bonding surfaces, adhesive application and curing, and daily quality control. The glue was assumed to be water-resistant, based on 1935 records from Unit Structures, Inc., which reportedly used such adhesives [21]. Timber Structures, Inc., the probable manufacturer, likely followed this practice [22]. According to APA (The Engineered Wood Association), fully water-resistant phenol-resorcinol adhesives were introduced in 1942, allowing glulam to withstand exterior exposure without glue line degradation [23].

By comparing the existing configuration with the original blueprints, they identified several discrepancies, most notably, a missing portal in the east wing and the absence of a canopy that was originally attached to the exterior columns and ran along all sides of the building (see Figure 4), as

confirmed by historical photographs (Figure 3) [17], [18]. The historical drawings do not include details of the timber connections, nor do they mention the bolted steel plates observed covering the face of all the inspected columns [18].

In order to be able to discuss the subjects of their analysis with each other and to increase the cohesion of their final report, the students developed a naming scheme to refer to the relevant columns and beams. A, B, C, and D refer to the sides of the buildings going from west to east, and portals were numbered from north to south for each building. So B8 (referred to in Figure 5) refers to the 8th column on the east side of the west wing. This system is used throughout their report and this paper.

Figure 34. From left to right A13 with damaged coating, B8 with a wood prosthesis, D15 with a metal prosthesis and extended bracket, and D7 with notable brown rot in addition to a metal prosthesis and extended bracket.

By comparing the existing configuration with the original blueprints, they identified several discrepancies, most notably, a missing portal in the east wing and the absence of a canopy that was originally attached to the exterior columns and ran along all sides of the building (see Figure 4), as confirmed by historical photographs (Figure 3) [17], [18]. The historical drawings do not include details of the timber connections, nor do they mention the bolted steel plates observed covering the face of all the inspected columns [18].

Most glulam columns exhibited some degree of surface delamination. Discolouration, likely due to ageing and prolonged UV exposure, was also observed in several columns. Coating degradation ranged from minor to severe, with only a few cases showing extensive damage. In some instances, visible repairs had been made using either wood or metal components (Figure 5). One column, in particular, showed significant fungal decay and deep delamination (Figure 5); this element was flagged at multiple points throughout the assessment and should be prioritised for remediation.

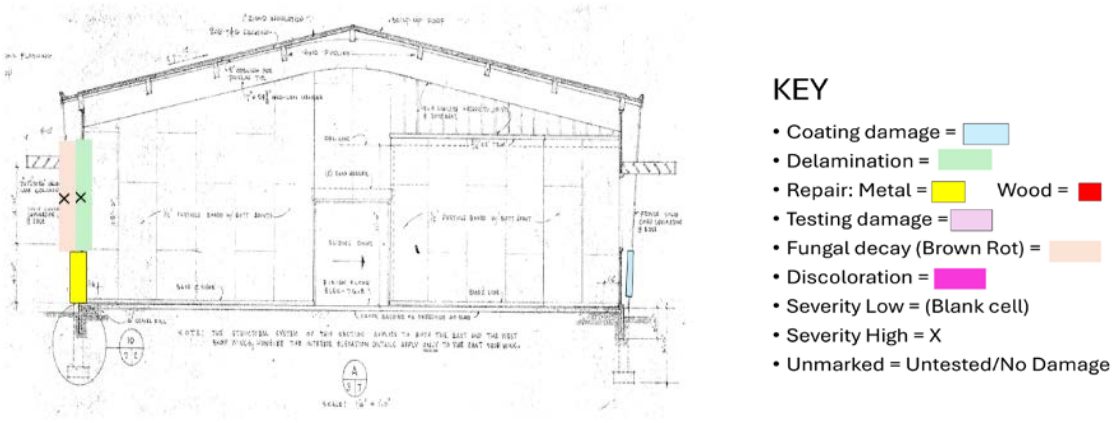

Figure 35. A sample condition assessment map for one of the portals overlayed on a diagram from the blueprints [18], detailing the nature and location of observed deterioration and damage, as well as including a key for identification of observed damage.

The visual inspection was conducted using the naked eye and a thermal camera. Figure 6 presents a single portal assessment which was made for all 31 portals included in the building. This one in particular showed severe delamination and fungal decay present. This portal has been flagged for high necessity of addressing to ensure the safety and health of the overall structure.

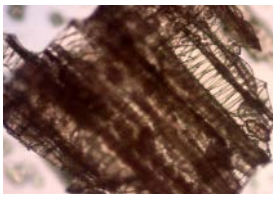

Figure 36. Helical thickenings identified in the wood samples show the likely species of Douglas-fir.

Douglas-fir (*Pseudotsuga menziesii*) was identified as the likely species based on anatomical analysis of a wood sample. Despite decay, the presence of helical thickenings (Figure 7), distinct to Douglas-fir among species listed in the 1954 AITC standards, confirmed the identification. These features are not caused by decay.

Figure 8 shows colour-scaled moisture content measurements by location. The west wing generally exhibits lower moisture content compared to the east wing, with the highest levels observed on the east side of the east wing. Additionally, columns in the south-eastern corner of the inner lot show elevated moisture levels. These variations may be influenced by factors such as higher precipitation exposure, reduced sunlight, or areas with more damaged protective coatings.

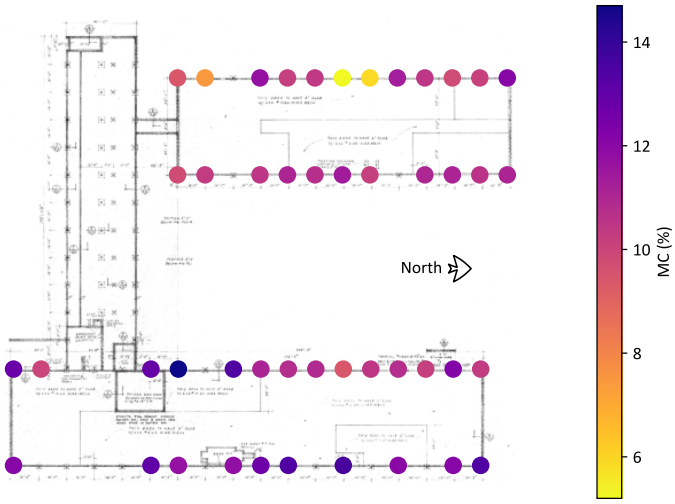

Figure 37. A modified blueprint of the Oak Creek Building [22] overlayed with each column's measured MC (if it was taken). Please note that the top row of measurements was taken five days before the rest and is not necessarily directly comparable.

Figure 9 presents all stress-wave velocity measurements used for variability analysis, adjusted for moisture content. Each point represents the average velocity for a given column, with the upper and lower markers indicating the maximum and minimum values measured, respectively. These results are compared to transversal stress-wave velocities for Douglas-fir reported in the literature [11], [12], [13].

Overall, the measured velocities in Figure 9 compare favourably with reference values, and moisture content appears to have minimal impact at this scale. Many columns show tightly clustered measurements, indicating good within-element homogeneity, though several outliers are also present. It is worth noting that some columns, such as column D7 (pictured in Figure 5), which was previously repaired with a metal prosthesis and appears to still retain significant decay damage, weren't tested. The test results, therefore, don't reflect the conditions of the most damaged elements.

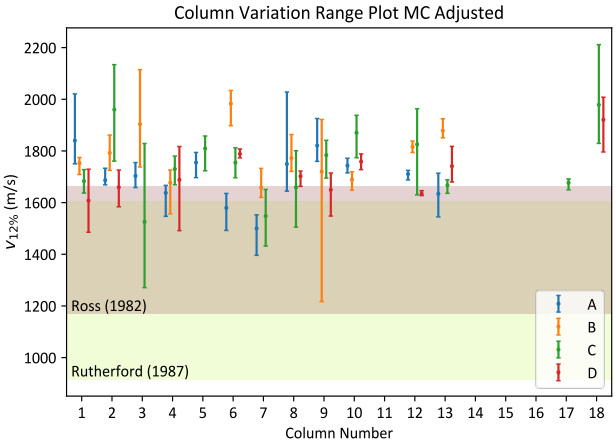

Figure 38. Stress-wave velocity readings for a 54 kHz transducer across the grain, compared to reference values [11], [12], [13], corrected for MC according to Equation 2.

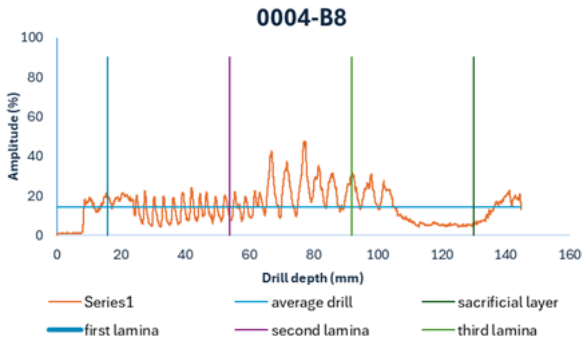

Figure 39. Resistance drilling graph with possible decay

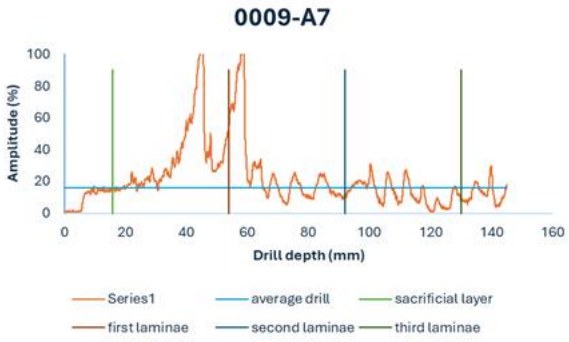

Figure 40. Resistance drilling graph with an area of very high density

Figures 10 and 11 show two resistance drilling profiles. In Figure 12, the third to fourth laminae of column B8 show flat signals, which are typically indicative of wood decay. From the table of averages above, the average percentage amplitude for this lamina is approximately 11.6% which is low compared to other laminae's percentage amplitude. In Figure 11, the first and second laminae of the column show very high signal intensity of approximately 34.4% and 26.6% respectively, as obtained from the table above, indicating the presence of knots or another highly dense material.

Table 1 reports the average amplitude values of drilling resistance torque required to drill through each tested column and beam, calculated for each lamina of columns tested, with highlighted extreme low and high average values.

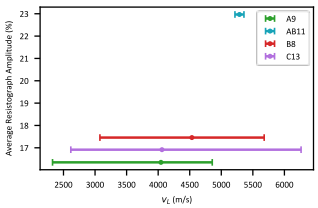

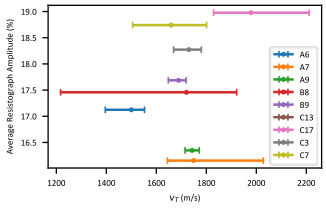

Figure 41. and Figure 42. Average resistance compared with velocities along the grain on the left and across the gran on the right.

Figure 12 and Figure 13 illustrate the relationships between average drilling resistance and stress-wave velocity measured parallel and perpendicular to the grain, respectively. As shown in the plots, no clear correlation emerges between drilling resistance and either orientation of stress-wave velocity. This outcome is expected, as the measurements were not taken at identical locations or along the same orientation within the members.

#	Column	Lamina 0	1	2	3
2	B9	5.67	22.24	17.86	16.50
3	B9	5.47	19.77	20.28	17.44
1	B9	7.22	32.01	19.53	17.42
4	B8	8.21	13.63	21.19	11.60
5	B8	7.68	17.60	21.36	21.12
9	A7	8.89	34.37	26.57	12.56
10	A7	5.61	26.78	20.59	13.19
11	A6	5.37	18.32	22.67	17.80
12	A6	5.23	17.91	20.84	17.10
13	C3	7.84	22.27	26.36	19.89
14	C3	8.96	20.24	22.86	19.36
15	C3	4.56	13.67	20.83	13.22
16	C7	9.16	16.85	19.01	22.16
17	C7	8.42	18.00	18.10	23.09
18	C17	8.67	18.93	20.26	37.15
21	A9	7.81	14.27	20.33	15.99
22	A9	7.11	17.05	20.23	18.01
23	C13	5.16	17.27	16.42	19.95
24	C13	5.61	17.02	17.25	19.79
25	D18	5.70	10.83	14.31	18.43
26	D18	7.27	11.60	16.51	21.46

Table 4. Average resistance amplitude (%) by lamella for each sample column and beam. Extreme low and high values are highlighted. Lamina 0 is called the sacrificial lamina in the blueprints and has about half of the thickness of the other laminas[18]. The number (#) refers to the resistograph sample the data was sourced form.

The results of the stress-wave velocity tests along the grain showed considerable variability within members, with an average absolute percent error per location

of 12.8%. This contrasts with the variability test of velocity across the grain, which had a lower error of 3.48%. When converted to the dynamic modulus of elasticity ($\boldsymbol{E}_{\mathrm{dyn}}$) using Equation 5: $\mathrm{E}_{\mathrm{dyn}} = \rho \mathrm{v}^2$ the average values fall slightly below the nominal values for common Douglas-fir species [15] (Figure 14).

This test used a 24 kHz transducer, which was later determined to be faulty. It generally reported a higher time-of-flight than expected according to the manufacturer. This was mitigated by subtracting the difference in time from a calibration rod, but the fault may extend further than a static time delta. This may account for the 24 kHz velocity values being significantly lower than the 54 kHz values in Figure 14.

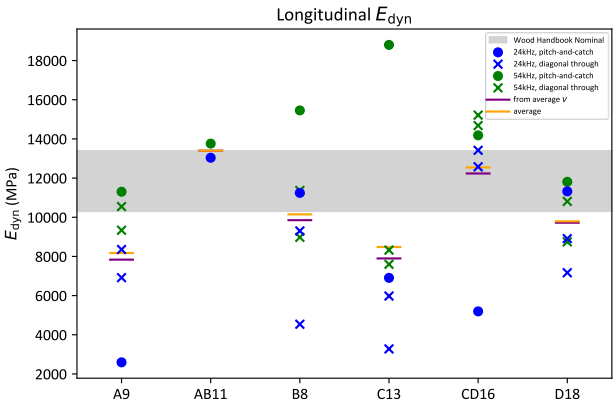

Figure 43. Calculated modulus of elasticity from measurements of velocity along the grain compared against nominal values given in the Wood Handbook for common Douglas-fir species [15].

To conclude, the structural assessment found the glulam members to be generally in adequate condition, with a few exceptions. Most non-decayed columns retained their mechanical properties, though widespread surface delamination, present in about 15% of columns, warrants further investigation. In contrast, the beams exhibited minimal deterioration. Regarding material reusability, the presence of embedded hardware on the column faces poses a challenge. Additionally, the structural reuse of integral beams is not supported by the results of the performed testing ($\boldsymbol{E}_{\mathrm{dyn}}$) and is currently limited by the absence of standardised procedures for re-certification.

CONCLUSION

By combining a desk survey, visual inspection, and various NDT and SDT testing techniques, valuable insights were obtained regarding the condition of the investigated structure. The analysis of historical standards helped identify key technological characteristics of the glulam materials, including the type of adhesive used. Microscopic examination of collected samples confirmed the wood species. Visual inspection revealed issues such as delamination and localised brown rot, one instance of which had compromised the load-bearing capacity of a structural element. Although some of the most deteriorated components could not be assessed using NDT methods, the tests performed did not indicate significant variability among the tested members, even in areas with suspected delamination. Overall, the findings provided the building owner with actionable information, highlighting areas requiring immediate intervention and others that should be monitored over time.

This course encouraged students to develop individual areas of expertise within the curriculum. By assigning specific research techniques or focus areas to each student and then having them share their findings with the class, the course ensured that every student contributed a unique and tangible value to the collective learning experience. A common challenge in collaborative projects, especially within single-department courses, is the overlap in students' educational backgrounds, which can make it difficult for individuals to feel they've made a distinct contribution. By distributing expertise intentionally, the course allowed students to take greater ownership and pride in their work if they chose to engage with it.

The structural health monitoring course has not only shown students the importance of proper diagnosis and prognosis of in-service structural members but has also demonstrated to them the need for collaborative effort in achieving greater results, both academic and in practice. The teamwork of the students has helped identify areas of concern in the structural members of a historical building, which will properly inform remediation or maintenance practices. Detection of decay and defects in timber structures is an essential skill that is constantly required in the construction industry, which can save companies the cost incurred from structural failures and protect lives and properties. This course has equipped its students with knowledge and skills that add value to the industry. In the future, more non-destructive or semi-destructive testing techniques may be explored to reduce the visually unappealing impact of destructive testing on the structural member.

REFERENCES

[1] H. Cruz *et al.*, "Guidelines for On-Site Assessment of Historic Timber Structures," *International Journal of Architectural Heritage*, vol. 9, no. 3, pp. 277–289, 2015, doi: 10.1080/15583058.2013.774070.

[2] M. Riggio *et al.*, "In situ assessment of structural timber using non-destructive techniques," *Materials and Structures*, vol. 47, no. 5, pp. 749–766, May 2014, doi: 10.1617/s11527-013-0095-4.

[3] M. Riggio, D. D'Ayala, M. A. Parisi, and C. Tardini, "Assessment of heritage timber structures: Review of standards, guidelines and procedures," *Journal of Cultural Heritage*, vol. 31, pp. 220–235, 2018, doi: 10.1016/j.culher.2017.11.007.

[4] M. Kloiber, M. Drdácký, J. S. Machado, M. Piazza, and N. Yamaguchi, "Prediction of mechanical properties by means of semi-destructive methods: A review," *Construction & Building Materials*, vol. 101, pp. 1215–1234, Dec. 2015, doi: 10.1016/j.conbuildmat.2015.05.134.

[5] T. Tannert *et al.*, "In situ assessment of structural timber using semi-destructive techniques," *Materials and Structures*, vol. 47, no. 5, pp. 767–785, May 2014, doi: 10.1617/s11527-013-0095-4.

[6] M. Riggio, J. Sandak, and S. Franke, "Application of imaging techniques for detection of defects, damage and decay in timber structures on-site," *Construction & Building Materials*, vol. 101, pp. 1241–1252, 2015, doi: 10.1016/j.conbuildmat.2015.06.065.

[7] U. Dackermann *et al.*, "In situ assessment of structural timber using stress-wave measurements," *Materials and Structures*, vol. 47, no. 5, pp. 787–803, May 2014, doi: 10.1617/s11527-013-0095-4.

[8] A. C. Senalik, G. Schueneman, and R. J. Ross, "Ultrasonic-Based Nondestructive Evaluation Methods for Wood: A Primer and Historical Review," U.S. Department of Agriculture, Forest Service, Forest Products Laboratory, 2014. doi: 10.2737/fpl-gtr-235.

[9] T. P. Nowak, J. Jasieńko, and K. Hamrol-Bielecka, "In situ assessment of structural timber using the resistance drilling method – Evaluation of usefulness," *Construction & Building Materials*, vol. 102, pp. 403–415, 2016, doi: 10.1016/j.conbuildmat.2015.11.004.

[10] L. Palaia, V. Lopez, J. Monfort, S. Esteve, P. Navarro, and M. Ángeles, "Procedure for NDT and Traditional Methods of Ancient Building Diagnosis, by Using Thermograph, Digital Images and other instruments data Analysis.," Jan. 2008.

[11] R. E. Pellerin and R. J. Ross, "Chapter 9; Inspection of Timber Structures Using Stress Wave Timing Nondestructive Evaluation Tools".

[12] R. J. Ross, “Quality assessment of the wooden beams and columns of Bay C of the east end of Washington State University’s football stadium,” Washington State University, Pullman, WA, Unpublished research, 1982.

[13] P. S. Rutherford, “Nondestructive stress wave measurement of incipient decay in Douglas Fir,” M.S. thesis, Washington State University, Pullman, WA, 1987.

[14] X. Wang, “Effects of Size and Moisture on Stress Wave E-rating of Structural Lumber,” 2008.

[15] D. E. Kretschmann, “Mechanical Properties of Wood,” in *Wood handbook : wood as an engineering material*, in General Technical Report, no. FPL-GTR-190. , Forest Products Laboratory: USDA Forest Service, 2010, p. Chapter 5. [Online]. Available: https://doi.org/10.2737/FPL-GTR-190

[16] B. Kasal and T. Tannert, Eds., *In situ assessment of structural timber*, vol. Vol. 7. Springer Science & Business Media, 2011.

[17] OSC News Bureau, *Forest Research Laboratory*. 1956. Accessed: Jun. 04, 2025. [Photograph]. Available: https://oregondigital.org/concern/images/df736r51h

[18] J. L. Payne, *Oregon Forest Research Center*. 1956.

[19] American Institute for Timber Construction, *Timber Construction Standards*, First Edition. Washington D.C., 1954.

[20] APA – The Engineered Wood Association, “Product Standard for Structural Glued Laminated Timber,” Tacoma, WA, Form A190.1-2022, Feb. 2022. [Online]. Available: https://www.apawood.org/publication-search?q=a190.1&tid=1

[21] I. Unit Structures, “An Oustanding Structural Achievement,” Peshtigo, WIS, Bulletin U-30. [Online]. Available: https://foresthistory.org/wp-content/uploads/2018/10/UnitStructures.pdf

[22] A. J. Rhude and A. Jordahl, “Structural glued laminated timber: History of its origins and early development”.

[23] APA – The Engineered Wood Association, “Glulam Product Guide,” Tacoma, WA, From X440E, 2017. [Online]. Available: https://www.apawood.org/publication-search?q=x440&tid=1

ASSESSMENT OF EXISTING TIMBER STRUCTURES - PORTUGUESE SELECTED EXAMPLES

Jorge M. BRANCO, Filipe SOUSA and Tiago S. LUÍS

ISISE, University of Minho

ABSTRACT

This paper seeks to showcase some of the latest studies involving the timber group at the University of Minho. The Sá de Miranda Secondary School, a large and impressive structure, exemplifies an old timber building affected by termite infestation. The ancient Braga Public Works building, one of the early projects by the renowned architect Marques da Silva, has been evaluated to accommodate new uses. These interventions required defining various repair and strengthening works. Although less complex, the assessment of the timber roof of the Póvoa de Varzim Town Council is also included, offering rich data and details. The objective is to discuss the procedures for assessing and diagnosing existing timber structures and how engineering, along with recent research and technical developments, can aid designers in their interventions.

KEYWORDS: Timber structures, assessment, repair, strengthening

INTRODUCTION

From the 18th to the early 20th century, traditional building construction in Portugal predominantly utilised timber for roof and floor structures, and occasionally for timber-reinforced masonry walls. As a result, the country's architectural heritage is abundant with timber-based structures, evident not only in historic and monumental buildings but also in the numerous edifices located in city centres. Many of these buildings remain in use today, despite having undergone significant modifications over time. Even with the widespread adoption of concrete, timber structures continued to play an important role, particularly in slab and roof construction. A substantial number of these timber structures now require structural intervention due to natural material degradation (ageing), inadequate maintenance, flawed design and/or construction, careless handling of wood, and/or accidental damage. Current understanding emphasises the importance of preserving and protecting existing wood systems as cultural assets, which offers considerable benefits for the overall performance of the building. Timber structures require meticulous analysis, akin to the scrutiny applied to structures composed of other materials. Given their significance and enduring role in construction, it is crucial not to overlook the proper analysis of traditional timber construction. Misunderstanding their behaviour could result in their disappearance within a few years. Designers must be well-versed in the material properties and adept at interpreting the performance of the structural system. Misinterpreting the global behaviour of traditional timber structures can lead to unacceptable stress distribution in the members, particularly due to inappropriate strengthening interventions, especially when connections are reinforced. The timber research group at the University of Minho, TimLab, boasts extensive experience in the assessment, diagnosis, and intervention of built timber heritage. This expertise stems from both research and engineering activities. This paper presents some of the most recent case studies in which TimLab has served as a consultant in recent years.

Sá de Miranda Secondary School

The Sá de Miranda Secondary School in Braga underwent renovations by Parque Escolar EPE in 2010, which included constructing new buildings and refurbishing existing ones. The original wooden floor beams and wall elements were preserved, while the floors, skirting boards, and wainscoting were replaced. Pine wood was used to replace the floors, whereas MDF was used for the panelling and some skirting boards. In 2015, signs of termite infestation were reported. A treatment was applied in March 2017. According to the Technical Specifications, this procedure involved: "Comprehensive treatment of the existing timber and timber to be used inside each room, including vacuuming of the air boxes, vacuuming and general cleaning of the entire structure, replacement of rotten or damaged solid timber in the existing slab structures (main beams, secondary beams, floor support beams and others), floors, skirting boards, wainscoting, door frames and trims. Treatment by spraying and injection with certified biocidal products such as XILIX GEL or equivalent, after removing the varnish and replacing the damaged areas" [1]. During a site visit in October 2018, signs of active infestation were still observed in untreated wood, although the effectiveness of the 2017 treatment is not necessarily in question. Specifically, in the Non-Teaching Staff Room, the removal of the false ceiling revealed the presence of termites in the structural elements of the ceiling/floor of Floor 1 (see Figure 1).

Figure 1. Cocoons on one of the main beams of the 1st floor structure (ceiling of the Non-Teaching Staff Room)

Based on this diagnostic phase, it was decided to propose an intervention in the staff room, intended to serve as a pilot intervention to define the actions to be implemented throughout the rest of the building. In addition, two complementary measures were recommended [1]: 1) the application of an anti-termite barrier along the exterior wall of the south façade, and 2) the implementation of a slow-acting colony control system and time monitoring of the risk of termite attack.

The chemical barrier should be applied externally to the south façade, as close to the ground level as possible. Injecting holes must be drilled exclusively into the masonry joints and properly sealed afterwards. This application must comply with the technical requirements provided by the supplier of the chemical compound that makes up the barrier, and the certified applicator for its proper execution.

The colony control and monitoring system involves the placement of soil stations in the main south courtyard, forming a perimeter around the building, particularly along the south façade. The soil traps should be spaced no more than five meters apart. Each station contains bait impregnated with a biocidal agent and is intended to act as a slow-acting mechanism for the medium-term eradication of the termite colony.

Braga Public Works Building

The building, designed by architect José Marques da Silva, dates to 1905. The construction began in 1906 and was officially inaugurated in 1931. Commissioned by Braga City Council, the building was intended to accommodate the post and telegraph services, public works department, and the industrial school (Figure 2) [2].

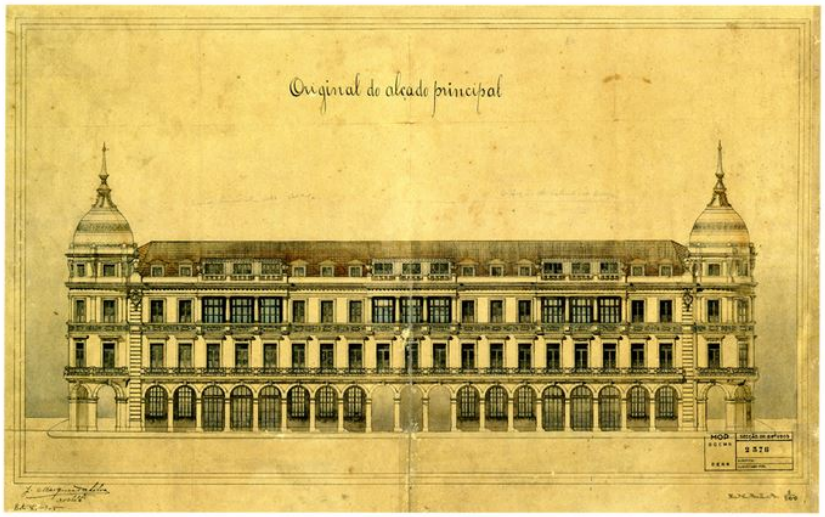

Figure 2. Original front view of the building

At an undetermined stage, the program was expanded to include the Bartolomeu dos Mártires Commercial and Industrial School, later called the Braga Commercial and Industrial School, which began operations in 1936 and operated there until 1981. The building occupies a footprint of approximately 500 m^2 and consists of four floors, with access via Rua do Castelo, Largo Barão de São Martinho and Largo de São Francisco. Currently, the building experiences two completely different realities. The public section, owned by the University of Minho, is currently vacant, having served over the years as reprographics, training rooms, and other functions. The private section is being assessed to evaluate a new use, potentially converting it into offices due to the building's central location in the city. The extended construction process (approximately 26 years) suggests that the architect treated the building as an almost permanent construction site and a formal laboratory for developing techniques, later applied in his buildings in the city of Porto.

In terms of its architecture, the building can be characterised as an example of the *Beaux Arts* style, stripped of ornamentation or with minimal decorative expression. The ornamental austerity observed in the treatment of the façades and the interior spaces is likely due to budget constraints and the functional nature of the program. The building's prolonged and uncertain construction process reflects limited resources, as evidenced by the project´s incomplete execution. In addition to the original simplicity, there were several low-quality interventions throughout the building, including half-height brick walls, chipboard doors, exposed electrical and plumbing systems, styrofoam and plasterboard ceilings, unsightly light fittings with no concern for integration, etc. These changes contribute to a general sense of disorder and improvisation. As a result, the interior of the building lacks architectural or heritage value. This area previously accommodated various services of the University of Minho, featuring a functional character. Successive interventions conducted over time have gradually reduced architectural significance. In clear contrast to the private section, where the original architectural qualities have been respected, the public section underwent significant alterations, including the construction of a reinforced concrete staircase and an elevator shaft (see Figure 3).

Figure 3. Reinforced concrete stairs and elevator shaft

From a construction standpoint, the building adheres to the conventional architectural model of its era. The outer perimeter is delineated by load-bearing stone masonry walls, which are interconnected with similarly load-bearing, albeit narrower, stone walls. These walls are cross-linked to support the wooden structural elements, such as beams, upon which the parquet flooring and partition walls are constructed. Certain interior partition walls also serve a structural function. The roof structure, including the cupolas of the turrets, is composed of wood. The thickness of the granite masonry load-bearing walls ranges from 0.50 to 0.80 meters. In addition to the granite masonry walls, the majority of the interior walls are constructed using Scots Pine (*Pinus sylvestris*) boards, oriented either vertically or diagonally (Figure 4). While the granite masonry walls support the primary structure, some partition walls also function as intermediate supports for the timber beams.

Figure 4. (a) Connection of floor beams with partition wall; (b) Partition wall with vertical planks; (c) Partition wall with diagonal planks

In general, it was observed that there are two semi-independent structures on each floor: one designed to support the loads on the upper floor and the other intended to support the ceiling on the lower floor. Both systems are anchored on the main beam structure made up of metal profiles and/or wooden beams. Floor Type 1 is made up of main beams made of metal profiles (IPN) embedded in the stone masonry walls. Two sets of wooden structures are laid perpendicular to these: one supporting the upper floor, and the other, the lower ceiling. The flooring system includes secondary sawn Riga Pine beams, which serve as support for the flooring beams and act as lateral support for the main beams. The structural system supporting the lower floor ceiling consists of secondary beams made of Riga Pine wood, onto which additional Riga Pine beams are fixed. The assembly is then enclosed by wooden boards, as illustrated in Figure 5, representing Floor Type 1 (a). The Type 2 Floor is a variation of the Type 1 Floor, where the metal beams are replaced by sawn chestnut (*Castanea sativa*) beams.

Accordingly, the main chestnut beams support both the upper floor and the lower ceiling structure, which remain identical to those described for Floor Type 1. Floor Type 3 differs from the others in that it has two completely independent structures. The structure that supports the upper floor consists of main chestnut beams embedded in the stone masonry walls, combined with dowel beams in Riga Pine, which support the beams that receive the flooring. On the other hand, the beamed ceiling is fixed to beams and dowels made of Riga Pine, which form a frame. For more details, the authors suggest reading [3].

Figure 5. Floor systems: (a) Type 1; (b) Type 2; (c) Type 3

The roof structure consists predominantly of wooden trusses, with different geometries, from simple to composite, varying according to the clear span to overcome and the function. The main trusses are composite, but there are also simple trusses (to support the corners), half trusses and others (see Figure 6).

Figure 6. The roof structure is made out of wooden trusses with various geometries

Made of Scots Pine, the trusses feature traditional single-tooth and double-tooth carpentry joinery, usually reinforced by metal elements (squares, T-squares, crowbars, etc.). The trusses and granite masonry walls are supported by the usual elements of Maritime pine (*Pinus pinaster Ait.*) wood roofs: row, purlins, sticks and slats. The cross-sections and spacing of these elements may vary according to the area of the building, but correspond to typical construction practices and dimensions of the period. The state of conservation of the Castle Building's structure was evaluated from the accesses generated by the inspection windows. It was initially possible to carry out a visual inspection of the structural elements, identifying the main pathologies, their current state (active or inactive), the extent of the damage and its probable cause. In addition, semi-destructive tests were employed as complementary tools to the visual inspection: controlled perforation test (Resistograph), surface hardness test (Pilodyn), thermographic imaging and hygrometer (see Figure 7). Overall, the structure of the Castle Building remains in a relatively good state, considering its date of construction. The identified pathologies were consistent with the construction system and the building's age. However, certain areas showed critical degradation, particularly due to water infiltration caused by inadequate maintenance.

Figure 7. (a) Controlled perforation test; (b) Surface hardness test; (c) Thermographic camera; (d) Water content measurement with hygrometer

Within the building, two areas were identified as being significantly compromised by advanced rot fungi, particularly in the encasement of wooden beams within masonry, as depicted in Figure 8. These pathologies remain active due to an unresolved source of moisture, which perpetually fosters conditions favourable for the proliferation of biological agents. In these affected areas, hygrometer measurements indicated a water content in the wood exceeding 30%. Conversely, in regions distant from the supports, the wood exhibited water content ranging from 10% to 12%, values that are consistent with the building's use and the prevailing environmental conditions (characterised by low relative humidity and high temperatures) at the time of measurement.

Figure 8. a) Beam of the chain that supports the ceiling of room S1.3 with damp and rot fungi; (b) Beam of the main beam of room S2.8 with rot fungi and beetle infestation; (c) Beam of the chain that supports the ceiling of room S2.2 with rot fungi and beetle infestation

In regions impacted by rot fungi, it is essential to recognise that decayed wood lacks any residual structural integrity, leading to a consequent reduction in the cross-sectional area of the structural elements at the supports. Surface hardness testing and controlled drilling have demonstrated that the depth of degradation is substantial, in some instances exceeding 40 mm, which is the maximum value measurable by Pilodyn. Consequently, in areas where the presence of rot fungi has been identified, it is advisable to reinforce the supports of the compromised beams, in addition to cleaning these areas and applying fungicidal treatments. Beetle infestations tend to affect structural elements more broadly than fungi, which typically exhibit localised degradation at the support areas. In the majority of the open inspection windows, generalised degradation by small woodworm was observed, and in specific areas, degradation by large woodworm was identified, particularly in elements made of pine (secondary beams, floor beams, and beams), which possess lower natural durability compared to chestnut.

Safety assessment

Based on the tests and visual inspection carried out, strength class D30 [4] was adopted for the main wooden beams of the floors, in chestnut, for the wooden elements of the roof and staircase, in Riga Pine, C24 [4] and for the metal profiles, S235 or Fe360. Permanent actions are composed of the materials' own weights, whether structural or non-structural elements, as well as other recommendations suggested by Eurocode 1 [5], and standard EN 338 [4]. The variable actions considered on the floors were as follows: 2.0 kN/m^2 for areas intended for private use (dwellings) and 3.0 kN/m^2 for stairs. The assessment was carried out on the most stressed structural elements in each room, on each of the building's floors, considering two overload situations:

- 2 kN/m^2, to which the building was subjected in the recent past (situation 1);
- 3 kN/m^2, which is the minimum overload recommended by European and national codes and standards for office use (situation 2).

Table 1. Ultimate Limit State verification of Floor 1 elements (Situation 1)

Element	Span (m)	Cross-section (mm^2)	Strength	Loads (kN/m^2)		Verification	
				G	Q	Bending	Shear
Barrotes	2,0	70x100	C24	1	2	0,46	0,22
VS2	2,8	120x250	C24	1	2	0,34	0,29
VS5	2,8	100x180	C24	1	2	0,74	0,47
VS8	2,7	100x220	C24	1	2	0,42	0,33
VS10	2,6	100x220	C24	1	2	0,35	0,28
VPA7	7,9	137x340	S235	1	2	0,35	0,07
VPA8	5,5	125x300	S235	1	2	0,36	0,08
VPM1	5,5	150x350	D30	1	2	0,54	0,34
VPM3	5,2	200x300	D30	1	2	0,68	0,39
VPA9	4,4	106x240	S235	1	2	0,36	0,10

Table 2. Ultimate Limit State verification of Floor 1 elements (Situation 2)

Element	Span (m)	Cross-section (mm^2)	Strength	Loads (kN/m^2)		Verification	
				G	Q	Bending	Shear
Barrotes	2,0	70x100	C24	1	3	0,65	0,31
VS2	2,8	120x250	C24	1	3	0,50	0,43
VS5	2,8	100x180	C24	1	3	1,10	0,68
VS8	2,7	100x220	C24	1	3	0,61	0,48
VS10	2,6	100x220	C24	1	3	0,51	0,41
VPA7	7,9	137x340	S235	1	3	0,51	0,11
VPA8	5,5	125x300	S235	1	3	0,53	0,13
VPM1	5,5	150x350	D30	1	3	0,78	0,50
VPM3	5,2	200x300	D30	1	3	1,00	0,58
VPA9	4,4	106x240	S235	1	3	0,53	0,14

Table 3. Service Limit State verification of Floor 1 elements (Situation 2)

Element	Span (m)	Cross-section (mm^2)	Strength	Loads (kN/m^2)		Deformation (mm)	
				G	Q	w_{inst}	w_{fin}
Barrotes	2,0	70x100	C24	1	3	3,80	6,02
VS2	2,8	120x250	C24	1	3	1,76	2,72
VS5	2,8	100x180	C24	1	3	4,99	7,83
VS8	2,7	100x220	C24	1	3	2,32	3,60
VS10	2,6	100x220	C24	1	3	1,85	2,87
VPA7	7,9	137x340	S235	1	3	18,95	-
VPA8	5,5	125x300	S235	1	3	10,47	-
VPM1	5,5	150x350	D30	1	3	4,52	7,10
VPM3	5,2	200x300	D30	1	3	6,32	9,96
VPA9	4,4	106x240	S235	1	3	8,60	-

The structural verification of the roof was performed under Ultimate Limit State (ULS), Service Limit State (SLS) and fire resistance for the trusses, their components, and the other elements supported by them that constitute the roof structure (slats, purlins, and rows). Resistance class C24 was considered for Riga Pine timber elements and C18 for Portuguese Maritime pine. However, some exceptions were made when assigning the strength class for Maritime pine: the elements that showed the best apparent quality were assigned strength class C24. A permanent load of 70 kg/m^2 and an overload during use of 60 kg/m^2 were assumed. For the verification of the trusses, the quantification of the acting forces was obtained from modelling in the SAP2000 software, as illustrated in Figure 9. For the verification of the other structural elements, they were considered to be bi-supported with simple supports, without moment transmission.

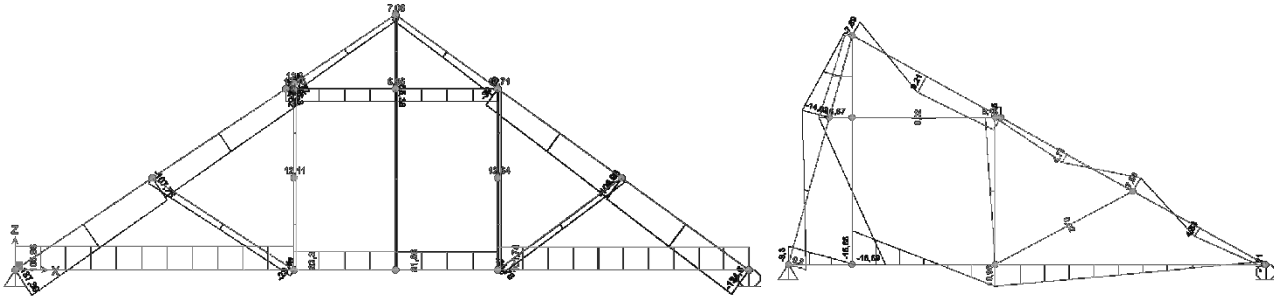

Figure 9. (a) Axial forces in a Queen-post truss and (b) bending moment in a half-truss

Póvoa Varzim Town Council

The roof of the Town Council is constructed with ceramic tiles arranged in eight slopes, corresponding to a square floor plan that includes a patio. This design aligns with the steel-framed skylight located above the central staircase of the building. Additionally, the front elevation of the building, which faces Praça do Almada, features two small dormers. Structurally, the roof's primary framework consists mainly of trusses that support the purlins, ridges and friezes. The secondary framework, comprising rafters and laths, rests upon the primary structure and supports the ceramic tile roof cladding (see Figure 10).

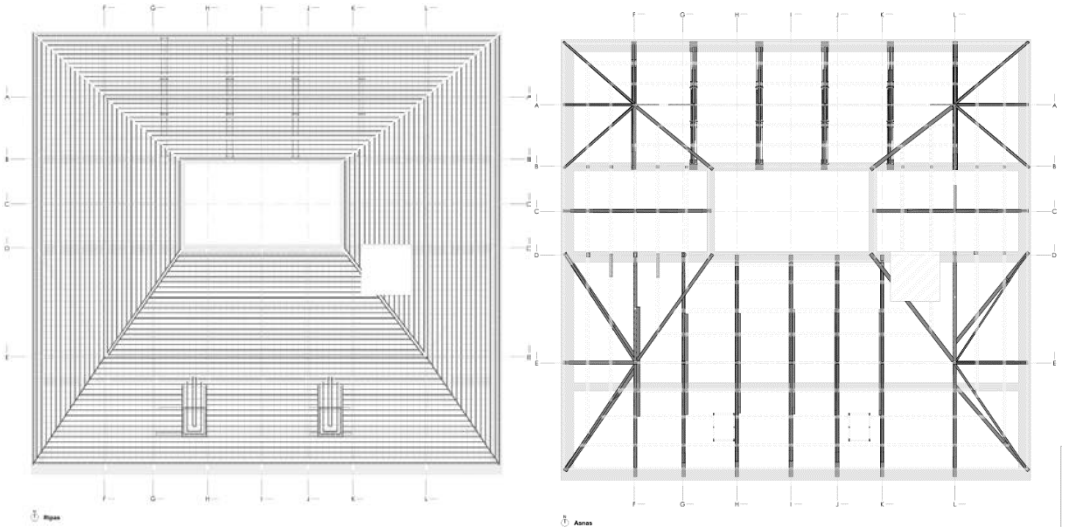

Figure 10. Roof of the Town council with (a) 8 slopes, 2 dormers and secondary structure and (b) main structure

The roof structure is composed of elements made from two wood species: Maritime pine and chestnut. It is noteworthy that, in recent years, certain local reinforcements of the structure have been implemented using components made from Eucalyptus wood (*Eucalyptus globulus*). In the case of Maritime pine, NP 4305 [6] facilitates the visual classification of wood elements by evaluating characteristics such as knots, fibre inclination, resin pockets, and sagging, among others. However, this standard applies to sawn timber after the sawmill process and not when it is utilised in existing structures. Furthermore, this standard categorises Maritime pine wood into two quality classes, E and EE, which correspond to strength classes C18 and C35, respectively. For safety considerations, it is recommended that Maritime pine elements be assigned to quality class E, which corresponds to a strength class of C18, as specified in EN 338 [4]. In Portugal, there is currently no established visual classification standard for chestnut wood. Consequently, the Italian standard UNI 11035 [7] has been adopted. This standard facilitates the classification of wood elements in existing structures and embraces various wood species prevalent in Italy, including chestnut and other coniferous species, a category that includes our pine. Through on-site visual inspection, it is feasible to assign the quality class S to the structural elements of chestnut wood. According to UNI 11035 [7], this classification corresponds to a strength class of D28, as defined in EN 338 [4]. Following the site visits conducted on the roof structure of the Póvoa de Varzim Town Council, it is observed that the overall structure is in satisfactory condition. However, minor interventions have been recommended to eliminate obstacles at the transition points between different sections of the roof structure and to widen and extend the existing walkways. These modifications aim to facilitate safer and more efficient access for inspection and maintenance purposes. Furthermore, the removal of these obstacles is anticipated to enhance the distribution of natural light within the roof space, thereby improving visibility during inspections and contributing to overall functionality (see Figure 11 and Figure 12).

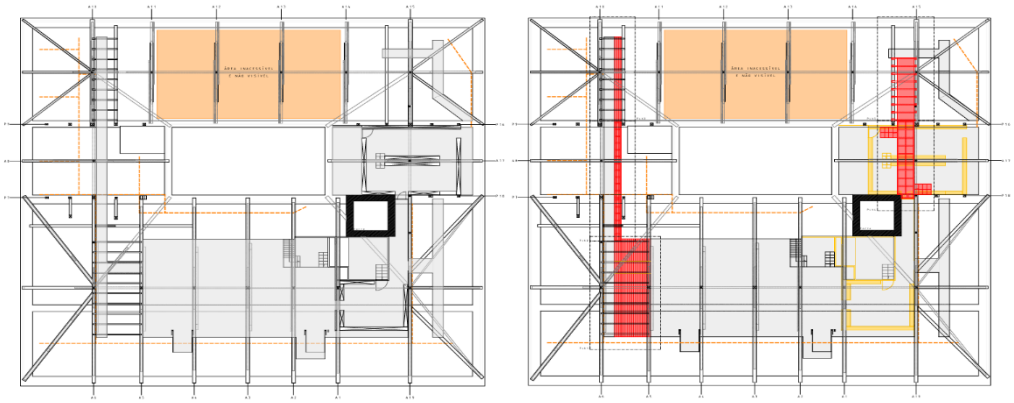

Figure 11. (a) Existing timber structures of the roof, including the available floor; (b) Proposal aimed to install an inspection walkway

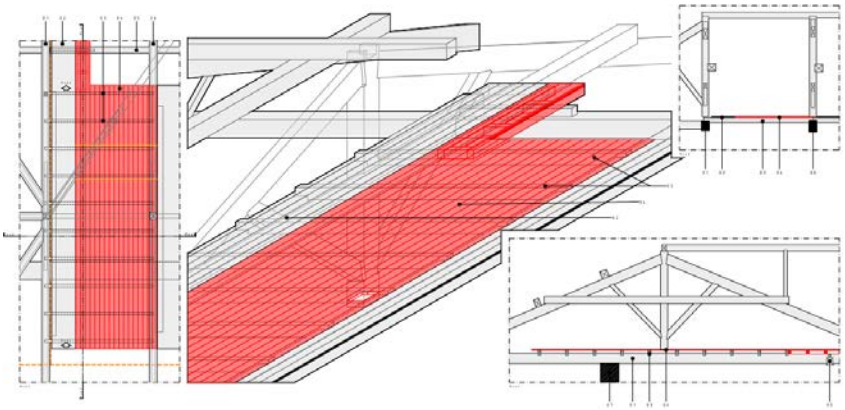

Figure 12. Details of the proposed inspection walkway

CONCLUSION

Various case studies on existing timber structures in Portugal have been presented. After a period in the recent past when timber structures were largely replaced by steel and concrete systems, current practices have shifted back toward the conservation of existing timber structures. This shift is facilitated by the combination of accumulated knowledge, inspection techniques, and structural analysis methods. For monuments, the type of wood (hardwood) and the quality of construction generally allow conservation. In contrast, in historical centres characterised by vernacular anonymous architecture, the combination of advanced deterioration and the original low-cost construction often makes conservation efforts unfeasible.

Recent studies on historical timber structures, led by TimLab, have significantly contributed to the assessment of existing Portuguese timber structures, offering a more reliable understanding of their structural behaviour and thereby minimising the extent of intervention and associated costs.

ACKNOWLEDGEMENTS

This research was supported by FCT/MCTES through national funds (PIDDAC) under reference UID/04029/Institute for Sustainability and Innovation in Structural Engineering (ISISE), and a grant with reference UMINHO/BII/2025/04 attributed to the third author is also acknowledged.

REFERENCES

[1] Branco J.M., Rodrigues L., Verbist M. (2019), Relatório de inspeção e verificação de segurança de um pavimento na Escola Secundária Sá de Miranda em Braga. TECMINHO. Requerente: Parque Escolar EPE, Guimarães, 40 pp.

[2] Branco J.M. (2024), Avaliação da condição dos elementos estruturais de madeira do Edifício do Castelo. TECMINHO. Requerente: UMinhoEXEC, 18 pp.

[3] Lima D.F., Aquino D.C., Rebouças A.S., Tenório M., Branco J.M. (2022), Avaliação da segurança estrutural para ações gravíticas do Edifício do Castelo. TECMINHO. Requerente: Uphold Unipessoal, Lda, Guimarães, 127 pp.

[4] EN 338:2003, Structural Timber. Strength classes. European Committee for standardization.

[5] EN 1991-1-1:2002, Eurocode 1: Actions on structures. European Committee for standardization.

[6] NP 4305:1995 - Madeira serrada de pinheiro-bravo para estruturas. Classificação Visual. CT 14 (LNEC).

[7] UNI 11035:2003, Structural timber - Visual strength grading rules and characteristics values for Italian structural timber population. UNI Ente Nazionale Italiano di Unificazione.

STRENGTHENING, STABILITY AND MODELLING

MASS TIMBER – PUSHING BOUNDARIES

Preetam BISWAS

Skidmore, Owings & Merrill, USA

INVITED LECTURE

With a focus on reduction of Embodied Carbon in Built Environment, there has been some movement in the use of Mass Timber on project types, project sizes and project location where timber has not been a predominant building material. Through a few case studies, this presentation aims to explore the realities of today and possibilities of tomorrow.

POST-EARTHQUAKE ASSESSMENT OF URM BUILDINGS WITH TIMBER ROOF AND FLOOR STRUCTURES

Mislav STEPINAC[1]

[1] Faculty of Civil Engineering, University of Zagreb

ABSTRACT

The European building stock is largely composed of unreinforced masonry structures with timber floor and roof systems. Such constructions shape the characteristic appearance of historic European cities, yet they exhibit pronounced vulnerability under seismic loading. In 2020, Croatia experienced two severe earthquakes that caused extensive damage, with approximately 26,000 buildings affected by the first event and more than 47,000 by the second. The urban landscape of continental Croatia is rooted in the Austro-Hungarian construction tradition of the early twentieth century. The majority of historic city cores were erected prior to the introduction of modern seismic regulations, and their buildings were therefore not conceived as earthquake-resistant structures. The present study examines the typology of unreinforced masonry buildings with timber floor and roof systems in Croatia and analyses the damage observed during the recent seismic events.

KEYWORDS: timber, roof, earthquake, floor, URM

INTRODUCTION

With the establishment of the Austro-Hungarian administration in Croatia, the widespread use of brick as the primary masonry material began. During this period, residential, public, and industrial buildings were constructed almost exclusively with industrially produced brick. Industrial production enabled increased output, consistent quality, and standardised dimensions of masonry units. Until 1932, the so-called solid Austrian brick (Austrian format) with dimensions of 14 cm in width, 29 cm in length, and 6.5 cm in height was employed. Buildings that today constitute an invaluable part of the cultural heritage within the historical core of Zagreb were predominantly constructed with brick and lime-based mortars. Timber played a significant role in residential construction in Zagreb between the late nineteenth and mid-twentieth centuries. It was predominantly incorporated in floor and roof structures, where its advantageous mechanical and physical properties were particularly evident. During the same period, timber was also extensively used for doors and window frames, as alternative materials were rarely applied. Floor and roof load-bearing systems were commonly built from silver fir and spruce, while in the case of specific buildings and wealthier investors, larch or oak could also be found. Historically, timber structures were constructed from hewn members, and this practice remained prevalent in Zagreb from the late nineteenth century until the mid-twentieth century.

This paper examines the typology of timber floor and roof structures in Zagreb and its surroundings. The following chapter addresses the damage observed in these structural systems, as well as the damage to unreinforced masonry buildings resulting from the performance of their timber components during earthquakes.

BUILDING TYPOLOGY AND DAMAGES

The building stock in the centre of Zagreb predominantly consists of traditional unreinforced masonry (URM) structures that were not designed to withstand seismic actions. These buildings were typically constructed with interconnected load-bearing masonry walls and timber floor systems [1, 2]. Structural deficiencies arise from irregular stiffness distribution, inadequate or absent wall-to-wall connections, and weak or missing links between walls, roofs, and floors. Their vulnerability is further increased by the lack of vertical and horizontal confining elements, which are required under current European seismic regulations for buildings subjected to high seismic demand. Limited in-plane resistance of the walls and insufficient load-bearing capacity of floor and roof structures further compromise their performance [3]. In addition, the advanced age of most buildings in Zagreb necessitates consideration of degraded mechanical properties. Typical earthquake-induced damage included the collapse or failure of chimneys, attic gable walls, and cantilever elements, as well as roof damage, wall cracking and failure (both in- and out-of-plane), detachment of gable walls, damage to lintels and vaults, partition wall failures, ceiling cracking, and stair damage [2]. Further details regarding the Zagreb earthquake, including preparedness, emergency response, and consequences, are provided in [4, 5, 6, 7, 8].

The roof structures are most commonly executed as king-post or queen-post trusses, although numerous hybrid forms of timber roof systems can also be found. The principal types of traditional timber roof structures in Zagreb are illustrated in Figure 1 [9]. Purlins are typically supported by brick or parapet walls, while spatial stabilisation through bracing is generally absent. In a limited number of cases, concrete slabs have been introduced beneath the roof systems as a result of later renovation works.

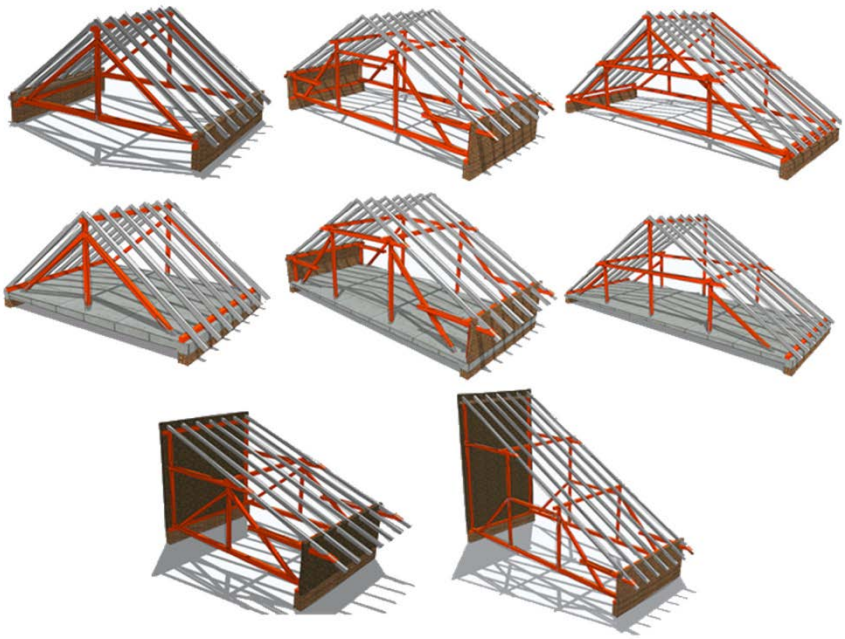

Figure 1. Representative timber roof systems in continental Croatia [9]

The floor structures of buildings erected in the late nineteenth and early twentieth centuries were typically constructed with timber beams spaced at intervals of up to 100 cm (typically 90 cm), with rubble fill placed between them (Figure 2). This fill served not only to protect the timber beams but also to provide sound and thermal insulation between residential units. Buildings erected in the mid-nineteenth century, which today survive in smaller numbers and are most often individually protected cultural monuments, were commonly built with three-sided hewn timber beams laid directly adjacent to one another without spacing. These structures also contained a rubble fill layer above the beams. A common characteristic of all such floor systems is the inadequate connection between the load-bearing

floor elements and the masonry walls. Timber beams were merely supported in prepared walls, without proper anchorage or stiffening, resulting in connections that lacked sufficient rigidity. Consequently, such structural systems display significant deficiencies in achieving the 'box effect' required for seismic performance.

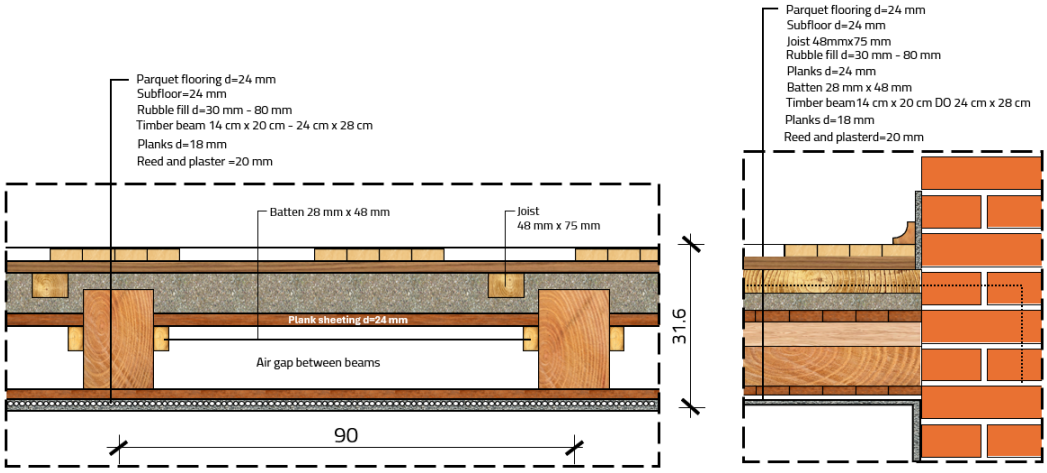

Figure 2. Representative timber floor systems for residential buildings in continental Croatia

Failures of non-structural elements, including chimneys and decorative façade features, were observed in nearly all buildings within the city centre. Collapse of gable walls, masonry columns, wall segments beneath or between windows, vaults, ceilings, and staircases was frequently recorded. In several cases, these failures also led to damage to the roof systems, which often became unstable due to the collapse of supporting masonry walls beneath them. Roof rafters and ridge beams commonly impacted gable walls, and in combination with their self-weight and the amplified seismic accelerations at gable height, substantial damage and partial or complete failure occurred. Post-earthquake inspections indicated that chimney failures had a predominant impact on direct roof damage. In certain cases, chimneys impaired the main load-bearing roof structure, while in most instances they fractured only the rafters, allowing the overall integrity of the roof to remain preserved. Significant damage was observed in large-span roofs, primarily due to the absence or inadequate design of out-of-plane bracing systems and the improper execution of carpentry compression joints, such as notched or mortise-and-tenon joints, which lacked reinforcement against tensile forces. Additional alterations of roof structures, often associated with attic conversions for residential use, considerably modified the original static system of these structures. Moreover, insufficient maintenance, particularly the prolonged ingress of moisture into timber elements, further weakened the structures and amplified the effects of seismic loading.

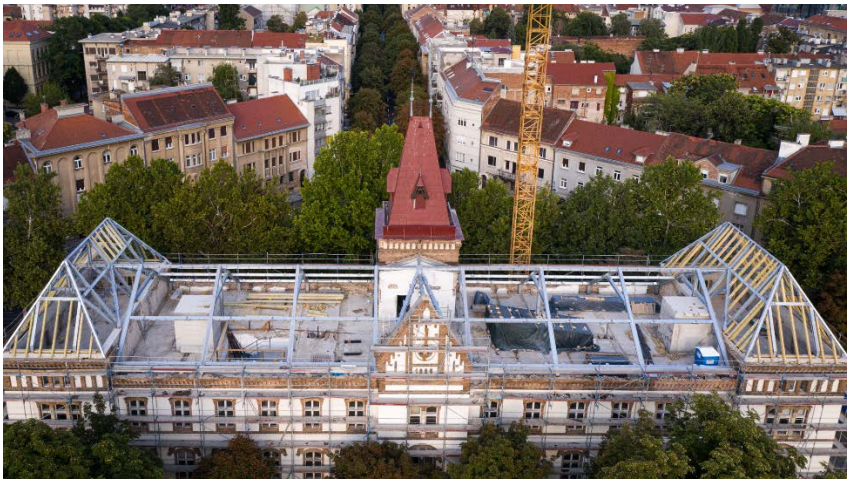

Figure 3. Representative timber floor systems for residential buildings in continental Croatia

CONCLUSION

The post-earthquake reconstruction in Zagreb is currently in full progress, with extensive efforts directed at the repair and renewal of damaged structures. Nevertheless, from the author's perspective, timber elements remain insufficiently protected within the ongoing interventions. Traditional timber roof structures, many of them remarkable examples of craftsmanship and engineering, are frequently replaced with steel systems in order to gain additional attic space (Figure 3). Furthermore, valuable timber components are often discarded as waste material instead of being preserved and reused. Greater attention should therefore be given to the safeguarding and reintegration of these elements, which constitute an irreplaceable part of architectural and structural heritage.

REFERENCES

[1] Lulić, L.; Ožić, K.; Kišiček, T.; Hafner, I.; Stepinac, M.

Post-Earthquake Damage Assessment-Case Study of the Educational Building after the Zagreb Earthquake. Sustainability 2021, 13, 6353.

[2] Stepinac, M.; Lourenço, P.B.; Atalić, J.; Kišiček, T.; Uroš, M.; Baniček, M.; Šavor Novak, M.

Damage Classification of Residential Buildings in Historical Downtown after the ML5.5 Earthquake in Zagreb, Croatia in 2020. Int. J. Disaster Risk Reduct. 2021, 56, 102140.

[3] Saloustros, S.; Pelà, L.; Contrafatto, F.R.; Roca, P.; Petromichelakis, I.

Analytical Derivation of Seismic Fragility Curves for Historical Masonry Structures Based on Stochastic Analysis of Uncertain Material Parameters. Int. J. Archit. Herit. 2019, 13, 1142–1164.

[4] Novak, M.Š.; Uroš, M.; Atalić, J.; Herak, M.; Demšić, M.; Baniček, M.; Lazarević, D.; Bijelić, N.; Crnogorac, M.; Todorić, M.

Zagreb Earthquake of 22 March 2020–Preliminary Report on Seismologic Aspects and Damage to Buildings. Gradjevinar 2020, 72, 843–867.

[5] Kišiček, T.; Stepinac, M.; Renić, T.; Hafner, I.; Lulić, L.

Strengthening of Masonry Walls with FRP or TRM. Gradjevinar 2020, 72, 937–953.

[6] Milić, M.; Stepinac, M.; Lulić, L.; Ivanišević, N.; Matorić, I.; Čačić Šipoš, B.; Endo, Y.

Assessment and Rehabilitation of Culturally Protected Prince Rudolf Infantry Barracks in Zagreb after Major Earthquake. Buildings 2021, 11, 508.

[7] Hafner, I.; Lazarević, D.; Kišiček, T.; Stepinac, M.

Post-Earthquake Assessment of a Historical Masonry Building after the Zagreb Earthquake—Case Study. Buildings 2022, 12, 323.

[8] Antonela Moretić, Mislav Stepinac, Paulo B. Lourenço,

Seismic upgrading of cultural heritage – A case study using an educational building in Croatia from the historicism style, Case Studies in Construction Materials, Volume 17, 2022, e01183, ISSN 2214-5095

[9] Perković, N.; Stepinac, M.; Rajčić, V.; Barbalić, J.

Assessment of Timber Roof Structures before and after Earthquakes. Buildings 2021, 11, 528.

PRESTRESSED TIMBER-TO-TIMBER COMPOSITES WITH A NOVEL 30° SCREW CONNECTION FOR THE RETROFIT OF EXISTING FLOORS: EXPERIMENTAL AND ANALYTICAL INVESTIGATIONS

Andrea BARTOLOTTI[1], Fabrizio FAES[2] and Ivan GIONGO[1]

[1] University of Trento, Department of Civil, Environmental and Mechanical Engineering
[2] Würth Srl / GmbH

ABSTRACT

This study investigates a new retrofit solution for existing timber floors based on a cambered and prestressed timber-to-timber composite (CP-TTC) approach. A novel 30° inclined screw connection, used with angled washers, was evaluated through an extensive experimental campaign including fastener compression tests, push-out shear tests, and full-scale floor bending tests. Hybrid Glued-Screwed (HGS) variants were also assessed to examine potential enhancements in the retrofit performance. Results confirm the screw system's ability to induce significant prestressing, and the retrofit method substantially improved both serviceability and ultimate limit states. Comparisons with benchmark solutions and numerical predictions evidence the effectiveness and feasibility of the CP-TTC strategy for floor rehabilitation. Analytical models were validated, and the impact of novel code provisions (FprEN1995-1-1:2025) was discussed.

KEYWORDS: timber-to-timber prestressed composites, inclined screw connections, floor strengthening, experimental testing

INTRODUCTION

Existing timber floors, particularly in historical or early 20th-century buildings, often fall short of current standards regarding stiffness, strength, and deflection control. Retrofit methods are essential to restore performance, accommodate modern usage demands, and preserve structural integrity without compromising heritage values. Among the viable strategies, Timber-to-Timber Composite (TTC) systems have gained attention as lightweight, effective, and reversible solutions.

TTC retrofitting is a well-established technique. Following early investigations that demonstrated the effectiveness of TCC solutions assembled using steel [1] or wooden dowels [2], [3], and [4] highlighted the benefits of inclined screw configurations in increasing the stiffness and load-bearing capacity of TTC strengthening. The long-term performance of TTC systems has also been extensively investigated by [5][6]. Building on these foundations, [7] further advanced the field by introducing a cambering and prestressing (CP) method, in which screws are inserted at an angle, starting from midspan and proceeding symmetrically toward the supports, inducing internal stresses and uplift. This CP procedure, supported by analytical formulations and validated through extensive experimental campaigns [8][9], was developed to enable more refined and efficient retrofit solutions. Further research has explored hybrid timber configurations, combining softwood and hardwood elements for optimised mechanical performance and material efficiency [10]. The use of hardwood in TTC systems has been further experimentally investigated, with [12] focusing on the connections, and [13] proposing prefabricated, prestressed floor modules adapted to different spans and usage scenarios. In this context, the present

work explores a novel TTC retrofit system utilising 30° inclined single-threaded screws (diameter 8 mm, [14]), installed with the aid of angled washers forming part of the connection system (as illustrated in Figure 1), in conjunction with cambering and prestressing techniques. Through a comprehensive experimental program, comprising fastener pressure tests, push-out shear tests, and full-scale floor bending tests, the study assesses both the localised connection behaviour and the global structural response. Screw-only configurations are compared with Hybrid Glued-Screwed (HGS) variants, in which epoxy resin mortar was applied locally near the supports to bond the interface and limit relative slip between the timber elements, to identify the potential benefits introduced by adhesive bonding. Experimental findings are further evaluated against analytical models and numerical simulations, with special attention to performance under serviceability and ultimate limit states as defined in both current [12] and forthcoming Eurocode 5 provisions [13]. The outcomes highlight the potential of this retrofit method to enhance the mechanical behaviour of existing floors while supporting practical implementation in renovation and conservation projects.

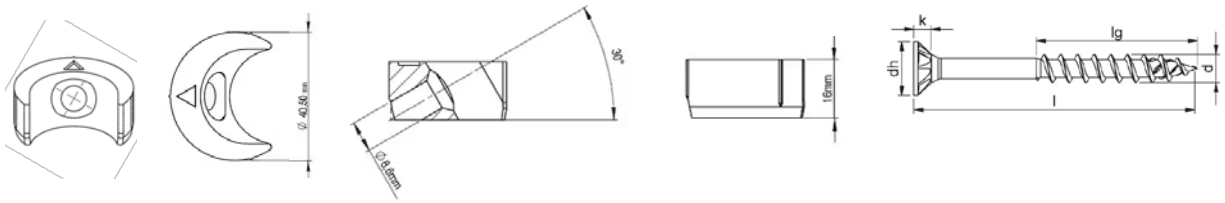

Figure 44. Connection system studied in the present paper: single-threaded screws and an angled washer

METHODOLOGY

The experimental program was designed to characterise and quantify the key mechanical parameters needed for the design of the prestressed TTC floor retrofit. The testing campaign was structured around three core objectives: (i) to evaluate the compressive force that inclined screws can induce, (ii) to determine the shear stiffness and strength of the screw-based connection system, and (iii) to assess the global structural performance of full-scale retrofitted timber floor specimens.

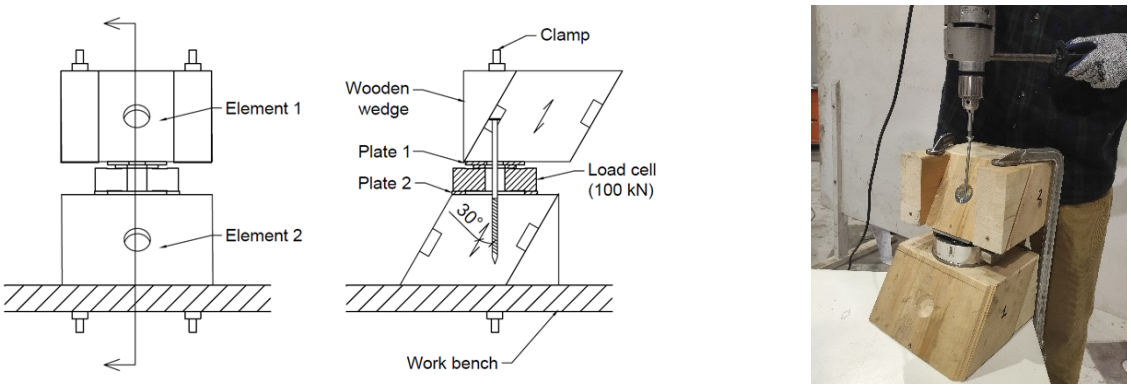

a) b)

Figure 45. Fastener pressure test: a) test setup, b) screw insertion.

The first phase consisted of fastener "pressure tests", which measured the compressive force generated by 30° inclined screws inserted into timber elements using angled steel washers. This force contributes to prestressing, resulting in axial compression in the joists and vertical uplift (camber) in the floor assembly. The capacity to generate and maintain this prestress is critical, as it defines the camber and uplift of the retrofitted floor. This initial camber can mitigate the early-stage deflection induced by

permanent loads, limiting potential damage to non-structural elements. Understanding the magnitude and time-dependent behaviour of this force is essential for design purposes. A total of 72 pressure tests were conducted. The setup involved load cells placed between two timber elements to record the compression force generated between them after the screw insertion (see Figure 2). Variables such as thread length and pilot hole presence were investigated. To investigate the evolution of the compressive force over time, three tests were monitored in the days following screw insertion to measure any drop in the fastener pressure.

In the second phase, push-out tests were carried out to assess the mechanical behaviour of the interface between the floor slab and the joists (Figure 3). The screw-only and HGS configurations were tested to compare their stiffness and strength characteristics. Twenty push-out shear tests were performed across four connection configurations: screw-only and HGS, each with and without a 23 mm timber planking interlayer. Additionally, three benchmark push-out tests were conducted using screws inserted orthogonally to the grain (90°) to quantify the influence of screw inclination on the stiffness and strength characteristics of the connection. Following EN 12512 protocols [9], the tests measured slip modulus and shear capacity of the fastener. The outcomes of these tests informed the definition of the design parameters needed for both analytical modelling and finite element simulations.

Table 5. Push-out test configurations.

Number of tests	Specimen type	Connection type	Screw length/thread length (mm)	Interlayer
3	A	Only screws 90°	220/100	None
5	B	Only screws 30°	220/100	None
5	C	Only screws 30°	260/100	Timber boards
5	BG	HGS	220/100	None
5	CG	HGS	260/100	Timber boards

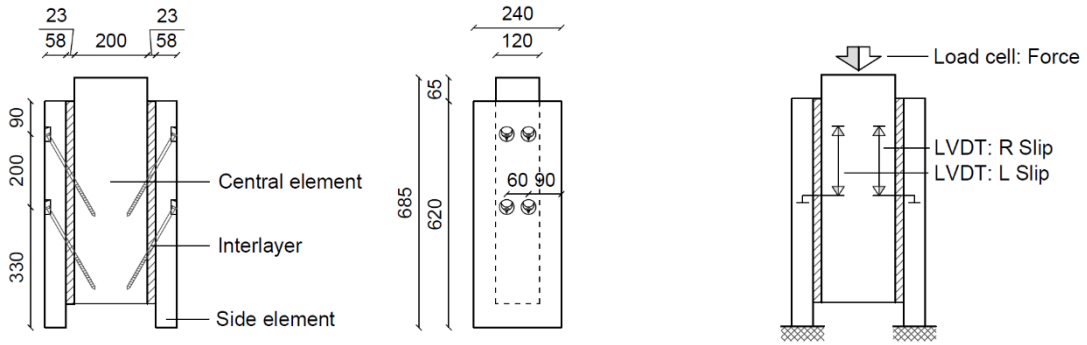

Figure 46. Push-out shear test: a) geometry of the specimens, b) test setup.

Finally, full-scale bending tests were performed on four TTC floor specimens (detailed in Table 2) with two different span lengths (4.5 m and 6.0 m). These tests evaluated the overall effectiveness and performance of the retrofit solution under service and ultimate loads. Instrumentation (see Figure 4) allowed for the measurement of midspan (f_M) and one-third span (f_L and f_R) deflection, interface slip (s_L, $s_{L1/4}$, $s_{L2/4}$, $s_{L3/4}$ and s_R) and joist strain distribution (ε_U and ε_U). The floor configurations included both span lengths, each tested in screw-only and HGS variants. Floors were cambered by inserting the inclined screws in a specific sequence from midspan toward the supports, introducing prestress and vertical uplift [3]. Load was applied using a six-point bending scheme, and deflections, slips, and strains were monitored throughout the tests.

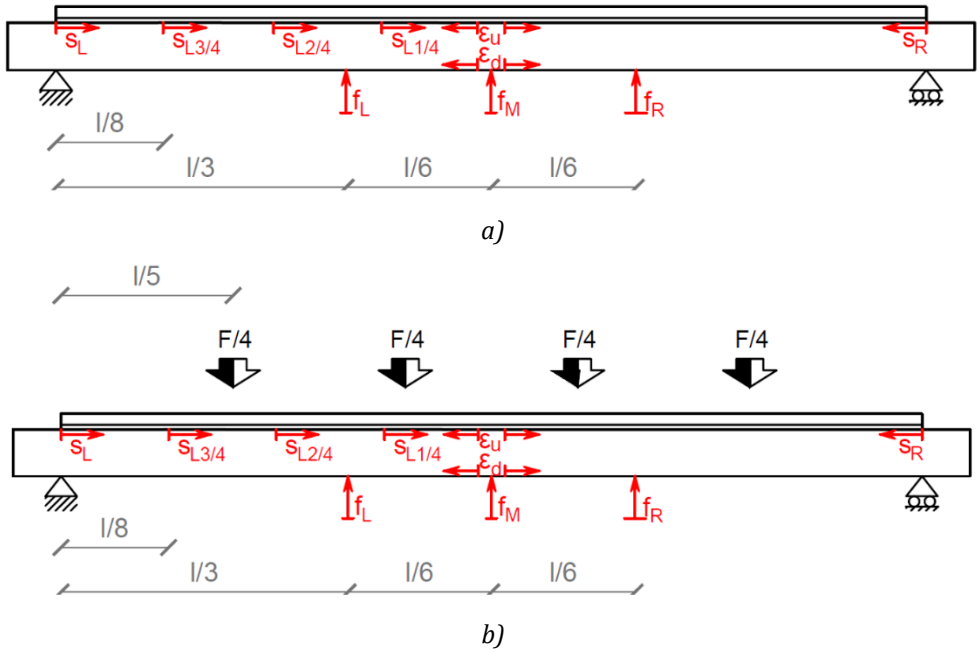

Figure 47. Full-scale test setup: a) CP procedure, b) load-to-failure test.

To ensure the experimental campaign addressed relevant structural conditions, the full-scale specimens were designed starting from a reference existing timber floor subjected to a permanent load equal to 1.5 kN/m² and a live load equal to 2 kN/m². The joist spacing was set to 50 cm and 60 cm for the 4.5 m and 6.0 m span floors, respectively. The structural capacity of these baseline configurations was initially checked under both serviceability and ultimate limit states, according to current code requirements (floor R4.5 and R6.0 in Table 3). Following this assessment, the loading conditions were upgraded to simulate more demanding use categories resulting from the renovation and refurbishment of the building, incorporating increased permanent loads (2.5 kN/m^2) and higher variable actions (3 kN/m^2) typically associated with intensified usage scenarios.

Based on the outcomes of the fastener pressure and push-out tests, the design of the retrofit configurations was carried out using the analytical model proposed by Giongo et al. [4], which accounts for the composite action in cambered and prestressed systems. The design of the screw-only configurations was intentionally based on the assumption of limited stiffness to explore the potential benefits and performance improvements achievable through HGS configurations. While the screw-only systems met ultimate limit state requirements, they intentionally did not satisfy the instantaneous deflection check at the serviceability limit state (SLS) to highlight the need for enhanced interface stiffness (see Table 3). To address this, the HGS configuration was specifically designed to overcome these limitations.

The HGS variant combined mechanical fasteners with adhesive bonding, and, due to the high stiffness of the latter, it was designed under the assumption of full composite interaction. This design approach enabled the HGS system to provide greater stiffness and deflection control, allowing it to satisfy SLS requirements in the design phase. The bonding was applied only along a designed length near the supports (35 cm and 45 cm for BG4.5 and BG6.0 6.0 respectively), calculated based on the interface shear force derived from the full-interaction hypothesis under ULS conditions. This design shear was compared with the adhesive shear strength as determined from the push-out tests, ensuring sufficient capacity within the bonded region. It is important to note that, although the adhesive length was calculated under ULS conditions, the contribution of the adhesive bonding in the HGS configuration was considered only for serviceability limit state (SLS) checks, whereas the ultimate limit state (ULS) verification of the floors relied solely on the mechanical contribution of the screws. The relatively short

bonding length was intentionally not extended, despite the potential benefits in terms of overall stiffness. This approach allowed the preservation of most of the original flooring by reinstating only a few of the outermost floorboards, thus providing a stable platform to stand on during retrofit application.

Table 6. Full-scale specimen details.

Test ID	Element 1 (b x h)	Element 2 (b x h)	Span length (m)	Timber board interlayer	Screw spacing (mm)	HGS (Yes/No)
B4.5	24 x 6 cm	12 x 12 cm	4.5	Yes	200	No
BG4.5	24 x 6 cm	12 x 12 cm	4.5	Yes	200	Yes
B6.0	24 x 6 cm	12 x 20 cm	6.0	Yes	200	No
BG6.0	24 x 6 cm	12 x 20 cm	6.0	Yes	200	Yes

Table 7. Design of the full-scale specimen considering reference existing floors (R4.5 and R6.0): ULS and SLS checks.

Floor ID	$w_{inst,Q}$ (mm)	w_{inst} (mm)	$w_{fin,net}$ (mm)	w_{fin} (mm)	Normal stress check (σ_d/f_d)
R4.5	27.2 > 12.9	49.2 > 15.0	67.3 >18.0	67.3 >30.0	1.79
R6.0	22.3 > 17.1	40.8 > 20.0	56.0 > 24.0	56.0 > 40.0	1.39
B4.5	10.1 < 13.0	19.2 > 15.0	1.2 < 18.0	28.5 < 30.0	0.97* | 0.99•
B6.0	12.8 < 17.1	24.5 > 20.0	8.5 < 24.0	35.6 < 40	0.91* | 0.92•
BG4.5	7.1 < 13.0	13.6 < 15.0	-4.9 <18.0	18.4 < 30.0	0.97* | 0.99•
BG6.0	9.5 < 17.1	19.6 < 20.0	6.6 < 24.0	26.6 < 40	0.91* | 0.92•

* short-term condition, • long-term condition

RESULTS

The experimental results provide a detailed evaluation of the connection system and its influence on the structural response of the CP-TTC retrofit strategy. The fastener pressure tests showed that the 30° inclined single-threaded screws, when inserted with angled washers, generated an average compressive force of approximately 6.5 kN per screw (see Table 4). This prestressing effect was stable over time, with short-term monitoring indicating a loss of less than 10% of the initial pressure over 12 days, more than 75% of which occurred within the first 24 hours. This represents a clear improvement compared to the findings in [13], where single-threaded screws with standard washers exhibited pressure losses of approximately 20% within 15 hours. The presence of pilot holes enhanced the induced force by approximately 13%, in contrast to the results in [13], where no appreciable variation was observed for the tested fastener types.

Table 8. Results of the fastener pressure tests.

	Number of tests	Mean force F ± σ (kN)
80 mm thread length:	**23**	**6.53 ± 1.53**
- With a pilot hole:	23	6.53 ±1.53
100 mm thread length:	**49**	**6.47 ± 1.45**
- Without a pilot hole:	7	5.77 ± 2.20
- With a pilot hole:	42	6.53 ± 1.40
Total:	**72**	**6.48 ± 1.44**

Push-out shear tests allowed for the comparison of mechanical performance between screw-only and HGS configurations (see Table 5). Bonding increased the average shear strength by more than 6 times

and the stiffness by over 19 times when comparing configurations B and BG. These results confirm the substantial role of adhesive bonding in improving connection performance. Additionally, the benchmark comparison between the 90° screw insertion (test A) and the 30° inclined configuration (test B) showed that stiffness improved nearly fivefold due to the inclined installation, confirming the potential of inclined screws to significantly enhance the stiffness of TTC floors.

The evaluation of the full-scale tests can be distinguished into two phases: the cambering and prestressing phase, and the loading phase until failure (Figure 5). During the cambering phase, the final camber measured at midspan showed good agreement with both analytical and numerical predictions (see Table 6). The analytical model slightly underestimated the camber in most cases, with deviations ranging from −11% to +6%, while the numerical model exhibited slightly higher discrepancies, with errors up to −20%. For instance, in the B4.5 and BG4.5 tests, the experimental camber was 33.7 mm and 33.4 mm, respectively, compared to analytical predictions of 30 mm and numerical predictions of approximately 27 mm. These results confirm that both analytical and numerical approaches can provide reliable estimations of the uplift induced by the CP assembly procedure, particularly for use in design applications. Another relevant observation concerns the comparable camber performance exhibited by the screw-only and HGS floor specimens, indicating that, in the HGS specimens, it was indeed possible to complete the CP assembly within the open time of the adhesive, despite the challenging conditions caused by summer temperatures. Had the adhesive begun to set, the resulting interface bond would have hindered the development of camber. This represented a critical technical challenge associated with the proposed retrofit strategy.

Table 9. Results of the push-out tests. Mean strength (f_{mean}) and stiffness ($k_{s,means}$) are expressed per fastener, based on total values divided by the number of fasteners (8).

Test ID	Number of tests	$f_{mean} \pm \sigma$ (kN)	$k_{s,mean} \pm \sigma$ (kN/mm)
A	3	12.64 ± 0.26	1.71 ± 0.04
B	5	9.19 ± 1.59	8.41 ± 0.73
C	5	11.68 ± 1.43	6.44 ± 0.69
BG	5	59.42 ± 8.72	163.82 ± 24.01
CG	5	29.01 ± 4.28	46.49 ± 13.72

Table 10. Final camber (in millimetres) at the end of the CP procedure resulting from experimental test, and accuracy of the analytical and numerical prediction.

Test ID	Experimental	Analytical	Numerical
B4.5	33.7	30 (-11%)	26.93 (-20%)
B6.0	27.2	26.7 (-2%)	22.78 (-16%)
BG4.5	33.4	30 (-10%)	26.93 (-19%)
BG6.0	25.1	26.7 (+6%)	22.78 (-9%)

Table 11. Summary of serviceability and ultimate limit state performance of the tested floor configurations according to EN 1995-1-1:2014.

Test	$w_{inst,Q}$ (mm)	w_{inst} (mm)	ULS normal stresses check (σ_d/f_d)
B4.5	10.6 < 13.0	21.4 > 15.0	0.89
B6.0	11.9 < 17.1	23.2 > 20.0	0.57
BG4.5	10.8 < 13.0	20.1 > 15.0	0.80
BG6.0	12.3 < 17.1	23.9 > 20.0	0.64

In the subsequent loading phase until failure, the structural response of the specimens was evaluated under increasing loads, resulting in the load-displacement behaviour presented in Figure 6. According to the EN 1995-1-1:2014 requirements, each configuration was assessed in terms of serviceability and ultimate performance, as summarised in Table 7. Normal stress levels in the joists were calculated from strain gauge measurements and compared against mean predicted values at the ultimate limit state (ULS). All tested specimens satisfied the ULS normal stress check, with stress-to-capacity ratios well below unity. Regarding SLS checks, the results related to the screw-only configurations (B4.5 and B6.0) showed that while instantaneous deflection limits under variable actions ($w_{inst,Q}$) were satisfied, total deflection under permanent and variable loads (w_{inst}) exceeded the serviceability threshold. These outcomes align with the design strategy, which intentionally assumed limited stiffness to demonstrate the potential benefits of improved composite interaction due to bonding. Conversely, the HGS configurations (BG4.5 and BG6.0) did not exhibit significant improvements in terms of global deflection control. The addition of epoxy bonding, applied over a limited interface length near the supports, had a negligible effect on the overall stiffness and deformation behaviour of the floor system within the target range compatible with serviceability conditions (see close-up in Figure 6). The impact of the epoxy bonding became noticeable only at higher force/deflection levels (compare, for example, the curves for B4.5 and BG4.5 at 50 mm midspan deflection).

To better understand the role of bonding, the interface slip profile was analysed at various locations along the span (at support and 1/8, 1/4, and 3/8 of the span length) and for different load levels corresponding to serviceability (w_{inst} and $w_{inst,Q}$) and ultimate limit states, as shown in Figure 7. The results highlight that the floors with HGS connections exhibited noticeably reduced slip at the support compared to the screw-only configurations, confirming the local effectiveness of the adhesive bond in reducing relative displacements at the bonded region. However, this local stiffening did not translate into a significant improvement in global deflection. This can be attributed to increased slip observed further along the span, beyond the bonded zones, suggesting a redistribution of deformation and strain accumulation away from the supports. These findings indicate that while the bonding locally improves the interface slip profile, its limited application length prevents it from meaningfully influencing the overall stiffness of the system. Thus, the addition of epoxy bonding, applied over a limited interface length near the supports, had a negligible effect on the overall stiffness and deformation behaviour of the floor system.

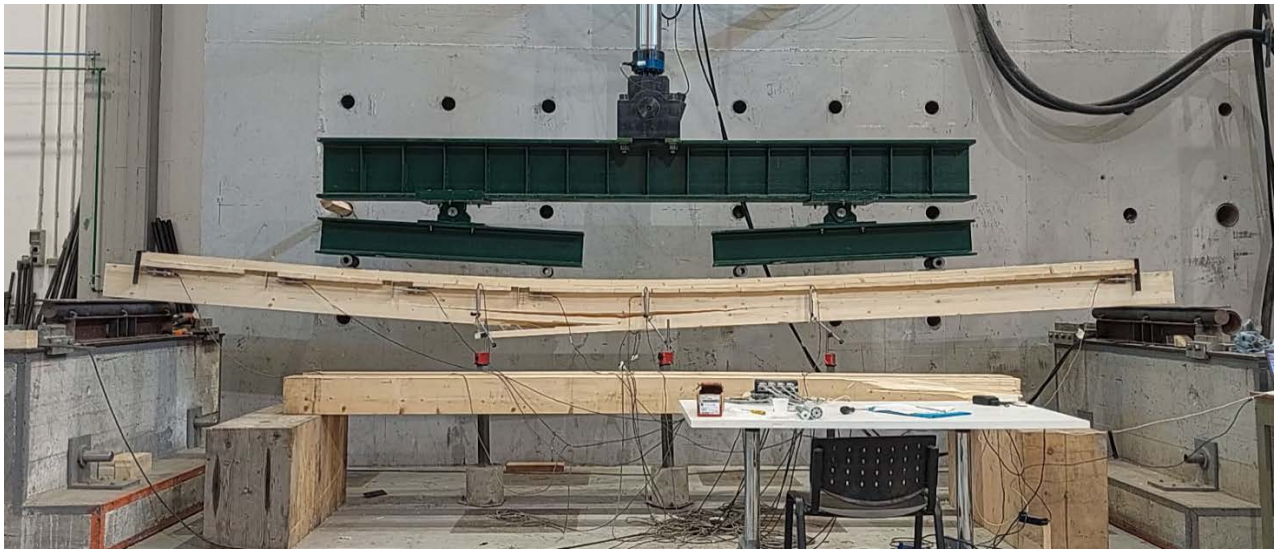

Figure 48. Full-scale TTC floor specimen at the end of the bending test

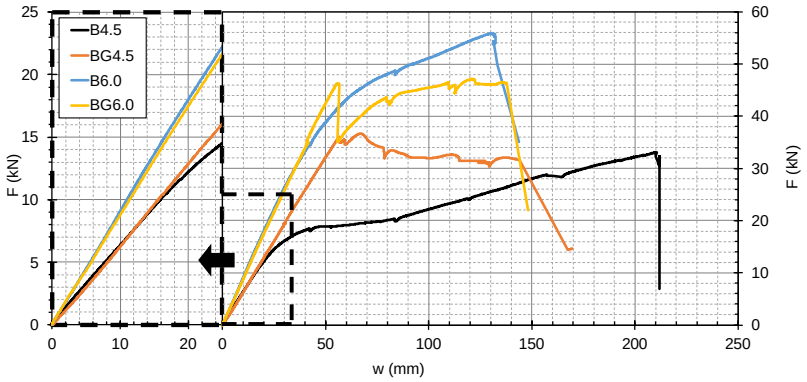

Figure 49. Applied load (F) versus midspan deflection (w) for specimens under six-point bending tests.

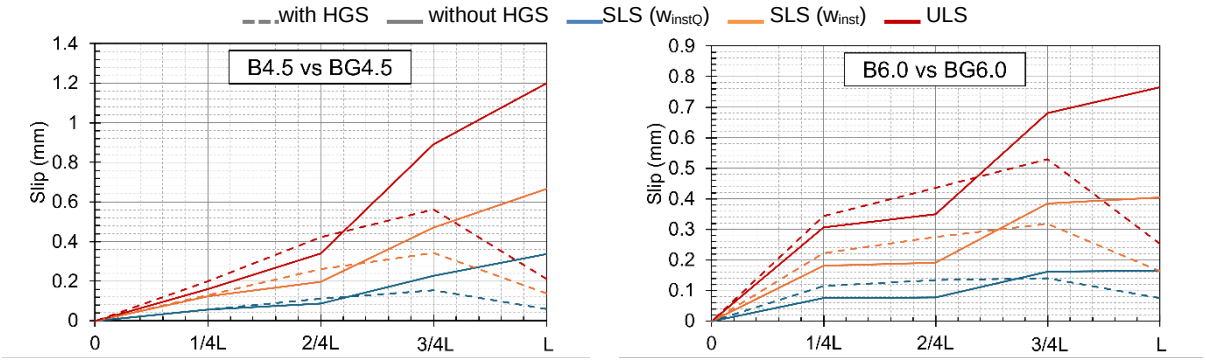

Figure 50. Interface slip profiles measured at various span locations under serviceability and ultimate load levels.

DISCUSSION

The experimental findings were examined in the context of recent developments in design codes and compared with existing retrofit strategies. In particular, attention was paid to the evolving serviceability limit state (SLS) requirements introduced in the upcoming revision of EN 1995-1-1:2014 and EN 1990:2002. The new code provisions [13][17] modify how deflections are treated in SLS checks, notably by excluding the initial deflection under permanent loads (w_1) from assessments concerning damage to non-structural elements and user comfort, except in cases involving non-brittle partitions or architectural appearance. In such cases, the beneficial effect of the initial camber can now be considered, offering an advantage for cambered and prestressed retrofit systems. According to this revised approach, the screwed-only specimens tested in this study satisfy the serviceability requirements when the updated criteria are applied.

The retrofit solution proposed in this work was also evaluated against several benchmark configurations featuring different screw types, inclinations, and interlayer conditions. The comparative analysis, based on analytical evaluations of both ultimate and service limit states (according to EN1995:1-1-2014) for 4.5 m and 6.0 m span floors, highlighted the superior performance of the tested system. Despite employing smaller diameter screws compared to some benchmark cases, the 30° inclined single-threaded screws combined with angled washers offered both high stiffness and strong prestressing capacity. This was attributed to the ability of single-threaded screws to generate greater tightening force during installation and to the enhanced connection rigidity provided by the inclined geometry. Results from push-out tests further reinforced these conclusions: when bonding was added (HGS configuration), stiffness increased by more than 19 times and shear strength by over six times compared to the screw-only equivalent. The comparison between the orthogonal screw insertion (benchmark test A) and the 30° inclined configuration (test B) demonstrated a nearly fivefold increase in stiffness, confirming the substantial influence of screw inclination on connection performance.

Table 12. Verification of serviceability limit state requirements for screw-only specimens according to the FprEN 1995-1-1:2025 and prEN1990:2022 provisions

Floor ID	Limiting damage to elements other than structural		Comfort of users	Appearance
	$w_2 + w_3$ (mm)	w_{max} (mm)	$w_2+w_{3,freq}$ (mm)	$w_1+w_2-w_c$ (mm)
B4.5	16.1 < 18.0	3.3 < 11.3	13.1 < 15	-3.7 < 18
B6.0	19.9 < 24.0	13.2 < 20.0	16.0 < 20.0	4.31 < 24.0

Table 13. Benchmark retrofit solutions.

Name	Screw angle	Screw type	Ø (mm)	Thread length (mm)	Floorboard interlayer	CP method	k_s (kN/m)	F (kN)
A	45°	Double thread	8.2	80+80	Yes	Yes	7840	2.1
B	45°	Double thread	8.2	80+80	Yes	No	7840	-
C	45°	Single thread	10	100	No	Yes	3740	4.6
D	90°	Single thread	8	100	No	No	1710	-

Table 14. Performance of the tested solution concerning the benchmarks: 4.5m floor.

ULS SHORT-TERM	**Test**	**A**	**B**	**C**	**D**
Element 2 tensile bending check:	96%	111%	113%	117%	175%
Element 1 compression bending check:	24%	28%	29%	28%	51%
Element 2 shear check	69%	65%	65%	84%	87%
ULS LONG-TERM					
Element 2 tensile bending check:	98%	113%	115%	120%	179%
Element 1 compression bending check:	25%	29%	37%	29%	63%
Element 2 shear check:	85%	80%	80%	105%	107%
SLS SHORT-TERM					
$w_{inst,Q}$ check:	78%	74%	74%	93%	156%
w_{inst} check:	127%	122%	122%	152%	256%
SLS LONG-TERM					
w_{fin} check:	94%	90%	90%	114%	-
$w_{fin,net}$ check	3%	111%	149%	71%	317%

Table 15. Performance of the tested solution with respect to the benchmarks: 6m floor.

ULS SHORT TERM	**Test**	**A**	**B**	**C**	**D**
Element 2 flexural tensile check:	93%	114%	117%	115%	162%
Element 1 flexural compression check:	20%	26%	28%	22%	33%
Element 2 shear check	66%	64%	64%	77%	78%
ULS LONG TERM					
Element 2 flexural tensile check:	95%	115%	119%	117%	165%
Element 1 flexural compression check:	20%	26%	36%	22%	40%
Element 2 shear check:	81%	77%	77%	94%	96%
SLS SHORT TERM					
$w_{inst,Q}$ check:	74%	72%	72%	84%	121%
w_{inst} check:	122%	119%	119%	138%	199%
SLS LONG TERM					
w_{fin} check:	89%	86%	86%	102%	-
$w_{fin,net}$ check	45%	118%	143%	94%	242%

CONCLUSION

This study investigated an innovative retrofit solution for existing timber floors based on the use of cambered and prestressed timber-to-timber composite (CP-TTC) systems. The core of the strategy relies on a novel connection configuration combining 30° inclined single-threaded screws and angled washers. Both screw-only and hybrid glued-screwed (HGS) variants were experimentally tested and analytically evaluated to assess their effectiveness in improving the structural performance of retrofitted floors.

The fastener pressure tests confirmed the ability of the inclined screws to generate significant compression forces (≈6.5 kN per screw on average), with losses of less than 10% over 12 days, most of which occurred in the first 24 hours. This prestressing contributed to the formation of camber, which plays a valuable role in mitigating early-stage deflection from permanent loads.

Push-out tests demonstrated that bonding significantly enhances the mechanical performance of the connection, increasing shear stiffness and strength by more than an order of magnitude when comparing HGS to screw-only setups. A benchmark test using 90° screw insertion confirmed the clear advantage of inclined installation in terms of connection stiffness, highlighting the importance of screw geometry in retrofit design.

Full-scale bending tests showed that the CP-TTC retrofit concept improves global stiffness and load-carrying capacity. Screwed-only specimens met ultimate limit state (ULS) criteria but exceeded the total serviceability deflection under combined permanent and variable loads. These results were in line with the design objective of exploring a lower-bound stiffness configuration. HGS variants, despite exhibiting reduced interface slip at the bonded regions, did not translate into significant global deflection improvements due to the limited bonding length and resulting strain redistribution.

The comparison with benchmark solutions demonstrated that the proposed retrofit system achieves superior performance in terms of strength, stiffness, and serviceability, even when compared to configurations using larger or more numerous fasteners. Analytical predictions aligned well with experimental results, confirming the reliability of the adopted design models. Moreover, under the forthcoming second-generation Eurocode provisions, the screw-only configurations are expected to meet SLS criteria, especially when the contribution of initial camber is considered.

Overall, the retrofit approach investigated in this study offers a promising, material-efficient, and constructible solution for upgrading existing timber floors. While adhesive bonding shows clear benefits at the connection level and proves compatible with the application of the CP assembly procedure, its global effectiveness remains uncertain, warranting further investigation. Future research should focus on optimising bonding layouts and evaluating long-term performance under cyclic and environmental loading.

ACKNOWLEDGEMENTS

The research was carried out within the framework of Timber-Engineering and NexTimber Projects sponsored by Würth Srl / GmbH.

REFERENCES

[1] Piazza, M. (1994). Restoration of timber floors via a composite timber-timber solution. In Proc. of the Technical Workshop RILEM" Timber: a structural material from the past to the future.

[2] Valluzzi M.R., Garbin E., Modena C., Flexural strengthening of timber beams by traditional and innovative techniques, J. Build. Appraisal 3 (2) (2007) 125–143.

[3] Giongo I, Piazza M, Tomasi R. Out of plane refurbishment techniques of existing timber floors by means of timber to timber composite structures. Proceedings of the world conference on timber engineering (WCTE), Auckland, New Zealand. 2012.

[4] Roensmaens, B., Van Parys, L., Carpentier, O., Descamps, T., 2018. Refurbishment of existing timber floors with screwed CLT panels. Int. J. Archit. Herit., 12(4), 622–631.

[5] Suárez-Riestra, F., Estévez-Cimadevila, J., Martín-Gutiérrez, E., Otero-Chans, D., 2022. Timber–timber composite (TTC) beam long-term behaviour: Full-scale experimental campaign and simplified analytical model. Construction and Building Materials, 361, 129649.

[6] Nie, Y., & Valipour, H. R. (2022). Experimental and analytical study of timber–timber composite (TTC) beams subjected to long-term loads. Construction and Building Materials, 342, 128079.

[7] Giongo I., Schiro G., Riccadonna D., 2019, "Innovative pre-stressing and cambering of timber-to-timber composite beams", Composite Structures, vol. 226, p. 111195.

[8] Giongo I., Schiro G., Walsh K., Riccadonna D., 2019b, "Experimental testing of pre-stressed timber-to-timber composite (TTC) floors" in Engineering Structures, v. 2019 vol. 201, (2019).

[9] Riccadonna D., Walsh K., Schiro G., Piazza M., Giongo I., 2020, "Testing of long-term behaviour of pre-stressed timber-to-timber composite (TTC) floors" in Con Build Mat, v. 236, (2020), p. 117596. - DOI: 10.1016/j.conbuildmat.2019.117596.

[10] Schiro G., Giongo I., Sebastian W., Riccadonna D., Piazza M., 2018, "Testing of timber-to-timber screw-connections in hybrid configurations", Construction and Building Materials, Volume 171, p. 170-186, DOI:10.1016/j.conbuildmat.2018.03.078.

[11] Chiniforush, A. A., Valipour, H. R., Ataei, A., 2021. Timber–timber composite (TTC) connections and beams: An experimental and numerical study. Con Build Mat, 303, 124493.

[12] Sciomenta, M., Gualtieri, P., Spera, L., Contu, F., Fragiacomo, M., 2024. Timber–timber composite (TTC) joints made of short-supply chain beech: push-out tests of inclined screw connectors. Materials and Structures.

[13] Schiro G, Giongo I, Riccadonna D, Enders-Comberg M, Piazza M. Prefabricated, prestressed composite timber floor modules for high performance applications. Seoul, Korea: Proceedings of the World Conference of Timber Engineering; 2018

[14] ETA (European Technical Approval) 11/0190: Würth self-tapping screws.

[15] European Committee for Standardization. EN 1995-1-1:2004+A2:2014: Eurocode 5 - design of timber structures, Part 1-1, General - Common rules and rules for buildings. Brussels.

[16] CEN (European Committee for Standardization), 2025, "Design of timber structures – Common rules and rules for buildings – Part 1-1: General". FprEN1995-1-1:2025. Brussels, BE.

[17] Giongo I., Piazza M., Tomasi R., 2013. "Investigation on the self tapping screws capability to induce internal stress in timber elements". Advanced Materials Research, vol. 778, pp. 604-611.

[18] CEN (European Committee for Standardization). 2001. Timber structures—Test methods—Cyclic testing of joints made with mechanical fasteners. EN 12512. Brussels.

[19] CEN (European Committee for Standardization), 2022, "Basis of structural and geotechnical design". prEN1990:2022. Brussels.

VERIFICATION OF SHORT-TERM AND LONG-TERM PERFORMANCE OF BEAM REINFORCEMENT SYSTEM USING DIAGONALLY DRIVEN LONG SCREWS

Shinya TAKANO, Yasufumi USHIO[2], Taito YAMAMURA[3], Shigefumi OKAMOTO[4] and Hiroki ISHIYAMA[4]

[1] Osaka Metropolitan University, Graduate school student, Division of Urban Engineering

[2] KANAI Group Co., Ltd,

[3] Osaka Metropolitan University (Graduated in March 2025)

[4] Osaka Metropolitan University, Graduate School of Urban Engineering

ABSTRACT

In this study, a Beam Reinforcement System using diagonally driven long screws was investigated to develop a reinforcement technique applicable to the renovation of wooden houses. The short-term structural performance of this method was experimentally verified, demonstrating that it ensures relatively high rigidity compared to existing techniques. Verification of the long-term performance suggested that the adjustment factor for the long-term allowable stress of this structure may significantly exceed the adjustment factor specified in the Japanese Building Standard Law[1]. This result may be due to the fact that the wood was stronger during the long-term test than during the short-term test due to drying. After the drying correction, the Duration of Load (DOL) factors were close to the adjustment factor specified in the Japanese Building Standard Law.

KEYWORDS: Duration of Load factor, Reinforced beam, Renovation, Screw

INTRODUCTION

In Japan, when renovating existing wooden houses, it is often required to remove columns to enhance design flexibility. However, to ensure sufficient structural strength after column removal, it is necessary to reinforce beams by increasing their depth to maintain rigidity and suppress deflection.

Existing beam reinforcement techniques include mechanical joints secured with bolts and chemical joints using adhesives. Generally, mechanical joints offer superior on-site constructability but require bolt holes, making it difficult to ensure rigidity. On the other hand, chemical joints can effectively ensure rigidity but have the drawback of inferior on-site constructability.

Therefore, we developed a Beam Reinforcement System (hereinafter referred to as "the present system") that uses long screws driven at an angle, which offers relatively high rigidity and easy on-site constructability [Fig. 1]. The present system enables highly efficient reinforcement because the long screws, when driven at an angle, counteract the horizontal shear forces generated by the sliding between the upper and lower chord members by exerting tensile forces along their axes. Additionally, long screws are easy to install on-site, cost-effective, and scalable for mass production, making them suitable for expanding the scope of application to small-scale wooden buildings and other structures.

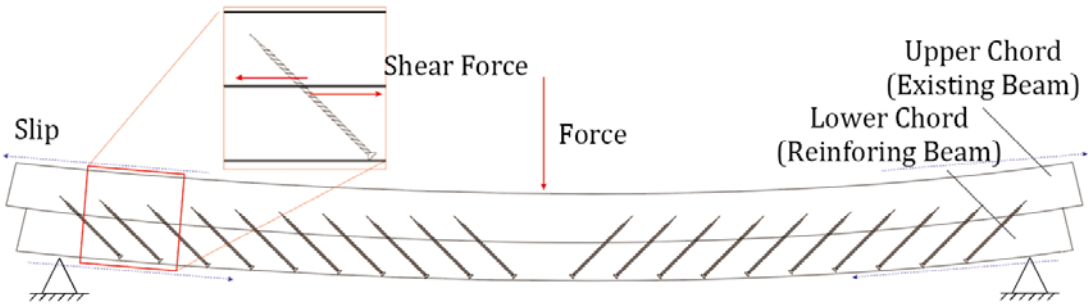

Figure 1. Overview of the present system

PURPOSE

Materials such as wood tend to gradually lose strength when subjected to long-term loads. In order to use this system in construction, it is necessary to understand its short-term structural performance and determine the adjustment coefficients for long-term allowable stress and rigidity. The relationship between the breaking strength and DOL of wood bending performance has been obtained by the Forest Products Laboratory (FPL) in the United States through seven years of bending tests on small flawless test pieces (Madison Curve)[2]. However, since shear and tensile forces act on the steel long screws at the joints, and compressive forces also act on the wood in the present system, it is not certain that the creep failure characteristics will necessarily match the Madison Curve obtained for wood alone. Therefore, in this paper, verification of short-term and long-term loads was conducted to determine the standard load required for setting the long-term load ratio, and the DOL coefficient was calculated.

VERIFICATION OF SHORT-TERM

Methodology

Figure 2 shows an overview of the test specimens for the short-term test. The dimensions of the test specimens were determined based on the assumption that the columns in the centre of the 2-ken (3636 mm) long beams would be removed. The number of test specimens shall be three composite beams reinforced with long screws [CB] and three unreinforced layered beams [LB]. The long screws were 280 mm long with a diameter of 9 mm, and pilot holes were drilled for driving them in. To prevent cracking due to drying, relief cuts were made, and the long screws were driven in in a staggered pattern. In all test specimens, the upper and lower chords were overlapped so that the relief cuts were on the lower side.

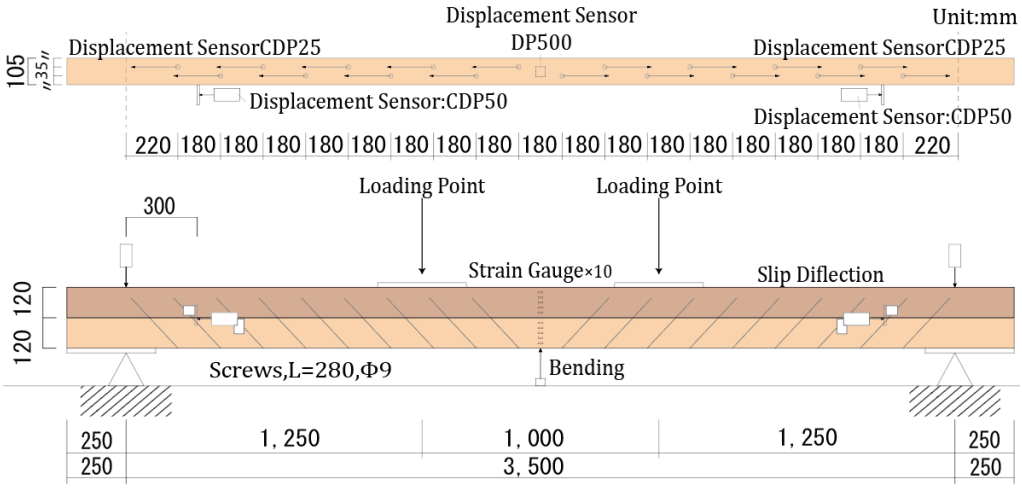

Figure 2. Overview of the test specimens for the short-term test

The density, moisture content, and Young's modulus of the test specimens for the short-term test were 495 ± 54 [kg/m^3], 25 ± 7 [%], and 8.2 ± 1.3 [kN/mm^2], respectively. Bending tests were conducted using a three-point load configuration with a monotonic loading method, and the maximum load and deflection at the span centre were measured. The tests were continued until failure occurred or the load decreased to 80% of the maximum load. The loading rate was set to 20 mm per minute, and the time required to reach the maximum load was approximately 5 minutes.

Results

Table 1 shows the result of short-term tests, and Fig. 3 shows the relationship between load - central deflection, and slip deflection. Fig. 4 shows a cross-sectional strain distribution diagram at the centre of the beam. The failure mode was predominantly bending failure with cracks propagating in the fibre direction near the centre of the lower chord. In particular, the composite beam exhibited increasing deflection accompanied by noise, eventually failing with a sound resembling the cracking of wood. CB-1 and CB-3 showed a significant decrease in load after reaching the maximum load, while CB-2 showed ductile behaviour. No deformation of the long screws in the composite beams was observed after the test. Therefore, it is considered that the wood yielded due to the combined bending and tensile stress of the lower chord rather than the long screws. Short-term test showed that the present system has relatively high rigidity, and beam reinforcement improved the maximum load capacity and reduced deflection. The increase in bending rigidity of the composite beams was approximately 2.2 times that of the layered beams. In addition, the strain at the centre of the beam was smaller for the composite beam than for the layered beam. Therefore, it can be considered that the reinforcement with long screws had the effect of integrating the upper and lower chords. However, it is difficult to completely suppress the amount of slippage between the materials because the stress distribution is not linear.

Table 1. Result of the short-term test

Specimen	P_{max} [kN]	δ_{Pmax} [mm]	EI ×10^8[kN·mm^2]	ε_{max} [N·mm^2]
CB-1	35.3	93	5.63	5613.8
CB-2	40.6	132	6.21	6027.6
CB-3	40.5	78	5.87	3657.7
LB-1	31.3	137	2.47	5539.0
LB-2	29.0	138	2.69	3775.2
LB-3	28.7	146	2.61	4518.4

Legend: CB: Composite Beam reinforced with long screws; LB: Layered Beam; P_{max} : Maximum load; δ_{Pmax} : Deflection at maximum load; EI : Bending stiffness; ε_{max} : Tensile edge strain at maximum load

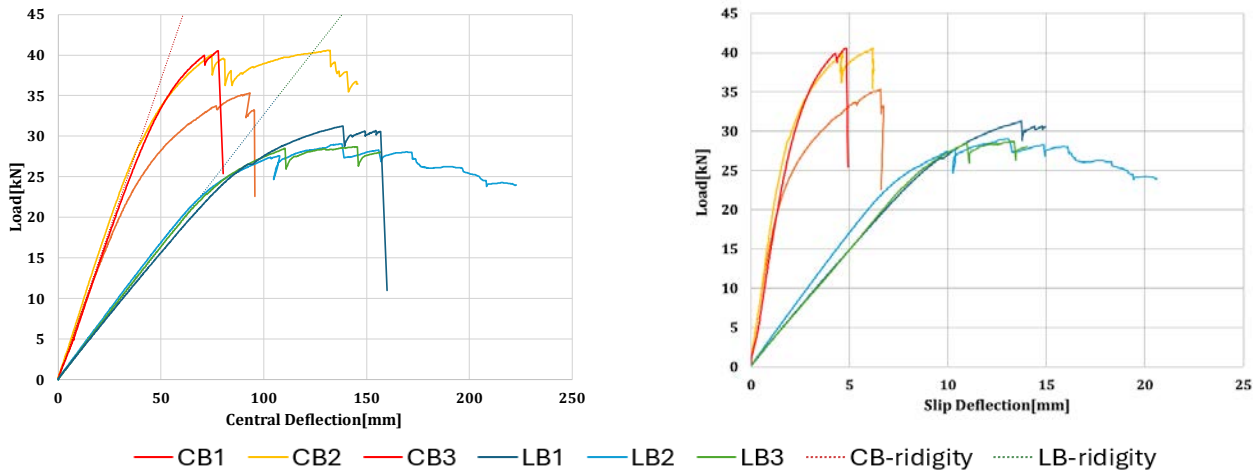

Figure 3. Relationship between load – central deflection, and slip deflection

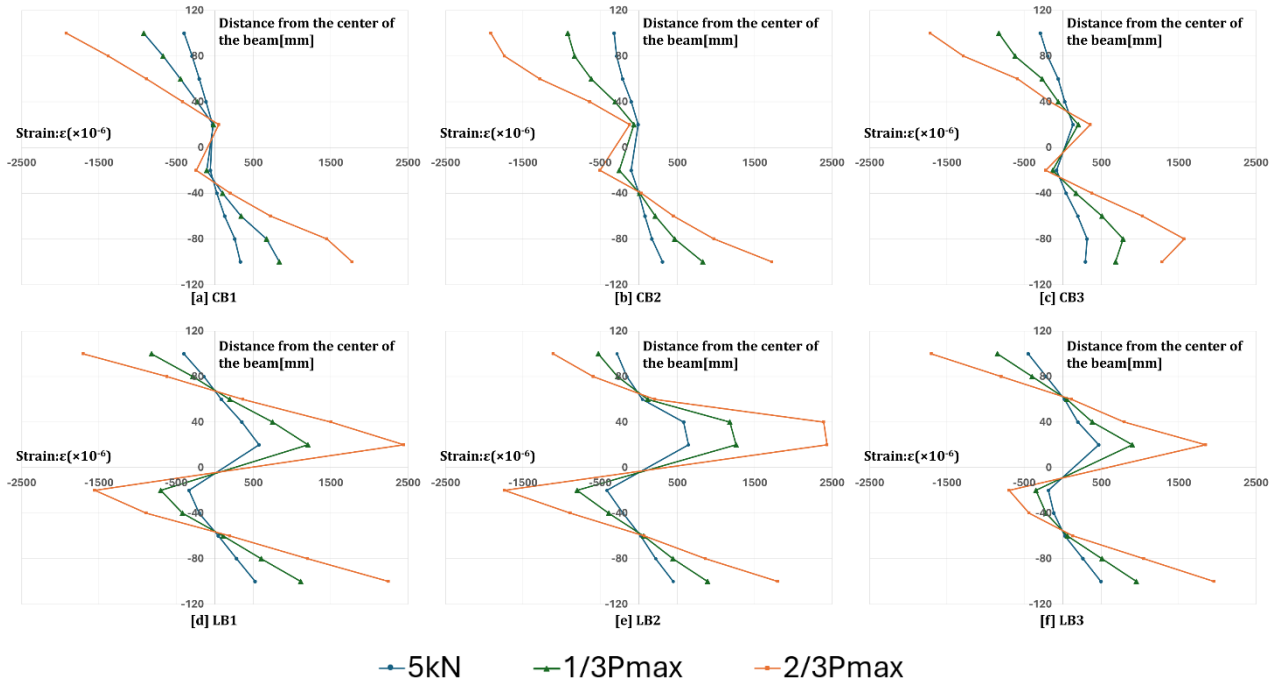

Figure 4. Cross-sectional strain distribution diagram at the centre of the beam

VERIFICATION OF LONG-TERM

Methodology

The average maximum load obtained in the short-term test was set as the reference load ratio of 1.0, and loads corresponding to load ratios of 0.9, 0.8, and 0.7 were continuously applied. In accordance with Japanese notification[3], the building's service life was set at 50 years, and the DOL coefficient after 50 years (medium to long term) was calculated. The time from loading to failure, the load, and the deflection at the centre of the test piece were measured. The number of test pieces was set at nine composite beams, with three for each load ratio. For comparison, three unreinforced layered beams were tested with a load ratio of 0.75.

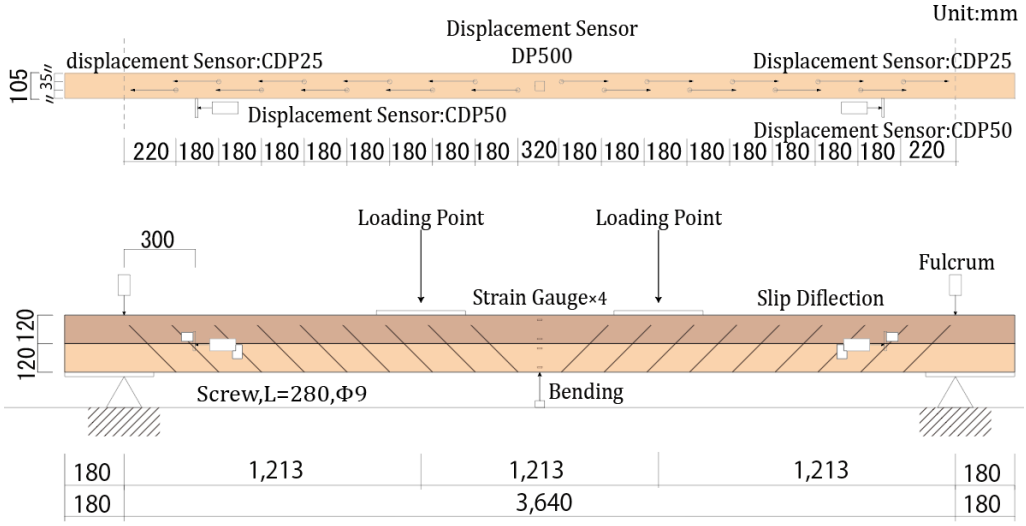

Figure 5. Overview of the test specimens for the long-term test

Figure 5 shows an overview of the test specimens for the long-term test. Since it was not possible to prepare the same environment for the short-term and long-term tests, the span was changed. The spacing of the long screws was changed in the centre of the beam because the shear stress is smaller than that at the ends of the material. Even if this causes a decrease in strength, the DOL coefficient is calculated on the safe side. The test specimen dimensions and test setup for the unreinforced layered beams were the same as those for the composite beams. The density, moisture content, and Young's modulus of the long-term test specimens were 498 ± 77 [kg/m^3], 23.1 ± 6.1 [%], and 8.2 ± 1.4 [kN/mm^2], respectively.

Figure 6 shows an overview of the test apparatus. Since long-term tests are expected to take a long time, a loading device was designed and manufactured that can continuously apply a constant vertical load to the test piece. This loading device uses a moment type that amplifies the load using the principle of leverage, enabling a load 20 times the weight to be continuously applied to the test piece. The load was measured using a strain gauge on the bolt of the loading section. The self-weight of the H-shaped steel, which is not included in the measured load, was pre-measured and added to the measured load to calculate the total load. Additionally, the test apparatus was installed in a constant temperature and humidity environment of 20 ±2[°C] and relative humidity of 65 ±5[%].

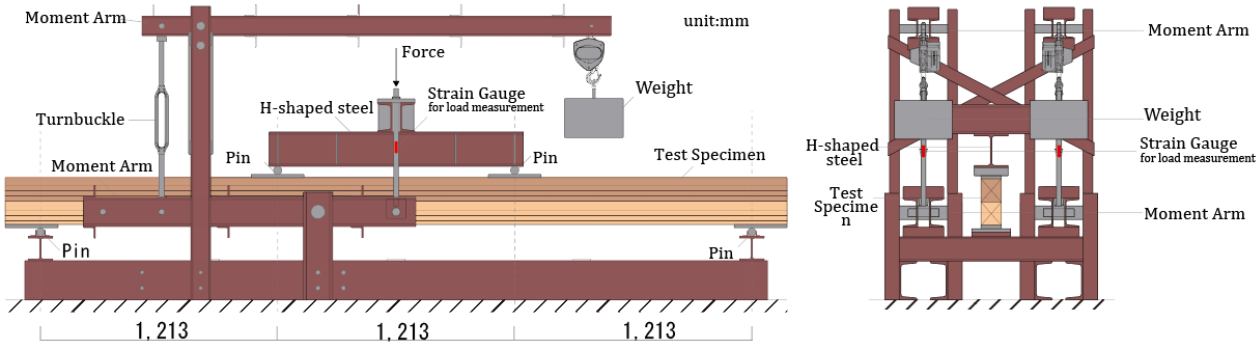

Figure 6. Overview of the test apparatus for the long-term test

Results

Three composite beam load ratios of 0.9 and three layered beam load ratios of 0.75 were applied. As of May 31, 2025, three composite beam load ratios of 0.9 and two layered beam load ratios of 0.75 had failed.

Table 2 shows the result of long-term tests. The criteria for determining destruction were set as “when deformation increased rapidly and load decreased.” Figure 7 shows the relationship between the duration of load and central deflection. All failures were dominated by bending failure with cracks in the fibre direction near the centre of the lower chord, as in the short-term test. CB-0.9-3 and LB-0.75-1 failed due to a short-term impact when the turnbuckle was rotated during loading. Therefore, these failures were considered to have occurred in a short period of time and were not taken into account in the calculation of the DOL coefficient. Other test specimens are considered to have failed in the third creep stage, in which progressive deflection occurred in the deflection curve and led to failure. In the CB-0.9 test, it was found that after the initial load was applied, the load fluctuated within a certain range. This was thought to be caused by the round steel at the fulcrum of the lever not moving smoothly due to rotational resistance caused by friction. Therefore, in the LB-0.75 test, grease and teflon sheets were inserted into the rotating parts to reduce rotational friction and suppress load fluctuations.

Table 2. Result of long-term test

Specimen	*Load mean* [kN]	*Time to failure* [hour]	*Stress level*	$\delta_{ultimate}$ [mm]
CB-0.9-1	35.15	1684	0.93	117.37
CB-0.9-2	34.89	1072	0.93	105.57
CB-0.9-3	-	0	-	90.64
LB-0.75-1	-	0	-	83.36
LB-0.75-2	24.74	95	0.86	95.72

Legend: CB: Composite Beam reinforced with long screws; LB: Layered Beam$\delta_{ultimate}$: Deflection at the centre of the beam when destroyed

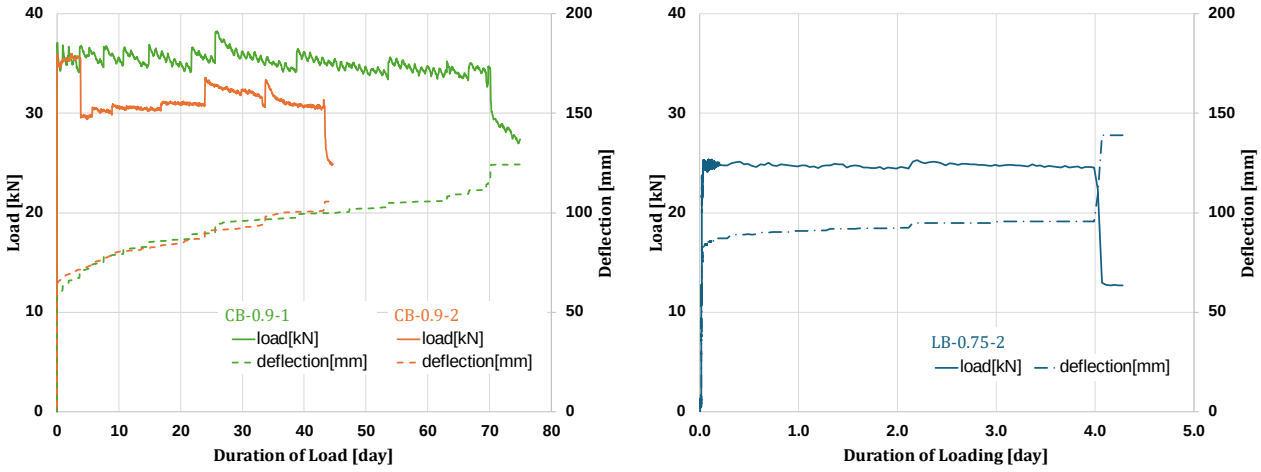

Figure 7. Relationship between duration of load - central deflection

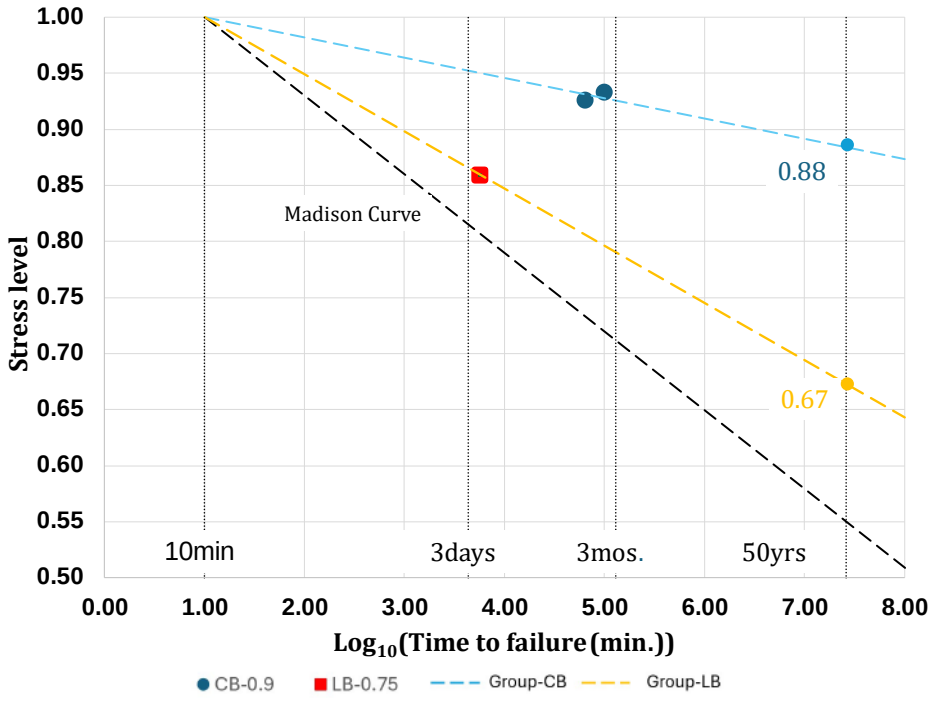

Figure 8. Relationship between time to failure and stress level

The regression line was determined based on the relationship between the common logarithm of the load duration and the stress ratio, and the strength ratio corresponding to a load duration of 50 years on the regression line was calculated as the DOL coefficient [Fig. 8]. Both composite beams and layered beams failed at times longer than the Madison curve. The DOL coefficient was 0.88 for composite beams

and 0.67 for layered beams. These results exceeded the standard value of 0.55 specified in the Building Standards Law.

DISCUSSION

The DOL coefficient obtained in the long-term test exceeded the standard value specified in the Building Standards Act because the short-term test was conducted in summer, whereas the long-term test was started in winter, resulting in improved strength due to drying. Therefore, it is necessary to reset the standard strength after making adjustments for drying.

The method for drying correction of composite beams is as follows. First, the reference strength of the tension string was calculated by substituting the average edge strain at maximum load obtained from the short-term test and the Young's modulus of the lower chord measured immediately before the start of the long-term test into the following equation [1]. Next, the standard load was obtained by substituting the standard strength into equation [2], which is an equation for calculating the elastic limit load of wooden built-up beams proposed by Kamachi et al[3] [Fig. 9].

$$ {}_F F_t = \varepsilon_{max} \cdot E_{ft} \quad [1] $$

$$ {}_F P_t = \left[\left(-\frac{1}{A_{ft} H} + \frac{E_{ft} h_{ft}}{2\Sigma \mathrm{E} I_\iota} \right) \frac{K \sinh \lambda(1-\alpha)L \cdot \sinh \lambda \alpha L}{\lambda \sinh \lambda L} + \left\{ \frac{K}{A_{ft} H} + \frac{(1-K) E_{ft} h_{ft}}{2\Sigma \mathrm{E} I_\iota} \right\} (1-\alpha)\alpha L \right]^{-1} \cdot {}_F F_t \cdot 2(1-\alpha) \quad [2] $$

$$ K = \frac{1}{1 + \dfrac{1 + (EA)_{fc}/(EA)_{ft}}{H^2 (EA)_{fc}} \Sigma \mathrm{E} I_\iota} \quad [3] $$

$$ \lambda = \sqrt{\frac{\Gamma H^2}{K \Sigma \mathrm{E} I_\iota}} \quad [4] $$

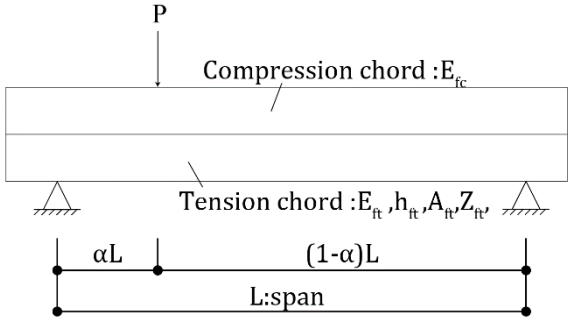

Figure 9: Schematic diagram

${}_F F_t$: Reference strength of tension chord

${}_F P_t$: Elastic limit load when the chord yields

ε_{max} : Short-term test Average edge strain on tensile side at maximum load

$(EA)_{fc}$: Compression stiffness of compression chord

$(EA)_{ft}$: Tensile stiffness of tension chord

E_{ft} : Young's modulus of tension chord

h_{ft} : Hight of tension chord

A_{ft} : Cross-sectional area of tension chord

$\Sigma \mathrm{E} I_\iota$: Total bending rigidity of each chord

α : Load center span ratio

L : Span

H : Distance between the neutral axes of the chords

The method for correcting for drying in layered beams is as follows. As with composite beams, the standard strength was calculated from [1] using the maximum strain at the outermost edge obtained from short-term tests and the Young's modulus of the lower chord measured immediately before the start of long-term tests. The standard strength of the lower chord was calculated by considering the load ratio between the upper chord and the lower chord, and the maximum load was calculated [5].

$$ {}_F P_t = \frac{2(E_{ft} + E_{fc}) Z_{ft}\ {}_F F_t}{E_{ft} L} \quad [5] $$

E_{fc} : Young's modulus of compression chord Z_{ft} : Cross-sectional coefficient of tension chord

Table 3 shows the Young's modulus measured at the start of the short-term test and long-term test, and the standard load after drying correction. Figure 10 shows the relationship between the load ratio after drying correction and the common logarithm of the load duration. However, composite beams 0.9-2 were not considered because their Young's modulus was not measured before the start of the long-term test. The DOL coefficient after drying correction was 0.58 for composite beams and 0.43 for layered beams, which are close to the Madison curve.

However, due to the small number of test specimens, it cannot be said that the estimated values obtained by drying correction are consistent. Therefore, future issues include increasing the number of test specimens and confirming the consistency of the estimated values obtained by drying correction.

Table 3. Result of long-term test

Specimen		E_{summer} [kN/mm2]	E_{winter} [kN/mm2]	Standard load After drying correction	Stress level After drying correction
CB-0.9-2	Upper Chord	6.18	6.85	46.29	0.75
	Lower Chord	9.01	8.91		
LB-0.75-2	Upper Chord	7.39	8.43	24.74	0.76
	Lower Chord	8.54	8.54		

Legend: E_{summer} : Young's modulus [2024.08.19]; E_{winter} : Young's modulus [2025.01.16]

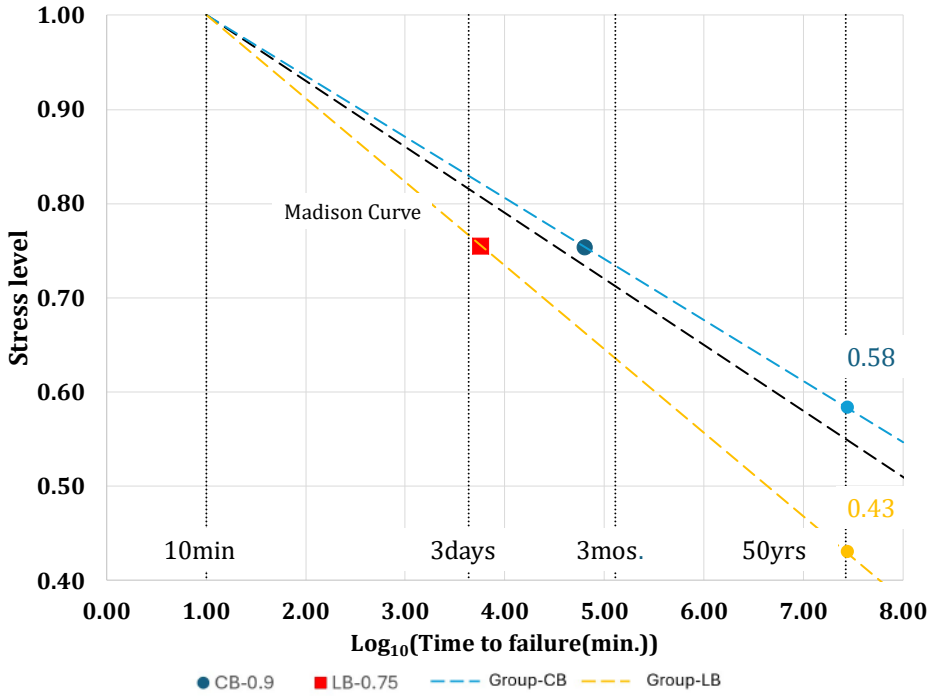

Figure 10. Relationship between time to failure and stress level after drying correction

CONCLUSIONS

In this study, the following findings have been obtained to date:

1. The short-term structural performance of the present system ensures relatively high rigidity and strength compared to existing technologies.

2. The long-term performance of the present system may greatly exceed the wood adjustment factor specified in the Building Standards Act of Japan. However, the improvement in strength due to drying of the wood was cited as a factor, and the DOL coefficient after drying correction was equivalent to the wood adjustment factor specified in the Building Standards Act of Japan.

Future issues include confirming the validity of estimates based on the increase in data and drying correction.

ACKNOWLEDGMENT

Part of this research was conducted with funding from the Osaka City Innovation Creation Support Grant.

REFERENCES

[1] The Building Standard Law of Japan, Article 89, April 2000

[2] Wood, L, W.: Relation of Strength of Wood to Duration of Load, FPL Report, No R1916, December 1951

[3] Ministry of Construction Notification No. 1446 and No.1459, May 2005

[4] Ken KAMACHI, Mashiro INAYAMA and Masafumi INOUE: Design Method for the Built-up-beams - Solution Method Based on the Parallel Chord Truss Model for the Multi-layered Built-up-beam Part 1-, J. Struct. Constr. Eng., AIJ Vol. 74 No.638, 691-700, April 2009

IN SITU MEASUREMENTS OF CLT FLOOR VIBRATION CONSIDERING EFFECTS OF NON-STRUCTURAL WALLS AND LONG-SPAN SUPPORTING BEAMS

Mohammadreza SALEHI[1], Ebenezer USSHER[1], Eli TOFTEMO[2], Daniel BØHN HAUG[2] and Roberto TOMASI[1]

[1] Norwegian University of Life Science (NMBU), Norway
[2] Brekke & Strand Akustikk AS, Norway

ABSTRACT

Cross-laminated timber (CLT) floors are gaining popularity in sustainable construction due to their high strength-to-weight ratio and environmental advantages. However, their vibration performance remains a key serviceability concern. This study investigates the influence of boundary conditions in terms of long-span supporting beams and non-structural walls on the dynamic behaviour of CLT floors. In-situ vibration tests were conducted on a CLT floor with two spans in a school building in Norway to identify its modal parameters. Results revealed that the long-span supporting beam lacked sufficient stiffness, causing coupled vibration behaviour with the floor system rather than independent span action. Non-structural walls were found to significantly enhance stiffness, raising natural frequencies beyond predictions by Eurocode 5 (EC5). Finite element models incorporating walls improved correlation with experimental data, but still underestimated floor stiffness, likely due to additional layers like screed. The findings highlight the critical role of non-structural walls and finishes in vibration design of a floor system and suggest the need for refined modelling approaches and updated design standards.

KEYWORDS: CLT floor, modal parameters, boundary conditions, serviceability

INTRODUCTION

Cross-laminated timber (CLT) has emerged as a sustainable and high-performance engineered wood product, increasingly utilised in modern construction. Its strength-to-weight ratio and environmental benefits make it particularly suitable for floor systems in timber buildings [1-3]. However, the vibration performance of CLT floor systems remains a critical serviceability concern. Despite meeting design stage criteria prescribed in standards such as Eurocode 5 (EC5), CLT floors can exhibit unexpected vibration behaviour in service due to the complexity of material properties, boundary conditions, and human-induced excitations.

Boundary conditions have a significant impact on the vibration performance of the CLT floor. Therefore, a comprehensive understanding of their role is essential for an accurate prediction of floor dynamic responses. A typical boundary conditions for CLT slabs are beams, as considered in design codes such as EC5. In recent years, most research has focused on simply rigid supports, as an idealised scenario, or elastic beam supports. Guo et al. [4] conducted experimental and numerical studies on timber floors with varying spans, slab and topping thicknesses, and boundary conditions, including rigid and elastic supports. Their findings highlight that boundary conditions significantly affect natural frequencies, mode shapes, and overall floor vibration performance. A numerical study by Huang et al. [5] was performed to model a CLT floor from a case study to validate the model against on-site measured data.

The study further assessed the dynamic behaviour of the CLT floor, considering various beam-supporting plans. An experimental modal analysis by Kawrza et al. [6] on a CLT slab demonstrates that accurately identifying both material properties and boundary conditions is essential to achieve good agreement between experimental and numerical results. Another study by Ussher et al. [7] on the vibration serviceability of lightweight timber floors emphasised that modal characteristics are highly sensitive to boundary condition details, including bearing surface contact, end and edge restraints, and the connection methods between CLT panels. These factors significantly influence floor performance and should be considered alongside conventional design parameters such as span, width, and CLT layup or configuration.

Compared to the supporting beam boundary conditions, the impact of non-structural walls on the dynamic behaviour of CLT floors has received relatively little attention and remains largely underexplored in the existing literature. Devin et al. [8] introduced a numerical modelling approach to account for the impact of non-structural elements, including internal partitions and exterior cladding systems. The study emphasises that partitions can serve as effective passive vibration control by adding not only mass and damping but also significant stiffness, which can be used to enhance floor vibration performance. Ussher et al. [9] investigated the influence of partition walls on the dynamic behaviour of CLT floors and demonstrated that such elements can significantly increase modal stiffness and alter vibration characteristics.

Despite these contributions, the combined effect of internal partition walls and supporting beams on the vibration performance of CLT floors remains largely overlooked in current research. This study aims to address this gap by investigating the dynamic behaviour of a CLT floor system through in-situ tests, focusing on supporting beams and non-structural walls under different boundary conditions. For this, in situ experimental tests were conducted on a CLT school building in Norway. A sensor-roving technique with dense accelerometer arrangements was used to capture floor modal parameters.

CASE STUDY

Aursmoen School is a three-story building in Aursmoen, Norway, under construction, shown in Figure 1. The building comprises five parts, totalling approximately 20,000 m^2, and includes a new kindergarten with 10 departments, a resource department, adult education, a leisure club, and a sports hall. The structural system consists of columns and beams in GLT, and CLT shear walls, in addition to CLT floors.

Figure 51. Aursmoen School

FLOOR MATERIAL AND GEOMETRY

Figure 2 illustrates the studied room and the corresponding floor drawings. The room is completely unfurnished, and the dimension is 8.0m x 7.8m. The tested area is marked in Figure 2 by a red dashed line. The floor is made of two separate CLT spans, named Span A and Span B. The supporting beams are

identical steel beams (S355). Both CLT spans have the same construction layout and CLT cross-section as shown in Table 1.

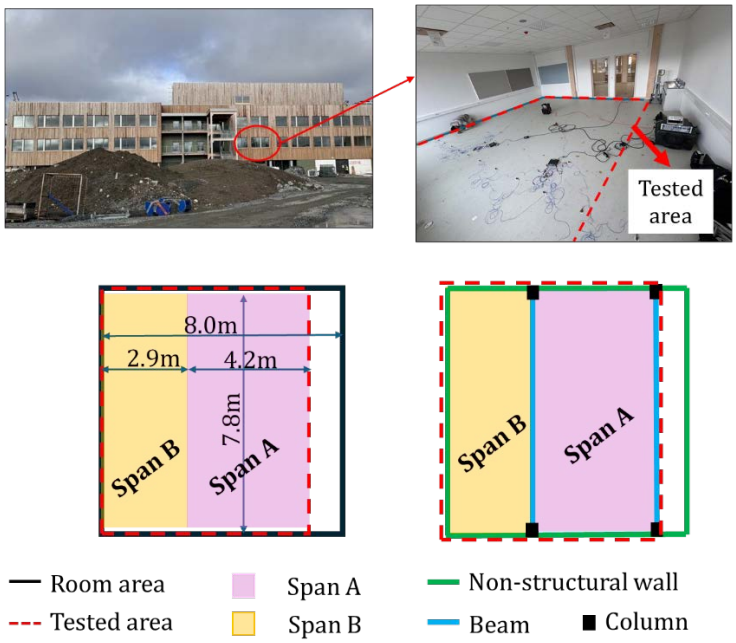

Figure 52. View of the tested floors and drawings

Table 16. Floor layout material

Layer	Thickness	Surface load (kN/m²)
Screed	60mm	1.20
Sound insulation	40mm	0.05
Insulation	-	0.30
Ceiling system	-	0.30
Other	-	0.15
CLT 160 L5s-2	160	0.72
Sum	-	**2.72**

EXPERIMENTAL SETUP

Vibration tests were performed to identify the modal parameters of the floors. These tests involved dynamic excitation induced by an individual weighing 79 kg.f through random walking and jumping on the floor. A dense sensor configuration using 16 accelerometers and a sensor-roving approach was employed to identify the modal parameters of the floors, as shown in Figure 3. For each span, two accelerometers were used as references, and the remaining six were used as roving sensors, with a total of 136 measurement points. The acquisition frequency was 200 Hz with a duration of 120 seconds for each excitation. The modal parameters have been obtained from the two well-known output-only identification algorithms: the Enhanced Frequency Domain decomposition (EFDD) and the Stochastic Subspace Identification (SSI).

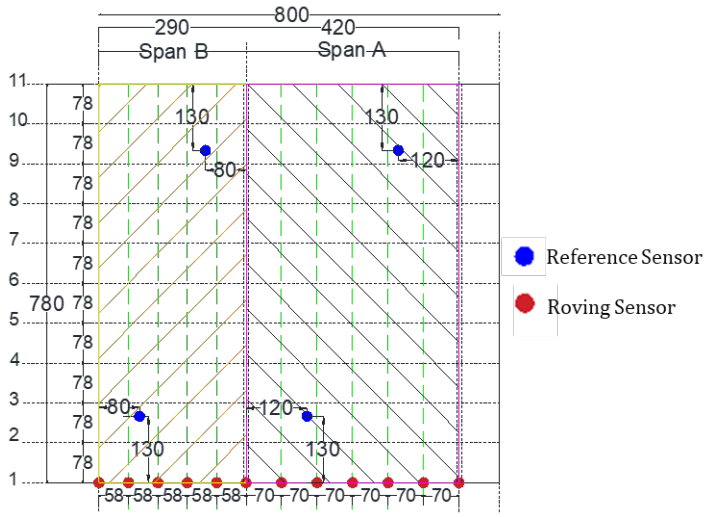

Figure 53. Experimental setup and measurement grids (unit in cm)

EXPERIMENTAL RESULTS

Figure 4 illustrates the first mode shape and corresponding frequency of the two CLT spans. Contrary to expectations, significant deformations are observed near the beams, which are designed to serve as a support. In contrast, much smaller deformations are evident near the walls. This suggests that the beams lack sufficient stiffness to effectively function as stiff boundary conditions. Instead of acting as a stiff support separating the two spans, the beam appears to participate in the global vibration of the floor system. Therefore, the two spans behave more like a single floor unit, vibrating together in a coupled manner.

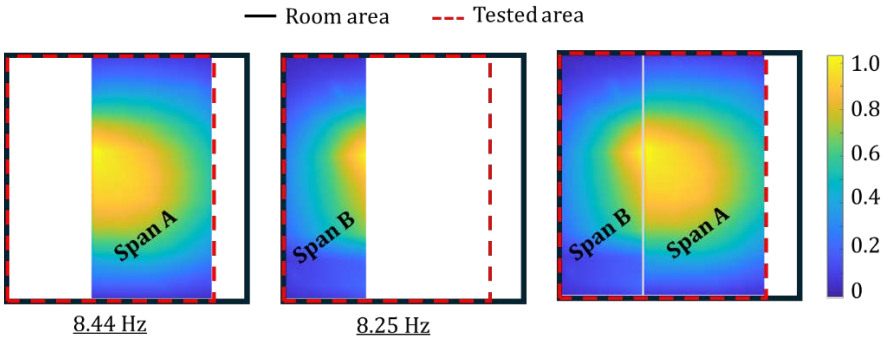

Figure 54. Identified the first mode shape and fundamental frequency

The proposed version of EC5 suggests Equation 1 for calculating the fundamental frequency of a single-span floor with rigid pinned supports at both ends. In this equation, L is the floor span, in m, EI_l is the bending stiffness along the floor span per meter width, in N.m²/m, and m is the floor mass per unit area, in kg/m². In the case of a single span $ke,_1$ = 1,0 and $ke,_2$ expresses the effect of transverse stiffness presented in equation 2, where b and EI_t are the floor width and the transverse stiffness, respectively. $ke,_2$ is set as 1 for a one-way spanning floor. Furthermore, equation 3 is provided to account for the effects of elastic supports, such as supporting beams at both ends.

$$f_1 = ke,_1 \; ke,_2 \; \frac{\pi}{2l^2} \sqrt{\frac{EI_l}{m}} \qquad (1)$$

$$ke,_2 = \sqrt{(1 + \frac{\left(\frac{l}{b}\right)^4 EI_t}{EI_l})} \quad (2)$$

$$f_1 = \sqrt{\frac{1}{f_{1,rigid}^2} + \frac{1}{3f_{1,beam1}^2} + \frac{1}{3f_{1,beam2}^2}} \quad (3)$$

In equation 3, $f_{1,rigid}$ is the floor fundamental frequency when supported on rigid supports, $f_{1,beam,1}$ and $f_{1,beam,2}$ are the fundamental frequencies of the supporting beams at two ends.

Table 2 presents the natural frequencies calculated using Equations 1-3, alongside those obtained experimentally, while the frequency predicted by EC5 is lower than the experimentally identified values. The first mode shape shown in Figure 4 reveals minimal deformations near the walls, suggesting that the non-structural walls act as additional boundary conditions, increasing the floor's stiffness. This restraining effect, which is not fully captured in the simplified analytical model, could lead to higher stiffness and, consequently, higher natural frequencies.

Table 17. Floor identified fundamental frequency (Hz) compared with EC5

	EC5	**Experimental**	**Diff.**
Span A	6.42	8.44	23.9%
Span B	6.42	8.25	22.1%

The Finnish National Annex to EC5 [10] proposes Equation 4 for two-way spanning floors, providing a more accurate estimation of the fundamental frequency for floors supported along all four edges. The natural frequency for Span A is calculated using Equation 4 and presented in Table 3. It shows a closer agreement with the experimentally identified values. This highlights the significant influence of additional boundary conditions, such as those provided by non-structural walls. It should be noted that, in the calculation with the assumption of a two-way spanning floor, the beams are considered as elastic supports and walls as rigid pinned supports.

$$f_1 = \frac{\pi}{2l^2}\sqrt{\frac{EI_l}{m}}\sqrt{1 + [2(\frac{l}{b})^2 + (\frac{l}{b})^4 (\frac{EI_l}{EI_t})]} \quad (4)$$

Table 18. Floor identified fundamental frequency (Hz) compared with EC5-Finland National Annex

	EC5	**Experimental**	**Diff.**
Span A	7.96	8.44	5.6%

FINITE ELEMENT MODELLING

Finite element (FE) models of the floor were developed based on the construction drawings using SAP2000 software. The CLT slab was modelled using a single-layer shell element with equivalent material properties. Columns and walls were represented as pinned supports, reflecting their significantly higher stiffness relative to the CLT slab. Supporting beams were also included in the model and defined as frame elements. The cross-section of the beam and its connection to the CLT slab are shown in Figure 6. Two models were developed for Span A: (i) assuming a single-span CLT slab with elastic beam supports, and (ii) assuming a single-span CLT slab with elastic beam supports and additional wall boundary conditions. Figure 6 illustrates the fundamental frequency and mode shape for Span A under two modelling conditions. The fundamental frequency, in the absence of the wall

(Figure 6a), deviates significantly from the experimentally identified value, a difference of 18%, indicating a limited accuracy of the simplified model.
When the effect of the walls is incorporated, the fundamental frequency increases to 7.69 Hz, and the deviation from the identified frequency is reduced to 8% (Figure 6b). Although the mode shape also improves and shows a closer agreement with its experimental counterpart, a noticeable difference still remains, indicating that further refinement of the boundary conditions or structural assumptions may be necessary.

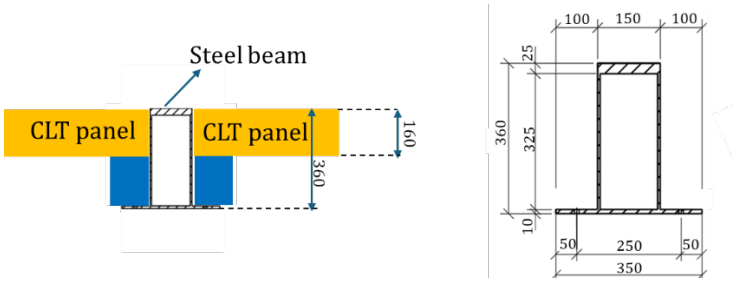

Figure 55. Beam cross-section and CLT slab (unit in mm)

In the subsequent modelling approach, the entire floor system, made of Span A and B, was modelled and analysed using the previously defined boundary conditions for the beams and walls. The resulting fundamental frequency and mode shape are presented in Figure 7. Despite adopting a pinned support assumption to represent the perimeter walls, the fundamental frequency was found to be 7.73 Hz, still lower than the values experimentally identified and presented in Figure 4. This suggests that the in-situ floor system exhibits greater stiffness than the numerical model. The discrepancy may be attributed to the additional stiffness caused by a 60 mm screed layer over the CLT slab.

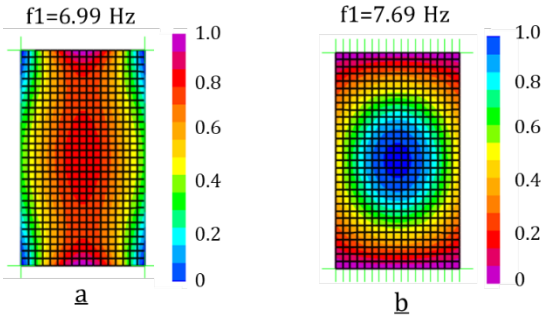

Figure 56. Fundamental frequency and mode shape for Span A: a) without the stiffening effect of walls, b) with the stiffening effect of walls

Compared to earlier models in Figure 6, the mode shape in Figure 7 exhibits improved agreement with its experimental counterpart, indicating a more accurate representation of the floor dynamic behaviour. Notably, Beam 1 (see Figure 7) does not appear to provide sufficient stiffness to the CLT floor. As a result, Spans A and B behave more like a single continuous span rather than acting independently. This coupled behaviour is evident in the mode shape and indicates that Beam 1 is deforming with the slab rather than constraining it. Although both beams have identical properties, Beam 1 exhibits greater deformation compared to Beam 2. This difference may be attributed to the proximity of Beam 2 to the stiffer boundary condition provided by the wall, which likely offers additional restraint and reduces the deformation of Beam 2.

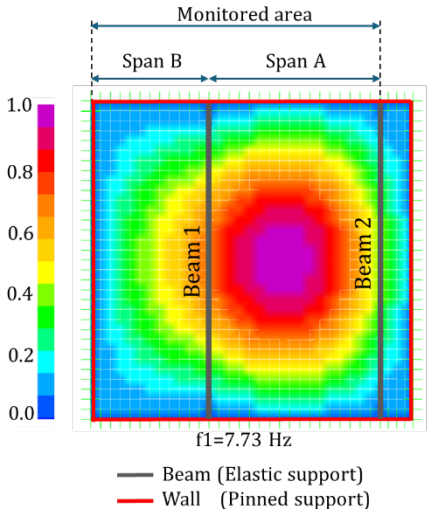

Figure 57. Numerical fundamental frequency and mode shape for the entire floor

A detailed comparison of the first mode shape deformation, illustrated in Figure 8, indicates that Beam 2 experiences approximately 43% less deformation than Beam 1. This notable difference supports the earlier observation that Beam 2 benefits from the added stiffness provided by its proximity to the perimeter non-structural wall. The additional boundary condition by the non-structural wall introduces additional restraint, thereby limiting the deformation of Beam 2. In contrast, Beam 1, which is located farther from the perimeter wall, lacks such support and thus deforms more significantly.

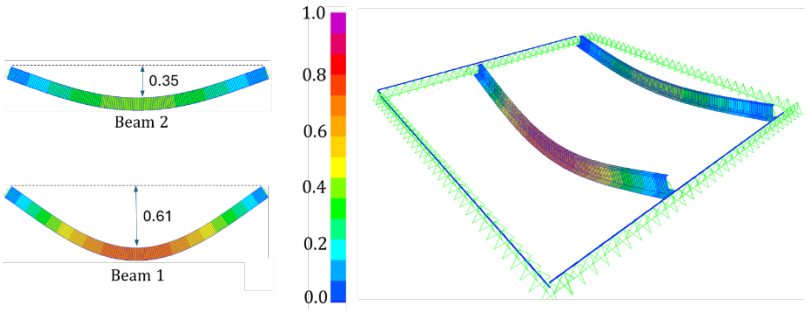

Figure 58. Deformation of the beams in the first mode

CONCLUSION

The fundamental frequencies identified experimentally were higher than those predicted by Eurocode 5 (EC5) using simplified analytical models. This discrepancy is primarily attributed to the influence of internal walls and the stiffening effect of additional layers, such as the 60 mm screed, which are not fully captured by the standard EC5 approach. When considering the floor as a two-way spanning system, as proposed in the Finnish National Annex to EC5, the calculated frequencies showed closer alignment with experimental values. This underscores the importance of accounting for additional boundary conditions by the non-structural wall.

Experimental results revealed that the two spans of the CLT floor system do not behave independently, as initially assumed. Instead, due to the insufficient stiffness of the supporting beam (Beam 1), the entire floor system behaves as a single, coupled system with significant deformation near the beam region.

Numerical simulations showed improved agreement with experimental results when the wall effects were included as an additional boundary condition. However, even with these added boundary conditions, the FE model still underestimated the in-situ fundamental frequency, highlighting the need for a more accurate modelling of actual construction conditions. Beam 2 exhibited significantly lower deformation for the first mode (43% less) than Beam 1, despite having identical properties. This was attributed to its proximity to a stiffer boundary condition, which offered additional restraint.

REFERENCES

[1] Hildebrandt, J., Hagemann, N., Thrän, D., 2017. The contribution of wood-based construction materials for leveraging a low-carbon building sector in Europe. Sustainable Cities and Society, 34, pp.405–418.

[2] IPCC, Summary for Policymakers, Cambridge University Press, Cambridge, UK, 2022, p. In Press, in Press.

[3] Dovetail Partners, 2013. Carbon in wood products – the basics. Dovetail Partners, Inc.

[4] Guo, C., Zhou, J., Chui, Y.H., 2025. Experimental and numerical investigations on vibration performance of mass timber slab floors with floating concrete toppings. Engineering Structures, 330, 119919.

[5] Huang, H., Gao, Y., Chang, W.S., 2020. Human-induced vibration of cross-laminated timber (CLT) floor under different boundary conditions. Engineering Structures, 204, 110016.

[6] Kawrza, M., Furtmüller, T., Adam, C., Maderebner, R., 2021. Parameter identification for a point-supported cross-laminated timber slab based on experimental and numerical modal analysis. European Journal of Wood and Wood Products, 79(2), pp.317–333.

[7] Devin, A., Fanning, P.J., Pavic, A., 2015. Modelling effect of non-structural partitions on floor modal properties. Engineering Structures, 91, pp.58–69.

[8] Ussher, E., Arjomandi, K., Smith, I., 2022. Status of vibration serviceability design methods for lightweight timber floors. Journal of Building Engineering, 50, p.104111.

[9] Ussher, E., Aloisio, A., Pasca, D.P., Hansen, S.L., Tomasi, R., 2024. Effect of partition walls on the vibration serviceability of cross-laminated timber floors. Journal of Building Engineering, 95, p.110001.
[10] SFS-EN 1995-1-1. Annex 16 – National Annex to standard SFS EN 1995-1-1, SFS, Finland.

FINITE ELEMENT MODELING OF HISTORICAL ROOF STRUCTURES IN CONSIDERATION OF REDUCED JOINT STIFFNESSES AND PLASTIC BEHAVIOUR

Beatrix ZRUBKA[1] and Dezső HEGYI[2]

[1] Wood preservation specialist and structural engineer
[2] Department of Mechanics, Materials & Structures, Faculty of Architecture, Budapest University of Technology and Economics, Budapest, Hungary

ABSTRACT

When analysing existing roof structures, it is often found that the results of Finite Element Models (FEM) do not match real-world conditions. Failure does not invariably occur at the point predicted by calculations, and deformations can also differ significantly from the calculated values. The highly statically indeterminate historical roof structures have a significant load redistribution capacity, which is not sufficiently exploited in general engineering practice. In our study, we analysed the main truss of a queen-post-type roof of the St George's Catholic Church in Romhány, Hungary. We collected the information on the mechanical damage of the chosen main truss and aimed to achieve a load distribution that reflected the emphasised conditions. We made a nonlinear analysis taking into account the plastic behaviour of the joints, and by adjusting the stiffness of the joints and nonlinear properties, we could influence the internal force distribution of the computational model. This approach is capable of producing more realistic results for historical roof trusses than linear elastic analysis, with the connection stiffness determined by recent codes and literature.

KEYWORDS: historical roof structures, nonlinear calculation, plastic limit analysis, timber connection stiffness

INTRODUCTION

As brittle failure limits the strength of wood in tension and shear, the use of linear elastic models has become common in the analysis of wood structures. Besides this practice, some research has shown that plastic deformations follow the elastic limits under compressive stress before the failure [1]. This fact will not change the elastic analysis of the rod elements under compression, as the brittle failure in tension affects the buckling resistance. However, a growing number of studies demonstrate that plasticity can be taken into account when analysing connections with compression or with metal dowel-type connectors. Oudjene and Rasneur analysed the elasto-plastic behaviour of compressed connections [2], [3], Tanadini pointed out that the plasticity affects the structural behaviour [4], [5]. Branco and Palma, with their colleagues, worked on the plastic behaviour of carpentry joints [6], [7]. Lokaj and Miller have gained experience on the plasticity of dowel-type connections [8], [9].

This circumstance opens up the possibility of the redistribution of loads due to plastic behaviour in statically indeterminate structures.

The load-bearing capacity can be calculated by the Eurocode 5 standard [10]. However, according to our research for existing roofs, the connection stiffness calculated by the code or the component method [6], [11] can only be considered as an upper limit, which may not be reached in reality. Softer connections

and plastic limits should be used to get closer to the real structural behaviour of historical roofs. Our goal is to develop a methodology for determining more realistic properties of connections in historical timber roof frames.

METHODOLOGY

A 2D FEM model was built in a software capable of nonlinear plastic analysis (the AXISVM 7 was used) for the main frame. The proper survey of the roof was used for geometry [12] (Fig.1).

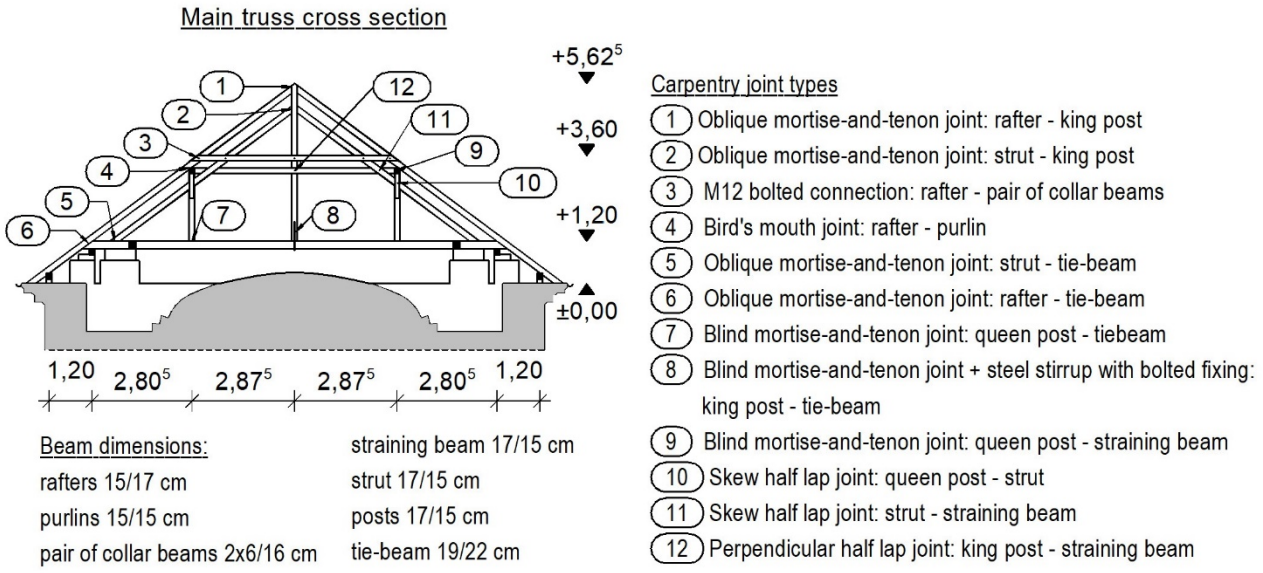

Figure 1. Dimensions of the main truss of the roof structure and numbering of the carpentry joints.

The load of the roof covering on the rafters was 0.21 kN/m^2, and the main frame was loaded with 3.94 kN vertical (downward) forces and 2.48 kN horizontal (inward) forces at the purlin points (a 3D model was used to express these values). The dead load of the roof frame was calculated at 410 kg/m^3.

In the initial model, we set the connections as perfect hinges with an axial stiffness of 10^{10} kN/m. A linear elastic analysis was run with this setup, but the results did not align with the onsite experiences in several contexts (for example, calculated and measured deflections or registered cracks and calculated stress peaks).

In the second phase, we calculated the stiffnesses of the bolted connections according to the Eurocode 5 [10]. The component method [6], [11] was used for the carpentry joints. The rotational stiffnesses were still free for all the connections [14]. The capacities of the connections were determined according to the Eurocode 5 to use it as the plastic limits of the connections (Tab. 1). We assumed that the connections would behave in a linearly elastic manner up to the yield point, and in an ideal plastic way thereafter, and we used a nonlinear calculation.

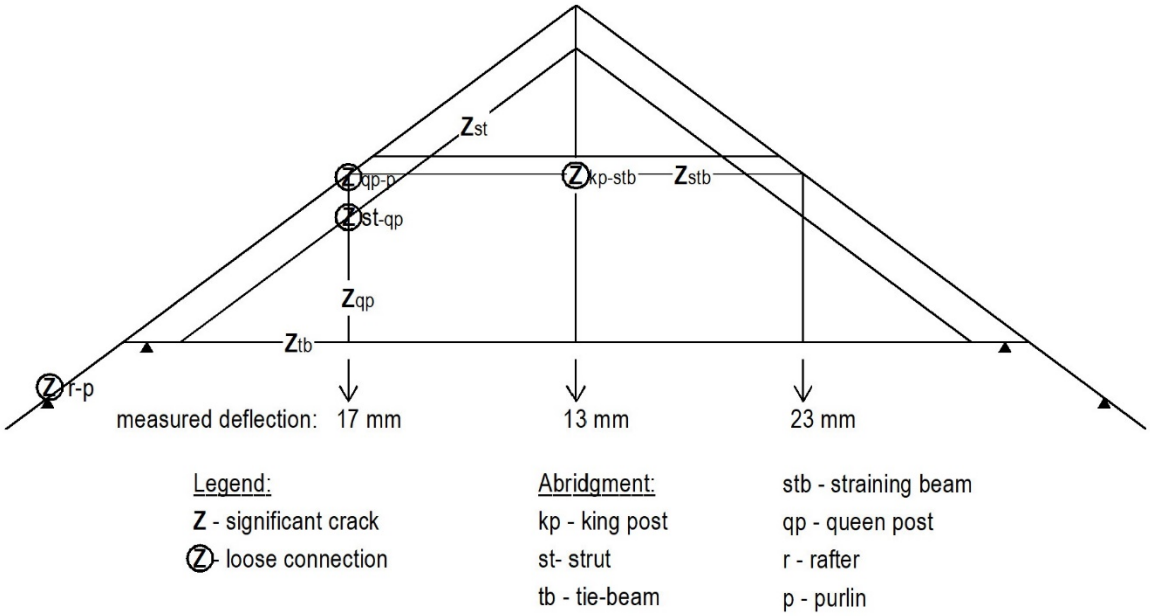

Figure 2. Damage map of the target main truss that was taken into consideration.

In the next phase, based on the onsite wood preservation observations [14] (Fig. 2), we intuitively adjusted the properties of the connections: the tension or compression limits were determined, and the stiffnesses were adjusted according to the gaps or the damage of the connections (Fig. 3-4).

Figure 3. Loose connection of the strut and queen post

Figure 4. Loose connection of the rafter and lower purlin

With these settings, we ran nonlinear calculations again. After the first analysis of this phase the results were reviewed and the model was corrected to avoid the forces and deformations that did not match reality: corrections were made on aspects such as the health condition of the rods, whether they allowed the calculated forces to be transmitted and weather they showed any signs of failure (crack or deformation). The settings were made one by one, and the results (stresses, utilizations and deformations) were continuously compared with the conditions on the site. The final setting is given in Table 1.

Table 1. Comparison of joint stiffnesses in the second and final phase

Joint Nr.	Axial stiffness of the connections in the second phase		Axial stiffness of the connections in the final phase		Load-bearing /plastic limit capacities of the connections in SLS		Load-bearing / plastic limit capacities of the connections in ULS	
	K_Y kN/m	K_Z kN/m	K_Y kN/m	K_Z kN/m	F_Y kN	F_Z kN	F_Y kN	F_Z kN
1	$125,5*10^3$	$51,5*10^3$	$125,5*10^3$	**132**	57	13	77	18
2	$132,8*10^3$	$58,4*10^3$	$132,8*10^3$	**$15,0*10^3$**	62	13	83	18
3	$5,8*10^3$	$5,8*10^3$	$5,8*10^3$	$5,8*10^3$	9		12	
4	$24,7*10^3$	$37,6*10^3$	**$24,7*10^2$**	$37,6*10^3$	14	19	19	26 **compres-sion only**
5	$85,7*10^3$	$90,6*10^3$	**$22,0*10^3$**	$90,6*10^3$	19	62	26	83
6	$507,1*10^3$	$21,4*10^3$	**$130,2*10^{-1}$**	$21,4*10^3$	120	14	0,5 **tension**	19
7	$24,2*10^3$	$54,0*10^3$	$24,2*10^3$	$54,0*10^3$	12	42	16	56
8	$24,2*10^3$	$22,3*10^3$	$24,2*10^3$	$22,3*10^3$	12	19	12	19 **tension**
9	$79,2*10^3$	$16,5*10^3$	$79,2*10^3$	**0**	42	9	56	12
10	$69,9*10^3$	$125,2*10^3$	$69,9*10^3$	**149**	35	37	47	50
11	$125,2*10^3$	$69,9*10^3$	**$148,9*10^3$**	$69,9*10^3$	37	35	50	47
12	10^{10}	10^{10}	-	-				

Legend: KY and KZ are the axial stiffnesses of the joints in horizontal and vertical directions; FY and FZ are the load-bearing or plastic limit capacity of the joints in horizontal and vertical directions.

RESULTS

Our goal was not to calculate the load-bearing capacity of the structure, but to demonstrate that the method we used was suitable for describing the on-site experiences of the structure. We chose symmetrical dead-load (SLS) (this load is on the structure for the lifetime), and dead-load + snow load combinations (ULS) (to demonstrate the higher usage of the elements according to the preliminary analysis) to present the results. In Figure 5, the comparison of the results of the initial linear and final nonlinear models can be seen under the (SLS) dead-load combination.

According to the onsite observations we expected: compression in the queen post-tie beam connection; compression or only small tension in the rafter-tie beam connection; big compression force in the (inner) struts and smaller in the (outer) rafters; bigger compression in the straining beam and smaller one or tension in the pair of collar beams (upper); 17mm deflection on the tie beam under the queen post.

Using the joint stiffnesses set by the code and the component method and linear elastic analysis (second phase), the results still did not meet the site conditions. With reduced stiffness in the linear elastic calculation, the internal force distribution of the structure was improved, but this was not yet sufficient to obtain the conditions recorded in situ. An important step in a more precise modelling was the inclusion of nonlinear properties (tension-only, compression-only) and plastic behaviour of the joints.

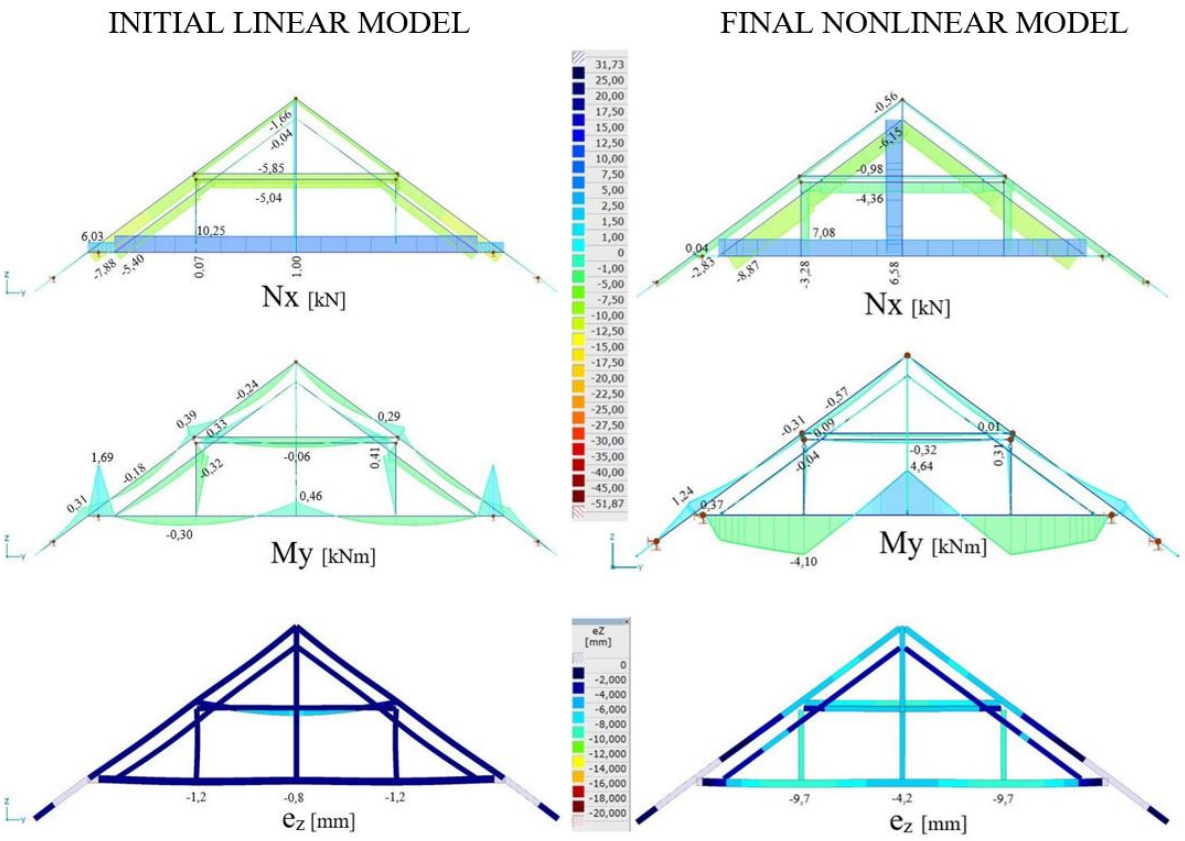

Figure 5. Comparison of the results of the initial and final model with the dead-load combination (SLS).

CONCLUSION

Despite the nonlinear calculation method and the plastic analysis being commonly used in the calculation of steel and reinforced concrete frames, it is not widespread in wood structures. There are only a few studies that take into consideration the plastic behaviour of the joints in the global structural modelling[15],[16]; however, plastic analysis leads to a more uniform stress distribution for statically indeterminate roof structures. Different stress peaks and sometimes higher load-bearing capacity can be achieved compared to the linear elastic calculations.

For existing roofs, this procedure offers a valuable opportunity to better describe structural behaviour and to identify the causes of damage.

Using this process intentionally and applying this knowledge in an informed way, interventions can be designed more effectively. Moreover, expensive and unnecessary reinforcements can be avoided. This is important both from a heritage preservation and an economic point of view.

REFERENCES

[1] Butterfield BG, Meylan BA, Peszlen IM: A fatest háromdimenziós szerkezezete, (Three dimensional structure of wood). Chapmann and Hall, London, UK. (1997)

[2] Oudjene M, Khelifa M: Elasto-plastic constitutive law for wood behaviour under compressive loadings. Construction and Building Materials 23.11 (2009) 3359-3366. https://doi.org/10.1016/j.conbuildmat.2009.06.034

[3] Rasneur, S., Zastavni, D., Misson, J. C., Jasienski J. P. 2024. On plastic development of timber structures based on 3D interactive vector-based graphic statics (VGS). Architectural Intelligence. 3, 10. http://dx.doi.org/10.1007/s44223-024-00054-3

[4] Tanadini, D., Schwartz, J., 2021. Analysis and design of timber-to-timber connections based on the lower bound theorem of the theory of plasticity. Santiago, Cile, World Conference of Timber Engineering (WCTE) 2020. https://doi.org/10.3929/ethz-b-000530140

[5] Tanadini, D. 2023. Limit analysis and timber plasticity. DSc thesis, ETH Zurich.

[6] Branco JM, Descamps T: Analysis and strengthening of carpentry joints. Construction and Building Materials 97 (2015) 34-47. https://doi.org/10.1016/j.conbuildmat.2015.05.089

[7] Palma P., Garcia H., Ferreira J., Appleton J., Cruz H. 2012. Behavior and repair of carpentry connections – Rotational behaviour of the rafter and tie beam connection in timber roof structures. Journal of Cultural Heritage, 13 (3): 64-73. http://dx.doi.org/10.1016/j.culher.2012.03.002

[8] Lokaj A., Dobes P., Sucharda O. 2020. Effects of loaded and distance and moisture content on the behavior of bolted connections in squared and round timber subjected to tension parallel to the grain. Materials 13 (23): 1-21. https://doi.org/10.3390/ma13235525

[9] Miller JF; Schmidt RJ, Bullei WM: New Yield Model for Wood Dowel Connections. Journal of Structural Engineering 136.10 (2010) https://doi.org/10.1061/(ASCE)ST.1943-541X.0000224

[10] Eurocode 5, EN 1995:2010, Design of timber structures (2010)

[11] Descamps T, Guerlement G: Component method for the assessment of the axial, shear and rotational stiffness of connections in old timber frames. Proc., 9ème Congrès National de Mécanique. Casablanca, Morocco (2009)

[12] Végh A.: Romhányi Szent György templom tetőszerkezetének felmérési terve (Survey plan of the roof structure of the St. George Church in Romhány, Hungary) Corvinterv Építőipari Tervező Bt. (2015) (in Hungarian)

[13] Kunecký J, Arciszewska-Kędzior A, Hasníková H: Mechanical performance of dovetail joint related to the global stiffness of timber roof structures. Materials and Structures 49.6 (2016) 1-13. https://doi.org/10.1617/s11527-015-0651-1

[14] Ugrinné Zrubka B: Faszerkezeti szakvélemény a romhányi Szent György templom tetőszerkezetéről (Timber structural inspection of the roof structure of the St. George Church in Romhány, Hungary) (2015). (In Hungarian)

[15] Hegyi D, Armuth M, Halmos B, Marotzy K: The effect of wind on historical timber towers analyzed by plastic limit analysis in the focus of a collapse. Engineering Failure Analysis 147 (2022) 105852. https://doi.org/10.1016/j.engfailanal.2021.105852

[16] Brühl F, Kuhlmann U, Jorissen A: Consideration of plasticity within the design of timber structures due to connection ductility, Engineering Structures 33 (2011) 3007-3017. https://doi.org/10.1016/j.engstruct.2011.08.013

BIODEGRADATION

BIM TOOL FOR MATERIAL OPTIMISATION BASED ON THE ONSET OF WOOD DECAY MODELING

Richard ACQUAH[1], Ana SANDAK[1], and Jakub SANDAK[1]

[1] InnoRenew CoE, UP IAM&UP FAMNIT, University of Primorska, Titov trg 4, 6000 Koper, Slovenia.

ABSTRACT

As the use of wood in construction grows due to its environmental and structural benefits, ensuring the durability of timber elements under diverse environmental exposures has become critical. This study presents a novel extension of a previously developed BIM-integrated service life estimation tool, introducing an automated material and treatment recommendation module designed to enhance timber durability during the design phase. Developed within Autodesk Revit and aligned with ISO 15686-4 guidelines, the plugin's underlying algorithm combines environmental inputs such as wind-driven rain, local climate, sheltering, and proximity to the ground with wood species properties, treatment types, and detailing conditions to generate element-specific service life duration predictions, focused on the onset of decay. A key innovation introduced in this study is a new algorithm that automatically recommends alternative wood species or treatment methods. These recommendations are context-sensitive, taking into account the availability of wood species and treatment options across different European countries to ensure practical and regionally relevant solutions. This integrated framework bridges the gap between analysis and design, providing architects and engineers with a BIM-integrated, data-driven decision support tool to optimise material selection and improve lifecycle performance.

KEYWORDS: Wood decay modelling, Material optimisation, Service life prediction, Timber durability, Building Information Modelling (BIM).

INTRODUCTION

Timber is a sustainable construction material valued for its low environmental impact, its potential for carbon sequestration, and its design flexibility. However, its durability remains a challenge, especially under varying environmental exposures and detailing conditions. Building Information Modelling (BIM) has emerged as a tool for integrating performance assessments into design workflows. In the WoodLCC project, Acquah et al. (2025) developed a BIM-based framework utilising a Revit plugin to estimate the service life of wood elements in accordance with ISO 15686-4. While effective for prediction, it lacked automated support for material optimisation when durability was insufficient. This study introduces a new module that recommends alternative wood species or treatments for the estimated service life duration. These suggestions are context-aware, taking into account species availability and performance across European regions. By integrating this functionality, the tool supports early-stage, data-driven decisions that improve durability and resource efficiency in timber construction.

METHODOLOGY

This study builds upon a previously developed BIM-integrated framework for predicting the service life of wood construction elements (Acquah et al., 2025). The existing model estimates the time until the onset of fungal decay using a dose-response approach compliant with ISO 15686-4. The core prediction

algorithm is defined by the relationship presented in Equation 2, as derived from extensive experimental research (Meyer-Veltrup et al., 2018; Niklewski et al., 2021):

$$SL \geq \frac{D_{Rd}}{D_{Ed}} \quad (1)$$

where:

SL = Service Life (years), the expected duration before the onset of decay.
D_{Rd}= Resistance Dose (days), quantifying the wood's inherent or enhanced capability to resist degradation due to its natural durability or protective treatments.
D_{Ed}= Exposure Dose (days/year), representing the annual cumulative impact of environmental factors that accelerate the degradation process.

The plugin, implemented in Autodesk Revit (via C#), embeds this model into the BIM environment using custom IFC property sets and element-level parameters. The plugin calculates and stores service life duration values for each wood component, utilising both pre-calculated climate data and project-specific inputs, such as overhang depth, ground clearance, and grain orientation, as shown in Figure 1. The novel contribution of this study is the integration of an automated material and treatment recommendation module that allows users to analyse alternative wood species and treatment options that can be used to improve the performance of the wood structure. The material and treatment algorithm are presented together with the user interface in Figure 1.

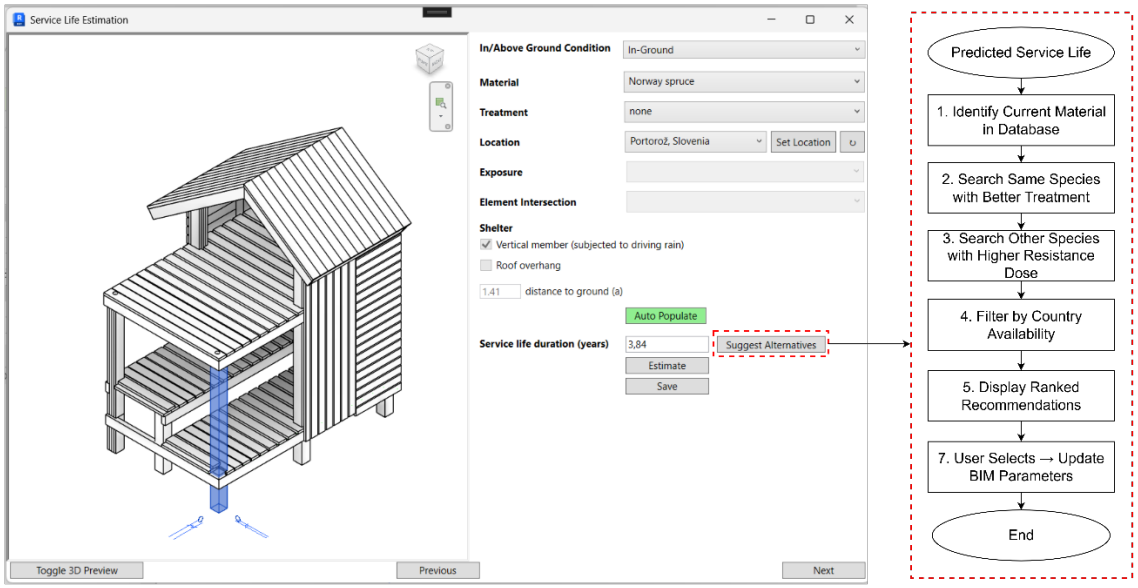

Figure 59. Integrated Revit Interface and Algorithmic Workflow for Service Life-Based Material Optimisation

This recommendation logic is visualised in Figure 1, which outlines the decision flow from detection of low service life to user-driven selection of alternatives. The methodology was validated using the same sensor-instrumented timber playhouse as in the original study by Acquah et al. (2025), demonstrating the successful application of substitution recommendations for high-risk elements. The new module enables early-stage design interventions by translating durability assessments into actionable material guidance directly within BIM workflows.

RESULTS

The extended plugin was tested using the same timber playground structure from the previous study (Acquah et al., 2025). The automated recommendation module was activated for elements with low predicted service life and successfully provided alternative wood species and treatment options with

improved durability outcomes. The system correctly prioritised regionally available materials and treatments, ranking them based on recalculated service life. Figure 2 shows an example output from the test model, where the tool generated multiple wood species and treatment alternatives for the wood element with an initially short service life. While environmental exposure monitoring of the playground structure is still ongoing, the plugin's predictions offer an early indication of high-risk components and feasible design adjustments.

CONCLUSION

This study enhances a previously developed BIM-based service life prediction tool by integrating an automated material and treatment recommendation module. The new functionality enables early-stage decision-making by suggesting context-specific alternatives when the predicted service life of timber elements is insufficient. By combining exposure-driven durability modelling with regionally relevant material data, the extended plugin bridges the gap between performance assessment and actionable design guidance.

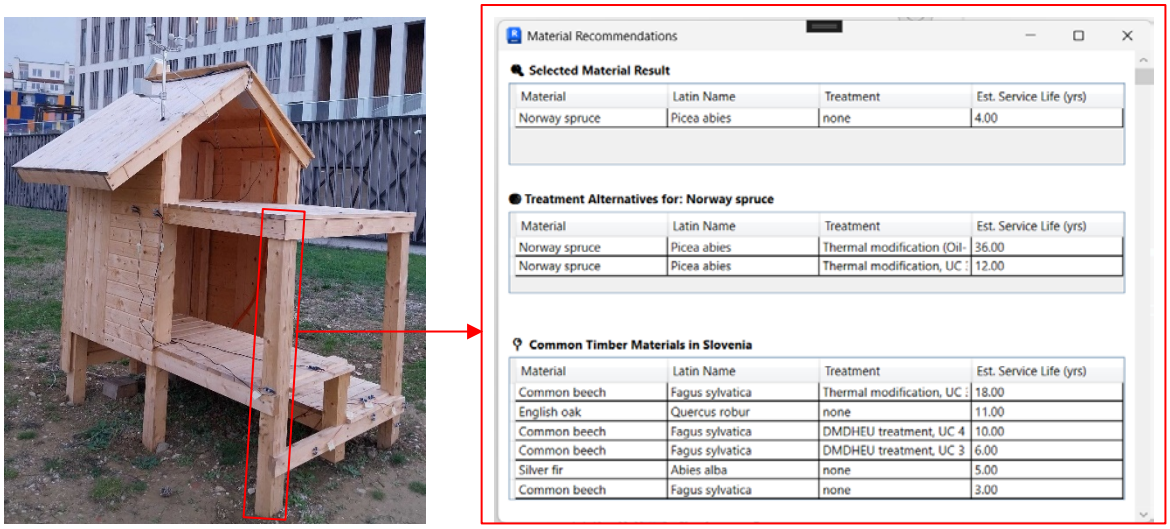

Figure 60. Example material recommendation results for an in-ground element in the playground structure

ACKNOWLEDGMENTS

The authors acknowledge the Slovenian Research and Innovation Agency for funding the infrastructural programme IO-0035 and the research programme WoDu. Authors also acknowledge the ForestValue Research Programme and the Republic of Slovenia's Ministry of Education, Science and Sport for financing the research project WoodLCC. Financial support for the conference was received from COST Action HELEN, CA20139, supported by COST (European Cooperation in Science and Technology).

REFERENCES

[1] Acquah, R., Sandak, A., Sandak, J., *RevitWoodLCC Plugin*. Zenodo, 2025. https://doi.org/10.5281/zenodo.14966455

[2] Meyer-Veltrup, L., Brischke, C., Niklewski, J., & Frühwald Hansson, E. (2018). Design and performance prediction of timber bridges based on a factorisation approach. Wood Material Science & Engineering, 13(3), 167–173. https://doi.org/10.1080/17480272.2018.1424729

[3] Niklewski, J., van Niekerk, P. B., Brischke, C., & Frühwald Hansson, E. (2021). Evaluation of Moisture and Decay Models for a New Design Framework for Decay Prediction of Wood. Forests, 12(6), 721. https://doi.org/10.3390/f12060721

A STUDY OF A SPACE-SAVING AND LOW-COST METHOD FOR PROMOTING WOOD DECAY FOR STRUCTURAL PERFORMANCE EXPERIMENTS

Yuki OTA[1] and Hiroki ISHIYAMA[2]

[1] Osaka Metropolitan University, Graduate school student, Division of Urban Engineering

[2] Osaka Metropolitan University, Graduate School of Urban Engineering

ABSTRACT

In order to develop experimental studies on the structural performance of wooden buildings during deterioration, it is necessary to promote decay in wood specimens in a space-saving and low-cost manner. Therefore, this study proposes a wood decay promotion method using silica sand and peptone. This method uses a solution of silica sand (to retain moisture) and peptone (to provide nitrogen), and expects the solution to provide the moisture and nitrogen necessary for the rot fungus to degrade the wood. The results showed that the peptone method was as effective in promoting decay as the conventional method, even though the frequency of water supply was reduced. The wood decayed the most when the peptone solution concentration was 0.5%. Furthermore, it is thought that more mycelia could be attached to the test specimens by placing them in sawdust in which the fungus was cultured, rather than by placing the PDA medium in which the fungus was cultured on the test specimens. However, future issues include the large variation in the degree of decay and the instability of mycelial attachment by the sawdust method.

KEYWORDS: fungi, decay, timber, peptone

INTRODUCTION

In Japan, a law promoting the use of wood has been enforced, and it is expected that the number of medium- and large-scale wooden buildings will increase in the future. To use them safely and in the long term, refining the method for estimating structural performance during deterioration is an urgent issue. There have been studies on the structural performance of decayed wood[1),2)] and on the structural performance of nail joints when wood is decayed or when both nail and wood have deteriorated[3)]. In addition, a formula was proposed to predict the structural performance of nail joints when both nails and wood deteriorate[4)]. However, no experiments have been conducted on plywood load-bearing walls when both wood and nails have deteriorated, and the consistency of the prediction equations has not been confirmed. The reason for this is that the currently adopted method of promoting the decay of wood specimens is time-consuming and costly, so that partial experiments can be performed, but full-scale experiments cannot. Therefore, to develop experimental research on the structural performance of deteriorated wooden buildings, a crucial problem to be addressed in the future is how to accelerate the decay of full-size specimens in a space-saving and low-cost manner. Therefore, in this study, a method for promoting the decay of wood using silica sand and peptone (hereinafter referred to as “the peptone method”) is proposed as an improved method of the decay source unit method, which is a conventional method. Then, the degree of decay of wood by the peptone method is quantitatively evaluated.

RESEARCH OF THE PAST

In a previous study, the decay source unit method was compared with a method using sawdust as an improvement on the decay promotion method. The following is an overview of each method and the results of decay experiments. The decay source unit involves filling a polypropylene container with agar medium containing nutrients and culturing a decay fungus (*Fomitopsis palustris*) on it as a decay source unit, which is placed in contact with the area to be decayed (Fig. 1). Previous studies[3)] have demonstrated that this method can reliably decay wood. However, a large static area and numerous containers are required to decay large specimens, as the decay source unit must be continuously installed in the decay area. In other words, it is possible to decay small specimens, but not full-size specimens.

Figure 1. The decay source unit

The sawdust method involves spreading a medium made from a mixture of sawdust, fusuma, and water on a fungus bed bag to culture the decay fungus, with wood placed on or inside the medium (Figs 2 and 3). This method utilises relatively inexpensive materials, such as sawdust and fusuma, and only requires leaving it standing on top of the doubling, allowing decay-promoting operations to be carried out in a small area and with fewer containers.

Figure 2. Placing the fungus in the growth medium.

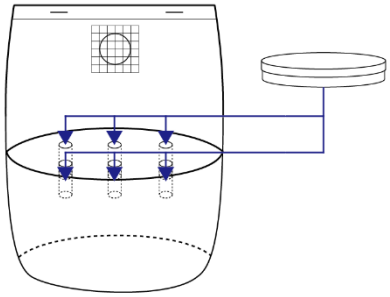

Figure 3. Install wood.

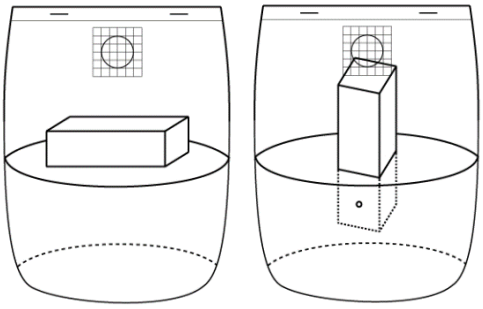

The results of quantifying the degree of decay of wood specimens after 8 weeks of accelerated decay using the decay source unit and sawdust methods are shown in Fig. 4. The depth of pilodyn was used to quantify the extent of wood decay. In the sawdust method, the fungus became so active that it overflowed the sterile bag, but the wood hardly decayed at all. This may be because sawdust and fusuma are easier for wood-decomposing fungi to decompose than wood.

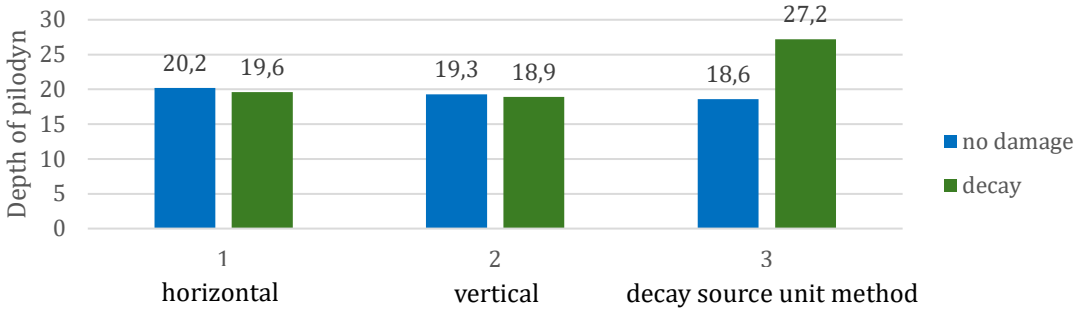

Figure 4. Comparison of the degree of decay between the sawdust method and the decay source unit method

As an improvement method, the use of silica sand (to retain moisture) and peptone (to provide nitrogen) solutions was proposed to provide the moisture and nitrogen necessary for the decay fungi to deteriorate the wood. More specifically, the concentration of the peptone solution is used as a parameter to determine when decay is most accelerated. This experiment aims to establish a method for reducing the location, cost, and container size of the specimen.

Table 1. Advantages and disadvantages of each decay promotion method

	Space	Cost	Container	Degree of decay
Setting up the medium	×	×	×	○
The sawdust method	○	○	○	×
The peptone method	○	○	○	○ (expectations)

EXPERIMENTAL METHOD

Outline of test specimen

Table 2 shows the list of specimens, and Fig. 5a shows the specimen shapes and dimensions.

Table 2. Specimen name and test content (including peptone aqueous solution concentration)

Group name	Evaluate content	a	b	c	d
0.5	Peptone solution concentration 0.5%	0.5-a	0.5-b	0.5-c	0.5-d
1	Peptone solution concentration 1%	1-a	1-b	1-c	1-d
2	Peptone solution concentration 2%	2-a	2-b	2-c	2-d
s-0.5	The sawdust method and peptone solution concentration 0.5%	s-0.5-a	s-0.5-b		
s-1	The sawdust method and peptone solution concentration 1%	s-1-a	s-1-b		
s-2	The sawdust method and peptone solution concentration 2%	s-2-a	s-2-b		
m1	Medium as it is installed 1	m1-a	m1-b	m1-c	m1-d
m2	Medium as it is installed 2	m2-a	m2-b	m2-c	m2-d
d	dry weight wood	d-a	d-b	d-c	d-d

Cedar (30 specimens in total) was used for the test specimens, and *Fomitopsis palustris*, which decay rapidly, were used for the decay manipulation. 4 specimens for total dry weight (group name: d) were

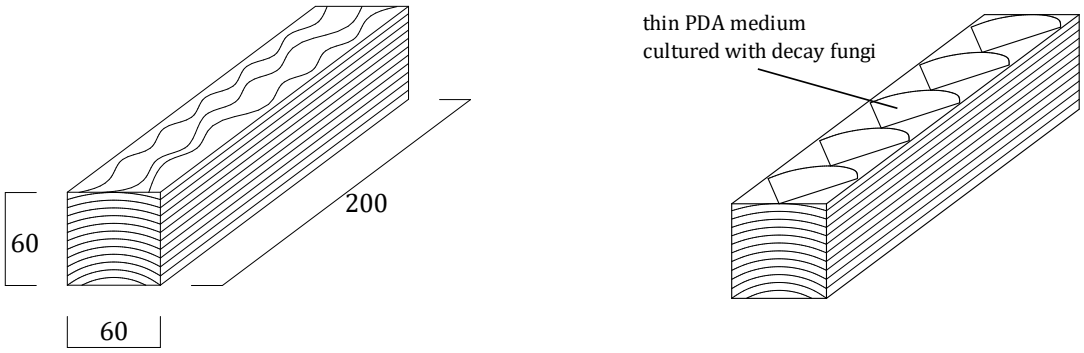

Figure 5. a) Specimen shapes and dimensions; b) 20 test specimens (groups: 0.5, 1, 2, m1, m2) were placed in a thin PDA medium cultured with decay fungi

weighed after being placed in a thermostatic incubator at 105°C for 24 hours, after measuring the air-dried weight. Twenty test specimens (group name: 0.5, 1, 2, m1, m2) were placed in a thin PDA medium cultured with decay fungi and left in a high humid environment at approximately 35°C for 2 weeks to allow mycelia to cover the specimens (Fig.5b)). In addition, six test specimens (group name: s-0.5, s-1, s-2) were placed in mycelium bags cultured with decay fungi by the sawdust method and kept in an environment of approximately 35°C for two weeks to allow the mycelium to cling to the specimens. The specimens (group names: 0.5, 1, 2, s-0.5, s-1, s-2, m1, m2) were then placed on silica sand containing peptone solution for 5 weeks (Fig.6). Peptone solution concentrations were 0.5%, 1%, and 2% based on 2% of the peptone concentration of the PDA medium.

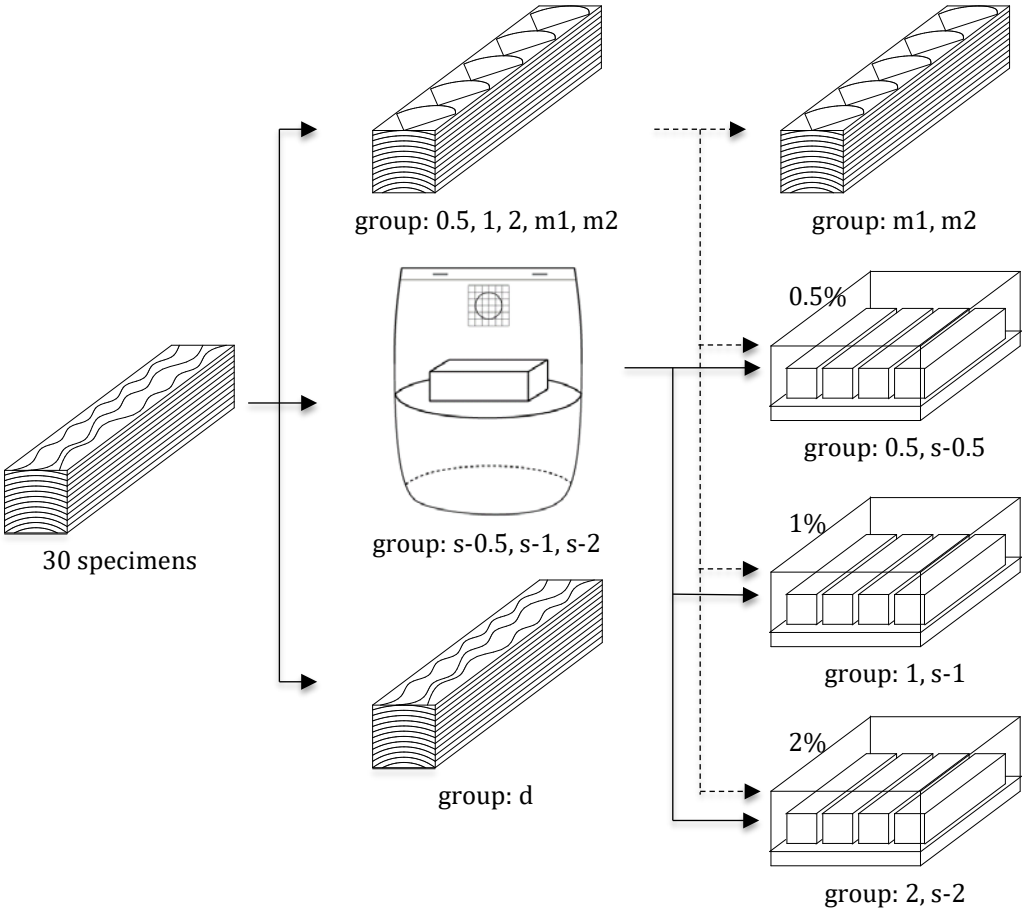

Figure 6. Test flow

Amount of peptone solution

According to AWPA[5], the optimum water saturation of a fungus cellar is 50-80%, so the silica sand is assumed to be the same, and the water saturation of silica sand was calculated. First, the maximum water retention of silica sand was measured to calculate water saturation. Filter paper was placed in a Buchner funnel, silica sand was placed in the funnel, and the silica sand was allowed to water for 24 hours. Next, after suction filtration for 15 minutes, the volume of silica sand after water supply (w_l) was measured. It was then dried at 105°C for 24 hours, and the total dry weight (w_0) was measured. From the above, the maximum water retention of the silica sand (H) was calculated from the following equation (1).

$$H\ [\%] = \frac{w_l - w_0}{w_0} \times 100 \quad (1)$$

Next, the degree of water saturation was calculated from the following equation (2). However, M [%] is the moisture content of silica sand.

$$degree\ of\ water\ saturation\ [\%] = \frac{M}{H} \times 100 \quad (2)$$

In addition, an attempt was made to use a gardening moisture meter to determine water saturation at any time and immediately. The relationship between water saturation and the moisture meter scale in water and peptone solutions of various concentrations is shown in Fig. 7. From Fig. 7, the peptone solution was to be fed when the water saturation was below 50%, i.e., when the moisture meter scale was below 2.3, 3.7, and 4.2 for the peptone solution concentrations of 0.5%, 1%, and 2%, respectively. As a result, the watering frequency of the peptone solution was about once a week, and the watering frequency of the fungus installation method was about once every two days in a 28°C environment.

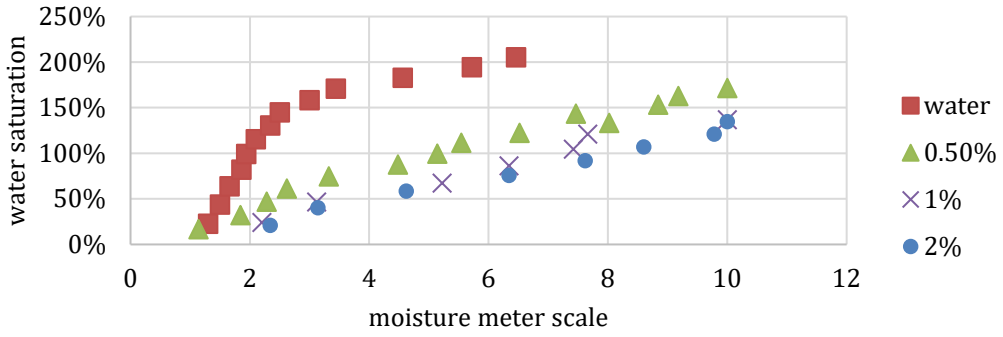

Figure 7. The relationship between water saturation and the moisture meter scale

Measurement items and deterioration diagnostic equipment

The air-dry weight of the specimens before accelerated deterioration, as well as the air-dry and total dry weights of the wood, were measured. Using these results, the total dry weight of each specimen was estimated before accelerated deterioration. Additionally, a pilodyn was used as a degradation diagnostic tool. Measurements were taken three times each at three locations, 50 mm, 100 mm, and 150 mm from the edge of the specimen, and the average value was recorded (Fig.8).

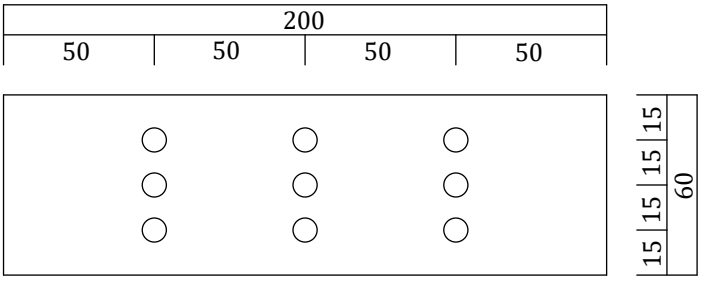

Figure 8. Pilodyn penetration depth measurement point

By comparing these results, the validity of the peptone method was verified, and the optimal peptone solution concentration was revealed.

RESULTS

The results for pilodyn penetration depth are shown in Fig. 9. From Fig. 9, it was confirmed that the peptone method was as effective as the medium installation method in promoting decay. However, it should be noted that in this study, no significant decay occurred due to the short decay acceleration period of 5 weeks, and there was no significant difference in the depth of the pilodyn penetration.

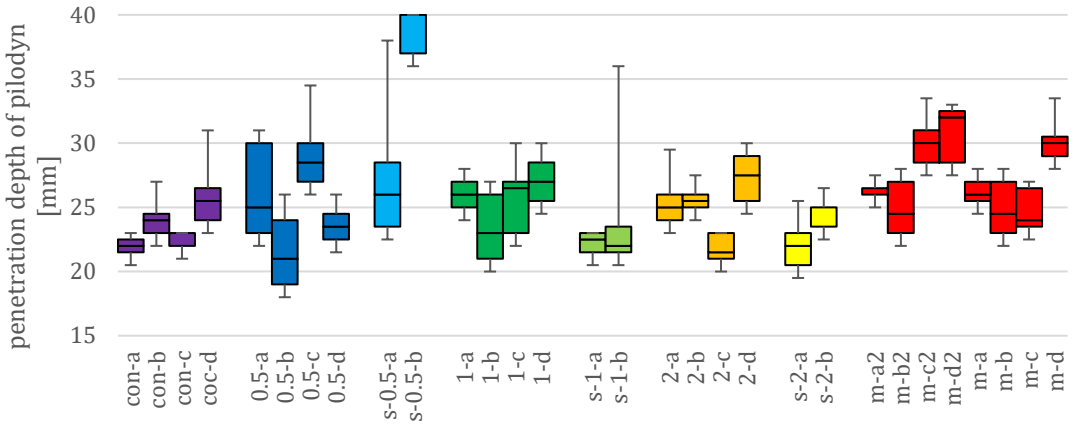

Figure 9. Pilodyn penetration depth

Fig. 10 also shows the relationship between the concentration of peptone solution and the depth of pilodyn penetration. Fig. 10 shows that the lower the peptone solution concentration, the greater the pilodyn penetration depth. However, when significance difference tests were conducted for groups 0.5 and 1, and 0.5 and 2, respectively, the P values were both 0.453, which is greater than the dominance level of 0.05 and not significantly different. In the case of 0.5% and 1% peptone solution concentrations, the sawdust method tended to have a greater pilodyn penetration depth than the fungus placement method when attaching the fungus to the test specimens. However, when significance difference tests were conducted for groups 0.5 and s-0.5 and 1 and s-1, respectively, the P values were 0.125 and 0.083, which were not significantly different. On the other hand, in the case of 2% peptone solution concentration, the depth of pilodyn penetration tended to be smaller when the sawdust method was used to attach the fungus to the specimens than when the fungus placement method was used, and significant differences were also observed between groups 2 and s-2 (P=0.008).

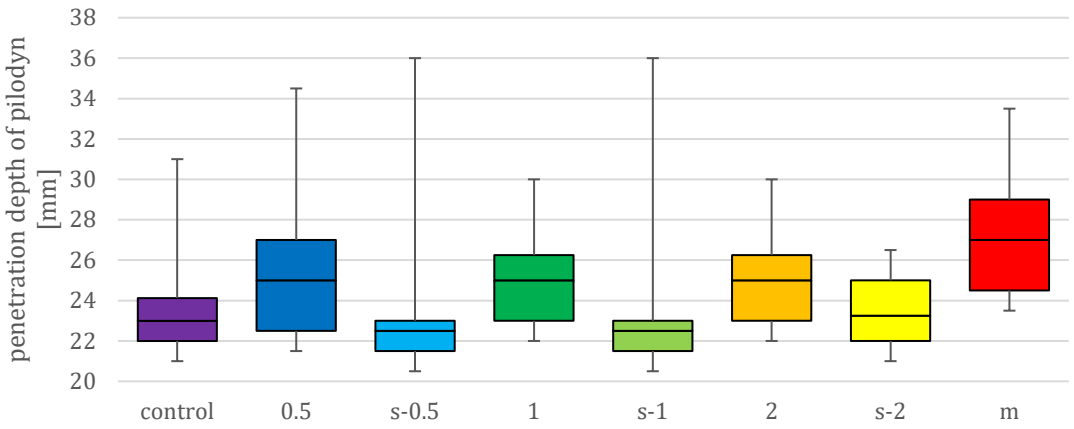

Figure 10. Relationship between the concentration of peptone solution and the depth of pilodyn penetration

Next, the results of the weight loss rate are shown in Fig. 11. From Fig. 11, the weight of the specimens decay-accelerated by the peptone method may increase, and there was no correlation between the concentration of peptone solution and the degree of deterioration. However, the rate of weight loss tended to decrease as the peptone solution concentration increased.

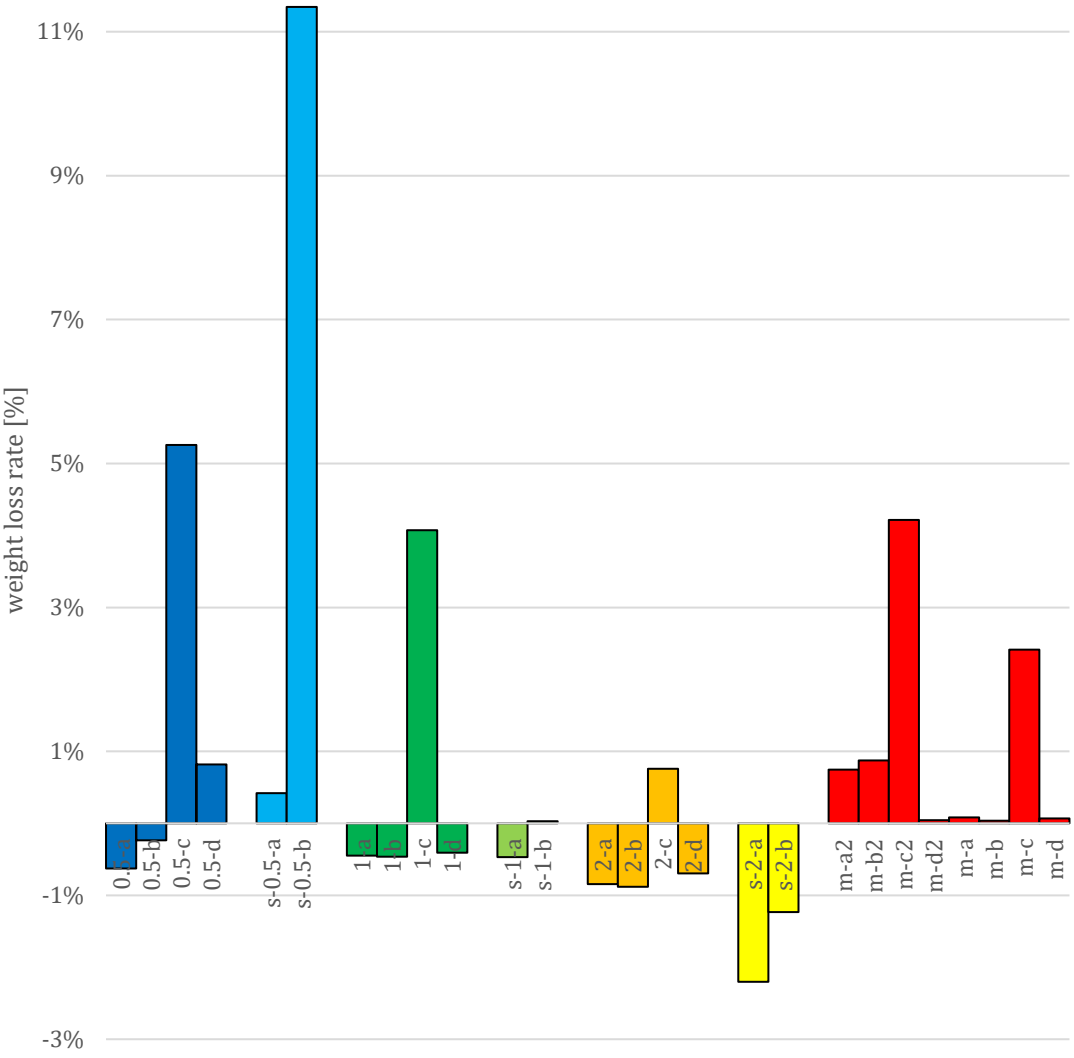

Figure 11. Weight loss rate

DISCUSSION

The osmotic pressure of the peptone solution on the wood is thought to be a factor that causes the wood to decay at lower concentrations of peptone solution. The lower the concentration of the peptone solution, the lower the osmotic pressure, and the higher the moisture content of the wood, the more active the wood-decomposing fungi. The variation in the depth of the pilodyn penetration was probably due to the difficulty of spreading the peptone solution uniformly over the silica sand, and the wood in contact with the silica sand that contained more peptone solution was more susceptible to decay. In addition, the smaller the peptone solution concentration, the smaller the amount of peptone that accumulates in the silica sand, and thus the error caused by the application of the peptone solution is considered to be greater. Due to these factors, it is believed that the lower the aqueous peptone solution, the greater the variation in pilodyn penetration depth, and therefore, no significant difference was determined. The reason the sawdust method tends to decay more than the fungus installation method

at 0.5% and 1% peptone solution concentrations is likely that the sawdust method allows fungi to grow faster and attach more to the specimens than the fungus installation method. However, the sawdust method is less stable in the placement of the fungi, as the sawdust method showed greater variation in the depth of the pilodyn than the fungi placement method, and the sawdust method showed less wood decay than the fungi placement method at a peptone solution concentration of 2%. The reason for this may be that the appropriate amount of moisture for the sawdust medium has not been clarified, and the growth of the fungi varies greatly depending on the variation in the amount of moisture. It should be noted, however, that the number of data points is small: 36 points for the four bodies, at 9 locations for the fungus installation method, and 18 points for the two bodies, at 9 locations for the sawdust method.

CONCLUSION

The following findings were obtained in this study:
(1) The peptone method is effective in wood decay promotion operations. Therefore, this method is likely to promote wood decay in a space-saving and low-cost manner.
(2) The smaller the concentration of peptone solution, the greater the depth of penetration is likely to be.
(3) When the mycelium is applied to the specimen, the sawdust method tends to attach more mycelium and promote wood decay more easily than the mycelium placement method.
Future issues include the development of a method for uniformly spreading peptone solution on silica sand and the clarification of the appropriate moisture content for the sawdust method.

ACKNOWLEDGEMENTS

The authors would like to thank all those who contributed to this study. In addition, this research was funded by a research grant from the public interest foundation PHOENIX.

REFERENCES

[1] Shogo NUMIMIZU, Yuji NOGUCHI, Risa TENKUMO, Takuro Mori, Kei TANAKA, Yushiyuki YANASE, Mitsunori MORI, Yasunobu NODA, Hiroshi KURISAKI, Tsuyoshi YOSHIMURA, Kohei KOMATSU, Masafumi INOUE (2011): Study on Surviving Strength Properties of Japanese Softwood with Biodeterioration Part.2 Compressive Strength Properties of Timbers with Biodeterioration, AIJ Kyushu chapter architectural research meeting, Vol.50, pp.713-716.

[2] Shogo NUMIMIZU, Kotaro KAWANO, Yuji NOGUCHI, Takuro MORI, Yoshiyuki YANASE, Kei TANAKA, Mitshunori MORI, Yasunobu NODA, Hiroshi KURISAKI, Tsuyoshi YOSHIMURA, Kohei KOMATSU, Masafumi INOUE (2012): Study on Surviving Strength Properties of Japanese Softwood with Biodeterioration Part.3 Bending and Compressive Strength Properties of Wood Damaged by Biodeterioration, AIJ Kyushu chapter architectural research meeting, Vol.51, pp.629-632.

[3] Ayaka IWAUCHI, Hiroki ISHIYAMA, Yasunobu NODA, Takuro Mori (2015): Structural performance of nailed joint with decay of wood and rust of nail, Summaries of technical papers of annual meeting, pp.99-100.

[4] Yuki OTA, Toru TOKUONO, Yuichiro NISHINO, Shigefumi OKAMOTO, Hiroki ISHIYAMA (2022): Study on the structural performance of wooden houses with the rusted nail and the decayed wood, Summaries of technical papers of annual meeting, pp.187-188.

[5] American wood-preservers' association standard (2000) E14-94, Standard method of evaluating wood preservatives in a soil bed.

BIOLOGICAL DEGRADATION IN HISTORIC TIMBER STRUCTURES: APPEARANCE, EXTENT, RELEVANCE AND SANATION

Hrvoje TURKULIN[1] and Marin HASAN[1]

[1] University of Zagreb, Faculty of Forestry and Wood Technology

ABSTRACT

Biological damage is one of the most destructive effects on historic wood structures (aside from fire, earthquakes, and structural collapse). It is commonly observed in varying degrees and intensities after only a few decades, and is virtually inevitable after centuries. Wood-destroying insects and fungi colonise wood in uninhabited areas (such as roofs or under-floors), but the extent of the damage depends on complex interactions among structural and environmental factors. Chief among these are the inherent durability of wood species, microclimatic conditions (especially air circulation), presence of liquid water (such as roof leaks), condensation at thermal bridges, or hygroscopic moisture absorption in cold, damp climates or where timber contacts masonry. Precise identification of infestation type and severity is only one aspect of assessing wood condition. Choosing appropriate remedial measures is another crucial factor. A wood technology expert with expertise in wood pathology must recommend to the structural engineer, investor, and carpenter the most effective intervention strategies for comprehensive remediation.
The paper presents our experience gained from more than thirty buildings in Croatia, assessed following the 2020 earthquakes. The paper outlines the most common forms of biological damage and proposes measures for the complete restoration of timber, ensuring the future longevity of the structures.

KEYWORDS: biological degradation, historic timber structures, identification, sanation

INTRODUCTION

BIODEGRADATION OF WOOD

Wood, as a natural material, serves as a sustenance source for various wood-destroying organisms, including bacteria, fungi, insects, and marine borers. Sapwood, pith, and juvenile wood (the area near the pith) are particularly rich in starch and accessible nutrients, making them highly vulnerable to attack by wood-decaying fungi, which preferentially degrade these tissues. Sapwood is also especially prone to insect infestation. In contrast, heartwood accumulates secondary metabolites, including tannins, resins, and other extractives, which possess fungicidal and insecticidal properties, providing natural defence against biodegradation. These compounds variably inhibit the growth of decaying fungi and restrict insect attack.
Certain xylophagous insect species specialise in attacking either sapwood alone or all wood types without distinguishing between heartwood and sapwood. Some insect species preferentially target either hardwoods or softwoods, while others, as well as wood-rotting fungi, are generally unselective regarding wood species and can cause extensive degradation in both types. Many xylophagous insect species that infest wood in service prefer the presence of fungal mycelium, which accelerates wood destruction when combined with fungal activity.

For wood to be susceptible to degradation by fungi or insects, certain conditions must be met: ample nutrient availability, the presence of oxygen in the wood, and specific temperature and moisture ranges suitable for organism activity.
For insect activity, the temperature range necessary for successful wood infestation and degradation is typically between 4 and approximately 45°C, with the wood's moisture content (MC) ranging from 10.5 to 65%. Fungi, in contrast, require a minimum moisture content of 20% in wood (except for dry rot fungi, which can survive and decay wood at lower moisture levels) and generally favour a temperature range of 5°C to 38°C. These environmental parameters are essential for the enzymatic breakdown of lignin, cellulose, and hemicellulose in the wood. Altering the temperature or moisture content substantially slows biological degradation [1], [5], [6], [7], [8], [11], [12], [13].

NATURAL (BIOLOGICAL) RESISTANCE OF WOOD

Due to its chemical composition, the durability of wood against biodegradation differs notably between species. Some, such as Quercus spp. (Oak), Robinia pseudoacacia L. (Black locust), Larix spp. (Larch), and Pinus sylvestris L. (Scots pine), exhibit higher resistance to biological decay due to specific heartwood extractives. In contrast, species like Populus spp. (Poplar), Salix spp. (Willow), and Fagus spp. (Beech) are much more susceptible to biodegradation because they contain fewer protective compounds.
The European Standard EN 350 [15] categorises wood into five durability classes based on its ability to withstand fungal and insect damage, with a specific focus on the durability of heartwood. Sapwood, regardless of species, is universally regarded as the most vulnerable portion due to its abundance of nutrients and absence of protective extractives.

CONDITIONS FOR DEVELOPMENT OF BIOLOGICAL DEGRADATION IN TIMBER STRUCTURES

Insects generally pose a smaller risk to timber structures, although the temperature and wood moisture ranges conducive to their infestation and growth are broader than those for fungi. Furthermore, the optimal conditions for insects overlap considerably with typical human comfort ranges. Only a few insect species dominate in structures in Croatia, mainly Common woodborers or beetles (Anobiidae), such as Anobium punctatum De Geer; House longhorn beetle (Hylotrupes bajulus Lin.); Powder-post beetle (Lyctus brunneus Stephens); and, on rare occasions in hardwoods, Deathwatch beetle (Xestobium rufovillosum de Geer). Regardless of how minor xylophagous insect attacks may be, they routinely permit moisture and water ingress through exit holes, which facilitates subsequent interactions between insects and wood-rotting fungi.
Fungal decay was consistently observed, as every historic structure contains zones where conditions favouring decay persist for several months or longer. The most common sites are wall plates (partially embedded in brick or plaster), corners with poor ventilation, and especially wood embedded in brickwork (such as ends of tie-beams and floor beams), where hygroscopic moisture and possible capillary action can cause wood moisture content (MC) to exceed the critical threshold of about 20%, even without roof leaks. Fungi were rarely detected on truss elements in the roof space, likely due to effective ventilation, regular summer temperatures exceeding 30–40°C, and rapid wood drying. However, the degree and rate of decay depend on numerous variables in the structure's history (type of roofing, leakage, available ventilation, accumulation of bird and bat excrement, water traps, gaps in joints, regular inspections and maintenance, etc.). All major types of fungal species were identified during inspections, including wet rot fungi (white rot and brown rot) and dry rot.

METHODOLOGY

Several methods were used to assess the health of wood. Table 1 details the step-by-step sequence for identifying biological damage, particularly when it is subtle or limited. Identifying specific fungi (such as through DNA analysis) was not undertaken, as this is not a required procedure according to EN 17121 (2019) [1]. The standard only necessitates recording the direct cause of biological damage (fungal decay, rot, or insect infestation). However, efforts were made to classify the type of fungus or insect more precisely, as this can guide the selection of curative measures for the structural engineer. Fungal presence was consistently associated with measurements of wood moisture content (using an electro-resistance moisture meter) and its depth gradient, surface temperatures of the wood and wall (measured with an infrared thermometer), as well as temperature and relative humidity readings taken by wired probes (around the member and within the wall bed). This enabled conclusions regarding the progression of the infestation (inactive and dormant in dry wood, or ongoing in moist wood with MC > (20) 22%). Insects were identified by evaluating the size and colour of exit holes, as well as the shape, colour, and texture of frass, when available. Detailed characterisation of damage type and severity was conducted using resistance drilling on-site (Resistance Drill IML 500) or on extracted cores (Ø 12 mm) in the laboratory, with macro-photography and optical reflectance microscopy. Occasionally, wood was checked for hidden infestation using small core drill tips, with fungal growth assessed in the lab (Petri dishes with nutrient agar at 25 °C for three weeks). The resulting fungal cultures could then be identified with greater accuracy.

Table 1. Sequences of different levels and tools for the evaluation of biological damage

Action	Damage confirmed	Decision
1. Visual inspection and examination by acoustic emission by tapping with a 250 g hard-plastic mallet (evidently present decay and/or dull sound):	- if yes, then:	Noted and photographed
	-if not, then:	Rejected, or:
2. Resistance drilling check:	- if yes, then:	Noted and demonstrated (resistogram)
	-if not, then:	Rejected, or:
3. Check on the Ø 12 mm drill cores	- if yes, then:	Noted, macro-photographed and additionally:
4. Microscopy or microbiological check		Final decision

RESULTS

The results section presents one example for each of the defined levels of health and degradation of the wooden beams (examined positions).

HEALTHY WOOD – SURFACE AGEING

Wherever the wood showed no insect exit holes or surface decay, the resistogram marked areas of sound structure. To validate the results, a Ø 12 mm core drill was extracted, polished, and examined microscopically at almost every measurement location (Fig. 1). The core was then refitted, polished, and photographed. Below the photo of the core, the resistogram was matched to evaluate the integrity of the wood at that site (top and centre images in Fig. 1). Micrographs of the core at two magnifications confirmed the healthy structure of the wood, with no evidence of decay (bottom two images in Fig. 1).

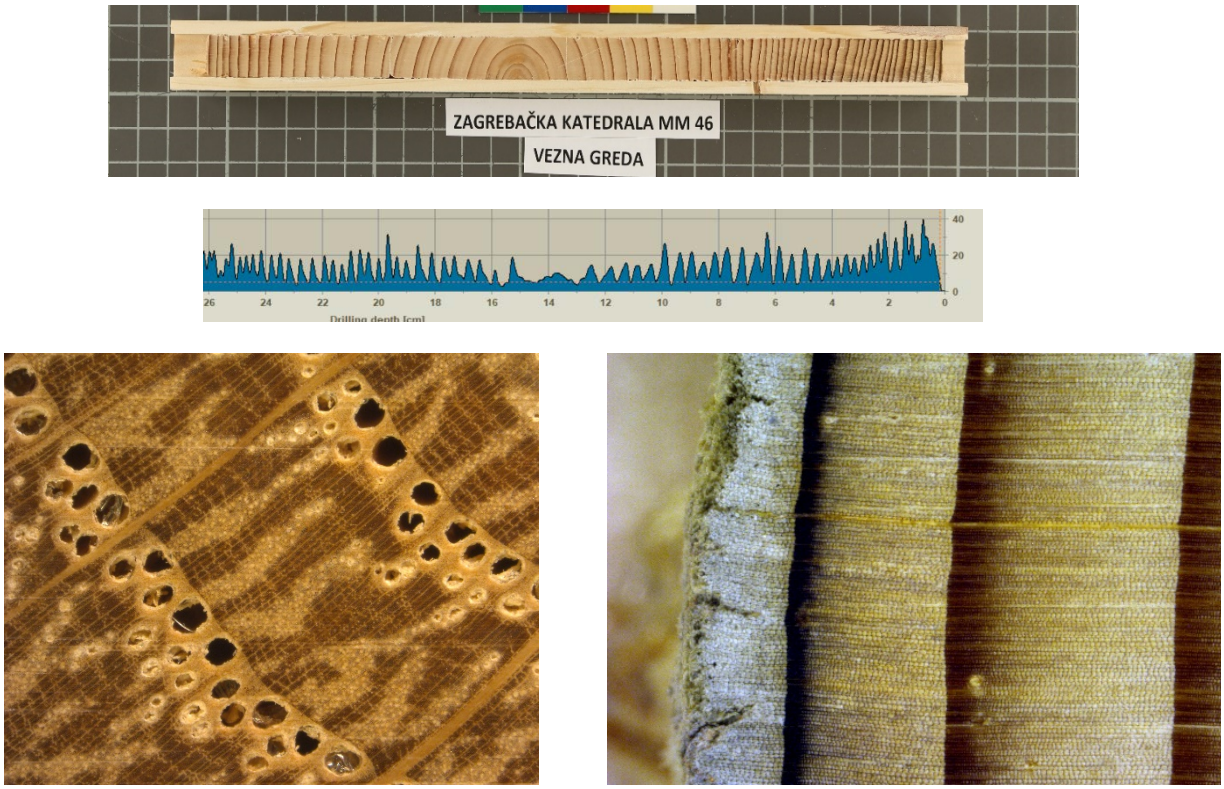

Figure 1. Top centre: fitted and polished core drill Ø 12 mm; Middle centre: belonging Resistogram of the visibly determined as sound element of the structure; Bottom left: sound and healthy oak-wood cross-section, with some tyloses in the vessels. Bottom right: Spruce surface damaged by ageing and mould down to the first latewood band. The effective cross-section of ½ cm was deemed unaffected.

INACTIVE, NOT SIGNIFICANT DAMAGE

Damage along the beam edges is visible only at scattered exit holes. Beam edges contain sapwood, which is heavily infested by the house longhorn beetle Hylotrupes bajulus (elliptical larval tunnels, approximately 3×5–7 mm, filled with coarse yellow frass). Circular larval tunnels of 1.0–1.5 mm, filled with white powdery frass, indicate infestation by Anobidae. The moisture content was below 16%, so such damage can be ignored, provided the wood remains dry and the roof is well-ventilated. Often, softwood beams were more severely damaged than oak beams; however, insect damage was mainly limited to the sapwood. In large-section elements, infestations may be ignored unless there is an ongoing risk of increased moisture (Fig. 2).

Figure 2. Left: half of the top surface of the beam was slightly planed to clean the dust and dirt. Damage can be seen only from sporadic exit holes, and only in sapwood-containing edges of the beam. Top right: polished cross-section of the edge of the beam containing a large amount of sapwood and larval tunnels. Bottom right: enlarged larval tunnel filled with coarse excrement.

INACTIVE, SIGNIFICANT DAMAGE

Frequent issues arise from the insertion of wood beams into walls (Fig. 3). When the beam is tightly embedded, lacking insulation or ventilation, complete deterioration develops after only 100-140 years, even in the absence of water ingress. Condensation in cold wall cavities elevates wood moisture, leading to a synergistic attack by insects and fungi that destroys the wood at its support. The sketch illustrates that inserts should be secure, insulated from moisture—at a minimum from below—and ventilated by alternating bricks, leaving gaps at the end grain and sides for summer drying (Fig. 3).

An example of fungal degradation, undetectable from the exterior, may persist deep within the element. The polished core drill of the tie-beam reveals microscopic evidence of previous infections (Fig. 4). At this location, a measured moisture content of less than 16% indicates dormant activity. The cross-section must be significantly reduced, since a 10% mass loss from fungal decay may lead to a 50–80% strength loss ([9], [14]).

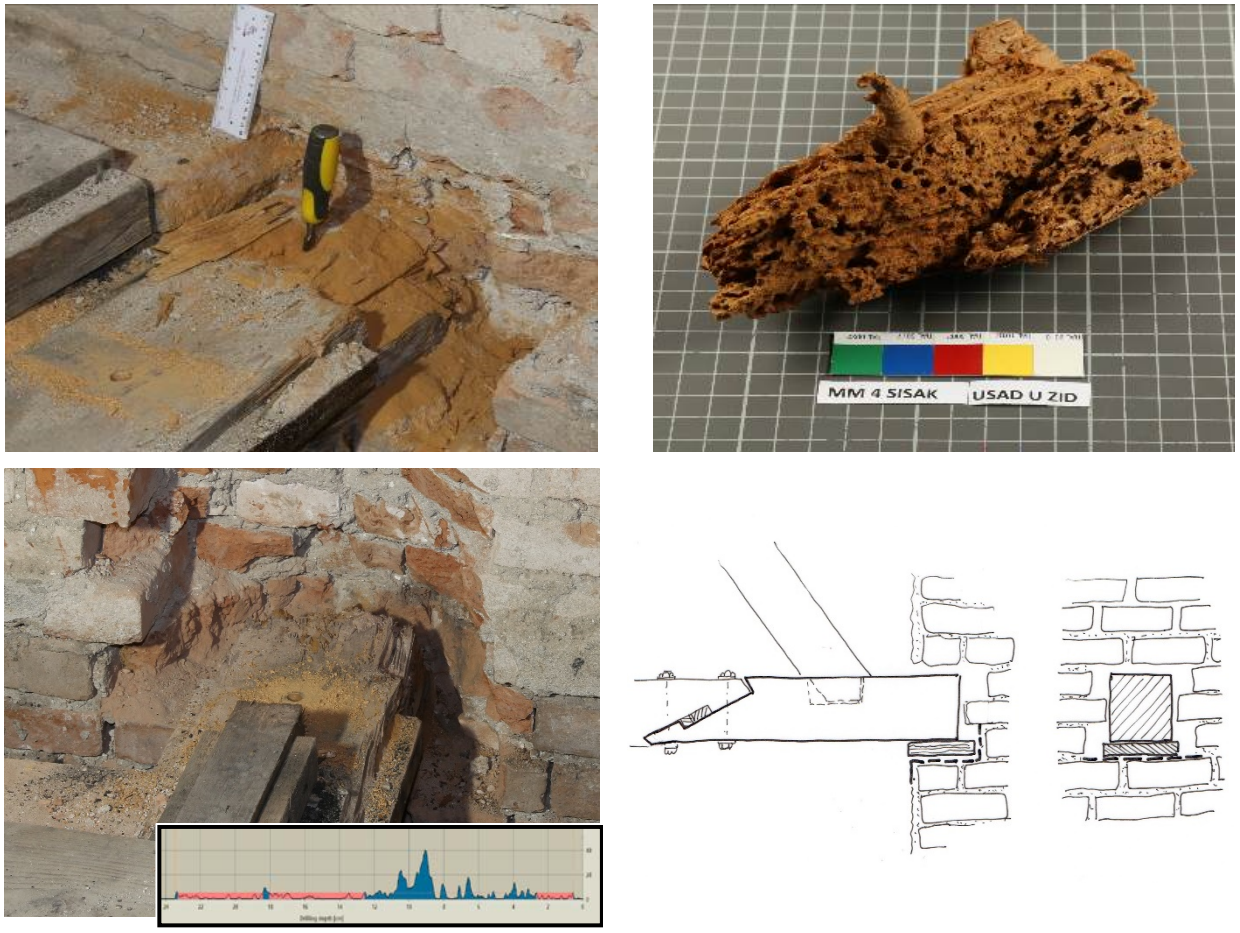

Figure 3. Regular problems with the wood beam inserts in the wall. Photographs: whenever the beam is built in tightly, with no insulation or ventilation, total damage occurs. The sketch represents the optimal firm insert of the beam into the wall, insulated from moisture at least from below, and ventilated by alternate shifting of bricks at the end grain and the sides.

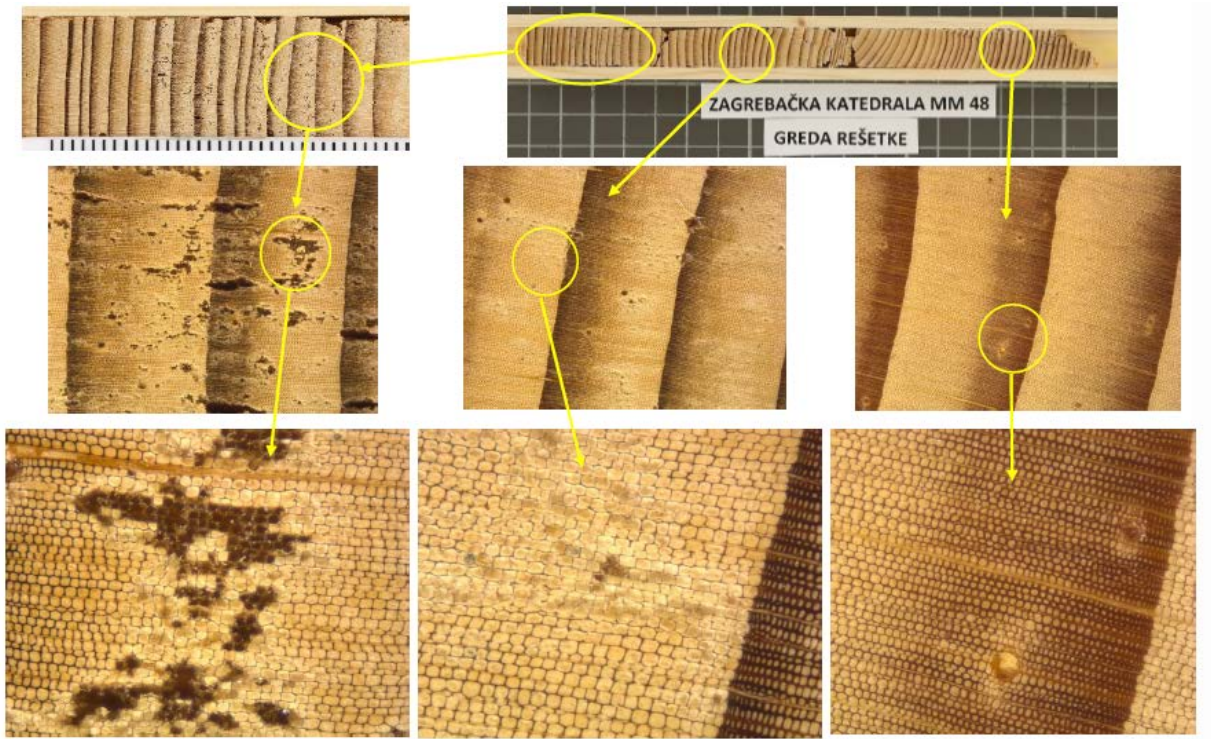

Figure 4. Polished core drill of the tie-beam, with microscopic evidence of earlier spread infection not seen from the outside.

An example of a tie beam, hewn from a small-diameter log, is presented. Consequently, a substantial portion of the upper surface and corners comprises sapwood. The upper section is almost entirely decayed, while the remaining 4 cm exhibits extensive insect damage and staining from bird droppings. The proposed reduction in cross-section (1 cm on both sides due to hewing inaccuracy and surface loss, and 9 cm from above) leaves only 53% of the original effective cross-section intact (Fig. 5).

Figure 5. The tie beam was hewn from a small-diameter log; consequently, the large portion of the upper surface and corners contained sapwood, which was completely eaten by insects, leaving only 53% of the effective cross-section.

ACTIVE, HEAVY DAMAGE

Damage to the support structure of the Zagreb Cathedral's central nave truss (1888) is classified as substantial and ongoing. The truss components (principal rafter, rafters, sprocket, and tie beam) consist of softwoods (SW, top left and right images, Fig. 6). Carpenters understood the risk of wood-brick contact and strategically used oak wood (OW) corbels to mitigate this risk. Visual inspection outside the wall reveals no deterioration. However, resistogram results (bottom left image, Fig. 6) show decay in the softwood, not the oak. Additional analysis was conducted. After partial brick removal (view from below, bottom right image, Fig. 6), extensive decay was evident on many corbels and wall plates. With a moisture content of 72% (middle left image, Fig. 6), the infection is deemed severe and active. These elements are recommended for replacement.

Microscopic analysis clearly demonstrates intact oak-wood structure on the outer portion of the beam's wall insert (left images at 40× and 140× magnification, tyloses visible in vessels, Fig. 7) and pronounced deterioration within the part embedded in the wall (right images at 40× and 140× magnification, Fig. 7). Microbiological testing on nutrient agar plates (bottom left image, Fig. 7) revealed robust growth of rot mycelium at the centre (SRED) and surface (POV) of the beam, with mould mycelia overtaking the rot, spreading over nearly the entire medium. This active mycelial growth confirms the ongoing vitality of rot fungi, while secondary moulds flourish, consuming residual sugars generated during cellulose decomposition.

Figure 6. Severe damage to the support of the truss of the central nave of the Zagreb Cathedral (1888), with still ongoing decay activity.

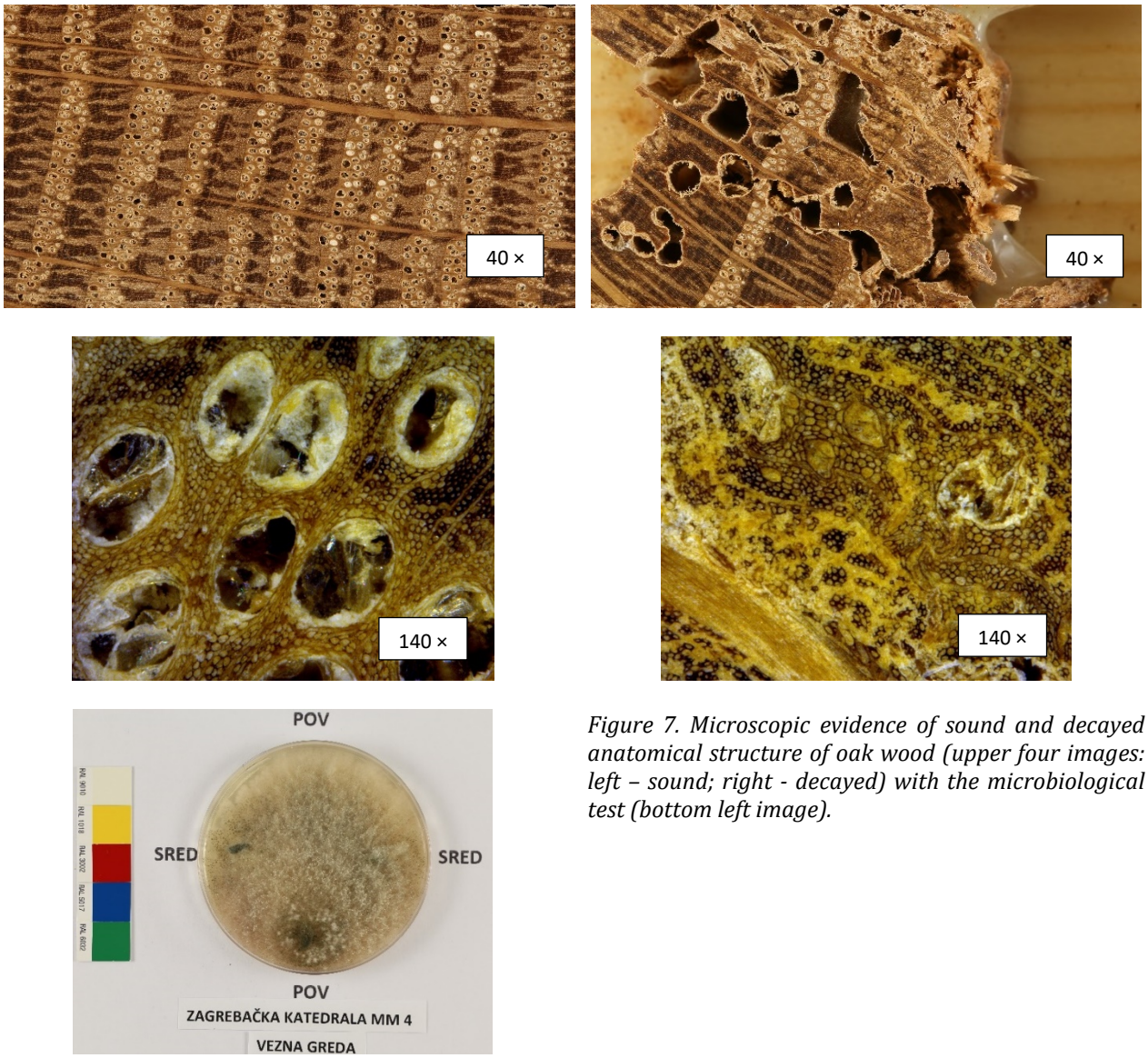

Figure 7. Microscopic evidence of sound and decayed anatomical structure of oak wood (upper four images: left – sound; right - decayed) with the microbiological test (bottom left image).

Another case demonstrating severe decay of the beam's insert in the wall is shown in Figure 8 and is examined here. Circular larval tunnels, measuring 2–4 mm in diameter (top right and middle left images, Fig. 8), and reddish-brown powdery frass (middle right image) indicate a heavy infestation, most likely by Xestobium rufovillosum, possibly occurring alongside fungal activity. A small sample of wood tissue from the inner part of the beam insert was placed on nutrient agar plates in Petri dishes. Uniformly colored rot fungal mycelium developed around this wood sample (left side of the Petri dish, marked "u ležaju"), confirming active fungal decay inside the beam insert. A second wood tissue sample was taken from the surface of the beam insert (right side of the Petri dish, also marked "u ležaju", Fig. 8). A third sample was collected from the outer part of the beam, situated outside but near the wall (upper part of the Petri dish, marked "van ležaja", Fig. 8). The appearance of multicolored mycelium around the two surface samples indicates both rot and mold fungi growth on the beam's exterior (bottom left image, Fig. 8). This pattern suggests that rot fungi originated inside the wall and have subsequently spread to the beam's outer regions. On the beam's surface, mildew is expected due to surface grime and dust. The insect infestation appears to have facilitated the spread of rot fungus within the beam.

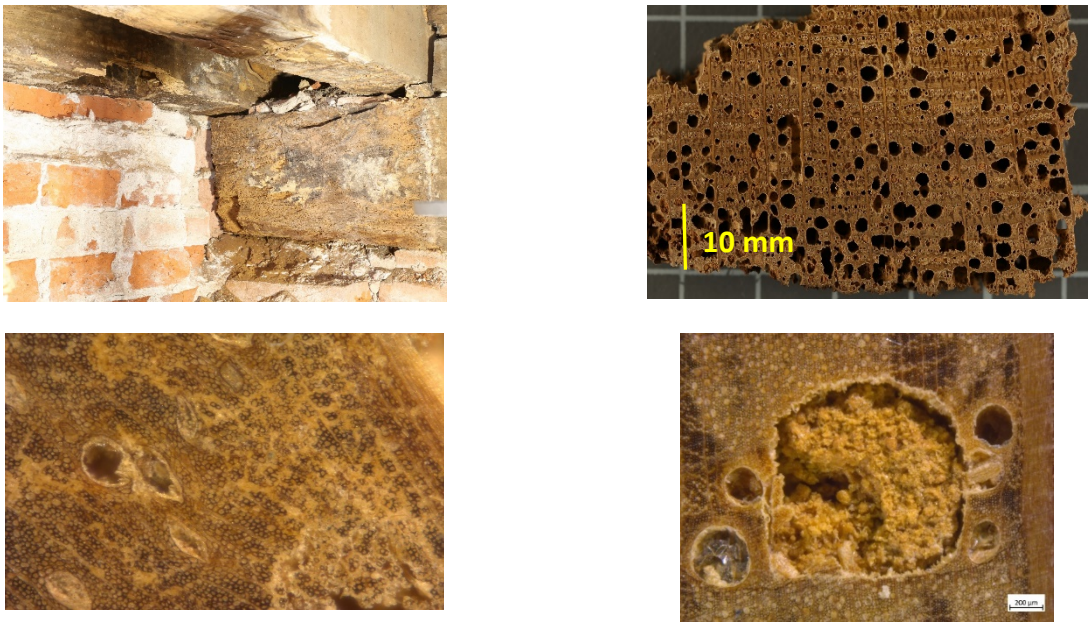

Figure 8. Confirmation of the finding of synergy of the lignicolous fungi and xylophagous insects in the critical zone of wooden beam insert into the wall: top left image – view to the beam insert in the wall; top right and both midle images – proof of insect attack; bottom lef image – developed different micelia over the nutrient medium plates in the Petri dish.

Catastrophic wet-rot damage (white fruiting body likely Rhodonia placenta (Fr.) Niemelä) developed beneath the leaking roof window. The fungus stains the surface brown, reddish-brown to dark brown, but leaves it apparently undamaged (top image in Fig. 9). This brown-rot fungus is notorious for causing internal wood decay. At the same time, the exterior remains visually intact or only slightly deteriorated, and it partially degrades lignin [16], [17], [18]. The micrographs (both bottom images in Fig. 9) corroborate the literature, showing that infection spreads via wood rays inward, destroying holocellulose and lignin in the inner earlywood layers. A detailed analysis of the bottom right image in Figure 9 reveals that the decayed wood tissue surrounding the cracks is darker brown than the adjacent tissue, likely due to a higher lignin concentration in these degraded areas (Fig. 9). Immediate remediation is required: repair the leak and replace the entire rafter.

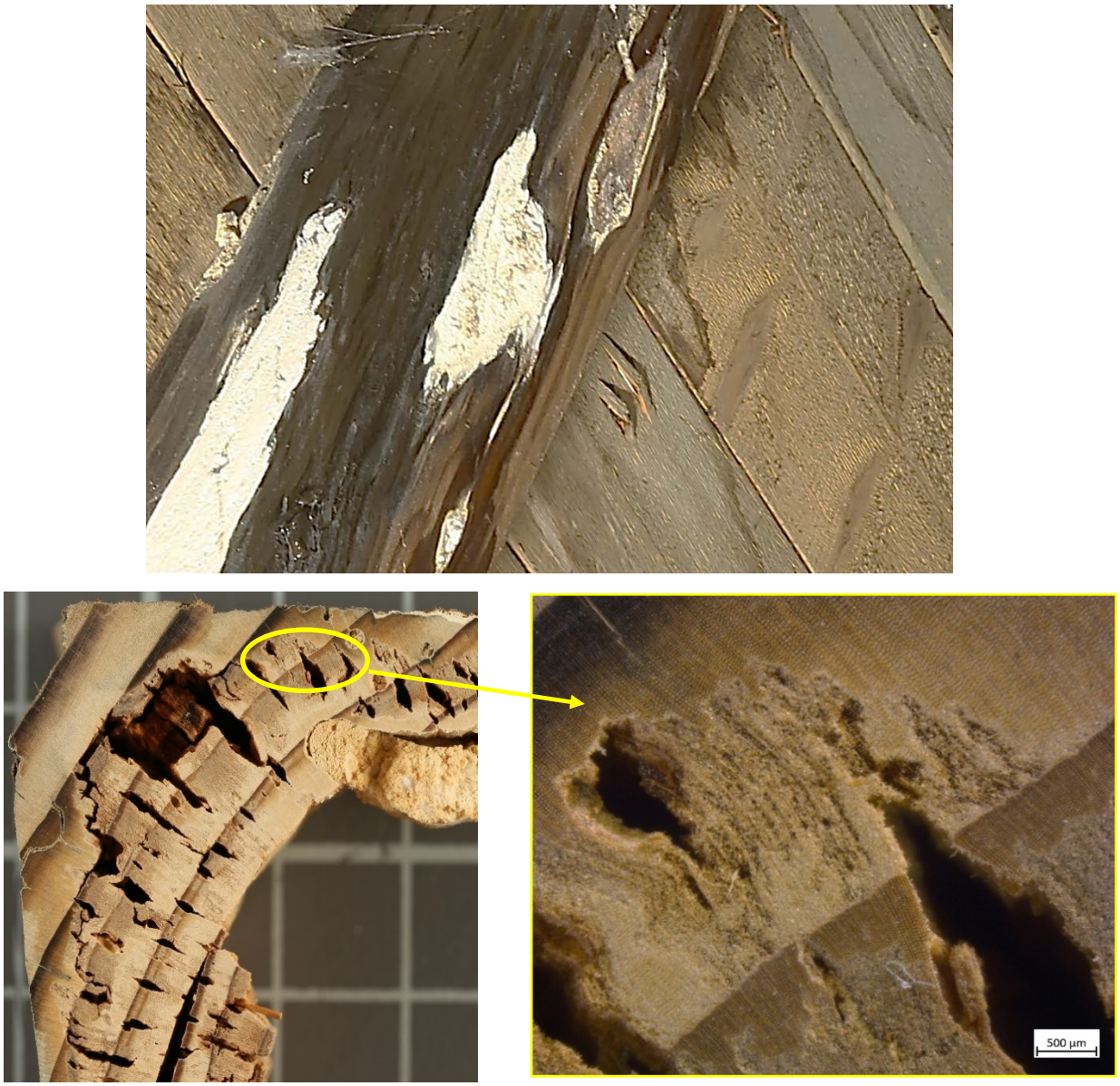

Figure 9. Catastrophic damage by wet-brown-rot: top-centre image – white fruiting body indicates most probably Rhodonia placenta (under the leaking roof window); bottom images – micrographs at different magnifications of decayed wood tissue in close to surface zone with lots of cracks.

DISCUSSION

It is important to determine the extent and intensity of biological damage, particularly for two reasons: firstly, this enables better-founded decisions about proposed curative measures. Secondly, in many cases, no biocidal treatment was applied; instead, the affected area was excised and substituted with a prosthesis.

Although many curative methods are available, it is generally opted to remove and replace infected and decayed tissue. Fumigation, heat treatment of the whole structure, or deep incision treatment with biocides are methods that are avoided because they can be highly demanding from an organisational, time-consuming, and cost perspective, yet still leave the formerly attacked wood mechanically weakened. Therefore, we generally opted for replacement of damaged wood with prostheses, improvements in hydro- and thermal insulation, and assurance of proper ventilation. The standard EN

17121 indicates that the insect attack on the surfaces of large cross-section elements can be ignored. However, whenever the wane is included in the cross section, and consequently the significant volume of sapwood is present in the elements, we discarded the infested part of the element and accordingly reduced the effective cross section. Generally, most insect damage was limited to sapwood. However, in cases involving insects that attack heartwood (e.g., Xestobium rufivillosum), the results align with the findings of Cruz and Machado [10], who concluded that even under extensive insect destruction throughout the cross-section, strength is diminished, but the remaining density still governs strength grading. If the timber is now dry and the infestation inactive, we recommend lowering the strength class for structural assessment.

Different actions were taken to combat the fungal attack. If even small cavities were found throughout the cross-section due to fungus, we recommended curative treatment or replacement for severe cases. Research [9] has shown that as little as 10% mass loss due to fungi can severely impair mechanical properties, including static bending by 70%, compression parallel to the grain by 45%, tension parallel to the grain by 60%, and shear by up to 20% [9]. Another study [14] showed that only 6% mass loss in birchwood led to a 59% decrease in impact bending strength. Although these results apply only to the studied species (pine and birch) and tests, they are alarming enough to warrant caution. Figure 9 demonstrates that damage may not be visible externally, and percussion may not detect decay; yet, microscopic inspection reveals perforations in nearly half of the cross-section. In such cases, intensive biocidal treatment with incisions or complete removal of the element was proposed.

In other cases, replacement was recommended as the most reliable option to prevent future fungal growth and the spread of spores. The challenge is determining how much of the remaining sound part should be removed beyond the evidently decayed section. Conservation principles stress that as much original material and texture as possible should be preserved. The general rule is to remove the decayed wood plus 1 m from the limit of visible decay (DIN 68800-4, [2]). However, splicing a prosthesis or adding timber splints can pose structural issues if the cut is far from the support. Commentary to DIN 68800-4 [3] thus recommends removing a minimum of 30 cm of sound wood, except in cases of dry rot (Serpula lacrymans), where 1 meter remains the standard. Removing 50 cm of unaffected wood beyond the decayed or infected zone is considered a safe compromise. Elements with extensive decay were recommended for complete replacement.

CONCLUSION

The inspection and assessment of biological degradation are essential steps in evaluating the integrity of timber structures. Virtually all historic structures exhibit some level of biological deterioration after 60-100 years, as wood was not kiln-sterilised and persistent moisture enabled insect and fungal colonisation, especially in poorly ventilated roof cavities and where timber is embedded in masonry. Utilising durable species such as oak enhances resilience, but only if the wood's moisture content remains below 20%. Nevertheless, roof areas in contact with masonry and lacking adequate drying during warm seasons retain moisture due to capillary absorption, condensation, or hygroscopic dampness in and near cold walls. Remedial measures may involve biocide application or resin consolidation of decayed wood; however, the preferred approach is the complete replacement of affected sections with prostheses or timber splints.

REFERENCES

[1] EN 17121 (2019): Conservation of cultural heritage – Historic timber structures – Guidelines for the on-line assessment of load-bearing structures. CEN, 28 pp.

[2] DIN 68800-4 (2020): Holzschutz - Teil 4: Bekämpfungsmaßnahmen gegen Holz zerstörende Pilze und Insekten und Sanierungsmaßnahmen (Wood preservation - Part 4: Curative treatment of wood destroying fungi and insects and refurbishment).

[3] Beuth-Kommentare: Holzschutz –baulich-chemisch-bekämpfend. Erläuterungen zu DIN 68800-2, -3, -4. Berlin: DIN Deutsches Institut für Normung e.V.; DGfH Deutsche Gesellschaft für Holzforschung e.V.

[4] Erler, K. (2004): Alte Holz-Bauwerke- Beurteilen und Sanieren. Berlin: HUSS-MEDIEN GmbH, Verlag Bauwesen

[5] Grosser, D. (1985): Pflancliche und tierische Bau und Werkholz-Schädlinge. Leinfelden-Echterdingen: DRW -Verlag.

[6] Scheiding, W. et al. (2016): Holzschutz. München: Carl Hanser Verlag

[7] Reinprecht, L. 2016): Wood deterioration, protection and maintenance. Chichester: WILEY Blackwell

[8] Binker, G. et al. (2014): Praxis-Handbuch Holzschutz. Köln: Rudlof Müller Verlag

[9] Wilcox, W.W.; Rosenberg, A.F. (1982): Architectural and Construction Deficiencies Contributing to Decay of Wood in Buildings. In: Meyer, R.W.; Kellog, R.M: Structural Uses of Wood in Adverse Environemnts. New York, Van Nostrand Reinhold. Original not seen, quoted from: Stalnaker, J., Harris, E.C. (1997): Structural Design in Wood. Dordrecht: Springer Science + Business Media.

[10] Cruz, H.; Machado, J.S. (2013): Effects of b beetle attack on the bending and compression strength properties of pine wood. Advanced Materials Research Vol 778: 145-151

[11] Eaton, R.A., Hale, M.D.C. (1993): Wood – Decay, pests and protection. Chapman & Hall, London, UK.

[12] Unger, A., Schniewind, A.P., Unger, W. (2001): Conservation of Wooden Artifacts – A Handbook. Springer-Verlag, Berlin Heidelberg, Germany.

[13] Reinprecht. L. (2007): Ochrana dreva – (Wood Protection). Technical University in Zvolen, Slovakia (in Slovak language).

[14] Langendorf, G. (1988): Holzschutz – (Wood Protection). Fachbuchverlag Leipzig, Germany, (in German language).

[15] EN 350:2016 durability of wood and wood-based products -- Testing and classification of the durability to biological agents of wood and wood-based materials. CEN, 68 pp.

[16] Niemelä, T. (1993). "Taxonomy of the genus *Postia* (Basidiomycota)." Mycological Research, 97(9), 1135–1147.

[17] Niemenmaa O, Uusi-Rauva A, Hatakka A (2007) Demethoxylation of [O(14)CH (3)]-labelled lignin model compounds by the brown-rot fungi *Gloeophyllum trabeum* and *Poria* (*Postia*) *placenta*. Biodegradation 19:555–565.

[18] Zabel, R. A., & Morrell, J. J. (1992). Wood Microbiology: Decay and Its Prevention. Academic Press, INC. London, UK.

STRUCTURAL, REINFORCEMENTS AND RETROFITTING

PREDICTION OF LOAD TRANSMISSION AND ANCHORAGE LENGTH OF WOOD SCREWS BASED ON PULL-OUT TESTS

Professor Dr.-Ing. Mazen AYOUBI[1]

[1] Chair of Building Materials, Frankfurt University of Applied Sciences, Frankfurt am Main, Germany

ABSTRACT

The reliable prediction of load transmission and anchorage length of wood screws used as reinforcement or connection elements is essential for their application in modern, filigree timber constructions. In particular, self-tapping screws with continuous threads have gained widespread use due to their favourable bonding behaviour, especially when installed at various angles to the grain. This study presents an extended model for describing the load distribution along the embedment length, based on an experimental program involving pull-out tests with long embedment depths. The tests investigated the influence of screw diameter and angle to the grain on the bond behaviour and anchorage performance. Special attention was given to the bond stress distribution around the screw axis, which was analysed using coloured crack patterns to visualise the internal stress state. These observations were integrated into the extended model, which introduces design-relevant parameters such as load transmission and anchorage length. This enables a more accurate prediction of the screw's withdrawal capacity and supports the optimisation of screw geometry to enhance structural performance. The findings enable more reliable and economical timber connection design and help define the requirements for load-bearing models in structural analysis. The proposed model establishes a clear link between thread geometry and mechanical behaviour, offering practical benefits for both design engineers and screw manufacturers.

KEYWORDS: load transmission, anchorage length, wood screws, bond behaviour, pull-out tests

INTRODUCTION

As a building material, timber offers numerous advantages in terms of sustainability, resource efficiency, and environmental performance. In practical applications, wood screws have become well established both for joining and reinforcing timber elements. For the design of slender and filigree timber structures, self-tapping fully threaded screws have proven to be an efficient and reliable reinforcement technique [5], [7].

An exemplary application is the pedestrian and bicycle bridge in Neckartenzlingen (cf. Figure 1). The evolution of screw thread design, particularly toward self-tapping variants, has significantly increased the use of wood screws in structural timber applications over the past years [2], [7].

In contemporary timber construction, self-tapping wood screws with continuous threads are increasingly employed beyond their traditional function of connecting timber components. These screws are now utilised to enhance the structural performance of timber members, particularly by increasing the load-bearing capacity of beam supports and mitigating tensile stresses perpendicular to the grain at notched support zones. Additionally, they are applied for the reinforcement of curved beams and members with transverse openings. Within these novel areas of application, the use of self-tapping

screws represents a structurally efficient, technically straightforward, and economically viable reinforcement technique [1-4].

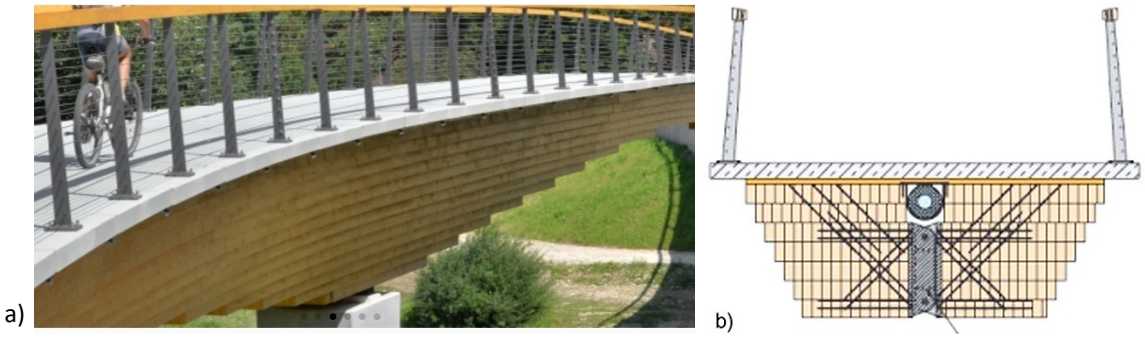

Figure 1. Use of wood screws as fasteners and for lateral pressure reinforcement on the example of the foot and cycle path bridge in Neckartenzlingen [10], as viewed in a) [11] and in cross-section b) [12].

The characterisation of the bond behaviour between self-tapping screws and the surrounding wood is essential for determining the effective load transmission and anchorage length. This, in turn, forms the basis for the development and validation of design methods for reinforcing timber structures using screws. However, the anisotropic and highly inhomogeneous nature of wood poses significant challenges for both analytical and numerical modelling of the screw–wood bond. Key parameters influencing the bond behaviour include the screw geometry, the angle between the screw axis and the grain (α), lateral pressure, timber density, screw diameter, and the penetration depth into the wood [4-6].

LOAD TRANSMISSION IN ANCHORAGE ZONE

To predict load transmission along the anchorage length of self-tapping screws used as reinforcement in glued-laminated timber elements, various experimental and numerical investigations have been carried out within different research projects, employing a range of test procedures. Key results can be obtained from pull-out tests, particularly regarding the withdrawal resistance of the screws. Beyond these basic parameters, pull-out tests have been modified and further developed to gain deeper insights into load transmission mechanisms and to determine the required anchorage length needed to utilise the material capacity efficiently, up to the maximum load-bearing potential of the steel used in the screws.

In contrast to tests with short embedment lengths, which are typically based on the assumption of a uniform average bond stress, tests with greater embedment lengths capture the bond mechanisms more accurately and are better suited for the practical implementation of modelling approaches. However, such tests are associated with increased experimental effort and cost. Furthermore, the derivation of the bond stress–slip relationship is considerably more challenging in these long embedment length tests.

The bond stresses along the anchorage length are not uniformly distributed; rather, they reach their peak under short-term loading—at the service load level—near the beginning of the load introduction zone. From this point onward, the bond stresses decrease progressively toward the end of the load transfer length in a nonlinear manner. The bond quality and the underlying mechanisms of force transmission mechanically influence both the maximum bond stress values and the degradation profile. In the anisotropic material wood, these mechanisms are significantly affected by the angle between the screw axis and the grain direction (α). Figure 2 schematically illustrates representative bond stress (τ) distributions in the end region of a screw embedded at three different angles to the grain direction (0°,

30°, and 90°). These distributions are based on strain profiles obtained from experimental investigations (cf. Pull-Out Tests) and from analytical results derived using the differential equations of the slip-based bond model (cf. Modelling of Bond Behaviour).

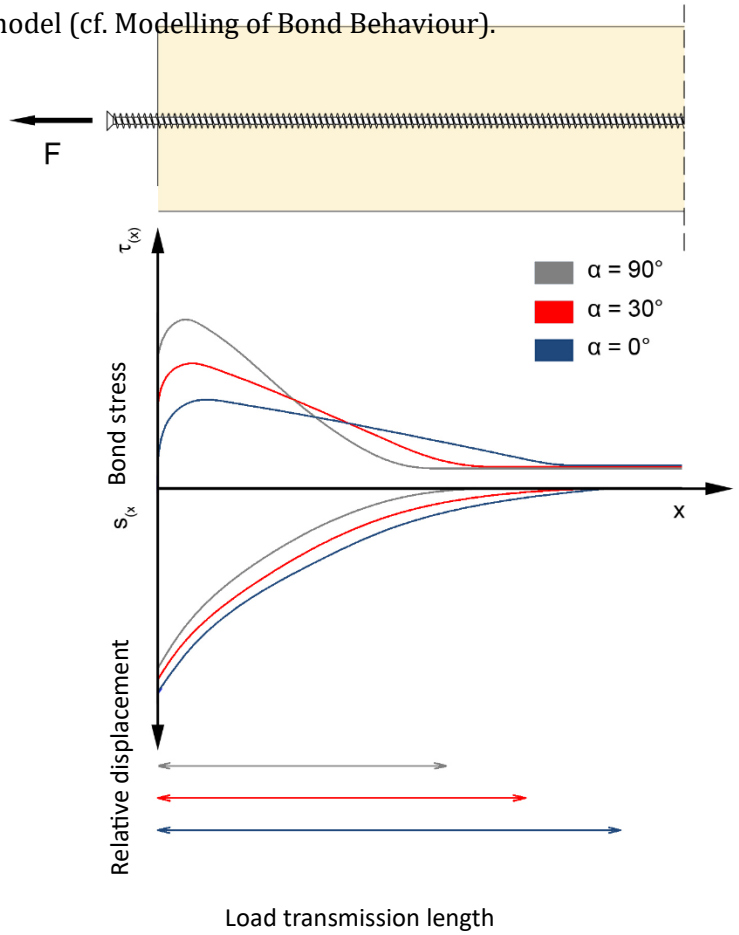

Figure 2. Bond stress distribution in the anchorage zone under short-term loading at service load level based on pull-out tests with long embedment length.

PULL-OUT TEST WITH LONG EMBEDMENT LENGTH

To investigate the anchorage behaviour of fully threaded screws with extensive embedment lengths under short-term loading, experimental investigations were conducted. Pull-out tests were used to examine the influence of screw diameter, embedment length, and the angle between the screw axis and the grain direction on the bond behaviour. These systematic investigations realistically capture the key parameters affecting the load-bearing behaviour of the screw–timber connection.

In all tests, the screws were inserted without pre-drilling into the timber specimens. To create a bond-free zone, a cylindrical borehole with a diameter of 50 mm and varying depths (5–12 cm) was introduced around the screw near the loaded end. This intentional interruption of the bond in the load introduction area effectively eliminates the influence of local transverse compression at the support, thereby preventing distortions of the measured results caused by unintended local effects in the anchorage zone.

After sufficient conditioning of the specimens under standard climate conditions, each test specimen was centrally fixed in the test apparatus. By varying the embedment length of the screws, and thus the bonded length of the specimen, the test setup (cf. Figure 3) was adjusted to match the respective specimen dimensions. Test series were conducted with short anchorage lengths of 15 d, medium embedment lengths of 20 d, and long embedment lengths of 25 d. Furthermore, for shallow angles

relative to the grain direction (0° and 15°), the embedment length was further increased until material failure of the screws occurred.

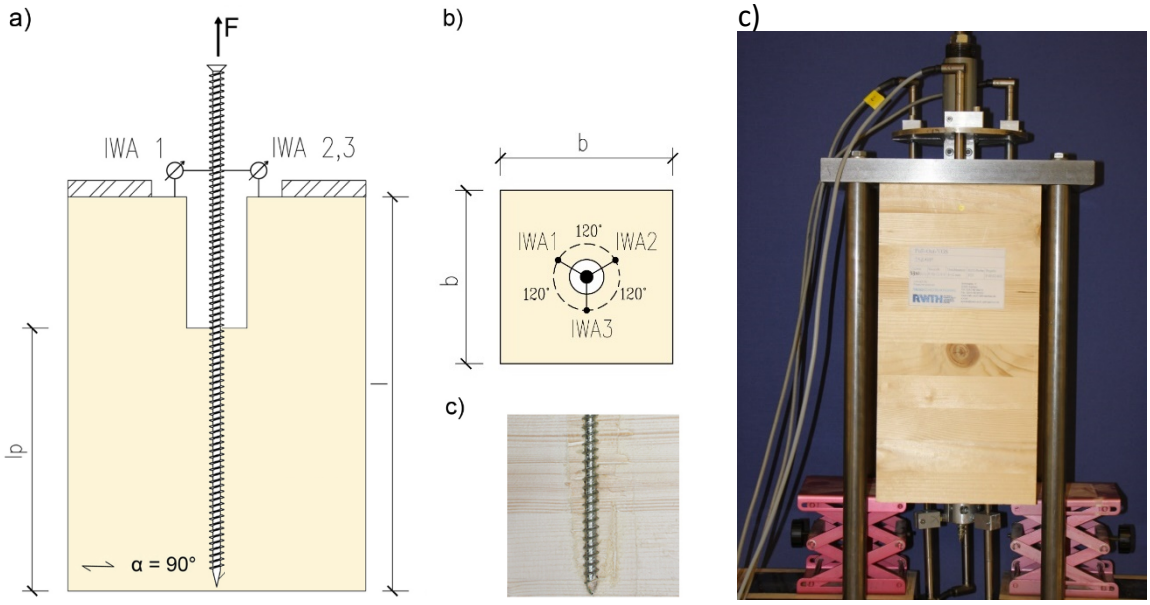

Figure 3. Pull-out test specimen with embedded tip: a) Vertical section, b) Section at the upper load application side, c) Saw cut at the location of the embedded tip, d) Overview of the test setup.

The test results reveal distinct withdrawal behaviours depending on the angle relative to the grain direction (cf. Figure 4). For short screw embedment lengths of 15 d and shallow insertion angles, force transmission is associated with larger relative displacements compared to specimens with a longer embedment length of 25 d. At insertion angles between 30° and 90°, the displacements and the maximum transferable forces tend to converge across the different angles. Once the maximum bond capacity is exceeded, the load-bearing capacity under the respective angles to the grain direction cannot be increased further, regardless of any additional increase in embedment length.

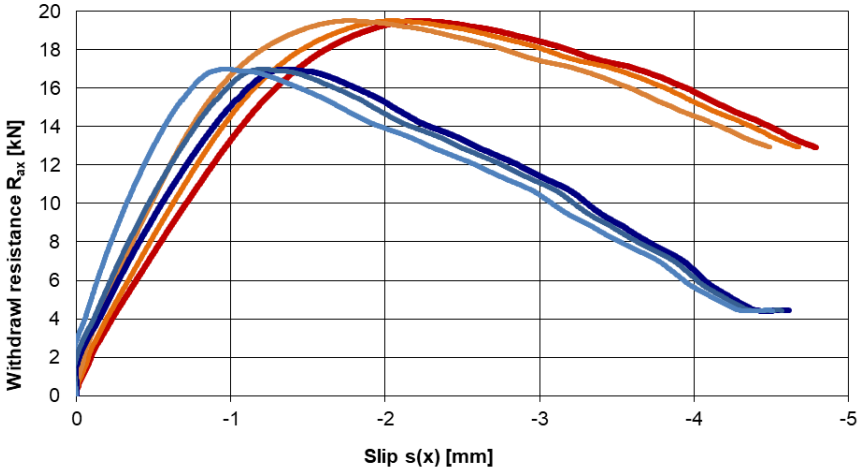

Figure 4. Results of Pull-out tests on fully threaded screws with a diameter of 8 mm and varying angles relative to the wood grain direction: red) a= 90°, blue) a=0°.

During the pull-out process, various bond mechanisms are activated. The decisive factor for their activation is the relative displacement of the screw with respect to the surrounding wood matrix. Figure 5 illustrates the processes occurring within the bond zone during the pull-out test of a fully threaded screw embedded in glued-laminated timber. The force to be transmitted increases in line with the bond stresses developing along the anchorage length. Based on insights gained from saw-cut sections of the pull-out tests conducted, the bond failure process can be described as a series of delamination and fibre-tearing processes within a nonlinear elastic material that exhibits varying strength properties in different material directions. The associated failure mechanisms are characterised by quasi-ductile behaviour under compressive loading and brittle failure under tensile and shear loading.

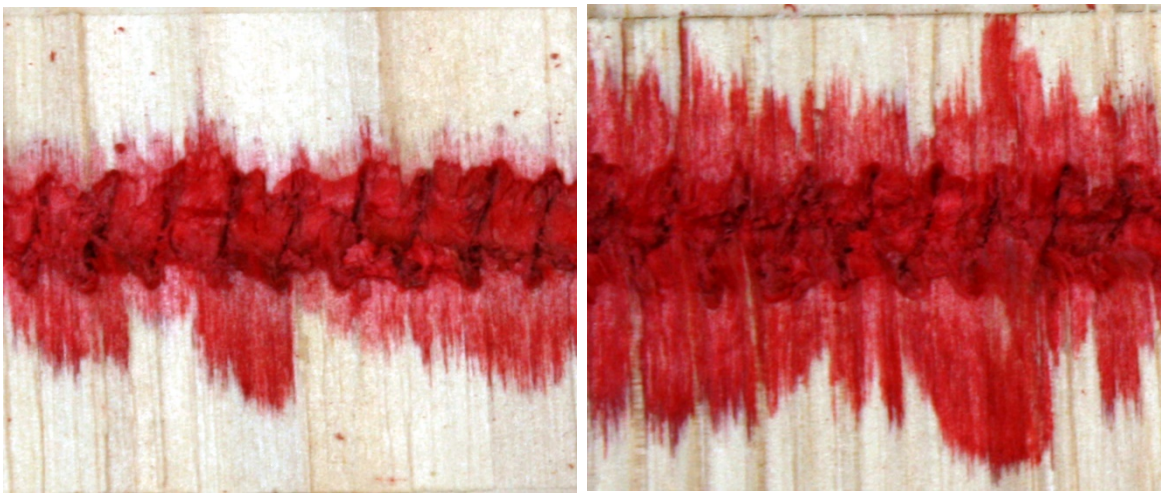

Figure 5. Visualisation of crack surface development based on bond damage, analogous to the crack propagation in the specimens under a load of 14.2 kN (left) and a load of 28.3 kN (right).

MODELLING BOND BEHAVIOUR FOR ANCHORAGE LENGTH PREDICTION

Wood screws are widely used as a cost-effective and efficient reinforcement method for glued-laminated timber elements as well as fasteners in timber-to-timber and timber-to-steel connections. However, there is still a deficiency of accurate models that effectively capture the influence of thread geometry on the load-bearing behaviour. Building upon extensive experimental investigations, current bond behaviour models for wood screws have been critically evaluated with a focus on their applicability in design. This assessment has led to the development of an improved model that extends existing approaches [8, 9].

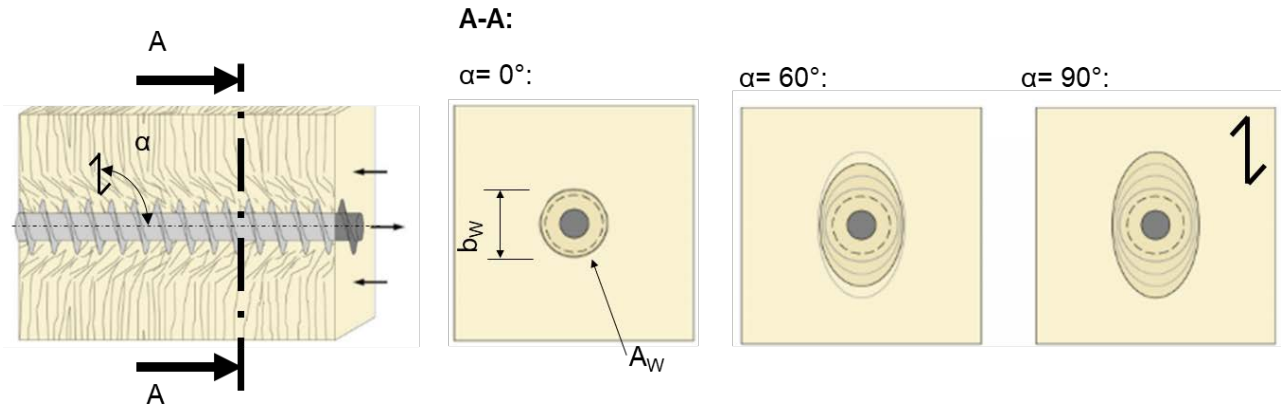

Figure 6. Gradient of the wood displacements of the load distribution tests of specimens with one screw (d= 12 mm) under tension loads at: a) tension load of 52,6 kN and angle to the grain of 30°, b) tension load of 20,4 kN and angle to the grain of 60° [5, 7].

The resulting shear strength distribution for a screw inserted parallel to the grain direction, which is a rectangular distribution with rounded corners, was obtained. In contrast, for a screw inserted perpendicular to the grain, a butterfly-shaped shear stress distribution emerges. This butterfly shape exhibits shear stress values that are approximately six times higher in the direction parallel to the grain compared to those in the transverse direction [7]. These varying shear strengths also lead to a non-uniform distribution of load transfer [5, 7]. The lower stiffness of wood results in a smaller radius of the tensile rings when screws are inserted parallel to the grain.
Furthermore, as illustrated in Figure 4, a change in the shape of the tensile rings is observed. For screws inserted parallel to the grain ($\alpha = 0°$), the tensile ring assumes a circular shape, whereas for perpendicular insertion angles ($\alpha = 90°$), it becomes elliptical (cf. Figure 6). The major axis of the ellipse aligns with the grain direction [5, 7].
This observation is based on experimental investigations using cross-sectional images of glued-laminated timber elements with fully threaded screws of 12 mm diameter and extensive embedment lengths [7]. Using a solution algorithm dependent on the insertion angle α, the lateral surface area of the screw was described by the parameters A_w (ranging from $16\pi d^2$ to $60\pi d^2$) and b_w (ranging from 4d to 10d) [5]. For intermediate insertion angles α, a linear relationship was assumed as an approximation (see Figure 6) [5, 7].

Figure 7 presents a comparison of withdrawal resistance values according to various standards and technical approvals for screws with a nominal diameter of 10 mm, a timber density of 460 kg/m^3, and an embedment depth of 200 mm (20d). The results of the numerical example, which reveal significant differences in withdrawal resistance depending on the insertion angle—both among the standards themselves and between the standards and different approvals—underscore the need for a precise characterisation and description of the bonding behaviour between screws and wood. This is essential for accurately determining the required anchorage length of the screws.

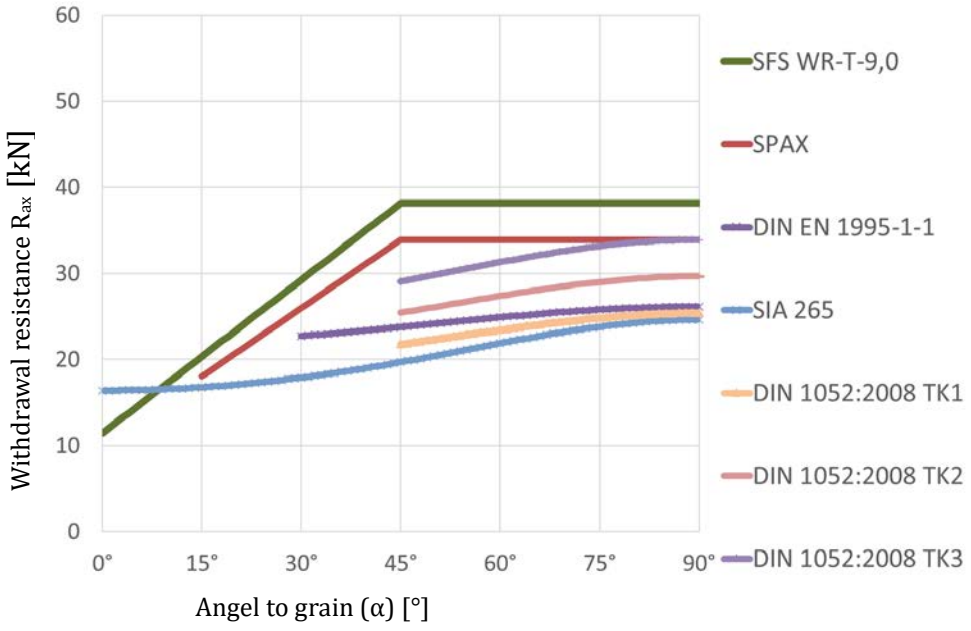

Figure 7. Exemplary Comparison of Axial Withdrawal Resistance (R_{ax}) of screws as a function of the angle α to the grain direction, for screws with a diameter of 10 mm and an embedment length of 20 d, at a wood density of 460 kg/m^3, based on various standards and approvals.

To assess current design approaches in the literature for the withdrawal resistance of fully threaded screws, the experimentally determined withdrawal capacities are compared with calculated values

according to DIN 1052, Eurocode 5 and SIA 265, as well as with values provided in technical approvals for screws that allow insertion at small angles to the grain direction (see Figure 8).

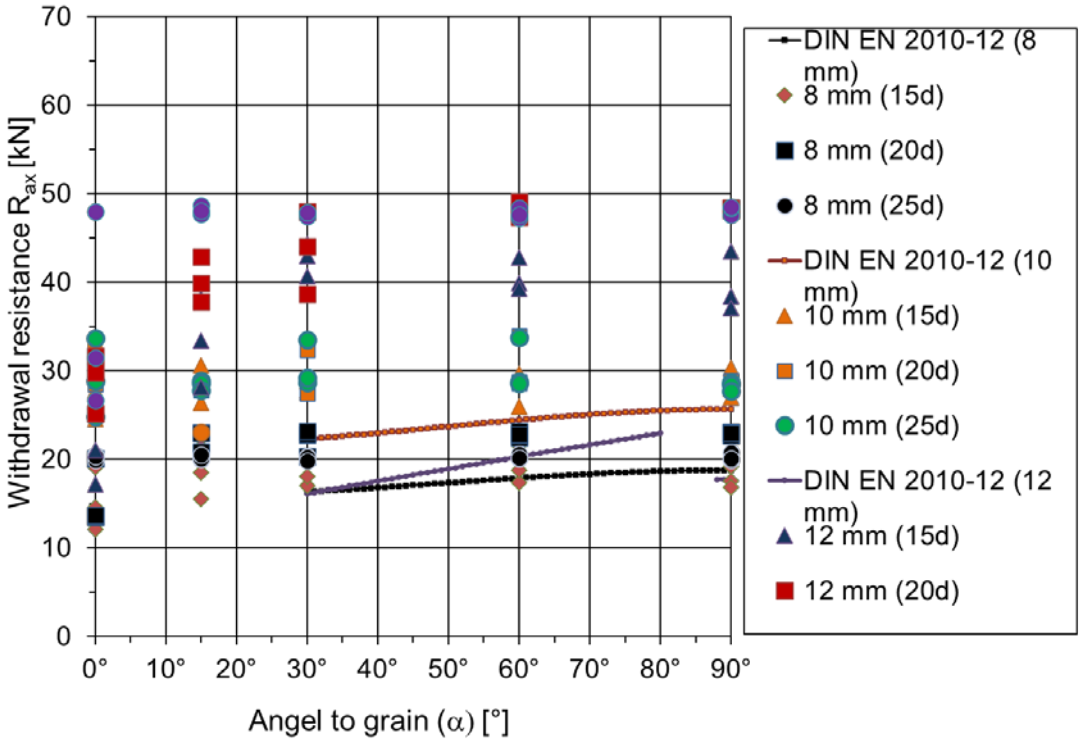

Figure 8. Comparison of the calculated axial withdrawal resistance R_{ax} according to Eurocode 5 (DIN EN 1995-1-1) *for an embedment length of l_{ef} =20d with the experimental values obtained from Pull-Out-Tests.*

The present test results also indicate that the withdrawal resistance of the screws does not increase proportionally with the embedment length. At insertion angles α < 15°, a reduction in bond load-bearing capacity was observed compared to larger angles. This affects both the frictional component of the bond resistance and, to an even greater extent, the remaining components—namely adhesion and shear bond. These effects must be taken into account when calculating the required anchorage length.

Based on the results of the experimental investigations and building upon the analyses presented therein, a mechanical model and a design concept for the anchorage length of fully threaded screws were developed [9]. The proposed design approach is aligned with the design principles of Eurocode 5 (EN 1995-1-1).

The anchorage length for screws (l_{ver} in mm) with varying diameters, insertion angles relative to the grain direction, and in different glued-laminated timber elements can be determined according to the Characteristic tensile load-carrying capacity ($R_{t,u,k}$ in N) for insertion angles between 15° and 90° using the following equation:

$$l_{ver} = \gamma_{Ma} \cdot \left(\frac{(R_{t,u,k} - 4200 \cdot d^{0,4}) \cdot}{\frac{(1,3 \cdot \cos^2 \alpha + \sin^2 \alpha)}{0,3 \cdot d^{0,5} \cdot \rho_k^{0,8}}} \right)^{1,11} \quad ; 15° \leq \alpha \leq 90°$$

At insertion angles α < 15°, a reduction in bond load-bearing capacity was observed compared to larger angles. This reduction affects both the frictional component of the bond resistance and, to a greater extent, the remaining components (adhesion and shear bond) [9]. Since no experimental data were available for the range between 0° and 15°, and the numerical analyses did not indicate a disproportionate decrease in bond performance within this range, a simplified linear relationship

between the reduction and the angle was assumed. The anchorage length can be calculated using the following equation:

$$l_{ver} = \gamma_{Ma} \cdot \left(\frac{(R_{t,u,k} - 4200 \cdot d^{0,4} + (540 - 36 \cdot \alpha) \cdot d) \cdot (1,3 \cdot \cos^2 \alpha + \sin^2 \alpha)}{0,3 \cdot d^{0,5} \cdot \rho_k^{0,8}} \right)^{1,11} \quad ; \alpha < 15°$$

The equations mentioned above consider screw diameters d between 8 mm and 12 mm, as well as the wood density in kg/m^3. In the absence of further experimental data, it is recommended to define the anchorage length of self-tapping fully threaded screws required to reach their maximum load-bearing capacity as at least 1.4 times the calculated values (γ_{Ma} = 1.4).

CONCLUSION AND OUTLOOK

The use of wood screws with continuous threads for reinforcing timber and glued-laminated elements represents an effective, straightforward, and economical method. Wood screws act as essential fasteners in timber-to-timber and timber-to-steel connections, and are also employed for the reinforcement of timber structures. For such joints and reinforcement techniques, the load-bearing capacity is the key performance parameter, primarily governed by the bonding mechanisms between the screw thread and the surrounding wood material. Understanding the bond behaviour and load transfer mechanisms between screw and timber is crucial for the safe and efficient design of screw connections in timber structures.

An extended model for describing the load distribution along the embedment length was developed based on an experimental program involving pull-out tests with extensive embedment lengths. The experiments focused on the influence of screw diameter and angle to the grain direction on the bond behaviour and anchorage performance. Special attention was given to rotational effects around the screw axis. These effects were investigated through coloured crack pattern analysis, which served to visualise the internal stress distribution within the wood matrix. The extended model incorporates these observations and introduces design-relevant parameters, such as the thread flank angle, allowing for a more accurate prediction of withdrawal capacity and supporting the geometric optimisation of screws for enhanced structural performance.

Furthermore, analysing the load transmission with respect to the angle to the grain provides additional insights that help refine existing models. These improved models of bond behaviour can support manufacturers in optimising screw geometries and facilitate the development of safe and cost-effective design approaches. Ultimately, the findings contribute to higher withdrawal capacities and increased reliability of screw connections in modern timber engineering.

Further research is required to enhance the efficiency of timber constructions reinforced or connected using wood screws, and to analyse in detail the results of ongoing long-term tests currently being conducted at the Frankfurt University of Applied Sciences (FRA-UAS). Particular attention should be given to the long-term performance, seismic resistance, and the structural behaviour of hybrid systems incorporating various types of screws.

REFERENCES

[1] Ayoubi, M.: Illustration of The Bond Behaviour of Wood Screws Using Extension Model. In: Proceedings of the SHATIS 2022 – 6th International Conference on Structural Health Assessment of Timber Structures, Editors: Jiří Kunecký & Hana Hasníková, ISBN: 978-80-86246-54-3, DOI: 10.21495/54-3, 7th – 9th September 2022, Prague, Czechia, 2022, pp. 07-15.

[2] Ayoubi, M.: Non-Destructive Testing Procedure for Determining Stress Distribution in with Self-Tapping Screws Reinforced Glue-Laminated Timber Elements. In: SHATiS'19, 5th International Conference on Structural Health Assessment of Timber Structures, Proceedings of the International Conference on Structural Health Assessment of Timber Structures SHATiS'2019, ISBN: 978-989-54496-2-0, Guimarães, Portugal, September 25-27, 2019, pp. 526-536.

[3] Ayoubi, M.; Trautz, M.: Bond Behaviour of Self-Tapping Screws being used as Reinforcement in Glue-Laminated Timber Elements. In: SHATIS' 15, the 3nd International Conference on Structural Health Assessment of Timber Structures, Proceedings of the International Conference on Structural Health Assessment of Timber Structures, ISSN 0860-2395, ISBN 978-83-7125-255-6, September 9-11, 2015, Wroclaw, Poland, pp. 859-871.

[4] Ayoubi, M.; Trautz, M.: Determination of the Stress Distribution in Timber Elements with Self-Tapping Screws using an Optical Metrology System. In: SHATIS' 13, the 2nd International Conference on Structural Health Assessment of Timber Structures, September 4-6, 2013, Trento, Italy, Book of Abstracts, pp. 117-118.

[5] Ayoubi, M.: Zum Verbundverhalten von Vollgewindeschrauben mit großen Einbindelängen beim Einsatz als Bewehrung in Brettschichtholzbauteilen, PhD Thesis, RWTH Aachen University, 2014.

[6] Ayoubi, M.; Rößler, G.; Trautz, M.; Raupach, M.: Experimental and Numerical Investigation of Bond between Glue-laminated Timber Elements and Self-Tapping Screws. In: 13 proceedings of the IASS 2013 Symposium, Wrocław, Poland, 23-27 September 2013, ed. Jan B. Obrębski and Romuald Tarczewski; International Association for Shell and Spatial Structures, Wrocław, Poland, 23-27 September 2013.

[7] Hölz, K.; Ayoubi, M.; Gwosch, T.; Matthiesen, S.: Theoretische Modelle zum Verbundtragverhalten von Holzschrauben für die Schraubengestaltung. In: Bautechnik (Zeitschrift für den gesamten Ingenieurbau), Volume 98, Issue 14, S. 86-94, 2021. DOI:10.1002/bate.202100003, https://onlinelibrary.wiley.com/doi/abs/10.1002/bate.202100003

[8] Ayoubi, M.; Trautz, M.: Bond behaviour of self-tapping screws being used as reinforcement in glue-laminated timber elements. Part 1: experimental investigations on self-tapping screws with continuous threads and long embedment length being used as reinforcement in glue-laminated timber elements. Bautechnik 92(11):790–799. https://doi.org/10.1002/bate.201400098

[9] Ayoubi, M.: Bond behaviour of self-tapping screws being used as reinforcement in glue-laminated timber elements. Part 2: Analytical and numerical investigations as well bond model derivation for the calculation of anchorage length. Bautechnik 93(11):817–827.

[10] Hölz, K.; Ayoubi, M.; Gwosch, T.; Matthiesen, S.: Theoretische Modelle zum Verbundtragverhalten von Holzschrauben für die Schraubengestaltung. In: Bautechnik (Zeitschrift für den gesamten Ingenieurbau), Volume 98, Issue 14, S. 86-94, 2021

[11] IB-MIEBACH (2020) Blockträgerbrücke Neckartenzlingen [online]. Lohmar: IB-MIE-BACH [Access: 09.07.2025].https://www.ib-mie-bach.de/de/projekte/holz-bruecken/holzdeckbruecke/blocktraeger br uecke-neckartenzlingen.html

[12] Miebach, F. (2019) Mit Holz zu neuen Ufern. Brücke über den Neckar in Neckartenzlingen lotet Grenzen aus in: dach+holzbau 2019, 1. S.40-45 5.

ASSESSMENT OF POST-TENSIONING REINFORCEMENT CONFIGURATIONS ON A TIMBER TRUSS

Kamryn E. WIESNER[1], Hélder S. SOUSA[1] and Jorge M. BRANCO[1]

[1] University of Minho

ABSTRACT

Post-tensioning with external steel cables is gaining popularity as a reversible, minimally invasive reinforcement method for historic timber structures. While its effectiveness in improving stiffness and reducing deflection has been demonstrated in beams and joists, its application for trusses has been less explored – particularly in terms of cable configurations and long-term prestressing losses.
This study presents an analytical and finite element (FE) investigation of different post-tensioning cable configurations applied to historic timber trusses. Using a parametric model built in SAP2000 that has been calibrated using experimental data, several cable configurations are analysed. For each layout, the effects on force redistribution, deflection, and overall capacity will be assessed and compared.

KEYWORDS: post-tensioning, timber trusses, finite element modelling, strengthening

INTRODUCTION

Timber trusses are central structural components in many historic buildings, particularly in large-span roofs. Over time, material degradation or increased load requirements can compromise their performance, prompting the need for strengthening interventions. In historic structures, it is important that interventions respect the original construction, meaning they should be non-invasive and reversible [1].
Post-tensioning with steel cables presents itself as an ideal solution for effectively strengthening timber members, reducing deflection and overall stresses, while respecting the original structure. Since the technique is applied externally, it is easily reversible and preserves the original structure geometry. This study investigates how different post-tensioned cable configurations affect the response of the structure, specifically through load redistribution and reducing deflection.

METHODOLOGY

The truss analysed in this study is a collar beam truss, shown in Figure 1, that spanned 15 m and was salvaged from an 18th-century building in Coimbra, Portugal [2]. The truss was reassembled and tested at the University of Minho laboratories in 2015.

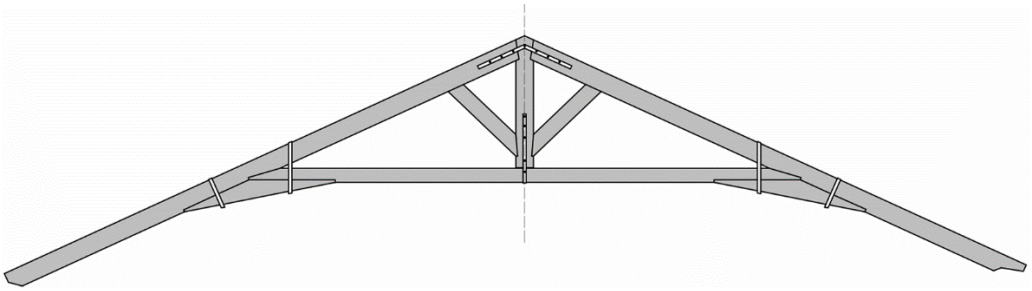

Figure 1. Geometry of Truss

An intervention using post-tensioning, shown in Figure 2, was installed and tested at that time. A finite-element model of the truss was created in SAP2000 and calibrated using the experimental test data. For the laboratory test setup, two actuators (ACT 842 and ACT 121) were used to simulate loads applied on the truss [3].

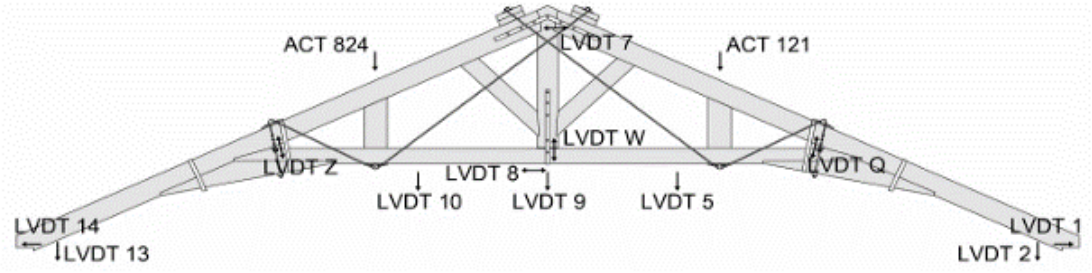

Figure 2. Post-tension cable layout used in [3]

Using this model as a base, a series of finite element models was created using different post-tension cable configurations and varying levels of prestressing force. Each strengthening method was analysed under dead and live load to simulate realistic loading conditions.

As mentioned in the introduction, structural interventions are designed when required to either resist new loads or to remediate issues. Therefore, when designing post-tensioning interventions, the cable layout is also determined in response to the loading of the truss and its current failure method.

In its original location, the truss supported purlins which spanned the distance between trusses. These, in turn, supported the roof rafters and tile roof. Since this is common for most trussed roofs, the cable configurations for this study were designed for this type of loading. The point loads from the purlins are shown in pink in the sketches shown in Table 1 below.

The first and second configurations aim to reinforce the whole truss without the need for adding extra truss members to support the new post-tension loads. Configurations 3 and 4 introduce new support members to avoid overstressing the tie beam and provide a path for the post-tension load to reach the truss rafter. Finally, the last two configurations look at cases where additional loads are introduced, particularly hanging loads from the underside of the truss.

For all post-tension cable configurations, a parametric study was performed to assess the influence of the amount of reinforcement (number of cables and level of tension). Moreover, the effect of the tension losses in the post-tension cable expected during the service life was simulated, incrementally decreasing the prestressing forces to see how the gradual loss of stress over time will affect the intervention. The level of prestressing force was decreased in increments of 5% (e.g. 5%, 10%, 15%) until failure or instability of the intervention was reached.

Table 1. Sketches of Cable Configurations

	Sketch	Description
1	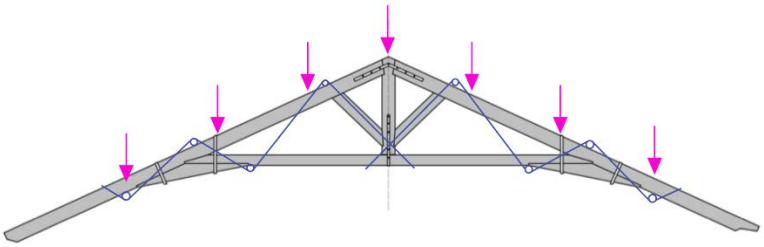	Two cables reinforcing the diagonal struts.
2	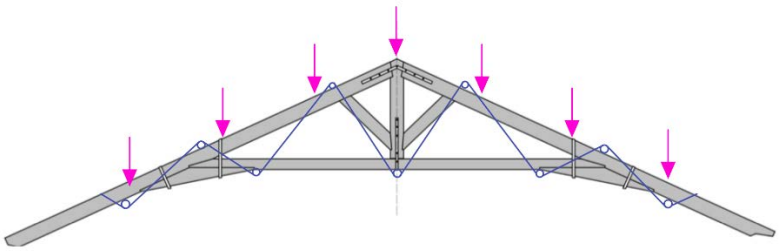	Single cable reinforcing the diagonal struts and the center post.
3	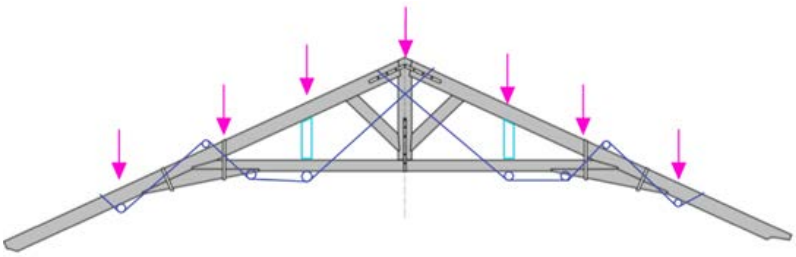	Two cables and new supports resisting the loading on the truss rafters.
4	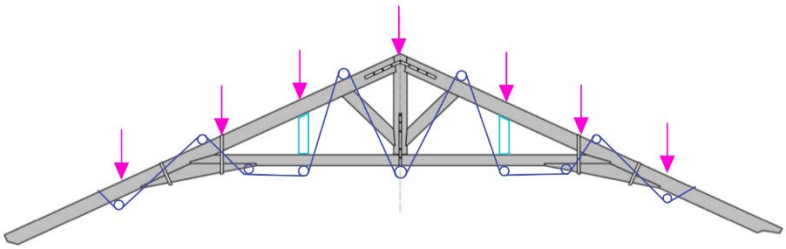	Single cable and new supports resisting all purlin point loads.
5	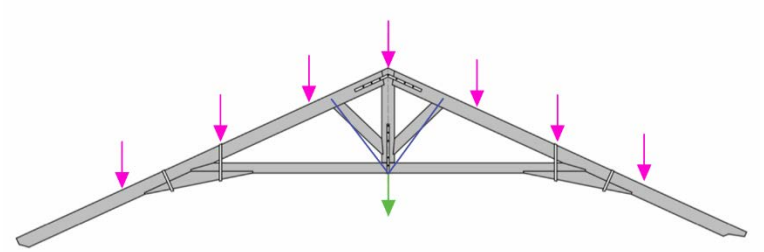	V-shaped cable resisting a hanging point load in the center of the truss.
6	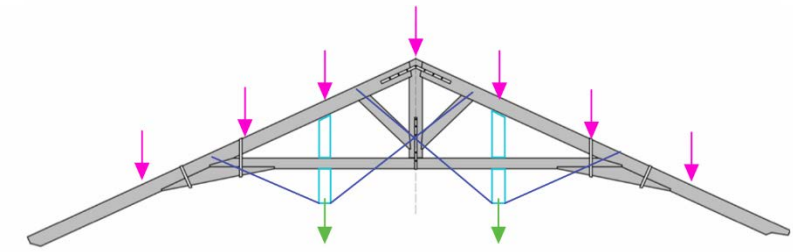	Two cables resisting two hanging point loads from the truss tie beam.

RESULTS

Under normal loading conditions, if the truss is in okay condition, as was the case for this case study, the prestressing cables do not have any positive effect. Even when the roof load was doubled, the truss without prestressing had less deformation than the prestressed trusses. However, in trusses 5 and 6, new loads totalling 35 kN per truss were added to the underside, and the cables greatly reduced the deflections. For truss 5, the maximum deflection at the centre of the tie beam decreased from 55.5 mm to 8.8 mm. While the overall cable reinforcing did not decrease deflections due to loading, it did help reduce the spreading of the truss, with configuration 1 performing the best.

CONCLUSIONS

Strengthening of timber trusses is increasing in popularity due to its effectiveness, balanced with its ease of installation and adherence to conservation principles. However, there are no guidelines yet for how to best use this technique. There is also uncertainty about how this intervention will hold up over time, due to the gradual loss of prestressing force that will inevitably occur due to cable relaxation, anchorage slip, and timber creep. This study helps answer some of the questions of both topics, providing guidance to structural designers who plan to use this technique.

REFERENCES

[1] ICOMOS International Wood Committee, "PRINCIPLES FOR THE CONSERVATION OF WOODEN BUILT HERITAGE," Dec. 2017.

[2] J. M. Branco, H. Sousa, and G. Crivellari, *Repair techniques used in two existing collar beam trusses: experimental results of full size scale tests, In: Proceedings of the World Conference on Timber Engineering (WTCE 2016 e-book)*. Vienna, 2016. [Online]. Available: http://shop.tuverlag.at/de/

[3] G. Crivellari, "Prestressing system for retrofitting a historical timber truss Advanced Masters in Structural Analysis of monuments and Historical Constructions i," Guimaraes, Jul. 2015.

TIMBER-BASED RETROFIT OF A URM HISTORIC CASE-STUDY BUILDING IN A HIGH SEISMICITY REGION

Giada ZAMMATTIO[1], Davide CASSOL and Ivan GIONGO[1]

[1] University of Trento, Department of Civil, Environmental and Mechanical Engineering, Trento, Italy.

ABSTRACT

The manuscript focuses on the application of timber panel overlays/claddings for the seismic retrofit of existing heritage masonry buildings by analysing a case-study building located in Italy, in an area of medium-high seismicity. The selected retrofit strategy consists of fixing cross-laminated timber (CLT) panels to the URM walls by using dry fasteners distributed over the wall surface. The panels are applied to the inside of the building to ensure enhancement in seismic performance while preserving the external façades. In this instance, the document examines the design and modelling (FME – Frame by Macro Element) decisions made to implement such reinforcement technique, identifying the optimal configuration in accordance with structural, architectural and conservation limitations. Pushover analyses were conducted to assess the global seismic performance of the structure. The results confirmed at the building scale what previous research had experimentally demonstrated at the wall-panel level: that timber overlays significantly improve the seismic resistance and deformation capacity of masonry buildings.

KEYWORDS: Unreinforced Masonry Building, Seismic Retrofit, Timber-based strengthening, macro-element modelling, CLT panels.

INTRODUCTION

Land in European countries is becoming increasingly anthropised, yet there is a growing recognition of the importance of preserving undeveloped areas. As a result, several governments have introduced guidelines aimed at protecting soil as a resource [1] and achieving net-zero land use by 2050 [2]. In parallel, the broader objective of achieving carbon neutrality by 2050 has also been established.
These targets have a direct impact on the building industry, which is responsible for 37% of global CO_2 emissions and accounts for 34% of global energy demand [3]. In Italy, these challenges are further compounded by the country's high seismic risk and the condition of its building stock, which includes a large portion of vintage unreinforced masonry (URM) buildings.
To address the need for net-zero land use, reduced carbon emissions, and enhanced seismic resilience, various innovative and sustainable retrofitting techniques have emerged in recent years. Among them, timber-based reinforcement systems have drawn increasing interest and are being actively explored by several research teams [4]-[15]. This discussion will focus specifically on the reinforcement of URM walls through the use of panel claddings or overlays. In this method, cross-laminated timber (CLT) panels are attached to URM walls using either mechanical or adhesive point-to-point connections [14]. Mechanical fixings typically involve 4–5 screw fasteners per square meter, supplemented by tension and shear anchors at the panel base (see Figure 1).

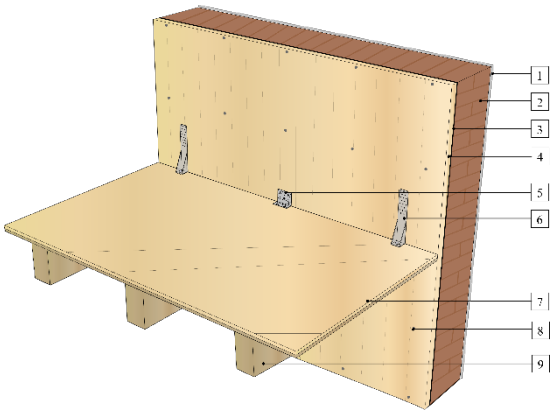

1. Plaster
2. Existing masonry (URM)
3. Waterproofing membrane
4. CLT panel
5. Shear anchor (e.g., angle bracket)
6. Tension anchor (e.g., hold-down)
7. New diagonal floorboard overlay
8. Mechanical timber-masonry screws
9. Existing joists

Figure 1. Reinforcement technique with CLT panel overlays

This modern solution offers numerous advantages. Firstly, timber possesses a high strength-to-density ratio, which allows for a significant improvement in structural performance with minimal additional mass. Unlike cement-based solutions, this characteristic reduces the seismic demand on the structure while enhancing both the load-bearing and displacement capacity of the walls. Importantly, this occurs without adversely affecting the building's overall dynamic behaviour. Secondly, the use of dry mechanical connections makes the intervention reversible. This facilitates not only quicker and more straightforward installation but also simplifies future maintenance and potential removal operations. Another key benefit of this approach lies in the positioning of the CLT panels on the interior side of the masonry. This placement protects the timber from environmental exposure and preserves the original appearance of the building's exterior façades, a critical consideration for heritage and listed buildings.
Finally, from an energy performance perspective, the natural thermal insulation properties of timber contribute positively to indoor comfort, particularly in colder climates. This makes the solution not only structurally effective and sustainable, but also energy-efficient.
The effectiveness of the proposed technique was assessed through an extensive numerical and experimental validation process consisting of multiple stages. A preliminary numeric study conducted to determine the viability of timber-panel retrofit strategies [1] was followed by extensive experimental testing performed mostly onsite and at various scales, addressing from the connections [16][17] to full-scale walls [14].
The results of these tests were then used to calibrate advanced numerical models, which could explore details (e.g., connection type and layout [18]), technique variants (e.g., by combining various engineered wood products [5][6]) and additional application scenarios such as external coatings exploiting possible panel inter-storey continuity [19].
In conclusion, the experimental and numerical evidence confirmed that CLT panel overlays can produce substantial improvements in structural performance. Specifically, the intervention leads to increases in bearing capacity of approximately 25–50% in shear and 20–40% in rocking, along with enhanced deformability, as evidenced by drift values exceeding 1.5%. Based on these promising results, the article proposes applying the CLT reinforcement technique to a real case study to check its applicability in heritage buildings and high seismic hazard areas.

EX MULINO TREVISAN. HYSTORY AND DESCRIPTION

The selected case-study building is the Ex Trevisan's Mill, part of the historic complex known as Villa Marini-Trevisan in Aviano. The site represents a notable example of a Friulian aristocratic house, a typology characteristic of the region [20]. The property is currently divided into two main areas: the renovated villa to the northwest (now operating as a bed and breakfast and vacation rental) and a group of disused rural buildings to the southeast, including the historical mill. In the absence of original

drawings, the construction history of the mill was reconstructed through surveys, archival documents and historical cartography. Recent findings indicate that the mill was erected between 1929 and 1930, replacing a late 19th-century stable. An extension on the southwest side was added in the 1940s. Milling operations terminated in 1972 due to the silting of the Roja watercourse, marking the beginning of the site's gradual abandonment and structural deterioration. The complex is currently in a state of ruin. However, it holds considerable historical and territorial value, demanding an intervention to preserve and enhance the site. The mill is situated within a broader context of ongoing restoration, evidenced by the demolition of adjacent buildings in 2008 and the recent restoration of the 17th-century villa.

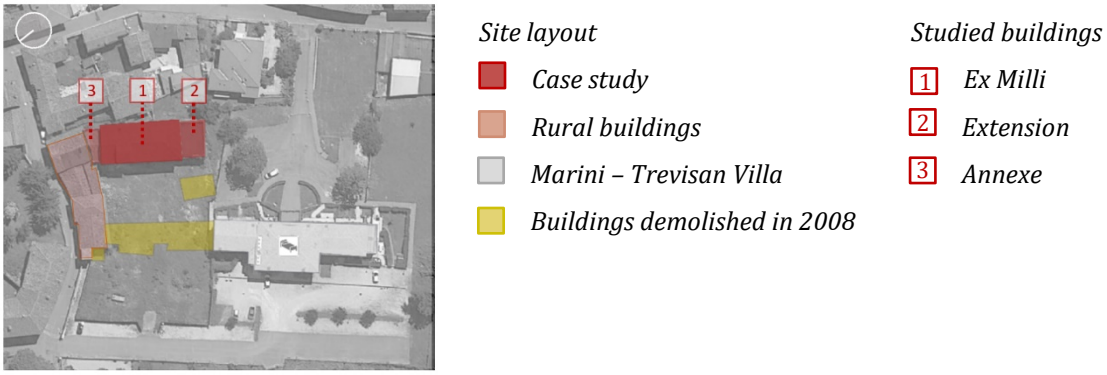

Figure 2. Villa Marini-Trevisan complex

The subject of this study is a building complex composed of three longitudinal structures aligned along an east-west axis (Figure 3). The complex measures approximately 37.5 metres in total length, 11.2 metres in depth (transverse direction), and reaches a maximum eaves height of about 11.5 metres. At the centre, there is a main body of the *mill*, which consists of three storeys above ground and includes a vertical extension. Regular openings mark the façades, while the structure features timber floors and roofing and masonry walls. Internally, two load-bearing masonry walls separate the central milling area from the space originally used for silos. Old timber stairs ensure vertical distribution.

To the southwest, an *extension* comprises a two-storey volume with timber flooring and a flat hollow clay-block and concrete roof. The ground floor is accessible only from the exterior, while the first floor connects to the main building through wall openings in the common wall. The third component, an *annexe* with a trapezoidal plan, is also two storeys high, built with masonry walls and timber floors. It should be noted, however, that there are no direct connections to the other volumes. Access to the site is currently only possible from the exterior, and the rooms are now in a state of degradation due to the severe deterioration of the horizontal structural elements.

Longitudinal section A-A

North view

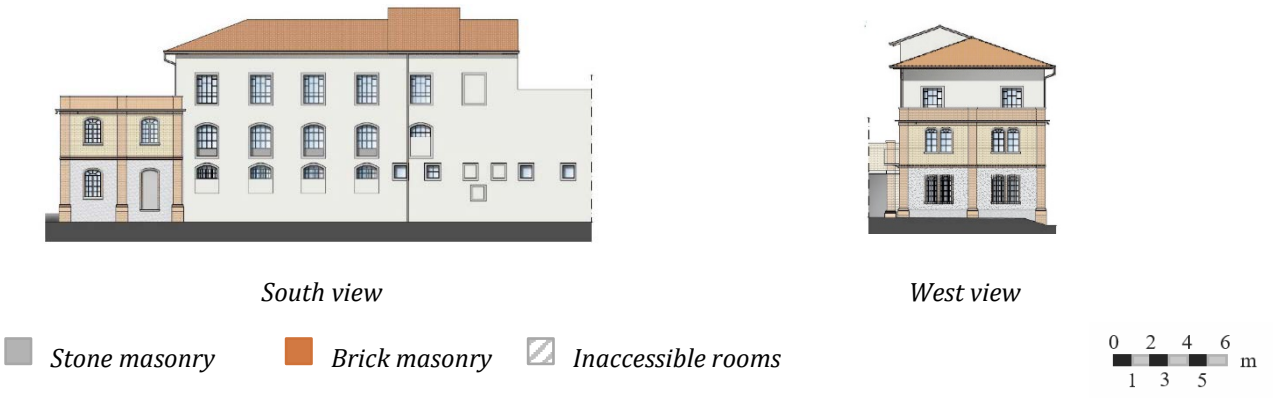

Figure 3. Case study building lateral views

The load-bearing walls (Table 1) of the ground floor of the mill (~50 cm thick) and the annexe (~50 cm thick) are composed of irregular dolomitic limestone, bedded with lime mortar. Starting from the first-floor level (approximately 3.80 m), the walls are constructed as three-leaf solid brick walls (45 cm thick), a construction technique consistent with the 1929 elevation of the original stable. The extension, built using traditional masonry techniques, features three-leaf walls at the ground floor and two-leaf walls at the first floor, with the addition of reinforced concrete columns supporting the floor structure.
The timber floors consist of a double-beam layer: primary chestnut beams and secondary spruce beams, with 2 cm thick wooden board flooring. The roofs of the mill and the annexe are made of timber with terracotta roof tiles. The extension has a flat roof made of one-way concrete joists with hollow blocks between the beams and an upper waterproof membrane as finishing.

Table 19. Characteristic values of masonry mechanical parameters for Knowledge Level 1 (KL1) according to [23]

Types of masonry	f_c **[MPa]**	τ_0 **[MPa]**	f_{v0} **[MPa]**	**E [MPa]**	**G [MPa]**
Irregular dolomitic limestone wall	1.4	0.028	-	1080	360
Regular brick and lime mortar wall	2.6	0.05	0.13	1500	500

f_c = masonry compressive strength; f_{v0d} = masonry shear strength/cohesion; τ_0 = shear stress; E = modulus of elasticity; G = modulus of rigidity

Photo 1 – Ground-floor wall

Photo 2 – 1st and 2nd floor wall

Photo 3 – First-floor ceiling

Photo 4 – Second floor of the extension

Photo 6 – Mill's roof

Figure 4. Photographic details

RENOVATION PROJECT

In light of the site context and with the aim of establishing an attractive focal point within the *Villa Marini-Trevisan* complex, it was decided to repurpose the building for receptive functions. The proposed use includes a bar and restaurant, with the flexibility to host events such as weddings, private parties, and corporate gatherings. As shown in Figure 4, the annexe was demolished. This was due to the horizontal structures being irremediably deteriorated. The 1950s extension was also removed for aesthetic reasons. The intervention was guided by the intention to enhance the architectural integrity of the site by eliminating incongruous elements.

To accommodate the planned new functions, a preliminary assessment of the existing floors was carried out. The assessment revealed the need to replace the old solid timber floors, characterised by small sections and large spans, with new glulam elements able to guarantee adequate structural performance. The new decking saw an additional diagonal board layer on top of the straight sheathing for an improved in-plane behaviour [15]. Out-of-plane stability of the face-loaded walls was then checked using linear kinematic analysis, assuming an effective wall-to-diaphragm connection.

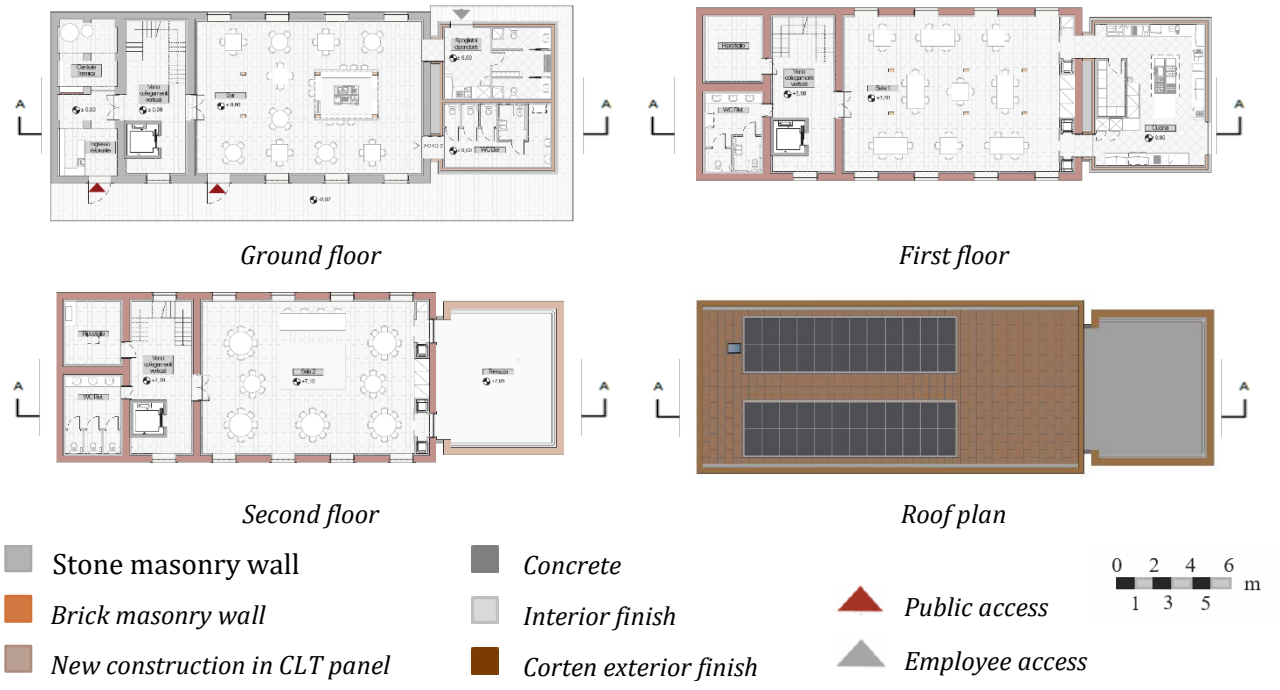

Figure 5. Project plans

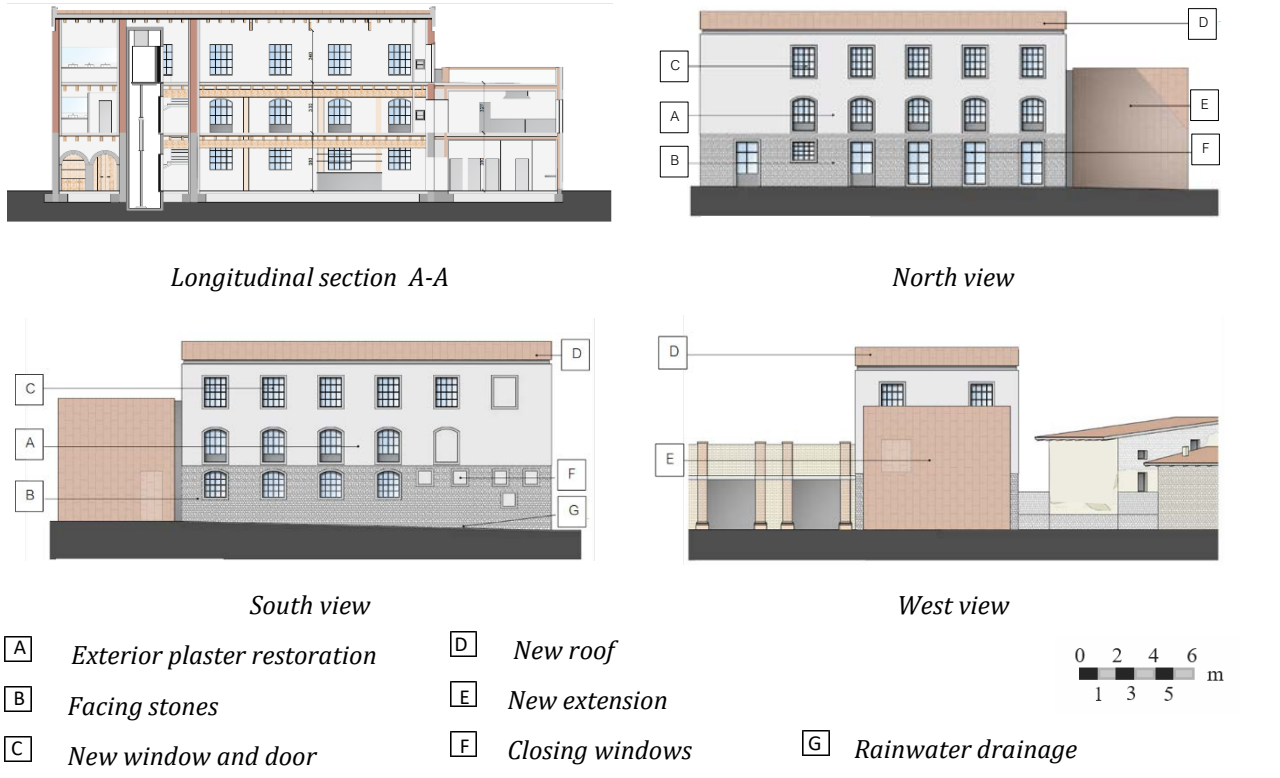

Figure 6. Project elevation views

In line with key architectural principles (i.e., distinguishability, material compatibility and preservation of historical memory), the intervention focused on maintaining the building's original forms, volumes, and external finishes ("skin"). A lateral building extension with a Cross-Laminated Timber (CLT) structure, seismically separated from the historic building, was designed using materials that are clearly identifiable even from the exterior and was positioned either detached or recessed in relation to the historic construction (Figure 6).
Then, non-linear static (pushover) analyses were conducted using macro-element modelling to assess the global seismic response. Eight analyses were carried out: four in the longitudinal (X) direction and four in the transverse (Y) direction. For each axis, two loading directions (+ and -) and two load distributions (uniform and modal) were considered.
The results are shown in Table 2 in terms of the safety index ζ_E calculated according to [21]. The table also reports the IS-V Class, which is derived from the safety index and reflects the building's seismic structural vulnerability (7 classes from A+ to F, with increasing vulnerability). Additionally, the Expected Annual Loss (EAL) Class is shown (8 classes, from A+ to G, with increasing expected losses). The seismic risk class is defined as the worst level between the IS-V and EAL classes [22].

Table 20: Assessment of the security level of the building

Local analyses	Damage limit state (DLS): $\zeta_{E,DLS}$=1,68 Life-saving limit state (LSLS) : $\zeta_{E,LSLS}$=1,63
Global analyses	Damage limit state (DLS): $\zeta_{E,DLS}$=0.494 (Analysis 6) Life-saving limit state (LSLS) : $\zeta_{E,LSLS}$=0.312 (Analysis 8)
Seismic risk class	IS-V Class : D EAL Class: F (EAL = 4,74%)

The new floor system, with improved connections between the masonry and horizontal elements, proved effective in preventing out-of-plane collapse of the walls. This is confirmed by a "local" safety index greater than 1 for both limit states considered. However, the pushover analyses resulted in a minimum vulnerability index of 0.312 for global in-plane behaviour at the Life Safety Limit State (LSLS), which falls below the threshold required for seismic retrofitting ($\zeta_E \geq 0.80$). This highlights the need for additional intervention on the masonry walls to enhance the building's overall load-bearing and deformation capacity.

MODELLING APPROACH

The global seismic behaviour of the building was evaluated in accordance with the Italian standards NTC 2018 [21] and Circolare n.7/2019 [23]. The analysis was conducted using the treMuri macro-element [24] available in the 3MURI software [25], which is specifically designed for masonry and mixed-structure buildings and employs the Frame by Macro Element (FME) method. To assess the impact on the building's global seismic response of the CLT-based overlay, a simplified modelling approach was adopted. In line with the approach adopted by Circolare n.7/2019 to account for reinforced plasters and other types of strengthening overlays, the reinforcement effect was represented by increasing the mechanical performance of the masonry piers/spandrels through coefficients enhancing the material properties. The adopted values were derived analytically, based on experimental evidence from the literature, and applied directly to the mechanical parameters of each masonry wall.

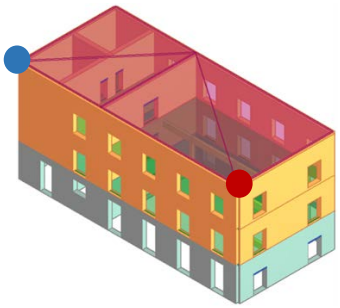

Figure 7. FME project model

The procedure adopted to simulate the CLT panel overlay (composed of three-layered 6 cm thick panels) is summarised as follows:

1. Identification of failure mechanisms: the primary failure modes of the masonry piers (rocking and shear) were first defined.
2. In-plane resistance estimation: the in-plane strength capacity of each pier was then calculated using the formulations provided by the standards. These calculations, summarised in Table 3, were based on the design strength of materials, determined by dividing the characteristic resistance values by the Confidence Factor (CF = 1.35, corresponding to Knowledge Level 1 – KL1).

Table 21. Lateral capacities

Racking failure (V_r)	$V_r = \frac{l^2 \cdot t \cdot \sigma_0}{2} \cdot \left(1 - \frac{\sigma_0}{0.85 \cdot f_{cd}}\right)$	For regular and irregular textures.
Stair-stepped failure (V_{st})	$V_{st} = \frac{l \cdot t}{b} \cdot \left(\frac{f_{v0d}}{1 + \mu \cdot \phi} + \frac{\mu}{1 + \mu \cdot \phi} \cdot \sigma_0\right) \leq V_{st,lim} = \frac{l \cdot t}{b} \cdot \frac{f_{bt}}{2.3} \cdot \sqrt{1 + \frac{\sigma_0}{f_{bt}}}$	For regular textures.
Diagonal cracking failure (V_{cr})	$V_{cr} = l \cdot t \cdot \frac{1.5 \cdot \tau_0}{b} \cdot \sqrt{1 + \frac{\sigma_0}{1.5 \cdot \tau_0}}$	For irregular textures.

l = pier length; t = pier thickness; σ_0= mean vertical stress; f_{cd}= masonry compressive strength; f_{v0d}= masonry shear strength/cohesion; μ = friction coefficient; ϕ = "interlocking coefficient", depending on the brick aspect-ratio; f_{bt}= brick tensile strength

3. Application of the retrofit: the capacity values obtained in Step 2 were then increased by a percentage derived from experimental results available in the literature and given in Table 4.

Table 22. Resistance percentage increase

Floor	Material	$+\Delta V_r$	$+\Delta V_{st/cr}$
Ground	Stone walls	30%	50%
1st	Brick walls	30%	40%
2nd	Brick walls	30%	40%

4. Back-calculation of "reinforced" material properties: using the inverse of the formulas from Step 2, the equivalent material strengths for the reinforced condition were derived. This was based on the increased resistance values calculated in Step 3. The resulting strengths were then compared with those of the unreinforced configuration to determine the corresponding improvement coefficients.
5. Application of improvement coefficients: these coefficients were applied to the material strength properties of each individual pier, depending on their expected failure mode (Table 5).
6. Drift limitation for reinforced piers: in accordance with supporting literature, a maximum drift of 1.5% was imposed on the reinforced piers - representing an expected deformation capacity increase relative to the unreinforced state.

The improvement coefficients obtained through this procedure fell within the following ranges:

Table 23. Range improvement coefficients

Floor	Rocking coefficient [φ_r]	Shear coefficient [$\varphi_{st/cr}$]
Ground	1.06 – 2.22	1.92 – 2.09
1st	1	1.69 – 1.95
2nd	1	1.49 – 1.62

As shown in Table 5, the improvement coefficient for rocking was conservatively assumed to be 1 for the upper storeys, neglecting the contribution of the reinforcement to the strength of walls subjected to rocking. This cautious approach stems from the fact that the method based on improvement coefficients cannot adequately capture the increase in resistant capacity provided by the reinforcement when the axial stress in the masonry is low, as is typically the case in upper storeys.

RESULTS AND DISCUSSION

Starting from the results of the model simulating the as-built conditions, the most stressed piers were identified through an analysis of the damage observed on the façade. An iterative procedure was then implemented: the previously defined improvement coefficients were selectively applied to the most critical piers, followed by updated pushover analyses. A series of incremental retrofit configurations was examined, revealing a progressive enhancement in the seismic response with the increasing number of panels. However, a saturation point was observed, beyond which the addition of further reinforcements to the piers no longer resulted in significant improvements (see Table 6).

Table 24. Vulnerability index and seismic risk classification for the various retrofit configurations

Design level		*As-built (As-B)*	*Retrofit 1 (R1)*	*Retrofit 2 (R2)*	*Retrofit 3 (R3)*	*Retrofit 4 (R4)*	*Retrofit 5 (R5)*	*Retrofit 6 (R6)*
$\zeta_{E\,(LSLS)}$	***3***	*0.449*	*0.751*	*0.928*	*0.949*	*0.949*	*0.949*	*0.949*
	7	*0.339*	*0.664*	*0.464*	*0.692*	*0.691*	*0.694*	*0.802*
IS-V Class		*D 31.49%*	*D 42.91%*	*C 46.41%*	*C 46.41%*	*B 69.14%*	*B 69.43%*	*A 80.20%*
EAL Class		*F 4.74%*	*E 3.59%*	*D 3.32%*	*D 3.32%*	*D 2.50%*	*D 2.50%*	*C 2.47%*

Note: Both analyses are based on uniform load distribution: Analysis 3 was conducted in the -X direction, and Analysis 4 in the -Y direction.

To meet the target of the seismic retrofitting (i.e., $\zeta_E \geq 0.8$), it became necessary to extend the intervention to the spandrels on the west façade, which were characterised by shear failure mechanisms. In accordance with the methodology used for the piers, the shear strengths of the spandrels (τ_0 for stone masonry and fv_0 for brick masonry) were increased by applying improvement coefficients of 1.4 and 1.6, respectively.

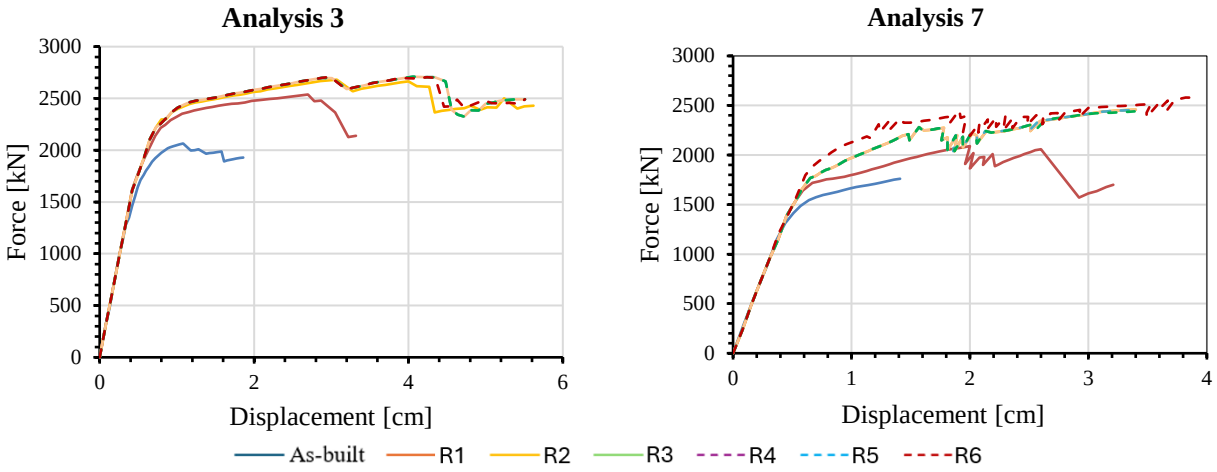

Figure 8. Capacity curves

Figure 8, Figure 9 and Table 6 present the capacity curves, vulnerability indexes at the Life-Safety Limit State (LSLS), and seismic risk classes, expressed in terms of Expected Annual Loss (EAL) and Safety Index (IS-V)[22], for the two most critical analysis scenarios. These results compare the as-built and retrofitted states. The analyses confirm that the progressive increase in reinforcement across the different phases generally resulted in improved capacity curves, higher vulnerability indices, and a clear upgrade in seismic risk classification. The iterative reinforcement procedure proved effective in identifying the optimal configuration, Retrofit 6, which includes CLT panels applied to all ground-floor piers, selected first-floor piers and four spandrels on the western perimeter wall. These findings highlight that full-coverage reinforcement is not always necessary to achieve suitable performance improvements.

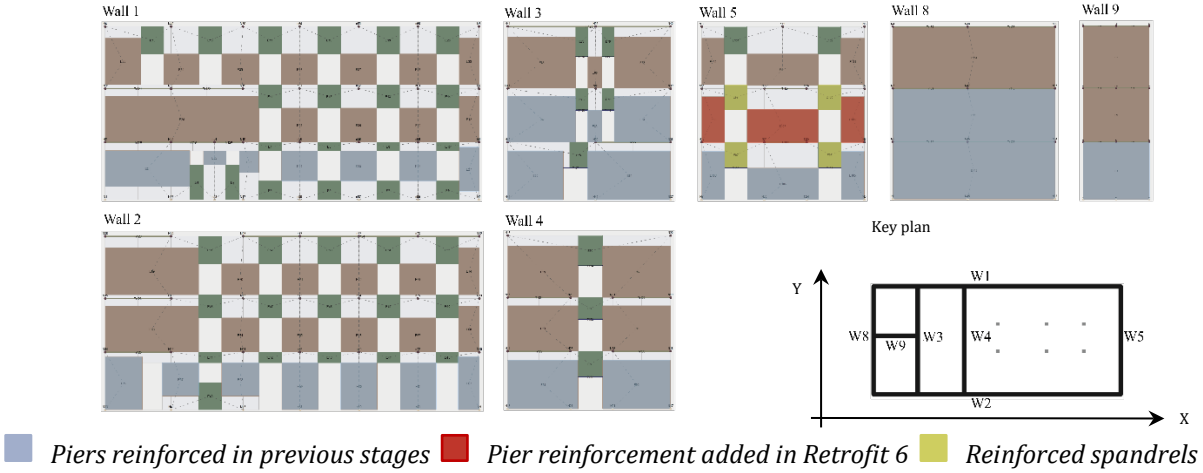

Figure 9. Best reinforcement configuration

CONCLUSION

This manuscript investigates the seismic performance of an integrated retrofit system for URM buildings, which involves the application of timber panel overlays to the internal surfaces of selected walls. A historic case-study building located in northern Italy was selected for the analysis. Following an overview of the renovation project, including hints to architectural aspects, a strengthening strategy featuring multiple configurations with incremental performance levels was examined in detail. The implementation of the optimised strengthening configuration led to a substantial increase in structural

performance, both in strength and displacement capacity. Notably, the IS-V index increased by up to 154%, and a reduction in the Expected Annual Loss (EAL) was achieved. The performance target of $\zeta_E \geq 0.8$ in both directions was successfully met, resulting in an upgrade of three risk classes. The results confirm the effectiveness of the adopted reinforcement strategy and are consistent with experimental findings reported in the literature. This suggests the potential applicability of the same approach to other buildings in similar conditions. However, it should be noted that the results obtained from the FME analysis are conservative, due to the simplified modelling of the reinforcement system. For more accurate and detailed design, more refined modelling approaches should be considered, incorporating variables such as the type and number of timber-to-masonry connections and anchoring devices at the base of the panels.

ACKNOWLEDGEMENTS

The reported research work was undertaken within the framework of the 2024–2026 ReLUIS-DPC network (Italian University Network of Seismic Engineering Laboratories and Italian Civil Protection Agency). Prof. A. Frattari is also thanked for sharing his expert opinion and providing guidance on the architectural aspects of the renovation project. The building's owner, Mr. Mario Marini, is also gratefully acknowledged for granting access to the site.

REFERENCES

[1] G. Larizza, I limiti della riqualificazione edilizia, PhD Diss., Univ. degli Studi di Ferrara, 2014

[2] European Commission, "*European Green Deal "*, Bruxelles, 2021

[3] V. Fronza, Edifici e neutralità climatica: proposta EPBD, Duegradi, 2023 (in Italian) https://www.duegradi.eu/news/edifici-neutralita-climatica/

[4] Maduh, U.J., et al., 2019. In-plane testing of URM wall panels retrofitted using timber strong-backs. Proc. Aust. Earthquake Eng. Soc. Conf., Newcastle.

[5] Dauda, J.A., Lourenço, P.B., Iuorio, O., 2020. Out-of-plane testing of masonry walls retrofitted with OSB timber panels. Proc. ICE Struct. Build.

[6] Cassol, D.; Giongo, I.; Ingham, J.; Dizhur, D. *Seismic out-of-plane retrofit of URM walls using timber strong-backs*. Constr. Build. Mater. 2021, 269, 121237.

[7] M. Busselli, D. Cassol, A. Prada, and I. Giongo. "Timber-based integrated techniques to improve energy efficiency and seismic behaviour of existing masonry buildings." In: Sustainability 13 (2021), 10379.

[8] D. Cassol, M. Danovska, A. Prada, I. Giongo. "Timber-based strategies for seismic collapse prevention and energy performance improvement in masonry buildings." *Sustainability* 16 (2024), 392.

[9] G. Guerrini, N. Damiani, M. Miglietta, F. Graziotti, Cyclic response of URM piers retrofitted with timber, Proc. ICE Struct. Build. 174 (2021) 372–388.

[10] M. Miglietta, N. Damiani, G. Guerrini, F. Graziotti, Full-scale shake-table tests on retrofitted cavity-wall URM buildings, Bull. Earthq. Eng. 19 (2021) 2561–2596..

[11] N. Damiani, G. Guerrini, and F. Graziotti. "Design procedure for a timber-based seismic retrofit applied to masonry buildings." In: Engineering Structures 301 (2024), 116991.

[12] Salvalaggio, M., and Valluzzi, M. R.. "Optimization of intervention strategies for masonry buildings based on CLT components." In: Heritage 5.3 (2022), pp. 2142–2159.

[13] M. R. Valluzzi, E. Saler, A. Vignato, et al., Nested buildings: integrated seismic and energy retrofit with CLT panels, Sustainability 13.3 (2021) 1188

[14] J. Zanni, S. Castelli, M. Bosio, et al., CLT exoskeleton and continuous monitoring, Procedia Struct. Integr. 44 (2023) 1164–1171

[15] J. Zanni, C. Passoni, A. Marini, et al., Wooden prefabcated exoskeleton for URM retrofit, WCTE, Oslo, 2023

[16] I. Giongo, E. Rizzi, D. Riccadonna, M. Piazza, On-site testing of timber-strengthened masonry shear walls, Proc. ICE Struct. Build. (2021). https://doi.org/10.1680/jstbu.19.00179

[17] CEN (European Committee for Standardization), 2024. "Earthquake resistance design of structures – Part 3: Assessment and retrofitting of buildings". prEN1998-3:2024. Brussels, BE.

[18] D. Riccadonna, I. Giongo, G. Schiro, E. Rizzi, M.A. Parisi, Shear testing of timber-masonry dry connections, Constr. Build. Mater. (2019).

[19] E. Rizzi, I. Giongo, D. Riccadonna, M. Piazza, Testing of stone masonry strengthened with CLT, Proc. 4th Int. Conf. PHC, Athens, 2021

[20] D. Cassol, I. Giongo, M. Piazza, Numerical study on seismic retrofit of URM walls with timber, ECCOMAS COMPDYN, Greece, 2021

[21] D. Cassol, E. Nagliati and I. Giongo, *"Seismic Retrofit of a URM Building with Timber-Based Coating: A Numeric Study".* In: Structural Analysis of Historical Constructions. SAHC 2023

[22] M.G.B. Altan, G. Gislon, Architettura d'arte in Aviano, Itinerari 37 (1977) 36–48

[23] Min. Infrastrutture, NTC 2018, D.M. 17/01/2018

[24] Min. Infrastrutture, Sisma Bonus, D.M. 07/03/2017 n. 65

[25] Min. Infrastrutture, Circ. 21/01/2019 n. 7, applicazione aggiornamento NTC

[26] Galasco A, Lagomarsino S, Penna A, Cattari S. TREMURI program: seismic analyses of 3D masonry buildings. University of Genoa; 2009.

[27] S.T.A. DATA, *"3muri brochure versione 12"*, 2020, Torino

EVALUATION OF SEISMIC RESISTANCE OF THE SISAK'S SYNAGOGUE MASONRY STRUCTURE STRENGTHENED BY CLT DIAPHRAGMS AND GLUE-LAMINATED TIMBER ARCHES

Roko ŽARNIĆ[1] and Vlatka RAJČIĆ[2]

[1] Slovenian Association for Earthquake Engineering, Jamova 2, 1000 Ljubljana, Slovenia

[2] University of Zagreb, Faculty of Civil Engineering, Fra Andrije Kačića-Miošića 26, 10000 Zagreb, Croatia

ABSTRACT

The detailed assessment and retrofitting of the historic masonry building in Sisak—originally constructed as a synagogue and later repurposed as a music school—demonstrate a comprehensive and effective seismic strengthening approach. The integration of reinforced concrete frames and lightweight timber structural elements, including CLT diaphragms and laminated timber domes, enables restoration of the original architectural layout while enhancing seismic resilience. Through nonlinear static analysis using the 3Muri software, the retrofitted structure was shown to achieve significant improvements in lateral stiffness and base shear capacity, fulfilling the seismic safety requirements of Eurocode 8. The observed damage patterns confirm the reliability of the structural model and indicate that the upgraded building can withstand future earthquake actions without critical structural failure. This project illustrates a successful balance between architectural conservation and modern engineering demands, offering a replicable model for seismic retrofitting of heritage buildings.

KEYWORDS: Seismic strengthening, Reinforced concrete frames, CLT diaphragms, Nonlinear static analysis, 3Muri software

INTRODUCTION

The main non-technical challenge in planning post-earthquake interventions for damaged historic and monumental buildings is related to their future function. This is also important from an investment perspective, as the overall funds needed for building rehabilitation are often limited.

In cases where buildings have a historic record of their functions during the pre-earthquake period, decisions may be easier. However, they can also be complex due to conservation requirements that consider the original configuration and initial purpose of the building. Returning a building to its original configuration may be very attractive from a conservation and architectural point of view. It opens up possibilities for reviving historic value, even if the new function cannot be equal to the original one for various reasons. However, returning a building to its original external and internal shape poses a serious challenge for structural retrofitting, which must satisfy the requirements of current national technical legislation [1], [2], [3].

The article provides a detailed overview of the retrofitting and partial reconstruction efforts for a historic building in Sisak, Croatia, which was originally built as a synagogue in 1892 and later served as a music school. The building sustained significant damage during the 2020 Petrinja earthquake [4], and the owner is now investing in restoring both its exterior and interior to their original state while maintaining its function as a music school. The efficiency of the proposed retrofitting measures has been

assessed using the 3Muri program, which is widely used for evaluating the seismic resilience of masonry structures.

DESCRIPTION OF DAMAGED BUILDING

The building's layout is of an orthogonal shape, measuring 20.15m in length and 16.15m in width. The height of the building is 15,5 m. Parts of the building, as originally constructed, are of burned clay solid bricks laid in lime mortar. Brick dimensions are l/d/h=30/15/7.5cm. Their characteristic compression strength is 15 MPa. Lime mortar varies in quality between the ground floor and first floor walls. Mortar on the first floor is of very poor quality, with an estimated compressive strength of 0.2 MPa, while the mortar of ground floor walls has an estimated compressive strength of 0.7 MPa.
During WW2, the synagogue ceased its function, and the state authorities repurposed it for public service. The ground floor interior was changed by adding partition walls of different thickness. The two-floor central hall was divided in height by massive new floor structures (Figure 2(a)). Façade windows were partially or entirely closed by masonry infills. The massive masonry arches supporting the timber domes and domes themselves were preserved in the original form, while passages between rooms were partially or entirely closed.

(a) (b)

Figure 1. Building before the earthquake (a) and its front western façade after the 2020 earthquake (b).

The earthquake on December 29, 2020, caused significant damage to the masonry walls. The western façade's gamble collapsed, and the façade walls developed severe cracks, especially along the contacts of the original and infilled parts of the walls in the original openings (Figure 1(b)). On the ground floor, cracks appeared along the contacts of the reinforced concrete floors and the supporting masonry walls (Figure 2(a)). On the first floor, damage occurred in the masonry arches and spandrel parts of the masonry walls (Figure 2(a)). The lightweight timber dome supported by masonry arches remained undamaged. Overall, the western massive part of the building sustained major structural damage, likely due to the tilting of the western part of the building caused by local ground properties where liquefaction might have occurred during the earthquake.

(a) (b)

Figure 2. The damaged interior: the south view of the ground floor(a) and west-north view of the first floor (b).

Learning from the building's earthquake response, a concept of partial reconstruction and retrofitting was developed as a joint endeavour of the asset owner, architects, conservators, and structural engineers. The main suggestion from the structural engineers was to use lightweight materials where possible to reduce future inertial horizontal forces due to earthquake excitation and to reduce vertical loading transferred to the problematic ground.

CONCEPT OF BUILDING RETROFITTING

Upon request of the owner, the layout of the building interior and the shape and dimensions of façade openings should be returned to the original shape of the building. It was a challenging task from the perspective of seismic resilience, especially because the conservator requested the preservation of original structural elements wherever possible. However, the general understanding of the need to introduce structural elements made of wood due to the reduction of masses has been achieved. Following the suggestion of team members responsible for structural issues, the intervention would encompass the following:

- Removal of ground floor inner walls, floor structures above the ground floor, and walls of the first floor, including masonry arches, timber domes, and roof structure.
- Restoring window openings on the ground floor to their original shape and adding reinforced concrete encirclements.
- Repairing ground floor façade walls by grouting and partially replacing weak mortar and constructing the inner reinforced concrete frames (Figure 3), and laying horizontal reinforced concrete tie beams atop the repaired ground floor façade walls.
- Construction of the first-floor inner masonry walls and façade walls extended to the roof knee and gable walls with horizontal reinforced concrete tie beams.
- Installation of laminated timber arches and domes on the first floor and CLT floor diaphragms (Figure 4). Pos.1 and 2 are 15 cm thick CLT panels, Pos. 3 is an 18 cm thick CLT panel, and Pos. 4, 5, and 6 are timber domes.

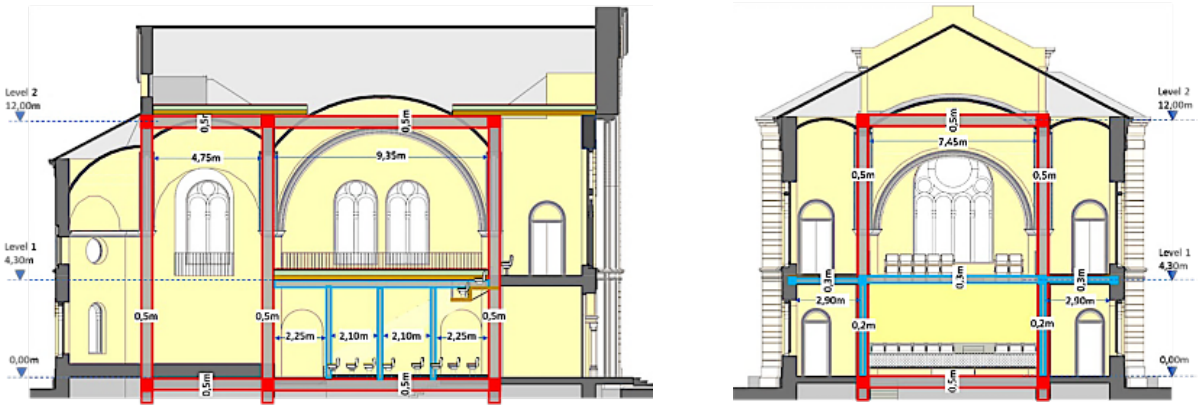

(a) (b)

Figure 3. Concept of retrofitted and added structural elements: longitudinal (East-West) (a) and lateral (South-North) (b) cross-section of building.

The thickness of the ground-floor masonry walls is 61 and 46 cm, while the first-floor walls will be 46 and 30 cm thick. Conservators request the use of bricks of the same type as originally used. The percentage of reinforcement of the main inner frame columns is equal to 3.5% of their cross-sectional area. The percentage of reinforcement of the main inner frame beams is equal to 1.2% of their cross-sectional area.

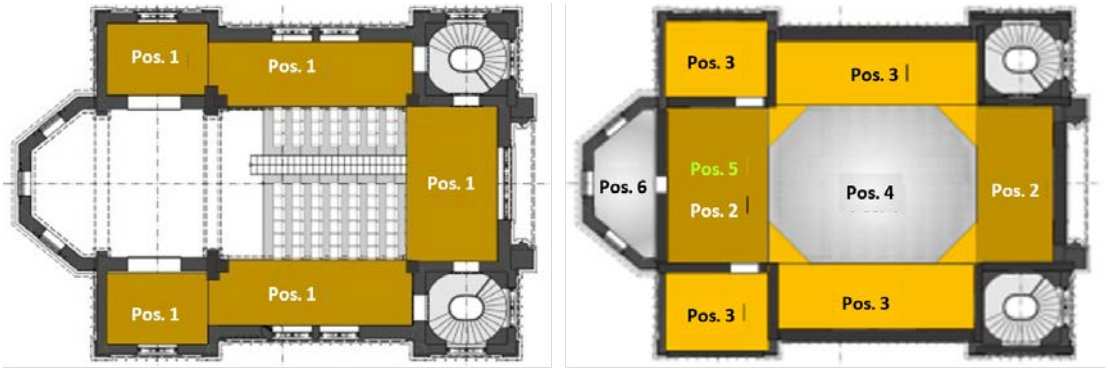

Figure 4. Added horizontal diaphragms on the first floor (a) and attic level (b), and timber domes on the attic level (b).

SEISMIC RESPONSE OF THE RETROFITTED BUILDING

The soundness and adequate earthquake resistance of the proposed structural concept were verified by seismic analysis of the equivalent frame model based on the discretisation in terms of piers and spandrels (SEM - Structural Elements Model). The simulation of the earthquake response of the structure was carried out using the 3Muri, v.13.9 software for the assessment of structures constructed of masonry and mixed materials through a nonlinear (pushover) and static analysis [5]. The theoretical background and practical application of the software are presented. Additionally, 3Muri is frequently used for assessing buildings affected by the 2020 earthquakes in Croatia [6].

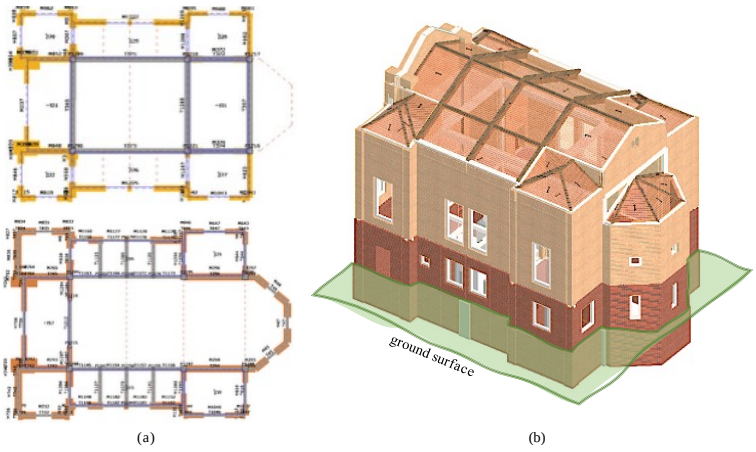

Figure 5. Ground floor and the first-floor layout of the building model (a) and its 3D model (b)

In the presented layouts of the ground and first floors (Figure 5(a)) and the 3D model of the building (Figure 5(b)), the positions of existing and new structural elements (masonry walls, reinforced concrete frames, and timber roof structure) are shown. The existing masonry, which will be repaired, is in a darker colour, while the new masonry is in a lighter colour.

In the equivalent frame approach, only the in-plane response of the URM walls is considered. Each wall is discretised by a set of masonry panels (piers and spandrels), where the nonlinear response is concentrated, connected by a rigid area (nodes).

The wall idealisation into an equivalent frame affects both the elastic field, as it alters the actual deformability of the wall due to the simplification of introducing rigid nodes, and the nonlinear phase of the response, as the regions where the cracks and nonlinearity are likely to develop are assumed a priori. Despite these simplifications, this approach is one of the most widely used in both engineering practice and research due to its computational efficiency in performing nonlinear analyses and its reasonable accuracy, as proven by various numerical simulations in the literature.

Table 25. Mechanical parameters assumed in the SEM model.

Solid brick and lime mortar	E [MPa]	G [MPa]	w [kN/m3]	f_m [N/cm2]	t_0 [N/cm2]
Existing masonry	1600	250	18	150	5
Newbuilt masonry	2100	350	18	230	7,6

E: modulus of elasticity, G: shear modulus, w: average specific weights, f_m: compressive strength, t_0: shear strength. The strength values must be divided by the CF, assumed equal to 1.2.

Table 1 presents the mechanical properties of masonry as used in the building model. The properties of the existing masonry have been derived from the results of standard on-site testing of masonry ("flat jack" compressive test, mortar joint shear test) and laboratory testing of bricks and mortars. The properties of the new masonry were derived from published sources. The shear strength of masonry macroelements was calculated according to Turnšek-Čačovič's theory [9].

RESULTS OF NONLINEAR STATIC ANALYSIS

Nonlinear static analysis was performed on the global equivalent frame model (Figure 5). Pushover curves were extracted by plotting the shear at the base of the building (V) as a function of the mean displacement of the nodes placed at the last floor (d). The control node was defined according to displacements calculated by modal analysis. The corresponding capacity curves (V* – d*) of the equivalent Single Degree of Freedom (SDOF) system were defined by following the general principles of, based on the evaluation of the participation coefficient Γ and the mass M* of each unit (having extracted from the 3D model the data related to each of them). Thus, each capacity curve was obtained by dividing the displacement d by Γ (d* = d/Γ) and the base shear by the product ΓM* (V* = V/(ΓM*)). Finally, for the seismic verification, the capacity curve was compared with the seismic demand. The analyses were performed by adopting, for each examined direction (+X, −X, +Y, and −Y), two different load patterns (LPs): proportional to masses (hereafter referred to as "uniform") and proportional to the product mass per height (hereafter referred to as "pseudo-triangular"). The results refer to the analysis step corresponding to a 20% decay of the base shear, assumed as representative of the Significant Damage limit state (SD) and Damage Limitation limit state (DL).

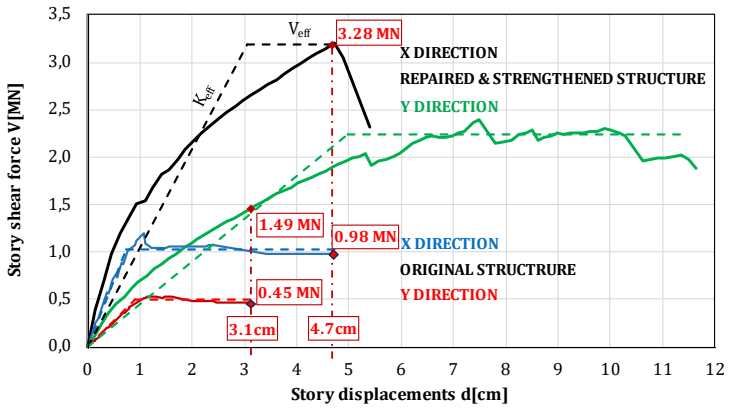

Figure 6. Comparison of modal capacity curves in direction -X and +Y obtained by the most significant analysis.

Table 2. Comparison of parameters of modal capacity curves

Direction of earthquake	Original structure		Strengthened structure	
	K_{eff} [kN/mm]	V_{eff} [MN]	K_{eff} [kN/mm]	V_{eff} [MN]
Direction X	135.3	1.01	104.0	3.19
Direction Y	53.2	0.48	45.0	2.24

K_{eff}: effective building stiffness, V_{eff}: effective building base shear strength

Nonlinear static analysis was performed on the global equivalent frame model (Figure 5). Pushover curves were extracted by plotting the shear at the base of the building (V) as a function of the mean displacement of the nodes placed at the last floor (d). The control node was defined according to displacements calculated by modal analysis. The corresponding capacity curves (V* – d*) of the equivalent Single Degree of Freedom (SDOF) system were defined by following the general principles of, based on the evaluation of the participation coefficient Γ and the mass M* of each unit (having extracted from the 3D model the data related to each of them). Thus, each capacity curve was obtained by dividing the displacement d by Γ (d* = d/Γ) and the base shear by the product ΓM* (V* = V/(ΓM*)). Finally, for the seismic verification, the capacity curve was compared with the seismic demand. The analyses were performed by adopting, for each examined direction (+X, −X, +Y, and −Y), two different load patterns (LPs): proportional to masses (hereafter referred to as "uniform") and proportional to the product mass per height (hereafter referred to as "pseudo-triangular"). The results refer to the analysis step corresponding to a 20% decay of the base shear, assumed as representative of the Significant Damage limit state (SD) and Damage Limitation limit state (DL).

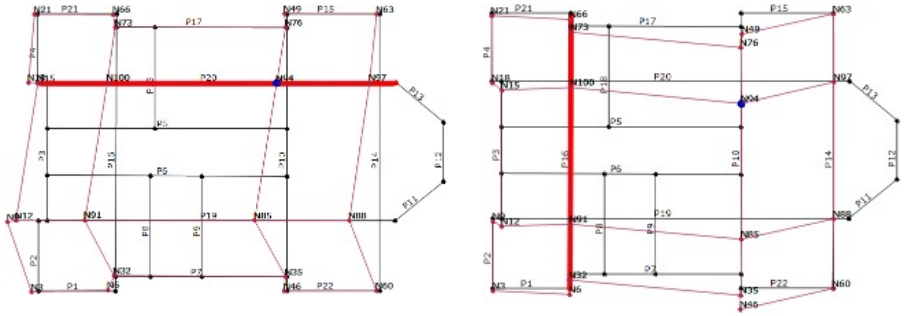

EARTHQUAKE ACTION IN X DIRECTION
dx = 4.7 cm, Vx = 0,98 MN

EARTHQUAKE ACTION IN Y DIRECTION
dy = 3.1 cm, Vy = 0,45 MN

ORIGINAL STRUCTURE

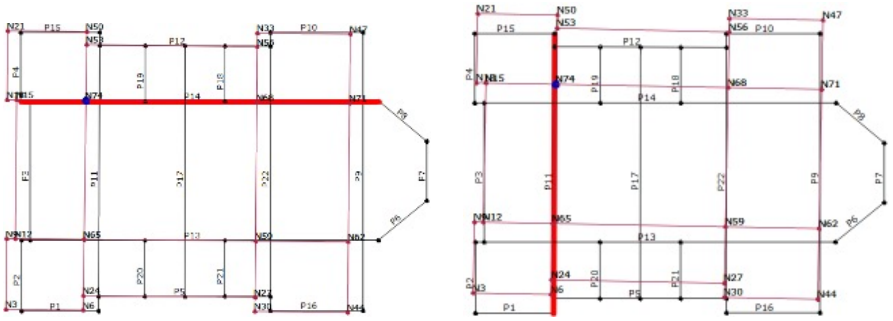

EARTHQUAKE ACTION IN X DIRECTION
dx = 4.7 cm, Vx = 3,28 MN

EARTHQUAKE ACTION IN Y DIRECTION
dy = 3.1 cm, Vy = 1,49 MN

STRENGTHENED STRUCTURE

Figure 7. Comparison of story displacements of the original and strengthened structure, with red line marked wall lines presented in Figure 8 below.

The original structure has a laterally softer upper story, which results in large deformations and severe damage to walls and arches, as shown in Figure 2(b). The lower, stiffer story suffered shear damage mostly along the contacts of reinforced concrete and supporting masonry walls (Figure 2(a)). The observed consequences of the earthquake are well simulated by the herein presented 3Muri assessment. Therefore, it can be presumed that the computation model and method of structural analysis give a realistic prediction of the strengthened structure's behaviour, as presented in Figures 6, 8, and 9. Figure 9 illustrates the distribution of damages at the significant damage (SD) limit state due to the action of the earthquake in the longitudinal (X) and transversal (Y) directions. The colour codification of damage levels is shown in Figure 8. More than half of the masonry piers and walls, as well

as all reinforced concrete columns and beams, are undamaged. The rest of the masonry piers suffered shear failures that did not jeopardise the stability and integrity of the structure. The strong inner reinforced concrete frames provide the global stability and integrity of the structure.

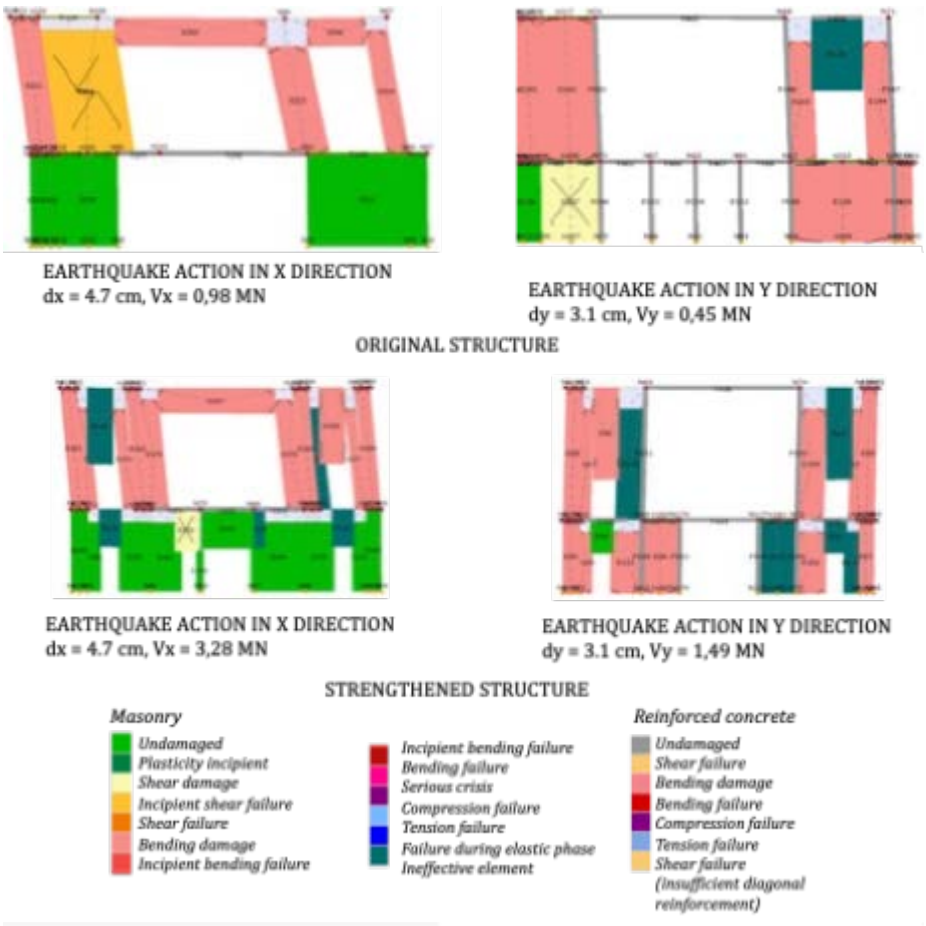

Figure 8. Comparison of deformations and damage levels in walls along the layout lines as depicted in Figure 7.

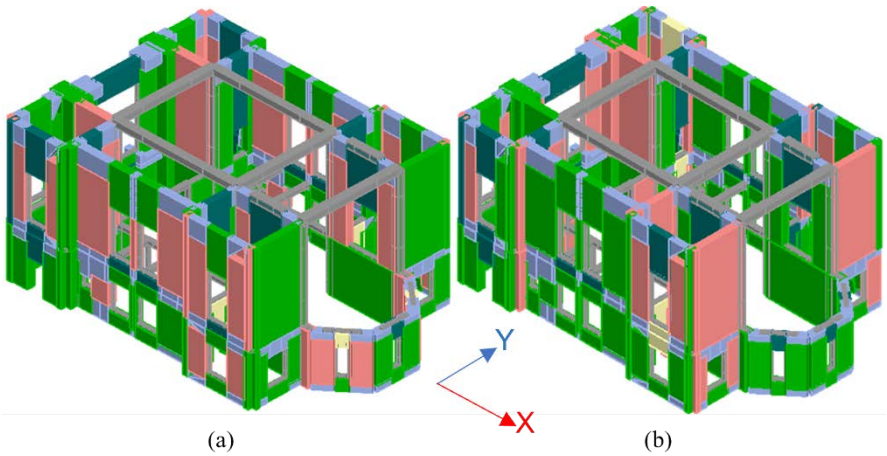

Figure 9. Damage pattern of structural elements resulting from the seismic analysis at achieved story displacement d of 47.1 mm and base shear force V of 3.28 MN in the X direction (a) and story displacement d of 115.0 mm and base shear force V of 2.39 MN in the Y direction (b).

The presented damage pattern of structural elements provides information on the critical parts of the building and its global response to earthquake action. This information is crucial for the design of the structure because the weak parts can be identified and strengthened if needed. However, in the

presented case, there is no need for further strengthening of structural elements because, in the configuration as presented, it fulfils the requirements of Eurocode 8.

CONCLUSION

The post-earthquake rehabilitation and seismic strengthening project of the monumental masonry building in Sisak, Croatia, represents a valuable case study in harmonising structural safety with architectural conservation. Originally constructed in 1892 as a synagogue and later adapted into a music school, the building sustained considerable structural damage during the 2020 Petrinja earthquake, particularly due to its vulnerability stemming from prior functional modifications and the poor quality of historical construction materials.

In response to the seismic damage, the retrofitting concept was carefully developed through a collaborative effort between structural engineers, architects, conservators, and the building's owner. The primary goals of the intervention were to restore the original spatial configuration and architectural identity of the building while significantly improving its seismic resistance in accordance with modern engineering standards. This dual objective introduced several challenges, notably the need to preserve historic elements and maintain architectural integrity, all while achieving compliance with current seismic codes.

The structural intervention strategy is centred around the integration of modern materials and systems that could reduce seismic mass and increase overall structural ductility and strength. Key components included the installation of inner reinforced concrete frames, the reconstruction of damaged masonry with materials matching the original in appearance but superior in strength, and the addition of engineered timber elements—laminated arches and CLT floor diaphragms—to reduce inertial forces and improve load distribution. Reinforced concrete tie beams and encirclements further enhanced structural continuity and confinement.

The efficiency and reliability of the proposed retrofit were rigorously evaluated using the 3Muri software, which employs the Equivalent Frame Model (EFM) to simulate the nonlinear seismic behaviour of masonry structures. Through pushover analysis and evaluation of capacity curves under different loading patterns, the study demonstrated a substantial increase in the structure's lateral strength and deformation capacity. Compared to the original building configuration, the strengthened structure showed a three- to fivefold improvement in base shear resistance, with significant reductions in critical damage zones. Most importantly, the analysis confirmed that the global structural integrity would be maintained under seismic loading conditions representative of Eurocode 8 performance objectives.

Damage pattern simulations at significant limit states showed that more than half of the masonry piers and all reinforced concrete elements would remain undamaged under design-level earthquake actions. The localised damage, primarily shear-related, did not compromise the overall stability or functionality of the structure. This outcome indicates that the intervention not only meets safety requirements but also achieves a high level of resilience, ensuring the continued use and preservation of the historic building in the long term.

Overall, the project exemplifies how modern engineering analysis and materials can be sensitively applied to heritage structures, ensuring both safety and cultural continuity. The methodology presented—balancing architectural restoration, material conservation, and advanced structural modelling—can serve as a model for similar rehabilitation efforts in seismically active regions. The success of this project underscores the importance of interdisciplinary collaboration and highlights the potential for integrating traditional masonry techniques with contemporary seismic design principles.

ACKNOWLEDGMENT

The presented case of earthquake resistance assessment of a repaired, strengthened, and partially reconstructed building is a part of the design documentation produced by PLANETARIS Ltd, Vodnikova 11, 10000 Zagreb, Croatia. The authors of this article contributed to the earthquake resistance assessment, while other involved experts, coordinated by the director of PLANETARIS Ltd., Natko Bilić, provided architectural content, data derived from the site investigations, and conservator's guidelines.

REFERENCES

[1] Act on Reconstruction of Earthquake-damaged Buildings in the City of Zagreb, Krapina-Zagorje County, Zagreb County, Sisak-Moslavina County and Karlovac County(Official Gazzette 21/23) https://mpgi.gov.hr/naslovna-blokovi-133/singled-out/reconstruction-of-the-city-of-zagreb-and-krapina-zagorje-county/reconstruction-of-earthquake-damaged-buildings-in-the-city-of-zagreb-and-krapina-zagorje-county/13723 Accessed on 20.6.2025

[2] Technical Regulation on amendments to the technical regulation for building structures, OG 75/20.

[3] Eurocode 8 (HRN EN 1998-1:2011; HRN IN 1998-3/NA),

[4] https://en.wikipedia.org/wiki/2020_Petrinja_earthquake. Accessed on 20.6.2025

[5] 3Muri Homepage, https://stadata.com/en/ Accessed on 20.6.2025

[6] Penna A.; Lagomarsino S.; Galasco A.: A nonlinear macro-element model for the seismic analysis of masonry buildings, Earthquake Engineering & Structural Dynamics, 43(2): 159-179, 2014. https://doi.org/10.1002/eqe.2335 Accessed: 15/06/2025.

[7] Ademović, N., Toholj, M., Radonić, D., Casarin, F., Komesar, S., & Ugarković, K. Post-earthquake assessment and strengthening of a cultural-heritage residential masonry building after the 2020 Zagreb earthquake. Buildings, 12(11), p. 2024, (2022). https://doi.org/10.3390/ buildings12112024. Accessed 15/06/2025.

[8] Marino, S.; Cattari, S.; Lagomarsino, S.; Dizhur, D.; Ingham, J.M. Post-Earthquake Damage Simulation of Two Colonial Unreinforced Clay Brick Masonry Buildings Using the Equivalent Frame Approach. Structures 2019, 19, 212-226. https://doi.org/10.1016/j.istruc.2019.01.010 Accessed 15/06/2025

[9] Turnšek, V.; Čačovič, F. Some experimental results on the strength of brick masonry walls. In: Proceedings of the 2nd international brick masonry conference. Stoke-on-Trent, UK: British Ceramic Research Association, p.149-156. (1971)

[10] Fajfar, P., Capacity spectrum method based on inelastic demand spectra. Earthquake Engineering & Structural Dynamics, 28(9), 979-993, (1999). https://doi.org/10.1002/(SICI)1096-9845(199909)28:9<979::AID-EQE850>3.0.CO;

CROATIAN EXPERIENCES

REPAIR AND STRENGTHENING OF HISTORIC CHURCH TIMBER ROOFS – STRUCTURAL ASPECTS

Juraj POJATINA[1] and David ANĐIĆ[1]

[1]Studio ARHING d.o.o., Zagreb

ABSTRACT

Following two major earthquakes in 2020 in the Zagreb and Petrinja areas, the Croatian Ministry of Culture undertook the repair and strengthening of damaged churches, most of which had timber roofs. The authors were engaged as structural engineers for renewal designs of more than 40 churches. In the presentation, the assessment and design procedure will be shown, with special emphasis on structural aspects. The presentation systematically delineates all phases involved in the restoration of historical timber roofs. It presents a range of implemented interventions for the load-bearing structure. It also shows detailed execution plans and shares practical insights from construction sites, emphasising the difficulties and challenges encountered during the restoration of this specific architectural and load-bearing structure.

KEYWORDS: historic timber roofs, structural repair and strengthening, structural assessment

INTRODUCTION

Historic timber roofs on churches predominantly consist of pitched roofs covered with tiles or, in more recent times, metal sheeting or asbestos-cement panels. In terms of load-bearing structures, historical roofs are situated beneath the covering, within the attic space, which is typically not visible from the usable parts of the building. Consequently, timber roof structures are frequently neglected or overlooked during conservation evaluations and structural assessments. From a structural perspective, these roofs are classical timber structures predominantly of the truss or rafter variety, spanning the width of the building, typically the distance between the external walls. Given that these structural components are generally as old as the buildings themselves, in the context of structural renovations undertaken following the earthquakes in Zagreb, Petrinja, and the surrounding areas, they primarily consist of timber roof structures that are between 100 and 300 years old.

Evaluating the condition of historical roofs required the collaboration of structural engineers, architects, and wood technology engineers with expertise in timber construction. In instances where the beams are decorated on their underside, it was essential to include a conservator-restorer in the team. Only through the integration of their specialised skills was the condition of the load-bearing structure comprehensively assessed, and the appropriate restoration intervention judiciously determined.

METHODOLOGY / ASSESSMENT

As with any verification of mechanical strength and stability, all foreseeable actions had to be considered, followed by a static calculation, and the load-bearing capacity assessment, along with actual strength classes, reduced cross-sections, and real boundary conditions. The initial deformed state of the

system, or any potential initial deformations, had been considered. During assessment, the following characteristics of historical timber structures were noted:

- The static systems were, in most cases, well-designed with notable redundancy in the system.
- The cross-sections of the bars and beams were generally over-dimensioned, which satisfies the load-bearing requirements. The main reason for over-dimensioning is the builders' awareness of the high impact of the robustness of timber element cross-sections on their durability. Specifically, the effect of moisture in the wood, as well as in the surrounding environment, had a significantly different impact on massive cross-sections compared to slender ones.
- The stabilising elements were also regularly functional and sufficient.
- Larger deformations or deflections mainly occurred due to the long-term creeping of the wood because of changes in the fluctuation content or due to loosening of the joints. In most cases, this loosening referred to local crushing at the point of the connecting material.
- However, the most common problem with exceeding load-bearing capacity is found in significantly reduced cross-sections, primarily due to decay (bearing sections of beams) or external abrasion and other damage.
- In some cases, additional actions were present due to poor original design, which caused increased deformations or deflections (e.g., eccentricity of connections).
- Some of the critical parameters negatively affecting durability and, in turn, load-bearing capacity, include unfavourable environmental conditions for the wood: lack of ventilation in the attic, local moisture and even water retention (accumulation), and parts of elements exposed to frequent changes in atmospheric conditions (sections near the waterline in bridge structures).
- Embedded parts of timber beams were also regularly critical sections of a roof structure due to capillary moisture uptake from the walls and environment, leading to decay of the cross-section.
- Joints are critical points of stability in the roof structure. The HRN EN 17212 (2016) standard notes that traditional carpentry joints can be considered adequate and sufficient for the imposed loads if no damage occurs or loads are not exceeded. In this regard, the joints were carefully examined: their selection (force transfer and adequacy of the cross-section), the interaction of the load on the joint with the anatomical directions of the wood, opening, loosening, crushing, or cracking of the wood at the joint or the joint as a whole. It was considered that the executed joint was not an ideal version, and the level of craftsmanship also had to be evaluated, as poor craftsmanship can significantly reduce the load-bearing capacity and stability of an otherwise good joint. From a conservation perspective, it was preferable to repair or replace joints with historical, contemporary variants, but this was not always possible, so the use of (less noticeable) modern engineering fasteners and materials had to be considered.

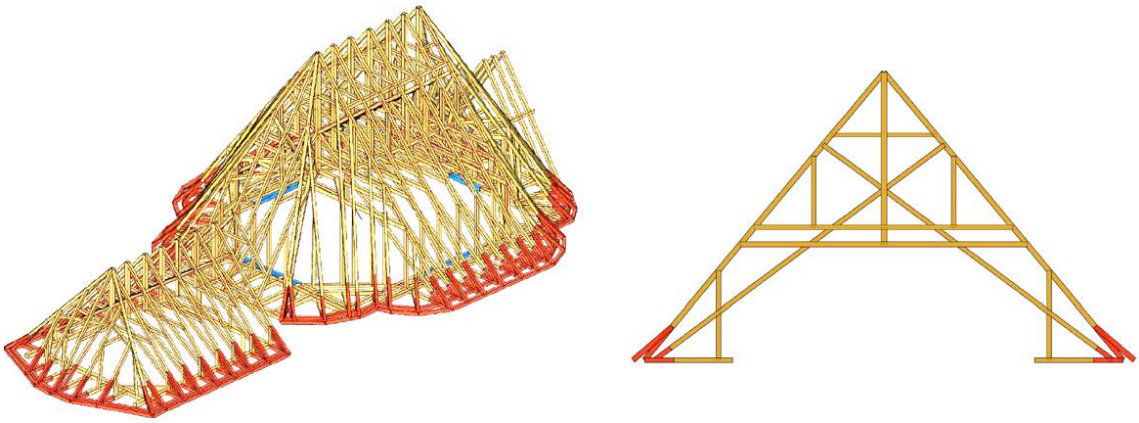

Figure 1. 3D model with marked parts of the elements for replacement.
Church of the Ascension of the Blessed Virgin Mary in Pokupsko (ca 1700).

REPAIR AND STRENGTHENING INTERVENTIONS

In accordance with the conservation valorisation of historical and protected structures, the principles established by ICOMOS for the structural restoration of architectural heritage were applied to these historical timber roofs. These principles prioritise the preservation of original static systems, the safeguarding of original elements and construction assemblies, the protection of original materials, and the reversibility of new interventions, among other considerations. In these structural restorations after the 2020 earthquake, the following interventions have been most frequently implemented:

- Replacement and reconstruction of supporting parts of the tie beam cross-sections;
- Replacement of wall plates along with the reconstruction of horizontal tie beams at the top of the walls.
- Replacement and reinforcement of purlins at the supports;
- Reinforcement, replacement, or addition of joint plates;
- Insertion or replacement of rafters or other worn-out bars or beams;
- Installation of steel stabilising ties;
- Insertion of steel rods to restore deflections or provide additional support;
- Replacement of roofing and roof sheet metal elements;
- Interpolation of steel horizontal ties at the level of the tie beams and horizontal tie beams.

CONCLUSION

The presentation follows a chronological survey of all the activities in preparation for the repair and reinforcement interventions, to the specifics of execution. Due to the complexity of the work and the responsibility involved in the approach to reconstructions, it can be concluded that these repair and strengthening projects of a large number of historic timber roofs present a solid example of a heritage retrofitting approach.

REFERENCES

Construction Restoration and Seismic Damage Projects:

[1] Assessment documents of the existing condition and restoration projects of buildings damaged in the Zagreb and Petrinja earthquakes of 2020. and other repair, strengthening, and extraordinary maintenance projects of wooden roof structures from the archives of Studio Arhing d.o.o., Zagreb.

[2] Assessment of the condition of wooden roof structures reports made as part of the renovation of buildings damaged in the earthquakes in Zagreb and Petrinja in 2020 from the archives of the Laboratory for Wood in Construction (LDG) of the Faculty of Forestry and Wood Technology of the University of Zagreb

POST-EARTHQUAKE CONDITION ASSESSMENT AND STRUCTURAL STRENGTHENING OF HERITAGE SACRAL AND CIVIL BUILDINGS IN CROATIA

Vlatka RAJČIĆ[1], Jure BARBALIĆ[1] and Nikola PERKOVIĆ[1]

[1] University of Zagreb, Faculty of Civil Engineering, Structural Department, Chair for timber structures

ABSTRACT

The global objective of sustainable development has been greatly directed toward preservation of the existing structures and protection of architectural heritage. Condition assessment of the existing timber structures have been gaining in importance in recent times. Bearing in mind that each building material is defined by specific mechanical properties, their distribution and damage mechanisms and degradation processes, it can be concluded that timber as a natural material requires a specific approach to condition assessment. Well collected, processed and formed in digital form, data on the current state is the basis for a reliable projection of the behaviour of the structure. The paper gives an overview of modern methods for determining the geometry of the structure, non-destructive and semi-destructive methods for the condition assessment and monitoring of existing timber structures. In conclusion, an overview of the modern way of storing data in global virtual databases is given as a basis for creating an artificial neural network that would potentially provide faster and more accurate interpretation of data. Typical examples include a museum building, a synagogue, and the roof of an office building.

KEYWORDS: timber structures, condition assessment, structural strengthening, post-earthquake

INTRODUCTION

Timber is often recognized as less durable material and timber structures as short-time lasting structures. While monitoring helps to continuously survey the condition of structures, non-destructive (NDT) methods aim to describe the existing condition of relevant areas of the structure [1]. There are two main areas of assessment and monitoring of timber structures: monitoring & assessment of historical timber structures and monitoring & assessment of relatively new structures erected recently as a result of significant advances and development with the field of new timber materials, timber structures and timber construction in general. The assessment of the structural health of old timber structures is different than the assessment of the new timber structures, e.g. large-span structures. Therefore, advantages in technology with requirements for preservation of both historical objects and new timber structures provoked an increased interest in scientific and professional community in assessment methods for timber structures.

The last decades were marked by a significant widening in the range of application of timber in structures and consequently a growing importance of the assessment of these structures. A wide variety of methods exist to assess timber structures, however, their frequency and scope, the decision-making approach concerning safety and the necessary interventions are far from being agreed upon.

During the INCEPTION HORIZON 2020 project, authors were obtained the assessment and digital capturing of the two case studies in Croatia.

The main purpose of this paper is to summarize the most important assessment methods for existing timber structures. In addition, use of unmanned aerial vehicles and photo digitization of the data which were gathered were used as an input for numerical model and structural analysis of the structure. The whole protocol is shown on actual case study of the H2020 Project INCEPTION, Technical Museum Nikola Tesla in Zagreb, Croatia.

The digital model is expected to become the representation and research needs to acknowledge the changing role that reconstruction, reservation and conservation now play in the representation of heritage and its analysis. INCEPTION models will be able to improve a greater understanding of European cultural assets as well as a direct reuse for innovative and creative applications.

The 3D representations should go beyond current levels of visual depictions, support information integration/linking, shape- related analysis and provide the necessary semantic information for in-depth studies by researchers and users. The generation of high-quality 3D models is still very time-consuming and expensive. Main aim of INCEPTION is to realise innovation in 3D modelling of cultural heritage through an inclusive approach for time-dynamic 3D reconstruction of artefacts, buildings, sites and social environments. More information about the project can be found on the webpage www.inception-project.eu.

Project is divided in eight work packages (WP) and the objective of WP5 is to show and describe use cases and to demonstrate new technologies in digitalizing a cultural asset. Croatian partners are responsible for two case studies: Cultural Heritage Municipality of Unešić (Dalmatian hinterland) and Technical Museum Nikola Tesla in Zagreb.

PROTOCOL OF THE ASSESSMENT ACCORDING TO H2020 INCEPTION project

In this chapter the majority of the NDT and semi-destructive methods to assess existing timber structures are listed, and the most common ones are briefly explained. Very broad overview is given by Colla et al. [2], in the reports of the FP7 European project SMooHS (www.smoohs.eu). Dietsch and Kreuzinger [3] summarized the most common methods: visual (hands-on) inspection, tapping (sounding), mapping of cracks, measurement of environmental conditions, measurement of timber moisture content, endoscopy, penetration resistance, pull-out resistance, drill resistance, core drilling, shear tests on core samples, stress waves, X-ray, dynamic response, load tests (proof loading), strain measurement, microscopic and chemical laboratory methods, macroscopic laboratory methods—testing of specimen. Systematic review of criteria to be used in the assessment and procedure for an assessment are presented by Cruz et al. [4] and Stepinac et al. [5]. Tannert et al. in [6] explained also several new techniques such as infrared thermography, glue line test, screw withdrawal, radial cores to determine compressive strength, pin pushing and surface hardness. Detailed explanations of every method can be found in [7-16]. New methods such as UAV and photo capturing of the objects were explained and presented in a way that they can be useful for structural assessment of buildings..

The simplest and most common NDT technique is visual inspection and it should be first step in assessing timber members in structure and whole structure itself. Obvious damages can be easily identified, including external damage, decay, crushed fibres, creep, or presence of severe cracks. Visual inspection has definite limitations: variability stems from differences in visual acuity and training/experience of personnel, problems with access, knowledge is limited to the exterior surface of the wood. Stress wave and ultrasound methods for investigating wood are based on the propagation of compression waves through wood. The performed tests are based on the time-of-flight measurement to determine wave propagation speed. In these measurement systems, a mechanical or ultrasonic impact is used to impart a wave into a member. The speed of propagation is directly correlated to the modulus of elasticity (MoE), but primary is correlated to the local singularities (knots, grain direction, degradation area...). When propagation velocity of the longitudinal stress wave is gained it is easy to

achieve value of MOE if density of member is known. Rajčić [22] proposes correlation between the ultrasound propagation velocity in a wooden element including other mechanical properties, i.e. strength of wood obtained by destructive laboratory testing. The correlation terms in [21-23] are provided for the velocity of ultrasound propagation for directions parallel and perpendicular to the grain, as derived from the "in situ" testing of very old wooden structures conducted in the scope of the FP7 project „Smart monitoring of historic structures" [21,22]. In the context of her master's thesis, Rajčić proposes in [24] correlations obtained by neural network analysis. Data for the study were obtained by testing the network on a large number of samples investigated using both non-destructive and destructive methods.

One of the most important factors affecting the performance and properties of wood is its moisture content. The amount of water present in wood can affect its weight, strength, workability, susceptibility to biological attack and dimensional stability in a particular end use. It is estimated that over 80% of the in-service problems associated with wood are in some way related to its moisture content. Two general approaches to determine wood moisture content can be distinguished. In direct measurements, the moisture content is determined by oven-drying or water extraction, whereby both are destructive methods with respect to timber members in-situ. Indirect measurement methods use physical properties of wood which are correlated to the wood moisture content [18].

To detect the quality of cross-sections, decay in timber elements and to determine density of timber elements drill/penetration techniques are used. Drilling resistance is classified as quasi-non-destructive because a small diameter hole remains in the specimen after testing. Drill resistance devices operate under the premise that resistance to penetration is correlated with material density. Plotting drill resistance versus drill tip depth results in a drill-resistance profile that can be used to evaluate the internal condition of timber member and identify locations of various stages of decay.

Infrared thermography (IRT) is a non-destructive investigation technique, which is becoming more frequently employed in civil and architectural inspections, in the diagnostic phase, in preventive maintenance or to verify the outcome of interventions. On historic structures, it allows investigating details of construction (e.g. hidden structure or masonry texture behind the plaster), damage and material decay (e.g. moisture, plaster detachment from a wall, cracks pattern evolution, temperature pattern evolution, microclimatic conditions mapping).

Digital photography is the most likely candidate for alternatives to laser scanning efforts. This applies also to cameras embedded on UAV or mobile robots, commonly used for terrestrial/aerial mapping and imagery. The challenges and importance of structural damage assessment, in particular its critical role in efficient post-disaster response, have placed this discipline in the spotlight of the remote sensing community [19]. For rapid damage assessment, remote sensing has been found to be very useful, however, so far it has not reached the level of detail and accuracy of ground-based surveys. Modern science and practice is aimed at maximizing the potential of modern multi-perspective oblique imagery captured from UAVs, using both the high-resolution image data and derived 3-D point clouds, resulting in a detailed representation of all parts of a building. Severe damage could be determined directly from the 3-D point cloud data, while for the distinguishing of lower damage levels structural engineering expertise remains necessary [20]. The aim of 3-D point cloud is that experts could visually identify a number of damage features that are related to a structure.

Nevertheless, problem in an assessment of timber structures are not the NDT principles but lack of guidelines and standards. Over the past years, a multitude of guidelines on how to approach the inspection and maintenance of existing timber structures have been published, however, only a few countries have published applicable code-type documents for the assessment of existing structures [3]. Systematic review of criteria to be used in the assessment of load-bearing timber structures in heritage buildings is presented by document issued by CEN TC 346 Conservation of Cultural Heritage WG10 Heritage timber and Cruz et al. [4].

Figure 1. Different NDT methods: ultrasound, moisture content measurement, drill resistance, infrared thermography

CASE STUDY I – THE TECHNICAL MUSEUM "NIKOLA TESLA", ZAGREB

The Nikola Tesla Museum is a complex scientific and technical museum founded as opposed to more specialized technical museums covering specific technical field. The idea of establishing such a museum dates back to the late 19th century, but the real history of the Technical Museum in Zagreb started in 1954 with the official decision of its establishment. In 1959 the museum, completely made of wood, was assigned to its present location. Facilities were built in 1948 for the temporary purposes - the Zagreb Fair. When the fair moved to a new location, facilities were used for a variety of social and sports activities and later donated to the Museum. Thus, the wooden buildings of the original temporary purpose, remained in constant, intensive use, with a very large number of annual visits by visitors from abroad and domestic people. Entire structure was designed and constructed as a timber structure and as such represents a rare existing example of European engineering concept of expo-halls timber structures with large span (85x40m) from the early 20 century. Object of interest, besides of the building, are individual exhibition specimens that are under the protection of the Conservation Department in Zagreb, Protection of Cultural Heritage [5].

The building which is a cultural property is under reconstruction/restauration for the last 10 years. Project of the condition assessment and reconstruction was finished in a period between 2010 and 2015 under the lead of Professor Vlatka Rajčić (University of Zagreb) [24].

Main objectives for the INCEPTION PROJECT regarding the museum were: to enhance the understanding of the history of institution, it's role in Republic of Croatia, the artistic value represented by the building and the artworks; 3d model, video presentation of the object and collection of exhibits; BIM model for condition assessment and improvement of energy efficiency in order to find solutions for thermal comfort.

External dimensions of the main hall are 87.75m (west facade) × 25.40m. Total area of ground plan is about 2137m2. East and west facade are partly glazed and partly covered with wooden panels, while the north and south facade are entirely covered with wooden panels. The main load-bearing system is 13 truss frames with spacing of 6.8 to 7.3m. Main timber frames are interconnected with 11 secondary trusses with spacing of 1.6m to 3m.

External dimensions of the main hall are 87.75m (west facade) × 25.40m. Total area of ground plan is about 2137m2. East and west facade are partly glazed and partly covered with wooden panels, while the north and south facade are entirely covered with wooden panels. The main load-bearing system is 13 truss frames with spacing of 6.8 to 7.3m. Main timber frames are interconnected with 11 secondary trusses with spacing of 1.6m to 3m.

The highest elevation of the hall from the front-eastern side of the building is 19.74m. Spatial stabilization of the building was done with three horizontal transverse, four longitudinal horizontal wind stabilizations and two vertical wind bracings [5].

Except the central hall, two side spaces exist. Side exhibition space is circling around the central part. Structural elements in these parts are small columns from the basement to the gallery and they support

gallery floor structure which consists of the horizontal beams 36/40 cm at distance of 1.25 m. Roof structure is timber truss.

Figure 2. Photos from the construction phase of the museum AND museum building filmed by UAV

Assessment of the structure started with visual control of the structural elements. Inspection activities revealed severe damage to the large number of facade columns. The western part of the facade had direct contact of the timber columns with foundation and decay was caused by a contact with rainwater or humidity. The specimen was taken from one of the damaged columns. Moisture measured in the given positions varied from 6% to the maximum moisture content of 20%. Tests by acoustic ultrasound were carried out to obtain modulus of elasticity of timber structural elements perpendicular to the fibres.

While assessing the structure, many defects were detected, not dangerous for the global bearing capacity, serviceability and structural stability, but this local damage can lead to local instability. Investigation work also revealed damage to the large number of columns of the west façade – the detail of the timber columns with direct contact with the ground which caused the decay of the lower part of the pillars where pillars due to damage on the system of the water drainage were constantly in contact with water. In many of the elements deep cracks were observed in longitudinal direction and in the vicinity of connectors. Examination revealed that a number of elements had visible torsion rotations of the cross section with respect to the vertical axis.

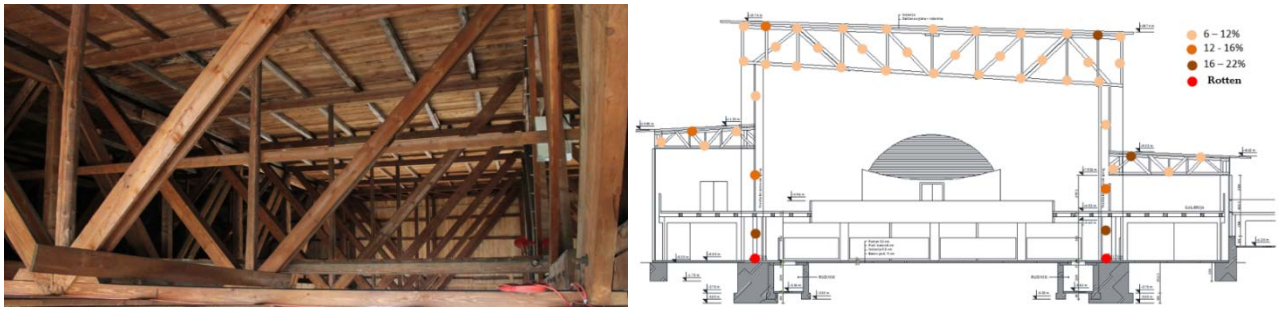

Figure 3. Measurement of the moisture content in roof timber trusses

The last part of the assessment of the timber structure was detailed survey of timber joints and connections between elements. Lot of connections in the structure were either poorly executed or their properties decayed over time. A number of joints were executed with improper installation of fasteners so their load bearing capacity is questionable. Several joints in the tensile zones of the timber trusses have been made by just a few fasteners. Carpentry joints were generally in good condition but some were not performing in the way in which they were intended to perform. The main reasons are the changes that have occurred over time and/or initial wrong execution of timber joints.

After the complete assessment of timber structure of the Technical Museum Nikola Tesla, proposals and recommendation for reconstruction, repair and/or strengthening of the structure were given.

In parallel with the structural and condition assessment of the museum, a 3-D model of the museum was created using UAV and photogrammetry. Data capturing was done and post processing of the gathered data is still ongoing. High resolution photographs were taken and point cloud models were created. The

flight height should be maintained the same for the entire duration of the shooting. After initial filming with UAV, photos were being processed in one of the photogrammetry programs. The photos were aligned and reference points were defined. Values of the coordinates for the corresponding points were entered and the entire area is georeferenced.

CASE STUDY II – THE SYNAGOGUE BUILDING, KOPRIVNICA

The building in question is a three-part synagogue from 1875, built on the model of the Viennese one. Throughout history, and as today, the building had the same sacral purpose. The building in question has been adapted several times for maintenance purposes, and the last major interventions were carried out in 1930.

The wooden part of the supporting ceiling structure of the ground floor is formed by the main assembled (three-part) beams laid along the perimeter of the gallery structure, i.e., parallel to the longitudinal facade and transverse portal (southern) facade wall, and secondary beams laid orthogonally to the longitudinal facade walls. The main beams are supported on wooden columns positioned as a continuation (above) the steel columns of the gallery structure, i.e., at the ends directly (without substructure) on/into the masonry walls. The secondary cross beams that span the span between the main beams and the facade walls are supported on the main beams in such a way that they are wedged between the lower and upper beams of the composite beam (the width of the middle beam of the composite beam in relation to the width of the upper and lower beams is smaller by the width of the cross beam support), or, at the ends, directly (without sub-means) on/into the masonry walls. The secondary cross beams that span the central span between the main beams are supported on the main beams. On the underside of the secondary beams, a board formwork with plaster on reeds is placed. The formwork boards are made of soft wood (spruce) and have an average thickness of 2.40 cm.

The roof structure consists of the main load-bearing systems laid orthogonally to the longitudinal facade walls. The roof structure is constructed in the form of a complex truss (a double truss at a higher level, the connecting beam of which is also the strut of the double truss at a lower level of the roof structure), whose connecting beam is supported on the main longitudinal beams of the ground floor ceiling structure in the axes of wooden columns positioned above the steel columns of the gallery structure, or at the ends directly (without substructure) on/into the masonry walls. The main load-bearing system consists of rafters, purlins, bay and ridge beams, trusses, clamps, struts, arms, columns, trusses and connecting beams, and lintels. Board formwork is placed on the rafters, on which battens, counter battens and covering (tiles) are laid. The formwork boards are made of softwood (spruce) and have an average thickness of 2.40 cm. All beams are sawn timber after processing and are made of softwood (spruce). The connection details of all elements are made in a classic way, with carpentry joints or with steel clamps, nails and metric screws.

The ground floor is unheated, dry and poorly ventilated, with a relative humidity of approximately 60%. The temperature varies in relation to the outside by approximately 30%. The attic is unheated, dry and poorly ventilated, with a relative humidity of approximately 60%. The temperature varies in relation to the outside by approximately 20%.

The condition of the structure was assessed based on a visual inspection, measurement of the equilibrium moisture content in the material (by indirect method), measurement of the dynamic modulus of elasticity of the material (by indirect method) and testing of the material density. Selection of reference measurement points based on visual assessment of the condition (elements where significant degradation was observed were selected). A sample of the timber was taken from the load-bearing element of the gallery structure, in a way that did not jeopardize its mechanical resistance and

stability and usability. This project determined the load duration class and the use class according to , determined the wood class and included an analysis of the condition of the wooden part of the load-bearing structure, indicating the critical properties of the structure in question.

The following conclusions were drawn from the investigation and analysis of the wooden part of the supporting structure of the gallery and the ceiling structure of the ground floor of the building in question. There was no degradation of the wooden structure during lateral impacts. The structure of the gallery structure is in good condition, with occasional local signs of degradation in the form of cracks along the element and significant cracks in the main cross beams at the points of connection with the steel column. The structure of the ceiling structure of the ground floor is in relatively good condition, with occasional local signs of degradation in the form of cracks along the element. The exception is certain elements where significant degradation in the form of rot and wormholes, twisting and/or deeper cracks along the element were observed. Also, the exception is the beam heads, where global degradation in the form of significant cracking and local degradation in the form of rot and wormholes was observed, and since they participate in the transfer of a significant part of the load, it is considered that even with reconstruction works, they will not meet the load-bearing and usability requirements. The same is true with the roof structure. Therefore, guidelines for reconstruction have been provided.

CASE STUDY III – THE ROOF STRUCTURE OF MINISTRY BUILDING , ZAGREB

The building in question is a city building from the second half of the 19th century, built in the style of early historicism. During its history, the building had various purposes, and today it houses the offices of the Ministry of Foreign and European Affairs of the Republic of Croatia.

Based on the survey and survey of the existing condition, the following was defined. The interfloor construction between the attic and the first floor consists of wooden beams laid in a direction parallel to the longitudinal axes of the building and directly (without substructure) supported on/in the masonry walls, or, on steel beams made of "I" profiles (laid in a direction orthogonal to the longitudinal axes of the building and directly (without substructure) supported on/in the masonry walls). The beams are sawn timber after processing and are made of soft wood (spruce). On the underside of the beams, a board formwork with plaster on reeds was placed, and on the upper side of the beams, reeds, and on the upper side of the beams, a load-bearing walkway system in the form of a ship's floor, or board formwork, on which a concrete screed was laid as a final layer. The formwork boards are made of softwood (spruce) and have an average thickness of 2.40 cm.

The roofs consist of the main load-bearing systems laid in a direction parallel to the transverse axes of the building. The roof structure is made in the form of a double hanger. The main load-bearing system consists of rafters, purlins, bay and ridge beams, hangers, clamps, struts, arms, columns, trusses and connecting beams and lintels. The connecting beams are raised from the attic floor level by approximately 10 cm and are directly (without substructures) supported on/in the masonry walls. The beams are sawn timber after processing and are made of softwood (spruce). The connection details of all elements were made in the classic way, with carpentry joints or steel clamps and screws. The rafters were covered with wooden formwork, battens, counter battens and roofing (tiles). The formwork boards were made of softwood (spruce) and had an average thickness of 2.40 cm.

Due to the functionality of the attic space, and due to the significant height of the roof structure itself, a service path of at least 80 cm wide was placed on the strut elements of the main load-bearing systems, consisting of wooden beams with a load-bearing walkway system in the form of a ship's floor, i.e. wooden formwork

The attic space is unheated, dry and ventilated (better at the top of the roof, and somewhat less so in the interfloor structure), with a relative humidity of approximately 60%. The temperature varies by approximately 20% compared to the outside.

The procedure for inspecting the condition of the wooden part of the roof structure of the building in question, as well as investigative tests, were carried out in accordance with all applicable regulations and standards. The condition of the structure was assessed based on a visual inspection, insight into the measured geometry of the structure (existing condition), measuring the equilibrium moisture content in the material (by indirect method), measuring the value of the dynamic modulus of elasticity of the material (by indirect method) and testing the density of the material. The selection of reference measurement points was based on a visual assessment of the condition (elements on which degradation was observed were selected). A sample of the timber was taken from the load-bearing element of the inter-storey structure, in such a way that the mechanical resistance and stability and usability of the same were not compromised. This project determined the load duration class and the use class, determined the wood class and included an analysis of the condition of the wooden part of the roof structure of the building in question, indicating the critical properties of the structure in question and degraded elements. The project also provided guidelines and recommendations for the renovation work of the structure in question.

The elements of the structure in question are mostly in an unworn condition, but for some elements it is considered that even with reinforcement work, they will not meet the load-bearing and usability requirements, therefore they need to be replaced in their entirety. The following conclusions were drawn from the investigation tests based on a visual inspection.

In some elements, cracks are visible along the axis of the element, resulting from changes in moisture content in the wood and shrinkage of the wood due to drying. Some cracked elements due to significant (deeper) degradation, i.e. excessive dimensions and the number and arrangement of cracks, need to be repaired/reinforced in order to achieve full load-bearing capacity. In some elements, twisting around the longitudinal axis was observed, but not to such an extent that they lost their load-bearing and usability function. During the investigation tests, no degradation was observed due to exceeding the mechanical resistance and stability of the elements. However, excessive permanent deformations of the elements were observed, but they do not significantly affect the mechanical resistance and stability and functionality of the structure in question.

The investigation revealed a lack of fasteners in the connection of the two elements, but this did not result in a loss of the load-bearing capacity of the connection. Furthermore, improperly executed connections were observed, which resulted in a loss of the load-bearing capacity of the connection, i.e., exceeding the mechanical resistance and stability of the elements and the appearance of a mechanism in the structure in question. Also, during seismic actions, there was degradation (failure) of the entire connection of the two elements, especially at the points of connection of the "bondruk" system and the roof structure (pulled out steel clamps). Also, in some places during seismic actions, there was degradation of the masonry (brick) filling of the "bondruk" system, as well as degradation of the wooden frame due to the appearance of wormholes and rot.

During the investigation, degradation of biological origin was observed. In some elements, a wormhole was observed, which is noticeable mainly on the surface, although in some elements, local degradation into wormholes is more significant and noticeable deeper in the cross section and along the element. In the elements near the positions where the roof leaks occur, rot was observed (along the bearings and along part of the span), which was noticeable both on the surface and in the depth of the cross section (up to 40% of the cross section).

CONCLUSIONS

At the moment lot of different assessment techniques exists and are representing promising methods for a quantitative description of the current condition of timber members in timber structures. This concerns material properties like modulus of elasticity, moisture content and density as well as structural properties like dynamic characteristics, localization of inhomogeneities, cracks, and biological attack [1].

Although some methods and instruments shown to be of very high quality and are necessary for the evaluation of structures, some devices do not guarantee value for which they were designed. Nevertheless, new techniques and devices are influencing the "classical" condition assessment of structures. For rapid damage assessment, remote sensing has been found to be very useful, however, so far it has not reached the level of detail and accuracy of ground-based surveys. Modern science and practice is aimed at maximizing the potential of mod-ern multi-perspective oblique imagery captured from UAVs, using both the high-resolution image data and derived 3-D point clouds, resulting in a detailed representation of all parts of a building.

The main focus of this paper was to present non-destructive and semi-destructive test methods which are highly in use for the assessment of old and under protection heritage objects and to show them on the special case study in Croatia. In addition to this practice, problems were pointed out in the state of the structure after the earthquake. More information and detailed procedure assessment can be found in [5, 22-25].

REFERENCES

[1] Krause, M. et al.: Needs for further developing monitoring and NDT-methods fir timber structures, Proceedings of the International Conference on Structural Health Assessment of Timber Structures, pp. 89-99 (2015)

[2] Colla, C. et al.: Laboratory and on-site testing activities part 3 - Historical timber elements, Report of SMooHS European FP7 project

[3] Dietsch, P. & Kreuzinger H.: Guideline on the assessment of timber structures: Sum-mary, Engineering Structures, Vol. 33 (2011), No. 11, pp. 2983-2986

[4] Cruz, H. et al.: Guidelines for On-Site Assessment of Historic Timber Structures, In-ternational Journal of Architectural Heritage, Vol. 9 (2015), pp. 277-289

[5] Stepinac, M., Rajčić, V., Barbalić, J. (2017). Inspection and condition assessment of existing timber structures, GRAĐEVINAR, 69 (9), 861-873

[6] Tannert, T. et al.; In situ assessment of structural timber using semi-destructive tech-niques, Materials and Structures, Vol. 47 (2014) No. 5, pp. 767-785

[7] Kasal, B.; Lear, G. & Anthony, R.: Radiography, In In Situ Assessment of Structural Timber. State of the art of the RILEM, Springer, 2011, pp. 39-50

[8] Pošta, J.; Dolejš J. & Vitek L.: In Situ Non-Destructive Examination of Timber ele-ments, Advanced material Research, Vol. 778 (2013), pp. 250-257

[9] Kuklik, P. & Kuklikova, A.: Methods of evaluation of timber elements, Wood Re-search, Vol. 46 (2001) No. 1, pp. 1-10

[10] Kasal, B. & Anthony, R.: Advances in in situ evaluation of timber structures. Progress in Structural Engineering and materials, Vol. 6 (2004) No. 2, pp. 94-103

[11] Carpentier, O. et al.: Active and quantitative infrared thermography using frequential analysis applied to the monitoring of historic timber structures, Proceedings of the International Conference on Structural Health Assessment of Timber Structures, pp. 61-70, 2015

[12] Hasnikova, H.; Vidensky J. & Kuklik P.: Influence of the device structure on the outputs ofsemi-destructive testing of wood by Pilodyn 6J, Proceedings of the Interna-tional Conference on Structural Health Assessment of Timber Structures, pp. 504-513, 2015

[13] Nowak, T.; Hamrol-Bielecka K. & Jasienko J.: Experimental testing of glued laminat-ed timber members using ultrasonic and stress wave techniques. Proceedings of the International Conference on Structural Health Assessment of Timber Structures, , pp. 523-534, 2015

[14] Sandak, J. et al.: An alternative way of determing mechanical properties of wood my measuring cutting forces. Proceedings of the International Conference on Structural Health Assessment of Timber Structures, pp. 543-552, 2015

[15] Yamaguchi, N. & Nakao M.: In-situ Assessment method for timber based on shear strength predicted with screw withdrawals, Proceedings of the International Confer-ence on Structural Health Assessment of Timber Structures, pp. 569-578, 2015

[16] Tannert, T.; Kasal B. & Anthony R.: RILEM TC 215 In-situ assessment of structural timber: Report on activities and application of assessment methods, Proceedings of the World Conference on Timber Engineering, , pp. 642-648, 2010

[17] Piazza, M. & Riggio M.: Visual strength-grading and NDT of timber in traditional structures, Journal of Building Appraisal, Vol. 3 (2008) No. 4, pp. 267-296

[18] Franke, B. et al.: Assessment and monitoring of the moisture content of timber bridges, available online

[19] Rastiveis, H., Samadzadegan, F., and Reinartz, P.: A fuzzy decision making system for building damage map creation using high resolution satellite imagery, Nat. Hazards Earth Syst. Sci., 13, 455–472, 2013

[20] Fernandez Galarreta, J., Kerle, N., Gerke, M.: UAV-based urban structural damage assessment using object-based image analysis and semantic reasoning, Nat. Hazards Earth Syst. Sci., 15, 1087–1101, 2015

[21] Rajčić, V. et al.: Smart Monitoring of Historic Structures Case study 3: Palazzo Malvezzi, Report of SMooHS European FP7 project, available from http:// www.smoohs.eu/tiki-in-dex.php?page = project %20results: (2012-02-14)

[22] Rajčić, V., Cola, C.: Correlation between destructive and four NDT techniques tests on his-toric timber elements, Proceedings of the 1st European Conference of Cultural Heritage Pro-tection, Berlin, Germany, (2012), pp. 148-155.

[23] Rajčić, V: Neural network for wood member clasification based on the results from nonde-structive testings of wood samples, Proceedings of the 4th International Conference of Slo-venian Society for Nondestructive Testing, Ljubljana, Slovenija, (1997), pp. 59-66

[24] Rajčić, V., Čizmar, D., Stepinac, M.: Reconstruction of the Technical Museum in Zagreb, Advanced material Research, 778, (2013), pp. 919-926